OPTIMISATION OF THE THERMAL DESIGN OF DISC-TYPE POWER TRANSFORMER WINDINGS

by Edward Patterson Childs, Jr., B.A., B.Sc., M.Sc.

Thesis Submitted to the University of London

for the Degree of Doctor of Philosophy

Department of Electrical Engineering

Imperial College of Science and Technology

February, 1984

© E. P. Childs, Jr. 1984

ABSTRACT

The purpose of this thesis is to present a computer program DISCNET written in FORTRAN which, given all the relevant constructional details of a disc-type power transformer winding and its operating conditions, will predict its thermal behaviour and in particular the location and value of its 'hottest spot' temperature. The software is restricted to ON, OF and OD transformers with flow-diverting washers. The horizontal and vertical cooling duct thicknesses, and the number of ducts per pass, appear to be the design parameters which influence the thermal behaviour most markedly. Significantly lower 'hottest spot' temperatures may be obtained using fewer ducts per pass, and vertical to horizontal duct thickness ratios greater than unity. A sample computation is made for an experimental winding rigged with 99 thermocouples and designed so that the oil flow distribution can be measured directly in each duct of an 8 duct pass, using a quartz insulated hot-film constant-temperature velocity probe. DISCNET prediction and experimental results agree well, given some uncertainty in the determination of the total flow rate in the measurement pass.

The theoretical and computational basis of DISCNET is given extensive treatment. The general purpose laminar Navier-Stokes and energy equation solver TEACH-L is described. The program was adapted as necessary to obtain tee-junction and corner flow pressure loss data, and to analyse the conjugated heat transfer which takes place at the oil-paper-copper interfaces in the horizontal ducts. These results were then assembled into an iteratively solved linear network which is the main part of DISCNET. Low Reynolds number flow in the winding permits essentially linear analysis of the flow distribution, but mostly weak

non-linearities due to junctions and corners, together with the variation of the fluid properties with temperature, necessitate iteration.

DEDICATION

I would like to dedicate this thesis to the memory of my father, Edward P. Childs, who died while the work was in progress.

ACKNOWLEDGMENTS

The author wishes to acknowledge the kind assistance and support of his supervisor, Dr. P. H. G. Allen. The work would have been impossible without the benefit of his extensive experience in thermal aspects of electrical machinery. The interest of Dr. O. Szpiro, who designed the facsimile winding, is also acknowledged.

Dr. A. D. Gosman kindly permitted the use of his computer program TEACH-L, and Dr. John Shemilt provided constant assistance at all stages of the computational work.

Mr. B. Gingell constructed the calibration duct, and the aluminium discs were expertly machined by Mr. W. Brown. Mr. R. Moore, the machine shop supervisor in the Electrical Engineering Department, was extremely helpful when the inevitable sudden or emergency jobs cropped up. Mr. R. B. Owen provided much helpful advice and assistance with laboratory apparatus.

Finally, the support of the National Science Foundation, Washington, D. C., U.S.A. and the Committee of Vice Chancellors and Principals, is gratefully acknowledged.

CONTENTS

		Page
ABSTRACT		3
DEDICATION		5
ACKNOWLEDGMENTS		6
LIST OF FIGURES		14
LIST OF TABLES		19
LIST OF SYMBOLS		20
CHAPTER ONE:	INTRODUCTION	32
1.1	Power Transformers and the Thermal Problem	32
1.2	Winding Designs and Cooling Configurations	35
1.3	Conventional Temperature Specifications and Attempts to Improve Them	39
1.4	Previous Treatments of the Transformer Thermal Problem	43
1.5	Overview of the Thesis	48
CHAPTER TWO:	THE PROBLEM DESCRIBED	50
2.1	Disc Winding Geometry	50
2.2	Problem Statement	53
2.3	Preliminary Observations	54
2.4	Governing Equations	58
2.5	Solution Strategy	61
CHAPTER THREE:	SIMPLE NETWORK MODEL	65
3.1	Simplifying Assumptions	65
3.2	Network Equations	72
3.3	Constant Property Disc Surface Temperature	76

		Page
3.4	Friction Loss and Buoyant Pressure Regain	77
3.5	Sample Calculations	78
3.6	Comparison with Experiment and Finite Difference Computations	82
3.7	Summary	84
CHAPTER FOUR:	FIELD EQUATION CALCULATIONS	85
4.1	Introduction	85
4.2	Generalised Field Equations	87
4.3	Control Volume Equations	89
4.4	Solution of Control Volume Equations	99
4.5	The SIMPLE Algorithm	100
4.6	Convergence, Underrelaxation and False Sources	105
4.7	Staggered Grid and Variable Spacing	108
4.8	Conclusion	110
CHAPTER FIVE:	TEE-JUNCTION FLOWS	111
5.1	Introduction	111
5.2	Flow Domain and Boundary Conditions	114
5.3	Micro vs. Mainframe Computing	117
5.4	Sample Output and Mesh Dependency Tests	119
5.5	Friction Constants	123
5.6	Conclusion	134
CHAPTER SIX:	CORNER FLOWS	135
6.1	Introduction	135
6.2	Flow Domain and Boundary Conditions	136
6.3	Definition of Friction Constants and Results	137

		Page
CHAPTER SEVEN:	DUCT FLOWS	139
7.1	Introduction	139
7.2	Initial Assumptions	141
7.3	Grid Arrangements and Boundary Conditions	143
7.4	Sample Output	151
7.5	Variable Viscosity Friction Constant	152
7.6	Mesh Dependency	153
7.7	Conclusion	154
CHAPTER EIGHT:	DISCNET	155
8.1	Introduction	155
8.2	Network with Junction and Corner Resistances	158
8.3	Sample Results	160
8.4	Conclusion	162
CHAPTER NINE:	EXPERIMENTAL WORK, INTRODUCTION	164
9.1	Introduction	164
9.2	The Experimental Winding	167
9.3	Hydraulic Circuit	170
9.4	Electrical Circuit	172
9.5	Concluding Remarks	173
CHAPTER TEN:	HOT-FILM VELOCITY PROBE MEASUREMENTS	174
10.1	Introduction	174
10.2	Calibration Apparatus	177
10.3	Calibration Procedure	180
10.4	Correlation of Results	184
10.5	Discussion	188

Page

CHAPTER ELEVEN: WINDING TEMPERATURE MEASUREMENTS 191

11.1 Introduction 191

11.2 Mean Winding Temperature Measurements by Resistance 193

11.3 Thermocouple Measurements 194

11.4 Horizontal Duct Centre-Line Temperatures Measurements 201

11.5 Thermal Characteristics of the System 201

11.6 Closure 203

CHAPTER TWELVE: COMPARISON OF THEORY AND EXPERIMENT 205

12.1 Overview of Experimental Programme 205

12.2 Cold Oil Velocity Measurements 205

12.3 Simultaneous Oil Velocity and Winding Temperature Measurements 211

12.4 Computer Prediction of Temperature and Oil Flow Distribution 215

12.5 Measurements with Third Flow-Diverter 223

12.6 Discussion and Conclusions 224

CHAPTER THIRTEEN: OPTIMISATION OF THE THERMAL DESIGN 225

13.1 Introduction 225

13.2 Optimisation of the 16 Duct Pass 226

13.3 Increasing the Number of Passes 227

13.4 Grading Horizontal Duct Thicknesses 230

13.5 Increasing Vertical Duct Thicknesses 238

13.6 Experimental Results 240

13.7 Assessment of Optimisation Techniques 243

13.8 Conclusion 245

		Page
CHAPTER FOURTEEN:	FURTHER WORK	247
14.1	Introduction	247
14.2	Circumferential Heat Flow	247
14.3	Radial Flow between Parallel Discs	249
14.4	Conclusion	253
CHAPTER FIFTEEN:	REFERENCES	254
APPENDIX A:	THERMOPHYSICAL PROPERTIES	260
APPENDIX B:	MATHEMATICAL DETAILS OF EQUATION (4.18)	269
APPENDIX C:	EQUIPMENT DETAILS	271
C1	Oil Cooling Circuit	271
C2	Winding Heating and Temperature Measurement Equipment	273
C3	Hot-Film Probe and Calibration Apparatus	277
APPENDIX D:	PROGRAM LISTINGS	287
D1	Simple Network	287
D2	FORTRAN Variable Definitions	290
D3	TEACH-L	299
	INIT	302
	PROPS	303
	CALCU	303
	CALCV	304
	CALCP	306
	CALCT	307

		Page
	LISOLV	308
	PRINT	309
D4	JUNCTION	310
	MAIN	311
	MODU	316
	MODV	317
	MODP	318
	Input File DATIN.DAT	318
	Output File RESULT.DAT	319
D5	CORNER	329
	MAIN	329
	MODU	334
	MODV	335
	MODP	336
	DUMP	336
	REST	336
	Input File CORNDAT.DAT	337
	Output File RESULT.DAT	338
D6	DUCT	349
	MAIN	350
	MODU	358
	MODV	358
	MODP	359
	MODT	360
	Output File RESULT.DAT	361
D7	DISCNET	374
	MAIN	376
	INPASS	377

	Page
CALDRS	378
CALFLO	379
PRNFLO	380
CALCK	381
CALJRS	382
CALCRS	383
SELCOR	384
SELCO	385
H	386
PE	386
RE	386
VISC	386
Input File DATIN.DAT	387
Output File RESULT.DAT	389

LIST OF FIGURES

	Page
Fig. 1.1 Schematic of Transformer (Allen (1960))	33
Fig. 1.2 Different Arrangements of Electric and Magnetic Circuits (Allen (1960))	35
Fig. 1.3 Disc vs. Layer Winding (Allen (1960))	36
Fig. 1.4 Sectional View of Transformer, Tank and Radiator with ONAN Cooling, adapted from Imre and Bitai (1978)	38
Fig. 1.5 Various Cooling Arrangements and Their Classification (Allen (1960))	39
Fig. 1.6 Section of Disc Winding with and without Flow-Diverting Washers	40
Fig. 1.7 Thermal Assumptions in CP1010:1975	42
Fig. 2.1 Plan View of the Winding	50
Fig. 2.2 Elevation of Sector A-A	51
Fig. 2.3 Vertical Section B-B	52
Fig. 2.4 Combined Heat Flow in Disc and Duct	56
Fig. 2.5 Combining Tee-Junction	62
Fig. 2.6 Dividing Tee-Junction	62
Fig. 2.7 Corner	63
Fig. 3.1 Simplified Domain	66
Fig. 3.2 Horizontal Duct	66
Fig. 3.3 Vertical Duct	66
Fig. 3.4 Network Analogue	73
Fig. 3.5 Duct Entrance Region	75
Fig. 3.6 Bulk Temperature vs. Height	80
Fig. 3.7 Symmetrical 8 Duct Pass	83
Fig. 3.8 Asymmetrical 8 Duct Pass	83

Page

Fig. 4.1 Control Volume 90

Fig. 4.2 Boundary Fluxes 92

Fig. 4.3 Line by Line Iteration 98

Fig. 4.4 Control Volume for Continuity Equation 101

Fig. 4.5 Singularity Condition 107

Fig. 4.6 Staggered Grid 108

Fig. 5.1 Two-Dimensional Tee-Junction 113

Fig. 5.2 Tee-Junction Flow Domain 114

Fig. 5.3 No-Slip Boundary Condition 115

Fig. 5.4 Treatment of Corners 116

Fig. 5.5 Dividing Junction, 10x8 Grid 120

Fig. 5.6 Dividing Junction, 17x13 Grid 120

Fig. 5.7 Dividing Junction, 22x18 Grid 121

Fig. 5.8 Dividing Junction, 30x25 Grid 121

Fig. 5.9 Mesh Dependence, Dividing Junction, High Re 122

Fig. 5.10 Mesh Dependence, Combining Junction, Low Re 123

Fig. 5.11 Mesh Dependence, Combining Junction, High Re 124

Fig. 5.12 Contour Plot of K_{cs} 129

Fig. 5.13 Contour Plot of K_{ct} 130

Fig. 5.14 Contour Plot of K_{ds} 131

Fig. 5.15 Contour Plot of K_{dt} 132

Fig. 5.16 Notation of Jamison and Villemonte (1971) 134

Fig. 6.1 Two-Dimensional Corner 135

Fig. 6.2 Corner Domain 136

Fig. 6.3 Contour Plot of K_c 138

Fig. 7.1 Disc/Duct Flow Domain 144

Fig. 7.2 10 Conductor Disc 150

Fig. 7.3 Temperature Distribution in 10 Conductor Disc 150

Page

Fig. 7.4 Surface Heat Flux Distribution in 10 Conductor Disc 151

Fig. 7.5 Comparison of DUCT with Analytical Solution 153

Fig. 8.1 Network with Junction and Corner Resistances Added 157

Fig. 8.2 Magnitude of Horizontal Duct Resistances 160

Fig. 8.3 Magnitude of Vertical Duct Flow Resistances 162

Fig. 8.4 Comparison of Simple Network and DISCNET Flow Prediction 162

Fig. 9.1 Possible Flow Pattern in Disc Winding without Flow-Diverting Washers 164

Fig. 9.2 Facsimile Winding 169

Fig. 9.3 Winding with Hot-Film Velocity Probe 170

Fig. 9.4 Schematic of Hydraulic Circuit 170

Fig. 9.5 Flow Rate Monitoring Arrangements 172

Fig. 9.6 Winding D.C. Supply Control Circuit 172

Fig. 10.1 Assembly Drawing of Calibration Duct 178

Fig. 10.2 Calibration Duct with Velocity Probe 181

Fig. 10.3 Calibration Duct, Tank and Pump Assembly 182

Fig. 10.4 Toothed Aluminium Disc and Opto-Switch 183

Fig. 10.5 Calibration Curve for Diesel Injector Pump 184

Fig. 10.6 Room Temperature Hot-Film Probe Calibration Curve 185

Fig. 10.7 March 1982 Probe Calibration 186

Fig. 10.8 Feb. 1983 Calibration 188

Fig. 10.9 March 1983 Calibration 188

Fig. 10.10 Correlation Coefficients as a Function of Pr 190

Fig. 11.1 Facsimile Winding Disc Voltage Taps 192

Fig. 11.2 Schematic of Disc Voltage Taps 194

Fig. 11.3 Thermocouple Calibration Curve 195

Fig. 11.4 Zone-Box Thermocouple Circuit 196

Fig. 11.5 Disc Thermocouple Locations 197

Page

Fig. 11.6 Thermocouple Installation 198

Fig. 11.7 Bottom Oil Thermocouple Locations 199

Fig. 11.8 Top Oil Thermocouple Locations 199

Fig. 11.9 Top Oil Thermocouples on Perspex Cylinder 200

Fig. 11.10 Hot Film Probe Resistance Temperature Calibration 201

Fig. 11.11 Warm-Up Curve of Experimental Winding 203

Fig. 11.12 Hot Spot, Mean Winding and Top Oil Rise vs. Flow Rate 204

Fig. 12.1 Cold Flow Measurements in Ducts 1-5 206

Fig. 12.2 Cold Flow Measurements in Ducts 6-8 207

Fig. 12.3 Gaps between Vertical Ribs and Discs 208

Fig. 12.4 Flow Distribution Showing Apparent Leakage 209

Fig. 12.5 Variable Viscosity Distortion of Velocity Profile 212

Fig. 12.6 Theory vs. Experiment, Disc 9 217

Fig. 12.7 Theory vs. Experiment, Disc 10 217

Fig. 12.8 Theory vs. Experiment, Disc 12 218

Fig. 12.9 Theory vs. Experiment, Disc 13 218

Fig. 12.10 Theory vs. Experiment, Disc 15 219

Fig. 12.11 Facsimile Winding with Third Flow-Diverter 223

Fig. 13.1 Datum Design -- 16 Duct Pass 227

Fig. 13.2 Two 8 Duct Passes 228

Fig. 13.3 Four 4 Duct Passes 228

Fig. 13.4 Comparison of 16, 8 and 4 Duct Pass 229

Fig. 13.5 Pressure Drop Through Pass vs. Number of Ducts per Pass 229

Fig. 13.6 Datum Design Compared with Graded Design 236

Fig. 13.7 $t_{hot,8}$ vs. c 238

Fig. 13.8 Pressure Drop vs. c 238

Fig. 13.9 $t_{hot,8}$ vs. a(b) 239

Fig. 13.10 Pressure Drop vs. a(b) 239

Page

Fig. 13.11 Effect of Duct Thickness Grading on Facsimile Winding 240

Fig. 13.12 Top Oil Rise vs. 1/Q, Graded and Ungraded Winding 242

Fig. 14.1 System for Analysis of Circumferential Heat Flow 248

Fig. 14.2 Radial Flow between Parallel Discs 250

Fig. A1 Kinematic Viscosity vs. Temperature 262

Fig. A2 Density vs. Temperature 263

Fig. A3 Dynamic Viscosity vs. Temperature 264

Fig. A4 Specific Heat vs. Temperature 265

Fig. A5 Thermal Diffusivity vs. Temperature 266

Fig. A6 Prandtl Number vs. Temperature 267

Fig. C1.1 Control Circuit for Pump Motor 272

Fig. C1.2 Circuit Diagram of Opto-Switch 273

Fig. C1.3 Pump Flow Rate Calibration 274

Fig. C2.1 Data-Logging Equipment 276

Fig. C3.1 Assembled Calibration Duct 279

Fig. C3.2 Filter Window, Spillway Side and Vertical Duct Side Wall 280

Fig. C3.3 Filter Chamber Side Cover 281

Fig. C3.4 Filter Chamber Rear Cover 282

Fig. C3.5 Filter Chamber Top Cover 283

Fig. C3.6 Filter Chamber Bottom Cover 284

Fig. C3.7 Spillway Bottom 285

Fig. C3.8 Vertical Duct Front and Rear Walls 286

Fig. D3.1 Flow Chart of TEACH-L 301

Fig. D7.1 Flow Chart of DISCNET 375

LIST OF TABLES

	Page
Table 1.1 Cooling Arrangement Symbols from B.S. 171 (1978)	37
Table 1.2 Cooling Arrangement Symbol Order from B.S. 171 (1978)	37
Table 3.1 SN Prediction of 4 Duct Pass	79
Table 3.2 SN Prediction of 8 Duct Pass	81
Table 3.3 SN Prediction of 16 Duct Pass	82
Table 5.1 Combining Junction Friction Constants	127
Table 5.2 Dividing Junction Friction Constants	128
Table 5.3 Comparison of Pipe Junction and Plane Junction Friction Constants	133
Table 6.1 Corner Friction Constants	138
Table 10.1 Least Squares Fit of Calibration Curves	189
Table 12.1 Comparison of SN, DISCNET, and Experiment	210
Table 12.2 Winding Temperature Measurements	214
Table 12.3 Comparison of DISCNET and Experiment, Hot Tests	221
Table 12.4 Comparison of Various Disc Hot-Spot Prediction Methods with Experiment	222
Table 12.5 Comparison of Probe Resistance Temperature Measurements with Theory	222
Table C2.1 Master List of Winding Thermocouples	277

LIST OF SYMBOLS

A reasonable effort was made to avoid using the same symbol for different physical quantities; this has occurred in a few isolated cases. The List of Symbols and context should eliminate any ambiguity. SI units have been used throughout, although Imperial Units are occasionally referred to in manufacturer's specifications. In Chapters 10-12, cm^3/s have been used for flow rates for numerical convenience.

Symbol	Physical Meaning	1st Used in Sec.	Units
a	left vertical duct thickness	2.1	m
A_c	flow cross-sectional area	2.2	m^2
$A_{P,N,S,E,W}$	combined convection/diffusion coefficients. For ϕ = u,v,t	4.3	kg/m s
	For ϕ = p'		s
A_P'	A_P - B	4.4	as A_P
A_p	surface area of probe	10.1	m^2
A_1	King's Law constant	10.4	V^2
A_2	King's Law constant	10.4	$V^2/(m/s)^{.5}$
$A_1, \ldots A_9$	Fluid property constants	A	see App. A
b	right vertical duct thickness	2.1	m
B	coefficient in source term	4.3	as A_P
B	constant of integration	A	dim'less
B_f	coefficient for false source	4.6	as B
c	horizontal duct thickness	2.1	m
c_p	specific heat at constant pressure	2.3	J/kg ^oC

Symbol	Physical Meaning	1st Used in Sec.	Units
C	constant of integration	8	dim'less
C	coefficient in source term	4.3	
	for ϕ = u, v		N/m
	for ϕ = p'		kg/m s
	for ϕ = t		kg ^{o}C/m s
C'	= C + $A_W\phi_W$ + $A_E\phi_E$	4.4	as C
C"	see (4.47)	4.4	as ϕ
C_f	coefficient for false source	4.6	as C
d	height of disc	2.1	m
d^*	d/($D_{l \text{ or } r}$ $Pe_{l \text{ or } r}$)	7.3	dim'less
D	diameter of hot film probe	10.1	m
$D_{e,w,n,s}$	pressure correction coefficient	4.5	m^2 s/kg
D_h	hydraulic diameter of flow passage	2.3	m
D_{hor}	hydraulic diameter of horizontal ducts	3.2	m
D_j	diagonal element in t.d.m.a. matrix	4.4	as A_P
D_l	hydraulic diameter of left vert. ducts	3.2	m
D_r	hydraulic diameter of r. vert. ducts	3.2	m
D_w	mean winding diameter	13.3	m
e	exponential function	4.4	dim'less
E	coefficient in King's Law correlation	10.4	dim'less
f	Fanning friction factor	3.1	dim'less
f_{app}	apparent Fanning friction factor	3.1	dim'less
$f_{n,s,e,w}$	factor used in control vol. equations	4.2	dim'less
$f_{\phi,u,v,p',t}$	underrelaxation factor	4.6	dim'less

Symbol	Physical Meaning	1st Used in Sec.	Units
F	coefficient in King's Law correlation	10.1	dim'less
g	gravitational acceleration	2.4	m/s^2
G'	correction to guessed G^*	4.5	$kg/m^2 s$
G_c	conductances between conductor nodes	7.3	W/m K
$G_{c,f}$	conductance between conductor and contiguous horizontal duct fluid temperature node	7.3	W/m K
$G^*_{e,w,n,s}$	mass fluxes due to guessed pressure	4.5	$kg/m^2 s$
G_l, G_r	conductances between disc-edge conductors and left and right vertical ducts	7.3	W/m K
G_x	mass flux in x-direction	4.2	$kg/m^2 s$
G_y	mass flux in y-direction	4.2	$kg/m^2 s$
h	convective heat transfer coefficient	2.3	$W/m^2 K$
h_l	mean value of h at left disc edge	7.3	$W/m^2 K$
h_r	mean value of h at right disc edge	7.3	$W/m^2 K$
i	current source in network model	3.2	m^2/s
$i_1, i_2, \ldots$	mesh currents in network model	3.2	m^2/s
I	conductor current	2.2	A
I_H	rms high voltage winding current	1.1	A
I_L	rms low voltage winding current	1.1	A
I_p	probe current	10.1	A
k	fluid thermal conductivity	2.3	W/m K

Symbol	Physical Meaning	1st Used in Sec.	Units
k_p	oil-impregnated kraft paper insulation thermal conductivity	7.3	W/m K
k_x	thermal conductivity in x-direction	2.4	W/m K
k_y	thermal conductivity in y-direction	2.4	W/m K
k_1, k_2,...	cubic duct thickness ratios	13.4	dim'less
K	friction constant	3.1	dim'less
K_c	corner flow friction constant	6.1	dim'less
K_{cs}, K_{ct}	combining flow friction constants	5.1	dim'less
K_{ds}, K_{dt}	dividing flow friction constants	5.1	dim'less
K_{m-1}	Jamison and Villemonte notation	5.5	dim'less
K_{m-2}	Jamison and Villemonte notation	5.5	dim'less
K_{1-m}	Jamison and Villemonte notation	5.5	dim'less
K_{2-m}	Jamison and Villemonte notation	5.5	dim'less
K'_{cs},K'_{ct}	modified K_{cs}, K_{ct}	5.5	dim'less
K'_{ds},K'_{dt}	modified K_{ds}, K_{dt}	5.5	dim'less
L	length of horizontal duct	2.1	m
L_{entry}	entrance length in JUNCTION	5.2	m
L_{exit}	exit length in JUNCTION	5.2	m
L_{horiz}	horizontal branch length in JUNCTION	5.2	m
L_{hy}	hydrodynamic entrance length	2.3	m
L_{th}	thermal entrance length	2.3	m
L'	modified L for pressure drop	7.5	m
L'_{entry}	modified L_{entry} for pressure drop	5.2	m
L'_{exit}	modified L_{exit} for pressure drop	5.2	m
L'_{horiz}	modified L_{horiz} for pressure drop	5.2	m

Symbol	Physical Meaning	1st Used in Sec.	Units
m	exponent in King's Law correlation	10.4	dim'less
$\dot{M}_{x,n,s,e,w}$	momentum flux across c.v. boundaries	4.3	N/m
n	exponent in King's Law correlation	10.4	dim'less
Nu	Nusselt number	2.3	dim'less
Nu_m	Nu averaged over probe surface	10.1	dim'less
$Nu_{m,H}$	duct-averaged Nu with constant wall heat flux boundary condition (parallel plate duct)	7.3	dim'less
$Nu_{x,H}$	local Nu with constant wall heat flux boundary condition (parallel plate duct)	3.3	dim'less
p	fluid static pressure	2.4	Pa
p_b	buoyant pressure regain	3.4	Pa
p_{ex}	pressure required by external agent to cause flow	3.5	Pa
p_{in}	average pressure at tee-junction entrance	5.3	Pa
p_1	average pressure at tee-junction exit	5.3	Pa
p_2	average pressure at tee-junction horizontal branch entrance/exit	5.3	Pa
p'	total pressure	3.1	Pa
p'	pressure correction	4.5	Pa
p^*	guessed pressure	4.5	Pa
$\bar{p}$	p defined mechanically	2.4	Pa

Symbol	Physical Meaning	1st Used in Sec.	Units
P	wetted perimeter of duct	2.3	m
Pe	Peclet number	2.3	dim'less
P_{in}	apparent input power	1.1	VA
P_{out}	apparent output power	1.1	VA
Pr	Prandtl number	2.3	dim'less
$\dot{q}'_j$	heat (per unit depth) from j^{th} conductor to fluid	7.3	W/m
$\dot{q}'''$	heat generation/volume	2.4	W/m^3
$\dot{q}''_w$	surface heat flux	2.3	W/m^2
$\dot{q}''_{w,m}$	average surface heat flux from probe	10.1	W/m^2
Q	pass inlet area flow rate	2.2	m^2/s
Q_{in}	junction inlet area flow rate	2.5	m^2/s
Q_l	left vertical duct area flow rate	7.3	m^2/s
Q_r	right vertical duct area flow rate	7.3	m^2/s
Q_1	junction exit area flow rate	2.5	m^2/s
Q_2	junction branch area flow rate	2.5	m^2/s
$\dot{Q}$	total winding dissipation	12.3	kW
$\dot{Q}'$	see (7.12)	7.3	W/m
$\dot{Q}'_j$	heat source per unit depth in j^{th} conductor	7.3	
r	distance from winding central axis	14.3	m
r_h	hydraulic radius of duct	2.3	m
$r_{h,horiz}$	horizontal duct hydraulic radius	5.1	m
$r_{h,vert}$	vertical duct hydraulic radius	5.1	m
R	mean winding radius	2.1	m

Symbol	Physical Meaning	1st Used in Sec.	Units
R_{avg}	mean winding resistance	11.1	Ω
R_c	temperature-dependent dissipation	7.3	W/m K
R_{CA}	cable resistance	10.4	Ω
R_{ch}	upper corner resistance	8.1	Pa s/m^2
R_{cl}	lower corner resistance	8.1	Pa s/m^2
R_{cs}	combining junction resistance	8.1	Pa s/m^2
R_{ct}	combining junction resistance	8.1	Pa s/m^2
R_{ds}	dividing junction resistance	8.1	Pa s/m^2
R_{dt}	dividing junction resistance	8.1	Pa s/m^2
Re	Reynolds number	2.3	dim'less
Re_{in}	junction entrance Re	5.2	dim'less
Re_1	junction exit Re	5.2	dim'less
Re_2	junction branch Re	5.2	dim'less
R_l	left vertical duct resistance	3.2	Pa s/m^2
R_o	mean winding resistance at t_o	11.1	Ω
R_p	probe resistance in 'operating' mode	10.1	Ω
R_r	right vertical duct resistance	3.2	Pa s/m^2
R_t	residual for t	7.3	kg K /m s
R_T	top resistance of DISA CTA Standard Bridge	10.4	Ω
R_u	residual for u	4.6	N/m
R_v	residual for v	4.6	N/m
R_ϕ	residual for ϕ	4.6	as R_u, etc.
R_1, etc.	resistance in duct 1, etc.	3.2	Pa s/m^2
R_{20}	probe resistance in 'resistance' mode at ambient temperature of 20 ^oC	10.3	Ω
R_∞	probe resistance in 'resistance' mode	10.3	Ω

Symbol	Physical Meaning	1st Used in Sec.	Units
s	slope of density vs. temperature curve	3.1	kg/m^3 K
S_f	false source	4.6	as C
S_M	mass source	4.5	kg/m^3 s
S_{MP}	mass residual	4.5	kg/m s
S_u	source associated with u	4.2	N/m^3
S_v	source associated with v	4.2	N/m^3
S_t	source associated with t	4.2	kg K/m^3 s
S_ϕ	source associated with ϕ	4.3	as S_u, etc.
t	local fluid temperature	2.2	^oC
t_a	cooling air or water temperature	1.3	^oC
t_{av}	arithmetic mean fluid temperature over a duct cross-section	3.1	^oC
t_b	bottom oil temperature	1.3	^oC
t_c	cooler top oil temperature	1.3	^oC
$t_{c,j}$	temperature of j^{th} conductor	7.3	^oC
t_e	duct entrance temperature	3.3	^oC
t_f	film temperature	10.1	^oC
t_h	hottest-spot temperature	1.3	^oC
$t_{hot,j}$	hot-spot temperature in j^{th} duct	3.3	^oC
t_m	bulk mean fluid temperature over a duct cross-section	2.2	^oC
$t_{mh,j}$	t_m at exit of j^{th} horizontal duct	3.1	^oC
$t_{m,in}$	t_m at pass entrance	2.1	^oC
$t_{m,out}$	t_m at pass exit	2.1	^oC
$t_{m,r}$	t_m in right vertical duct	7.3	^oC
$t_{m,j}$	$t_{m,r}$ in j^{th} right vertical duct	3.1	^oC

Symbol	Physical Meaning	1st Used in Sec.	Units
t_o	datum or reference temperature	3.1	^oC
t_r	mean winding temperature by resistance	1.3	^oC
$t_{r,1-2}$	mean temperature by resistance of disc-pair 1-2, etc.	11.1	^oC
t_t	tank top oil temperature	1.3	^oC
t_w	winding top oil temperature	1.3	^oC
t_{wall}	duct wall temperature	2.3	^oC
$t_{w,m}$	mean probe surface temperature	10.1	^oC
t_∞	undisturbed fluid temperature	10.1	^oC
u	fluid x-direction velocity component	2.2	m/s
u_{in}	mean velocity at junction entrance	5.5	m/s
u_m	fluid mean axial velocity	2.2	m/s
u_1	mean velocity at junction exit	5.5	m/s
u'	correction to u^*	4.5	m/s
u^*	guessed u derived from p^*	4.5	m/s
U	free stream or duct centre-line velocity	10.1	m/s
v	fluid y-direction velocity component	2.4	m/s
v_m	mean vertical duct velocity	3.1	m/s
V_H	r.m.s. L.V. winding voltage	1.1	V
V_L	r.m.s. H.V. winding voltage	1.1	V
V_{out}	output voltage from DISA bridge	10.3	V
V_p	voltage across the probe	10.1	V
w	horizontal duct width	2.1	m
x	axial (flow direction) component	2.4	m

Symbol	Physical Meaning	1st Used in Sec.	Units
x^*	dimensionless x for thermal entrance region	3.3	dim'less
x^*	dimensionless x	B	dim'less
y	coordinate normal to flow direction	2.4	m
z	overall width of insulated conductor	7.3	m
z	cartesian coordinate in circumferential direction	14.2	m

α	fluid thermal diffusivity	A	m^2/s
α_j	$A_{N,j}$ in t.d.m.a. matrix	4.4	kg/m s
α_{20}	resistivity-temperature at 20 ^oC	7.3	K^{-1}
α'_j	see equation (4.46)	4.4	dim'less
β	coefficient of thermal expansion	3.1	K^{-1}
β_j	$A_{S,j}$ in t.d.m.a. matrix	4.4	kg/m s
Γ_ϕ	transport property associated with ϕ	4.2	kg/m s
γ	a large constant (10^{30})	5.2	dim'less
δ	distance from disc surface to nearest temperature node	7.3	m
δx	grid spacing	4.2	m
δy	grid spacing	4.2	m

Symbol	Physical Meaning	1st Used in Sec.	Units
Δ	prefix denoting a difference	3.1	dim'less
Δp	static pressure drop in the flow direction between two cross-sections of interest	3.1	Pa
Δp_c	see equation (6.1)	6.3	Pa
Δp_{ct}	see equation (5.8)	5.5	Pa
Δp_{dt}	see equation (5.9)	5.5	Pa
Δp_s	see equation (5.7)	5.5	Pa
$\Delta \dot{p}_c$	see equation (6.2)	6.3	Pa
$\Delta \hat{p}_{cs}$	see equation (5.10)	5.5	Pa
$\Delta \hat{p}_{ct}$	see equation (5.11)	5.5	Pa
$\Delta \hat{p}_{ds}$	see equation (5.12)	5.5	Pa
$\Delta \hat{p}_{dt}$	see equation (5.13)	5.5	Pa
$\Delta\theta_{wo}$	$\theta_r - \theta_{mc}$	1.3	^oC
ε	thickness of insulation	7.3	m
η	thickness of conductor	7.3	m
θ_b	bottom oil rise	1.3	^oC
θ_c	cooler top oil rise	1.3	^oC
θ_h	hottest spot rise	1.3	^oC
θ_{mc}	mean cooler oil rise	1.3	^oC
θ_{mw}	mean winding oil rise	1.3	^oC
θ_r	mean winding rise by resistance	1.3	^oC
θ_t	tank top oil rise	1.3	^oC
θ_w	winding top oil rise	1.3	^oC

Symbol	Physical Meaning	1st Used in Sec.	Units
θ'_h	$t_h - t_b$	11.5	^oC
θ'_r	$t_r - t_b$	11.5	^oC
θ'_w	$t_w - t_b$	11.5	^oC
λ	coefficient of bulk viscosity	2.4	Pa s
μ	fluid dynamic viscosity	2.3	Pa s
ν	fluid kinematic viscosity	4.3	m^2/s
ϱ	fluid density	2.4	kg/m^3
ϱ_o	ϱ at t_o	3.1	kg/m^3
ϱ_{20}	resistivity at 20 ^oC	7.3	Ω m
σ	half-height of conductor	7.3	m
τ_w	wall shear stress	5.2	Pa
ϕ	solved-for variable in generalised field equation	4.2	as u,v,t
$\phi_{N,S,E,W}$	value of ϕ stored at neighbouring nodes of ϕ_p to the north, south east and west	4.3	as ϕ
ϕ_p	value of ϕ at node being considered	4.3	as ϕ
ϕ_p^{old}	value of ϕ_p from previous iteration	4.6	as ϕ
ϕ_p^{r}	new value of ϕ_p using relaxation	4.6	as ϕ
ϕ_p^{wr}	new value of ϕ_p without relaxation	4.6	as ϕ

CHAPTER 1

INTRODUCTION

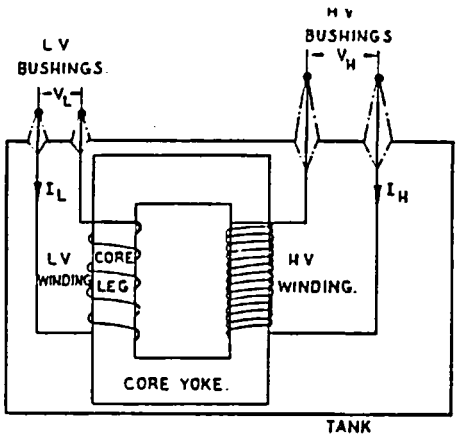
1.1 Power Transformers and the Thermal Problem The power transformer, as used in the transmission and distribution of electricity, is a large electromagnetic device for converting power between two voltages. Its use is associated with the practice in most developed countries of highly centralised generation of electricity and the need to transmit the power at as high a voltage as possible so as to minimise losses in transmission lines over long distances.

In the U.K., the largest units (typically 800 MVA) step-up the generator output line voltage (typically 22.5 KV) to the transmission line voltage (typically 400 KV). Smaller units (typically 200 MVA) are used at intermediate distribution points to step-down to 132 KV and lower. Further step-down to 11 KV occurs using (typically) 50 MVA units, where the latter voltage may be used directly in industrial plant, or is stepped-down finally to the 'mains' voltage used in homes.

The essential elements of the transformer are shown in Fig. 1.1. The low and high voltage windings are wound from insulated conductors (copper or aluminium) onto a magnetic core, made of laminated sheet steel, which enhances the flux linkage. The assembly is enclosed in a steel tank, generally filled with transformer oil.

As the equation in Fig. 1.1 suggests, most of the apparent input power $P_{in} = I_L V_L$, (where I and V are the rms values of current and voltage) is transmitted as useful apparent output power $P_{out} = I_H V_H$. The

efficiency, P_{out}/P_{in}, of most transformers is typically 95 - 100%. The power loss, however, though a small percentage of P_{in}, appears as an amount of heat which is very large in absolute terms, and turns out to be the critical factor in determining the maximum power at which a given unit may be safely and economically operated. It arises in the core, due to 1.) the hysteresis of the ferromagnetic material, and 2.) eddy currents which tend to resist flux alternation; and in the conductors due to I^2R losses from main and eddy currents induced by leakage fluxes.



I_L = LOW VOLTAGE CURRENT. I_H = HIGH VOLTAGE CURRENT.
V_L = LOW VOLTAGE (L.V.) V_H = HIGH VOLTAGE (H.V.)
APPROXIMATELY, $I_L V_L = I_H V_H$ = APPARENT POWER TRANSMITTED

Fig. 1.1 Schematic of Transformer (Allen (1960)

Generally speaking, larger transformers are more efficient. If all linear dimensions of a given design are increased by a factor $F > 1$, whilst maintaining the flux density in the core and the current density in the conductors approximately the same, both flux and current will increase by F^2, leading to an increase in the VA rating of F^4 (Stein and Hunt (1979), p. 73). The power losses, however, only increase by F^3. Larger transformers are also substantially cheaper per KVA.

The penalty is that the available core and conductor surface area for the dissipation of these losses will increase by only F^2. This purely thermal consideration is important both for reasons of safety and economy. The greatest hazard arises from localised overheating in the conductor insulation, the 'hot-spot' temperature. Experiments on both solid and stranded conductors wound with kraft-paper insulation and then immersed in oil by McNutt, et al. (1979) have shown that at temperatures above 140 ^{o}C, gas is evolved from the insulation with concomitant reduction of its dielectric strength. In severe cases, this could lead to catastrophic failure. British Standard Code of Practice 1010 (CP 1010:1975) forbids hot-spot temperatures in excess of this value.

The enormous capital cost of large transformers (£2 - £4 per KVA at 1982 prices, private communication) leads to careful consideration of the factors affecting their useful life, normally expected to be 'some tens of years' (CP 1010). It is widely agreed that the life of the transformer is determined by the life of the conductor insulation. Insulation aging rate is primarily governed by temperature, in accordance with Arrhenius' Law (Allen and Tustin (1972)), and investigators generally concur that in the range 80 ^{o}C to 140 ^{o}C, the rate of using life is doubled for every temperature increase of approximately 6 ^{o}C (CP 1010). 98 ^{o}C is defined by CP 1010 as the temperature at which aging occurs at a 'normal' rate.

Knowledge of the location and value of the hot-spot temperature for a transformer of a given design and rating is clearly desirable, and might logically be expected to form part of the manufacturer's guaranteed specification. In practice, transformers are manufactured

with so many different winding designs and cooling configurations that, as B.S. 171 states, "The hot-spot temperature cannot normally be measured directly".

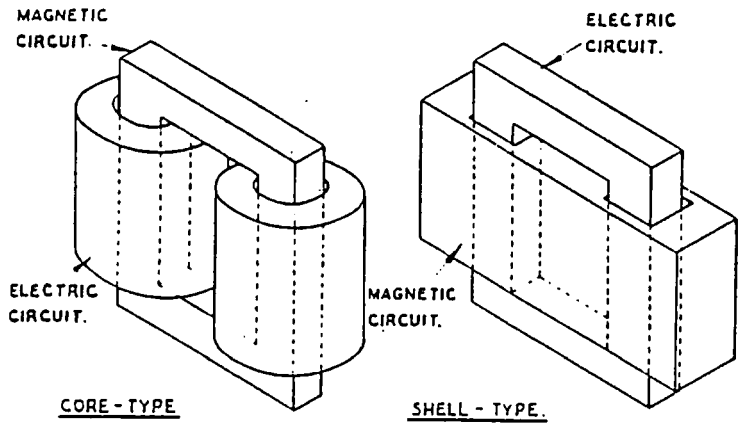


Fig. 1.2 Different Arrangements of Electric and Magnetic Circuits (Allen (1960))

1.2 Winding Designs and Cooling Configurations The electric and magnetic circuits in large power transformers may be arranged in two different ways, illustrated schematically in Fig. 1.2. The shell-type construction is used in the U.S. for the largest units rated up to 1,300 MVA. The electrical circuit consists of flat 'pancake' coils. Only the core-type arrangement is used in the U.K. Fig. 1.1 shows a simple core-type transformer in which the l.v. and h.v. windings are arranged on different legs of the core; however, it is far more common to install the h.v. and l.v. windings concentrically on the same leg as shown in the section and plan views at the top of Fig. 1.3.

The coils may be wound axially, in concentric cylindrical shells (the layer winding) or radially, in parallel discs (the disc winding). The two are illustrated at the bottom of Fig. 1.3. Disc windings have

largely supplanted the layer-type in the U.K., and are widely used in the U.S. for medium power applications. Some disc-type windings are air-cooled, with or without a protective enclosure which may or may not be ventilated. This thesis, however, will be concerned only with oil-immersed disc windings.

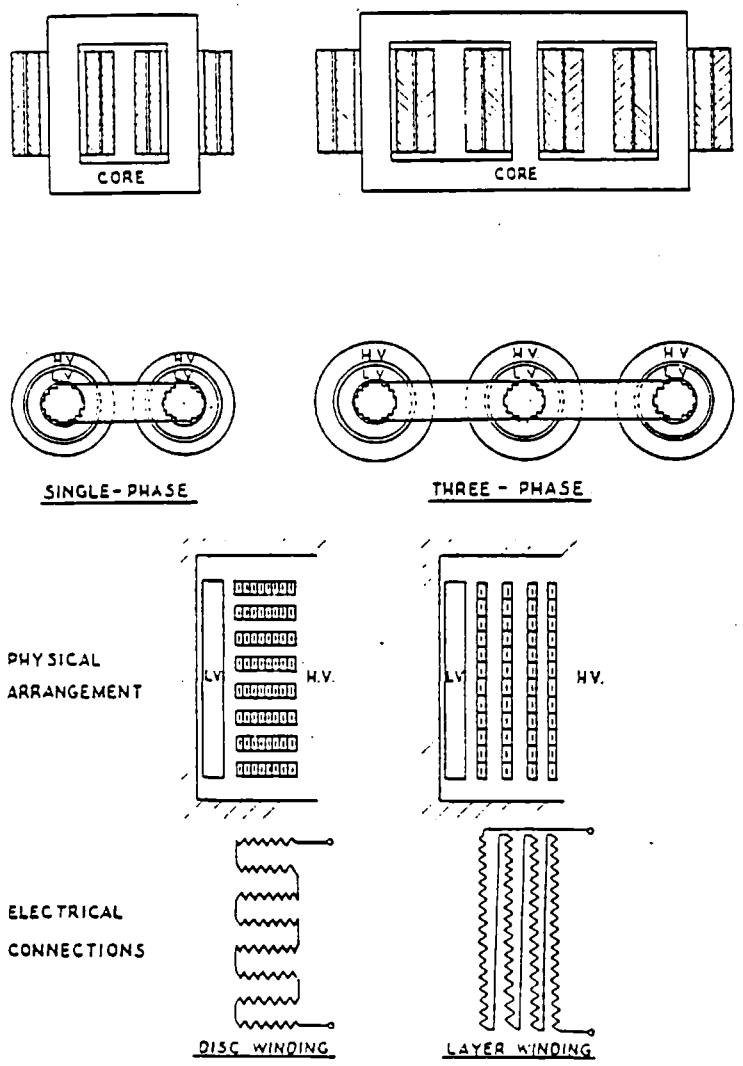


Fig. 1.3 Disc vs. Layer Winding (Allen (1960))

Considerable variation in the cooling arrangements of oil-immersed

LETTER SYMBOLS	
Kind of Cooling Medium	Symbol
Mineral oil or equivalent flammable synthetic insulating liquid	O
Non-flammable synthetic insulating liquid	L
Gas	G
Water	W
Air	A
Kind of Circulation	
Natural	N
Forced (oil not directed)	F
Forced-directed oil	D

Table 1.1 Cooling Arrangement Symbols from B.S. 171 (1978)

ORDER OF SYMBOLS			
1st Letter	2nd Letter	3rd Letter	4th Letter
Indicating the cooling medium that is in contact with the windings		Indicating the cooling medium that is in contact with the external cooling system	
Kind of cooling medium	Kind of circulation	Kind of cooling medium	Kind of circulation

Table 1.2 Cooling Arrangement Symbol Order from B.S. 171 (1978)

windings is possible and these are systematically classified (B.S. 171) by a four-letter designation explained in Tables 1.1 and 1.2. A simplified sectional view of an ONAN arrangement is shown as Fig. 1.4. In this case a radiator has been fitted to the tank which cools the oil by natural air circulation. The cooled oil in the lower portion of the tank is 'free to choose' an upward flow path through the core cooling channel, windings, or in the space between the windings and the tank walls. The various streams then mix in the upper part of the tank. The addition of a pump in the oil circuit would convert the arrangement to OFAN. If, in addition, baffles were fitted at the bottom of the tank to direct the oil either through the windings or the core, the

classification would be ODAN. Other variations are shown in Fig. 1.5. Dual classifications are common, e.g. ONAN/ONAF, to give a double rating.

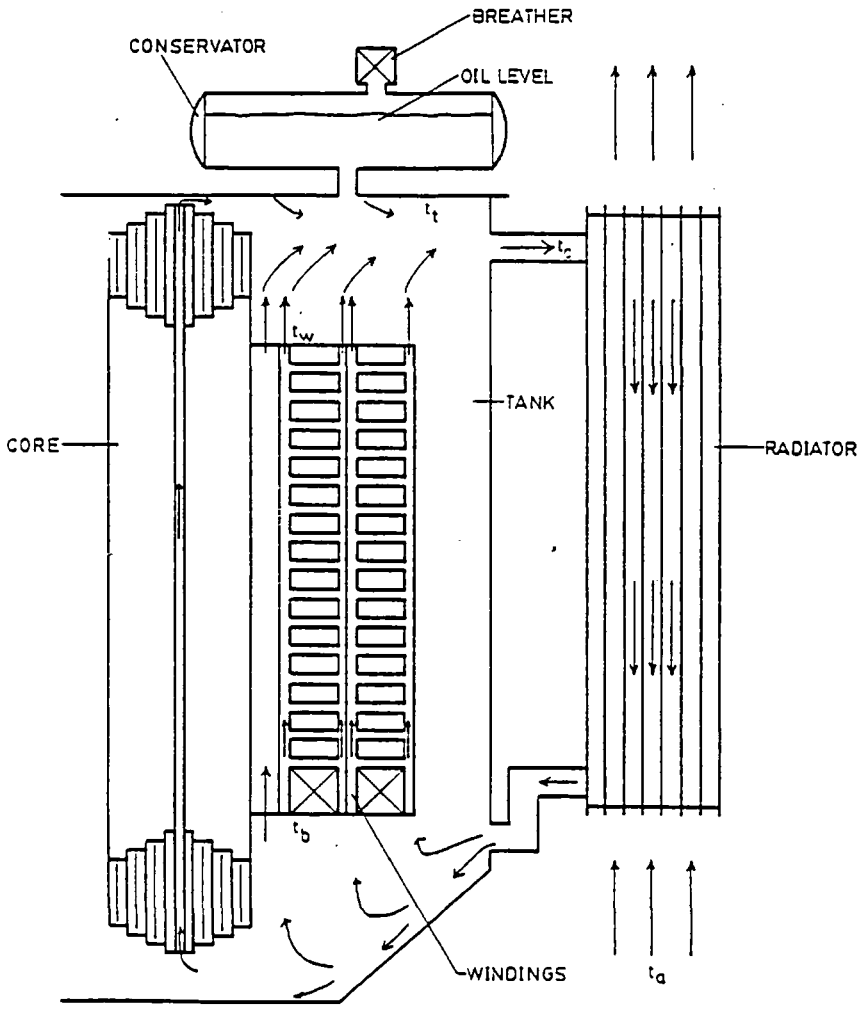


Fig. 1.4 Sectional View of Transformer, Tank and Radiator with ONAN Cooling, adapted from Imre and Bitai (1978)

The oil flow within individual disc-windings may or may not be guided, using flow-diverting washers, in a prescribed direction through groups of the horizontal ducts between successive discs. The two possibilities are shown schematically in Fig. 1.6. Flow-diverting

washers are normally used in disc windings of the OD class. Each group of discs between successive washers is called a 'pass'.

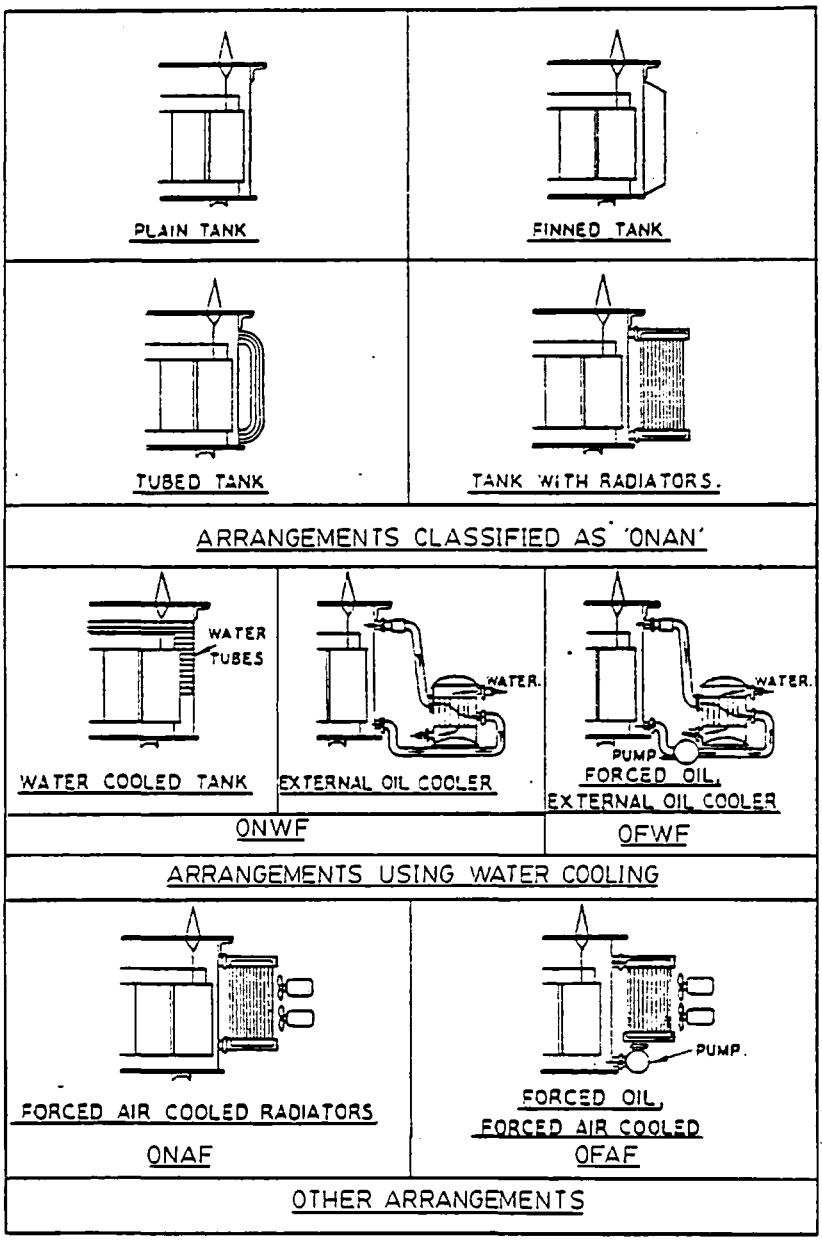


Fig. 1.5 Various Cooling Arrangements and Their Classification (Allen (1960))

1.3 Conventional Temperature Specifications and Attempts to Improve Them The transformer manufacturer is usually required to specify

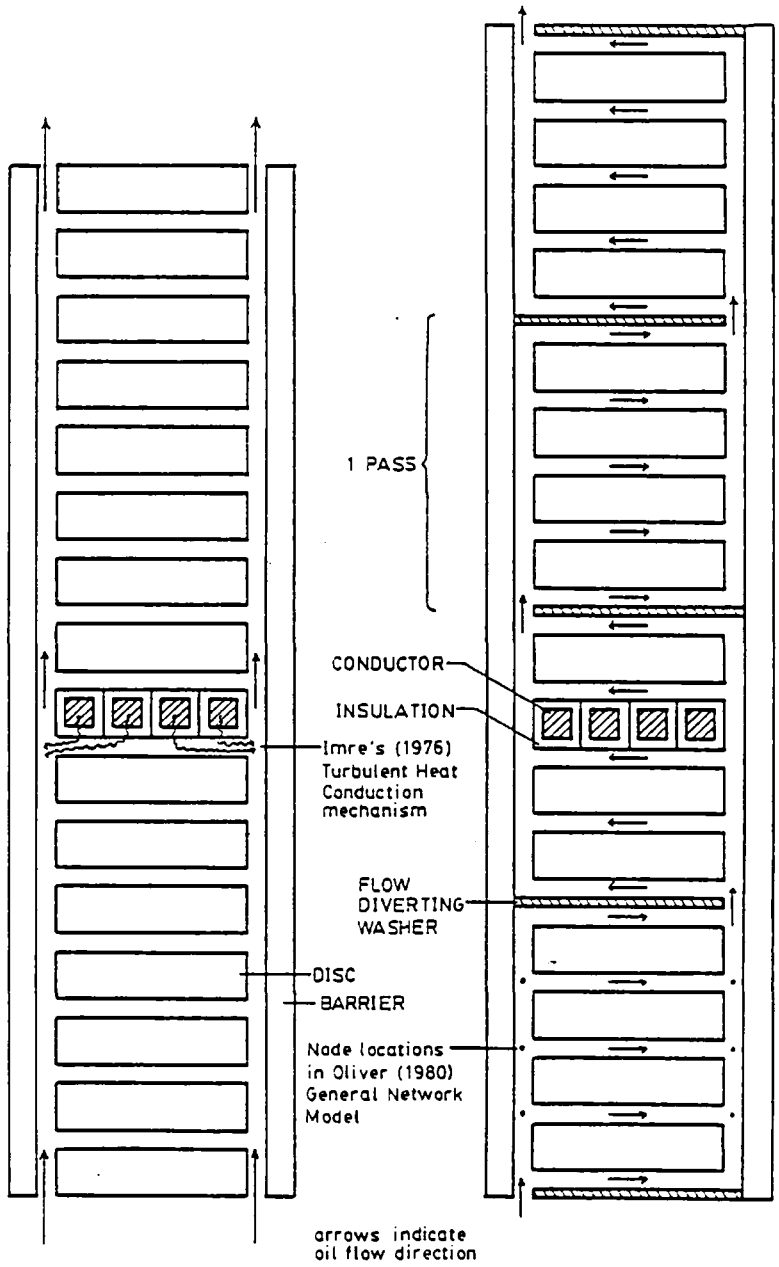


Fig. 1.6 Section of Disc Winding with and without Flow-Diverting Washers

temperature as a difference, or 'rise' above the ambient temperature t_a. The hottest spot temperature in the winding t_h would thus be reported as $\theta_h = t_h - t_a$. The nominal value of t_a in the U.K. is considered to be 20 ^{o}C. No attempt in fact is made to specify θ_h either by direct measurement or theoretical prediction. Several devices have been

proposed which could be permanently installed in a winding and register t_h (see Allen (1975), Pratt (1972), Allen and Havlicek (1974), Yannucci and Thompson (1979) and EPRI (1979)). These devices, however, are of little value without a priori knowledge of the hottest spot location.

B.S. 171 instead requires the specification of θ_r, the temperature rise of the winding determined by resistance measurements and θ_c or θ_t, the rise in the top of the cooler or the tank (see Fig. 1.4). B.S. 171 regards θ_c and θ_t as equivalent, designating either simply as the 'top-oil' temperature rise. It is also customary to measure the temperature rise of the 'bottom oil', θ_b, from which the mean oil temperature rise in the cooler is presumed to be

$$\theta_{mc} = 0.5(\theta_c + \theta_b). \tag{1.1}$$

CP 1010 then asserts that θ_h may be found from

$$\theta_h = \theta_c + 1.1\Delta\theta_{wo}, \tag{1.2}$$

where $\Delta\theta_{wo}$, the difference between the mean winding temperature rise and the mean oil temperature rise (in the coolers) is

$$\Delta\theta_{wo} = \theta_r - \theta_{mc}. \tag{1.3}$$

The thinking behind equations (1.1) - (1.3) is shown schematically in Fig. 1.7. θ_c or θ_t are assumed equal to θ_w, the temperature rise of the oil as it emerges from the windings (all windings are assumed to have equal θ_w). The winding and oil temperature rises are assumed to increase linearly with height, the difference between them being

constant and equal to $\Delta\theta_{wo}$. The top coil is always assumed to have the maximum average temperature, the hottest spot in it being greater by 10% of $\Delta\theta_{wo}$.

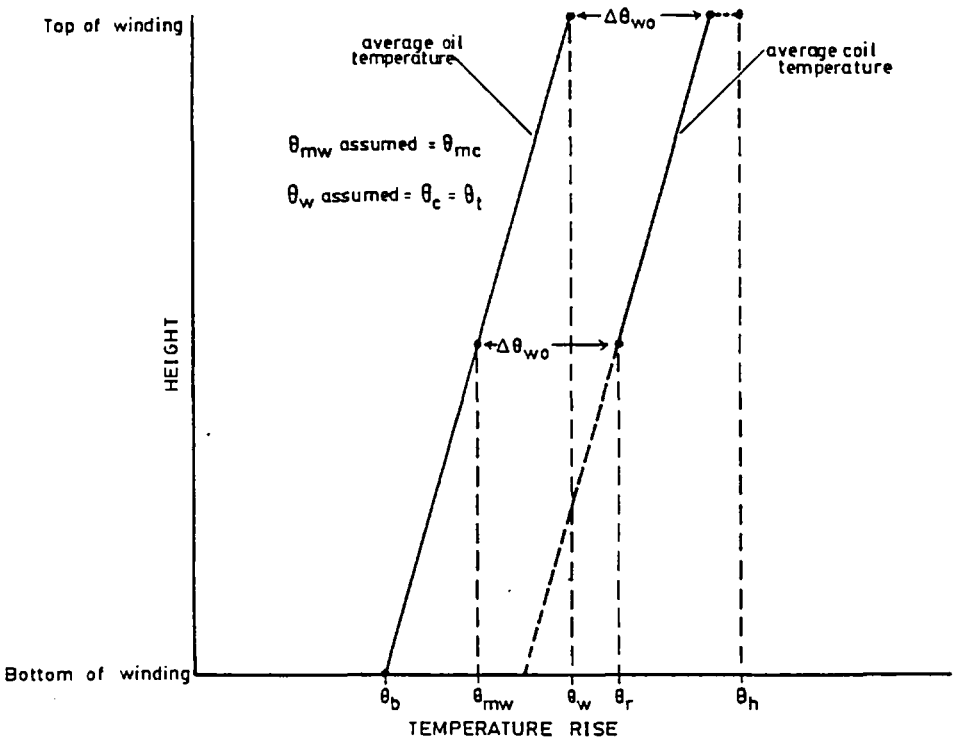


Fig. 1.7 Thermal Assumptions in CP1010:1975

It is not surprising that many of these assumptions have been challenged. Examination of Fig. 1.4 should suggest that, e.g., θ_w may differ substantially from θ_c and θ_t. Carruthers and Norris (1969) cite evidence that only 25 - 50% of the oil flow in the coolers can be expected to go through the windings under forced conditions. θ_w will thus be considerably greater than θ_c or θ_t, because of the mixing of the winding oil with the stagnant layer of oil in the top of the tank. Their proposed remedy is to obtain θ_w from what they believe to be a direct measurement of the mean oil temperature rise in the winding, θ_{mw}. When a

transformer is tested under full load, θ_r is measured by plotting the resistance of the winding against time from the shut down of the current, extrapolating backwards to obtain the value before time zero (B.S. 171). Their assertion is that as the mean winding temperature falls, it will, if 'corrected' for the concomitant fall in θ_{mc}, approach a constant value, namely θ_{mw}. In later papers (Norris (1971) and Norris (1974)), this 'multiflow' principle evolved into a proposal for a new standard specification, but was correctly regarded to have little solid basis either in theory or experimental evidence (Allen (1972, 1975), discussion of Norris (1971, 1974)). Allen's criticisms were confirmed by the experimental work of Lampe, Persson and Carlsson (1972) who proposed instead that θ_w be measured directly, using a teflon hose inserted into the top of each winding, and connected outside the tank to a pressure sensing instrument. The volumetric expansion of the oil in the hose would, after calibration, yield accurate values of θ_w. Determination of θ_h, however, would still depend on (1.2) being correct (which is open to considerable doubt). Experimental work by Pivrnec and Havlicek (1972), for example, demonstrated that the winding temperature does not necessarily increase linearly with height nor is the top coil necessarily the hottest.

Clearly there is a need to put the thermal specification of power transformers on a sounder basis. The guidelines set out in B.S. 171 are bound to underrate some designs and overrate others. To predict θ_h accurately for a given design clearly requires a far more detailed analysis of the heat transfer and fluid flow in the winding itself. Some of the prior work in this field will now be considered.

1.4 Previous Treatments of the Transformer Thermal Problem The

earlier attempts to predict the thermal behaviour of transformers mostly involve empirical formulae derived from correlations of test data. These have been extensively reviewed by Allen (1960). A more recent example of this kind of approach is Eastgate (1965). An early exception is the work of Steckler (1928, 1929), in which he analyses the temperature distribution in a single disc of a winding without flow-diverting washers (see Fig. 1.6).

Some papers treat the windings in their tank together with the external radiators as a single thermal/hydraulic system. A particular application is to determine the oil flow rate in naturally cooled transformers (Muur (1962) and Yamaguchi, et al., (1980)). The latter work appears to be of very high technical quality; the flow rate is measured through a window in the pipe of the bottom radiator using laser doppler anemometry. The experimental results agree well with the prediction of a computer program which iterates on the flow rate until the calculated pressure drop around the circuit is equal to the calculated natural convective pressure gain. The final result, however, consists only of a prediction of the mean winding temperature.

It appears that Allen was the first to apply the field equations of fluid mechanics and heat transfer to transformer winding analysis. In Allen and Allan (1963) the layer-type winding is analysed (see Fig. 1.3), in which the oil flows up long vertical ducts. The individual duct, together with its immediately surrounding conductors, insulation and spacing material, is treated as the elemental thermal system. The velocity and temperature profiles are assumed fully developed, but full account is made of variable fluid properties and anisotropic thermal conductivity in the surrounding insulation. A resistance network

analogue computer was used to solve the momentum and energy equations. Much pioneering work was also accomplished in the measurement of the relevant thermophysical properties (Allen 1957, 1959). In later work (Allen and Finn (1969)) thermal entrance effects were included in the analysis and a digital computer was used. Additional references to Allen's work are made throughout the thesis.

Extensive work has been done by Imre on disc-type windings without flow-diverting washers. In this case there is theoretically no established flow direction in the horizontal ducts, therefore Imre assumed that the oil there was static, moving only up the vertical ducts. A 'turbulent' heat conduction mechanism (see Fig. 1.6) was postulated to operate from the horizontal winding surfaces, through the static oil, to the oil flowing in the vertical ducts. Assuming symmetrical boundary conditions on the four sides of any disc, he obtained an analytical solution of the heat conduction equations in a quarter-disc, for an arbitrary temperature distribution on the half-disc surface in contact with the static oil (Imre and Dankò (1976)). In later work, (Imre (1976), Imre et al. (1978), Imre and Bitai (1978), Imre (1981), he preferred to proceed using a hierarchical network approach. Each conductor pair in a disc was modelled as a node, coupled to neighbouring pairs and through the static horizontal duct oil to a single node in the nearest vertical duct. Mass and heat flow networks for the oil in the vertical ducts of each winding were then formulated, and interconnected at their inlets and exits to an overall network comprising the oil flow in the core, tank and cooler. Regretfully he does not appear to have applied his techniques to disc windings with flow-diverting washers.

Preiningerova (1983) solved the temperature and magnetic fields simultaneously in disc windings, also without flow-diverting washers. This procedure allows for non-uniform dissipation, caused by leakage flux-induced eddy currents in the windings. One of the weaknesses of the approach is the assumption of uniform oil temperature and heat transfer coefficient around each disc. (Only the conduction problem in the disc is solved, not the fluid flow in the ducts).

Howe (1978) was concerned with the effect of moisture on the kraft paper conductor insulation. He proposed the simultaneous numerical solution of the unsteady concentration, temperature, momentum and electric field equations to obtain the partial vapour pressure of water diffusing from insulation to oil as a function of time and load. Important to his analysis is the internal heat generation in the insulation due to dielectric losses. To include this affect the electric field equations must be solved. Though he makes reference to the oil flow distribution in disc-type windings, his experimental system more closely resembles a layer-type winding, comprising 2 windings and 3 vertical ducts. He assumed fully-developed, but time-dependent velocity profiles.

Haggblad and Mattsson (1983) used the finite element computer program NACHOS, designed for incompressible flow problems, to solve the flow at the junctions in disc windings between the vertical and horizontal ducts. Isothermal conditions were assumed, and it was not stated whether or not flow-diverting washers were used.

Oliver (1980) used a general network model to estimate transformer winding temperatures and oil flows in a disc winding with flow-diverting

washers. His important contribution bears comparison with the present work on many points. A single pass (see Fig. 1.6) is taken as an elemental system, and a node is located at the entrance and exit of each horizontal duct. The solution provides values of the pressure and bulk temperature at each node, and the velocity and mean wall temperature in each duct connecting the nodes. The hottest local wall temperature in each horizontal duct is then estimated, from which the hottest conductor temperature in each disc may be found.

The success of any network model depends on the accuracy of the assumptions made and the coefficients used in formulating the flow resistances, etc. In the ducts, Oliver used the friction factor for fully developed, constant property flow in parallel plate ducts (an approximation of rectangular cross-sectioned ducts with a very high aspect ratio), modified for variable viscosity by a correction factor. At the junctions between vertical and horizontal ducts, pressure loss coefficients were derived from pipe tee-junction data (see Chapter 5). Conservation of mass and energy at each node, together with pressure drop estimates along the paths between nodes, then yield values of the flow rate in each duct and the bulk oil temperature at each node. In particular, the flow-rate and bulk oil temperature at the entrance of each horizontal duct is obtained, from which may be calculated the mean wall temperature. Oliver used the Nusselt number from the analytical solution for constant property, parallel plate ducts with constant wall heat flux, assuming a fully developed velocity profile, but a developing temperature profile, assumed flat at the duct entrance. The duct-averaged Nusselt Number is used, modified, as with the friction factor, by a variable viscosity correction factor. The local wall and local conductor hot spot temperature is assumed to be highest at the

exit of every horizontal duct. The is because heat loss from the vertical edges of the disc, and conduction along the duct wall, is ignored. Circumferential conduction in the conductors is also neglected, and no allowance appears to have been made for the 'masking' effect of the pressboard spacers which separate the discs. A sample calculation is made, but no experimental confirmation of the method is provided; however, the flow distribution results bear qualitative resemblance to measurements made in a perspex model by Allen, Szpiro and Campero (1981).

1.5 Overview of the Thesis The purpose of the present work is essentially the same as Oliver's, to predict the location and value of the hottest spot temperature in a disc winding with directed flow and flow-diverting washers. A network method, based on a single pass, is used, however the formulation is quite different. Extensive use is made of finite difference field calculations on a digital computer to obtain more accurate estimates of pressure loss coefficients in the ducts and junctions, and the conductor temperatures in the discs. The overall solution is 'hybrid', using lumped parameter networks where possible, and full field solutions where necessary. Direct experimental confirmation is provided from measurements of oil velocities and temperatures in a facsimile disc winding. In conclusion, an attempt is made to assess the influence of the various design parameters on the hot-spot temperature, and so to optimise the thermal design.

Chapters 2 - 8 develop the theoretical and computational basis of the work, and the experimental work is presented in Chapters 9 - 12. Design optimisation is discussed in Chapter 13, and the suggested direction of further work is outlined in Chapter 14. In the next

chapter, the geometry of the disc winding will be presented in greater detail, and various approaches to the solution of the problem will be discussed.

CHAPTER 2

THE PROBLEM DESCRIBED

2.1 Disc Winding Geometry The geometry of a single disc-type transformer winding will now be considered in detail, noting in particular the important dimensions which will influence the thermal analysis.

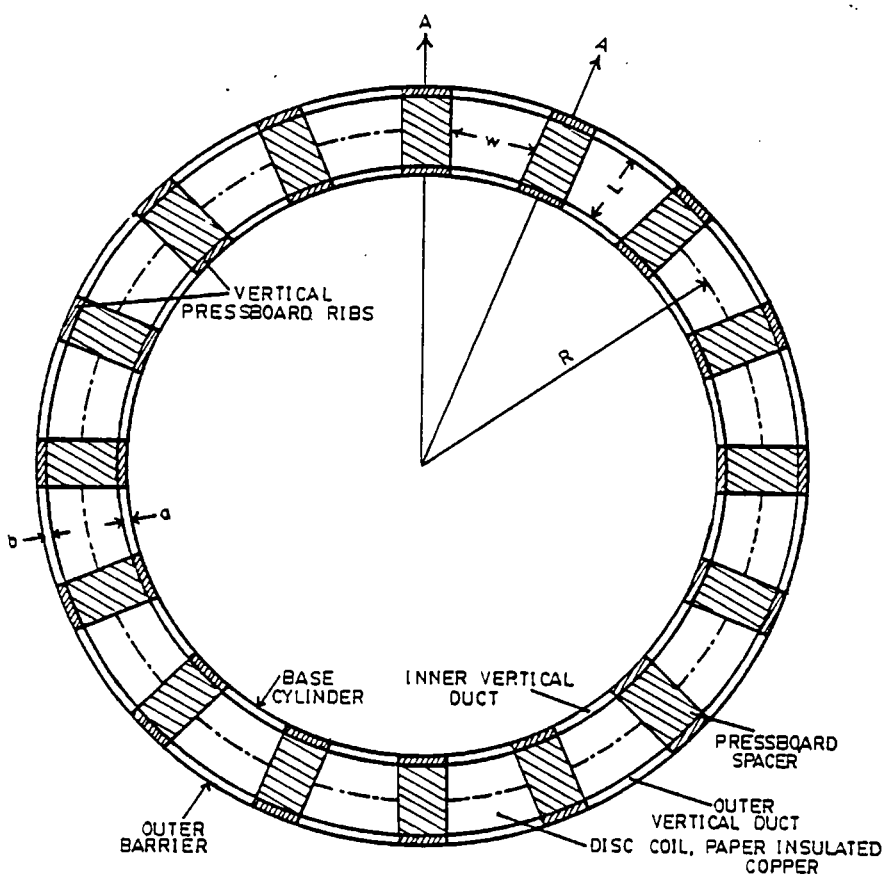


Fig. 2.1 Plan View of Disc Winding

A plan view of a typical winding is shown as Fig. 2.1. To avoid clutter, the individual conductors in the disc coil are not shown and the base cylinder and outer barrier are represented as single lines. In

the sector contained between radial lines A-A, it is seen that the pressboard spacers form a horizontal duct of mean width w and length L. Although the mean winding radius R will vary in practice, it is usually assumed large enough (typically 0.5 - 1.0 m) to enable neglect of the variation of width in the horizontal ducts. This assumption will be more closely considered in Chapter 14.

The inner and outer vertical ducts, of thicknesses a and b respectively, are also seen (in cross-section) to be formed by vertical pressboard ribs which set the outer barrier and base cylinder off from the winding.

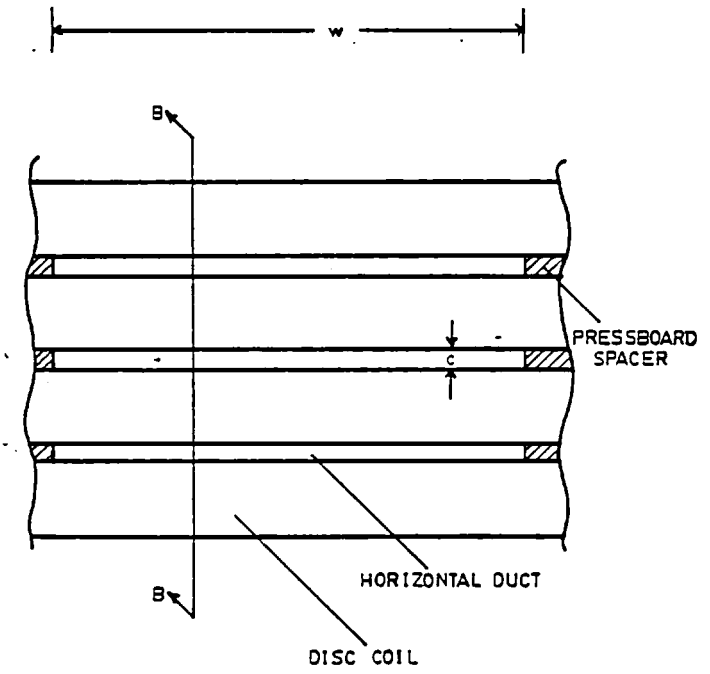


Fig. 2.2 Elevation of Sector A-A

In this example there are 16 geometrically equivalent sectors, and it is usually assumed that the oil flow distributes itself evenly around the circumference (swirling is ruled out). An elevation view of a part of sector A-A is shown as Fig. 2.2. 4 discs and 3 ducts of thickness c

are shown. The aspect ratio of the ducts w/c (or w/a, w/b for vertical ducts) is usually large enough (typically 20-25) to assume that they are hydrodynamically equivalent to infinite parallel plate ducts. The result may be seen as vertical section 8-8 in Fig. 2.3.

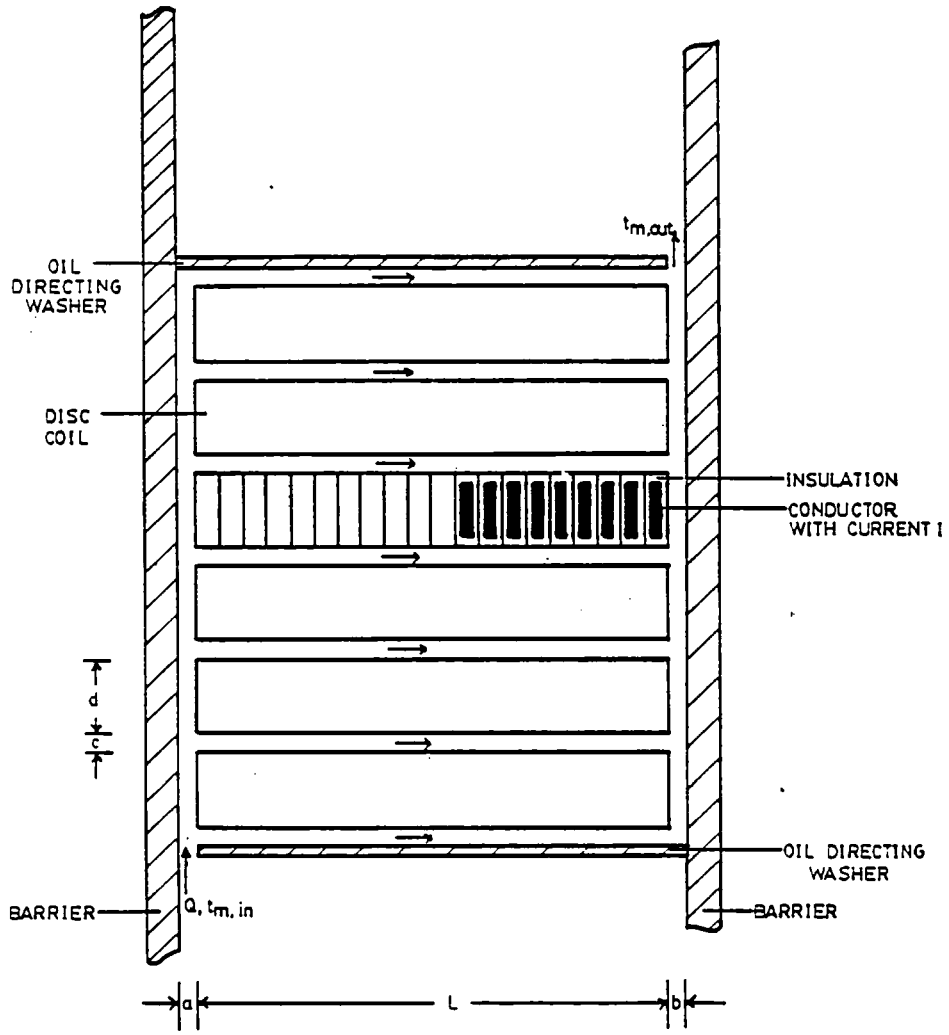


Fig. 2.3 Vertical Section 8-8

Here, a "pass" comprising 6 discs and 7 ducts is shown. The oil-directing washers at the top and bottom force the oil to flow in the direction indicated by the arrows. (An alternative method of diverting the flow, apparently used in some Japanese designs (see Yamaguchi, et al. (1981)) is pictured in Fig. 3.1.) In the U.K., a pass may contain as

many as 36 discs, and a winding may have several passes. The thickness c of the horizontal ducts may vary within a pass due to tapping arrangements or for the purpose of maintaining an ampere-turn balance between the high and low voltage windings. This latter point will be considered further in Chapter 13.

Assuming that the geometrical simplifications made thus far are reasonable, it follows that the thermal performance of the entire transformer may be determined from bottom to top analysis of each pass in each winding. Since successive passes are connected by only one path, exit conditions for the first become entry conditions for the second, and so on. The problem then reduces to solving a one-pass system.

2.2 Problem Statement Referring again to Fig. 2.3, it is assumed that the oil flow rate Q into the pass, its bulk fluid temperature $t_{m,in}$ and all dimensions and relevant thermophysical properties are known. In general, the bulk fluid temperature t_m of a fluid flowing at mean velocity u_m in a duct of cross-sectional area A_c is defined as

$$t_m = \frac{1}{A_c u_m} \int_{A_c} ut \, dA_c, \tag{2.1}$$

where u and t are the local axial velocity and temperature. (Since the problem is 2-dimensional, Q is an area flow rate which has units of m^2/s). Each conductor is assumed to carry a steady current I and to have reached thermal equilibrium with its environment. It is further assumed that the heat flux through the barriers and oil-directing washers is negligible.

Given the above knowledge it is desired to calculate the average

temperature of each conductor in each disc of the pass, and hence to find the location and value of the hottest spot temperature. The pressure drop through the pass is also required. The solution of this problem is the main purpose of this thesis, as to the author's knowledge there is no published work which accurately predicts individual conductor temperatures and for which experimental verification has been obtained.

2.3 Preliminary Observations The pass shown in Fig. 2.3 is seen to be composed of an interconnected series of relatively long (L = 100 mm) horizontal and relatively short (d = 14 mm) vertical ducts, all relatively thin (a = b = c = 4 mm). These dimensions are typical. The flow rates generally used, and the viscosity of most insulating fluids ensure, low duct Reynolds numbers (Re = 20 - 200). The definition of Re throughout this thesis is based on the hydraulic diameter D_h of the duct, defined as

$$D_h = \frac{4A_c}{P} = 4r_h, \tag{2.2}$$

where A_c is the cross-sectional area, P the wetted perimeter and r_h the hydraulic radius of the duct. In the case of, e.g., a horizontal duct

$$D_h = 2c. \tag{2.3}$$

Low Reynolds numbers and long thin ducts ensure laminar flow and small hydrodynamic entrance effects. The hydrodynamic entrance length L_{hy}, defined as "the duct length required to achieve a duct section maximum velocity of 99% of the corresponding fully developed magnitude

when the entering flow is uniform" (Shah and London (1978), p. 41), is given by Atkinson et al. (1969), for the parallel plate geometry, as

$$L_{hy}/D_h = 0.3125 + 0.011Re, \qquad (2.4)$$

which will give $L_{hy} << L$ in the horizontal ducts. The highest Re in fact occur in the vertical ducts near the entrance and exit of the pass, which presents complications to be further discussed in Chapter 5. Furthermore the dynamic viscosity of most insulating oils decreases sharply with temperature (see Appendix A), causing doubt about the concept of fully developed velocity profiles. This point will be taken up in Chapter 7.

Setting these difficulties aside for the moment, and bearing in mind that $L >> d$, it is reasonable to assume that most of the heat transfer will occur by conduction and convection in the horizontal ducts, and that each duct could be analysed individually if its inlet flow rate were known. Hence it is necessary to consider the factors which affect the distribution of flow between the several horizontal ducts of a pass.

In general, as will be presented later, both experiment and theory demonstrate that the distribution of flow is unequal and in some cases highly non-uniform. The pressure drops along each parallel path from inlet to outlet which in combination govern this distribution will consist of a.) friction losses, primarily in the long horizontal ducts and b.) momentum losses (or regains) in the short vertical ducts and at all connecting junctions. Because both Re and L_{hy} are small, friction losses are expected to predominate; in fact, it will be shown in Chapter

3 that total neglect of momentum effects gives a reasonably accurate prediction of the flow distribution in some cases. In Chapters 5 and 6, the momentum effects at junctions and corners will be considered in detail. Their influence on the pass flow distribution is discussed in Chapter 8.

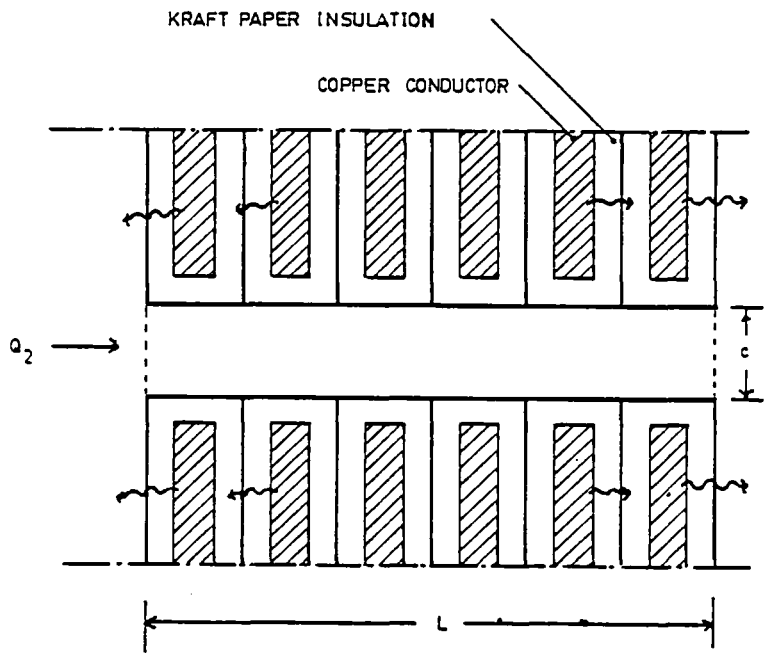


Fig 2.4 Combined Heat Flow in Disc and Duct

Assuming that the flow rate and bulk fluid temperature at the inlet of each horizontal duct is known, knowledge of individual conductor temperatures will require analysis of a region such as that of Fig. 2.4. Each half disc contains only 6 conductors, which would be common in a low voltage winding. Two observations will be made.

First, most insulating fluids have high viscosities and specific heats but low thermal conductivities, see Appendix A, resulting in high Prandtl numbers (typically 400-80). Thus even though the duct Reynolds numbers are low, the Peclet numbers Pe will be high:

$$Pe = RePr, \tag{2.5}$$

where Pr is the Prandtl number

$$Pr = \frac{\mu c_p}{k}, \tag{2.6}$$

where μ, c_p and k are the dynamic viscosity, specific heat at constant pressure and thermal conductivity. These parameter values indicate that thermal entrance effects will be present; in particular, the Nusselt number will vary considerably along the horizontal surface of the disc. As is standard, the Nusselt number

$$Nu = \frac{hD_h}{k}, \tag{2.7}$$

where the convective heat transfer coefficient h is given by

$$h = \frac{\dot{q}''_w}{t_{wall} - t_m}, \tag{2.8}$$

where t_{wall} and t_m are the local (disc) surface and bulk fluid temperatures and $\dot{q}''_w$ is the local surface heat flux.

The thermal entrance length L_{th}, defined as "the duct length required to achieve a value of local Nu equal to 1.05 Nu for fully developed flow" (Shah and London (1978), p. 50), depends not only on flow geometry but also on the thermal boundary conditions. In the case of the parallel plate duct with constant wall heat flux, Shah (1975) gives

$$L_{th} = 0.0115439 D_h Pe. \qquad (2.9)$$

Except for the very lowest values of Pe (low flow rates combined with high oil temperatures, hence low Pr), this will give $L_{th} >> L$.

The second observation is that some heat transfer may be expected to occur from the surface of the disc edges to the vertical ducts, which will result in some heat conduction within the disc as suggested in Fig. 2.4 by the serpentine arrows. Hence the heat transfer problem is a conjugated one. Further complications arise from the non-homogeneity of the materials in the discs (oil-impregnated kraft paper and copper).

2.4 Governing Equations The solution of the flow and temperature fields in the region of Fig. 2.3 necessitates detailed consideration of the governing partial differential equations commonly referred to as the continuity, momentum (Navier-Stokes) and energy equations. (Navier (1823) derived the momentum equations for incompressible flow using molecular arguments. Stokes (1845) rederived them using concepts of continuum mechanics more common in today's textbooks, incorporating compressible flows.) Derivations of these equations are available in many standard fluid mechanics texts, e.g. Batchelor (1967), and will not be reproduced here.

In the case of steady, two-dimensional flow, the continuity (conservation of mass) equation is:

$$\frac{\partial}{\partial x}(\rho u) + \frac{\partial}{\partial y}(\rho v) = 0. \qquad (2.10)$$

Local fluid velocities u and v are in the x and y directions

respectively. ϱ is the local fluid density. Although transformer oil is generally considered to be an incompressible fluid, the variable density form of the continuity equation has been retained for later convenience.

The momentum equations are, for the x direction:

$$\varrho u\frac{\partial u}{\partial x} + \varrho v\frac{\partial u}{\partial y} = - \frac{\partial p}{\partial x} + \frac{\partial}{\partial x}(2\mu\frac{\partial u}{\partial x}) + \frac{\partial}{\partial y}(\mu[\frac{\partial u}{\partial y} + \frac{\partial v}{\partial x}]), \qquad (2.11)$$

and for the y direction

$$\varrho u\frac{\partial v}{\partial x} + \varrho v\frac{\partial v}{\partial y} = - \frac{\partial p}{\partial y} - \varrho g + \frac{\partial}{\partial x}(\mu[\frac{\partial v}{\partial x} + \frac{\partial u}{\partial y}]) + \frac{\partial}{\partial y}(2\mu\frac{\partial v}{\partial y}), \qquad (2.12)$$

where g is the acceleration due to gravity.

The symbol p requires brief additional discussion. Strictly speaking it is imprecise to label p in equations (2.11) and (2.12) as the thermodynamic or fluid static pressure (as is customary) except in the case of a stationary fluid in thermodynamic equilibrium. In the derivation of the momentum equations, p is defined <u>mechanically</u> as the average compression on a fluid element which is not necessarily at thermodynamic equilibrium. Furthermore, in a moving fluid, compression stresses arise due to viscosity which are absent in a stationary fluid. As pointed out by White (1974), p. 70, the <u>difference</u> between the thermodynamic pressure p and the mean mechanical pressure $\bar{p}$ is

$$\bar{p} = p - (\lambda + \frac{2}{3}\mu)(\frac{\partial u}{\partial x} + \frac{\partial v}{\partial y}) \qquad (2.13)$$

where λ is the coefficient of bulk viscosity. Stokes's (1845) hypothesis was to set

$$\lambda + \frac{2}{3}\mu = 0. \tag{2.14}$$

This assumption has caused controversy, but chiefly in dealing with compressible flows. In the case of transformer oil, as

$$\frac{\partial u}{\partial x} + \frac{\partial v}{\partial y} \approx 0, \tag{2.15}$$

the distinction between mechanical and thermodynamic pressure is unimportant. In this thesis, then, p will be taken to mean throughout the thermodynamic or fluid static pressure.

It will also be noted that equations (2.11) and (2.12) allow for variable viscosity. Unfortunately this makes analytical solution of the equations virtually impossible even in simple geometries.

The energy conservation equation for the fluid is

$$\varrho c_p (u\frac{\partial t}{\partial x} + v\frac{\partial t}{\partial y}) = \frac{\partial}{\partial x}(k\frac{\partial t}{\partial x}) + \frac{\partial}{\partial y}(k\frac{\partial t}{\partial y}), \tag{2.16}$$

where it has been assumed that heat generated through viscous dissipation and fluid compression is negligible. Allen (1959) has shown that the thermal conductivity k of transformer oil can both increase and decrease with temperature, hence this possibility is retained in the equations.

In solid areas of the domain, the energy equation becomes

$$\frac{\partial}{\partial x}(k_x\frac{\partial t}{\partial x}) + \frac{\partial}{\partial y}(k_y\frac{\partial t}{\partial y}) + \dot{q}''' = 0, \tag{2.17}$$

where k_x and k_y are thermal conductivities in the x and y directions and $\dot{q}'''$ is the energy generation per unit volume. The former complication results from the anisotropic thermal conductivity of some conductor insulation, the latter from the I^2R losses present in the copper conductors.

2.5 Solution Strategy In deciding how to solve the field equations most efficiently in a domain such as Fig. 2.3, first note that analytical methods would be extremely difficult to apply. The flow domain is multiply-connected, the momentum and energy equations are coupled through temperature-dependent viscosity, and finally the solid areas are non-homogeneous.

Second, while numerical solution using a digital computer is possible, it would be somewhat inefficient and less accurate to treat the pass as a whole. Any numerical computation depends for its accuracy, on, among other things, the fineness of the grid spacing. No computations can be considered complete without some sort of "grid-independence test", in which successive refinements of the grid are carried out until the quantity desired from the calculation is only slightly altered. In the flow domain under consideration, considerable refinement is required at corners and tee-junctions, while in the long horizontal ducts, where the flow is likely to be fully developed, the grid could be quite coarse. In any case a very large number of grid points would be required to treat the pass as a whole, and this would unduly increase storage requirements and central processor unit time.

Finally, it should be remembered that the ultimate aim of the analysis is to predict the location and value of the hot-spot

temperature. It is reasonable to expect that the hot-spot will occur somewhere in the interior conductors of the disc (not near the edges, which are cooled by the vertical ducts). Therefore, minute details of recirculation flow patterns at tee-junctions and corners are not required, only insofar as they influence the overall flow distribution.

The above considerations have suggested the strategy adopted in this thesis. First, the overall flow distribution is to be predicted from a "network" model which makes use of lumped flow-resistances. Second, each duct is then solved individually using the full field equations, and extending the calculation into the disc, to yield finally the individual conductor temperatures.

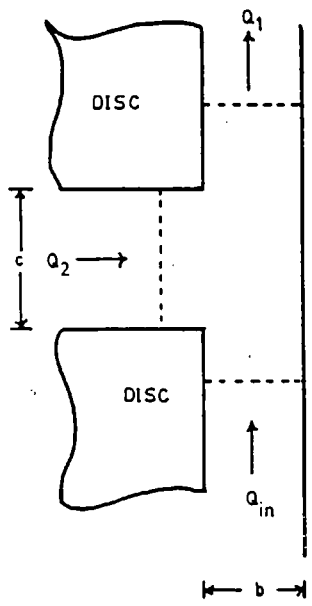


Fig. 2.5 Combining Tee-Junction

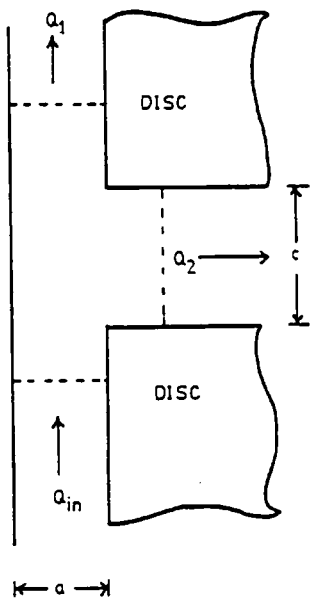


Fig. 2.6 Dividing Tee-Junction

In Chapter 3, a simple network model will be described, in which variable viscosity and corner and tee-junction losses are ignored, and it is assumed that the flow is fully developed throughout. The flow

resistances are derived from constant property parallel plate friction factors which are well known. In Chapter 5, the continuity and momentum equations will be numerically solved in combining and dividing tee-junctions, within a region enclosed by the dashed and solid lines in, respectively, Figs. 2.5 and 2.6. A similar computation is detailed in Chapter 6 for the corner region shown as Fig. 2.7. Concentrating on simplified regions reduces computer time and storage requirements and provides higher resolution. From these computations are extracted flow resistances which are then added to the simplified network. Examination of Figs. 2.3 - 2.7 will confirm the following convention for labelling flow rates:

Q = area flow rate into pass,

Q_2 = area flow rate in horizontal ducts,

Q_{in} = area flow rate in vertical ducts entering a junction,

Q_1 = area flow rate in vertical ducts leaving a junction.

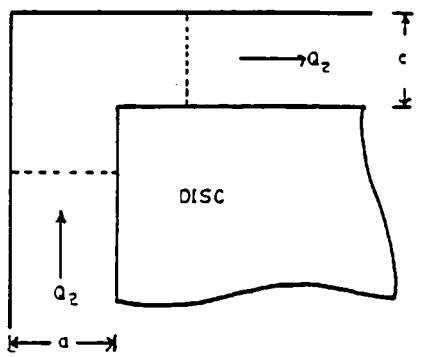


Fig. 2.7 Corner

In Chapter 7, the flow region of Fig. 2.4 (but invoking duct centre-line symmetry) is calculated to determine a.) the effect of variable viscosity on the pressure drop and b.) to obtain the details of

the individual conductor temperatures. The results of a.) are used to revise the friction factor used in Chapter 3. The result of all of these refinements is the full disc network model DISCNET which iteratively determines the flow distribution by successively adjusting all flow resistances for variable viscosity and momentum effects. DISCNET is fully described in Chapter 8.

CHAPTER 3

SIMPLE NETWORK MODEL

3.1 Simplifying Assumptions The continuity, momentum and energy equations stated in Chapter 2 (2.10) - (2.12), (2.16) can be easily applied to the flow domain of Fig. 2.3 provided that additional assumptions are made:

1.) The flow is fully developed in all vertical and horizontal ducts.

2.) Fluid properties are constant, except for density in the body force term, in the vertical ducts.

3.) Junction and corner losses are ignored.

4.) The thermal boundary condition on the disc surface is constant heat flux on all horizontal surfaces. Heat flux from the vertical edges of the discs is ignored.

These assumptions are presented graphically in Fig. 3.1. Assumption 3.) is indicated by cross-hatching in the junction and corner areas. Assumption 4.) is represented by the serpentine arrows and single hatchings on the disc edges. This assumption ignores any conduction within the discs, ensuring that the problem is not conjugated. Assumption 2.) is sometimes referred to as the "Boussinesq" or "quasi-incompressible" assumption and will be further qualified in due course.

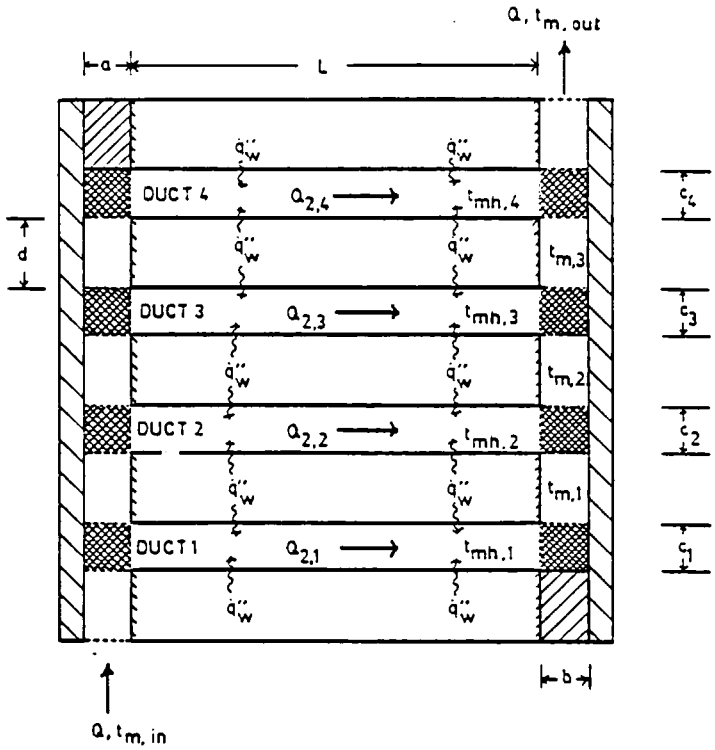


Fig. 3.1 Simplified Domain

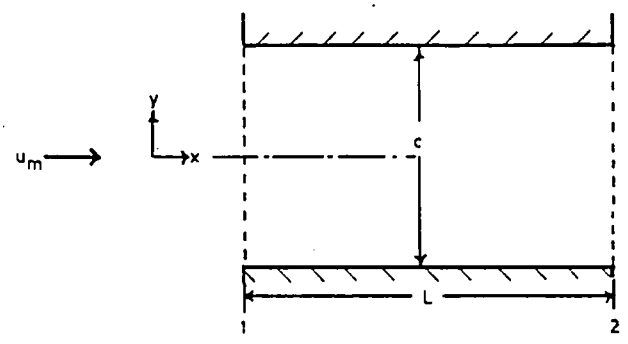


Fig. 3.2 Horizontal Duct

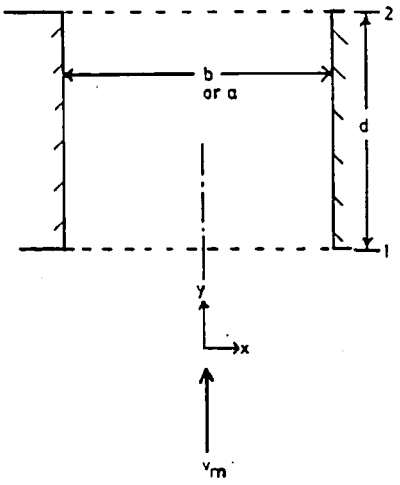


Fig. 3.3 Vertical Duct

If assumptions 1.) and 2.) are applied to one of the horizontal ducts, Fig. 3.2, equation (2.11) simplifies greatly to:

$$0 = -\frac{dp}{dx} + \mu \frac{d^2u}{dy^2}, \tag{3.1}$$

whose solution is

$$u = \frac{3}{2}u_m\left(1 - \frac{4y^2}{c^2}\right), \tag{3.2}$$

where

$$u_m = \frac{1}{c}\int_{-c/2}^{c/2} u \, dy. \tag{3.3}$$

The details of the derivation are omitted as they may be found in any fluid mechanics text, e.g. Schlichting (1979), p. 84. The pressure drop from station 1 to 2 (Fig. 3.2) is then given by

$$p_1 - p_2 = \frac{12u_m\mu L}{c^2}. \tag{3.4}$$

If the pressure drop through the entire pass is required, it is necessary to include the effects of buoyancy in the right hand vertical ducts. The oil flowing in each horizontal duct of Fig. 3.1 will enter at at bulk temperature $t_{m,in}$, and because of the wall heat flux will exit at $t_{mh,1}$, etc. At the combining junctions, mixing will occur: e.g. at the exit of duct 2, oil at $t_{mh,2}$ mixes with oil at $t_{m,1}$ (= $t_{mh,1}$) to yield oil in the vertical duct 2 at $t_{m,2}$. As the oil in the right-hand vertical duct increases in temperature, its density will decrease, generating a buoyancy force which tends to assist upward flow. The exact value of the force is related to the area underneath a graph of <u>mean</u> oil density vs. height. The mean oil density in turn would be determined, in

this case, from the arithmetic mean temperature t_{av} at each level in the right-hand vertical duct (see Allen, 1960). Strictly speaking, t_{av} is not the same as t_m, however, in this simplified analysis, it is assumed that t does not vary <u>across</u> the vertical duct, i.e., the temperature profiles are assumed to be flat. In this special case, t_{av} and t_m are the same, and the latter quantity will be used in subsequent calculations of the buoyancy force.

If the flow is assumed to be fully developed in the vertical ducts, but the gravitational body force term is retained, equation (2.12) becomes, for the domain of Fig. 3.3

$$0 = - \frac{dp}{dy} - \varrho g + \mu \frac{d^2v}{dx^2}. \qquad (3.5)$$

The density of most transformer oil decreases linearly with temperature, (see Appendix A), which may be expressed:

$$\varrho = \varrho_o + s(t-t_o), \qquad (3.6)$$

where ϱ_o is the density at some datum temperature t_o and s (negative) is the slope of the density vs. temperature curve. It is more common to express density-temperature variation using the coefficient of thermal expansion β, defined as

$$\beta = - \frac{1}{\varrho}\left(\frac{\partial \varrho}{\partial t}\right)_p, \qquad (3.7)$$

where the partial derivative is to read "$\partial\varrho/\partial t$ at constant pressure", however Allen (1960) has pointed out that, for transformer oil, β is less convenient to use since it varies with temperature (s does not).

Although equation (3.5) differs from (3.1) due to the addition of the body force term $\rho \underset{\wedge}{g}$, the dissimilarity can be removed by defining a "total" pressure p' such that

$$\frac{dp'}{dy} = \frac{dp}{dy} + \rho g, \tag{3.8}$$

which upon substitution into (3.5) yields an equation identical in form to (3.1), whose solution yields the total pressure drop from station 1 to 2 (see Fig. 3.3) which is

$$p_1' - p_2' = \frac{12 v_m \mu d}{b^2}. \tag{3.9}$$

The relationship between the total and static pressure drop may be found by integration of (3.8) from 1 to 2 in Fig. 3.3:

$$p_2' - p_1' = p_2 - p_1 + \rho_o g d + sg \int_{y_1}^{y_2} (t - t_o) dy, \tag{3.10}$$

where t_o must be set equal to the temperature at y_1. Substitution of (3.9) in (3.10) yields

$$p_1 - p_2 = \frac{12 v_m \mu d}{b^2} + \rho_o g d + sg \int_{y_1}^{y_2} (t - t_o) dy. \tag{3.11}$$

The static pressure drop on the L.H.S. is what would be measured by a differential manometer connected between stations 1 and 2. It is the pressure difference which must be supplied by a pump or some other external agent to overcome the friction loss (1st term, R.H.S.) and raise the fluid through height d (2nd term, R.H.S.). If t increases from y_1 to y_2 (heating) then the 3rd term on the R.H.S. will be negative

(since $s < 0$). Hence the buoyancy term tends to decrease the pressure drop, and to assist upward flow.

In the case of a transformer cooling circuit, the above integration is carried out around the closed loop path up the windings and down the radiator (see Fig. 1.4). The result will yield the total friction loss and the total thermal driving force (terms 1 and 3, R.H.S. of (3.11)) around the circuit. The <u>difference</u> (term 1 - term 3) will represent the pressure needed from a pump. In naturally cooled transformers, the mean velocity of the fluid around the circuit will adjust itself until term 1 = term 3. Allen (1960) was the first to demonstrate these principles rigorously and to apply them to transformer design.

To conclude this section, three additional points will be made about the development of equations (3.1) - (3.11). First, in order to be consistent with the assumption of fully developed flow in the vertical ducts, it has been tacitly assumed that $t = t(y)$ only. At any cross-section, uniform temperature across the vertical duct will ensure an isothermal, parabolic velocity distribution. Temperature variation across the duct will distort this profile. The effect is ignored here, but Allen and Finn (1970) have considered it in detail. It is important in the analysis of <u>long</u> vertical ducts.

Second, since in horizontal ducts, no change in height occurs, the total pressure drop is the same as the static pressure drop, i.e.,

$$p_1 = p_2 = p_1' - p_2' = \frac{12 u_m \mu L}{c^2}. \qquad (3.12)$$

This fact will be of use in the formulation of the network equations.

Finally, the dimensionless friction factor f will be defined. For fully developed flow in ducts of uniform cross-section, the pressure drop Δp is due solely to the action of the wall shear stress on the fluid. When Δp over a length L of duct of hydraulic radius r_h is normalised with respect to the mean kinetic energy per unit volume of the fluid $\varrho u_m^2/2$, the definition of f emerges:

$$\frac{\Delta p}{\varrho u_m^2/2} = f \frac{L}{r_h}. \tag{3.13}$$

In the case of parallel plane ducts, we may substitute the expression for Δp from equation (3.4), bearing in mind that $c = 2r_h$:

$$f = \frac{24\mu}{\varrho u_m 4 r_h}, \tag{3.14}$$

whence it is evident that

$$f = \frac{24}{Re}, \tag{3.15}$$

where Re is based on the hydraulic diameter $D_h = 4r_h$:

$$Re = \frac{\varrho u_m D_h}{\mu}. \tag{3.16}$$

The friction factor for fully-developed, constant property fluid flow in ducts of arbitrary but uniform cross-section is of the form

$$f = \frac{K}{Re}, \tag{3.17}$$

where K is called a "friction constant", and is a function only of the duct geometry. It should be noted (see Shah and London (1978), p. 40) that the "large" or Darcy friction factor sometimes used in the literature is 4 times f, and will not be used in this thesis.

It is frequently convenient to define an "apparent" friction factor f_{app} in flow situations where a pressure drop Δp over length x occurs due to <u>both</u> friction and momentum effects,

$$\frac{\Delta p}{\rho u_m^2/2} = f_{app} \frac{x}{r_h}. \tag{3.18}$$

This quantity will be used in Chapters 5 - 8.

<u>3.2 Network Equations</u> Equations (3.4) and (3.9) will now be rewritten in terms of the friction constant K, flow rate Q and hydraulic diameter $D_{hor} = 2c$ for horizontal ducts,

$$\Delta p' = \frac{4KQ_2\mu L}{D_{hor}^3}, \tag{3.19}$$

$D_l = 2a$ for left hand vertical ducts

$$\Delta p' = \frac{4KQ_1\mu d}{D_l^3}, \tag{3.20}$$

and $D_r = 2b$ for right hand vertical ducts

$$\Delta p' = \frac{4KQ_1\mu d}{D_r^3}, \tag{3.21}$$

where the use of the total pressure drop $\Delta p'$ for both horizontal and vertical ducts is for reasons of convenience and is justified by (3.12).

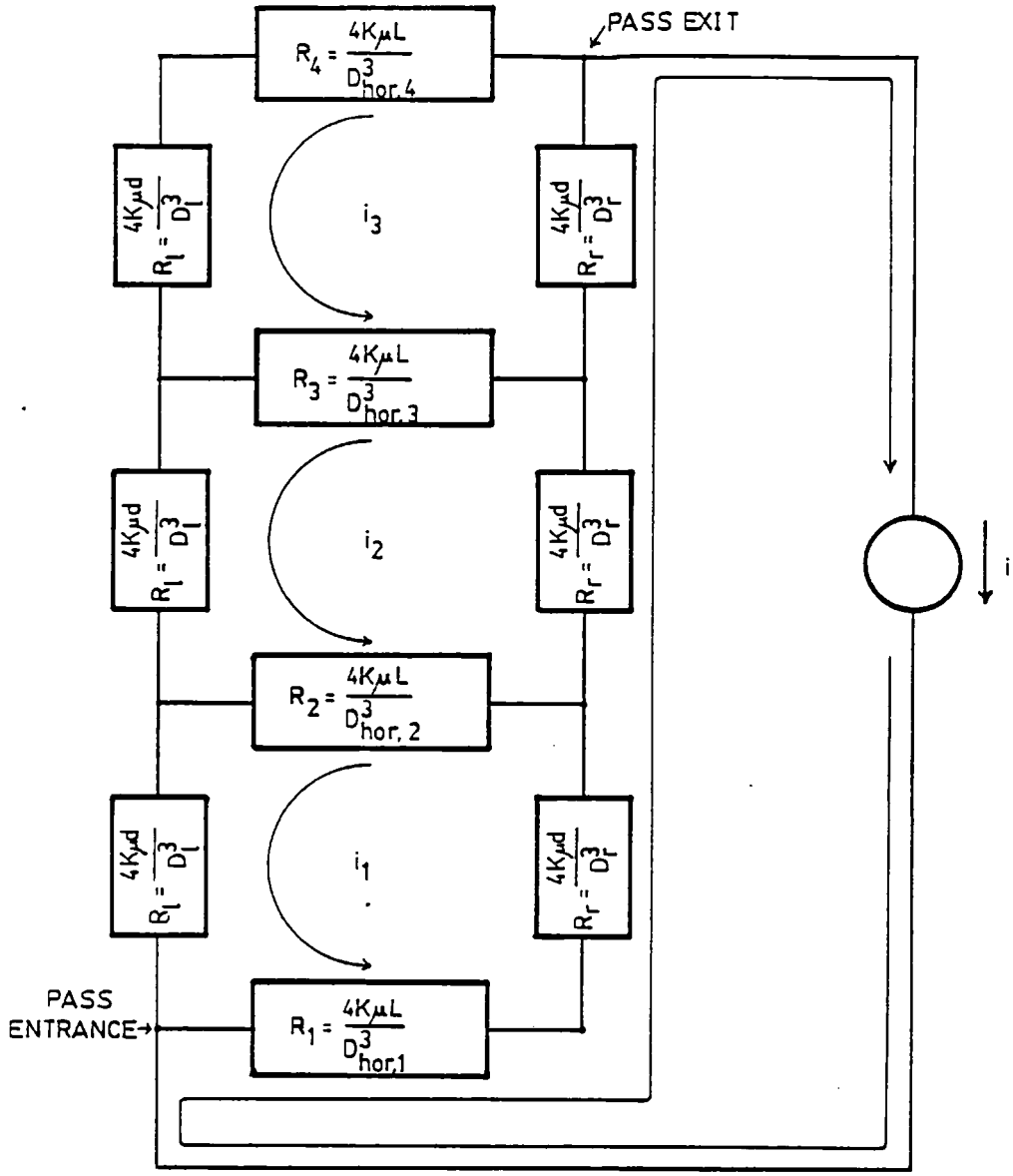


Fig. 3.4 Network Analogue

The form of these equations suggests an Ohm's Law type electrical analogy, in which: volt drop = $\Delta p'$, current = Q and resistance = e.g. $4K\mu L/D^3_{hor}$ for horizontal ducts. At combining junctions, Fig. 2.5, an analogous Kirchoff current law may be written

$$Q_1 = Q_{in} + Q_2. \tag{3.22}$$

and for dividing junctions, Fig. 2.6

$$Q_{in} = Q_1 + Q_2. \tag{3.23}$$

Hence the four duct system of Fig. 3.1 may be replaced by the equivalent circuit shown as Fig. 3.4. R_{1-4} are the resistances for horizontal ducts 1 - 4, which may differ due to the hydraulic diameters $D_{hor,1-4}$. R_l and R_r are the resistances for the left and right hand vertical ducts, i_{1-3} are the mesh currents (chosen for convenience). The flow through the pass is represented by a current source i, where i is numerically equal to the area flow rate into the pass. The area flow rate in horizontal ducts 1 - 4, $Q_{2,1-4}$ are related to i, i_{1-3} as follows:

$$\begin{aligned} Q_{2,1} &= i + i_1 \\ Q_{2,2} &= i_2 - i_1 \\ Q_{2,3} &= i_3 - i_2 \\ Q_{2,4} &= -i_3. \end{aligned} \tag{3.24}$$

Mesh currents i_{1-3} may be easily calculated from the following set of mesh equations, written down by inspection from Fig. 3.4:

$$
\begin{aligned}
i_1(R_1+R_2+R_1+R_r) \; -i_2R_2 \qquad\qquad &= -i(R_1+R_r) \\
-i_1R_2 \qquad +i_2(R_2+R_3+R_1+R_r) \; -i_3R_3 \qquad &= -iR_r \qquad (3.25) \\
-i_2R_3 \qquad +i_3(R_3+R_4+R_1+R_r) \; &= -iR_r
\end{aligned}
$$

These equations may easily be expanded by inspection to a system of N ducts comprising N-1 mesh currents. A tri-diagonal matrix always results, which may be solved easily on a digital computer. However, for passes of up to 10 ducts (which will generate 9 mesh equations) a Texas Instrument model TI-59 pocket calculator could be used. The TI-59 will invert up to a 9x9 matrix, requiring about 12-15 minutes for the computation.

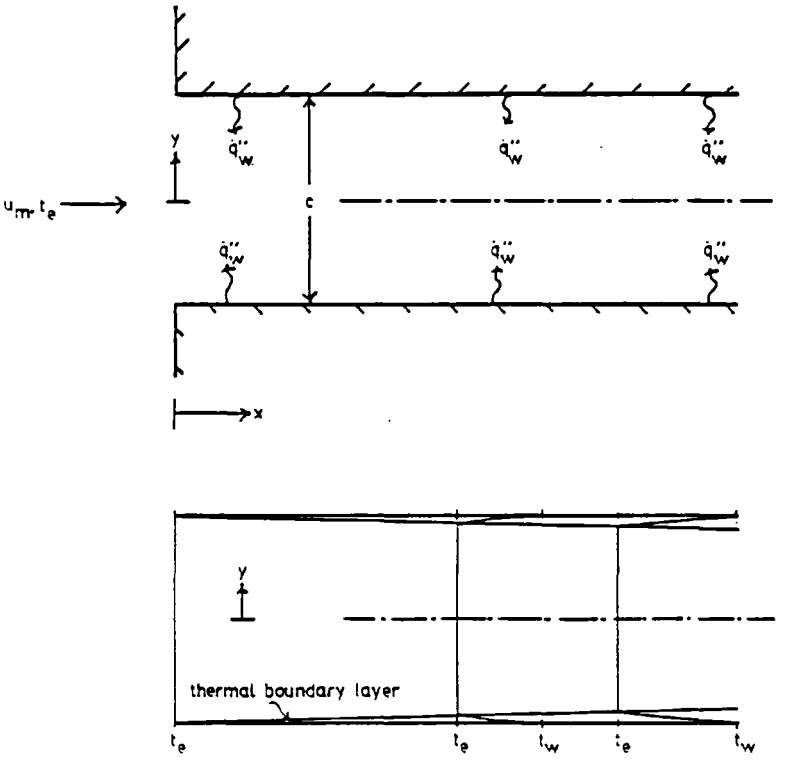


Fig. 3.5 Duct Entrance Region

3.3 Constant Property Disc Surface Temperature The solution of (3.25) will yield, by (3.24) the area flow rates in the horizontal ducts $Q_{2,1-4}$. The disc surface temperatures in each duct may then be calculated using the known analytical solution for the parallel plane duct with constant wall heat flux and a constant property fluid. The velocity profile is assumed parabolic (fully developed) while the temperature profile is developing. The inlet temperature (t_e) profile is uniform. The entrance region of the duct is shown in Fig. 3.5, together with a sketch, underneath, of the developing temperature profile and thermal boundary layer. The infinite series solution obtained by Sparrow et al. (1963) has been approximated by Shah (1975) as follows:

$$Nu_{x,H} = 1.490(x^*)^{-1/3} \quad \text{for } x^* \leq 0.0002$$

$$Nu_{x,H} = 1.490(x^*)^{-1/3} + 0.4 \quad \text{for } 0.0002 < x^* \leq 0.001 \qquad (3.26)$$

$$Nu_{x,H} = 8.235 + 8.68(10^3 x^*)^{-0.506} e^{-164x^*} \quad \text{for } x^* > 0.001,$$

where $Nu_{x,H}$ is the local (subscript x) Nusselt number for the constant wall heat flux boundary condition (subscript H), defined, as earlier

$$Nu_{x,H} = \frac{hD_h}{k}, \qquad (3.27)$$

where

$$h = \frac{\dot{q}''_w}{t_{wall} - t_{mh}}, \qquad (3.28)$$

and where x^* is defined as

$$x^* = \frac{x}{D_h Pe}. \tag{3.29}$$

The bulk fluid temperature rise $t_{mh} - t_e$ along the length L of the duct may be easily derived from energy conservation principles, (see Kays (1966), p. 109) from which we obtain:

$$t_{mh} - t_e = \frac{2\dot{q}''_w L}{\varrho c_p Q_2}. \tag{3.30}$$

This simplified model will predict that the hot-spot temperature $t_{hot} = t_{wall}$ at x = L, i.e. at the right edge of the disc. This somewhat implausible result, due to the second part of assumption 4.) at the beginning of this chapter, will be rectified in Chapter 7. Since in reality t_{wall} will increase with x over most of the duct, but decrease sharply as x approaches L, the value of t_{hot} predicted from $Nu_{x,H}$ will be higher than observed, although this error will be compensated by the fact that, in practise, t_{hot} is measured in the interior of the disc (see Chapter 11) and will be greater than the hottest surface temperature. In any case the $Nu_{x,H}$ solution, in conjunction with the flow rates from (3.24) and (3.25), give useful preliminary results.

3.4 Friction Loss and Buoyant Pressure Regain The friction loss from entrance to exit of the pass shown as Fig. 3.1 may be calculated once i_{1-3} have been obtained from the network of Fig. 3.4. Any path from entance to exit may be used, in this example the path is taken through R_1 and up through the three R_r resistors. To this must be added the iR drops in the entrance and exit vertical ducts. (As these resistances do not affect the value of i_{1-3}, they are not included in the network.) The total pressure drop is then

$$\Delta p' = iR_1 + (i+i_1)(R_1+R_r) + (i+i_2)R_r + (i+i_3)R_r + iR_r. \quad (3.31)$$

The buoyant pressure regain p_b through the same pass may be calculated once $t_{m,1-3}$ are known, by evaluating the integral in (3.11) along any path up the pass. For convenience, the friction loss calculation path will be taken. Since t is assumed to be a function of y only, $t_m(y) = t(y)$, and t_o must be set to $t_{m,in}$:

$$p_b = -sg\int_{entrance}^{exit}(t_m(y) - t_{m,in})dy \quad (3.32)$$

A graphical illustration of this integral will appear in the next section.

3.5 Sample Calculations The equations presented in the previous two sections can be implemented on a programmable calculator such as the TI-59, and this was done in the early stages of the research. However, the process is lengthy and somewhat tedious, and more recently an Acorn BBC Model B microcomputer has been used. The program, written in BASIC, is listed in Appendix D1, but a brief outline of the calculation procedure and some sample results will be given here.

First, all relevant fluid properties, pass dimensions and inlet conditions are input, so that network resistances R_{1-4}, R_l and R_r (see Fig. 3.4) can be computed. The matrix of simultaneous equations (3.23), being tri-diagonal, may be solved by a tri-diagonal matrix algorithm (T.D.M.A.), yielding the "mesh currents" i_{1-3} from which horizontal duct flow rates $Q_{2,1-4}$ are obtained. The Peclet number Pe is then calculated

in each duct to obtain x^* (3.29), from which $Nu_{x,H}$ (3.26) and t_{wall} (3.28) are obtained once t_{mh} in each horizontal duct has been found from (3.30).

Referring to Fig. 3.1, it is assumed that uniform mixing of the oil occurs at the three combining junctions, from which $t_{m,2}$, $t_{m,3}$ and $t_{m,out}$ are calculated. ($t_{m,1}$ is simply equal to $t_{mh,1}$, see Fig. 3.1.) The buoyant pressure regain p_b may then be calculated by evaluating the integral (3.32). Finally the pressure drop due to friction is obtained from (3.31).

In the following three examples, the flow distribution and t_{hot} (t_{wall} at x = L) for each duct are calculated for passes of 4, 8 and 16 ducts. In all cases the pass inlet temperature $t_{m,in}$ = 40°C, pass area flow rate Q = 1.2 x 10^{-3} m^2/s, surface heat flux $\dot{q}''_w$ = 3,000 W/m^2, disc dimensions d = 16 mm, L = 100 mm, and all duct hydraulic diameters D_{hor}, D_l, D_r = 8 mm. These dimensions are typical of U.K. industrial design. The properties of the fluid, a naphthenic transformer oil conforming to B.S. 148, are given in Appendix A. The results for the first example are given as Table 3.1.

Duct No.	% Flow	$t_{hot,j}$ °C	$t_{mh,j}$ °C	$t_{m,j}$ °C
4	28.45	55.3	41.0	41.2
3	21.55	56.8	41.4	41.2
2	21.55	56.8	41.4	41.2
1	28.45	55.3	41.0	41.0
$\Delta p'$ = 213.3 Pa, p_b = 0.6 Pa, p_{ex} = 212.7 Pa				

Table 3.1 SN Prediction of 4 Duct Pass

$t_{hot,j}$, $t_{mh,j}$ and $t_{m,j}$ are t_{hot} and t_{mh} in the j^{th} horizontal duct, and t_m in the j^{th} vertical duct, so that $t_{m,4} = t_{m,out}$. p_{ex} is the

difference between $\Delta p'$, the total pressure drop due to friction, and p_b, the buoyant pressure regain. Hence p_{ex} must be supplied by some external agent to cause flow in the pass. In order to evaluate p_b from (3.32), some reasonable assumption needs to be made about the variation of t_m with y. If it is assumed that y = 0 at the pass entrance (see Fig. 3.1), the simplest form of temperature variation with height is given as Fig. 3.6. Here, e.g., $t_{m,1}$ is assumed to change suddenly to $t_{m,2}$ upon entering the combining junction at the end of duct 2, where y = 36 mm. The shaded area under the curve is proportional to p_b. In this example, typical of forced convection, p_b provides only about 0.3% of the total pressure requirement. Note that, since $t_{mh,2} = t_{mh,3}$, and $t_{mh,4} < t_{mh,3}$, $t_{m,2}$, $t_{m,3}$ and $t_{m,4}$ are all roughly equal. In the next two examples, t_m actually <u>decreases</u> slightly towards the top of the pass, as cooler oil from the upper ducts combines with hotter oil from the starved central ducts.

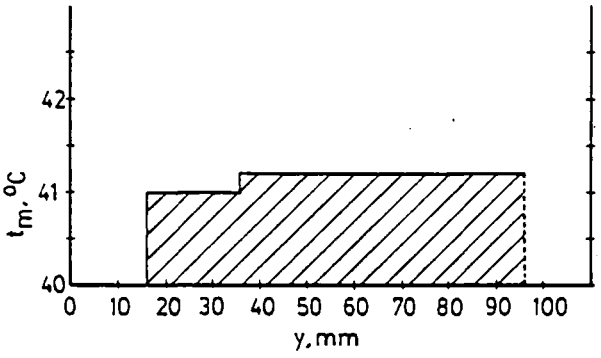


Fig. 3.6 Bulk Temperature vs. Height

In a 4-duct pass the flow distribution is seen to be roughly uniform, and t_{hot} only slightly higher in the middle ducts. The situation for an 8-duct pass, Table 3.2, is not as good. There is a difference of 10°C between t_{hot} in the middle and outer ducts, due to

"starvation" of oil in the middle two ducts. On the positive side, Δp' has increased only 30% over the 4-duct case, while p_b represents slightly more (0.9%)of Δp'.

Duct No.	% Flow	$t_{hot,j}$ °C	$t_{mh,j}$ °C	$t_{m,j}$ °C
8	22.08	56.7	41.4	42.4
7	13.14	60.1	42.3	42.7
6	8.41	63.5	43.6	42.8
5	6.37	66.0	44.7	42.6
4	6.37	66.0	44.7	42.4
3	8.41	63.5	43.6	42.1
2	13.14	60.1	42.3	41.7
1	22.08	57.0	41.4	41.4
$\Delta p' = 278.0$ Pa, $p_b = 2.5$ Pa, $p_{ex} = 275.6$ Pa				

Table 3.2 SN Prediction of 8 Duct Pass

In the case of 16 ducts, Table 3.3, the effects of maldistribution are far more drastic. t_{hot} in the middle ducts is over 50°C higher than in the outer ducts, due to extremely low flows in ducts 8 and 9. The slightly increased role of buoyancy (2.2% of the total pressure requirement) does not really compensate for the excessive hot-spot temperatures.

Although the above examples are based on a simplified model they can be expected to give a reasonable qualitative comparison of the thermal behaviour of passes of different mumbers of ducts. The model should prove of value to suggest the direction of design improvement, which will be discussed at length in Chapter 13.

Duct No.	% Flow	$t_{hot,j}$, °C	$t_{mh,j}$, °C	$t_{m,j}$, °C
16	21.40	56.9	41.4	44.8
15	12.25	60.6	42.4	45.7
14	7.02	65.1	44.3	46.3
13	4.03	70.5	47.4	46.6
12	2.34	77.2	52.8	46.5
11	1.39	86.3	61.5	46.2
10	0.89	98.5	73.6	45.8
9	0.67	109.2	84.3	45.3
8	0.67	109.2	84.3	44.8
7	0.89	98.5	73.6	44.2
6	1.39	86.3	61.5	43.7
5	2.34	77.2	52.8	43.2
4	4.03	70.5	47.4	42.7
3	7.02	65.1	44.3	42.2
2	12.25	60.6	42.4	41.8
1	21.40	56.9	41.4	41.4
$\Delta p'$ = 438.0 Pa, p_b = 9.8, p_{ex} =428.2				

Table 3.3 SN Prediction of 16 Duct Pass

3.6 Comparison with Experiment and Finite Difference Computations

The simplified network model does appear to give reasonably quantitative results in the prediction of % flow in each duct, when compared with the room temperature perspex model measurements and companion finite-difference calculations of Szpiro, Allen and Richards (1982). A full-scale perspex model of a single 8-duct pass was constructed, and through it was pumped transformer oil at room temperature (the model contained no heating elements). Oil velocities in each duct were measured directly using a DISA constant temperature hot film probe. Concurrent finite-difference computations were made on a digital computer using a stream-function vorticity formulation of the constant property, two-dimensional Navier-Stokes equations. Since the grid points were spread throughout the 8-duct pass, resolution was fairly coarse (about 5 grid points across each duct). Nevertheless, good agreement between experiment and prediction was obtained.

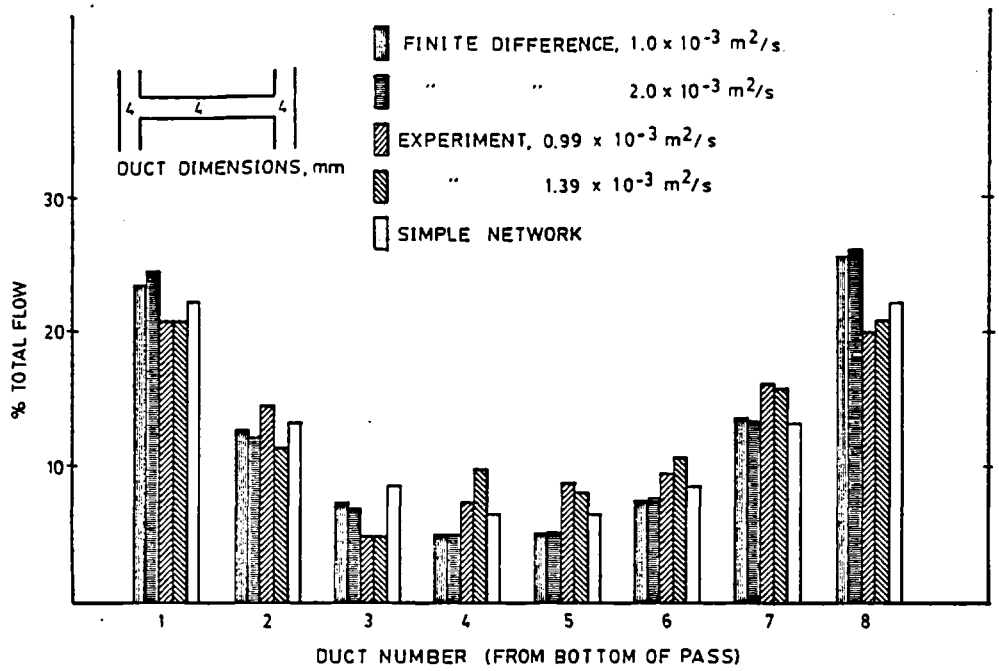


Fig. 3.7 Symmetrical 8 Duct Pass

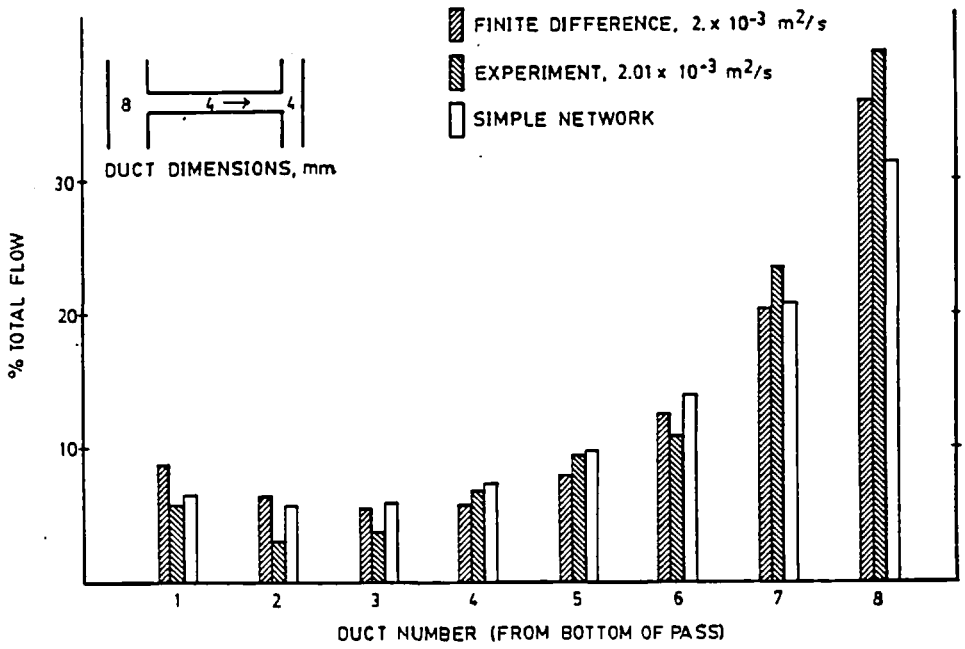


Fig. 3.8 Asymmetrical 8 Duct Pass

In Fig. 3.7 and 3.8, the network prediction is compared with their

results. All three appear to be reasonably close. Fig. 3.8 illustrates the effect of unequal left and right-hand vertical ducts. It should also be noted that the simple network model will predict the same flow distribution at any flow rate, since resistances R_i, R_r and R_l are all independent of flow rate, i.e. they are linear.

3.7 Summary The main purposes of this chapter have been to:

1.) Describe a simple network model which will serve as the basis for further refinements.

2.) Illustrate the marked difference in the thermal behaviour of passes with large (16) and small (4) numbers of ducts.

3.) Compare the results of the model with published work.

The refinements needed require a method of solving the continuity, momentum and energy equations (2.10) - (2.12), (2.16) in corners, junctions, heated ducts, etc. In the following chapter, the physical and mathematical basis of the 'general purpose' FORTRAN program used in this research will be described in detail.

CHAPTER 4

FIELD EQUATION CALCULATIONS

4.1 Introduction Refinement of the simple network model requires the relaxation of assumptions 1.) to 4.) in section 3.1, in particular noting that

1.) The flow in vertical and horizontal ducts is not fully developed at the entrances and exits of junctions and corners.

2.) Fluid properties are not constant, particularly viscosity. The decrease of viscosity with temperature tends to distort the parabolic velocity profile, reducing the friction factor when the oil near the disc surface is heated. This distortion influences in turn the energy equation and temperature field.

3.) Junction and corner losses may be significant when local Reynolds numbers are relatively high (at the entrance and exit of a pass). Recirculation zones may occur near corners.

4.) Since there is heat flux from the vertical edges of the discs, heat flow within the discs will occur, and the constant heat flux boundary condition (b.c.) can no longer apply.

A method of solving equations (2.10) - (2.12) and (2.16) - (2.17) is therefore required which can cope with two-dimensional laminar flows, allowing for variable properties and recirculation, i.e. capable of implementation in the geometries of Figs. 2.4, 2.5 - 2.7, with appropriate b.c.'s.

The development of computer software for the numerical solution of

heat transfer and fluid mechanics problems has been the subject of growing numbers of Ph.D. theses. As Patankar (1982) has pointed out in a recent survey paper, some duplication and "reinvention of the wheel" has resulted. General purpose solvers have become increasingly attractive to large industrial users since computer simulation is becoming cheaper and more flexible than prototype construction and testing. Hence commercial packages such as PHOENICS (see Spalding (1981)) have become available.

There is considerable debate among workers as to whether the current state of the art warrants marketing of "all-purpose" fluids packages such as PHOENICS. It is not the purpose of this thesis to enter the debate or to attempt a survey of a rapidly changing field. The emphasis will rather be to report experience in solving a particular problem.

It was decided in the early stages of the research to make use of any appropriate existing software that was readily available provided that 1.) the accuracy of the program could be verified and 2.) its physical and mathematical basis, and subsequent implementation in a computer code, could be thoroughly understood. The choice of locally available software which could be applied to <u>all</u> of the flow situations was between TEACH-L (Gosman, et al. (1975)) and PHOENICS. The latter has the advantage of being a highly developed "user friendly" research tool. It must be used, however, as a "black box", the source listings being unavailable (and unalterable). TEACH-L is used primarily as a teaching tool in the Mechanical Engineering Dept. at Imperial College. Though not as versatile as an all-purpose package, it has all the necessary features and its source listings, in FORTRAN, are available. The task of the user is to understand the program fully, then to adapt it as

necessary to his/her particular problem. In particular, the user must program the boundary conditions, fluid property equations, grid spacing, etc.

The decision was therefore taken to use TEACH-L, not because PHOENICS was judged inadequate or inaccurate, but to ensure full understanding and verification of the results. Doubtless other users might have arrived at different decisions depending on their circumstances. The purpose of this chapter will then be to explain fully the physical and mathematical basis of TEACH-L. Subsequent chapters will detail the adaptation of the program to particular geometries and boundary conditions. Except as otherwise indicated, most of this chapter has been compiled and expanded upon from lecture notes and other unpublished material.

4.2 Generalised Field Equations Equations (2.11), (2.12) and (2.16) may be arranged in the following equivalent forms:

$$\frac{\partial}{\partial x}(\rho uu) + \frac{\partial}{\partial y}(\rho vu) - \frac{\partial}{\partial x}(\mu\frac{\partial u}{\partial x}) - \frac{\partial}{\partial y}(\mu\frac{\partial u}{\partial y}) - S_u = 0, \qquad (4.1)$$

$$\frac{\partial}{\partial x}(\rho uv) + \frac{\partial}{\partial y}(\rho vv) - \frac{\partial}{\partial x}(\mu\frac{\partial v}{\partial x}) - \frac{\partial}{\partial y}(\mu\frac{\partial v}{\partial y}) - S_v = 0, \qquad (4.2)$$

$$\frac{\partial}{\partial x}(\rho ut) + \frac{\partial}{\partial y}(\rho vt) - \frac{\partial}{\partial x}(\frac{k}{c_p}\frac{\partial t}{\partial x}) - \frac{\partial}{\partial y}(\frac{k}{c_p}\frac{\partial t}{\partial y}) - S_t = 0, \qquad (4.3)$$

where

$$S_u = - \frac{\partial p}{\partial x} + \frac{\partial}{\partial x}(\mu \frac{\partial u}{\partial x}) + \frac{\partial}{\partial y}(\mu \frac{\partial v}{\partial x}), \qquad (4.4)$$

$$S_v = - \frac{\partial p}{\partial y} - \varrho g + \frac{\partial}{\partial x}(\mu \frac{\partial u}{\partial y}) + \frac{\partial}{\partial y}(\mu \frac{\partial v}{\partial y}), \qquad (4.5)$$

$$S_t = - k \frac{\partial t}{\partial x} \frac{\partial}{\partial x}(\frac{1}{c_p}) - k \frac{\partial t}{\partial y} \frac{\partial}{\partial y}(\frac{1}{c_p}). \qquad (4.6)$$

The motivation for this rearrangement is to be able to generalise (4.1)-(4.3) as follows:

$$\frac{\partial}{\partial x}(G_x \phi) + \frac{\partial}{\partial y}(G_y \phi) - \frac{\partial}{\partial x}(\Gamma_\phi \frac{\partial \phi}{\partial x}) - \frac{\partial}{\partial y}(\Gamma_\phi \frac{\partial \phi}{\partial y}) - S_\phi = 0, \qquad (4.7)$$

where

G_x = mass flux in the x-direction = ϱu [kg/m^2 s]

G_y = mass flux in the y-direction = ϱv [kg/m^2 s]

$$\phi = \begin{cases} \text{x-direction momentum/mass} = u \text{ [m/s]} \\ \text{y-direction momentum/mass} = v \text{ [m/s]} \\ \text{energy/mass-heat capacity} = t \text{ [}^{o}\text{C]} \end{cases}$$

$\Gamma_{u,v}$ = dynamic viscosity = μ [Pa s, kg/m s]

Γ_t = thermal exchange coefficient = k/c_p [kg/m s]

S_ϕ = sources associated with ϕ (4.4) - (4.6).

It is evident that the strategy is to combine everything which does not fit into the first four terms of (4.7) into the "source" term S_ϕ. No physical connotation is intended in using the word "source". However, if the viscosity and specific heat are constant and the fluid incompressible, the sources simplify to

$$S_u = -\frac{\partial p}{\partial x}, \tag{4.8}$$

$$S_v = -\frac{\partial p}{\partial y}, \tag{4.9}$$

$$S_t = 0, \tag{4.10}$$

so that at least in the case of the momentum equations one might want to think of the pressure gradients as a "source" of momentum. In the absence of internal heat generation in the fluid, S_t is zero; energy input arises only through the boundary conditions. In subsequent computations, these simplified source expressions will be used; justification will be included as each flow situation is discussed. The continuity equation (2.10) may also be cast in the form of (4.7) if ϕ is taken as a constant equal to unity. However (2.10) will be accorded different treatment, as will be shown later.

4.3 Control Volume Equations In order to solve equation (4.7) on a digital computer, a grid must be imposed on the flow field, and a set of algebraic equations derived, each of which is accurate at or near a specified grid point. Finite difference equations, e.g., are obtained by using Taylor's series expansions about each grid point. In TEACH-L, however, the algebraic equations are derived by integration of (4.7) over a small control volume, one of which is shown as the shaded area bounded by dashed lines in Fig. 4.1. The grid, represented by the solid lines, has been taken to be two-dimensional cartesian with equal spacing δx, δy for illustration in the first instance. The values of ϕ_P and its nearest neighbours ϕ_N, ϕ_S, ϕ_E and ϕ_W are stored at the indicated intersection points of the grid lines. (TEACH-L in fact allows for

variable grid spacing and uses a "staggered" grid; these complications will be incorporated later.)

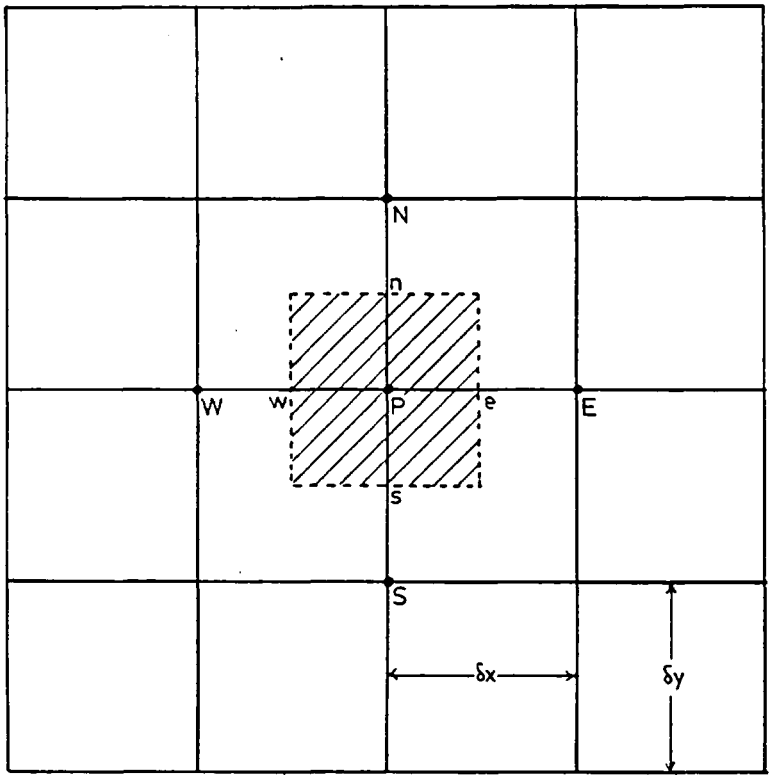


Fig. 4.1 Control Volume

Term by term integration of (4.7) gives, e.g., for the first term

$$\int_s^n \int_w^e \frac{\partial}{\partial x}(G_x \phi) dx dy = \int_s^n [(G_x \phi)_e - (G_x \phi)_w] \, dy, \qquad (4.11)$$

where the limits of integration n, s, e, w are intended to suggest the more formal procedure of establishing the origin of a coordinate system at the lower left-hand corner of the control volume, then integrating from x = 0 to x = δx and from y = 0 to y = δy. Evaluation of the R.H.S. of (4.12) requires assuming that $(G_x \phi)_e$ and $(G_x \phi)_w$ are constant along the east and west boundaries:

$$\int_s^n [(G_x\phi)_e - (G_x\phi)_w]dy = [(G_x\phi)_e - (G_x\phi)_w]\delta y. \qquad (4.12)$$

The accuracy of (4.12) will depend on the fineness of the grid. The final result for the rest of (4.7), making analogous assumptions, is

$$[(G_x\phi - \Gamma_\phi\frac{\partial\phi}{\partial x})_e - (G_x\phi - \Gamma_\phi\frac{\partial\phi}{\partial x})_w]\delta y + [(G_y\phi - \Gamma_\phi\frac{\partial\phi}{\partial y})_n - (G_y\phi - \Gamma_\phi\frac{\partial\phi}{\partial y})_s]\delta x$$

$$- \int_s^n \int_w^e S_\phi dxdy = 0. \qquad (4.13)$$

One advantage of the control volume formulation is the ease with which each term may be understood physically. The first term, e.g., of (4.13) using the variables and constants associated with u becomes:

$$(\rho uu - \mu\frac{\partial u}{\partial x})_e \delta y = \dot{M}_{x,e}, \qquad (4.14)$$

which represents the amount of x-direction momentum per second (per unit depth) leaving the control volume through the east boundary ($\dot{M}_{x,e}$) from the combined effects of convection (ρuu) and diffusion ($-\mu\partial u/\partial x$). (Recall that $\mu = \rho\nu$, kinematic viscosity ν being the momentum diffusion coefficient, and that momentum diffuses in the direction of negative velocity gradients). When the source integral is evaluated using (4.8), and the other terms of (4.13) are similarly identified, (4.13) becomes (for $\phi = u$)

$$\dot{M}_{x,e} - \dot{M}_{x,w} + \dot{M}_{x,n} - \dot{M}_{x,s} = (p_w - p_e)\delta y, \qquad (4.15)$$

which says in other words

net outflow of x-direction momentum from control volume = net force in x-direction (4.16)

One could in fact have begun with statement (4.16), the control volume statement of Newton's 2nd Law, working backwards to finally obtain (4.13).

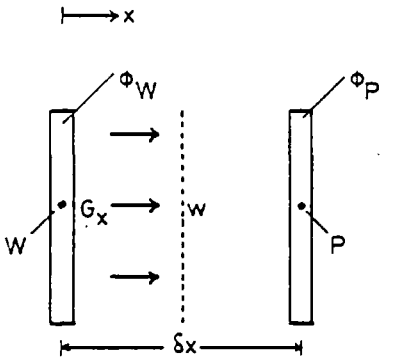


Fig. 4.2 Boundary Fluxes

Having identified the first four terms of (4.13) as boundary fluxes, it remains to find suitable expressions for them involving the quantities stored at P and its neighbours N, S, E, W. Considering the situation at the west boundary, evaluation of

$$(G_x\phi - \Gamma\frac{\partial\phi}{\partial x})_w , \qquad (4.17)$$

requires expressions for ϕ_w and $(\partial\phi/\partial x)_w$ in terms of ϕ_P and ϕ_W. The difficulty may be appreciated by taking the case in which ϕ stands for

temperature. One may imagine, as shown in Fig. 4.2, a one-dimensional problem in which two thin porous plates separated by a distance δx are being cooled by a uniform and constant mass flux G_x. If $\phi_P > \phi_W$, heat will diffuse by conduction in the negative x-direction; if G_x is positive heat will be convected in the positive x-direction. The interplay of these two effects will determine conditions at the west boundary of the control volume, which in Fig. 4.2 is the dashed line between the two plates, and this may be analysed by solving the one-dimensional equation

$$G_x \frac{d\phi}{dx} - \Gamma_\phi \frac{d^2\phi}{dx^2} = 0, \tag{4.18}$$

$$\text{with b.c.'s } \phi = \phi_W \text{ at } x = 0, \ \phi = \phi_P \text{ at } x = \delta x,$$

where G_x and Γ_ϕ are assumed constant. The solution (see Appendix B for details) at $x = \delta x/2$ (the west boundary) is

$$\phi_w = (\phi_P - \phi_W)\left[\frac{e^{Pe/2} - 1}{e^{Pe} - 1}\right] + \phi_W, \tag{4.19}$$

and

$$\left(\frac{d\phi}{dx}\right)_w = \frac{(\phi_P - \phi_W)}{\delta x} Pe\left[\frac{e^{Pe/2}}{e^{Pe} - 1}\right], \tag{4.20}$$

where the local grid Peclet number Pe is here defined as

$$Pe = \frac{G_x \delta x}{\Gamma_\phi}. \tag{4.21}$$

When Pe is large, (4.19) and (4.20) become, respectively

$$\phi_w = \phi_W, \tag{4.22}$$

and

$$\left(\frac{d\phi}{dx}\right)_w = 0. \tag{4.23}$$

In this case, conditions at x = δx/2 are entirely dictated by the upstream node at x = 0. Assuming that (4.22) and (4.23) apply invariably is called "upwind differencing". If on the other hand, Pe is very small, (4.19) and (4.20) revert to

$$\phi_w = \frac{\phi_P + \phi_W}{2}, \tag{4.24}$$

and

$$\left(\frac{d\phi}{dx}\right)_w = \frac{(\phi_P - \phi_W)}{\delta x}. \tag{4.25}$$

Here, diffusion dominates and conditions at the west boundary depend on ϕ_P and ϕ_W in equal measure; this is known as "central differencing".

Spalding (1972) proposed the use of (4.19) and (4.20) as a "hybrid" scheme. Upwind differencing alone leads to numerically stable solutions but causes errors in the results known as "false diffusion". Central differencing alone gives implausible results at high Peclet numbers and can lead to numerical instability (see Patankar (1982)).

The above one-dimensional analysis is equally applicable when ϕ is taken to be u or v, in which case $G_x \delta x/\Gamma_\phi$ = Re, the grid Reynolds number. It is not quite as easy to formulate an analogous one-dimensional problem, however. In the following development, the combined convection and diffusion terms will continue to be written in terms of the grid Pe (which is appropriate when ϕ = t). It is to be understood that Re should be substituted for Pe if ϕ = u or v.

Using (4.19) and (4.20), (4.17) in terms of ϕ_P and ϕ_W may be written down:

$$(G_x\phi - \Gamma_\phi \frac{\partial \phi}{\partial x})_w = G_w[f_w\phi_W + (1 - f_w)\phi_P], \tag{4.26}$$

where

$$f_w = \frac{e^{Pe_w}}{e^{Pe_w} - 1}, \tag{4.27}$$

where the subscript w on Pe and G is now introduced to distinguish it from the Pe's and G's which must be calculated at the other boundaries n, s, and e. (Since it is obvious that the mass flux entering through the west boundary must be x-direction, the subscript x has been dropped.) To economise on the use of computer time, it is better to approximate f_w as follows:

$$f_w = 1 \text{ for } Pe_w > 2,$$

$$f_w = \frac{1}{2}(\frac{2}{Pe_w} + 1) \text{ for } -2 \leq Pe_w \leq 2, \tag{4.28}$$

$$f_w = 0 \text{ for } Pe_w < -2.$$

This avoids the frequent computation of exponentials. The corresponding expressions for the remaining boundaries are obtained in a similar manner and are

$$(G_x\phi - \Gamma_\phi \frac{\partial \phi}{\partial x})_e = G_e(\phi_P(1 + f_e) - \phi_E f_e), \tag{4.29}$$

$$(G_y\phi - \Gamma_\phi \frac{\partial \phi}{\partial y})_n = G_n(\phi_P(1 - f_n) - \phi_N f_n), \tag{4.30}$$

$$(G_y\phi - \Gamma_\phi \frac{\partial \phi}{\partial y})_s = G_s(f_s\phi_S + (1 - f_s)\phi_P), \tag{4.31}$$

where f_e, f_n, f_s are approximated in a similar manner as:

$$\begin{aligned} f_e &= 0 \text{ for } Pe_e > 2, \\ f_e &= \frac{1}{2}(\frac{2}{Pe_e} - 1) \text{ for } -2 \leq Pe_e \leq 2, \\ f_e &= -1 \text{ for } Pe_e < -2, \end{aligned} \tag{4.32}$$

$$\begin{aligned} f_n &= 0 \text{ for } Pe_n > 2, \\ f_n &= \frac{1}{2}(\frac{2}{Pe_n} - 1) \text{ for } -2 \leq Pe_n \leq 2, \\ f_n &= -1 \text{ for } Pe_n < -2, \end{aligned} \tag{4.33}$$

$$f_s = 1 \text{ for } Pe_s > 2,$$

$$f_s = \frac{1}{2}\left(\frac{2}{Pe_s} + 1\right) \text{ for } -2 \leq Pe_s \leq 2, \tag{4.34}$$

$$f_s = 0 \text{ for } Pe_s < -2.$$

Assembly of all components of (4.13) requires a more general expression for the integrated source term:

$$\int_s^n \int_w^e S_\phi dxdy = B\phi_p + C. \tag{4.35}$$

When the simplified source expressions (4.8) - (4.10) are used, B in (4.35) is zero and we have

$$C = (p_w - p_e)\delta y \text{ for } \phi = u, \tag{4.36}$$

$$C = (p_s - p_n)\delta x \text{ for } \phi = v, \tag{4.37}$$

and

$$C = 0 \text{ for } \phi = t. \tag{4.38}$$

The control volume equations may be written down more compactly using the following definitions for the combined convection and diffusion coefficients:

$$A_N = G_n \delta x f_n$$

$$A_S = G_s \delta x f_s$$

$$A_E = G_e \delta y f_e \tag{4.39}$$

$$A_W = G_w \delta y f_w$$

$$A_P = \sum_C A_C \phi_C = A_N + A_S + A_E + A_W$$

where $\sum_C$ indicates a summation over the cluster of nodes N, S, E, W. Insertion of identities (4.26) - (4.38) in (4.13) finally yields:

$$(A_P - B)\phi_P - \sum_C A_C \phi_C = C. \tag{4.40}$$

Equation (4.40) must be written at each node where the value of ϕ_P is required; doing so will generate an NxN matrix of simultaneous equations where N is the number of nodes in the solution domain. The line by line iterative method of matrix inversion used in TEACH-L will be discussed in the next section.

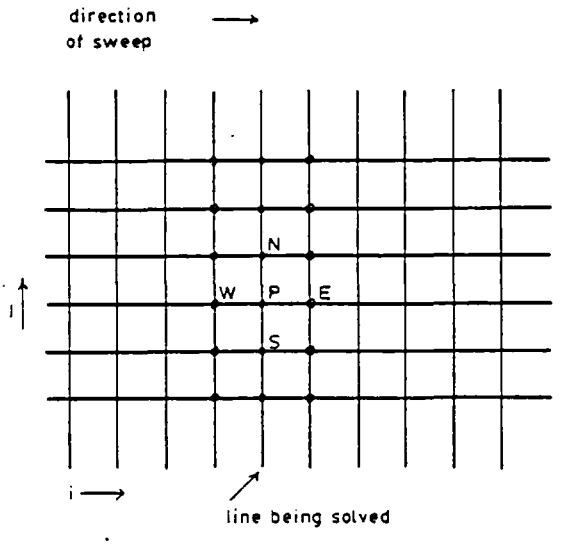


Fig. 4.3 Line by Line Iteration

4.4 Solution of Control Volume Equations Equation (4.40) as it stands will give rise to a sparsely banded matrix. A typical node P, as shown in Fig. 4.3, will have four neighbours and hence its row of the matrix will contain five entries. If however, the grid is solved line by line (LBL), taking ϕ_W and ϕ_E to be temporarily known, (4.40) becomes, for a given line i (see Fig. 4.3)

$$A_P'\phi_P - A_N\phi_N - A_S\phi_S = C', \tag{4.41}$$

where

$$A_P' = A_P - B, \tag{4.42}$$

and

$$C' = C + A_W\phi_W + A_E\phi_E, \tag{4.43}$$

which will generate a tri-diagonal matrix:

$$\begin{aligned}
&- \beta_2\phi_1 + D_2\phi_2 - \alpha_2\phi_3 && = C_2' \\
&- \beta_3\phi_2 + D_3\phi_3 - \alpha_3\phi_4 && = C_3' \\
&\qquad\vdots && \qquad\vdots \\
&- \beta_j\phi_{j-1} + D_j\phi_j - \alpha_j\phi_{j+1} && = C_j' \\
&\qquad\vdots && \qquad\vdots \\
&- \beta_{n-1}\phi_{n-2} + D_{n-1}\phi_{n-1} - \alpha_{n-1}\phi_n && = C_{n-1}',
\end{aligned} \tag{4.44}$$

where

$$D_j = A_{P,j}',$$

$$\alpha_j = A_{N,j}, \tag{4.45}$$

$$\beta_j = A_{S,j},$$

and it is assumed that ϕ_1 and ϕ_n are known. Matrix (4.44) may be easily solved from the following recurrence relations:

$$\alpha'_j = \frac{\alpha_j}{D_j - \beta_j \alpha'_{j-1}}, \quad j = 2, n-1, \ \alpha'_1 = 0, \tag{4.46}$$

$$C''_j = \frac{C'_j + \beta_j C''_{j-1}}{D_j - \beta_j \alpha'_{j-1}}, \quad j = 2, n-1, \ C''_1 = \phi_1, \tag{4.47}$$

$$\phi_j = \alpha'_j \phi_{j+1} + C''_j, \quad j = n-1, 2, \tag{4.48}$$

which can be easily translated into FORTRAN. The procedure is then to sweep repeatedly through the solution domain line by line, as indicated in Fig. 4.3.

All of the above assumes that the source term C is known. This presents no problem in the energy equation where C is zero, however in the momentum equations, C contains the pressures at the boundaries of the control volume, which must themselves be solved for. A separate equation is needed, but none exist which yield the pressures explicitly. The appropriate procedure for overcoming this difficulty is described next.

4.5 The SIMPLE Algorithm Patankar and Spalding (1971) proposed the Semi Implicit Method for Pressure Linked Equations which makes use of

the continuity equation to obtain the pressure field iteratively. The procedure is to begin with a "guessed" pressure field, solving the momentum equations for u and v. These velocities may not satisfy the continuity equation, which is then applied to each node to determine the "correction" which needs to be made to the "guessed" pressure field. The final result, after repeated iteration, yields values of u,v and p which satisfy <u>both</u> the momentum and continuity equations.

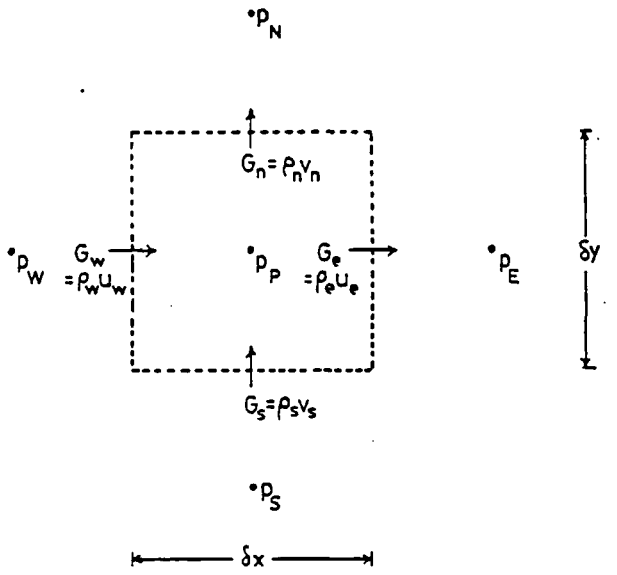


Fig. 4.4 Control Volume for Continuity Equation

As mentioned earlier, the continuity equation emerges from (4.7) if ϕ is set to unity:

$$\frac{\partial}{\partial x}(G_x) + \frac{\partial}{\partial y}(G_y) - S_M = 0, \qquad (4.49)$$

where S_M is the "mass source". In most applications real mass sources and sinks will not be present, but the term will be retained for later convenience (see Chapter 5). When (4.49) is integrated over the control

volume of Fig. 4.4, we obtain

$$(G_e - G_w)\delta y + (G_n - G_s)\delta x = \int_s^n \int_w^s S_M \, dxdy. \tag{4.50}$$

We now divide the G's into two components:

$$\begin{aligned} G_e &= G_e^* + G_e' , \\ G_w &= G_w^* + G_w' , \\ G_n &= G_n^* + G_n' , \\ G_s &= G_s^* + G_s' , \end{aligned} \tag{4.51}$$

where the G^*'s are obtained from solving the momentum equations with a guessed pressure field. (They do not, however, satisfy continuity (4.50).) The G''s are corrections which, when added to the G^*'s yield G's which do satisfy continuity). Substitution of (4.51) in (4.50) gives, after rearrangement:

$$(G_e' - G_w')\delta y + (G_n' - G_s')\delta x = \int_s^n \int_w^e S_M \, dxdy - S_{MP} \tag{4.52}$$

where

$$S_{MP} = (G_e^* - G_w^*)\delta y + (G_n^* - G_s^*)\delta x. \tag{4.53}$$

The pressure p is divided into two similar components

$$p = p^* + p', \tag{4.54}$$

where p^* is the guessed pressure (giving rise to the G^*'s), and p' is the pressure correction. For example, writing the control volume equation (4.40) for u_w at the west boundary of the control volume of Fig. 4.4, the guessed values of p_W^* and p_P^* have resulted in a value of u_w^* ($G_w^* = \varrho_w u_w^*$):

$$(A_P - B)u_w^* - \sum_C A_C u_C^* = \delta y(p_W^* - p_P^*). \tag{4.55}$$

Solving for u_w^* and taking differentials of both sides

$$du_w^* = \frac{\delta y}{(A_P - B)} d(p_W^* - p_P^*), \tag{4.56}$$

where any effect of a small pressure change on $\sum_C A_C u_C^*$ has been ignored. We may therefore write approximately

$$u_w' \approx \frac{\delta y}{(A_P - B)} (p_W' - p_P'), \tag{4.57}$$

and in terms of G_w'

$$G_w' \approx \varrho_w D_w (p_W' - p_P'), \tag{4.58}$$

where

$$D_w = \frac{\delta y}{(A_P - B)_w}. \tag{4.60}$$

where the subscript w on $(A_P - B)$ indicates that the bracketed

coefficients are for the u node located on the west boundary of the control volume surrounding p_P. Similar expressions for the other boundaries are:

$$\begin{aligned} G'_e &\approx \varrho_e D_e (p'_P - p'_E), \\ G'_s &\approx \varrho_s D_s (p'_S - p'_P), \\ G'_n &\approx \varrho_n D_n (p'_P - p'_N), \end{aligned} \tag{4.61}$$

where

$$\begin{aligned} D_e &= \frac{\delta y}{(A_P - B)_e}, \\ D_s &= \frac{\delta x}{(A_P - B)_s}, \\ D_n &= \frac{\delta x}{(A_P - B)_n}, \end{aligned} \tag{4.62}$$

where $(A_P - B)_n$ and $(A_P - B)_s$ are the coefficients for the $\underline{v}$ nodes located on the north and south boundaries, respectively. Substituting (4.57) - (4.62) into (4.52) yields

$$(A_P - B)p'_P - \sum_C A_C p'_C = C - S_{MP} \tag{4.63}$$

where

$$\int_s^n \int_w^e S_M \, dxdy = Bp'_P + C, \tag{4.64}$$

and

$$A_N = \varrho_n D_n \delta x, \text{ etc.} \tag{4.65}$$

Equation (4.63) is of the same form as (4.40) and may therefore also be solved by the LBL procedure. Once the p' field has been obtained, the corrections to the u and v fields may be obtained from, e.g. (4.57). The complete solution procedure may now be summarised:

1.) Initial values of all variables (u,v,p,t) are specified.

2.) Coefficients for u and v are assembled and the equations are solved.

3.) The pressure correction field is obtained, and the u, v and p fields are adjusted.

4.) Coefficients for t are assembled and the equations are solved.

5.) Convergence is checked, and, if not obtained, the procedure is repeated from 2.) using the new fields.

4.6 Convergence, Underrelaxation and False Sources The criterion for a converged solution is that equation (4.40) for u, v, and t and equation (4.49) for mass be simultaneously satisfied at every node within a specified error. The procedure is to sum the absolute values of the residuals R_ϕ at each node over the domain and require that this sum be less than a given percentage of some reference value. For u, v, t:

$$R_\phi = C + \sum_c A_c \phi_c - (A_p - B)\phi_p \tag{4.66}$$

for mass,

$$R_\phi = S_{MP} \quad \text{(see equation (4.53))}. \tag{4.67}$$

A suitable reference value must be chosen for each variable, and usually is, e.g., for $\phi = u$, the total flow of x-direction momentum into the solution domain.

Since equation (4.40) is non-linear (the A's contain u's and v's from the previous iteration), divergence might occur if there is too large a change in the ϕ's from one iteration to the next. In most cases this can be avoided by modifying (4.40) as follows:

$$\frac{(A_P - B)}{f_\phi}\phi_P^r - \sum_C A_C \phi_C = C + \frac{(1 - f_\phi)}{f_\phi}(A_P - B)\phi_P^{old}, \tag{4.68}$$

where f_ϕ is the underrelaxation factor for ϕ, ϕ_P^r is the new value of ϕ_P with relaxation, and ϕ_P^{old} is the value of ϕ_P from the previous iteration. Subtracting (4.40) from (4.68) yields

$$\phi_P^r = f_\phi \phi_P^{wr} + (1 - f_\phi)\phi_P^{old}, \tag{4.69}$$

where ϕ_P^{wr} is the new value of ϕ_P which would have been obtained without relaxation. Common values for f_u and f_v are 0.5, f_t and f_p, are usually 1.0 (no relaxation).

It may occur in the early stages of the iteration process that a particular node has a net outflow of mass from its control volume. If this outflow takes the form shown in Fig. 4.5, and

$$Pe_w,\ Pe_s < -2,\ Pe_e,\ Pe_n > 2 \tag{4.70}$$

then

$$f_e = f_w = f_s = f_n = 0, \text{ see (4.28) - (4.34)}, \tag{4.71}$$

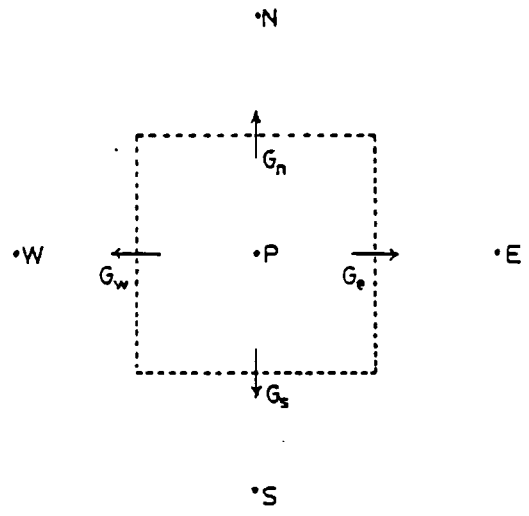


Fig. 4.5 Singularity Condition

rendering A_p zero at that node. If B is also zero, then a singularity will result in the matrix equations, in which an attempt would be made to divide by zero, see (4.46) - (4.47). This difficulty may be overcome by the "trick" of using a false source

$$S_f = B_f \phi_p + C_f, \tag{4.72}$$

where

$$B_f = -S_{MP} \text{ (see (4.53))}, \tag{4.73}$$

and

$$C_f = S_{MP}\phi_P^{old}, \tag{4.74}$$

modifying (4.40) to yield

$$(A_P - B - B_f)\phi_P - \sum_C A_C\phi_C = C + C_f. \tag{4.75}$$

If there is a net outflow, S_{MP} will be positive, hence the coefficient of ϕ_P will be non-zero even if $(A_P - B)$ is zero. This device will not affect the converged solution since B_f and C_f will tend to zero as convergence is approached.

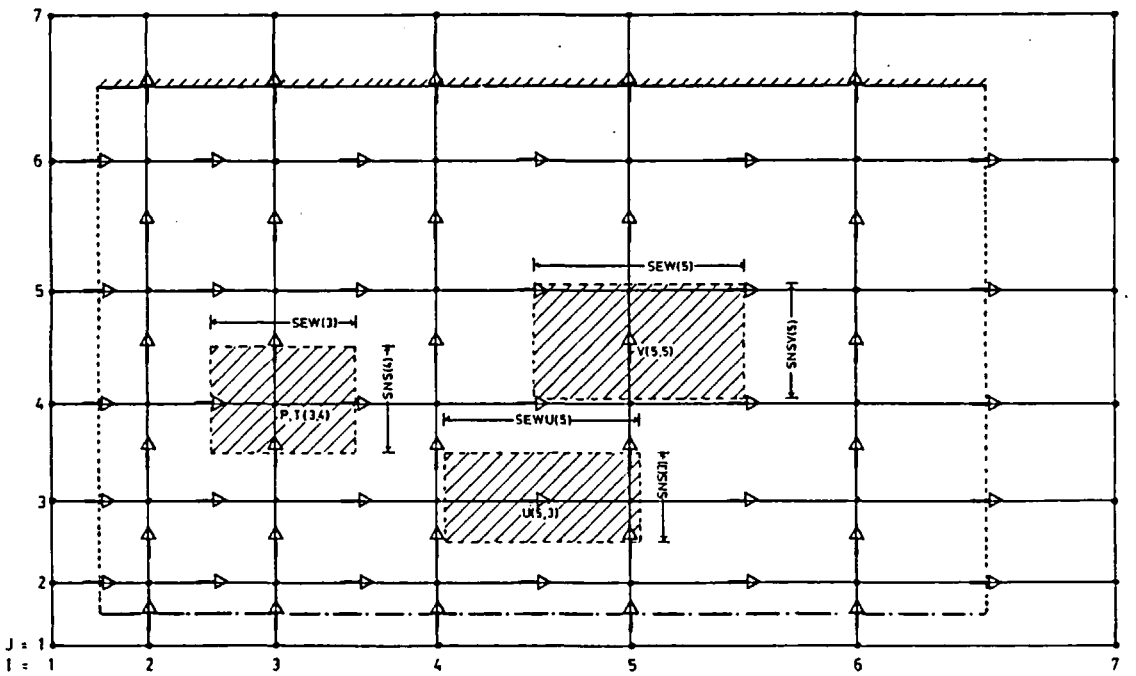


Fig. 4.6 Staggered Grid

4.7 Staggered Grid and Variable Spacing TEACH-L has provision for variable spacing between grid lines. This feature is useful as it is frequently necessary to refine the grid in flow areas where steep

gradients of ϕ exist, e.g. near corners. A typical 7x7 grid is shown in Fig. 4.6. The grid boundaries enclose the solution domain, which in the figure comprises an upper wall, a line of symmetry at the bottom, and an entrance and exit section at the left and right. The system might represent the upper half of a horizontal duct. The thermodynamic variables p, t and all fluid properties are stored at the intersection points of the grid lines, while the u and v velocities (represented by the arrows) are stored on the grid lines between the points.

In FORTRAN, p or t stored at I = 3, J = 4 (see Fig. 4.6) becomes P or T(3,4), whereas u and v derive their indices from the grid point in front of the tip of the velocity arrow. U(5,3) and V(5,5) are identified in Fig. 4.6 for illustration. The shaded areas surrounding these three variables are their respective control volumes. Note that, because of the combined effect of variable grid spacing and staggered variable locations, the dimensions of the control volumes must be carefully determined. The east-west dimension of the control volume for a P or T cell is computed in the same manner as for a V cell; compare, e.g. SEW(3) for T(3,4) and SEW(5) for V(5,5). That is because P's and T's with the same I index as V's are both located on a common 'longitudinal' grid line. The same applies to the north-south dimension of P or T cells and U cells. Here, P's, T's or U's with the same J index are on a common 'latitudinal' grid line. Compare, e.g., SNS(4) for T(3,4) in the figure with SNS(3) for U(5,3). The east-west dimension of the control volume for U, SEWU and the north-south dimension of the control volume for V, SNSV, however, do not correspond to SEW and SNS for P or T. SEWU(5) and SNSV(5) in the figure are shown for illustration. The general rule is that the boundary of a control volume for a given variable ϕ_P is located half-way between, e.g. ϕ_P and ϕ_W. In TEACH-L, an entire subroutine,

INIT, is devoted to the computation of all these dimensions, and full details may be found in the listings in Appendix D3.

This staggering of the variable locations is convenient in calculating the coefficients for the control volume equations. The fluid velocities needed for e.g. P or T(3,4) are conveniently stored at the boundaries of their control volume. The pressures required for the source terms for e.g., U(5,3) and V(5,5), are stored at their respective control volume boundaries. Note that the boundaries of the solution domain coincide with the location of the normal velocities.

The penalty for these conveniences is a more complicated geometry. The dimensions of each control volume (e.g. SEW(3) X SNS(4)) must be individually calculated and stored.

4.8 Conclusion The physical and mathematical basis of TEACH-L has been presented. The program uses primitive variables, control volume equations with hybrid differencing to represent fluxes at the boundaries, and the SIMPLE algorithm to obtain the pressure field. Listings with further documentation will be found in Appendices D2 and D3.

Implementation of the boundary conditions has not been discussed -- this is best done in Chapters 5, 6 and 7 as each flow situation is described.

CHAPTER 5

TEE-JUNCTION FLOWS

5.1 Introduction Dividing and combining tee-junction flows commonly occur on the "sucking" and "blowing" sides of manifolds, of which the transformer pass shown in Fig. 2.3 is one example. The latter is in fact atypical of most industrial manifolds which operate at high Reynolds numbers (e.g. distributing pipes in water-filtering systems, see Keller (1949)), in which the flow is usually turbulent. Thus much of the literature on manifold and tee-junction flows (Favre (1937), McKnown and Hsu (1950), Acrivos, Babcock and Pigford (1959), to name a few) is not applicable to the present work. An experimental study by Jamison and Villemonte (1971), though partly conducted at low Reynolds numbers, measured losses in a three-dimensional system consisting of short radius galvanized screwed tees connecting sections of 3/4 inch black iron pipe. Their measured losses, although used by Oliver (1980) in his network model of a transformer pass are nonetheless very much higher than those predicted in a two-dimensional system and are entirely unsuitable for the present work, as will be shown.

The earliest work which appears to have been published on two-dimensional laminar tee-junctions was that of Blest (1972). He used perturbation methods to study the situation (applicable to arterial blood flow) in a dividing junction when the branching flow is slight and through a smaller side vessel. Blowers (1972), later in the same year used the stream function-vorticity formulation of the Navier-Stokes equations to analyse numerically combining flows at Reynolds numbers of 180 and 900. He used an "upwind" finite difference scheme, concentrating

most of his investigation on the effects of varied meshes on numerical stability and the location of recirculation zones. No pressure data was reported.

Further computer investigations were carried out in the late 1970's in the Mechanical Engineering Department at Imperial College, using programs very similar to TEACH-L. Vlachos's (1978) work dealt with dividing junctions over a Reynolds number range of 496 - 1130. The application of his work was to the human recirculatory system. As blood is a non-Newtonian fluid, a power viscosity law had to be incorporated into the computer code. Companion measurements of velocity profiles using laser-doppler anemometry (LDA) were carried out and the agreement was found to be good. Some pressure loss data was reported, but the values of Re used were too high for the data to be useful to the present study. Pollard and Spalding (1980) investigated three-dimensional combining flow in a square cross-sectioned tee-junction, obtaining reasonable agreement with LDA measurements by Simitovic (1977). Reynolds number ranges were not cited, although the flow was stated to be laminar. No pressure data was given.

In general, the pressure loss (or regain) through a two-dimensional combining or dividing tee-junction, in the absence of heat transfer, appears to be influenced by three independent parameters: $r_{h,vert}/r_{h,horiz}$, Q_{in}/Q_2 and Re (see Fig. 5.1). The "friction constants" (to be defined shortly) along the indicated paths, labelled, e.g., $K_{cs} = K_{combining,straight}$ and $K_{dt} = K_{dividing,turning}$, are therefore functions of three variables. In a disc-type winding appropriate values of the first parameter will depend on design practice; $r_{h,vert}$ is generally greater than or equal to $r_{h,horiz}$. Four values of $r_{h,vert}/r_{h,horiz}$ were

selected: 0.5, 1.0, 2.0 and 3.0. The second parameter will depend on the number of discs in the pass. As was seen in Chapter 3, passes of large numbers of ducts will result in extreme maldistribution of flow and hence large values of Q_{in}/Q_2 (> 100). As most of the experimental work in this thesis is based on an 8 duct pass, values of Q_{in}/Q_2 were taken to be 1.5, 2.14, 4.0, 6.0, 8.0, and 10.0. The third parameter Re will be largely dependent on the flow rate into the pass; appropriate values were selected as 9.4, 17.6, 52.0 93.6, and 176. Varying each parameter independently requires 4x6x5 = 120 runs for each type of junction, for a total of 240. The results of these extensive calculations will be presented in this chapter.

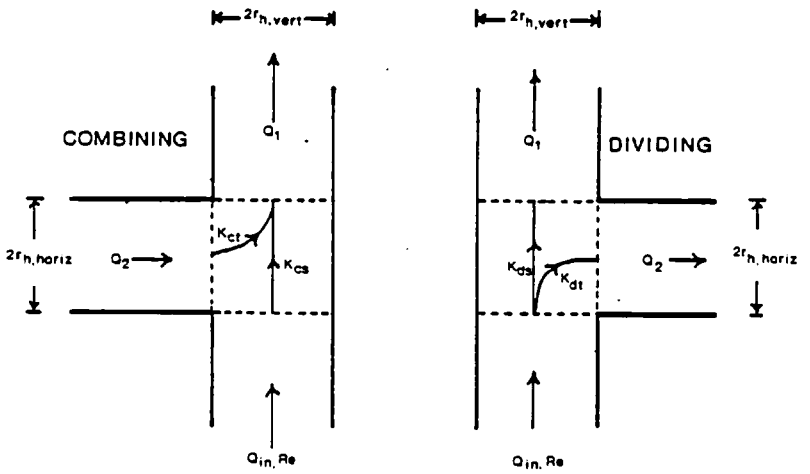


Fig. 5.1 Two-Dimensional Tee-Junction

First, the flow domain and the implementation of the boundary conditions will be described. Comparison of micro and mainframe computing speeds will be made. Sample graphical output will then be presented together with the results of mesh dependency tests. Finally, the friction constants will defined, and the results of the parametric study will be discussed.

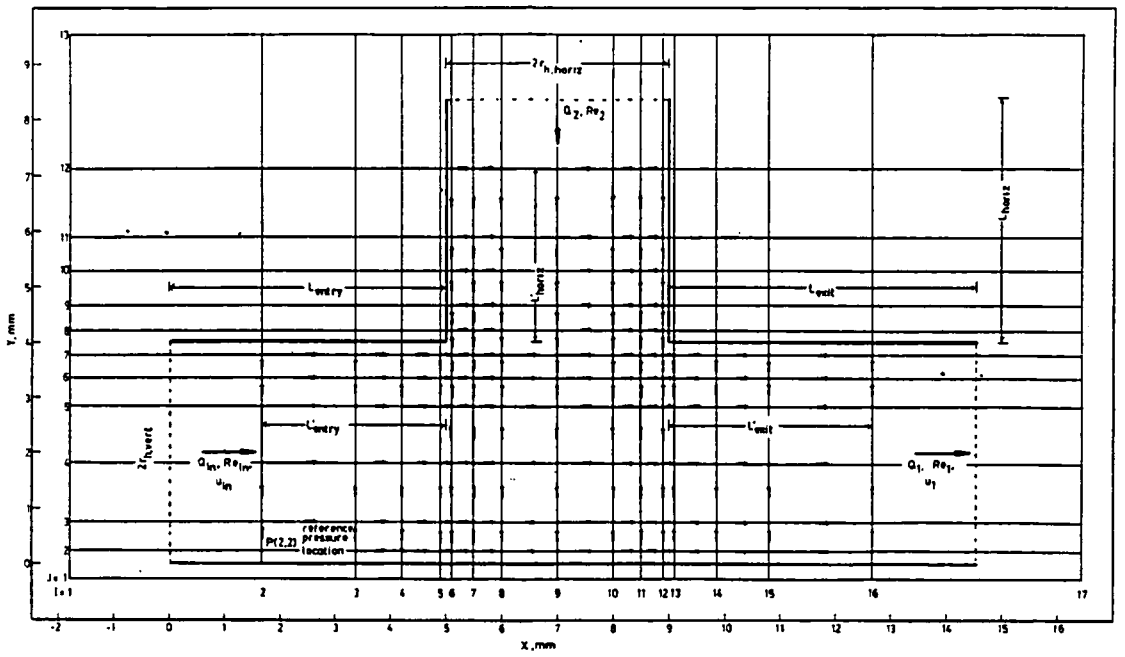


Fig. 5.2 Tee-Junction Flow Domain

5.2 Flow Domain and Boundary Conditions A sample flow domain from one of the 240 combinations is shown with overlaid grid as Fig. 5.2. It is a combining junction, in which Re_{in} = 9.4, Q_{in}/Q_2 = 2.14 and $r_{h,vert}/r_{h,horiz}$ = 1.0. For convenience, the junction has been laid on its side, hence u and v are the vertical and horizontal duct axial velocities, respectively. Parabolic profiles are assumed at all entrances/exits. L_{entry}, L_{horiz} and L_{exit} are adjusted (using (2.4)) according to Re_{in}, Re_2 and Re_1 (see Fig. 5.2) to make this boundary condition reasonable. Within and on the solid portions of the domain, the u and v velocities and pressure corrections p' are set to zero. This is easily done by setting the source coefficients B and C in (4.40), as follows:

$$B = -\gamma, \quad C = 0 \qquad (5.1)$$

where γ is a very large number (10^{30}). This will result in

$$\phi_p = 0. \tag{5.2}$$

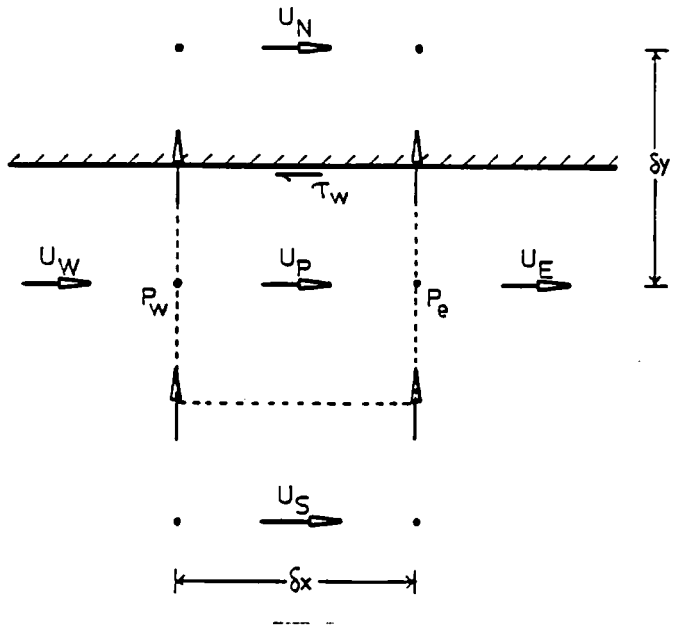


Fig. 5.3 No-Slip Boundary Condition

The "no-slip" condition is used for the u velocities on the vertical duct walls and v velocities on the horizontal duct walls. A control volume for a u cell at the wall is shown in Fig. 5.3, where it is seen that there is no convection of x-direction momentum through the north boundary since the v velocities stored at the upper left and right hand corners are zero. Also u_N is zero from (5.1) and (5.2). The procedure for incorporating the wall shear stress τ_w is first to set A_N to zero. Then, provided that u_p is close enough to the wall, τ_w may be approximated as

$$\tau_w = \mu \frac{u_p}{\delta y/2}, \tag{5.3}$$

and the total momentum source is

$$Bu_P + C = (-\mu \frac{u_P}{\delta y/2})\delta x + (p_w - p_e)\delta y, \qquad (5.4)$$

whence

$$B = -\mu \frac{\delta x}{\delta y/2}, \qquad (5.5)$$

and

$$C = (p_w - p_e)\delta y, \qquad (5.6)$$

as before (see (4.35) and (4.36)).

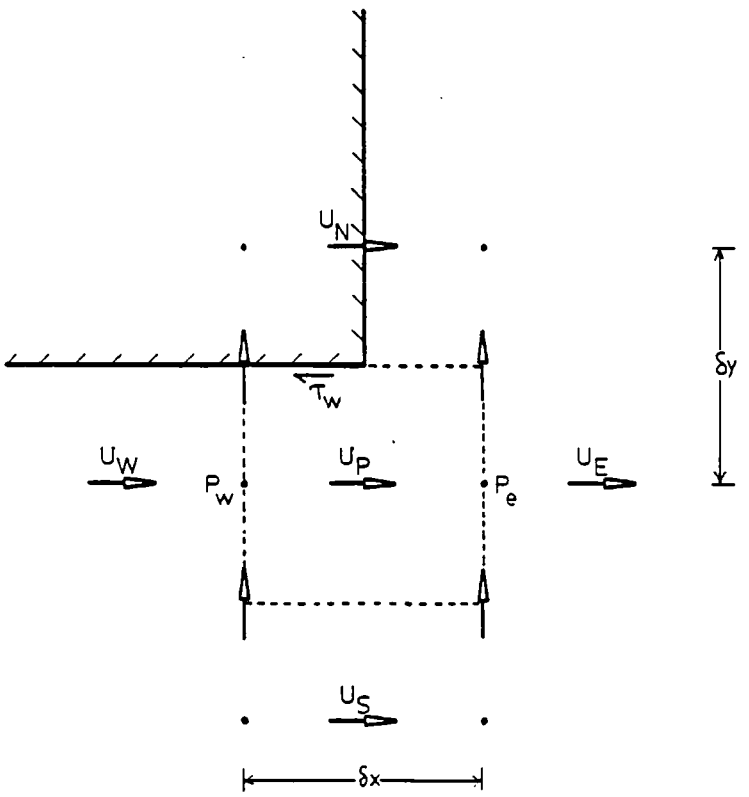


Fig. 5.4 Treatment of Corners

The corners require slightly different treatment, as is evident

from Fig. 5.4. Here, convection proceeds through the right half of the north boundary of the u_p cell, while shear stress τ_w acts only on the left half. The solution is to set A_N to one-half of its current value, while reducing 8 to one-half of the expression given in (5.5).

Though heat transfer will take place in the junctions in a transformer pass, and will thus have some influence on the pressure drop (through variable viscosity), the effect, expected to be slight, is ignored here, and the calculation is isothermal. The implementation of the various boundary conditions in FORTRAN is incorporated together with TEACH-L into a program called JUNCTION. Listings may be found in Appendix D4.

5.3 Micro vs. Mainframe Computing Faced with prospect of 240 computer runs in addition to debugging and mesh dependency tests as only one part of the total computational requirements of the project, alternatives to expensive mainframe computer use were explored. Companion runs were carried out on the CDC Cyber 174 mainframe computer, the DEC LSI 11/23 16 bit microcomputer, and the Research Machines RML 380Z 8 bit microcomputer. The test case used was a dividing junction, Re_{in} = 9.4, Q_{in}/Q_2 = 2.14 and $r_{h,vert}/r_{h,horiz}$ = 1.0. A 17x13 grid was used (see Fig. 5.2), and 39 iterations were required to reduce the absolute sum of all residuals to 1% of their reference values. The RML 380Z required 43 minutes, the LSI 11/23 14 minutes and the Cyber 174 1.48 minutes, giving a time ratio of 29:9.5:1. In spite of their slowness, it was far more convenient to use the RML's. The jobs on the mainframe had to be submitted in batch mode and generally took several hours or overnight to turn around. Submitting the jobs via a ponderous and continually evolving operating system was often frustrating and the

computer centre staff lost patiently awaited output on several occasions. Using a dedicated micro interactively was found to be far more congenial. The progress of the job could be observed and, if necessary, aborted. The output could be saved on a portable floppy disc or sent to a local printer as required. (The LSI 11/23 machines shared all of these advantages, but the RML's were used as the Microcomputer Unit at Imperial College maintains 12 for general college use and provides excellent support.)

Possible objections to the use of microcomputers for field calculations are a.) insufficient memory to handle large arrays, b.) loss of accuracy due to lower precision, c.) less sophisticated compilers, particularly for debugging purposes, d.) much slower speeds. For this particular case a 17x13 grid was found to be adequate (justification will follow in the next section), and this was easily accomodated on the RML (which has 56 Kilobytes (K) of memory available for compiled programs) requiring only about 39 K. In general, larger memory requirements can be handled using overlays. The RML, with two double-sided single-density disc drives, has about 1 Mbyte of disc storage on line. In the course of the companion runs mentioned earlier, and the mesh dependency tests discussed in the next section, no loss of accuracy was noted from mainframe (which uses 60 bits for each real variable) to micro (which uses 32 bits). If difficulties were to occur with accuracy, double precision (64 bit words) could be used. Some difficulty was encountered with the Microsoft FORTRAN-66 compiler available on the RML, especially with input format specifications. In general, the user is advised to build up a library of small program modules (subroutines) which are more easily debugged individually. (This is considered good programming practice anyway). Finally, slowness of

speed is more than compensated by the convenience of having a totally dedicated machine; this was judged preferable to sharing a mainframe which is only 30 times faster with up to 200 users simultaneously and systems operators who quite often pick an awkward moment to interrupt the service for "development work".

5.4 Sample Output and Mesh Dependency Tests Since the end result desired from the calculation was overall junction pressure loss data, the pressure fields were examined in detail. A mesh dependency test was done for a dividing junction, with $Q_{in}/Q_2 = 2.14$, $r_{h,vert}/r_{h,horiz} = 1$ and $Re = 9.4$ (Re with no subscript implies Re_{in}). The output is presented graphically as isobar plots in Fig. 5.5 - 5.8, comparing different meshes. The 10x8 and 17x13 runs were done on the RML, the 22x18 on the LSI 11/23 and the 30x25 on the CDC mainframe. Each isobar is labelled with the pressure in Pa.

In TEACH-L, an arbitrary reference pressure (chosen to be 1.00 Pa) is fixed at a specified node (P(2,2), see Fig. 5.2). As will be seen from comparison of Figs. 5.5 - 5.8, the position of P(2,2) varies as the mesh (shown as fine solid lines) is refined. This is particularly noticeable in the 30x25 plot (Fig. 5.8) and must be borne in mind whilst assessing the effects of mesh refinement on the location and value of the isobars. The 10x8 mesh is clearly inadequate as it gives exit pressures substantially higher than those of the other three meshes. The pressure ridge on the corner further from the entrance is absent, with no suggestion of an adverse gradient just around the corner nearer the entrance. These features appear clearly on the three finer meshes, the 30x25 affording somewhat more detail of the latter. Detail, however, is not needed, only reasonable estimates of the pressure differences from

the entrance(s) to the exit(s).

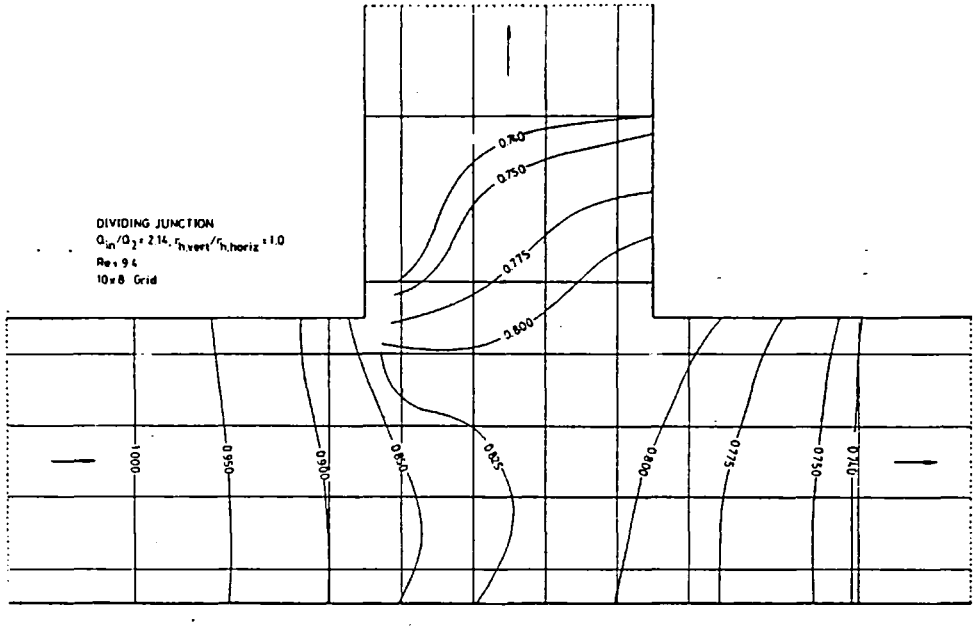


Fig. 5.5 Dividing Junction, 10x8 Grid

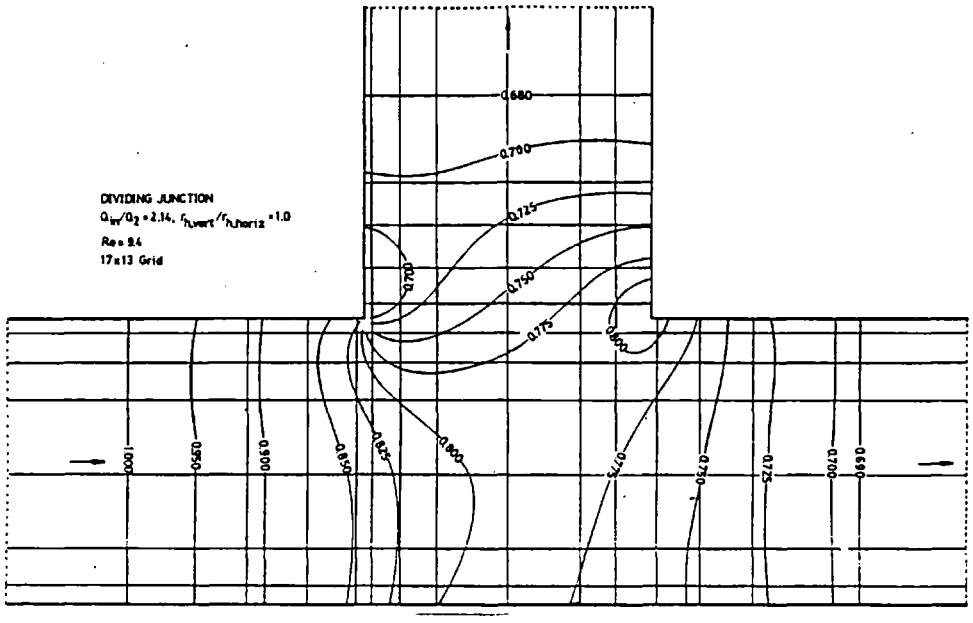


Fig. 5.6 Dividing Junction, 17x13 Grid

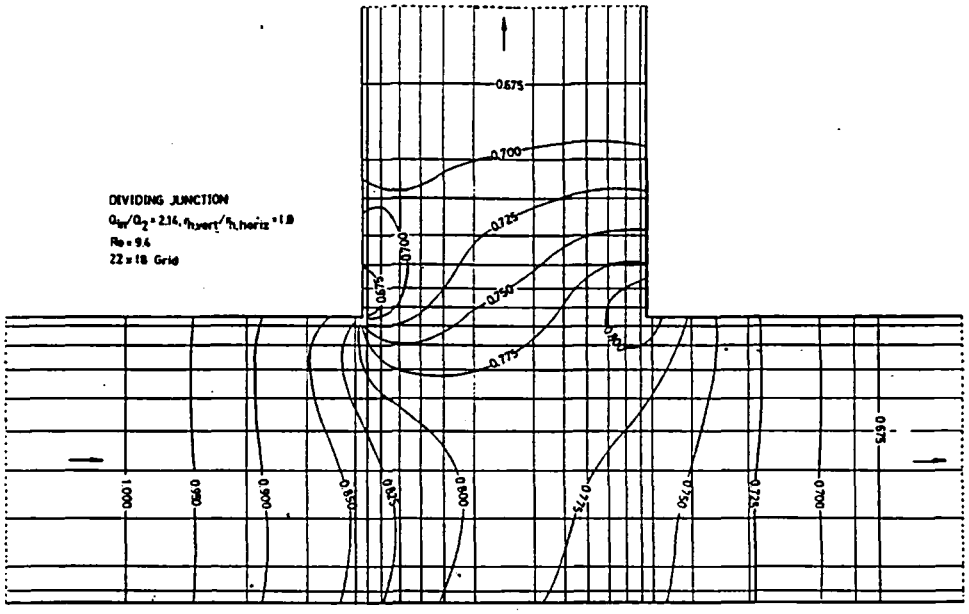


Fig. 5.7 Dividing Junction, 22x18 Grid

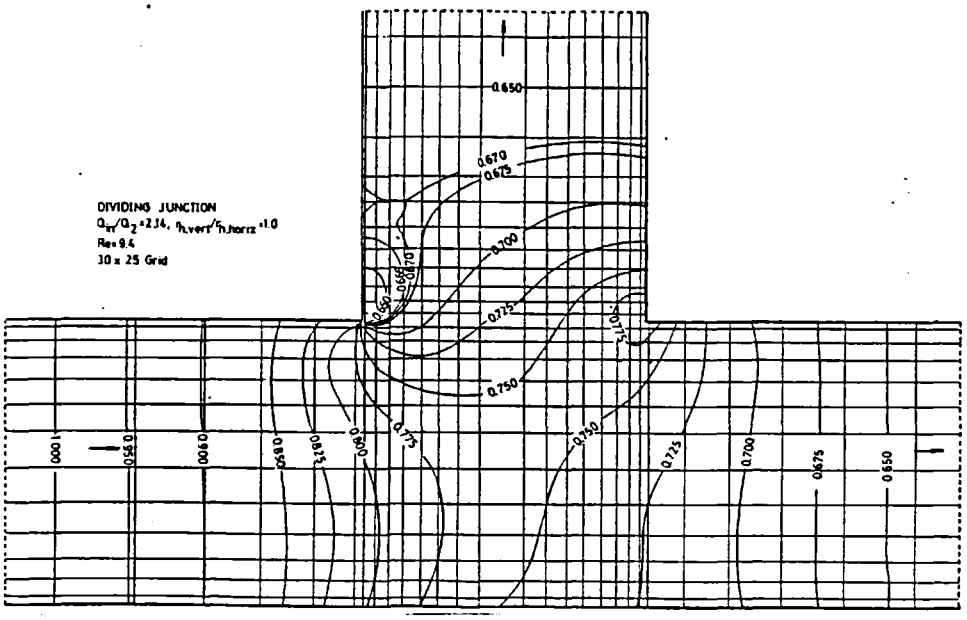


Fig. 5.8 Dividing Junction, 30x25 Grid

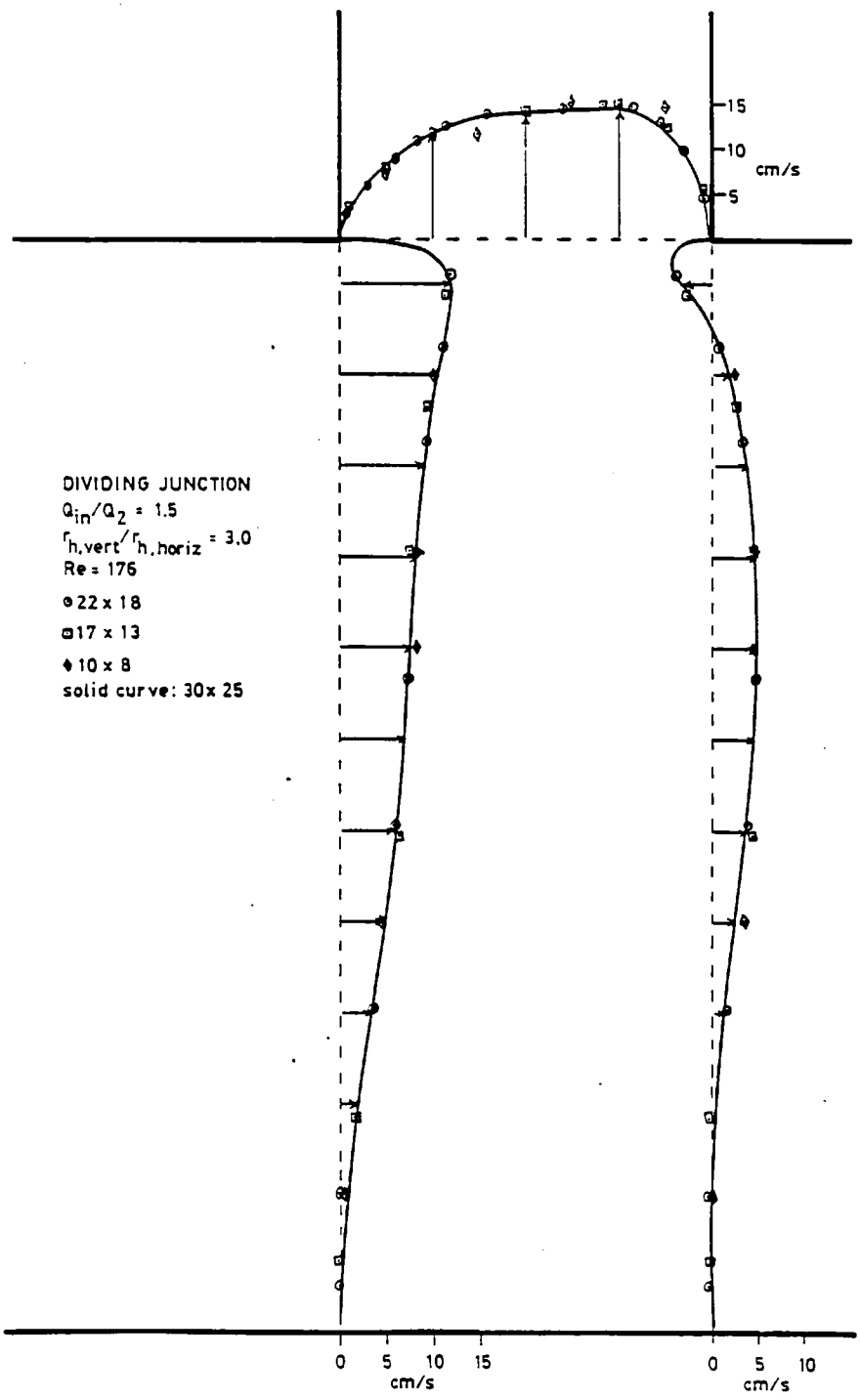


Fig. 5.9 Mesh Dependence, Dividing Junction, High Re

As the computation covered a wide range of Reynolds numbers, etc., mesh dependency tests were also done for three other representative cases. Velocity profiles on the three sides of the junction are compared

in Figs. 5.9 - 5.11. In all three cases only the 10x8 points appear to depart significantly from the solid curves drawn from the 30x25 runs. On the basis of these tests the 17x13 grid was judged adequate for providing an estimate of overall pressure drop through the combining and dividing junctions.

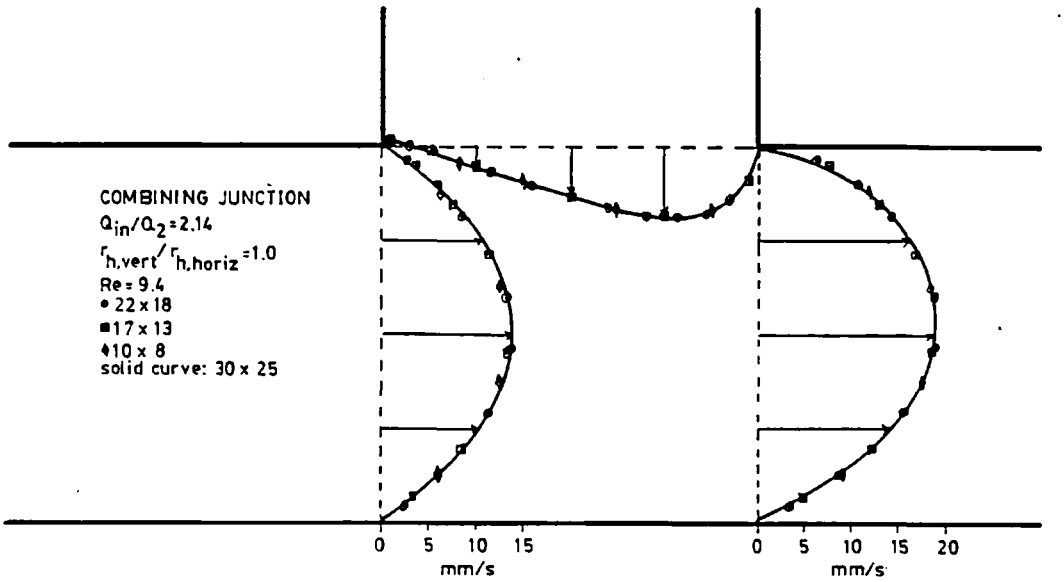


Fig. 5.10 Mesh Dependence, Combining Junction, Low Re

5.5 Friction Constants It was desired to define friction constants so that the junction and corner losses could be easily incorporated into the network model as additional resistances. This was done as follows. The inlet and outlet pressures were taken to be the average of the node pressures along lines I=2 (p_{in}), I = 16 (p_1) and J = 12 (p_2) (see Fig. 5.2). The pressure drops along lengths L'_{entry}, L'_{exit} and L'_{horiz} were then computed assuming fully developed flow:

$$\Delta p_s = \frac{1.5\mu}{r^3_{h,vert}}(Q_{in}L'_{entry} + Q_1 L'_{exit}), \qquad (5.7)$$

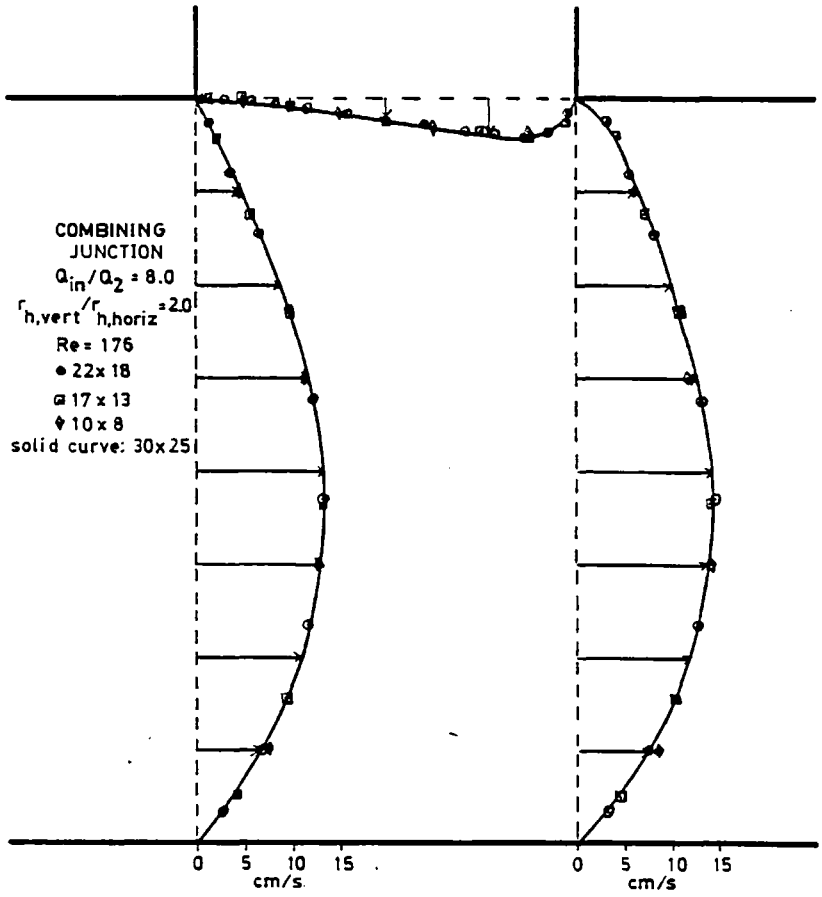


Fig. 5.11 Mesh Dependence, Combining Junction, High Re

where Δp_s is the 'straight-through' pressure drop along the portions of vertical ducts at the entry and exit of the junction. For combining flow, the fully developed flow pressure drop along the section of horizontal duct L'_{horiz} and the section of vertical duct L'_{exit} which it turns into is

$$\Delta p_{ct} = 1.5\mu\left[\frac{Q_2 L'_{horiz}}{r^3_{h,horiz}} + \frac{Q_1 L'_{exit}}{r^3_{h,vert}}\right], \qquad (5.8)$$

and for dividing flows, the analogous turning 'fully-developed' pressure

drop is

$$\Delta p_{dt} = 1.5\mu \left[\frac{Q_{in} L'_{entry}}{r^3_{h,vert}} + \frac{Q_2 L'_{horiz}}{r^3_{h,horiz}} \right]. \qquad (5.9)$$

Δp_s, Δp_{ct} and Δp_{dt} would already have appeared in the simple network; the <u>differences</u>, though between these pressure drops and what is computed by TEACH-L as $p_{in} - p_1$, etc. are the "excess" pressure drops, namely

$$\Delta \hat{p}_{cs} = (p_{in} - p_1)_{cs} - \Delta p_s, \qquad (5.10)$$

$$\Delta \hat{p}_{ct} = (p_2 - p_1)_{ct} - \Delta p_{ct}, \qquad (5.11)$$

for combining flows, and

$$\Delta \hat{p}_{ds} = (p_{in} - p_1)_{ds} - \Delta p_s, \qquad (5.12)$$

$$\Delta \hat{p}_{dt} = (p_{in} - p_2)_{dt} - \Delta p_{dt}, \qquad (5.13)$$

for dividing flows. These excess pressure drops contain 1.) the drops through the junctions themselves and 2.) the drops in the entrance and exit sections due to momentum redistribution (settling, etc.). It is convenient to normalise them following the concept of an "apparent" friction factor (3.18), and to further assume that this will take the form of equation (3.17). The only uncertainty is the assignment of a suitable length x in equation (3.18). It was decided arbitrarily to set $x = 2r_{h,vert}$ since this is of the same order as the distance though the junction itself. Doing so leads to the following definitions of the

"friction" constants:

$$K_{cs} = \frac{8\Delta\hat{p}_{cs} r_{h,vert}^2}{\mu Q_1}, \qquad (5.15)$$

$$K_{ct} = \frac{8\Delta\hat{p}_{ct} r_{h,vert}^2}{\mu Q_1}, \qquad (5.15)$$

$$K_{ds} = \frac{8\Delta\hat{p}_{ds} r_{h,vert}^2}{\mu Q_{in}}, \qquad (5.16)$$

$$K_{dt} = \frac{8\Delta\hat{p}_{dt} r_{h,vert}^2}{\mu Q_{in}}, \qquad (5.17)$$

where it may be noted that the excess pressure drops for combining junctions are normalised with respect to the fluid dynamic pressure at the exit ($\varrho u_1^2/2$); for dividing junctions, ($\varrho u_{in}^2/2$) is used (see (3.18)). u_1 and u_{in} are mean velocities.

Defining the friction constants in this way makes them directly comparable with the friction constant K (= 24), for fully developed flow. The only drawback is that, at high Reynolds numbers (176) the values of L'_{entry} and L'_{exit} may exceed d (see Fig. 3.1). Physically this suggests that neighbouring junctions may be interfering with each other, an effect which is entirely neglected here. Whether the values of K_{ds}, etc. obtained in such a case are reasonable is open to doubt. They are presented here nevertheless as "first estimates", in the absence of anything better.

The results of the 240 runs are given as Tables 5.1 and 5.2 and as Figs. 5.12 - 5.15. In the latter, lines of constant (e.g.) K_{cs} are

plotted as a function of $r_{h,vert}/r_{h,horiz}$ and Q_{in}/Q_2, at Re_{in} = 9.4, 52 and 176.

$\frac{r_{h,vert}}{r_{h,horiz}}$	0.5		1.0		2.0		3.0	
$\frac{Q_{in}}{Q_2}$	Re	K_{cs}/K_{ct}	Re	K_{cs}/K_{ct}	Re	K_{cs}/K_{ct}	Re	K_{cs}/K_{ct}
1.5	9.4	32.6/ 26.4	9.4	26.7/ 22.9	9.4	21.4/ 28.4	9.4	19.3/ 39.3
	17.6	42.8/ 37.4	17.6	36.3/ 32.3	17.6	32.3/ 33.9	17.6	29.5/ 43.0
	52.0	89.7/ 84.5	52.0	81.2/ 75.4	52.0	76.0/ 68.9	52.0	74.7/ 68.2
	93.6	151.9/146.5	93.6	142.9/138.1	93.6	137.9/128.1	93.6	137.4/121.2
	176	286.7/280.1	176	278.9/274.8	176	282.4/266.3	176	290.2/263.2
2.14	9.4	31.3/ 24.5	9.4	25.0/ 20.8	9.4	19.3/ 23.9	9.4	17.4/ 37.2
	17.6	39.3/ 33.5	17.6	32.5 28.3	17.6	26.9/ 29.1	17.6	25.0/ 37.2
	52.0	75.2/ 70.2	52.0	66.5/ 62.1	52.0	60.7/ 57.0	52.0	59.2/ 58.9
	93.6	121.9/116.3	93.6	111.1/108.1	93.6	105.9/102.0	93.6	105.1/ 98.6
	176	223.4/217.0	176	212.8/208.8	176	211.1/202.8	176	213.8/198.0
4.0	9.4	30.3/ 22.6	9.4	23.3/ 18.1	9.4	16.8/ 18.2	9.4	14.4/ 27.6
	17.6	35.8/ 29.5	17.6	28.0/ 23.4	17.6	21.7/ 22.6	17.6	19.4/ 27.8
	52.0	59.0/ 53.8	52.0	48.7/ 44.8	52.0	42.0/ 41.4	52.0	40.0/ 44.5
	93.6	87.7/ 82.0	93.6	76.0/ 73.3	93.6	69.3/ 51.2	93.6	67.8/ 70.8
	176	148.2/141.2	176	135.2/133.7	176	129.4/127.6	176	129.2/125.6
6.0	9.4	30.0/ 21.7	9.4	22.7/ 16.9	9.4	16.0/ 16.4	9.4	13.4/ 22.1
	17.6	34.4/ 27.8	17.6	26.2/ 21.4	17.6	19.4/ 19.4	17.6	17.0/ 24.0
	52.0	52.7/ 47.6	52.0	41.8/ 38.0	52.0	34.5/ 34.8	52.0	32.2/ 36.4
	93.6	74.2/ 68.3	93.6	61.5/ 58.4	93.6	54.2/ 53.5	93.6	51.8/ 55.6
	176	117.9/110.2	176	104.4/101.7	176	97.7/ 98.0	176	95.1/ 95.2
8.0	9.4	29.9/ 21.4	9.4	22.4/ 16.2	9.4	15.3/ 14.3	9.4	12.8/ 18.8
	17.6	33.6/ 26.9	17.6	25.2/ 20.3	17.6	18.3/ 18.3	17.6	15.7/ 18.7
	52.0	49.8/ 44.5	52.0	38.3/ 34.4	52.0	30:5/ 30.5	52.0	28.7/ 32.2
	93.6	67.0/ 61.0	93.6	53.9/ 50.4	93.6	46.4/ 46.3	93.6	43.8/ 47.4
	176	102.4/ 94.3	176	88.4/ 84.9	176	80.8/ 81.6	176	78.6/ 81.7
10.0	9.4	29.9/ 21.2	9.4	22.2/ 15.8	9.4	15.3/ 13.6	9.4	12.7/ 12.2
	17.6	33.2/ 26.4	17.6	24.8/ 19.5	17.6	17.6/ 16.0	17.6	14.6/ 18.4
	52.0	47.4/ 42.2	52.0	36.0/ 32.1	52.0	28.3/ 27.6	52.0	25.6/ 28.7
	93.6	63.3/ 57.2	93.6	49.8/ 46.4	93.6	41.6/ 40.7	93.6	39.0/ 41.6
	176	93.7/ 85.6	176	78.8/ 74.9	176	70.4/ 70.6	176	68.2/ 71.5

Table 5.1 Combining Junction Friction Constants

$\frac{r_{h,vert}}{r_{h,horiz}}$	0.5		1.0		2.0		3.0	
$\frac{Q_{in}}{Q_2}$	Re	K_{ds}/K_{dt}	Re	K_{ds}/K_{dt}	Re	K_{ds}/K_{dt}	Re	K_{ds}/K_{dt}
1.5	9.4	12.9/ 10.3	9.4	6.5/ 14.9	9.4	1.1/ 45.0	9.4	1.0/100.5
	17.6	8.1/ 7.6	17.6	.7/ 14.3	17.6	-5.4/ 54.6	17.6	-7.4/126.4
	52.0	-10.6/ 4.0	52.0	-20.2/ 20.2	52.0	-25.9/106.6	52.0	-28.2/259.1
	93.6	-31.0/ 6.2	93.6	-39.1/ 37.9	93.6	-43.7/189.9	93.6	-45.7/446.2
	176	-64.0/ 16.2	176	-70.1/ 86.2	176	-73.7/384.4	176	-76.2/861.4
2.14	9.4	17.1/ 10.0	9.4	10.1/ 11.9	9.4	3.9/ 30.2	9.4	1.2/64.9
	17.6	13.6/ 7.2	17.6	5.4/ 10.3	17.6	-1.3/ 33.8	17.6	-4.1/76.3
	52.0	-1.5/ 3.4	52.0	-13.1/ 10.5	52.0	-20.3/ 55.4	52.0	-23.0/138.5
	93.6	-20.0/ 3.9	93.6	-31.7/ 19.0	93.6	-38.1/ 94.6	93.6	-40.8/229.2
	176	-52.0/ 9.1	176	-61.8/ 42.1	176	-66.9/197.7	176	-69.7/448.8
4.0	9.4	22.4/ 9.6	9.4	14.8/ 9.4	9.4	7.9/ 17.0	9.4	5.3/ 33.7
	17.6	21.0/ 7.1	17.6	12.3/ 7.5	17.6	5.1/ 16.8	17.6	2.3/ 35.5
	52.0	13.8/ 4.1	52.0	1.2/ 5.5	52.0	-7.0/ 21.0	52.0	-10.3/ 51.1
	93.6	3.4/ 4.3	93.6	-11.5/ 7.3	93.6	-20.1/ 32.9	93.6	-23.1/ 76.8
	176	-19.4/ 7.7	176	-33.1/ 16.5	176	-41.4/ 62.9	176	-45.2/141.6
6.0	9.4	24.7/ 9.5	9.4	16.9/ 8.7	9.4	9.6/ 12.7	9.4	6.7/ 23.0
	17.6	24.3/ 7.1	17.6	15.4/ 6.8	17.6	8.0/ 12.2	17.6	4.7/ 23.4
	52.0	21.6/ 4.4	52.0	8.7/ 4.5	52.0	.2/ 12.8	52.0	-2.8/ 29.5
	93.6	15.7/ 5.1	93.6	.5/ 5.6	93.6	-8.6/ 18.4	93.6	-12.0/ 40.8
	176	1.7/ 7.6	176	-15.4/ 11.8	176	-24.7/ 35.1	176	-27.5/ 74.6
8.0	9.4	25.9/ 9.6	9.4	18.0/ 8.3	9.4	10.6/ 10.6	9.4	8.0/ 17.4
	17.6	25.1/ 7.2	17.6	17.1/ 6.5	17.6	9.4/ 10.0	17.6	6.5/ 18.0
	52.0	25.6/ 4.7	52.0	12.8/ 4.1	52.0	4.4/ 9.8	52.0	1.2/ 20.5
	93.6	22.6/ 5.4	93.6	7.4/ 5.0	93.6	-1.8/ 13.6	93.6	-5.2/ 27.6
	176	13.5/ 8.0	176	-3.6/ 9.6	176	-13.5/ 24.6	176	-17.0/ 48.6
10.0	9.4	26.6/ 9.6	9.4	18.7/ 8.2	9.4	11.6/ 9.3	9.4	8.6/ 14.6
	17.6	27.2/ 7.2	17.6	18.1/ 6.4	17.6	10.6/ 8.6	17.6	7.5/ 14.5
	52.0	28.1/ 4.8	52.0	15.5/ 4.0	52.0	7.0/ 8.3	52.0	3.7/ 16.5
	93.6	27.6/ 5.6	93.6	11.8/ 4.8	93.6	2.8/ 11.5	93.6	-0.8/ 21.6
	176	21.8/ 8.3	176	4.1/ 9.2	176	-6.0/ 19.6	176	-9.9/ 36.7

Table 5.2 Dividing Junction Friction Constants

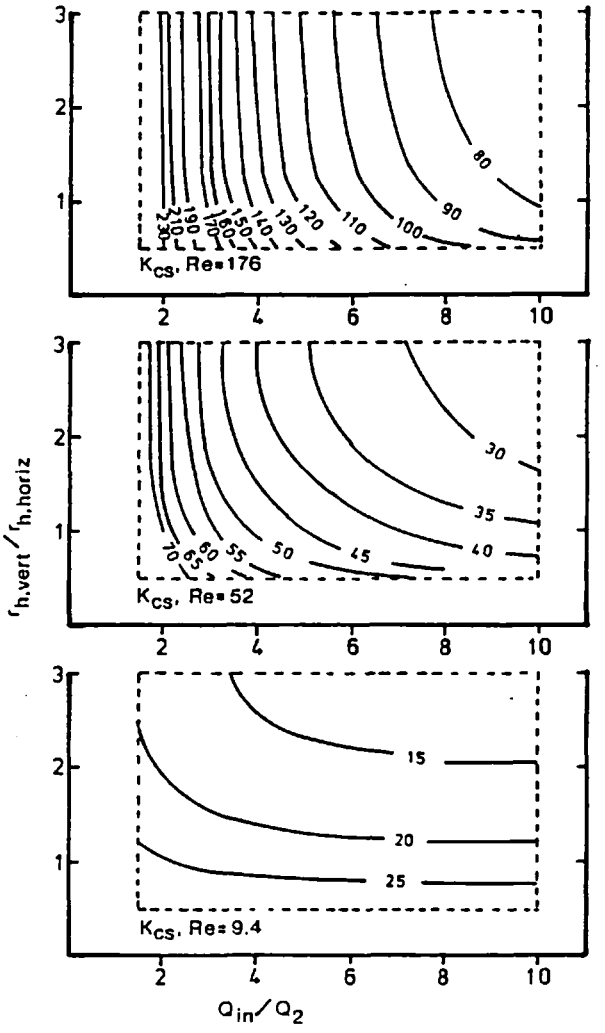


Fig. 5.12 Contour Plot of K_{cs}

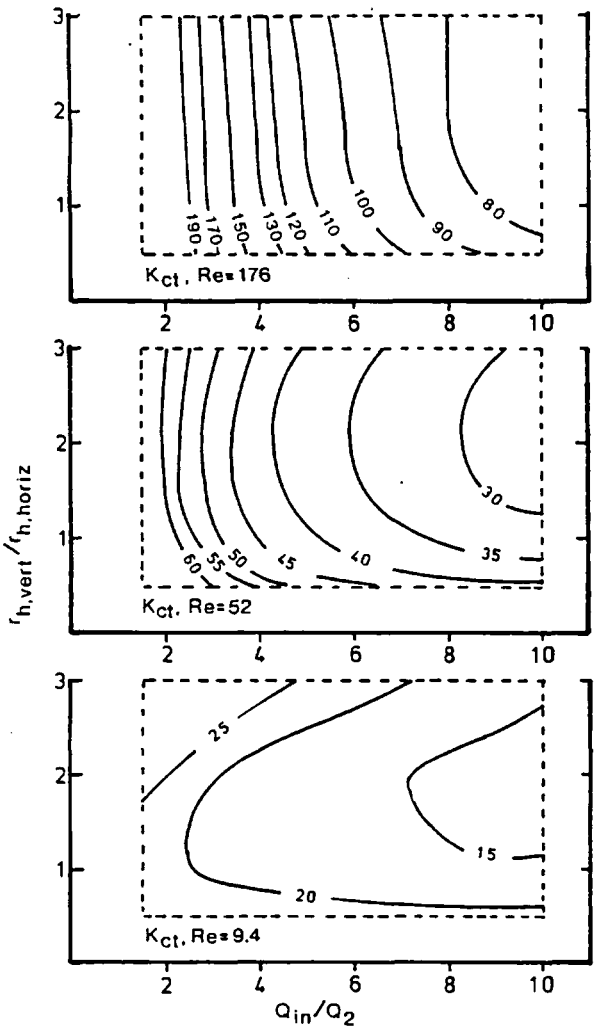


Fig. 5.13 Contour Plot of K_{ct}

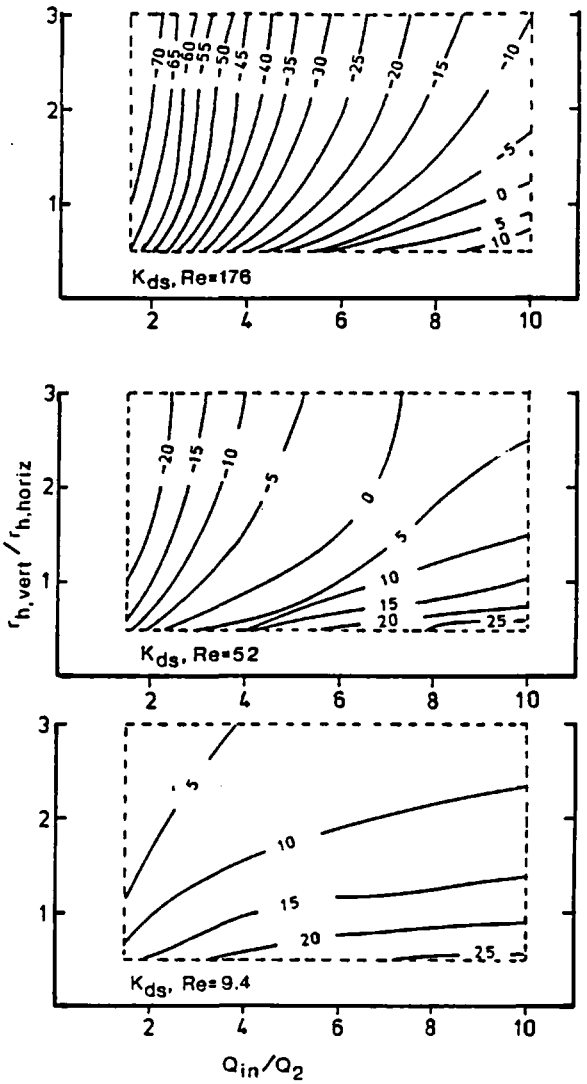


Fig. 5.14 Contour Plot of K_{ds}

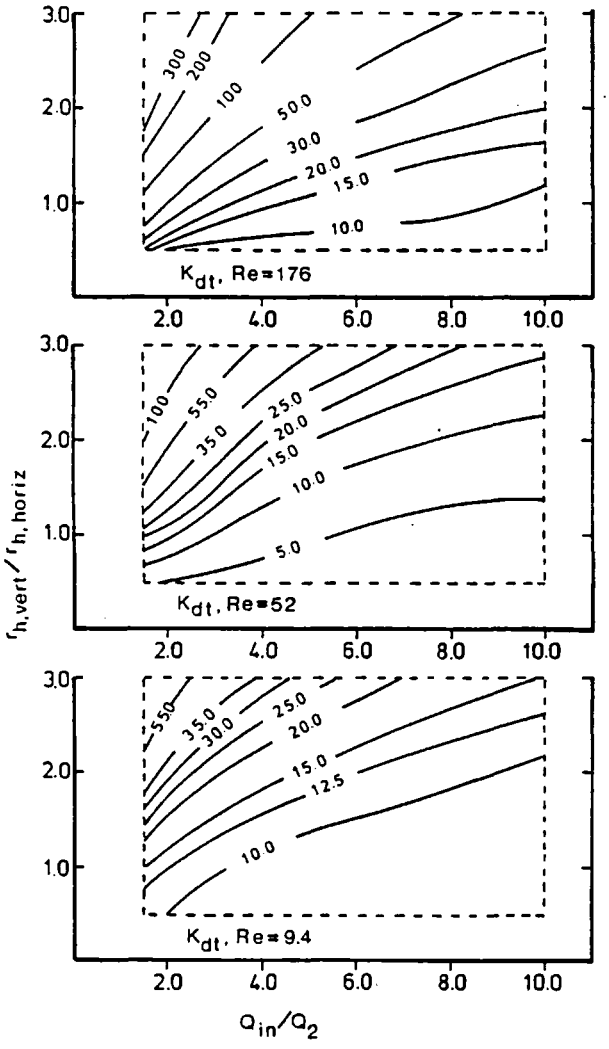


Fig. 5.15 Contour Plot of K_{dt}

In all four figures it is evident that the K's are themselves functions of Re; resistances formed from them will therefore be non-linear. In some cases, as will be seen later, these resistances are smaller than R_1, R_2, etc. and their non-linearity is weak. In combining junctions, fluid velocities will always increase, and pressure loss due to acceleration will add to friction losses. Thus only positive values of K_{cs} and K_{ct} occur, increasing with Re and decreasing with Q_{in}/Q_2. In dividing junctions, however, the fluid decelerates, causing pressure regain which compensates for friction losses. At higher Re, negative

values of K_{ds} occur (Fig. 5.14), although momentum never sufficiently outweighs friction to drive K_{dt} negative (Fig. 5.15). Areas of recirculation along turning paths, causing greater viscous dissipation, are increasingly likely at higher Re, especially in the horizontal duct entrance.

The section will close with a comparison of K_{cs}, etc. and the experimentally obtained coefficients of Jamison and Villemonte (1971) derived from measuring losses in 3/4 inch pipe tees. Their notation for K_{m-1}, etc. is explained in Fig. 5.16, and the comparison is tabulated in Table 5.3. The Jamison and Villemonte values listed are as used by Oliver (1980) to compute the flow distribution in a disc-type winding. The primes on K'_{dt}, etc. indicate that corrections have been made to define K_{dt}, etc. in the same way as K_{m-2}, etc.

Dividing Junction				
$\frac{Q_{in}}{Q_2}$	K_{m-1}	K_{m-2}	K'_{ds}	K'_{dt}
			Re=9.4/176	Re=9.4/176
∞	2090	7000	-	-
4	2130	7000	40/-88	60/120
2	3570	7000	40/-260	50/200
1.3	6140	7000	-	-
1	10650	7000	-	-
Combining Junction				
$\frac{Q_{in}}{Q_2}$	K_{1-m}	K_{2-m}	K'_{cs}	K'_{dt}
			Re=9.4/176	Re=9.4/176
∞	2090	7300	-	-
3	2130	7300	48/330	160/1360
1	3570	7300	-	-
.33	6140	7300	-	-
0	10650	7300	-	-

Table 5.3 Comparison of Pipe Junction and Plane Junction Friction Constants

In most cases, the two-dimensional coefficients are two orders of magnitude lower than those from the pipe tee data. Furthermore, even though Jamison and Villemonte state that negative values of K_{m-1} did occur, these values are not included in their data summaries and graphs. Finally, it is interesting to note that substantial values of K_{1-m} and K_{m-1} were obtained even when Q_{in}/Q_2 approached infinity (i.e. no horizontal branch flows). This would suggest that a substantial portion of the measured losses were due to the roughness and sudden expansions of the screwed fittings, making the data even less applicable to disc windings.

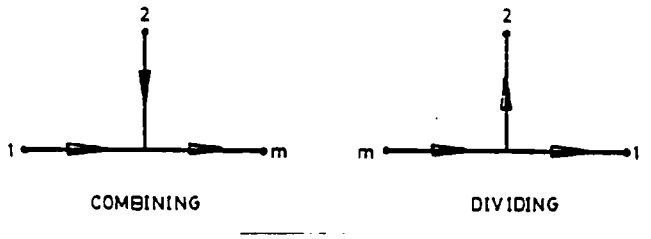


Fig. 5.16 Notation of Jamison and Villemonte (1971)

5.6 Conclusion Friction constants for two-dimensional combining and dividing junctions have been obtained by using TEACH-L. Rigorous mesh-dependency tests could not be made for all 240 cases, but the representative cases chosen indicated that the 17x13 grid was adequate. In any case, the accuracy needed is not necessarily known until the constants have been incorporated into the network model. The aim here has been to produce "useable" constants, believed to be much more accurate than the pipe data in Table 5.3.

CHAPTER 6

CORNER FLOWS

6.1 Introduction At the top left and bottom right of the pass shown as Fig. 3.1 the fluid is forced to turn through 90^{o}, which will give rise to a pressure drop along the path shown in Fig. 6.1. As was the case for the tee-junction flows, no pressure loss data was found in the literature for two-dimensional, laminar corner flows. Laminar flow in a circular pipe was studied by White (1929), but for the same reasons as outlined in Chapter 5, the results are expected to be substantially different from the two-dimensional case.

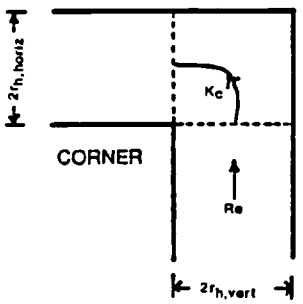


Fig. 6.1 Two-Dimensional Corner

A parametric study similar to that for tee-junctions was therefore made using TEACH-L, however far less computation was required. The pressure drop appears to be governed by only two parameters, $r_{h,vert}/r_{h,horiz}$ and Re, which were varied over four and five levels, respectively, requiring only 20 runs. All calculations were done on the RML 380Z. The program incorporating the necessary boundary conditions was named CORNER.

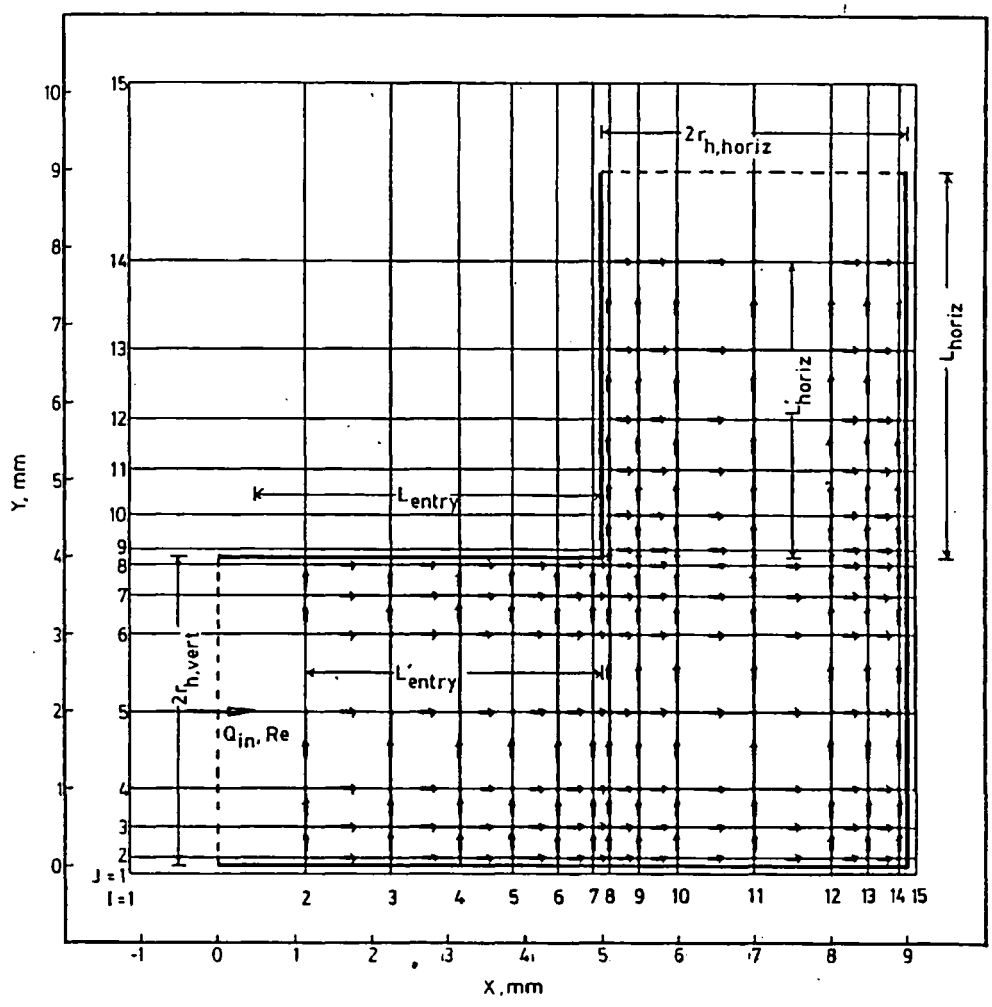


Fig. 6.2 Corner Flow Domain

6.2 Flow Domain and Boundary Conditions A 15x15 grid was used with refinement near the walls and the two (270^{o} and 90^{o}) corners. (See Fig. 6.2). The no-slip condition for all velocity components parallel to the walls is applied as described in Sec. 5.2. The 270^{o} corner is handled exactly as in the tee-junctions (see Section 5.2.) The 90^{o} corner requires no special treatment other than prescribing the usual no-slip condition for the tangential velocity components near the wall; thus the source coefficients B and C for U(14,2) and V(14,3) (see Fig. 6.2) are set in exact analogy with (5.3) to (5.6). A parabolic velocity profile at entrance and exit is assumed, with L_{entry} and L_{horiz} set according to

Re, using (2.4). A listing of CORNER with further documentation may be found in Appendix D5.

6.3 Definition of Friction Constants and Results K_c is defined similarly to K_{cs}, etc. in Chapter 5. The pressure drop Δp_c due to fully developed flow is determined from

$$\Delta p_c = 1.5\mu Q_{in}\left[\frac{L'_{entry}}{r^3_{h,vert}} + \frac{L'_{horiz}}{r^3_{h,horiz}}\right], \tag{6.1}$$

(see Fig. 6.2 for definitions of L'_{entry} and L'_{horiz}). The excess pressure drop $\Delta\hat{p}_c$ due to entrance, cornering and exit effects is then

$$\Delta\hat{p}_c = (p_{in} - p_2) - \Delta p_c \tag{6.2}$$

where p_{in} and p_2 are the average pressures on the entrance line I = 2 and exit line J = 14 (see Fig. 6.2). The definition of K_c follows as

$$K_c = \frac{8\Delta\hat{p}_c r^2_{h,vert}}{\mu Q_{in}}. \tag{6.3}$$

The results of the 20 runs are given in Table 6.1 and plotted in Fig. 6.3. K_c increases substantially with $r_{h,vert}/r_{h,horiz}$, indicating that it is "difficult" for the fluid to turn the corner from a wider to a narrower duct, the converse being "easy". No claim of mesh independence is made for these results. A 15x15 grid was assumed adequate since it is of comparable size to the 17x13 grid used for the tee-junction calculations. Further investigation was not made due to the relatively slight influence of K_c expected on the overall pass flow distribution.

Confirmation of this assumption must await the incorporation of K_c into the network model, to be done in Chapter 8.

$r_{h,vert}/r_{h,horiz}$	0.5	1.0	2.0	3.0
Re				
9.4	11.3	22.3	86.1	205.0
17.6	8.6	23.9	109.8	266.5
52.0	5.6	44.5	235.6	578.5
94.0	9.2	78.2	408.3	990.6
176.0	23.4	167.6	805.6	1902.0

Table 6.1 Corner Friction Constants

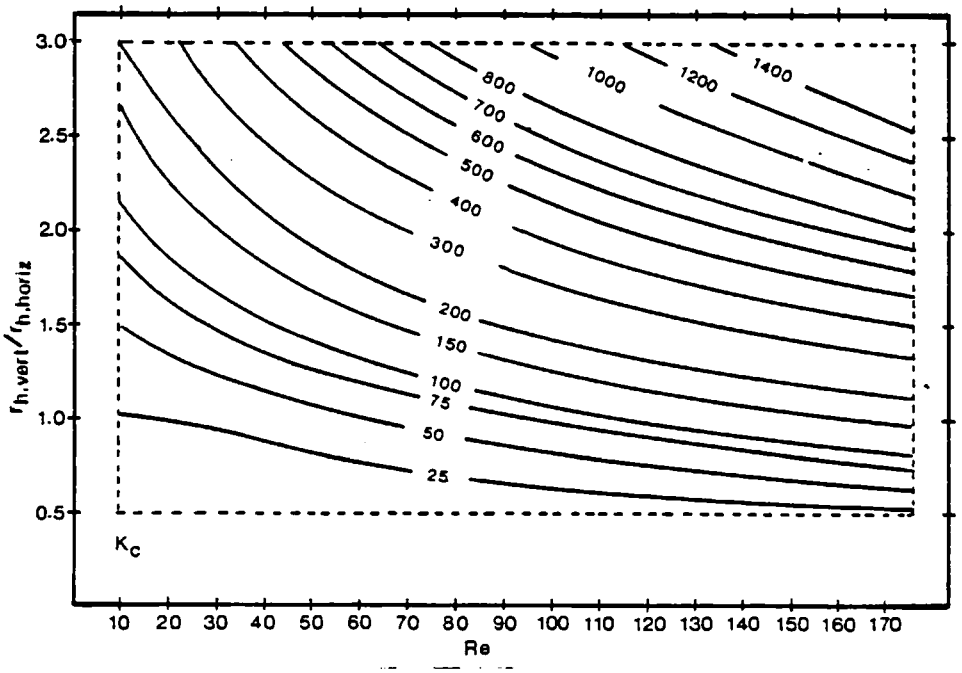


Fig. 6.3 Contour Plot of K_c

CHAPTER 7

DUCT FLOWS

7.1 Introduction The study of fluid flow and heat transfer in ducts of various cross-sectional shapes, with numerous boundary conditions and flow regimes, has generated so many technical papers that several Ph.D theses would be required to provide an adequate survey of the field. Shah and London (1978) produced 536 references in their excellent book whilst limiting themselves to laminar flow forced convection and constant property fluids.

Their book contains many examples of classical analytical solutions for simple geometries and boundary conditions; variable property flows, however, even in simple situations, generally require numerical methods. The results are usually reported as "correction" factors to the constant property friction factors and Nusselt numbers (see Kays (1966), p. 258). Since, in many liquids, notably oils, viscosity is the most variable property, the correction factors usually consist of a ratio of the viscosity at the wall to the viscosity at the bulk fluid temperature raised to some power. These correlations appear to be useful when both temperature and velocity profiles are fully developed, and when only the mean Nusselt over the length of the duct is required.

As stated in Chapter 2, the flow in the horizontal ducts of a disc winding will be well within the thermal entry region, where the local Nusselt number may vary considerably. A computer-based numerical method yielding local wall temperatures, and also able to cope with variable

fluid properties and various boundary conditions, in a two-dimensional (parallel plane) geometry, would seem called for. The hot-spot temperature could then be obtained by extending the solution domain into the disc itself and solving for the individual conductor temperatures.

Again, it is likely that more computer codes have been written to deal with ducts than any other flow situation, and a comprehensive survey cannot be made here. Most of these codes treat duct flows as a "parabolic" rather than "elliptical" phenomenon (see White (1974), p. 81). In the former, axial diffusion of heat and momentum is neglected, permitting a "marching" solution. Boundary conditions need only be specified at the duct entrance and walls. In elliptical flows, heat and momentum may diffuse axially as well as across the duct. Boundary conditions must be specified all round the flow domain (i.e. at the exits as well). Axial diffusion may be neglected as long as the Peclet number is greater than 100, according to Kays (1966), p. 121. Below that an elliptical method such as TEACH-L is required.

In high Prandtl number fluids, Peclet numbers below 100 would only occur at extremely slow flows (Re < 1-2), hence marching solutions have been successfully used in many transformer applications. Of especial note is the "truncation" method invented by Allen (1970), which assumes that "all partially developed temperature profiles are truncated versions of the fully developed one, developing outward from the wall and only changing shape where it meets fluid at its initial temperature." This method has been successfully compared with the results of experiment and other more complex computer solutions, in ducts of various geometries, and is particularly suited to the analysis of the long vertical ducts which occur in layer-type windings (see Allen

(1968), Preiningerova and Allen (1974) and Collins, Allen and Szpiro (1977)).

In the relatively short horizontal ducts of a disc-type winding (see Fig. 2.4), marching methods cannot be used because of pronounced edge effects on the discs. Substantial diffusion of heat will take place in the disc in a direction parallel to the axis of the duct. Furthermore, although the current in each conductor is fixed under steady state conditions, the wall heat flux will vary with the conductor temperature (due to copper resistivity-temperature variation), which will depend on the flow conditions in the duct. It appears that while the duct flow itself is essentially parabolic, the disc heat conduction problem is definitely elliptic, and the two interact. The decision was therefore taken to adapt TEACH-L to solve the conjugated problem. The implementation of these complex boundary conditions, the DUCT program, will be presented in this chapter together with some sample results. Listings with documentation may be found in Appendix D6.

7.2 Initial Assumptions In addition to the general assumptions mentioned in section 2.4, the following additional assumptions peculiar to the duct/disc problem will be made. The expressions (4.4) - (4.6) for sources S_u, S_v and S_t will be simplified to (4.8) - (4.10). This involves the removal of 1.) the "extra" variable viscosity terms from S_u and S_v, 2.) the body force term from S_v and 3.) the "extra" variable heat capacity terms from S_t. These three actions may be justified as follows.

1.) Applying (2.15) to the variable viscosity terms in (4.4) and (4.5) gives

$$\frac{\partial}{\partial x}(\mu\frac{\partial u}{\partial x}) + \frac{\partial}{\partial y}(\mu\frac{\partial v}{\partial x}) \approx - \frac{\partial}{\partial x}(\mu\frac{\partial v}{\partial y}) + \frac{\partial}{\partial y}(\mu\frac{\partial v}{\partial x}), \qquad (7.1)$$

and

$$\frac{\partial}{\partial x}(\mu\frac{\partial u}{\partial y}) + \frac{\partial}{\partial y}(\mu\frac{\partial v}{\partial y}) \approx \frac{\partial}{\partial x}(\mu\frac{\partial u}{\partial y}) - \frac{\partial}{\partial y}(\mu\frac{\partial u}{\partial x}), \qquad (7.2)$$

where it may be seen that permission to interchange the order of partial differentiation in either term of the R.H.S. of the two equations would cause it to cancel with the other term. Such permission would require, of course, constant viscosity; nevertheless it can be expected that both (7.1) and (7.2) will be very small. Alternatively it could be argued that in a duct the axial velocities u will greatly exceed the normal velocities v, hence the v terms in (7.1) may be ignored. In the case of S_v, since the v velocities are expected to be very small, all components of S_v will be negligible and neglect of (7.2) will make no difference.

2.) In horizontal ducts of rectangular cross-section, free convection effects appear to give rise to twin vortices whose axes run parallel to the duct axis. In their theoretical study, Cheng and Hwang (1969) state that as the aspect ratio (w/c, see Fig. 2.2) of the duct increases, the vortices tend to move out towards the vertical side walls, presumably vanishing as w/c approaches infinity (i.e. the parallel plane duct.) Experimental results are reported by Akiyama, Hwang and Cheng (1971) but their investigation used air at Reynolds numbers less than 100. Cheng, Hong and Hwang (1972), in a more relevant theoretical study, examined buoyancy effects in the thermal entrance region of horizontal rectangular channels with uniform wall heat flux for a large Prandtl number fluid. Their analysis indicated that vortex

generation depends on the existence of a temperature gradient across the width of the duct. Such a gradient will, of course, vanish as the aspect ratio approaches infinity. Hence, these published results indicate that, in the parallel plane geometry, the effect of free convection will be negligible, especially for high Prandtl number fluids. The body force term ρg in (4.5) is therefore neglected. Examination of the sample output provided in Appendix D6 confirms that, since the ducts are short, density variation sufficient to give rise to a substantial buoyancy force does not arise.

3.) Though the heat capacity c_p of transformer oil does vary with temperature, the effect is secondary compared with viscosity variation. Hence the terms in (4.6) are neglected, although variation of k/c_p is allowed in (4.3). Examination of some sample output will confirm that the variation of k/c_p is slight (see Appendix D6, where it is referred to as the 'thermal exchange coefficient').

7.3 Grid Arrangement and Boundary Conditions In Fig. 7.1, a coarse 6x6 grid is shown which comprises a half-duct and half-disc containing four conductors. The y-axis in the region of the duct is scaled up 20 times over the x-axis to make the drawing readable. The conductors are not drawn to scale in the y-direction, but in the x-direction it is intended that the surface of each insulated conductor coincides exactly with the shaded t-cells at the oil interface. The very sharp refinement of the grid near the disc surface is required because of the high Prandtl number of the oil and the consequently thin thermal boundary layer. The grid ultimately used was 22x9, to coincide with the experimental winding, each disc of which contained 20 conductors. At the top and bottom of the solution domain it will be seen that lines of

symmetry have been assumed at the disc and duct centre-lines. The accuracy of this assumption will be discussed further in Chapter 12.

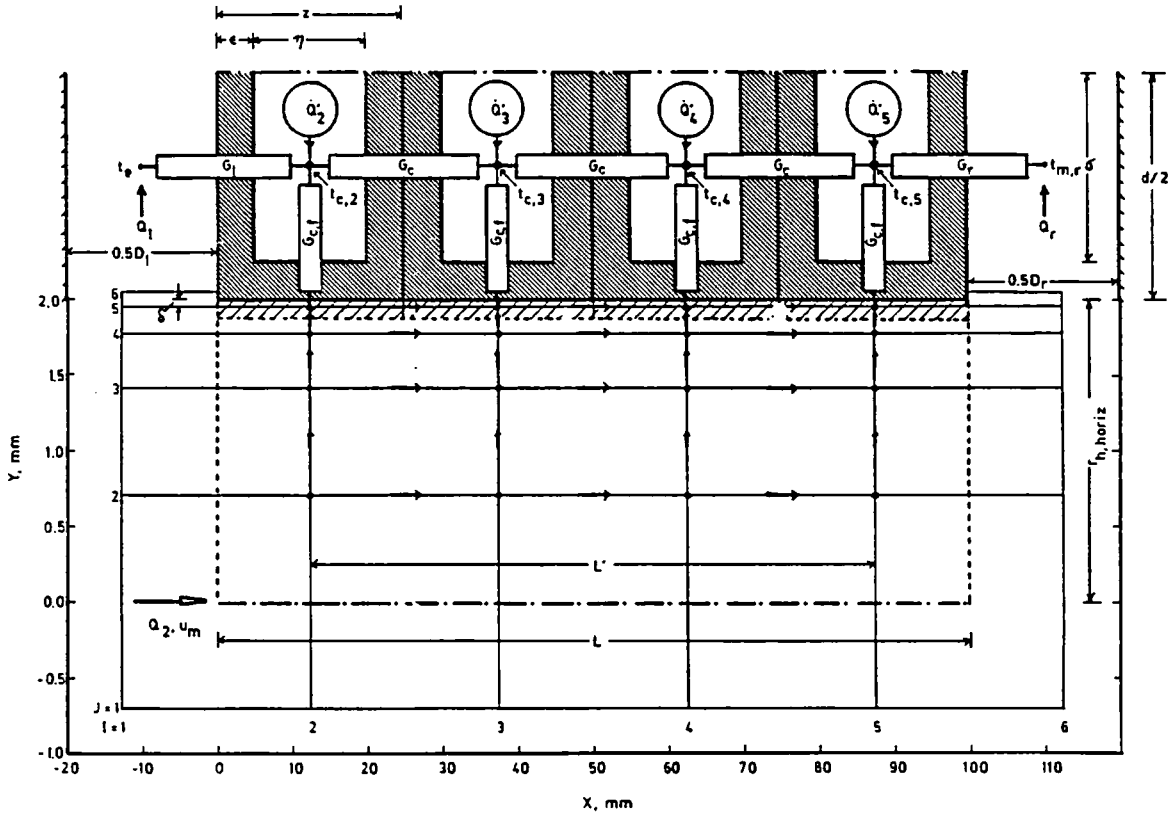


Fig. 7.1 Disc/Duct Flow Domain

Each half-conductor is modelled as a single node whose average temperature is $t_{c,2}$, etc., and is connected to its neighbouring conductors through conductances G_c, to the nearest temperature nodes in the fluid T(2,5), etc., through conductances $G_{c,f}$ and to the bulk fluid temperatures t_e and $t_{m,r}$ in the left and right vertical ducts through conductances G_l and G_r. (The uniform duct entrance temperature t_e, and the bulk temperature in the left-hand vertical duct are assumed equal. The expression for each of these conductances is:

$$G_c = \frac{k_p \sigma}{2\varepsilon} , \tag{7.3}$$

$$G_{c,f} = \frac{(k_p z/\varepsilon)(kz/\delta)}{(k_p z/\varepsilon + kz/\delta)} , \tag{7.4}$$

$$G_l = \frac{(h_l \sigma)(k_p \sigma/\varepsilon)}{(h_l \sigma + k_p \sigma/\varepsilon)} , \tag{7.5}$$

$$G_r = \frac{(h_r \sigma)(k_p \sigma/\varepsilon)}{(h_r \sigma + k_p \sigma/\varepsilon)} , \tag{7.6}$$

where

k_p = thermal conductivity of kraft paper insulation (through the laminations, see Appendix A) [W/m K]

σ = half-height of uninsulated conductor [m]

ε = thickness of insulation [m] (same on all sides)

z = overall width of conductor [m]

k = thermal conductivity of fluid [W/m-K]

δ = distance from disc surface to nearest temperature node [m]

h_l = mean convection conductance at left disc edge [W/m^2-K]

h_r = mean convection conductance at right disc edge [W/m^2-K]

As indicated by the grid lay-out in Fig. 7.1, the flow field is not solved for in the left and right hand vertical ducts, therefore h_l and h_r must be assumed. It was decided to use the <u>mean</u> Nusselt number $Nu_{m,H}$ based on $Q_{l \text{ or } r}$ and $D_{l \text{ or } r}$ averaged over the height d of the disc, available from the constant property, parallel plane, constant wall heat flux solution given by Shah (1975)

$$Nu_{m,H} = 2.236(d^*)^{-1/3} \quad \text{for } d^* \leq 0.001,$$

$$Nu_{m,H} = 2.236(d^*)^{-1/3} + 0.9 \quad \text{for } 0.001 < d^* < 0.01, \tag{7.7}$$

$$Nu_{m,H} = 8.235 + 0.0364/d^* \quad \text{for } d^* \geq 0.01,$$

where

$$d^* = d/(D_{l \text{ or } r}\, Pe_{l \text{ or } r}). \tag{7.8}$$

This was deemed adequate, as the constant property Nusselt number does not depart significantly from the variable property Nu over short duct lengths. It was also found that in any case the solution of the conductor temperatures is not very sensitive to small variations in the values of h_l and h_r.

Conductance $G_{c,f}$ is a series combination of the conductances from the conductor to the oil-insulation interface $(k_p z/\varepsilon)$ and from the oil-insulation interface to the nearest fluid temperature node (kz/δ). G_l and G_r are similar combinations. The I^2R losses in the conductors are modelled by injecting into each half-conductor node a heat source per unit depth $\dot{Q}'_2$, etc. (see Fig. 7.1), where, e.g.

$$\dot{Q}'_2 = \frac{\rho_{20}[1 + \alpha_{20}(t_{c,2} - 20)](I/2)^2}{\eta\sigma}, \tag{7.9}$$

where

η = width of uninsulated conductor [m]

ϱ_{20} = resistivity of conductor at $20^{o}C$ [Ω-m]

α_{20} = resistivity-temperature coefficient of conductor at $20^{o}C$ [$^{o}C^{-1}$]

I = rms current in each conductor [A]

Equating the energy input to the energy output at each node leads to

$$\begin{aligned}
(G_c+G_{c,f}+G_1)t_{c,2} - G_c t_{c,3} &= \dot{Q}_2' + G_{c,f}T(2,5) + G_1 t_e \\
- G_c t_{c,2} + (2G_c+G_{c,f})t_{c,3} - G_c t_{c,4} &= \dot{Q}_3' + G_{c,f}T(3,5) \\
- G_c t_{c,3} + (2G_c+G_{c,f})t_{c,4} - G_c t_{c,5} &= \dot{Q}_4' + G_{c,f}T(4,5) \\
- G_c t_{c,4} + (G_c+G_{c,f}+G_r)t_{c,5} &= \dot{Q}_5' + G_{c,f}T(5,5) + G_r t_{m,r}
\end{aligned} \tag{7.10}$$

The arrangement of (7.10) is inconvenient due to the fact that $\dot{Q}_2'$, etc. are functions of $t_{c,2}$, etc. To eliminate this, define

$$R_c = \frac{\varrho_{20}\alpha_{20}(I/2)^2}{\eta\sigma}. \tag{7.11}$$

and

$$\dot{Q}' = \frac{\varrho_{20}(1 - 20\alpha_{20})(I/2)^2}{\eta\sigma}, \tag{7.12}$$

so that, e.g.

$$\dot{Q}_2' = \dot{Q}' + R_c t_{c,2} \tag{7.13}$$

(7.10) may now be rearranged to yield

$$\begin{aligned}
(G_c+G_{c,f}+G_l-R_c)t_{c,2} - G_c t_{c,3} &= \dot{Q}' + G_{c,f}T(2,5) + G_l t_{m,l} \\
- G_c t_{c,2} + (2G_c+G_{c,f}-R_c)t_{c,3} - G_c t_{c,4} &= \dot{Q}' + G_{c,f}T(3,5) \\
- G_c t_{c,3} + (2G_c+G_{c,f}-R_c)t_{c,4} - G_c t_{c,5} &= \dot{Q}' + G_{c,f}T(4,5) \\
- G_c t_{c,4} + (G_c+G_{c,f}+G_r-R_c)t_{c,5} &= \dot{Q}' + G_{c,f}T(5,5) + G_r t_{m,r}
\end{aligned} \tag{7.14}$$

The set of equations (7.14) is again tri-diagonal, and may be solved by the TDMA. The sequence of events in the solution procedure is then:

1.) Equations (7.14) are solved using current values of T(2,5) etc. (t_e if it is the first iteration).

2.) The values of $t_{c,2}$ etc. obtained from 1.) are used to evaluate the heat flux from each conductor into its contiguous fluid temperature cell (shaded, Fig. 7.1), e.g.

$$\dot{q}_2' = G_{c,f}[t_{c,2} - T(2,5)]. \tag{7.15}$$

This heat flux is incorporated as a boundary condition for the T(2,5) cell using the source expression (4.35). Here B = 0 and

$$C = \dot{q}_2'/c_p. \tag{7.16}$$

It is necessary to divide by the heat capacity c_p to maintain consistency with (4.3). The procedure for obtaining the heat flux boundary condition for T(3,5), etc. is the same. For reasons analogous with specification of the no-slip conditions on the u-velocity (see Section 5.2), A_N must be set to zero for all shaded T-cells.

3.) Using the heat fluxes calculated in 2.) the temperature field in the fluid may now be solved, yielding in particular new values of T(2,5) etc.

4.) The process is repeated beginning from 1.) until convergence is attained. In this case the reference value used for R_t (see (4.66)) will simply be

$$(\dot{q}_2' + \dot{q}_3' + \dot{q}_4' + \dot{q}_5')/c_p. \tag{7.17}$$

The thermal boundary conditions required on the other three boundaries are: uniform inlet and outlet temperatures equal to t_e and $t_{m,r}$ respectively, and zero heat flux across the duct centre-line, obtained by setting A_S to zero for centre-line T-cells.

The hydrodynamic boundary conditions on u are: at the inlet, a parabolic velocity profile, at the wall, the no-slip condition (see Sec. 5.2), and zero momentum flux across the duct centre-line (by setting A_S to zero for all centre-line u-cells). At the outlet, a difficulty arises

since the outlet velocity profile (which will not be parabolic due to variable viscosity) is not known. To get round this difficulty the exit profile is adjusted to satisfy the overall continuity requirement, a practice used in some of the TEACH-L sample problems. (See the listing of MODU, Appendix D6, for details). Velocity v is set to zero at the wall and duct centre-lines.

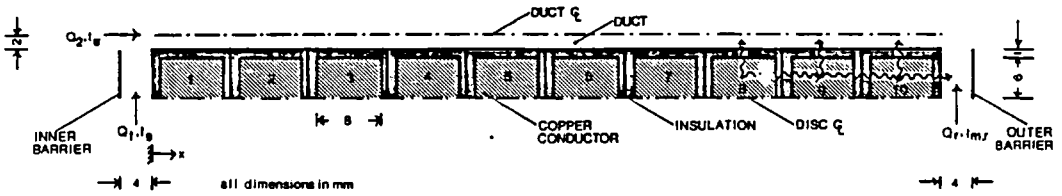


Fig. 7.2 10 Conductor Disc

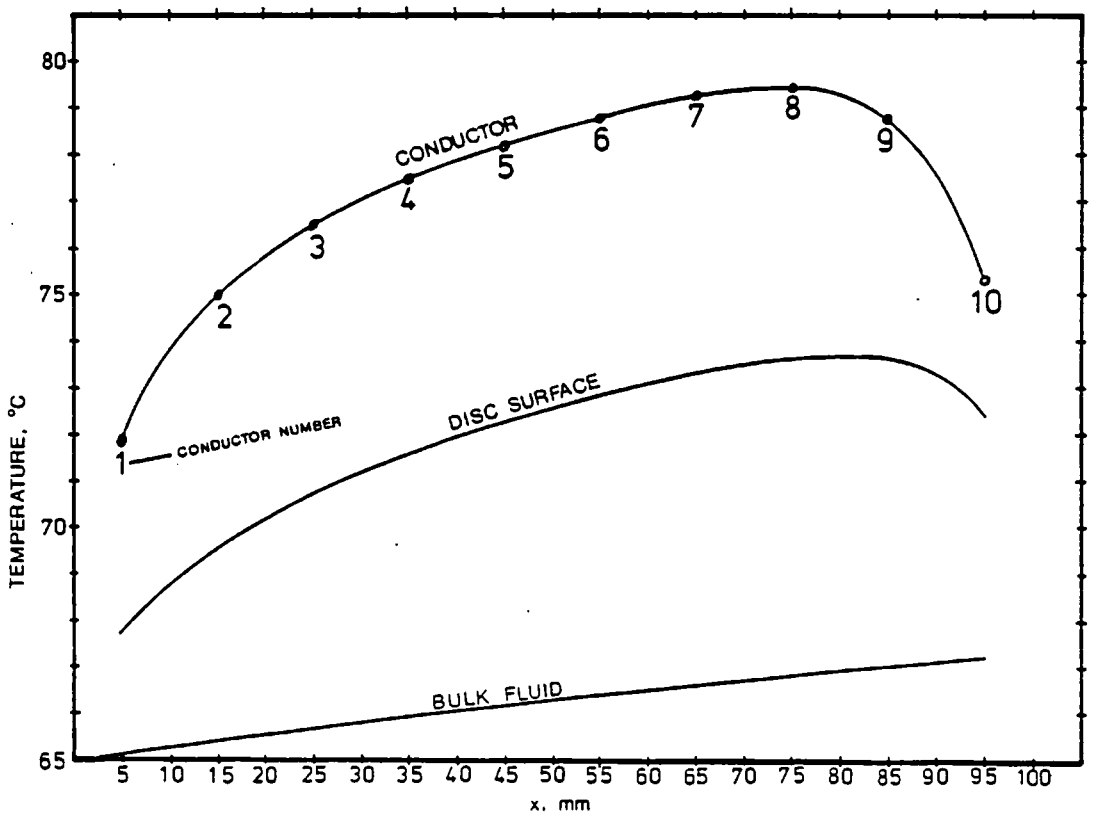


Fig. 7.3 Temperature Distribution in 10 Conductor Disc

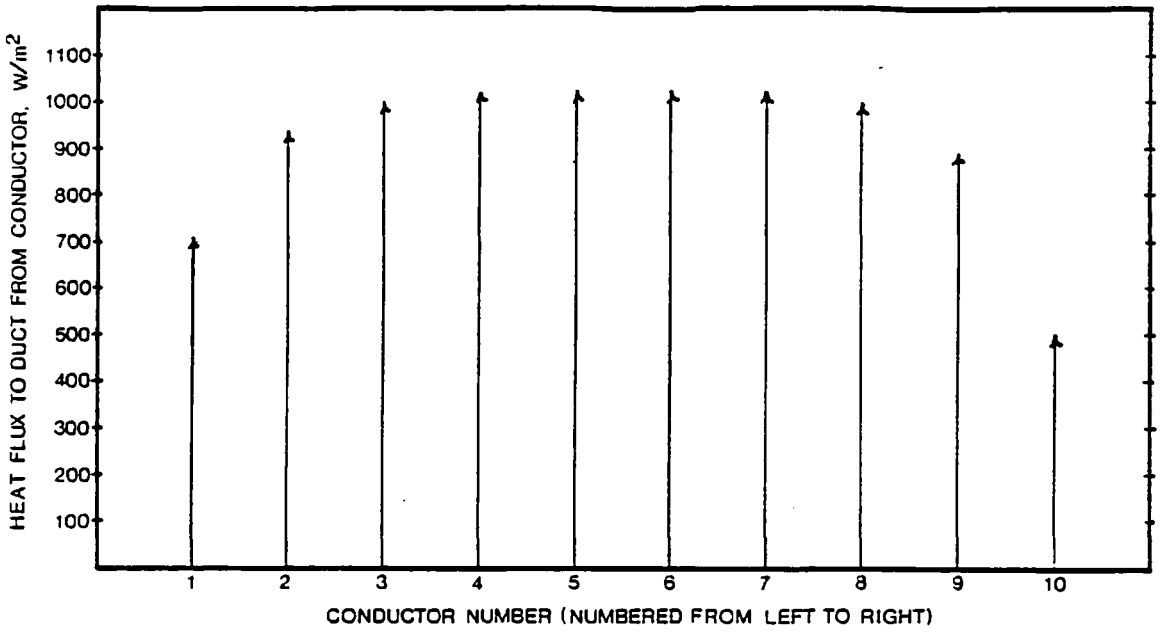


Fig. 7.4 Surface Heat Flux Distribution in 10 Conductor Disc

7.4 Sample Output A sample half-disc/duct system, shown as Fig. 7.2, comprising ten conductors and using a 12x6 grid, was solved. The results are given as Figs. 7.3 and 7.4. The operating conditions were

$$Q_2 = Q_1 = Q_r = 5 \times 10^{-5} \ m^2/s$$

Inlet Re = 16.5

Inlet Pr = 88.7

Inlet Pe = 1,468

$$t_{m,r} = t_e = 65.0 \ ^{o}C$$

I/2 = 152.6 A

The solution is characterised by a sharp decrease in conductor temperature at the outlet edge of the disc (Fig. 7.3). This accords well with experimental measurements and will be elaborated in Chapter 12. In

Fig. 7.4, the conductor fluxes (here $\dot{q}'_2$ to $\dot{q}'_{11}$) are plotted. The winding current was chosen to give a surface heat flux of 1000 W/m^2 in the absence of edge effects. Whilst conductors 3 to 8 deliver approximately 1000 W/m^2, conductors 1, 2, 9 and notably 10 give far less. Hence the latter 4 conductors must be delivering a significant amount of heat to the side vertical ducts.

7.5 Variable Viscosity Friction Constant The pressure drop through a heated horizontal duct in which a variable viscosity fluid is flowing will generally be lower than in a constant property flow. Even in ducts with a simple thermal boundary condition such as constant wall heat flux, the velocity profile will never, strictly speaking, be fully developed. As the temperature along the wall of the duct increases, and the viscosity there decreases, the velocity profile will continually undergo adjustment. The more complex thermal boundary conditions presented in Sec. 7.4 will cause the viscosity near the wall to decrease over most of the duct, but to increase again as the wall temperature falls off near the exit due to disc edge effects.

It is still meaningful to define a friction constant K under these circumstances, based on (3.18) and (3.17):

$$K = \frac{8r_{h,horiz}^2 \Delta p}{L' u_m \mu} \quad , \tag{7.18}$$

where μ is determined at t_e, Δp is the difference between the average pressures at I = 2 and I = 5, and L' is the distance between these pressure "lines" (see Fig. 7.1). However, K will now depend not merely on the geometry of the duct cross-section (as in the constant property

solution) but on flow rate, fluid properties, inlet temperature, thermal boundary conditions, duct length, etc. In the example of Sec. 7.4, K was 21.68, about 9.7% lower than the constant property fully developed value (K = 24). In the pass of a disc winding, K will vary from one duct to another. In general, the lower the flow rate and the higher the wall heat flux, the lower the resultant value of K, all other conditions being equal. The effect of this will be assessed in Chapters 8 and 12.

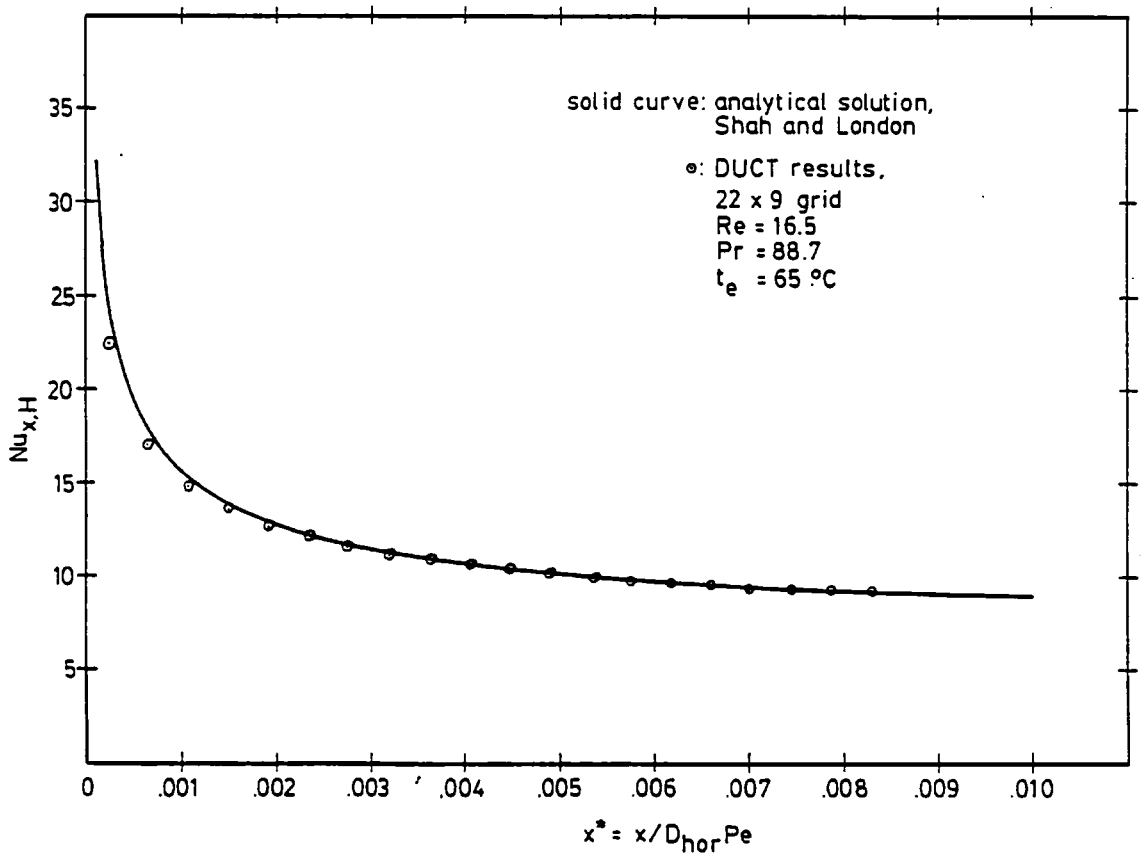


Fig. 7.5 Comparison of DUCT with Analytical Solution

7.6 Mesh Dependency It is possible to alter the boundary conditions stated in Section 7.3 (by setting h_l and h_r to zero) so that a constant wall heat flux system is approximated. If constant fluid properties are also imposed, the results of the computation can be compared directly with the published analytical solution tabulated by

Shah (1975). This has been done in Fig. 7.5, where a 22x9 grid was used. The agreement is seen to be adequate, hence the 22x9 grid was judged acceptable for the variable property and wall heat flux computations reported in Chapter 12. The excercise was repeated for coarser grids: 6x6, 12x6 and 22x6; all gave results very close to the analytical solution.

7.7 Conclusion TEACH-L has been modified to predict individual conductor temperatures, allowing for variable fluid properties, in a single disc of a transformer winding, and the pressure drop in the adjacent duct, assuming that the flow rate is known. The pressure drop data, expressed as a friction constant K, is required for the refined network model DISCNET, to be described in Chapter 8. The final results, being the flow distribution in the pass, and the conductor temperatures in each disc, are compared with experimental measurements in Chapter 12.

CHAPTER 8

DISCNET

8.1 Introduction In this chapter the FORTRAN program DISCNET (Disc Network) will be outlined (listings, sample output and further documentation may be found in Appendix D7). DISCNET incorporates the junction and corner loss data of Chapters 5 and 6, and the variable viscosity friction constant calculation described in Chapter 7 into the simple network model outlined in Chapter 3, enabling a more accurate determination of the pass flow distribution.

From the friction constants K_{ds}, etc. calculated by JUNCTION and CORNER, resistances R_{ds}, etc. are formed which are added to the network of Fig. 3.4. The program DUCT is included as a subroutine of DISCNET, and the K's required for R_1, R_2, etc. (see Fig. 3.4) are evaluated in each horizontal duct as the overall computation proceeds. (It was decided that a once-and-for-all parametric study on K would be impractical, since, in variable property fluid flows, K is affected by so many parameters). A very coarse grid (6x6) is used to run DUCT, so as not to prolong the calculation unnecessarily (a sample comparison with a 22x9 grid found the value of K to differ by only about 5%). The procedure used by DISCNET is then:

1.) The relevant geometric data for the pass is read in, together with the fluid properties, the friction constants from Tables 5.1, 5.2 and 6.1, and the operating conditions: winding current I, oil inlet temperature $t_{m,in}$ and flow rate Q.

2.) The K's for all horizontal and vertical ducts are initialised to 24 (constant property value), the junction and corner resistances to 0.

3.) The bulk oil temperature at the inlets to all horizontal ducts (and in the left-hand vertical ducts (see Fig. 3.1)) is set to the pass inlet temperature $t_{m,in}$ and remains so throughout the calculation. The bulk temperature in the right-hand vertical ducts ($t_{m,1}$, etc., Fig. 3.1) is initialised to $t_{m,in}$.

4.) The network resistances are assembled and the network solved for the flow rate in each duct. At this point, because of the initial values set in 2.), the result will be exactly equal to that of the simple network model.

5.) Using the current values of horizontal duct flow rates $Q_{2,1}$, etc. the variable viscosity K's for each duct are calculated using the 6x6 version of DUCT. $t_{m,1}$, etc. are updated.

6.) The junction and corner resistances are calculated. Using current values of $Q_{2,1}$, etc., Q_{in}/Q_2 and Re_{in} are determined for each junction and K_{ds}, K_{dt}, etc. are obtained by linear interpolation in Tables 5.1, 5.2 and 6.1.

7.) The duct resistances are calculated (R_1, R_2, etc.) using the variable viscosity K's from 5.)

8.) The network is solved for the flow rates $Q_{2,1}$, etc.

9.) Repeat the procedure from step 5.) until convergence is reached. In DISCNET, this happens when the sum of the absolute values of the changes in the Q_2's from one iteration to the next is less than 1% of the pass inlet flow rate Q. 5 iterations may be required in a typical case.

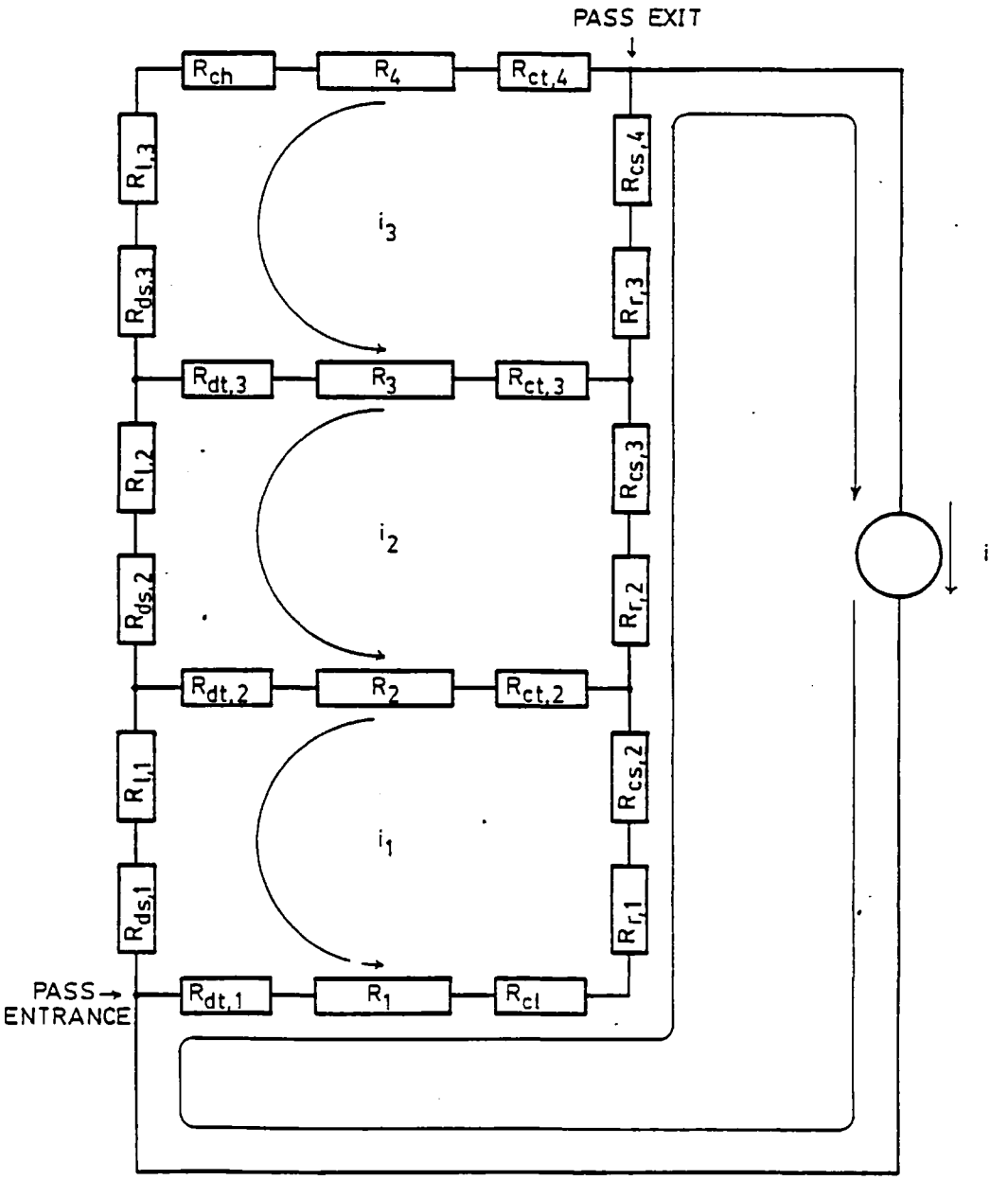


Fig. 8.1 Network with Junction and Corner Resistances Added

DISCNET is thus a "hybrid" scheme. The overall formulation remains

that of a lumped parameter network, but some of the resistances must be calculated using field equations as a sub-operation. Iteration is necessary since the junction, corner and duct resistances are all non-linear. Fortunately the non-linearity is weak enough so that the computation converges readily (in all cases attempted) without need for underrelaxation.

8.2 Network with Junction and Corner Resistances The "improved" network is shown as Fig. 8.1. The horizontal duct resistances R_1, etc. are defined exactly as in Fig. 3.4, except that K is set to its variable viscosity value (different for each duct). μ is determined at $t_{m,in}$ (see Fig. 2.3). $R_{l,1}$, etc. and $R_{r,1}$, etc. are also defined as R_l and R_r in Fig. 3.4, except that the value of μ used will be dependent on the temperature at the inlet of the vertical duct in question. K, however, is assumed to be 24 in the vertical ducts. Since the temperature in the left vertical ducts is assumed to remain at $t_{m,in}$, the R_l's will all be equal. The R_r's, however will vary according to $t_{m,1}$, etc.

The junctions are numbered according to the connecting horizontal duct. Dividing junctions hence are numbered from 1, combining junctions from 2. R_{cl} and R_{ch} are the lower and higher corner resistances. These resistances are then defined as follows:

$$R_{ds} = \frac{2K_{ds}(Q_{in}/Q_1)\mu}{D_1^2}, \tag{8.1}$$

$$R_{dt} = \frac{2K_{dt}(Q_{in}/Q_2)\mu}{D_1^2}, \tag{8.2}$$

$$R_{cs} = \frac{2K_{cs}(Q_1/Q_{in})\mu}{D_r^2}, \tag{8.3}$$

$$R_{ct} = \frac{2K_{ct}(Q_1/Q_2)\mu}{D_r^2}, \tag{8.4}$$

$$R_{cl} = \frac{2K_c\mu}{D_{hor,1}^2}, \tag{8.5}$$

$$R_{ch} = \frac{2K_c\mu}{D_{1,1}^2}, \tag{8.6}$$

where, in equation (8.1) - (8.4) the junction/duct number subscripts have been dropped to avoid excessive clutter (the full numbering scheme may be extracted from the listings, found in Appendix D7). As with the vertical and horizontal duct resistances, μ in (8.1) - (8.6) will depend on the bulk temperature at the designated junction/corner.

In equations (8.1) to (8.4), K_{ds}, e.g., has been multiplied by flow rate ratio Q_{in}/Q_1. This has been done to correct an error, made without the benefit of hindsight, in the original definitions of K_{ds}, etc. It will be recalled from Chapter 5 that K_{ds} and K_{dt} are defined in terms of Q_{in}, K_{cs} and K_{ct} in terms of Q_1 (see (5.15) - (5.17)). In formulating the resistances, it was realised (see Fig. 8.1) that R_{dt} and R_{ct} would have in fact to be defined according to Q_2 (horizontal duct flow rate), R_{ds} in terms of Q_1 (flow rate exiting from dividing junction in vertical duct) and R_{cs} in terms of Q_{in} (flow rate entering combining junction from vertical duct). The error is easily put right as in (8.1) - (8.4) and the difficulty does not arise in the corner resistances.

The solution to the network proceeds exactly as in the simple

network model, except that, of course, the coefficients of the matrix equations (3.25) will contain the additional junction corner resistances.

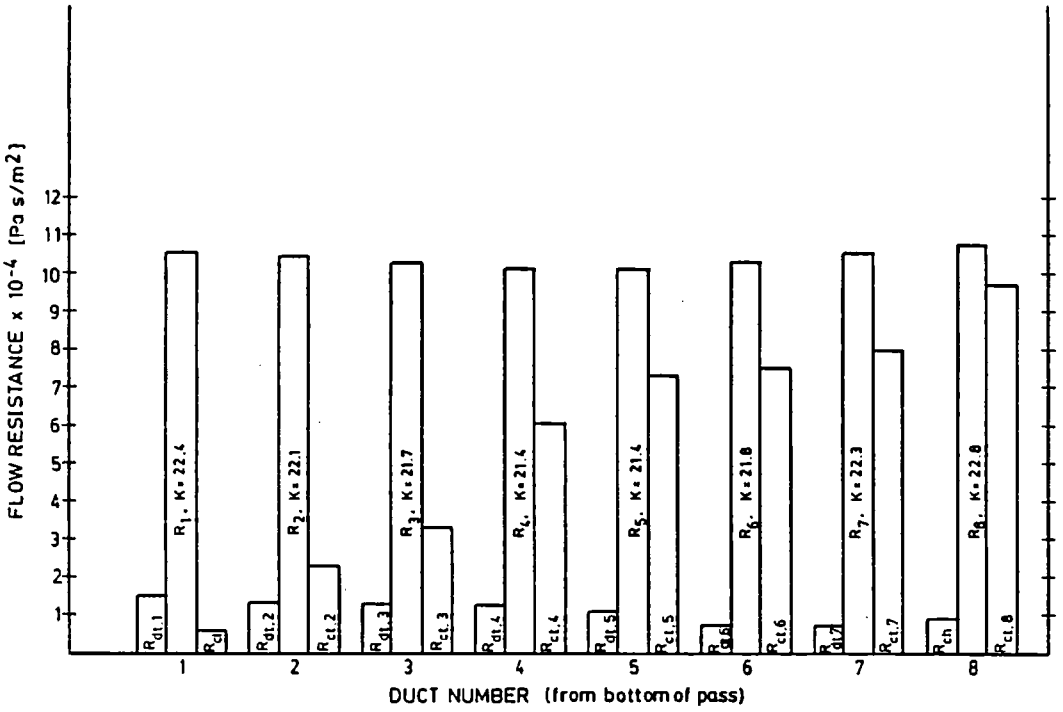


Fig. 8.2 Magnitude of Horizontal Duct Resistances

8.3 Sample Results The effect of these additional or modified resistances may be seen from detailed consideration of a sample calculation. An 8 duct pass is examined, with $t_{m,in}$ = 58.9°C, Q = 7.0 x 10^{-4} m^2/s and I = 800 A (in the coarse 6x6 grid, large conductors are used, see Fig. 7.1; this value of I gives a wall heat flux of about 1000 W/m^2). Under these conditions, the pass inlet Reynolds number (based on D_l) is 196, a value typical of forced convection cooling. The disc dimensions were L = 100 mm, d = 14 mm, and all duct hydraulic diameters $D_{hor} = D_l = D_r$ = 8 mm. Referring to Fig. 8.1, it will be seen that the total flow resistance in, e.g., horizontal duct number 2 is the sum of $R_{dt,2}$, R_2 and $R_{ct,2}$. The corresponding 3 resistances for each of the 8

ducts in the sample calculation are compared in Fig. 8.2. It is interesting to note that while R_{dt} is relatively small in each duct, R_{ct} increases from the bottom to the top of the pass. As the oil in the right vertical ducts accumulates through the combining junctions, the resistance to entrant flows from the horizontal ducts increases, reaching a maximum at duct number 8. The horizontal duct resistances R_1, etc., are approximately equal notwithstanding slight variations in K, as shown. Thus the action of the combining junctions introduces a marked asymmetry, especially at relatively high Re. The total flow resistance in duct 8 turns out to be almost twice that of duct 1. The situation in the left and right vertical ducts is presented in Fig. 8.3. In the dividing junctions at the entrances to ducts 1, 2 and 7, R_{ds} is actually negative. Pressure regain has occurred due to deceleration, enough to overcome frictional dissipation. At the other junctions, R_{ds} is positive, but small compared to R_1. A marked difference is evident in the combining junctions. Here R_{cs} is of the same order as R_r, and increases so that $R_{cs,8}$ is almost three times the magnitude of $R_{r,7}$. In the combining junctions, fluid acceleration causes a pressure drop which adds to frictional losses. The consequence of this asymmetry is that the total resistance to flow in the right hand vertical ducts is almost twice that of the left, and this has a marked effect on the flow distribution, as may be seen in Fig. 8.4. The prediction of the simple network model (the starting point of DISCNET's iterations) is compared with the DISCNET final results. The imbalance of the left and right vertical duct resistances leads to a skewed distribution. The oil finds it "easier" to proceed up the left vertical ducts, and so "accumulates" in duct number 8.

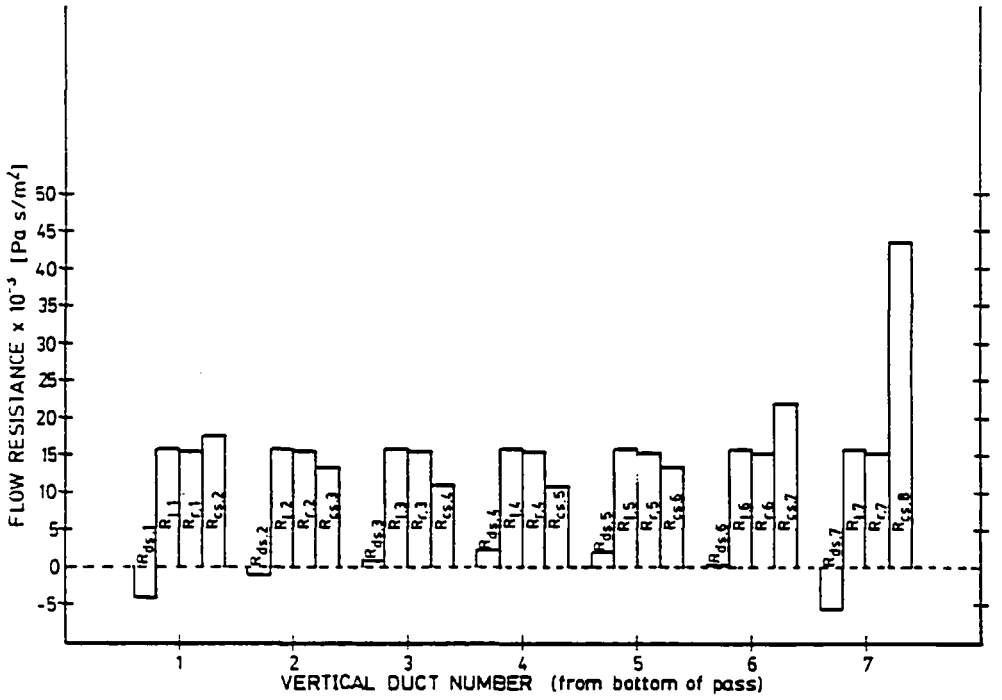


Fig. 8.3 Magnitude of Vertical Duct Flow Resistances

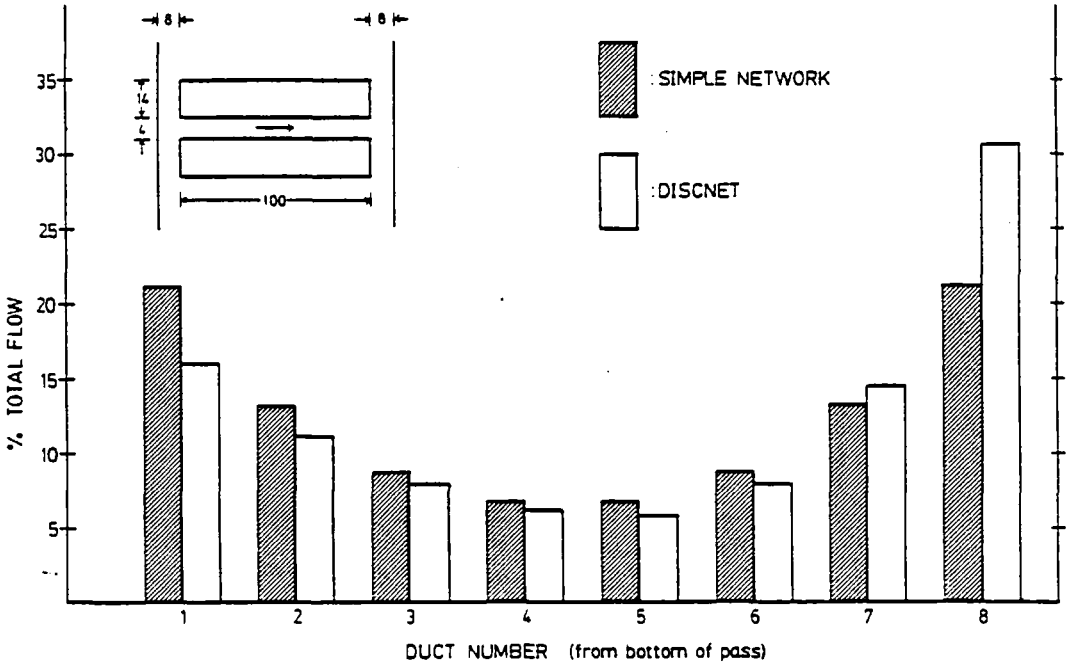


Fig. 8.4 Comparison of Simple Network and DISCNET Predictions

8.4 Conclusion The program DISCNET has been outlined and sample

calculations have been provided. It is evident that several important factors which significantly influence the flow distribution are introduced by including the effects of variable viscosity, junctions and corners. The example given here is that of a relatively high Reynolds number condition typical of forced convection, and it is evident that the momentum effects in the junctions predominate over variable viscosity effects. At lower flow rates typical of naturally cooled transformers, the reverse would probably occur. More examples of DISCNET calculations are given in Chapter 12.

It should be mentioned that, once the flow rate in each duct has been obtained using DISCNET, the local conductor temperatures in each disc are obtained using a fine-mesh (e.g. 22x9) version of DUCT. Examples of complete calculations are given in Chapter 12 also.

CHAPTER 9

EXPERIMENTAL WORK, INTRODUCTION

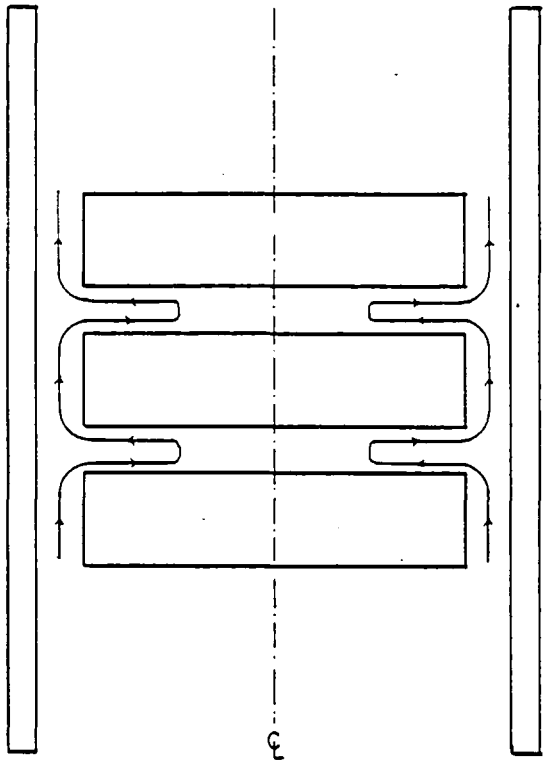


Fig. 9.1 Possible Flow Pattern in Disc Winding without Flow-Diverting Washers

9.1 Introduction Little experimental work has been published which involves the measurement of individual conductor temperatures and the flow distribution in horizontal ducts of disc-type transformer windings. Since it is highly inadvisable to embed thermocouples in windings intended for service, most thermal measurements have been made in models of various kinds or in expensive purpose-built experimental windings. Most of the studies are of disc windings without flow-diverting washers, Fig. 9.1 (see also Fig. 1.6), where in a perfectly symmetrical design and a perfectly horizontally located transformer the direction of flow

in the horizontal ducts is indeterminate and possibly proceeds as suggested by the arrows. Thiele (1941) carried out flow visualization studies in a model of a vertical sector of such a system under natural convection conditions. He found that by introducing thermal or geometrical asymmetries, a transverse flow in the horizontal ducts could be induced. In the absence of such a flow, one would expect the temperature distribution in the disc to be symmetrical about its centre-line. Lobenstein (1967) carried out similar experiments under forced convection conditions; his model consisted of 120 coil sections in some of which individual conductor temperatures appear to have been measured. He observed transverse flows in the horizontal ducts, with and without flow-diverting washers, and reports a disc temperature distribution qualitatively resembling that predicted by the DUCT program (Fig. 7.3). Brechna and Tschudi (1962) measured the temperature distribution, using thermocouples, in a model of a sector of a single disc. Their investigation was an attempt to improve the thermal design by using various baffling arrangements around the disc and by leaving 'gaps' of conductor pairs in the disc. Most of the flow configurations used bear little relation to a pass with flow-diverting washers. Taylor, Berger and Western (1958) performed experiments on both layer and disc windings. Their disc model consisted of a vertical section (only two discs in height) comprising (in the circumferential direction) an entire horizontal duct, two spacers on either side of it, and one-half of the two horizontal ducts on the outside of the two spacers. The section was flattened (as if the winding had an infinitely large mean radius). No flow diverting-washers were used. They report only mean disc temperatures, and assume an oil-flow pattern as shown in Fig. 9.1. Pivrnec and Havlicek (1972), built a similarly flattened model but containing 96 discs. Among their results are the mean disc temperatures,

under both natural and forced convection, for a winding configuration using flow-diverting washers, with 6 passes of 16 ducts each. Their results indicate substantial flow starvation at the top of each pass in which the flow is radially outward (from left to right, Fig. 3.1). The situation in the other passes was the converse of this. This asymmetry could have been caused by vertical duct dimensions b > a (see Fig. 3.1), although these dimensions are not specifically stated in the paper. Pivrnec (1973), made a further study of the flow characteristics in the same model. His results confirm an asymmetrical flow distribution. Oddly, he states that the vertical duct thicknesses were equal. The method of flow measurement is not described. Preiningerova and Pivrnec (1977), using (presumably) the same model, but without flow-diverting washers, report local conductor temperatures for selected discs. Lampe, Persson and Carlsson (1972), in their excellent critique of current practice in hot-spot and top-oil temperature measurement, mention a similar flattened model, placed between plexiglas (for flow visualization). The model contained 108 thermocouples and 400 tests were performed. Unfortunately, none of the detailed results of individual tests appear to have been published.

The intention of the experimental investigation presented in this thesis is to provide detailed information on individual conductor temperatures and horizontal duct flow rates in an 8 duct pass with flow-diverting washers, over a range of flow rates to include natural and forced convection conditions. The results are intended to provide verification of the computer analysis presented in Chapters 5 through 8. In this chapter, the experimental winding and ancillary apparatus will be described. In Chapter 10, the measurement of oil velocities using a hot-film probe will be discussed and in Chapter 11, the measurement of

temperature in the winding by thermocouples and resistance is described. The results of the tests, comparison with prediction, and conclusions are presented in Chapter 12.

9.2 The Experimental Winding The facsimile winding shown schematically in Fig. 9.2, designed by Szpiro (1980), differs from the other models mentioned in Sec. 9.1 in that it is a complete winding, not a sector or "slice". At the top of the figure, a plan view is shown, where it may be seen that the winding has 6 sectors. The base cylinder and outer barrier are both made from perspex, and are set off from the winding by 6 pressboard ribs on the inner diameter and 12 on the outer. The pressboard spacers are of an unusual shape. Due to the size of the experimental tank, the mean radius of the winding (177 mm) was made smaller than would normally be found in practice. The spacers were therefore designed to ensure that the width of the horizontal ducts would be uniform (here w = 100 mm), thus approximating more closely the situation in windings of larger mean radius. The draw-back of the design is that a greater proportion of the surface area of the discs is "masked" by the spacers (i.e. not in contact with the oil), than would be the case in commercial transformers.

The experimental winding has 16 discs, of 20 conductors each (with dimensions shown in the inset of Fig. 9.2), and was configured with 2 flow-diverting washers (each 2 mm pressboard) to have 2 passes of 8 ducts each. The upper pass, with the flow-diverting washers at top and bottom, may be seen in section A-A. Thus the oil, entering through the inlet pipe/flange is assumed to divide itself equally between the 6 sectors and enters the bottom of each lower pass through one of 6 circumferential slots in the steel base plate. The lower flow-diverting

washer forces most of the oil in the lower pass to flow radially inward; upon entering the upper pass the top flow-diverting washer causes the flow to proceed radially outward.

The spacers, nominally 2 mm thick, were installed in pairs to give a nominal horizontal duct thickness of 4 mm. Upon assembly and compression of the winding, however, considerable variations were noted and are shown in section A-A. 2 pairs of perspex cylinders were supplied, intending to provide inner and outer vertical duct thicknesses of 4 and 8 mm in any combination. Although valiant attempts were made to machine them to this specification, the smallest of the outer cylinders upon assembly resulted in an average vertical duct thickness of 8 not 4 mm. The problem was exacerbated by some circumferential variation in the radial width of the discs.

To measure the oil velocities in the 8 ducts of the upper pass, tapped holes were made in the outer cylinder (the top 4 are shown in the partial elevation of Fig. 9.2) to enable the hot-film velocity probe to be inserted into the horizontal ducts, about 30 mm in from the outer circumference of the disc. The photograph in Fig. 9.3 shows the assembled winding raised out of its tank, with the probe inserted in the top duct but one. Brass knurled plugs with neoprene O-rings were fitted to the other tapped holes. Visible in the photograph on the top of the upper flow-diverting washer are 12 spacers, a (grey) steel pressure ring and a (blue) steel top plate. An outer circle of short threaded rods bolted to the top plate compress the pressure ring. An inner circle of longer rods within the inner cylinder bolt the top plate to the base plate. These were tightened as necessary to prevent slippage of the discs whilst raising the winding from the tank to change the position of

the probe.

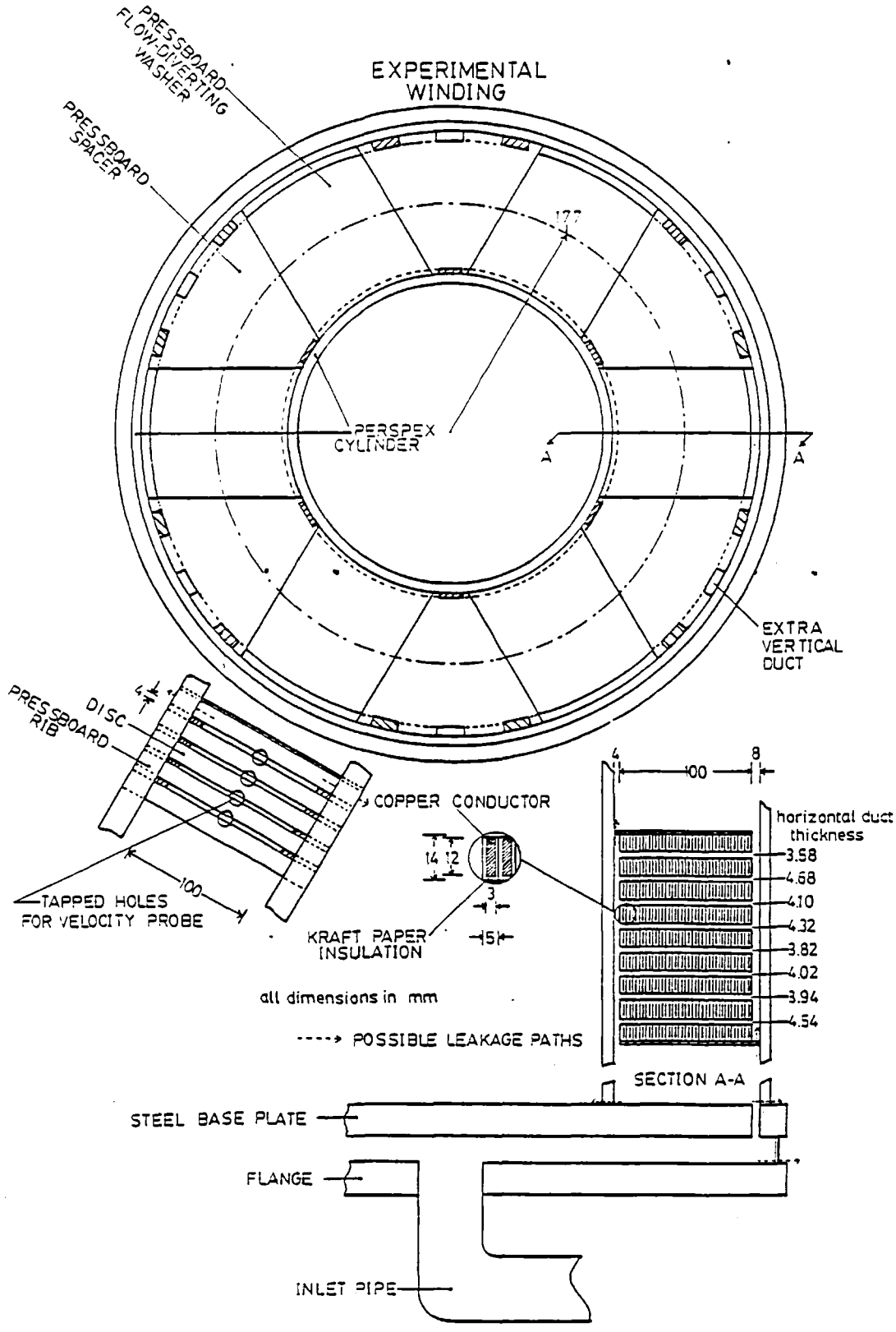


Fig. 9.2 Facsimile Winding

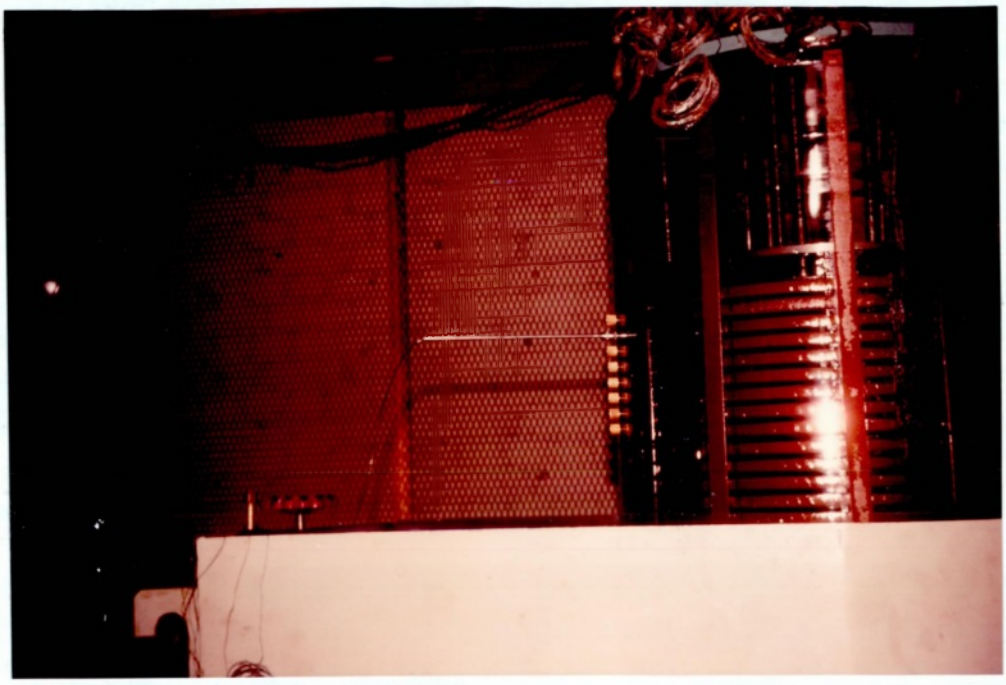


Fig. 9.3 Winding with Hot-Film Velocity Probe

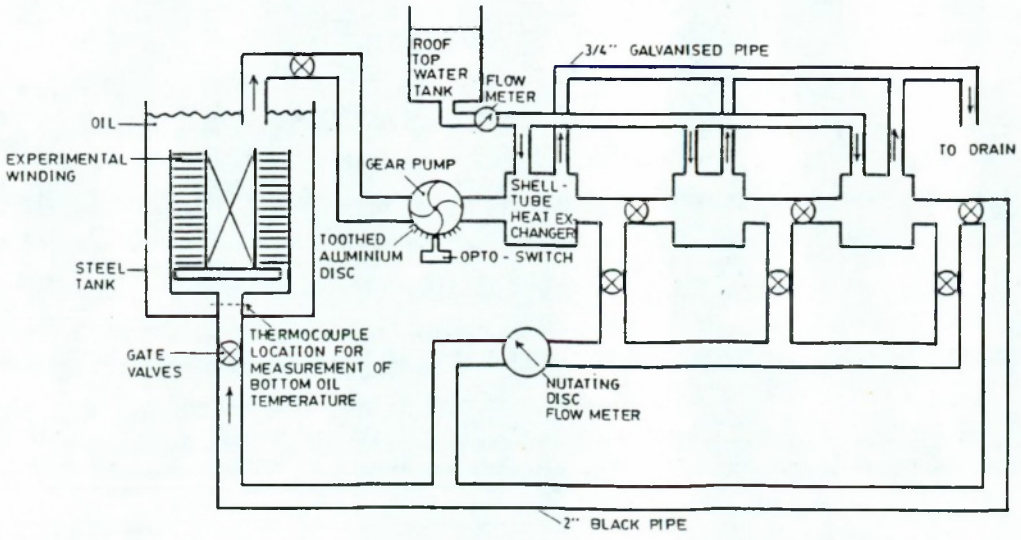


Fig. 9.4 Schematic of Hydraulic Circuit

9.3 Hydraulic Circuit A schematic of the hydraulic circuit is shown in Fig. 9.4. Oil flow was maintained by a gear pump, coupled, via pulleys and a timing belt in a 4:1 reduction to a compound wound D.C.

motor whose speed was controlled by a Ward-Leonard system (see Appendix C1). This arrangement afforded precise, even control of the flow rate over a wide range. The R.P.M./ flow rate characteristic of this positive displacement pump was linear, and independent of the oil temperature. A toothed aluminium disc was fitted to the pump shaft to measure the R.P.M. in conjunction with an Opto-Switch, an integrated circuit in a slot-shaped package. An infrared beam is directed across the slot to a detector on the other side; when interrupted by a passing tooth, a change in voltage occurs at the output of the device. As the pump shaft turns, a square wave is generated which is input to a frequency counter. The R.P.M., and therefore the flow rate (after calibration), may thus be easily monitored. The arrangement is shown in the photograph, Fig. 9.5. The pump motor (B 62) is shown in the foreground. The pump itself is behind the aluminium disc. The Opto-Switch (not visible) is fitted to the pump frame at the top of the disc. (A better view of the device may be found in Chapter 10, and details of its circuit are in Appendix C1). An R.P.M. vs. flow rate calibration was obtained using the nutating disc flow meter (Fig. 9.4), see Appendix C1. Visible in the background of the photograph are the 3 oil-to-water heat exchangers shown in Fig. 9.4. Each one is rated to dissipate 3.5 kW at an oil flow rate of 3.79×10^{-3} m^3/s (50 g.p.m.) They are arranged with by-passing valves so that 1, 2 or 3 may be used in series, for a total cooling capacity of 10.5 kW. This was far in excess of what was needed; only one was ever used. Cooling water was obtained from the nearest tap, being supplied from a roof top storage tank. 2" black pipe was used for the oil circuit, 3/4" galvanised on the water side (connected by 3/4" garden hose to the tap and drain). The system had been used previously by Finn (1971) for experiments involving layer windings. Extensive rearrangement was necessary to eliminate leaks and adapt the circuit for its present use.

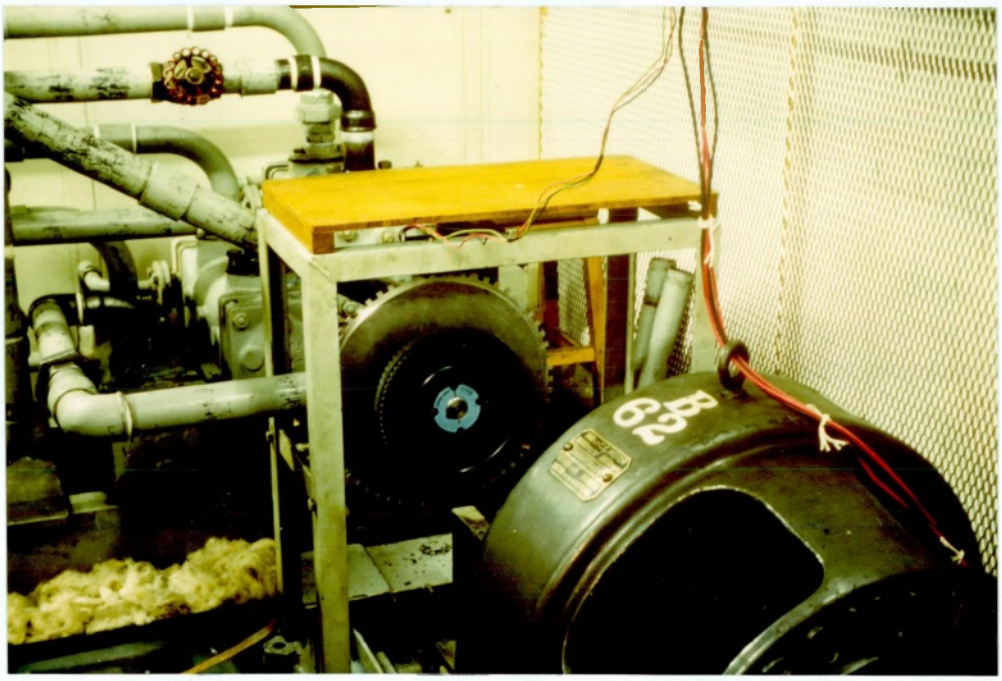


Fig. 9.5 Flow Rate Monitoring Arrangements

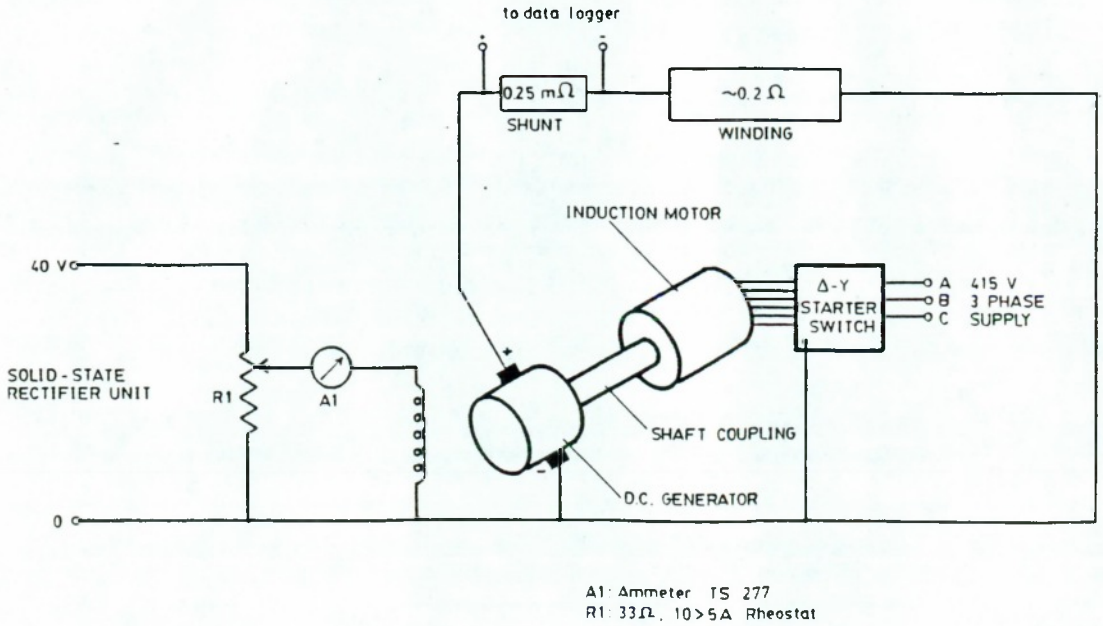


Fig. 9.6 Winding D. C. Supply Control Circuit

9.4 Electrical Circuit To simulate the I^2R losses in a transformer

under load, the winding was connected to a D.C. welding generator rated at up to 20 kW (40 V/500 A). The field was excited by a large solid-state rectifier unit, and the output current (normally set at about 150 A), was monitored using a 300 A (75 mV) shunt. The shunt volt drop was input directly to the data logger used to monitor the thermocouple voltages (see Chapter 11). The generator was shaft-coupled to a 3-phase (415 V) induction motor, which was started using a star-delta switch. The circuit is shown in Fig. 9.6, and more detailed equipment specifications are given in Appendix C2.

9.5 Concluding Remarks The apparatus described provided steady winding currents and flow rates. The heat exchangers (thanks to a water supply at approximately constant temperature) enabled the system to reach a stable steady-state in a few hours.

CHAPTER 10

HOT-FILM VELOCITY PROBE MEASUREMENTS

10.1 Introduction The measurement of local fluid velocities by the technique of hot-wire anemometry is now well established. The method is based on the existence of a simple empirical correlation, due to Kramers (1946), for the heat transfer from a stationary circular cylinder of infinite extent whose surface temperature is constant and is immersed in a steady stream:

$$Nu_m = 0.42Pr^{0.2} + 0.57Pr^{1/3}Re^{1/2}, \tag{10.1}$$

where

$$Nu_m = \frac{\dot{q}''_{w,m} D}{k(t_{w,m} - t_\infty)}, \tag{10.2}$$

where D is the diameter of the cylinder, $\dot{q}''_{w,m}$ is the average surface heat flux from the cylinder, $t_{w,m}$ is the average wall temperature and t_∞ is the temperature of the undisturbed free stream. Here,

$$Re = \frac{UD}{\nu}, \tag{10.3}$$

where U is the (uniform) free stream velocity, and the fluid properties are evaluated at the film temperature t_f:

$$t_f = \frac{t_{w,m} + t_\infty}{2} . \qquad (10.4)$$

Equation (10.1) is usually referred to as King's Law because it is of the form predicted by an early theory due to King (1914). The correlation is good over a wide range ($0.1 < Re < 10^4$). A thin wire mounted between two slender prongs approximates an infinite cylinder well, provided that conduction off the ends of the wire to the probe supports is negligible. The small wire diameter (typically 25 μm) ensures that, according to Hinze (1959), the hot wire probe (in air) can be used over a velocity range $4.0 < U < 4.0 \times 10^4$ m/s. A common application of the probe has therefore been the measurement of turbulent air flows.

If a probe of resistance R_p and surface area A_p carries a current I_p, then

$$\dot{q}''_{w,m} = \frac{I_p^2 R_p}{A_p} . \qquad (10.5)$$

Modern hot-wire anemometers use a 'bridge-feedback amplifier' (see Perry and Morrison (1971)) which effectively maintains the wire at a constant temperature (hence constant R_p) by varying I_p according to U (t_∞ is assumed constant). The voltage drop across the probe V_p is therefore proportional to $U^{1/4}$. The exact relationship in a specific instance is always obtained by calibration.

Use of hot-wire anemometry in liquids, particularly oils, is far less common. Eckelmann (1972) found that wire probes were unsuitable for measurements in Shell 3101 mineral oil. If $t_{w,m}$ was maintained above

200 ^{o}C, cracking of the oil would occur, and subsequent polymerization would cause honey-like dirt deposits to form on the wire. Below that temperature, a temporary desensitizing coating forms, only a few μm thick. The above two effects rendered the velocity measurements totally unreliable.

Eckelmann also conducted experiments using quartz-insulated hot-film probes and found them to be free from the above problems, and capable of yielding reproducible calibration curves. Based on his experience, it was decided to use the same probe type for the transformer oil velocity measurements in the horizontal ducts of the experimental disc winding.

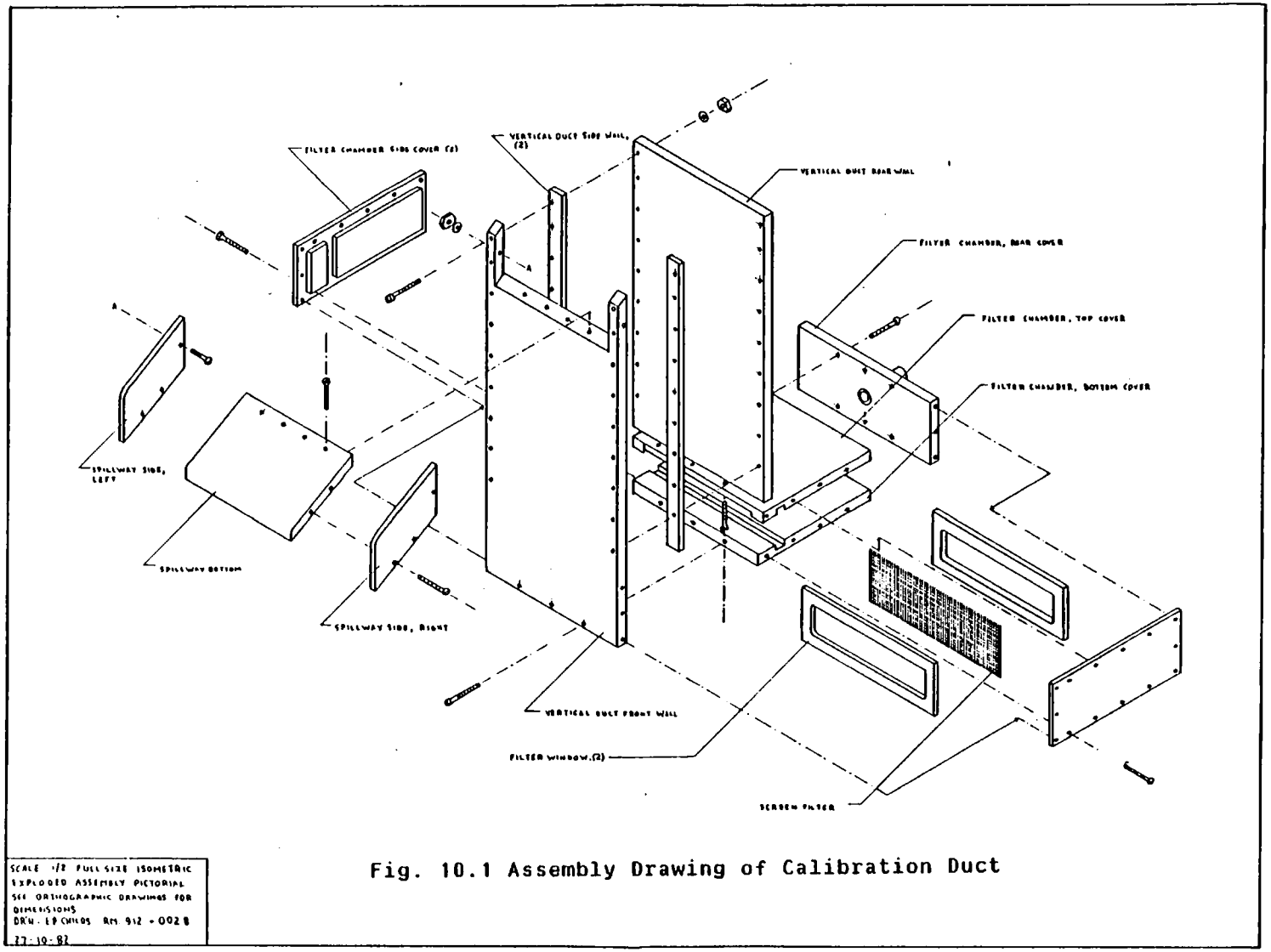
There were three other problems specific to the present application. First, the reclaimed transformer oil (B.S. 148) used in the experiments contained 'lint': very fine fibers which tended to wrap themselves around the probe and cause desensitization. Second, the probe was to be used to measure the centre-line velocity in a thin (4 mm) duct, and there was concern about the influence of the nearby disc surface (2 mm away) on the probe response. Finally, the measurements had to be made over a temperature range of about (20 - 80 ^{o}C).

The first difficulty was partly resolved by filtering the oil through a 100 mesh phosphor bronze screen. Some lint still collected on the probe but the much smaller fibers were easily dislodged by tapping the probe holder. The second circumstance led to the design and construction of a novel calibration duct. To deal with the wide temperature range of the measurements, in which the Prandtl No. of transformer oil varies from 400 - 60, an attempt was made to find a

correlation similar to (10.1), and valid over the operating range of Reynolds and Prandtl numbers in the experiments.

10.2 Calibration Apparatus The calibration of hot-wire probes in air is usually easily done in a wind-tunnel where there is ample room to install other devices (e.g. Pitot tubes) for comparison purposes. In liquids, the situation is not as straightforward. A common method is to use a cylindrically shaped container of liquid on a rotating turn-table. After spinning at constant speed for a while, the liquid assumes the motion of a solid body. The probe may be dipped quickly into the liquid at a specified distance from the center of rotation. Examples of this technique may be found in Bertrand and Couders (1978) and Gourdon, et al. (1981).

It is generally recommended that a probe be calibrated in an environment as similar as possible to the one in which the measurements will be made. Though hot-film probes are designed to be used in very close proximity to solid surfaces (e.g. in boundary layer applications), their influence on the local temperature and velocity profles must be taken into account. The correlation (10.1) strictly applies to uniform, free-stream conditions; if significant velocity and temperature gradients are present at the point of probe measurement, errors may occur. Wills (1962) discusses the increased rate of heat loss from a hot-wire probe in air in close proximity to a wall having a much higher thermal conductivity than the fluid. The increased $\dot{q}''_{w,m}$ will give rise to a higher apparent velocity.



SCALE 1/2 FULL SIZE ISOMETRIC
EXPLODED ASSEMBLY PICTORIAL
SEE ORTHOGRAPHIC DRAWINGS FOR DIMENSIONS
DRW. EP CHILDS REF. 912 - 002 B
27-10-82

Fig. 10.1 Assembly Drawing of Calibration Duct

Wills's work is not strictly applicable to the situation in disc windings since the surface material, kraft paper insulation, has a thermal conductivity of the same order as transformer oil. If anything, one would expect $\dot{q}''_{w,m}$ to be reduced by the wall heat flux $\dot{q}''_{w}$, leading to lower apparent velocities. Presumably this would only occur if the thermal boundary layer had extended to the centre-line of the duct, i.e. if the temperature profile were fully developed, an unlikely situation in this application. The decision was therefore taken to build a calibration duct of exactly the same cross-section (4 mm x 100 mm) as the disc winding ducts out of perspex. The surface of the calibration duct was unheated, therefore the effect of $\dot{q}''_{w}$ on $\dot{q}''_{w,m}$ was neglected. The oil was to be circulated into and out of a tank equipped with a heater stirrer by means of a positive displacement pump with a linear r.p.m. vs. flow rate characteristic which was independent of temperature. To accomplish these ends, a novel design was required.

An exploded isometric assembly pictorial of the duct is shown as Fig. 10.1. The dimensioned orthographic drawings may be found in Appendix C3. The oil enters through the tube in the filter chamber rear cover, passes through the filter, and proceeds up the vertical duct. The probe is inserted through the opening in the top of the duct, and centred with respect to the duct walls about 200 mm from the bottom of the duct. It was assumed that the velocity profile was fully developed at that section. The oil, emerging through the top, runs down the spillway into the tank. A photograph of the duct with the probe inserted is shown as Fig. 10.2. Fig. 10.3 shows part of the duct and the tank, both of which are normally lagged. At the rear is the small diesel injector gear pump (covered with lagging). The pump R.P.M. were

monitored exactly as for the larger flow circuit described in Chapter 9. The pump, toothed aluminium wheel and Opto-Switch are shown as Fig. 10.4. The pump was coupled to a 200 V D.C. shunt motor, run at full field, but varying the armature volts by means of a rheostat. The speed control was reasonably smooth and reliable over a range of 13 - 800 R.P.M. The flow rate vs. R.P.M. calibration was obtained using a stop-watch and a graduated cylinder. The calibration curve is given as Fig. 10.5.

10.3 Calibration Procedure A DISA 55M10 CTA Standard Bridge was used in conjunction with a 55R11 quartz-insulated hot-film probe. The constant temperature bridge in its 'operating mode' maintains the probe at a resistance R_p which is preset by the operator. In 'resistance mode', a small current (0.8 mA) is put through the probe so that its resistance R_∞ at the ambient fluid temperature t_∞ can be determined. The overheat ratio, O.H.R., is related to the temperature difference between the probe and the ambient, and is defined as

$$O.H.R. = \frac{R_p - R_\infty}{R_\infty}. \qquad (10.6)$$

The resistance-temperature relationship is assumed to be of the form

$$R_p = R_{20}[1 + \alpha_{20}(t_{w,m} - 20)], \qquad (10.7)$$

where R_{20} and α_{20} are respectively the resistance and temperature coefficient for the probe at 20 ^{o}C, and are usually specified for each probe supplied by the manufacturer.

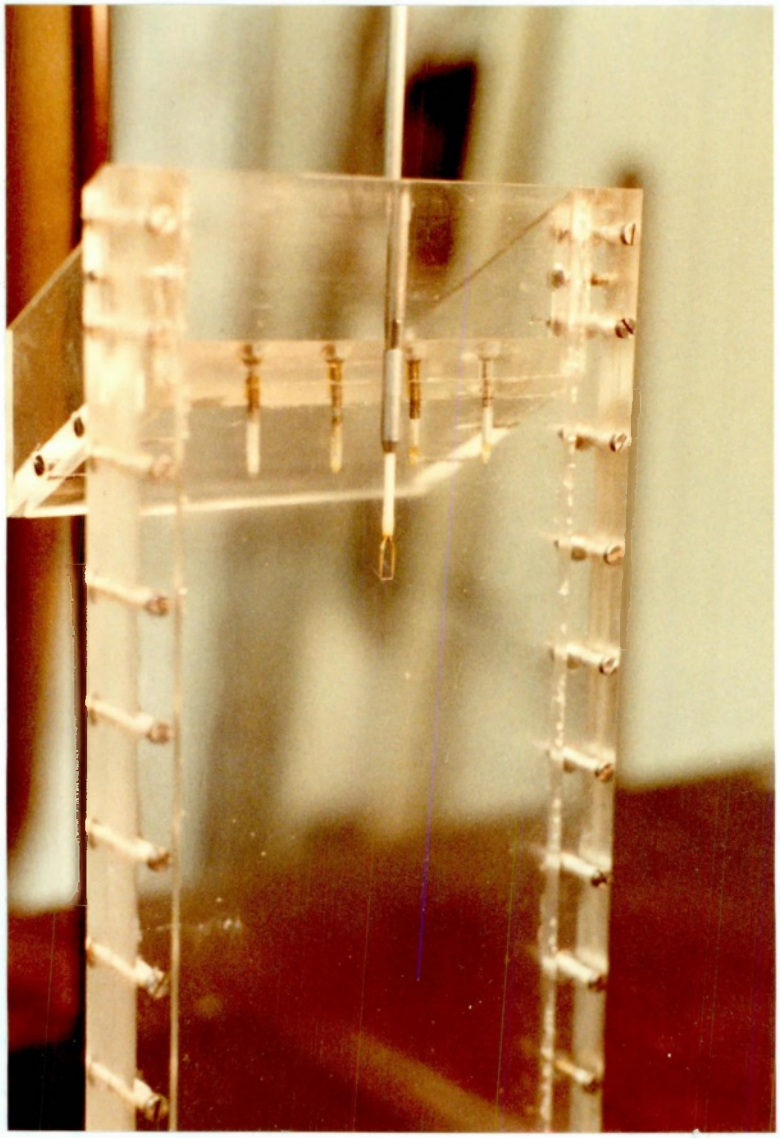


Fig. 10.2 Calibration Duct with Velocity Probe

The O.H.R. is inconvenient to use if R_∞ varies substantially in the course of the measurements, and it is desired to maintain a constant temperature difference $t_{w,m} - t_\infty$ over the whole range of t_∞. Here, the resistance difference $R_p - R_\infty$ was maintained constant at 1.2 Ω, corresponding to a temperature difference of 58.5 ^{o}C. Tests were carried out varying t_∞ in 20 ^{o}C increments from 20 ^{o}C to 80 ^{o}C. Thus the maximum probe temperature was 138.5 ^{o}C. The hot film probe could not be operated

above 150 ^{o}C.

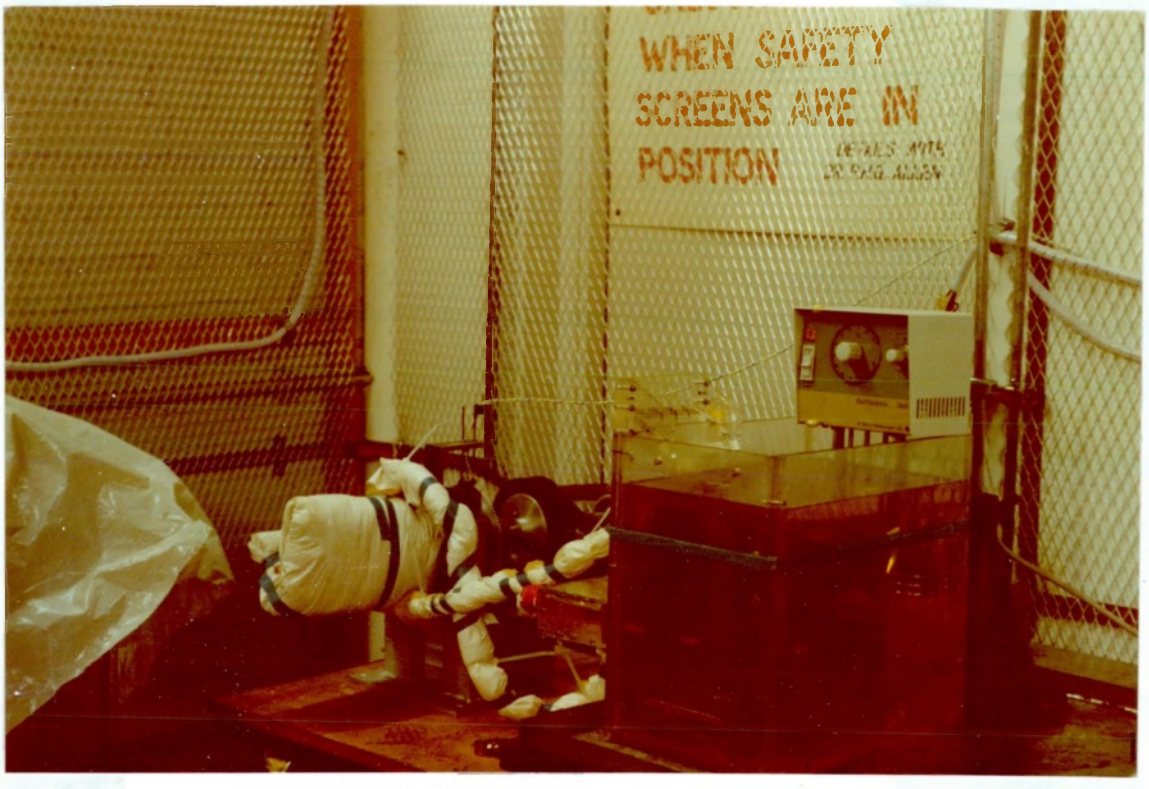


Fig. 10.3 Calibration Duct, Tank and Pump Assembly

Once the oil in the tank had come to the selected temperature as controlled by the heater-stirrer, the output voltage from the bridge V_{out} (which is proportional to V_p, the voltage drop across the probe) was recorded, together with R_p and R_∞, while varying the flow rate in the calibration duct from 0.2 - 30.0 cm^3/s. As the flow in the calibration duct was assumed fully-developed (and isothermal) at the probe measurement section, the analytical solution due to Dryden, et al. (1932) and Marco and Han (1955) was used to determine the value of the duct centre-line velocity U as a function of duct mean velocity u_m. Natarajan and Lakshmanan (1972), provide a formula for determining U/u_m at various duct aspect ratios. Here, the aspect ratio (100/4) is 25 and their formula gives

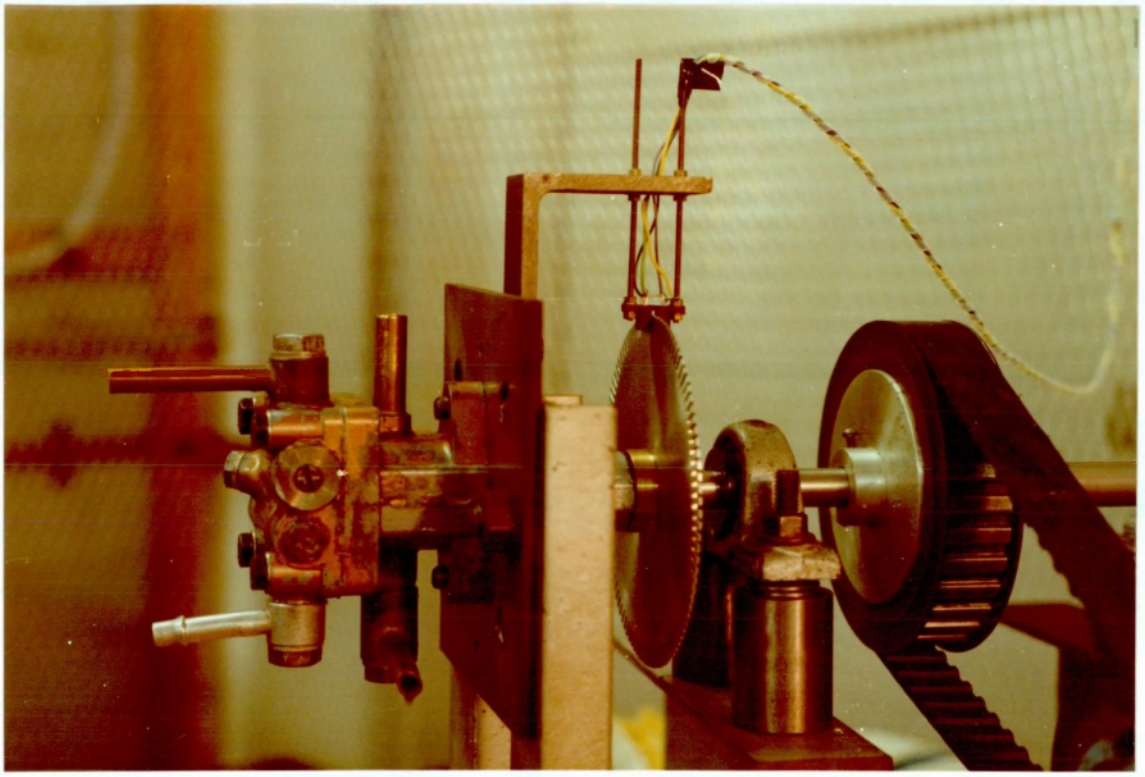


Fig. 10.4 Toothed Aluminium Disc and Opto-Switch

$$U/u_m = 1.54, \qquad (10.8)$$

which is very close to the parallel plane duct value of 1.5. Taking (10.8) in conjunction with the calibration curve, Fig. 10.5, and given the cross-sectional area of the calibration duct (10 cm x .4 cm = 4 cm^2), one obtains

$$U\ [cm/sec] = R.P.M. \times 0.0120. \qquad (10.9)$$

5 readings each were taken of R.P.M. and V_{out} at each flow rate setting and the results averaged. The standard deviation was typically less than ±0.5%. A linear plot of V_{out} vs. U obtained at room temperature is given as Fig. 10.6. This curve was used for the first set of flow measurements

in the unheated winding described in Chapter 12.

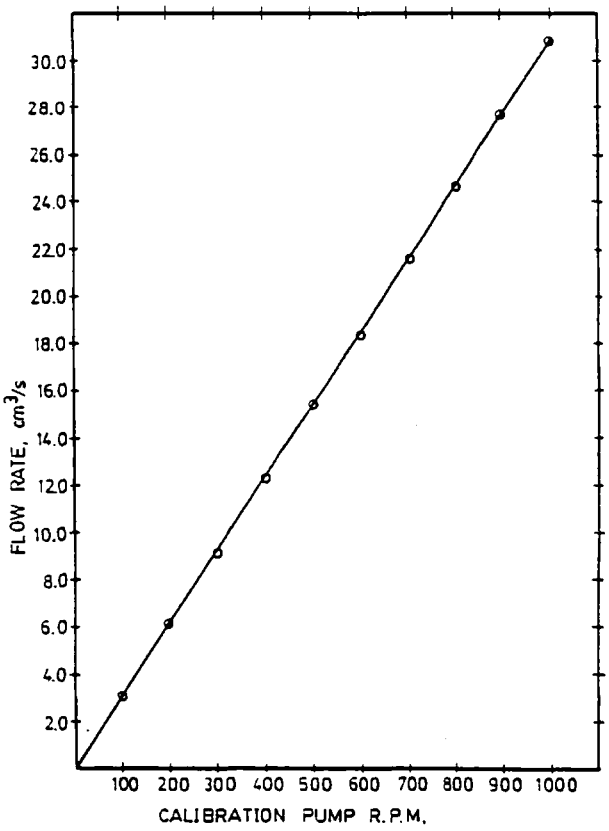


Fig. 10.5 Calibration Curve for Diesel Injector Pump

10.4 Correlation of Results The calibration results are usually correlated in the King's Law form,

$$V_{out}^2 = A_1 + A_2 U^{1/2}, \qquad (10.10)$$

where A_1 and A_2 are numerical constants to be determined. This is a useful form provided that all measurements are carried out at the same temperature. Most methods of compensation for variations in t_∞, e.g. Hollasch and Gebhart (1972), assume that A_1 and A_2 are only weak functions of t_∞. This is impossible in the case of transformer oil. It was therefore necessary to seek a more general correlation of the form

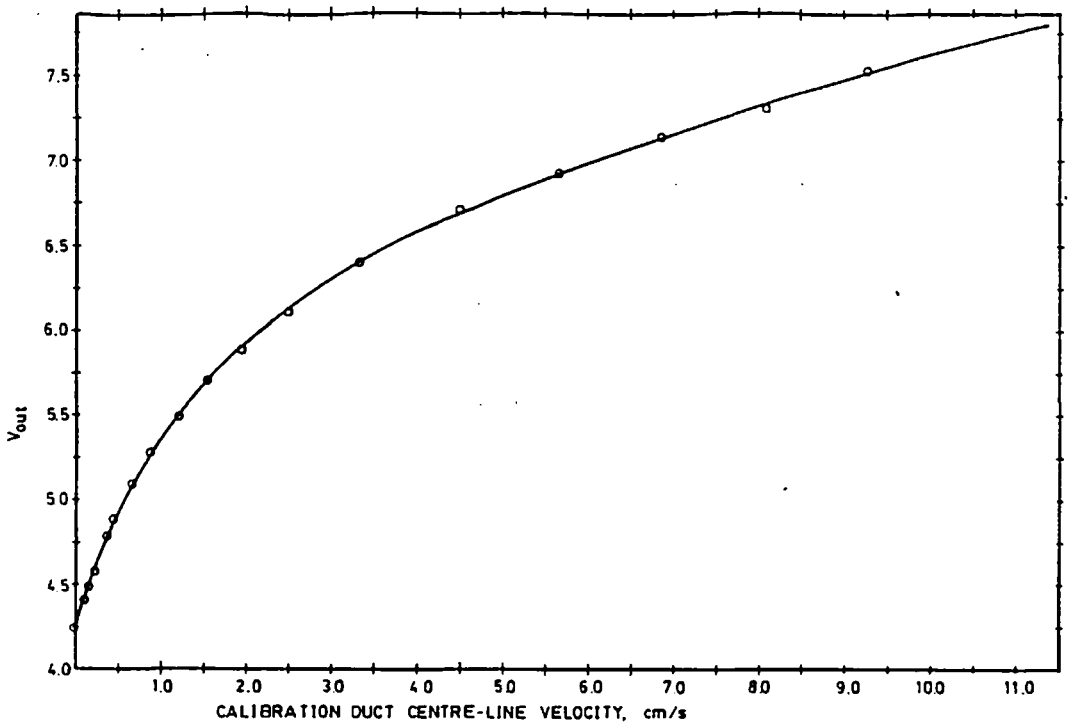


Fig. 10.6 Room Temperature Hot-Film Probe Calibration Curve

$$Nu_m = EPr^m + FPr^n Re^{1/2}, \qquad (10.11)$$

where E and F are constants to be determined, as are exponents m and n. (10.11) is in the same form as (10.1), with Nu_m, Re and Pr all defined in the same way. To use this correlation, a relationship was needed between V_{out} and V_p (from which $\dot{q}''_{w,m}$ is determined). This was obtained from the DISA 55M10 CTA (1977) instruction manual as

$$V_p = \frac{V_{out} R_p}{R_p + R_T + R_{CA}}, \qquad (10.12)$$

where R_T is the 'top' bridge resistance (50 Ω) and R_{CA} is the resistance of the cable and probe leads up to and including the probe supports (0.5 Ω). Since R_p varies with t_∞ (from about 6.0 Ω to 7.3 Ω), V_p and V_{out} are

not related in a fixed ratio.

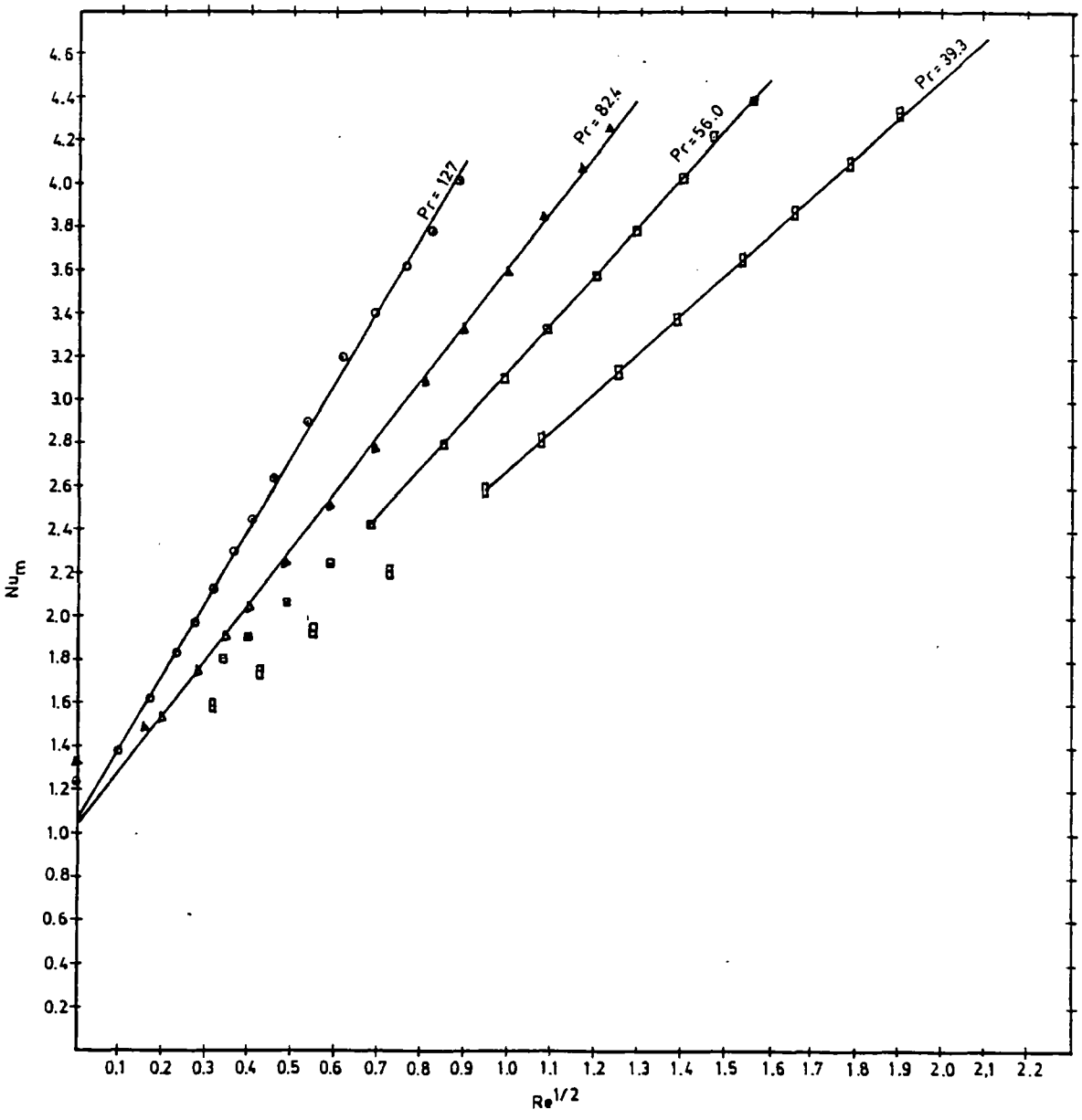


Fig. 10.7 March 1982 Probe Calibration

The correlation procedure was to take the results of the constant temperature runs (in which, in particular, Pr is constant, or nearly so), plotting, for each, Nu_m vs. $Re^{1/2}$. A family of straight lines was obtained over the entire temperature range, although while working at the high temperatures and low flow rates, it was difficult to maintain

t_∞ constant. Despite the lagging applied all round the circuit, the oil would cool by as much as 2 - 3 ^oC under the worst conditions while flowing up the calibration duct. The calibration curves are plotted, for a total of 10 runs conducted over a period of one year (using the same probe), in Figs. 10.7 - 10.9. (The manufacturer advises regular recalibration of the probe, as its response tends to deteriorate with age). The calibration runs included as Fig. 10.7 were done in an early prototype of the calibration duct, in which extreme difficulties were encountered with cooling of the oil (as much as 10 ^oC) at low flow rates and oil bath temperatures of 60 - 80 ^oC (Pr = 56.0 and 39.3). Thus the lower points on these two curves do not fall on the straight line drawn through the upper portion of the data. This situation improved with the later runs of Figs. 10.8 and 10.9. In general, the scatter is minimal, and the correlation appears to be good as low as Re = 0.01. A linear least-squares fit on the data is given as Table 10.1. To determine E, F, m and n in equation (10.11), log-log plots were made of the slopes and y-intercepts in Table 10.1, and a least squares fit was again made. The result (plotted with linear axes) is shown as Fig. 10.10, and considerable scatter is evident. The final expression obtained was

$$Nu_m = .5407Pr^{.1395} + .2216Pr^{.5585}Re^{1/2} \quad . \qquad (10.13)$$

This one expression would be used as follows. A single reading of the DISA bridge, in both operating and resistance mode, would yield R_p, R_∞ and V_{out}. t_f would be obtained from (10.7) and (10.4), and all property values would be calculated at this temperature. Nu_m would then be found from (10.2), (10.5) and (10.12). Solving (10.13) for $Re^{1/2}$, U would finally be obtained from (10.3). The accuracy of the correlation was checked by attempting to reproduce the calibration data. A random sample

of data from all 10 calibration runs was used, and the error in predicted U was found to be as much as ±17%.

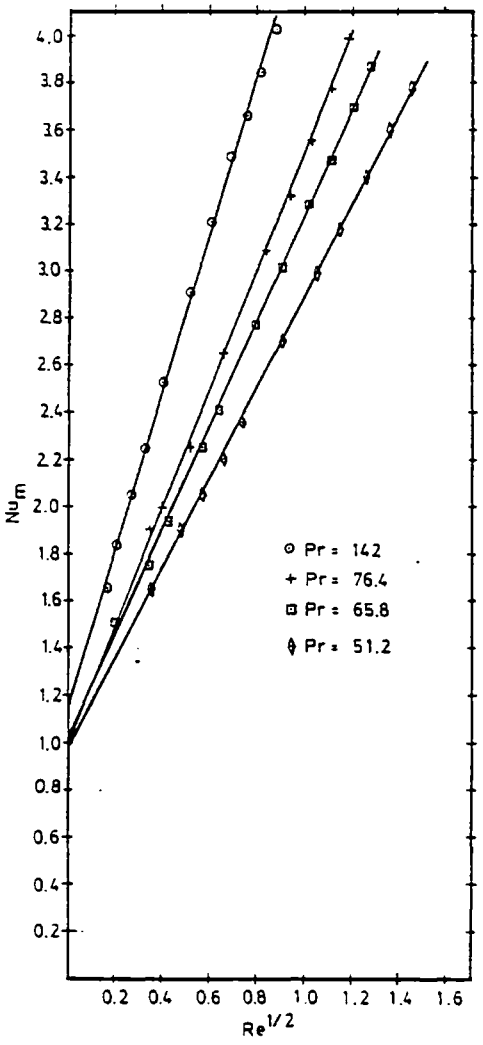


Fig. 10.8 Feb. 1983 Calibration

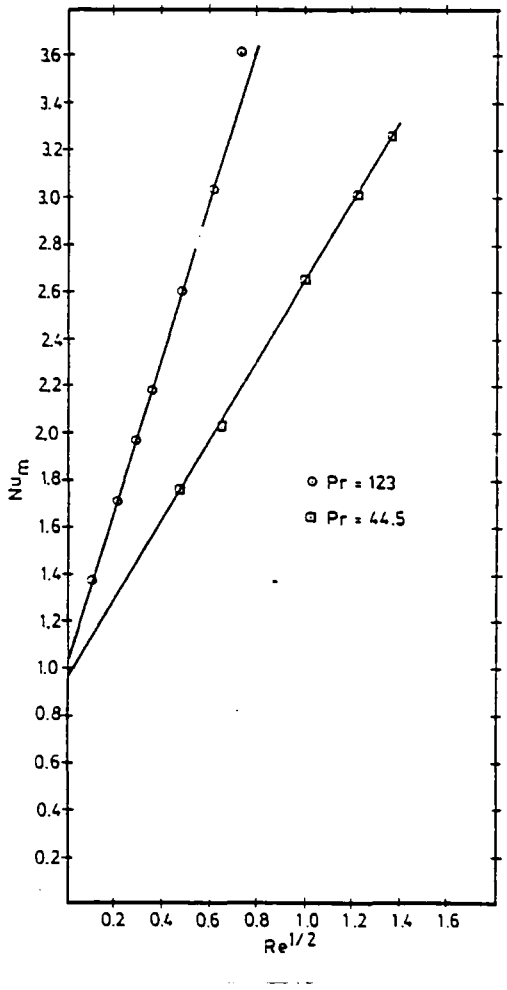


Fig. 10.9 March 1983 Calibration

10.5 Discussion This result, from long tests and tedious correlation, is somewhat disappointing, and means that the measurement of horizontal duct flow rates, as reported in Chapter 12, was subject to considerable uncertainty. The major sources of error were presumed to be 1.) failure to keep Pr exactly constant in each run, 2.) variations in the response of the probe over a year of use, 3.) undetected fouling of the probe by lint in the oil and 4.) possible departure from the

correlation at Re < 0.1. The latter is suspected as the error in reproducing the lower values of U was usually greater. Matters could presumably be improved through the use of a more precisely controlled, perhaps automated hydraulic circuit, interconnected with a data logger or dedicated microcomputer, and using more sophisticated correlation, especially for lower values of U. This was unfortunately beyond the time and resources allocated to the project. As will be seen, however, the hot-film probe provides useful, if not highly accurate information about the actual flow distribution in the winding. This will be discussed in Chapter 12.

Pr = 141.9,	$Nu_m = 1.124 + 3.415Re^{1/2}$
Pr = 127.0,	$Nu_m = 1.048 + 3.393Re^{1/2}$
Pr = 123.0,	$Nu_m = 1.013 + 3.266Re^{1/2}$
Pr = 82.4,	$Nu_m = 1.020 + 2.601Re^{1/2}$
Pr = 76.4,	$Nu_m = 0.979 + 2.546Re^{1/2}$
Pr = 65.8,	$Nu_m = 0.996 + 2.265Re^{1/2}$
Pr = 56.0,	$Nu_m = 0.900 + 2.243Re^{1/2}$
Pr = 51.2,	$Nu_m = 0.967 + 1.949Re^{1/2}$
Pr = 44.5,	$Nu_m = 0.950 + 1.685Re^{1/2}$
Pr = 39.3,	$Nu_m = 0.875 + 1.810Re^{1/2}$

Table 10.1 Least Squares Fit of Calibration Curves

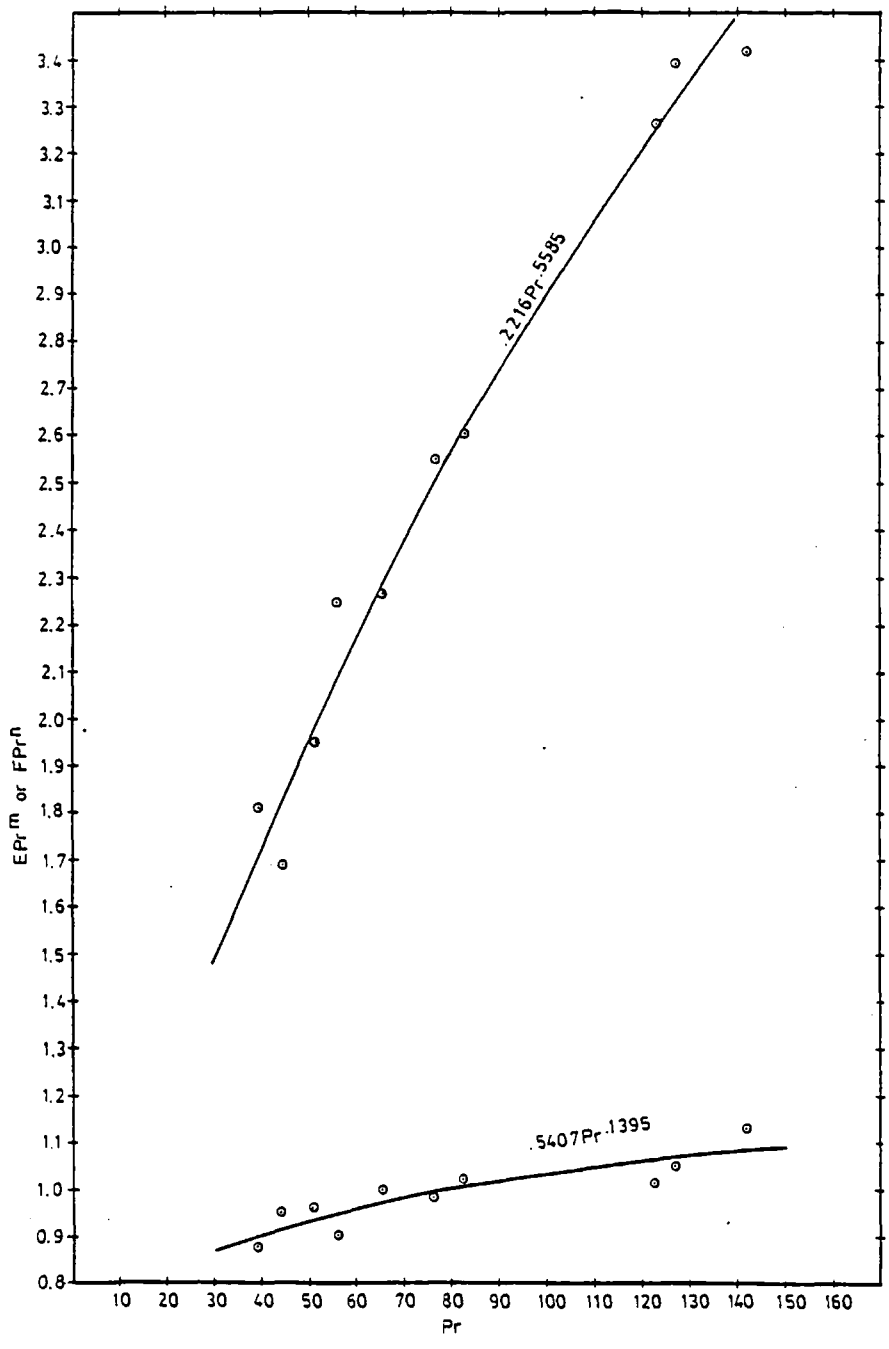


Fig. 10.10 Correlation Coefficients as a Function of Pr

CHAPTER 11

WINDING TEMPERATURE MEASUREMENTS

11.1 Introduction When oil-immersed transformers are tested for service, only two temperature measurements are required under B.S. 171:Part 2:1978, the winding temperature rise $\theta_r = t_r - t_a$ and the top-oil temperature rise (θ_t or θ_c, see Chapter 1). t_r is obtained by the resistance method from the formula

$$t_r = \frac{R_{avg}}{R_o}(235 + t_o) - 235, \qquad (11.1)$$

where R_{avg} is the mean winding resistance under test conditions, and R_o is the cold winding resistance at some datum temperature t_o. The ambient temperature t_a may be the cooling air or water temperature, depending on the type of cooler fitted. t_t or t_c is measured with a thermometer placed in an oil-filled thermometer pocket on the cover or in the outlet pipe to the cooler (see Fig. 1.4). These measurements are made in lieu of a direct determination of the hot-spot temperature, for which no reliable and safe method has yet been devised.

The experimental winding described in Chapter 9 is supplied with a D.C. current at low voltage, hence thermocouples could be safely embedded in the individual discs as desired, the intention being to measure the hot-spot temperature directly. The hot-film probe, installed as described in Chapter 9, was also used to measure, whilst in resistance mode the centre-line oil temperature 70 mm from the entrance of each horizontal duct in the top pass of the winding.

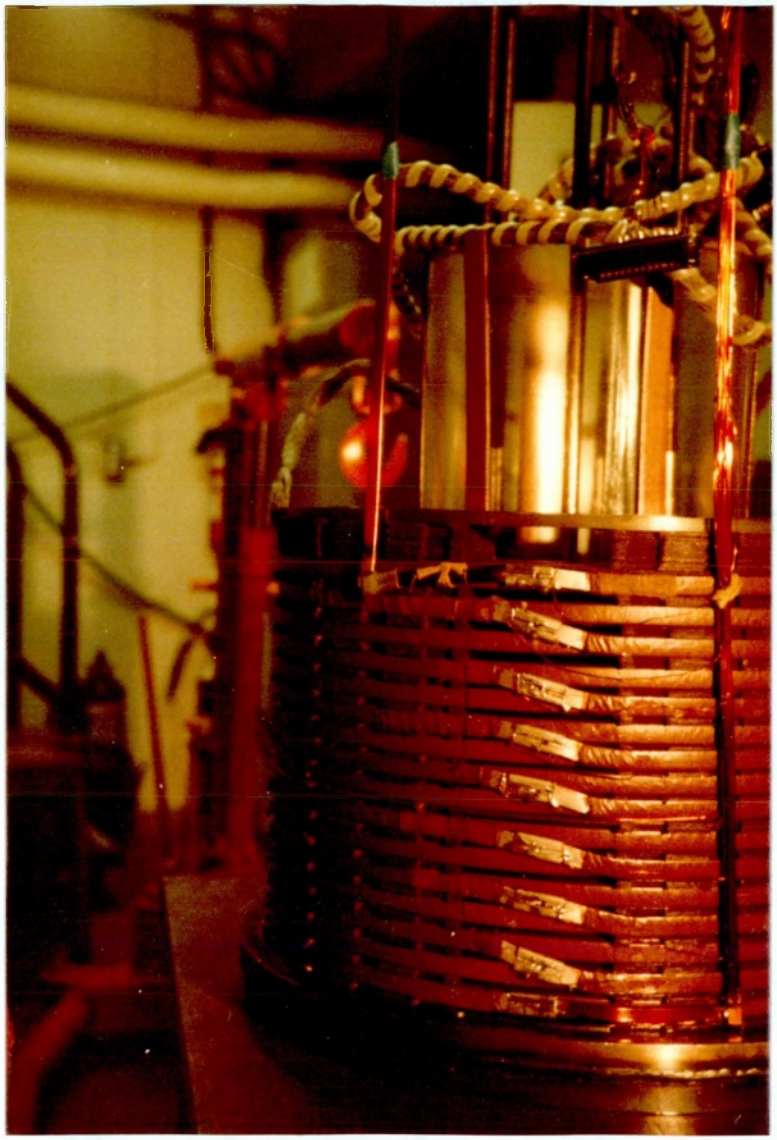


Fig. 11.1 Facsimile Winding Disc Voltage Taps

Successful computer prediction of the local temperatures in the winding requires knowledge of the bulk oil temperature at the bottom of the winding t_b and an attempt was made to measure it. For overall energy conservation checks, measurement of the bulk temperature of the oil as it emerges from the top of the winding (t_w) was also attempted. As Lampe, Persson and Carlsson (1972) have pointed out, t_w generally does not equal t_t or t_c, since the oil emerging from the top of the windings

mixes with a substantial amount of stagnant oil at the top of the tank, only some of which may flow into the cooler (see Fig. 1.4). Yamaguchi, et al. (1980) provide an excellent discussion of this point. The cooling water temperature t_a was noted and found to be 15 - 20 ^{o}C, depending upon the time of year. The mean winding temperature t_r, as well as the mean temperature $t_{r,1-2}$, etc. of each disc pair was also recorded for completeness. In this chapter, various aspects of these temperature measurements will be discussed, concluding with a description of the overall test procedure and thermal characteristics of the experimental system.

11.2 Mean Winding Measurements by Resistance The B.S. 171 formula for calculating the mean winding temperature (11.1) is based on a resistance-temperature coefficent α_{20} = .00392 $^{o}C^{-1}$. The winding was manufactured as 8 coil pairs, each wound from a continuous insulated conductor, the cross-over from disc to disc in each pair occurring on the inside diameter. The 8 pairs, upon final assembly, were soldered at the cross-over points on the outer diameter, as shown in the photograph Fig. 11.1. The voltage measurement taps at each outer cross-over, consisting of light gauge enamelled copper wire, are also visible. The arrangement is shown schematically in Fig. 11.2. The volt-drop across each disc pair, and across the 0.25 mΩ current shunt, were input to the first 9 channels of the data-logger, as shown. (Further details of the equipment may be found in Appendix C2). The resistance of each disc pair was calculated from the measured volt drop and current. R_o in (11.1) was determined by allowing the winding to come to room temperature overnight, then passing a current through it too small (11.5 A) to disturb its equilibrium temperature t_o taken to be the average of the 99 embedded thermocouple readings (25.2 ± 0.4 ^{o}C).

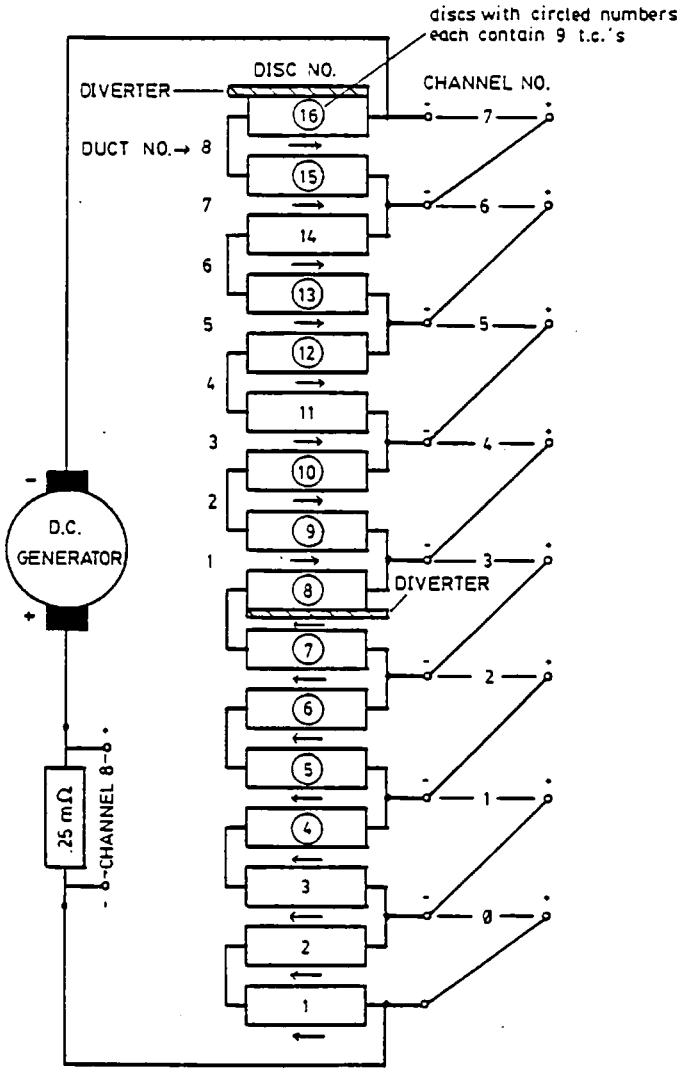


Fig. 11.2 Schematic of Disc Voltage Taps

11.3 Thermocouple Measurements 106 thermocouples in all were fitted, 99 in the winding itself, 2 and 5 to measure the bottom and top oil temperatures, respectively. The thermocouples (t.c.'s) were all made from 2 batches of 33 SWG Type J (iron-constantan) wire, insulated with glass fibre. A calibration check of one of the t.c.'s was made using a manufacturer-calibrated Type K digital thermometer. The curve, Fig. 11.3, is seen to be in close agreement with the values given in the CRC Handbook (1977), p. E-110. The slope of the curve was 52.9 $\mu V/^{o}C$.

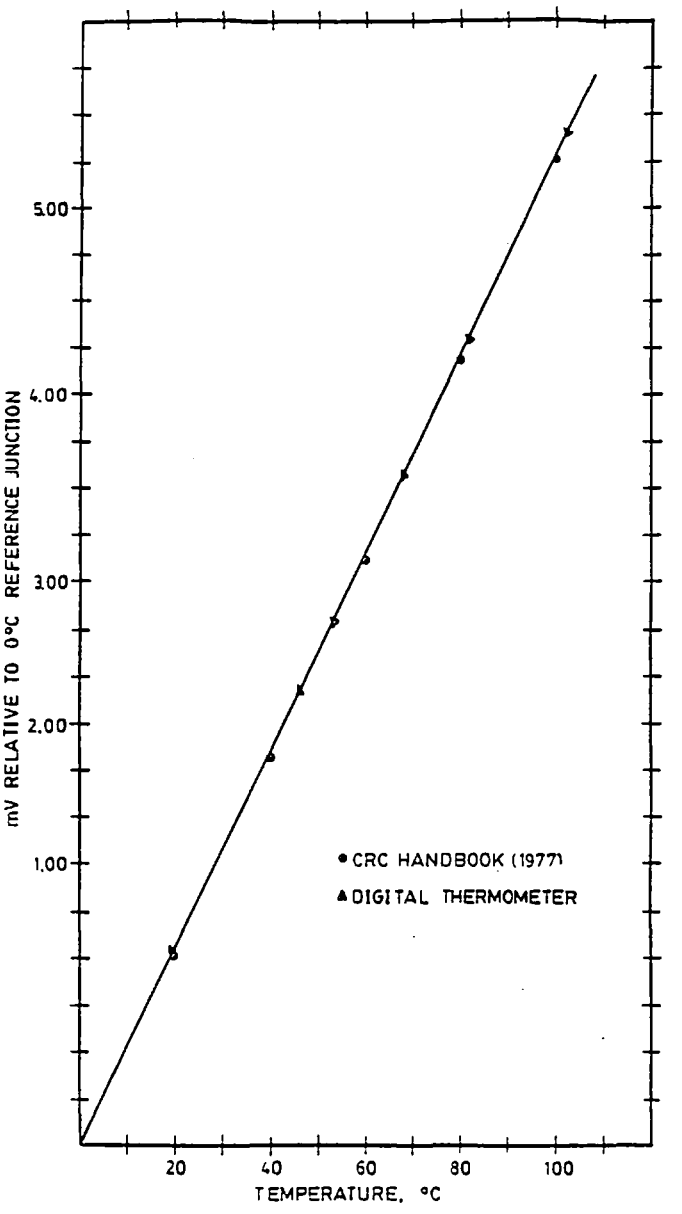


Fig. 11.3 Thermocouple Calibration Curve

Ideally, each thermocouple pair should be run continuously from the measurement junction to its own cold junction. Given the large number of t.c.'s, a compromise was sought, and the 'zone-box' circuit was used, in which all t.c.'s share a common reference junction. A schematic of the circuit is given as Fig. 11.4. Benedict (1977) maintains that, provided all junctions in the shaded zone are at the

same temperature, the uncertainty in this circuit is of the order of 0.5 ^{o}C.

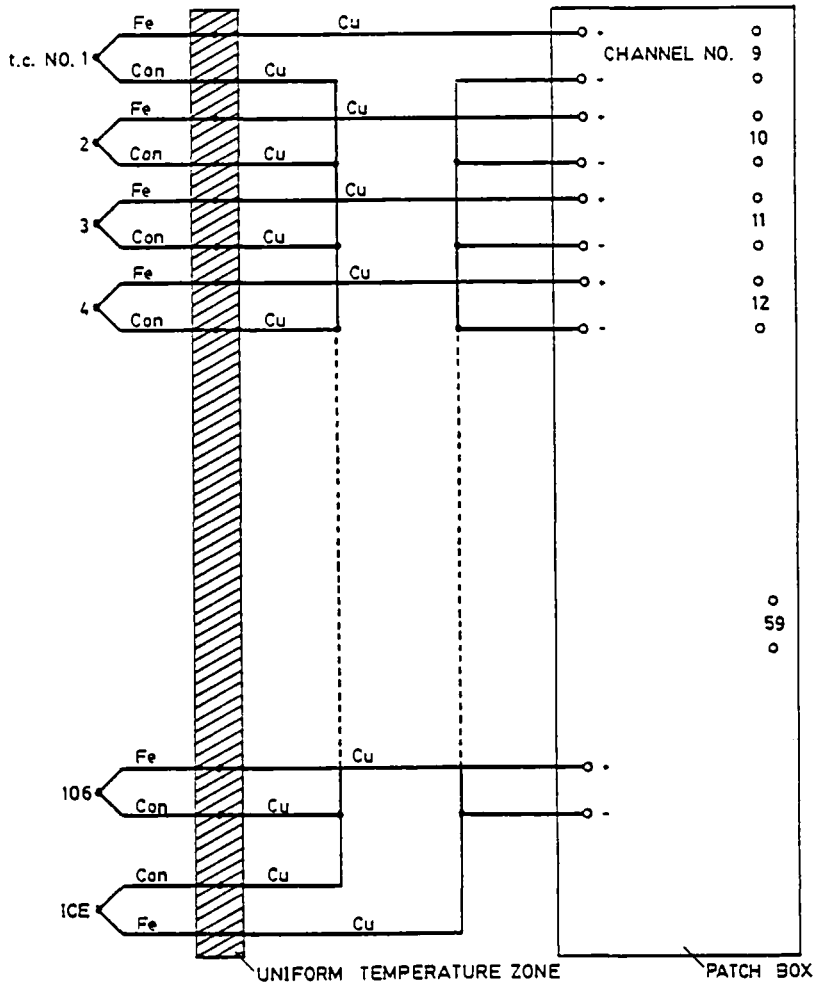


Fig. 11.4 Zone-Box Thermocouple Circuit

To enable removal of the winding assembly from the test area, the 4 m long t.c. wires were soldered to gold-plated, 24-way Amphenol connectors, to the mates of each of which were soldered the copper extension wires. All connectors were immersed in an oil bath equipped with a stirrer to maintain an approximately uniform temperature.

The data-logger used in the experiments had 60 channels, the first 9 of which were used for the winding resistance measurements. To enable

the recording of all 106 t.c.'s, a 'manual' patch box (see Fig. 11.4) was constructed using 13 'female' 24-way connectors. 5 'male' connectors were permanently wired to the 60 channel inputs. The data-logger scanned any range of channels selected, at user-specified time intervals. Each analogue (D.C.) channel voltage was input to a digital voltmeter, filtered to remove A.C. components caused by generator noise, converted to digital form, and output to a mechanical printer, the whole process requiring about a second per channel. Allowing for manual patching, all signals could be printed in a few minutes.

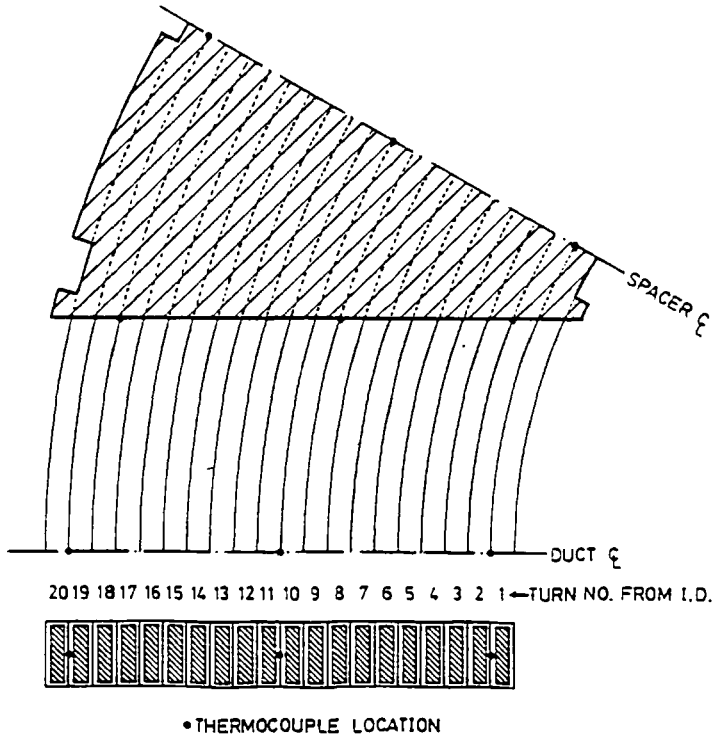


Fig. 11.5 Disc Thermocouple Locations

Before the winding was immersed in oil, 99 t.c.'s were installed at the manufacturer's works between turns in 11 of the 16 discs (the circled disc numbers in Fig. 11.2). As seen, only 6 of the 8 discs in the upper pass contained t.c.'s. The 9 in each disc were located, in

groups of 3, along the duct and spacer centre-lines, after turns 1, 10 and 19 from the inside diameter, and along the spacer-duct boundary (side wall of the horizontal duct), after turns 2, 9 and 18. The arrangement is shown schematically in Fig. 11.5, and a photograph appears as Fig. 11.6. A master list of t.c. numbers and their locations may be found in Appendix C2.



Fig. 11.6 Thermocouple Installation

Measurement of the bulk temperature of a fluid flowing in a duct is not straightforward, and frequently the average of several temperatures across a duct section is used as an approximate substitute. The approximation is strictly speaking only valid if the velocity profile is 'flat', in which case the bulk and arithmetic mean temperatures are the same.

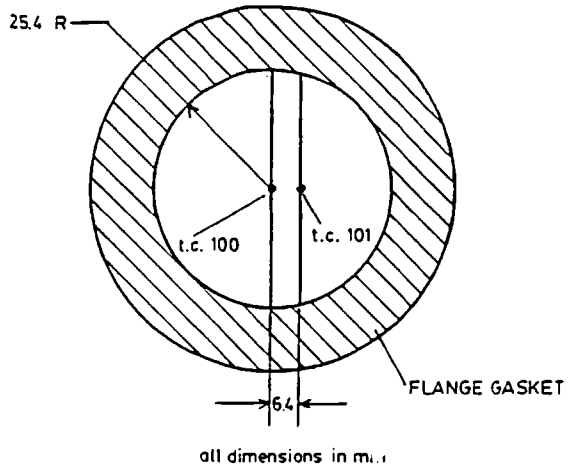


Fig. 11.7 Bottom Oil Thermocouple Locations

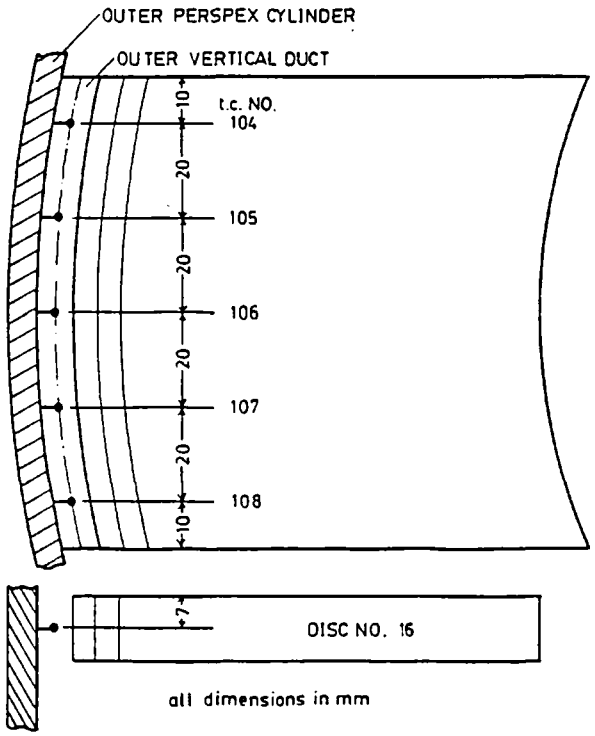


Fig. 11.8 Top Oil Thermocouple Locations

The bottom oil temperature was measured from 2 t.c.'s inserted through the gasket of a bolted flanged coupling on the winding inlet pipe. Their location is shown in Figs. 11.7 and 9.4, and readings from

the two invariably agreed within a few microvolts. Presumably the temperature profile at the gasket was approximately flat, as the oil there would have been well mixed by the heat exchanger.



Fig. 11.9 Top Oil Thermocouples on Perspex Cylinder

An attempt was made to measure the top oil as it emerged from the exit of the upper pass adjacent to disc 16 (see Fig. 11.2). This was done by cementing 5 t.c.'s along the circumference of the outer perspex cylinder spaced 20 mm apart, as shown in Fig. 11.8. They may also be

seen in the photograph, Fig. 11.9. Their average value would approximate the circumferential mean centre-line temperature, and can only therefore be regarded as an estimate of the bulk top-oil temperature.

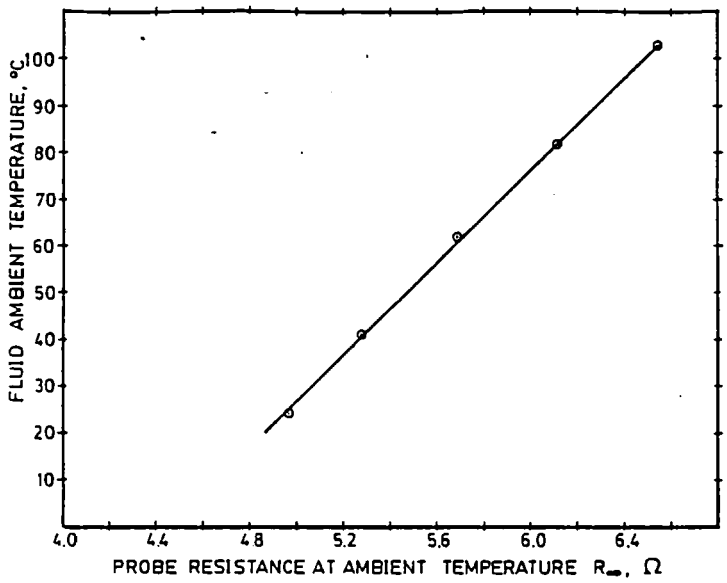


Fig. 11.10 Hot Film Probe Resistance-Temperature Calibration

11.4 Horizontal Duct Centre-Line Temperature Measurements While measuring the centre-line velocities of the 8 ducts in the upper pass, the centre-line temperature was also recorded using the probe in resistance mode. The value of the this temperature was found from equation (10.7) (substituting R_∞ for R_p). The resistance-temperature calibration curve for the probe, Fig. 11.10 was obtained using the manufacturer-calibrated digital thermometer from which was obtained α_{20} = .00414 $^oC^{-1}$ and R_{20} = 4.866 Ω. The DISA (manufacturer) supplied values for the probe were α_{20} = .0042 $^oC^{-1}$ and R_2 = 4.88 Ω.

11.5 Thermal Characteristics of the System Attainment of a thermal steady state, essential before taking any temperature readings, depended on choosing a power input to the winding matched by the dissipation

capacities of the heat exchanger and the surroundings. After trial and error, 5.14 kW was found to be about right. The winding current at this power was approximately 150 A, somewhat over the rating of the winding under forced cooling conditions (126 A). After equilibration, the bottom oil temperature usually settled out at about 56 ^{o}C. During warm-up, excess current (200 A) was input and the cooling water left off. When the bottom oil had attained 56 ^{o}C or exceeded it, the current was reduced to about 150 A, the water turned on (1.26 - 2.52 x 10^{-4} m^3/s or 100 - 200 g.p.h.), the oil flow rate adjusted to the desired value, and nothing else was touched until the system had come to equilibrium. The sudden injection of cooling water reduced the winding resistance slightly, allowing the winding current to increase slightly, after which the system smoothly approached a thermal steady state. The behaviour is seen from Fig. 11.11 where the bottom, top oil and mean winding temperatures are plotted against time. Approximately 2.5 hours was required to bring the system to the desired steady state. During the warm-up period, the plotted temperatures were logged every 10 minutes.

All tests were run at 5.2 kW, but the oil flow rate was varied from 2.46 - 8.62 x 10^{-4} m^3/s (3.25 - 11.4 g.p.m.). Approximately 2 hours was required for the system to re-stabilise after a flow rate change. The dissipation in the heat exchanger did not appear to be a function of oil flow rate over this range.

The hottest t.c. was found to be in the top disc, in the middle, on the spacer centre-line (see Fig. 11.5). Its value, expressed as $\theta'_h = t_h - t_b$ along with $\theta'_r = t_r - t_b$ and $\theta'_w = t_w - t_b$, is plotted as a function of the pass inlet flow rate (presumed to be 1/6 of the total flow rate) in Fig. 11.12. The data is taken from the second series of

tests mentioned in Chapter 12.

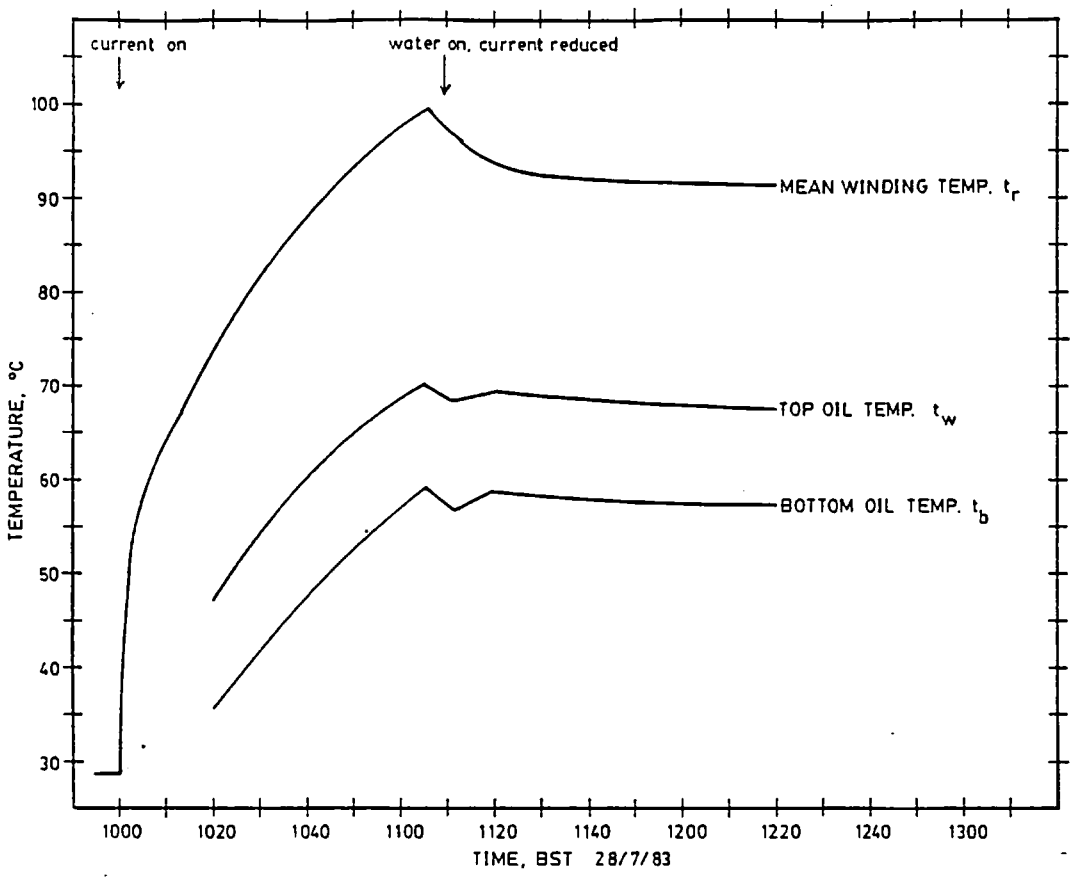


Fig. 11.11 Warm-Up Curve of Experimental Winding

11.6 Closure Temperature measurements in the winding were obtained using 3 different techniques: winding resistance, t.c.'s and a hot-film probe in resistance mode. A winding dissipation rate of 5.14 kW proved compatible with the heat-exchangers, and the thermal time constant of the system enabled measurements at 3 different oil flow rates during the course of a working day.

The test results, and their comparison with the predictions of DISCNET and DUCT, will be described in the next chapter.

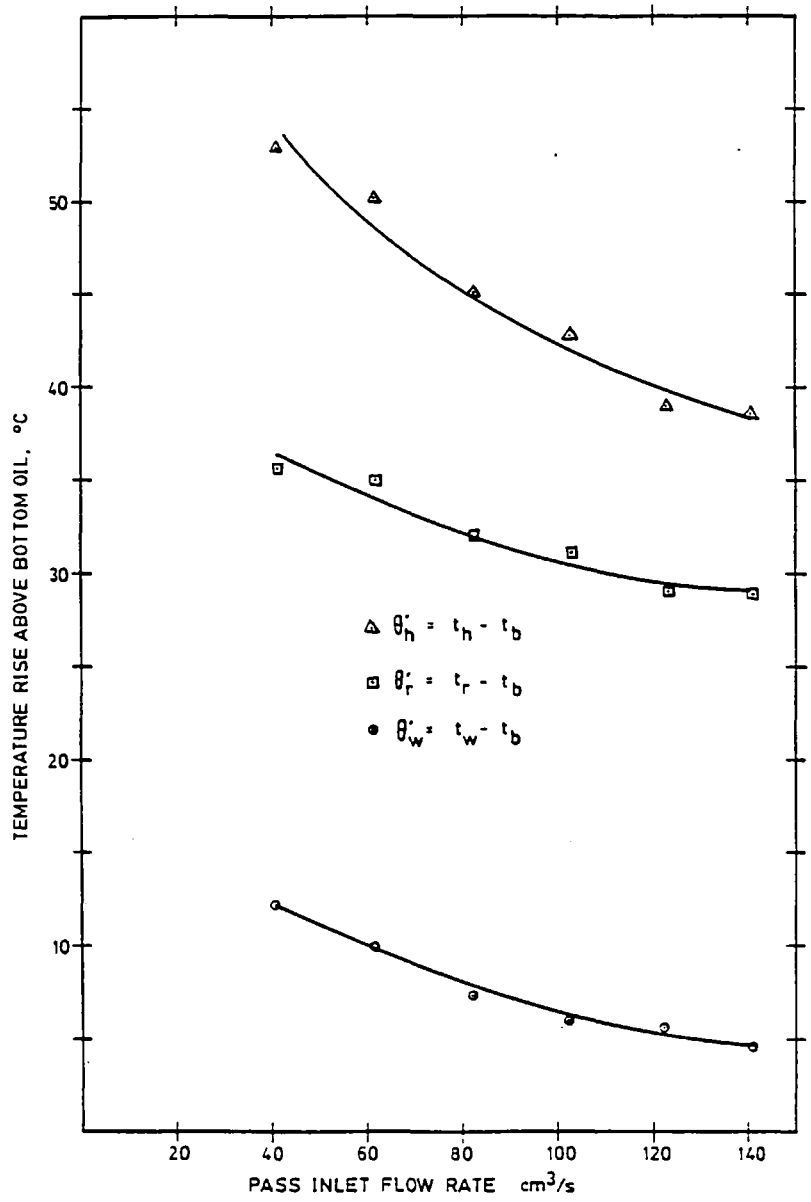


Fig. 11.12 Hot Spot, Mean Winding and Top Oil Rise vs. Flow Rate

CHAPTER 12

COMPARISON OF THEORY AND EXPERIMENT

12.1 Overview of Experimental Programme The first set of experiments consisted of oil velocity measurements in an unheated winding at room temperature. The winding was set up exactly as shown in Fig. 9.2. In the second set, the winding was unaltered, but was heated, as described in Chapter 11, and simultaneous oil velocity and winding temperature measurements were made. The winding was then modified slightly by the addition of a third flow-diverting washer just under the grey steel pressure ring (see Figs. 9.3 and 12.11) and on top of the 12 spacers. Its purpose was to eliminate suspected 'leakage' oil flow. The cold and hot tests were then repeated as in the first and second set. The final set of experiments consisted of measurement of temperature only, in a heated winding in which the horizontal duct thicknesses were graded to improve the oil flow distribution. These latter results will be presented in Chapter 13.

12.2 Cold Oil Velocity Measurements The DISA CTA bridge had provision for input from only one probe, hence measurement of the oil velocity in each of the 8 ducts involved raising the winding out of the tank for each duct and exchanging the threaded probe holder with one of the knurled plugs (see Fig. 9.3). The tapped holes in the outer perspex cylinder were lined up as precisely as possible with the centre-line of each horizontal duct.

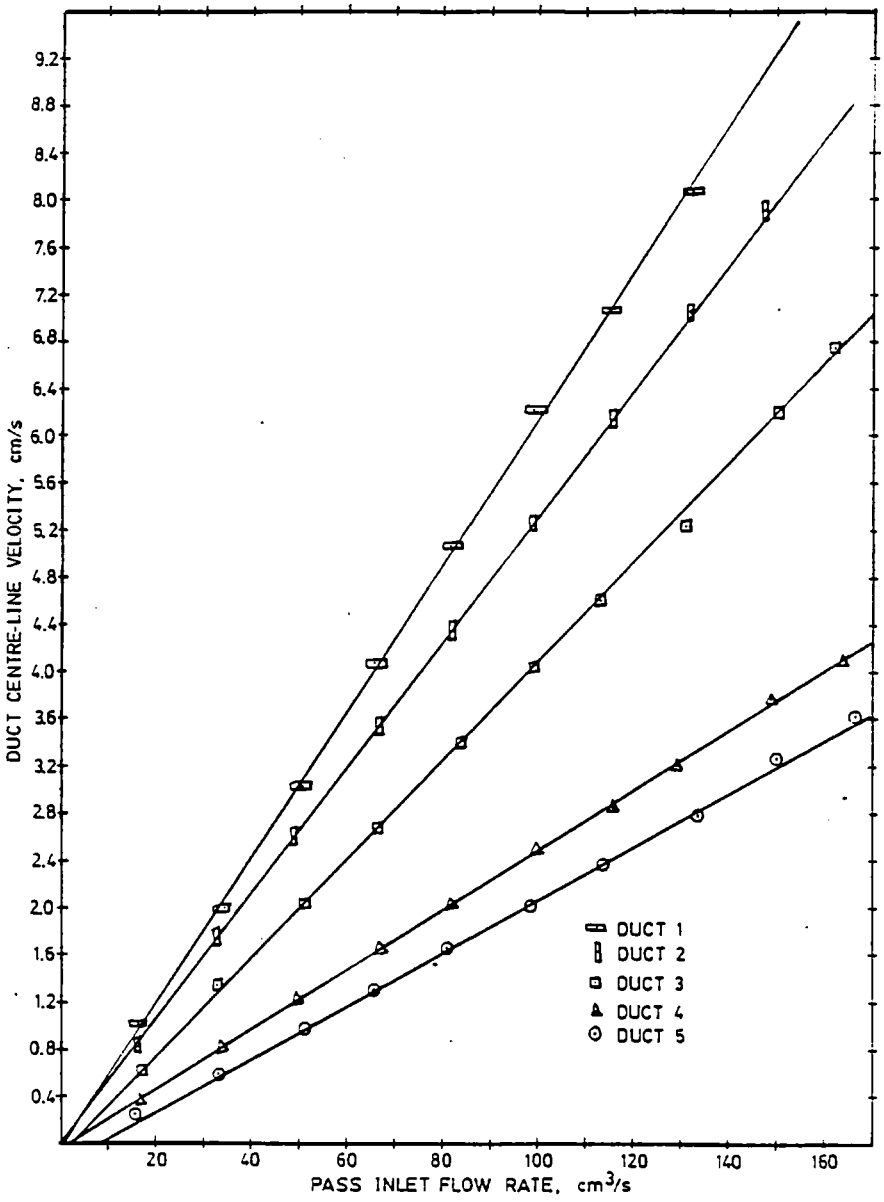


Fig. 12.1 Cold Flow Measurements in Ducts 1 - 5

The volume of oil delivered by the gear pump was found to be 4.925 cm^3/s per R.P.M., and this was presumed to divide itself equally between the 6 circumferential sectors in the winding (see Fig. 9.2). The pass inlet flow rate was thus assumed to be 0.821 cm^3/s per R.P.M., and was varied from 16.4 - 164 cm^3/s (20 - 200 R.P.M.). In terms of area flow rate, this corresponded to 1.64 - 16.4 x 10^{-4} m^2/s, or assuming a

vertical inlet duct thickness of 4 mm, a mean inlet velocity range of .041 - .41 m/s. This range of mean oil velocities is representative of both ON and OF transformers.

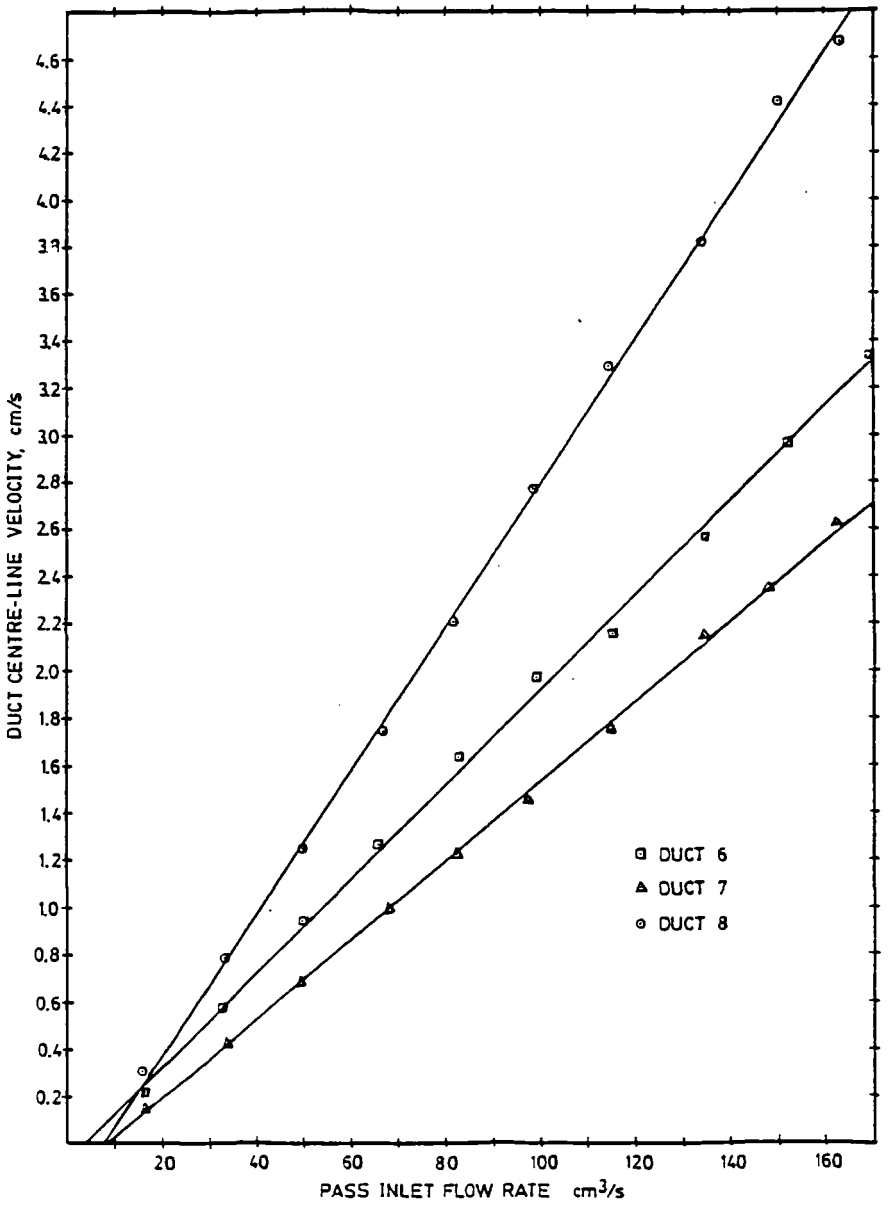


Fig. 12.2 Cold Flow Measurements in Ducts 6 - 8

The cold measurements with the film probe were not subject to the ± 17 % uncertainty reported in Section 10.4, since the oil temperature was fairly steady at 20 - 23 °C. The calibration curve given as Fig.

10.6 was used. In Figs. 12.1 and 12.2, the duct centre-line velocity of the 8 ducts are plotted as a function of pass inlet flow rate. It is interesting to note that the relationship is linear, i.e. the flow distribution expressed as the % total flow in each duct is approximately invariant with flow rate within the specified range. The result suggests that in this case the local Reynolds numbers at the various junctions and corners are too low for significant momentum effects to arise.



Fig. 12.3 Gaps between Vertical Ribs and Discs

As mentioned in Chapter 9, the probe was inserted so as to measure the centre-line velocity about 70 mm from the duct entrance, where it

was assumed that the profile was fully developed. The flow rate in each duct was calculated using equation (10.8) and the duct dimensions shown in Fig. 9.2. When the sum of the duct flow rates was compared with the pass inlet flow rate as indicated by the pump R.P.M., a shortfall of 29.2% emerged. Thus only 70.8% of 1/6 of the total oil pumped appears to have gone through the 8 horizontal ducts in the top pass in which the probe was inserted. The remainder was presumed to have leaked out 1.) Through the flanged pipe joints before entering the slots in the steel base plate, 2.) Underneath the bottom edges of the inner and outer perspex cylinders 3.) through the 1st flow diverting washer at the top of the lower pass, 4.) through gaps between the vertical pressboard ribs and individual discs in the upper or lower pass. These possible leakage paths are indicated in Fig. 9.2, and the gaps of item 4.) are visible in the photograph, Fig. 12.3. The flow distribution, including leakage, is shown as Fig. 12.4 (result A.).

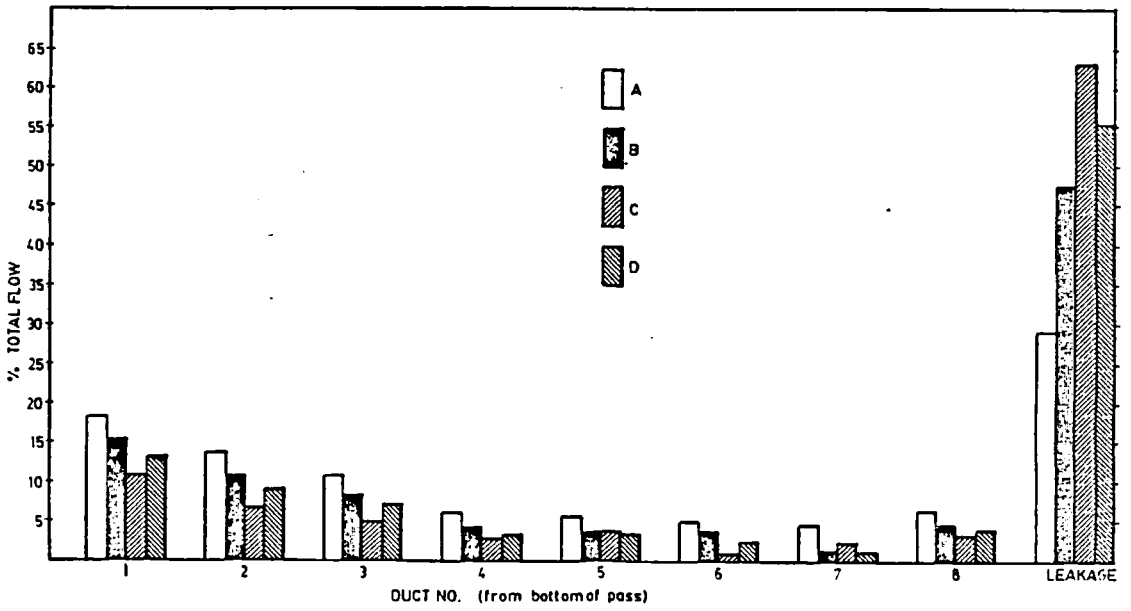


Fig. 12.4 Flow Distribution Showing Apparent Leakage

Leakage can be a significant handicap to accurate prediction of

the thermal behaviour of a particular design. It may vary between two otherwise identical units due to construction anomalies. Carruthers and Norris (1969) suggest that even in OD designs, it is safe to assume that only 50% of the total oil flow actually goes through the windings. This is due to the flabbiness of the pressboard baffles used to direct the flow. The experimental winding would be expected to (and does) have less leakage due to the steel base plate and perspex cylinders.

	% TOTAL FLOW							
		Discnet Prediction $Q_{in} \times 10^4$, m^2/s						
Duct No.	SN	1.	3.	5.	7.	9.	11.	EXP.
8	4.34	4.52	4.64	4.84	5.06	5.31	5.57	9.2
7	8.12	7.68	7.90	8.19	8.50	8.84	9.20	6.6
6	5.72	5.23	5.49	5.65	5.82	6.02	6.22	7.2
5	8.07	7.41	7.56	7.75	7.96	8.18	8.37	8.2
4	7.60	7.24	7.35	7.50	7.66	7.80	7.94	8.7
3	12.37	12.18	12.28	12.43	12.52	12.63	12.74	15.2
2	16.73	17.07	17.04	17.03	16.96	16.91	16.88	19.2
1	37.06	38.66	37.44	36.60	35.52	34.30	33.09	25.6

TABLE 12.1 Comparison of SN, DISCNET, and Experiment

Since the network model does not allow for leakage flow paths, considerable discrepancy may be expected between its prediction and experiment. To provide some basis of comparison, it was arbitrarily decided to 'correct' the results as if all the leakage had occurred prior to the measurement pass. DISCNET was then used to predict the flow distribution at various pass inlet area flow rates (Q = 1, 3, 5, 7, 9, 11 x 10^{-4} m^2/s) corresponding to pass inlet Reynolds numbers of 7.1, 21.2, 35.3, 49.4, 63.5 and 77.6. All fluid properties were evaluated at room temperature (21.5 ^{o}C) and of course the winding current was set to zero. All dimensions were obtained from Fig. 9.2.

The results are presented in Table 12.1, where the simple network (SN) prediction and 'corrected' experimental results are included for comparison. It is interesting to note that the DISCNET results vary only slightly with flow rate and are close to SN except in duct 1 at the higher flow rates. This result broadly follows the findings of Figs. 12.1 and 12.2. These low Reynolds number results are due to the markedly higher viscosity at room temperature. The situation is quite different when the winding is heated.

The comparison of DISCNET with experiment is fair over all, the most serious discrepancy being in the % flow prediction in duct number 1. Whether this is due to leakage from that duct or deficiencies in DISCNET is not clear. More significantly, DISCNET predicts that the minimum flow occurs in duct 8, whereas measurement shows it to be in duct 7.

12.3 Simultaneous Oil Velocity and Winding Temperature Measurements This second set of measurements was considerably lengthier, as ample time had to be allowed for the system to come to thermal equilibrium. Changing the velocity probe to a different duct necessitated a shut-down of the winding current and pump. In practice, a full day was required for each duct measurement. The measured flow distribution (Fig. 12.4, Result 8) was obtained from 8 days of tests, in each of which every attempt was made to achieve thermal equilibrium under the same operating conditions, which were:

$$t_b = 55.9 \pm 2.3\ ^{o}C$$

$$\dot{Q} = 5.137 \pm .11\ kW\ (I = 150\ A)$$

$$Q = 8.23 \pm .03 \times 10^{-4} \ m^2/s \ (R.P.M. = 100)$$

where t_b is the bottom oil temperature, whose measurement is described in Chapter 11, Q is the total winding dissipation, and Q is the pass inlet area flow rate inferred from the pump R.P.M.

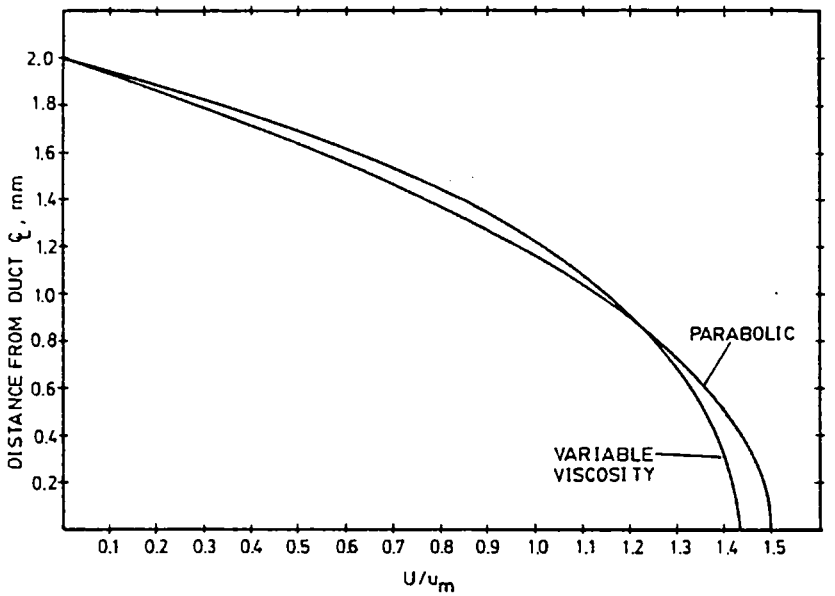


Fig. 12.5 Variable Viscosity Distortion of Velocity Profile

The probe velocity measurements were derived from equation (10.13) and were hence subject to an uncertainty of ± 17%. An additional uncertainty in computing the individual duct flow rates from the centre-line velocity arose due to the departure of a variable viscosity velocity profile from the assumed, isothermal, parabolic shape. This effect was estimated by using DUCT to predict the variable viscosity profile 70 mm from the duct entrance at various flow rates, and with an inlet temperature and surface heat flux close to those expected in the winding ducts. In Fig. 12.5, U/u_m is plotted against distance from the duct centre-line. The parabolic profile is included for comparison. U/u_m (U being the centre-line velocity) was found to be typically, 1.43

rather than 1.5, hence this effect could lead to a 5% underestimate of the duct flow rate.

In any event the measured flow distribution (Fig. 12.4, Result 8) shows a marked increase in the 'leakage' flow (from 29% in the cold tests to about 48%). Whilst it is possible that heating the winding may substantially change the flow resistances along some of the leakage flow paths, perhaps by expansion/deformation of the perspex/pressboard, it is probable that some of the increased apparent leakage arises from the uncertainties mentioned in the previous paragraph.

In Table 12.2, the temperature measurements in the winding during one of the 8 runs are summarised. The probe temperature (from R_∞) was read before and after the scan of the t.c. voltages. All voltages (t.c. and disc pair volt drop) were recorded 5 times (this took about 10 minutes) and the average taken. The standard deviation was at most 0.2 ^{o}C. t_w was estimated from the average of the 5 t.c.'s located at the exit of the measurement pass (see Chapter 11). The standard deviation was typically 1.5 - 2.0 ^{o}C. For the numbering scheme of the discs and ducts, see Fig. 11.2. Whilst the temperatures in discs 8 - 16 will be considered presently in detail, the reversal of flow direction in the horizontal ducts brought about by the flow-diverting washer underneath disc 8 (see Fig. 11.2) may be clearly seen by comparing the radial temperature distribution in the discs above and below this washer. The former are skewed radially outward, whilst the latter are skewed radially inward.

Date: 17-2-83 Winding Current 153.8 A Winding Dissipation 5.15 kW

Pass Inlet Area Flow Rate From Pump R.P.M.: 8.26 X 10^{-4} m^2/s

Mean Winding Temp.: 87.8 ^{o}C Bottom Oil: 55.8 ^{o}C Top Oil: 62.8 ^{o}C

Disc Pair Mean Temperatures, ^{o}C:

Disc 1-2: 82.6 Disc 3-4: 86.3 Disc 5-6: 84.7 Disc 7-8: 86.3
Disc 9-10: 87.8 Disc 11-12: 90.8 Disc 13-14: 90.9 Disc 15-16: 93.0

	THERMOCOUPLE MEASUREMENTS, ^{o}C					
Location: Disc No.	After Turn No. From I.D.	Duct C-L	After Turn No. From I.D.	Corner	After Turn No. From I.D.	Spacer C-L
4	1	77.9	2	81.8	1	79.2
	10	87.4	9	88.1	10	90.1
	19	70.5	18	77.3	19	74.0
5	1	77.2	2	82.0	1	78.0
	10	89.2	9	87.2	10	85.9
	19	74.7	18	77.3	19	66.8
6	1	75.2	2	79.9	1	78.3
	10	84.5	9	85.8	10	88.1
	19	69.9	18	77.2	19	74.4
7	1	75.2	2	79.9	1	76.7
	10	83.4	9	84.4	10	86.0
	19	69.7	18	76.6	19	73.3
8	1	74.1	2	80.1	1	74.6
	10	92.6	9	91.8	10	94.7
	19	77.9	18	86.2	19	77.7
9	1	69.3	2	74.0	1	70.6
	10	89.7	9	86.4	10	85.9
	19	---*	18	87.6	19	80.4
10	1	70.5	2	75.4	1	71.9
	10	87.4	9	87.9	10	91.4
	19	81.9	18	89.0	19	83.4
12	1	72.3	2	78.3	1	73.3
	10	91.1	9	91.5	10	94.2
	19	83.4	18	92.2	19	84.5
13	1	72.9	2	78.6	1	74.4
	10	91.2	9	91.7	10	94.5
	19	85.0	18	92.7	19	86.8
15	1	73.5	2	78.5	1	74.7
	10	92.9	9	93.1	10	96.3
	19	84.4	18	93.9	19	90.1
16	1	78.8	2	84.0	1	78.5
	10	98.5	9	98.2	10	100.4
	19	87.8	18	96.6	19	88.4

Table 12.2 Winding Temperature Measurements

*faulty t. c.

12.4 Computer Prediction of Temperature and Oil Flow Distribution

Prediction of the temperatures and oil velocities in the upper pass of the experimental winding (discs 8 - 16, ducts 1 - 8, see Fig. 11.2) was attempted in two ways. Firstly, use was made of the measured flow distribution to calculate the disc temperatures directly, using DUCT (see Chapter 7). Secondly, the DUCT calculations were repeated, using the flow distribution predicted by DISCNET (see Chapter 8). Comparison of the two methods afforded, among other things, a means of assessing the accuracy of DUCT and DISCNET separately.

In the first calculation, the input required by DUCT for each duct is Q_2, Q_1 and Q_r, t_e and $t_{m,r}$ and I/2 (see Chapter 7 and Fig. 7.1). Q_2 for each of the 8 horizontal ducts was available from the hot film measurements, and by continuity, Q_1 and Q_r in each adjacent vertical duct were easily calculated. t_e was assumed equal to the pass inlet temperature $t_{m,in}$ (see Fig. 2.3), which was estimated from the measured values of t_b and t_w given in Table 12.2, as follows. The 7 ^oC temperature rise ($t_w - t_b$) was apportioned 7/16 to the lower pass and 9/16 to the upper pass (see Fig. 11.2) so that $t_{m,in}$ was assumed equal to $t_b + 7/16(t_w - t_b) = 58.9\ ^oC$. $t_{m,r}$ is normally calculated by DISCNET, however in this first calculation it was assumed equal to t_w.

Determination of the appropriate value of I/2 required consideration of the 'masking' effect of the pressboard spacers. The total surface area of the 16 discs (excluding edges, but including the areas covered by the spacers) was 3.55 m^2, however, the total area exposed to oil flow was only 1.92 m^2, or 54% of the total. If all of the heat transfer is considered to occur in the horizontal ducts, then I/2

must be set so as to give an average surface heat flux of 5.153 kW/1.92 m^2 (see Table 12.2) = 2.68 kW/m^2. Setting I/2 to half the actual experimental winding current (153.8/2 = 76.9 A), would assume uniform heat flux over the whole disc surface area, and would thus yield an average heat flux of (5.153 kW/3.55 m^2 = 1.45 kW/m^2).

This masking effect, plus the considerable uncertainty in the flow rate measurements, led to a consideration of 'best' and 'worst' cases. Assuming, for example, that all values of Q_2 were +17% in error (and should therefore be lowered), and that the maximum value of I/2 be used (about 105 A) gives the 'worst' case, and predicts temperatures much higher than those measured. The 'best' case, assuming all values of Q_2 were 17% low due to probe calibration uncertainties, and an additional 5% low due to velocity profile distortion (and should be raised accordingly), and using the minimum value of I/2 (76.9 A), predicts temperatures much lower than measured. Within these extremes, several combinations of I/2 and Q_2 were found to give good agreement with experiment; in the sample calculations to be presented, one such was used consistently for all of the computer runs. I/2 was set to 97.5 A, to give a value of average surface heat flux of 2.3 kW/m^2. This assumes that 86% of the total winding dissipation flows directly to the horizontal duct oil. The measured velocities are assumed underestimated by 17%, and the individual ducts flow rates a further 5%. Thus whereas the total measured pass inlet flow rate Q was found to be 4.3×10^{-4} m^2/s, this was revised upward to 5.46×10^{-4} m^2/s. All 8 of the measured values of Q_2 were revised upward proportionately. This combination was favoured, since the increased apparent leakage flow in the hot flow measurements suggested that the probe velocities were too low rather than too high. Taking the revised value for Q gives an apparent leakage

of about 33% -- which is comparable with 29% observed in the cold tests.

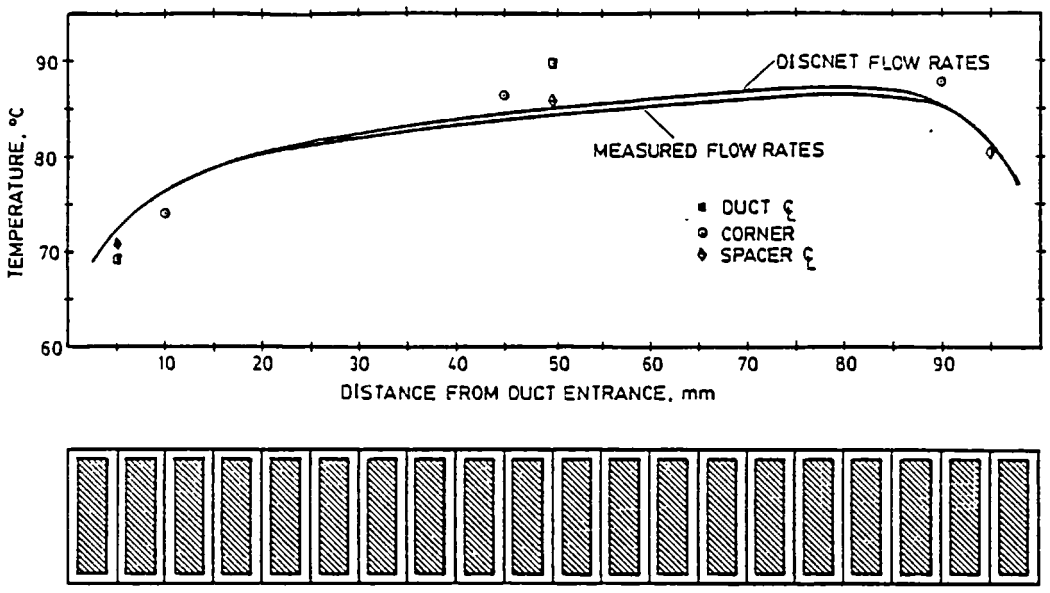


Fig. 12.6 Theory vs. Experiment, Disc 9

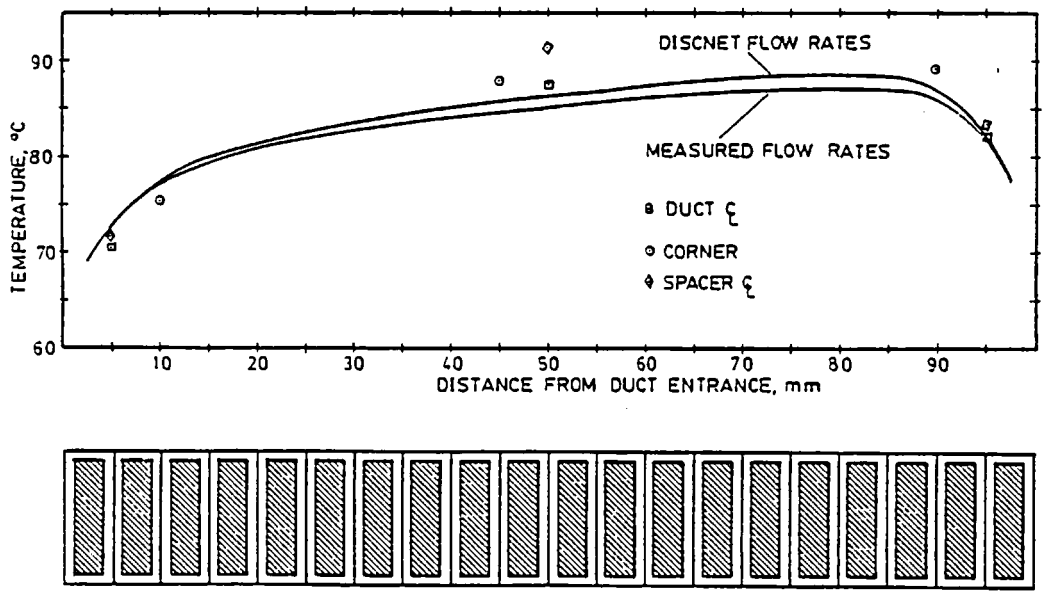


Fig. 12.7 Theory vs. Experiment, Disc 10

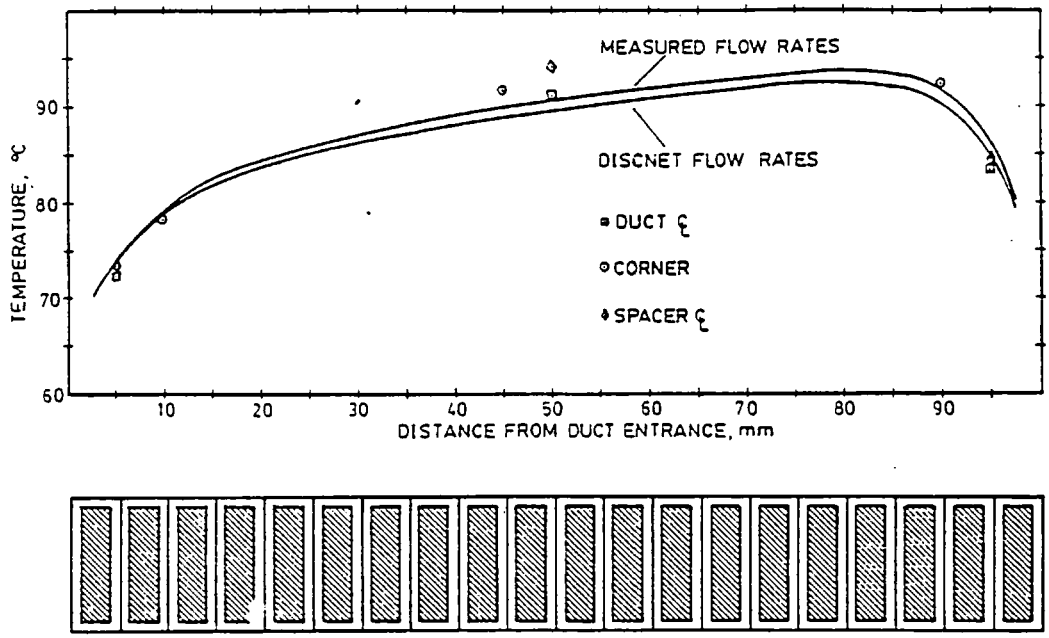


Fig. 12.8 Theory vs. Experiment, Disc 12

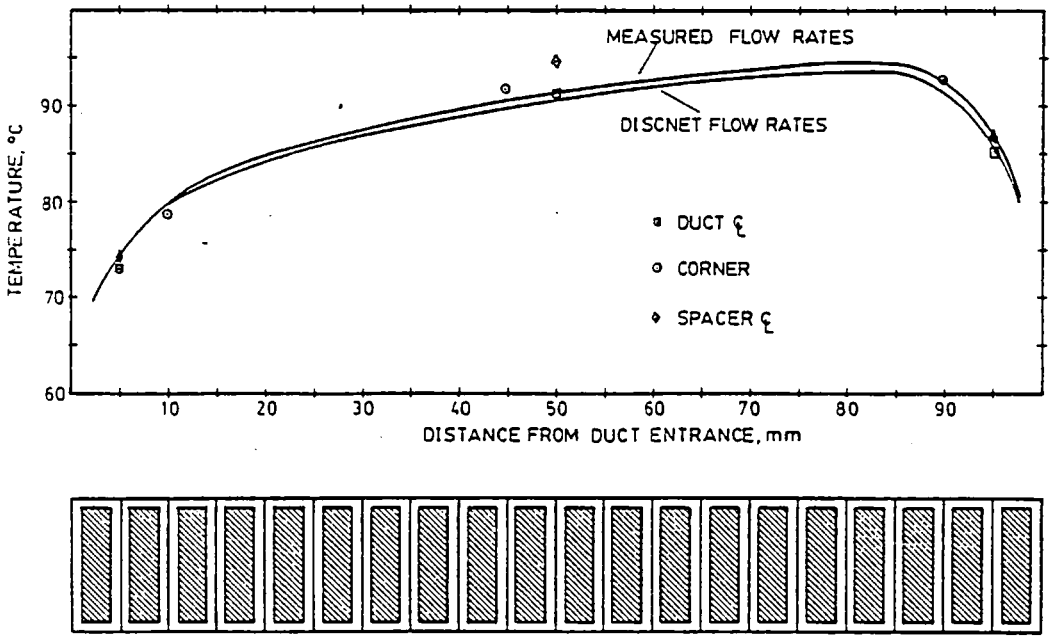


Fig. 12.9 Theory vs. Experiment, Disc 13

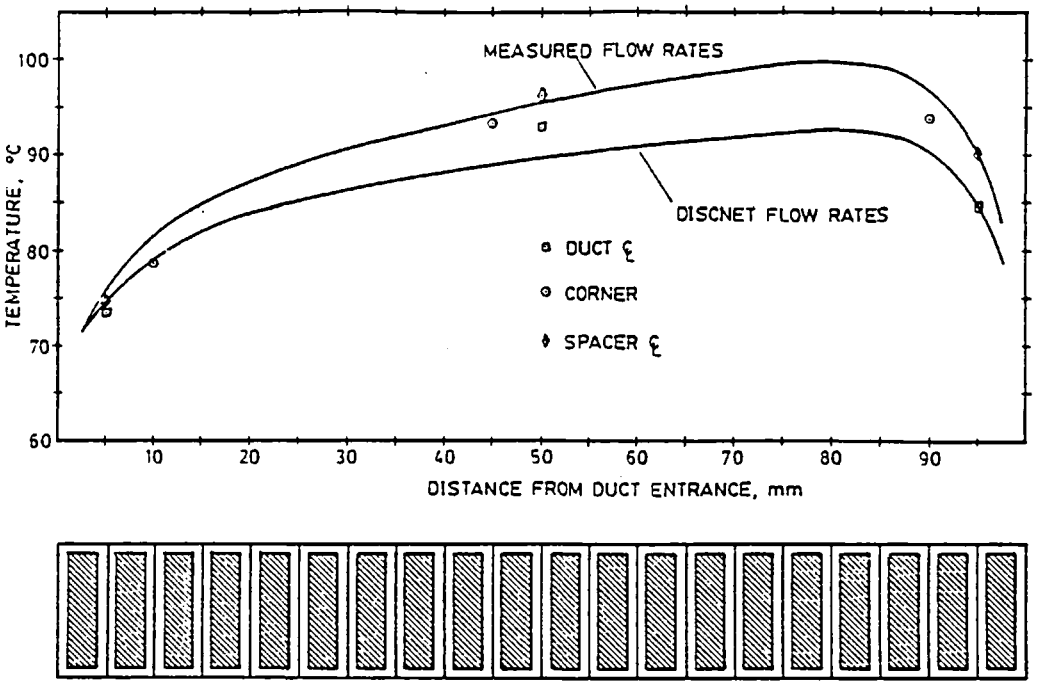


Fig. 12.10 Theory vs. Experiment, Disc 15

In the upper pass of the experimental winding, t.c.'s were fitted only in discs 8, 9, 10, 12, 13, 15 and 16. Discs 8 and 16 could be expected to run hotter than predicted because the pressboard flow-diverting washers were fitted flush to these discs (see Fig. 11.2). This, in retrospect, was a mistake, and would not be done in a commercial winding. Efforts were thus concentrated on predicting the temperatures in the remaining discs. As DUCT assumes a symmetry plane through each disc, it was decided to compute each disc temperature distribution twice, using the flow rate at the top and bottom, and then to average the conductor temperatures obtained from the two runs. This was deemed necessary since some discs had substantially different flow rates on their top and bottom surfaces, and the disc conductor temperatures, as computed with the two flow rates, differed considerably. Such a circumstance calls into question the assumption of

the symmetry plane through the disc; however in the present calculation, the averaging procedure seemed to work quite well. The results for discs 9, 10, 12, 13 and 15 are plotted in Figs. 12.6 - 12.10

DUCT can be expected to predict most accurately the temperature in the centre-line of the horizontal duct (the squares). The temperatures in the duct corners (circles) and in the spacer centre-line (diamonds) will be higher. The only exception, assumed due to a faulty or mislabelled t.c., occurs in disc 9, Fig. 12.6, where the duct centre-line t.c. in the middle of the disc actually appears to read higher than the corresponding spacer centre-line t.c. In general, the agreement with experiment is very good; in particular the sharp temperature drop-off at the exit of the duct predicted by the theory matches up very well with the experimental points. The fact that the spacer centre-line temperature is only 2 - 4 ^{o}C higher than at the duct centre-line (in the middle of the disc) suggests that most of the heat generated in the conductors masked by the spacers flows circumferentially by conduction until, when adjacent to the duct oil, it is then convected away. All 5 of the cases shown, given a somewhat arbitrary choice of I/2 and Q, demonstrate consistently good agreement between theory and experiment (within 1 - 2 ^{o}C).

The second stage of the computer verification involved the prediction of the duct flow distribution using DISCNET. The same values of surface heat flux and pass inlet flow rate were used as in the first computation. The comparison of DISCNET and experiment (corrected, as in Table 12.1, to assume that all leakage occurred prior to the pass entrance) is given in Table 12.3. Here, the most serious discrepancy occurs in duct 7, whereas, unlike the cold measurements, the agreement

in duct 1 is quite good. Further, the departure of DISCNET from the Simple Network prediction is greater, due to the substantial increase in the pass inlet Re, caused by reduced viscosity. (Pass inlet Re = 153 in the present computation at $t_{m,in}$ = 58.9 ^{o}C, compared to just about 38 - 40 at the same pass inlet flow rate at room temperature).

	% TOTAL FLOW	
Duct No.	DISCNET	Experiment
8	7.39	9.0
7	10.47	2.5
6	7.05	7.1
5	9.07	6.9
4	8.68	8.4
3	13.13	16.3
2	16.30	20.9
1	27.92	30.4

Table 12.3 Comparison of DISCNET and Experiment, Hot Tests

The disc temperature distributions were recalculated, using DUCT and the flow rates supplied by DISCNET, and the results are shown alongside the previous calculation in Figs. 12.6 - 12.10. Except for disc 15, where the experimental points fall between the two curves, the temperature distributions are quite close. Evidently the winding temperatures are not markedly dependent on the individual duct flow rates in this particular case, which would typically occur in an OF design. The DISCNET flow prediction, and the hot film measurements, though imprecise, are good enough to afford reasonably accurate temperature predictions.

In all discs considered, the hottest spot occurs in the 16th and 17th turns from the inside diameter. Because the Simple Network model neglects the disc edge effects, it predicts the hottest spot in the 20th turn. A comparison of the SN disc hot-spot prediction with the 2

computations just described is given as Table 12.4. In-general, the SN prediction, though on the high side, is not bad, and might serve as an adequate, if conservative guide. (Whereas in Chapters 3 and 13, SN is used to predict the duct wall temperatures, here, to afford direct comparison with the DUCT prediction, the temperature drop across the conductor insulation has been added.)

Disc No.	HOTTEST TEMPERATURE IN DISC, °C			
	SN Prediction	DISCNET Prediction	Measured Flow Prediction	Experiment
16	100.9	--	--	101.5
15	100.0	92.5	100.0	96.5
14	99.6	--	--	--
13	99.0	93.5	94.5	94.5
12	97.0	92.5	94.0	95.0
11	94.8	--	--	--
10	92.0	88.5	87.0	89.5
9	89.2	87.5	86.5	88.5
8	87.6	--	--	95.0

Table 12.4 Comparison of Various Disc Hot-Spot Prediction Methods and Experiment

DUCT NO.	DUCT CENTRE-LINE TEMPERATURE 70 mm FROM ENTRANCE, °C		
	MEASURED FLOW PREDICTION	DISCNET PREDICTION	EXPERIMENT
8	59.8	60.3	62.2
7	66.6	59.4	72.5
6	60.2	60.2	67.9
5	60.2	59.6	70.4
4	59.9	59.8	63.6
3	59.1	59.2	60.1
2	59.0	59.1	60.0
1	58.9	58.9	57.2

Table 12.5 Comparison of Probe Resistance Temperature Measurements with DUCT Prediction

Finally, an attempt was made to predict the duct centre-line temperatures at the probe location (70 mm form the duct entrance) using the temperature profiles computed by DUCT. These results are summarised

in Table 12.5, where very considerable discrepancies are seen to arise in ducts 5, 6 and 7. It is unclear why this whould be, as the agreement in the other 5 ducts is fair.

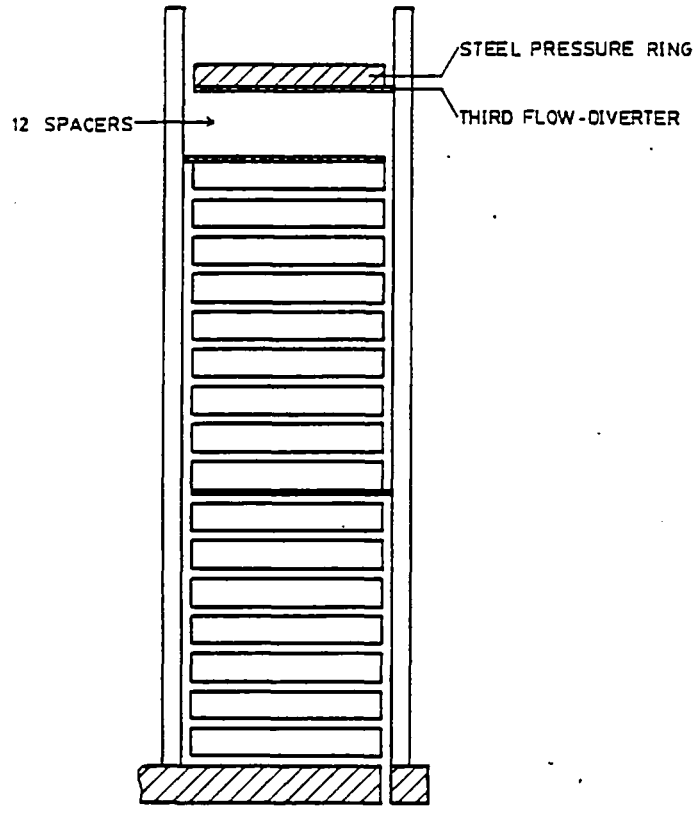


Fig. 12.11 Facsimile Winding with Third Flow-Diverter

12.5 Measurements with Third Flow-Diverter The leakage described in section 12.2 was believed to occur predominantly between the outer disc edges and the vertical pressboard ribs (Fig. 12.3), thereafter proceeding up the 'extra' vertical duct formed between the 2 ribs on the outer side of each spacer column (see Fig. 9.2). It was thought that this flow path could be sealed off by fitting a 3rd flow-diverter, shown schematically in Fig. 12.11. This, however, (C., cold tests; D., hot tests, Fig. 12.4) served to increase rather than decrease the leakage flow. Upon later inspection of the winding, it was found that the outer

perspex cylinder tended to 'ride' up the winding during thermal cycling, allowing the oil to leak directly into the tank upon emerging from the circumferential slots in the steel base plate. To reduce leakage significantly, a major refit would probably have been required; none was undertaken, since the end result would probably behave quite differently from a commercial winding.

12.6 Discussion and Conclusion DISCNET and DUCT, and for that matter SN, appear, in the test case described, to have provided reasonably accurate predictions of the hot-spot temperature. The results, however, were subject to considerable uncertainty about leakage, and the 'masking' effect of the spacers. The former difficulty is apt to be even more severe in commercial practice, where leakage may vary considerably between units of similar or identical design. The latter difficulty could be resolved by considering circumferential heat flow, and is mentioned in Chapter 14 as an area of further work.

In the next chapter, various ways of improving and optimising the thermal design will be discussed.

CHAPTER 13

OPTIMISATION OF THE THERMAL DESIGN

13.1 Introduction The results of the previous chapter have shown that DISCNET and DUCT may be used to predict with reasonable accuracy the thermal behaviour of a given winding. The next logical step is to use the software as a design tool, and in particular to identify, if possible, the best thermal design which is compatible with other requirements, e.g. electromagnetic efficiency, ability to withstand surge and short-circuit conditions, economic viability and practicality of manufacture.

Various ways of improving the thermal design of a disc winding with flow-diverting washers have been considered by other workers. Some of these involve the removal of one or two turns from each disc to create additional vertical ducts. Brechna and Tschudi (1962) conducted a large number of experiments on a single disc with single turns removed in various locations. Baffling arrangements around the disc, however, resembled in most cases a disc winding without flow-diverting washers. Lobenstein (1967) was concerned with the ratio c/L (see Figs. 2.1 and 2.2), stating that its optimal value was 0.1. Szpiro, Allen and Richards (1982) experimented with variation of the vertical duct thicknesses a and b (see Fig. 3.1).

In general, the dimensions of the disc, and therefore the ratio L/d (see Fig. 3.1) will be governed by electromagnetic considerations, e.g. the turns ratio and whether the winding is high or low voltage. The thermal designer has some flexibility, however, in determining the

number of ducts in a pass, and the duct dimensions a, b and c_1, c_2, etc. In this chapter, it will be assumed that L/d is given, but optimal values of the vertical and horizontal duct dimensions will be suggested. The Simple Network model (SN) will be used for these calculations as it is more amenable to optimisation studies. Although of course not as accurate as DISCNET and DUCT, it is good enough to indicate that one arrangement is better than another. The design of Table 3.3, in Chapter 3 will be taken as the 'datum', and various ways of improving this very poor arrangement will be considered. Experimental results arising from an attempt to improve the thermal design of the top pass of the facsimile winding will also be presented.

13.2 Optimisation of the 16 Duct Pass The datum design, shown as Fig. 13.1, consists of a single pass of 17 discs and 16 ducts. The SN prediction of this design, given in Table 3.3, shows extreme starvation in ducts 8 and 9 and very high values of t_{hot} there. (Recall that SN gives the maximum wall temperature in each duct, rather than the maximum conductor temperature in each disc).

Three ways of improving the thermal behaviour will be examined independently, although these could, if desired, be used in combination: 1.) increasing the number of passes by adding flow-diverting washers, 2.) grading the horizontal duct thicknesses so as to equalise the flow rate in each duct and 3.) increasing the thickness of both vertical ducts while leaving the horizontal ducts with their original dimensions. Each method has its advantages and disadvantages, and will be discussed in turn.

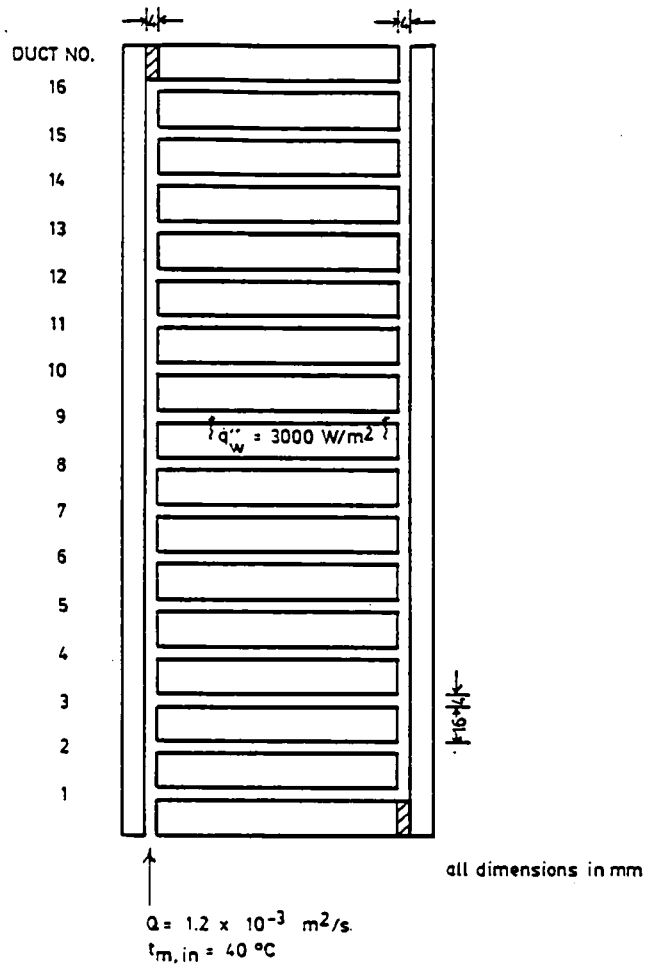


Fig. 13.1 Datum Design -- 16 Duct Pass

13.3 Increasing the Number of Passes This first and most obvious method is already suggested by the preliminary results of SN in Chapter 3. The datum design could be converted to 2 passes of 8 ducts, Fig. 13.2, or 4 passes of 4 ducts, Fig. 13.3. The results of these improvements are compared with the original design in Fig. 13.4. The difference between 16 and 8 ducts per pass is dramatic; between 8 and 4 ducts, less so. If the 'Japanese' form of blocking washers is used, as shown in Fig. 13.1 - 13.3, this modification could be carried out without altering the overall height of the 17 discs or any of the duct dimensions. Other arrangements, e.g. Fig. 2.3, would increase the

overall height, a possible disadvantage. The penalty for adding washers is a substantial increase in the pumping pressure required, as seen in Fig. 13.5. The buoyant pressure regain is also less for 4 passes of 4 ducts than 1 pass of 16 ducts. These latter considerations might militate against increasing the number of passes in ON windings.

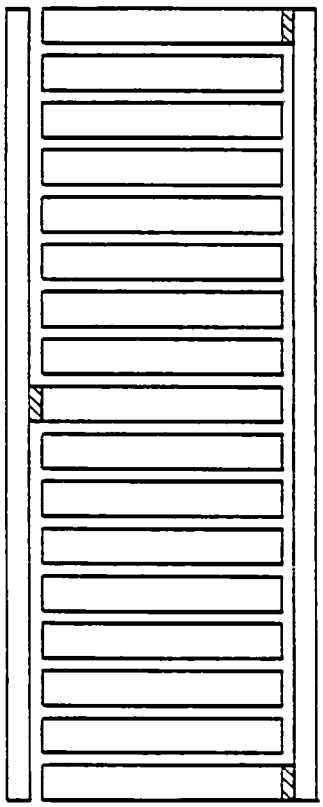


Fig. 13.2 Two 8 Duct Passes

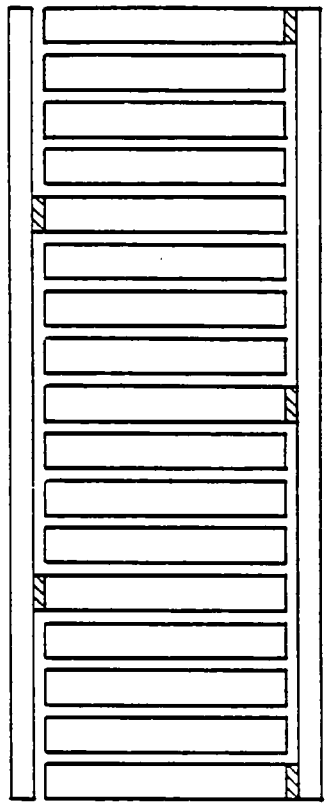


Fig. 13.3 Four 4 Duct Passes

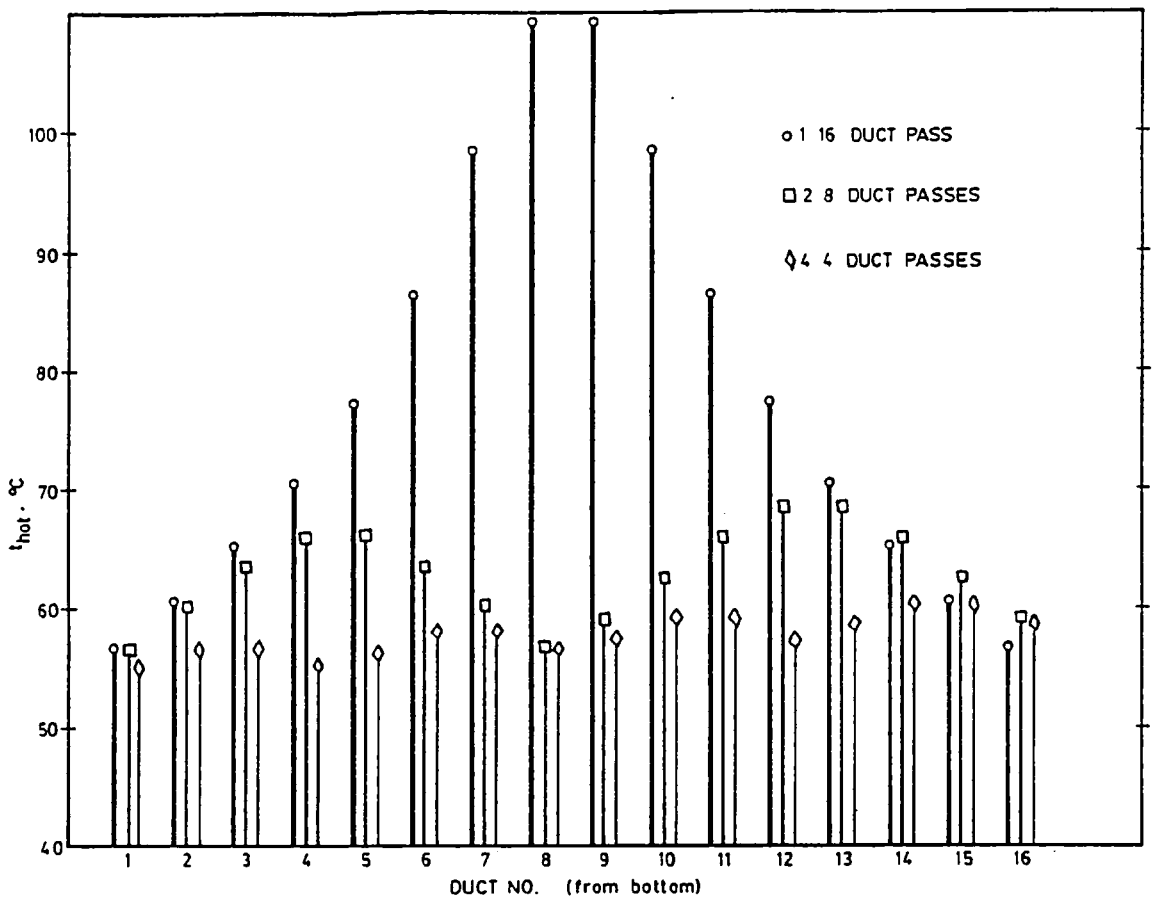


Fig. 13.4 Comparison of 16, 8 and 4 Duct Pass

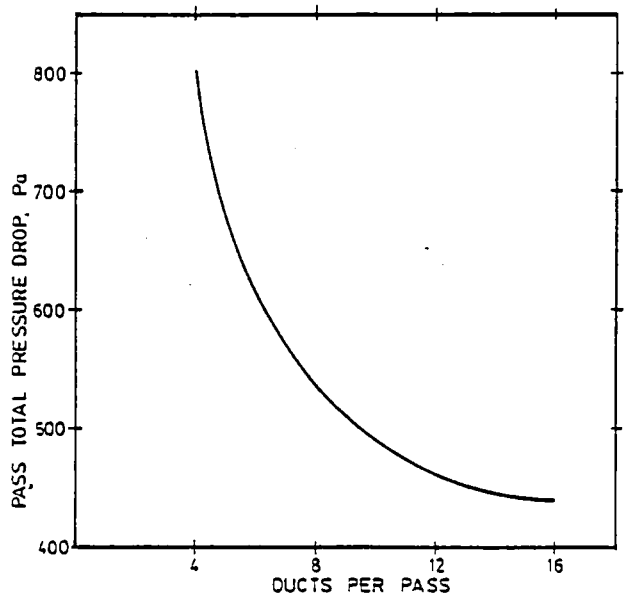


Fig. 13.5 Pressure Drop through Pass vs. Number of Ducts per Pass

13.4 Grading Horizontal Duct Thicknesses The second method of improving the thermal behaviour is to adjust the horizontal duct thicknesses c_1, c_2, etc., leaving a and b unchanged (see Fig. 3.1), so as to equalise the flow in each duct. The appropriate values of c_1, c_2, etc. may be calculated directly from the SN equations (3.25) if a = b. Assuming, for convenience, a 4 duct pass, we may define all of the resistances R_1, R_2, etc. in terms of R_1 (= R_r if a = b) by introducing the following dimensionless cubic duct thickness ratios k_1, k_2, etc.

$$k_j = \left(\frac{a}{c_j}\right)^3 , \qquad j = 1,2,\ldots 4, \tag{13.1}$$

where j is an index running in this case from 1 to 4 in increments of 1. R_j may now be defined in terms of R_1 as

$$R_j = \frac{L}{d} k_j R_1 , \qquad j = 1,2,\ldots 4, \tag{13.2}$$

(see definitions of R_j, R_1 and R_r in Fig. 3.4). If (13.2) is substituted in (3.25) and both sides are divided by iR_1, the outcome is

$$\begin{aligned}
&\frac{i_1}{i}\left[\frac{L}{d}(k_1+k_2) + 2\right] - \frac{i_2}{i}\frac{L}{d}k_2 && = -\left(\frac{L}{d}k_1 + 1\right),\\
&-\frac{i_1}{i}\frac{L}{d}k_2 + \frac{i_2}{i}\left[\frac{L}{d}(k_2+k_3) + 2\right] - \frac{i_3}{i}\frac{L}{d}k_3 && = -1,\\
&-\frac{i_2}{i}\frac{L}{d}k_3 + \frac{i_1}{i}\left[\frac{L}{d}(k_3+k_4) + 2\right] && = -1.
\end{aligned} \tag{13.3}$$

Imposing the constraint of equality of flow in each duct leads to (see (3.24)):

$$\frac{i + i_1}{i} = \frac{1}{4} ,$$

$$\frac{i_2 - i_1}{i} = \frac{1}{4} ,$$

$$\frac{i_3 - i_2}{i} = \frac{1}{4} , \qquad (13.4)$$

$$- \frac{i_3}{i} = \frac{1}{4} ,$$

from which

$$- \frac{i_1}{i} = \frac{3}{4} ,$$

$$- \frac{i_2}{i} = \frac{1}{2} , \qquad (13.5)$$

$$- \frac{i_3}{i} = \frac{1}{4} ,$$

and for a pass of N ducts

$$\frac{i_j}{i} = - \frac{N - j}{N} , \qquad j = 1,2,\ldots N-1. \qquad (13.6)$$

Substitution of (13.5) into (13.3) yields, after rearrangement

$$\frac{1}{4}\frac{L}{d}k_1 - \frac{1}{4}\frac{L}{d}k_2 = \frac{1}{2},$$

$$+\frac{1}{4}\frac{L}{d}k_2 - \frac{1}{4}\frac{L}{d}k_3 = 0, \qquad (13.7)$$

$$+\frac{1}{4}\frac{L}{d}k_3 - \frac{1}{4}\frac{L}{d}k_4 = -\frac{1}{2}.$$

Generalising for a pass of N ducts, N - 1 equations are obtained which are in fact recurrence relations

$$k_j = k_{j+1} + \frac{d}{L}(N - 2j), \qquad j = N-1, N-2, \ldots 1. \qquad (13.8)$$

If one assumes that, say k_N is known, (13.8) may be applied N - 1 times to obtain K_{N-1}, k_{N-2}, ... k_1 in terms of k_N. Upon doing so, an arithmetic progression results which may be summed, to obtain

$$K_{N-j} = k_N + \frac{d}{L}j(j + 1 - N), \qquad j = 1, 2, \ldots N - 1. \qquad (13.9)$$

To determine the value of k_N, an additional equation is needed. It may be obtained by imposing the constraint that the height of the pass remain unaltered as a result of varying c_1, c_2, etc. In the case of a pass which is initially dimensioned as $a = b = c_j$, the sum of the horizontal duct thicknesses will be Na, for N ducts. Thus, it must be required that

$$Na = \sum_{j=1}^{N} c_j, \qquad (13.10)$$

or, substituting (13.1) in (13.10),

$$N = \sum_{j=1}^{N} k_j^{-1/3}. \tag{13.11}$$

In the case of the datum design, d/L = 0.16, so that if N = 4, (13.9) gives

$$\begin{aligned} k_1 &= k_4, \\ k_2 &= k_3 = k_4 - 0.32, \end{aligned} \tag{13.12}$$

whereupon (13.11) yields

$$2(k_4)^{-1/3} + 2(k_4 - 0.32)^{-1/3} - 4 = 0. \tag{13.13}$$

Equation (13.13) may be solved numerically by any convenient method. Here, the 'graphical bisection method', as implemented on the TI-59 calculator was used, which yielded $k_1 = k_4 = 1.177$ and $k_2 = k_3 = 0.857$. Assuming a = 4 mm, the graded duct dimensions turn out to be

$$\begin{aligned} c_1 &= c_4 = 3.79 \text{ mm}, \\ c_2 &= c_3 = 4.21 \text{ mm}. \end{aligned} \tag{13.14}$$

For a = b = c = 4 mm and N = 8, the graded duct thicknesses are

$$c_1 = c_8 = 3.01 \text{ mm}$$

$$c_2 = c_7 = 3.55 \text{ mm},$$

$$c_3 = c_6 = 4.32 \text{ mm},$$

$$c_4 = c_5 = 5.14 \text{ mm}. \qquad (13.15)$$

Finally, for N = 16,

$$c_1 = c_{16} = 1.92 \text{ mm},$$

$$c_2 = c_{15} = 2.11 \text{ mm},$$

$$c_3 = c_{14} = 2.34 \text{ mm},$$

$$c_4 = c_{13} = 2.70 \text{ mm},$$

$$c_5 = c_{12} = 3.17 \text{ mm},$$

$$c_6 = c_{11} = 3.96 \text{ mm},$$

$$c_7 = c_{10} = 5.52 \text{ mm},$$

$$c_8 = c_9 = 10.28 \text{ mm}. \qquad (13.16)$$

As N increases, the grading necessary to equalise the flow becomes more drastic.

At this stage it must be recognised that it would be impractical to expect a manufacturer to produce pressboard spacers to a tolerance of 0.01 mm. The finest variation one might expect from one duct to another is 1 mm, and a more likely gradation is 2 mm. Given these realities, a 4 duct pass would not benefit from grading, and an 8 duct pass would only if 1 mm variation was available. The 16 duct pass could be graded by 1 mm by rounding off the dimensions in (13.16) to the nearest mm:

$$c_1 = c_{16} = 2 \text{ mm},$$

$$c_2 = c_{15} = 2 \text{ mm},$$

$$c_3 = c_{14} = 2 \text{ mm},$$

$$c_4 = c_{13} = 3 \text{ mm},$$

$$c_5 = c_{12} = 3 \text{ mm},$$

$$c_6 = c_{11} = 4 \text{ mm},$$

$$c_7 = c_{10} = 6 \text{ mm},$$

$$c_8 = c_9 = 10 \text{ mm}. \qquad (13.17)$$

If the minimum variation permissible was 2 mm, an improvement could still be made using the following dimensions:

$$c_1 = c_{16} = 2 \text{ mm},$$

$$c_2 = c_{15} = 2 \text{ mm},$$

$$c_3 = c_{14} = 2 \text{ mm},$$

$$c_4 = c_{13} = 2 \text{ mm},$$

$$c_5 = c_{12} = 4 \text{ mm},$$

$$c_6 = c_{11} = 4 \text{ mm},$$

$$c_7 = c_{10} = 6 \text{ mm},$$

$$c_8 = c_9 = 10 \text{ mm}. \qquad (13.18)$$

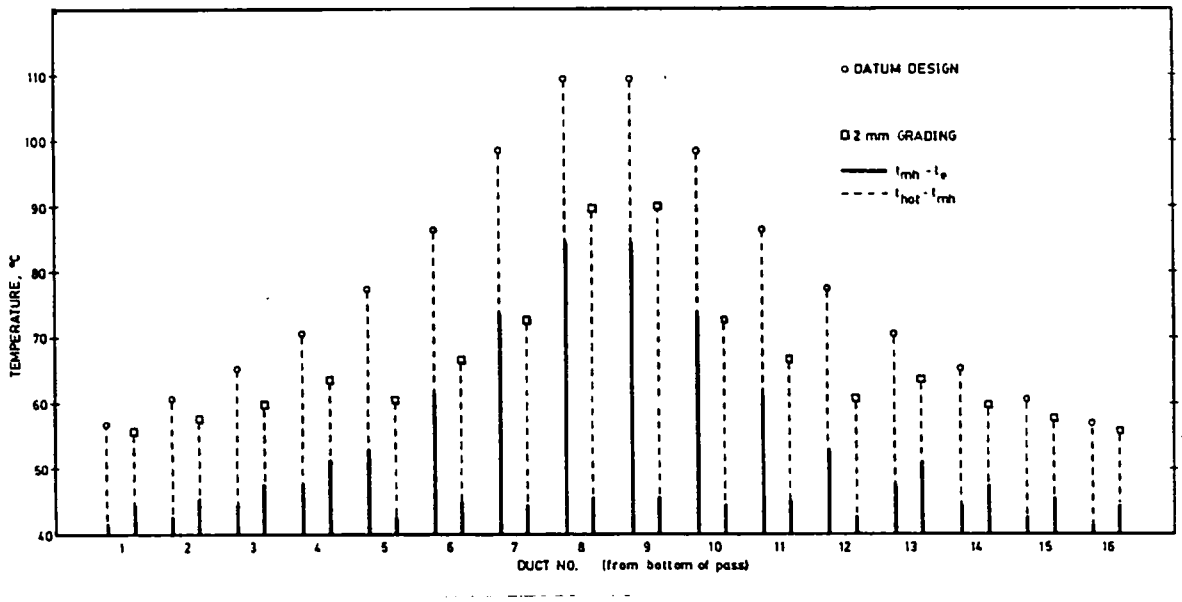


Fig. 13.6 Datum Design Compared with Graded Design

In Fig. 13.6, the datum design (circles) is compared with a pass graded in increments of 2 mm (as (13.18), squares). The solid portion of each bar represents the bulk temperature rise ($t_{mh} - t_e$) in each duct. The dashed portion represents the hottest wall temperature rise above the maximum bulk temperature ($t_{hot} - t_{mh}$).

In the datum design the extremely high t_{hot} in the middle ducts is seen to be due to a correspondingly high t_{mh} caused by maldistribution of flow. The variation in the Nusselt number (as evidenced by the variation in $t_{hot} - t_{mh}$ represented by the length of the dashed line) is only slight. In the graded design, flow maldistribution is essentially cured as evidenced by an approximately equal $t_{mh} - t_e$ in each duct. However, though the graded design certainly is an improvement ($t_{hot,8}$ reduced by 20 ^{o}C), it is thermally less successful than the division of the pass into two 8 duct passes, where the greatest t_{hot} is reduced by 40 ^{o}C. The total pressure drop for the graded and two 8 duct passes is

also about the same.

The graded design is less successful due to the fact that increasing the hydraulic diameter of the middle ducts leads to a substantial decrease of the mean velocity there. Since, in the thermal entrance region, the temperature field is essentially a boundary layer phenomenon, the local Nusselt number will be influenced by the mean velocity (not the flow rate). Hence equality of flow rate in ducts 1 and 8 yields equal bulk temperature rises (see Fig. 13.6), yet since $c_8/c_1 = 5$, the Nusselt number is substantially lower in the middle ducts, and $t_{hot,8} - t_{hot,1} = 24\ ^{o}C$. A similar effect may be expected, even when the temperature profiles are fully developed. Rearranging (2.7) and (2.8), (setting $t_{wall} = t_{hot}$ and $t_m = t_{mh}$) leads to

$$t_{hot} - t_{mh} = \frac{\dot{q}''_w D_h}{Nu\ k}\ , \qquad (13.19)$$

from which it may be seen that two ducts, in which the flow is fully developed thermally and hydrodynamically (Nu constant), with the same surface heat flux and bulk temperature rise, will have different $t_{hot} - t_{mh}$ in direct proportion to the difference in the hydraulic diameters.

It would thus seem that the optimal design for a transformer pass would be one that produces equality of flow rate and mean velocity in every duct while maintaining uniform horizontal duct thickness. Such a design would distribute the thermal loading evenly through a pass whether or not the temperature fields were fully developed or developing, and would thus be applicable to both natural and forced oil flow conditions. Although it cannot be achieved exactly, this very

desirable situation can be closely approached by increasing the ratio a/c (or b/c).

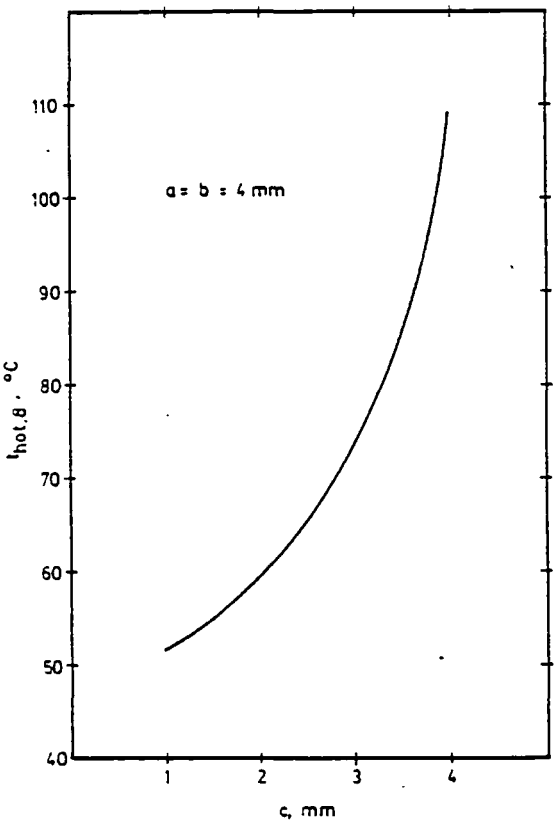


Fig. 13.7 $t_{hot,8}$ vs. c

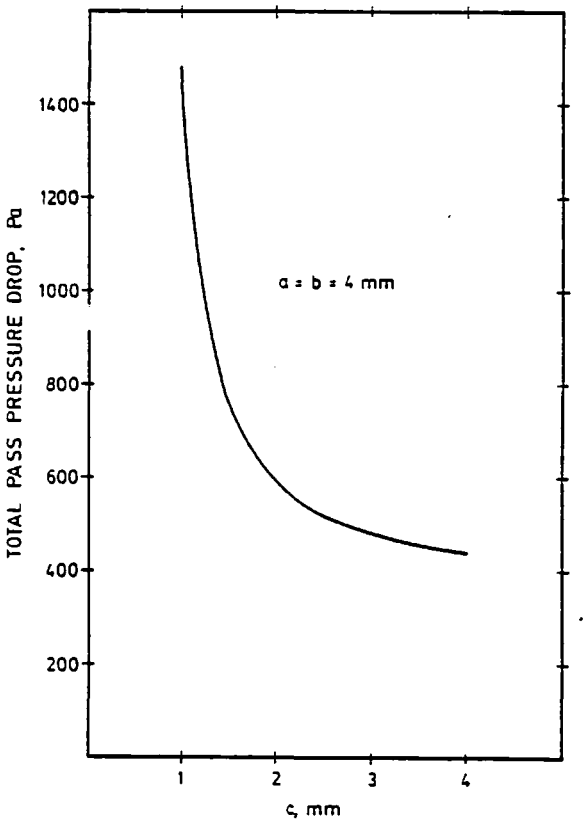


Fig. 13.8 Pressure Drop vs. c

13.5 Increasing Vertical Duct Thickness A third method of correcting maldistribution of flow may be seen by consideration of the network analogue, Fig. 3.4. If $R_1 = R_2 = R_3 = R_4$, which is the case when all the horizontal duct thicknesses are equal, then equal 'current' will flow in these 'resistors' provided that the 'volt' drop across each is the same. This condition will be nearly attained if R_l and R_r are small relative to R_1, R_2, etc. Since all of the 'resistors' are inversely proportional to the cube of the duct thicknesses, increasing the ratio a/c (and b/c) is the most effective way of decreasing R_l/R_j (and R_r/R_j).

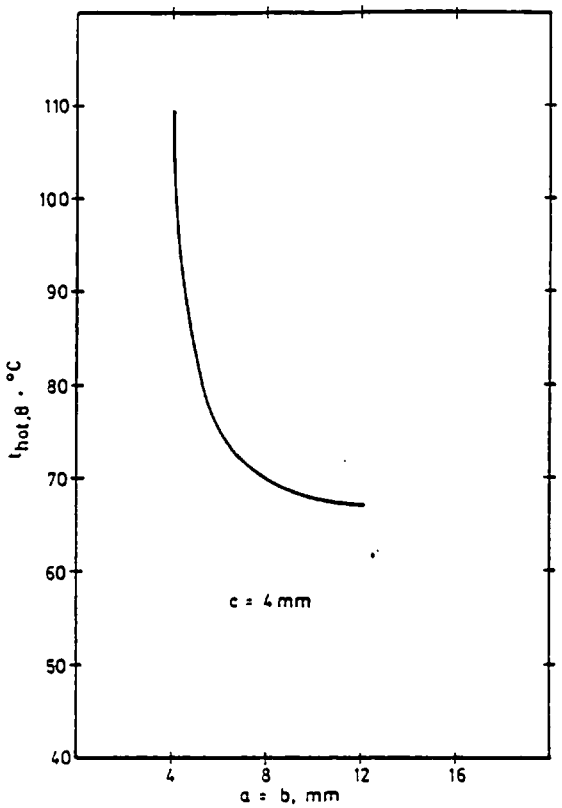


Fig. 13.9 $t_{hot,8}$ vs. a (b)

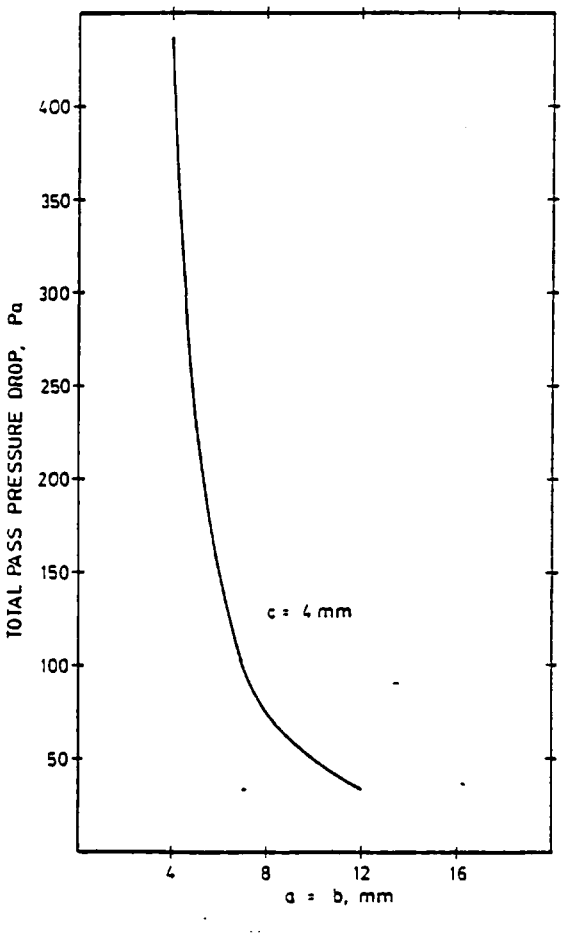


Fig. 13.10 Pressure Drop vs. a (b)

Working from the datum design, one could either increase a and b leaving c = 4 mm or decrease c by the same in all ducts leaving a = b = 4 mm. The effect of the latter is seen in Fig. 13.7, where $t_{hot,8}$ is plotted against c. The dramatic decrease in $t_{hot,8}$ with c is accompanied by an equally dramatic increase in the total pressure drop through the pass, as seen in Fig. 13.8. Alternatively increasing a and b equally, while leaving c = 4 mm causes <u>both</u> $t_{hot,8}$ and the total pass pressure drop to <u>decrease</u>, as seen in Figs. 13.9 and 13.10. In both cases, a dramatic improvement is obtained for a relatively minor change (0.5 mm) in either a (and b) or c.

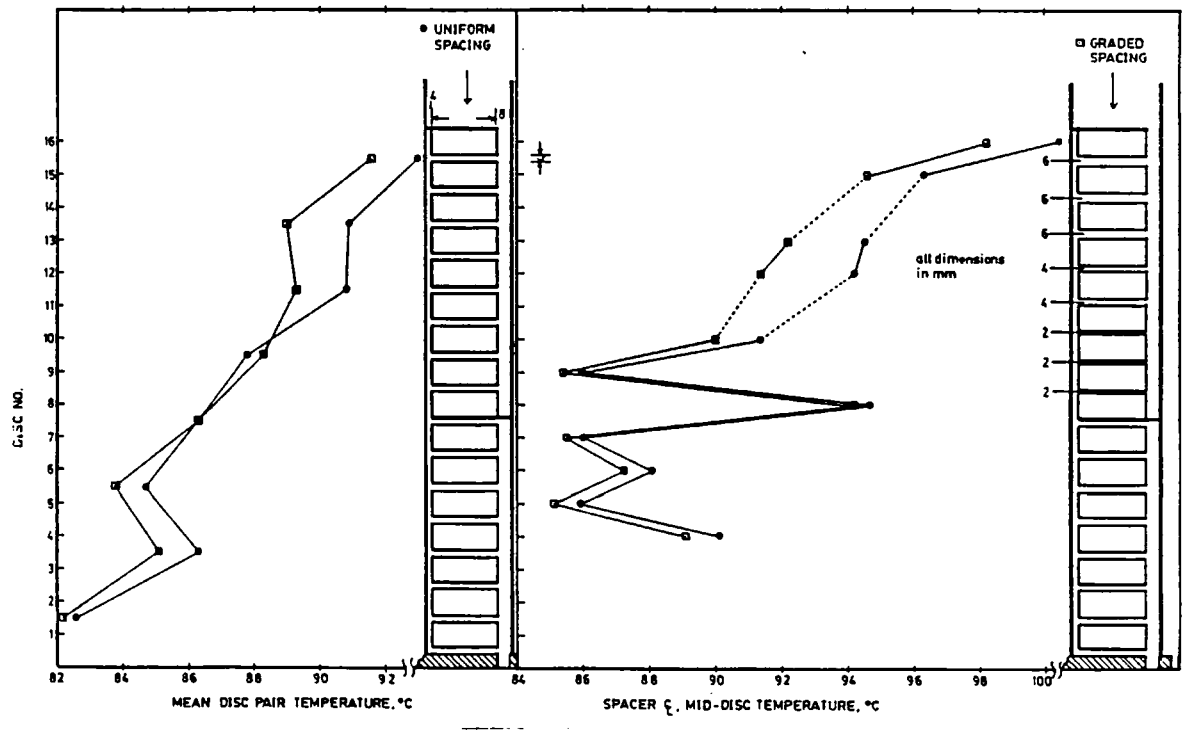


Fig. 13.11 Effect of Duct Thickness Grading in Facsimile Winding

13.6 Experimental Results The three above mentioned optimisation methods, especially the last two, assume equal left and right vertical duct thicknesses, and hence a symmetrical flow distribution. In the experimental duct, since a = 4 mm and b = 8 mm, the flow was asymmetrical, nonetheless it was desired to attempt improvement of the thermal design by one of the above methods. In the early stages of the theoretical work (when this experiment was planned), grading the horizontal duct thicknesses appeared to be the most promising optimisation method.

The spacers supplied by the manufacturer were all 2 mm thick -- too thick to effect any improvement in a symmetrically arranged 8 duct pass (as (13.15) and accompanying discussion). Nevertheless, an attempt was made to force more oil to flow through the top starved ducts, and

the arrangement shown as Fig. 13.11 was used (see the right side of the figure). The lower pass was left unaltered. No attempt was made to measure the flow distribution in the top pass, or to predict flow or temperature using DUCT or DISCNET. The object of the excercise was merely to illustrate experimentally the effect of grading on the winding temperature distribution and to assess whether grading in this case afforded any improvement.

The graded and ungraded designs are compared in Fig. 13.11. On the left are plotted the mean disc pair temperature distributions, obtained by resistance, and on the right, the local temperatures (read from the t.c.'s) in the middle of each disc and the centre of the spacer column. (Recall that t.c.'s were installed only in discs 4, 5, 6, 7, 8, 9, 10, 12, 13, 15 and 16). The circular points in both plots are taken from the data given as Table 12.2.

The graded winding was tested under the same conditions and over the same range of flow rates as the second set of tests described in Chapter 12, however upon examining the results, it was found that the winding oil temperature rise above the bottom oil temperature $\theta'_w = t_w - t_b$ was much higher than in the ungraded winding. If the approximate assumption is made that t_w and t_b are both bulk fluid temperatures (see Chapter 11) then θ'_w at the same flow and dissipation rate should be the same for the graded and uniform spacing. In Fig. 13.12, where θ'_w is plotted against 1/Q (Q being the pass inlet flow rate in cm^3/s inferred from the pump R.P.M.), it can be seen that the slopes of the lines from the two sets of results are quite different. After the tests on the graded winding, it was discovered that the outer perspex cylinder had worked its way up from the steel base plate. A similar difficulty was

noted in the third set of measurements described in Chapter 12.

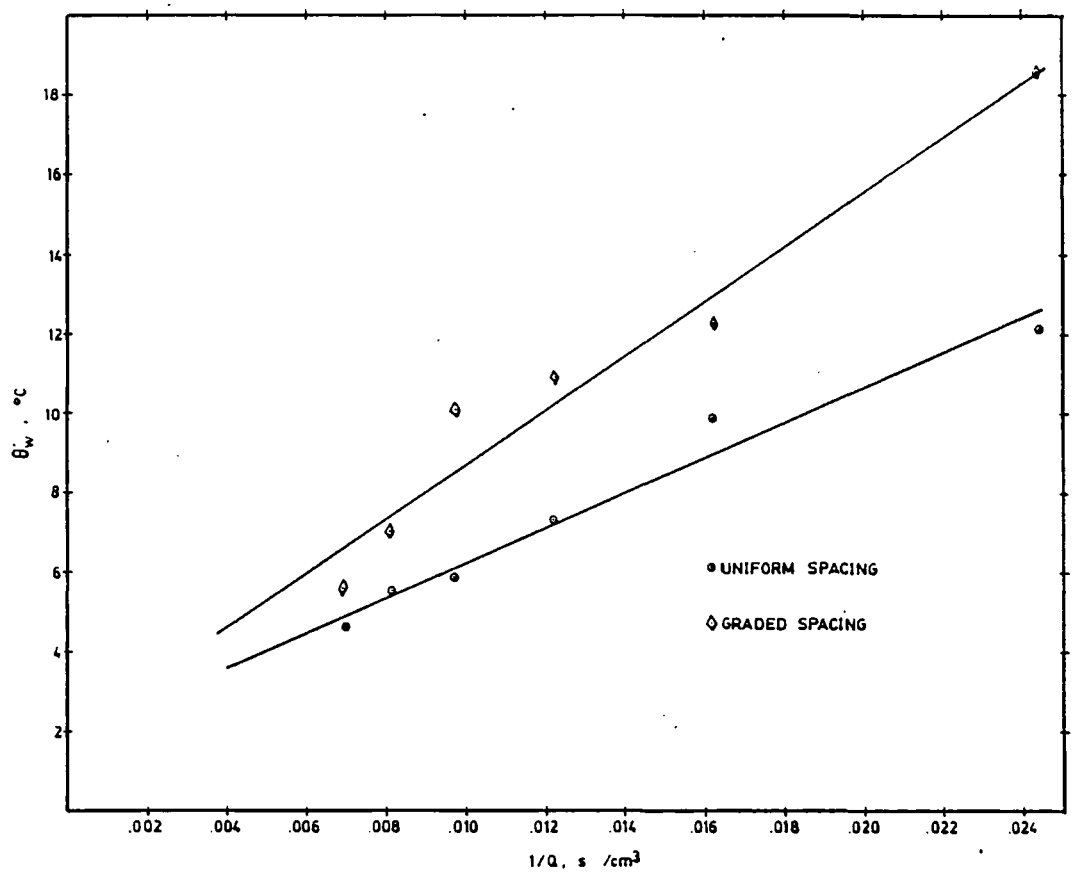


Fig. 13.12 Top Oil Rise vs. 1/Q, Graded and Ungraded Winding

To salvage the results ; it was decided to compare the results of Table 12.2 with a corresponding set from the graded measurements which which had the same θ'_w (7 ^{o}C). The flow rate, of course, was higher (123.4 cm^3/s for the graded set, compared to 82.65 cm^3/s for the ungraded set). This 49% increase corresponds reasonably well with the 56% increase in the slope of the graded curve over the ungraded, Fig. 13.12. t_b for the graded set was 56.0 ^{o}C, very close to that of the ungraded set (55.8 ^{o}C).

The comparison in Fig. 13.11 of the two measurements, especially the t.c. readings on the right-hand side, do show that in the bottom

pass, the temperatures are very close (within 1 ^{o}C), whereas near the top of the upper pass, the temperatures in the graded case are about 2 ^{o}C lower. Though this is a small difference, it is believed to be significant enough to at least illustrate the effect of grading.

13.7 Assessment of Optimisation Techniques Of the three methods described, all appear to offer some improvement in the thermal performance. In a given design situation, the effect of a specific thermal design modification may actually decrease the reliability or performance of the winding in some other respect. For example, increasing the ratio a/c would seem the most effective method of correcting maldistribution, especially by increasing a or b (since both the hot-spot temperature and the pressure drop are reduced). This however, will increase the gap between the core and the l.v. winding, or between the l.v. and h.v. windings, and may reduce the electromagnetic efficiency of the transformer. The alternative, viz. reducing c might lessen the ability of the winding to withstand surge conditions without failure. Standring and Hughes (1956) measured the puncture voltage of pressboard sheets of various thicknesses, with and without oil gaps. Their results, plotted as puncture voltage vs. oil gap, had slopes ranging from 4 - 12 kV/mm. Modest reductions in c might therefore be acceptable, if the manufacturer could achieve greater precision in this aspect of the assembly process.

Any design modification which alters the spacing between discs, viz. grading, or inserting U.S./U.K.-type flow-diverting washers, will also alter the spatial distribution of the ampere-turns in that winding and could affect the short-circuit strength of the transformer. According to Waters (1966), a typical power transformer must be designed

to withstand short-circuit currents up to 25 times the base current. Since the forces developed within the windings are proportional to the square of the current, they must be analysed with great care.

The ideal design is to have exact ampere-turn balance between the l.v. and h.v. windings, and to have the spatial ampere-turn distributions uniform and precisely aligned axially. In particular, the 'electrical' centers of each winding must be at precisely the same height. If one winding is lower than the other, additional radial magnetic fluxes are generated which give rise to an axial thrusting force tending to displace the windings even further from the correct position. Any displacement which does occur gives rise to a even larger thrusting force, and so on. Gibbs (1950) states that a 2,500 kVA 44 kV core-type transformer may have an end thrust of ~~4046~~ 80,071 N (18,000 lb) per leg for displacement of as little as 13 mm.

In practice, displacement of electrical centers is never an intentional design, however it is common for some variations within a winding in the spatial ampere-turn distribution to occur due to tapping arrangements. Assuming that all tapping occurs in the h.v. (outer) winding, 'gaps' occur in it which are absent in the l.v. winding. The effect of these gaps is to introduce thrusting forces against the top and bottom clamps of the h.v. winding, and to increase the forces on individual coils within both windings. (Even in a perfectly aligned transformer, axial compression forces are generated within each winding, being highest on the end coils). These forces can be reduced by tapping the h.v. coil symmetrically, in small amounts, at several locations and by introducing compensatory gaps in the l.v. winding at the appropriate locations.

In view of short-circuit considerations, thermal design improvement by grading is not recommended as a first choice (although the slight variation in duct thickness brought about by grading is generally far less drastic than in tapping arrangements). Also Japanese-type flow-diverting washers are recommended over the U.S./U.K.-type. In any event, it would clearly be advantageous to assess the thermal effect of a particular tapping arrangement and, if possible, to arrange the location of flow-diverting washers so as to use it to advantage. Under no circumstances should an asymmetrical grading arrangement as shown in Fig. 13.11 be used as this will displace the electrical centre of the winding. In fact, there appears to be little advantage in the asymmetrical flow distribution brought about by unequal vertical duct thicknesses.

13.8 Conclusion The best thermal optimisation procedure would probably be a combination of method 1 (using Japanese-type washers) and method 3. If, in using method 3, it is decided to reduce the horizontal duct thicknesses c, this should be done in both windings. In that case, no short-circuit design modification would be needed. This combination of methods should have sufficient flexibility to accommodate electromagnetic and surge design considerations. In any event, the potential for thermal improvement and consequent uprating of an improved design, is very high.

The above calculations also demonstrate how sensitive the thermal performance of a given design is to small departures from nominal duct thicknesses. These departures easily occur in the course of winding construction, and might explain the considerable variation, noted by

some manufacturers, in the performance of windings of identical design.

CHAPTER 14

FURTHER WORK

14.1 Introduction Most of the effort in this thesis has been, on the one hand, concerned with the physical and mathematical basis of the software: TEACH-L, JUNCTION, CORNER, DUCT and DISCNET, and on the other, with the development of an experimental programme to confirm the theory. An attempt has been made to point out shortcomings at each stage of the work, and no doubt some investigation of these would be required before a commercial user would want to use the software directly in his design process. Increasing the grid refinement in the JUNCTION and CORNER codes might yield more accurate values of the friction constants, and interaction between neighbouring junctions could also be analysed. In addition to the junction and corner pressure drops, losses along known leakage flow paths could be modelled using TEACH-L, as well as those through particular baffling arrangements in OD designs. DISCNET could be incorporated into an overall mass and heat flow network which included the flow in the core and the radiators, enabling a prediction of the flow rate through the winding under ON conditions.

More basic to the physical analysis are two effects which have been ignored, and might well be included in any further research programme. They will be briefly discussed in this concluding chapter.

14.2 Circumferential Heat Flow The thermal analysis of Chapter 7 neglected any circumferential variation of temperature within a disc, and thus can be expected to predict temperatures accurately only at the horizontal duct centre-line. Even if this is deemed adequate, problems

can arise in setting the appropriate value of winding current in DUCT, due to the masking effect of the spacers, as was seen in Chapter 12.

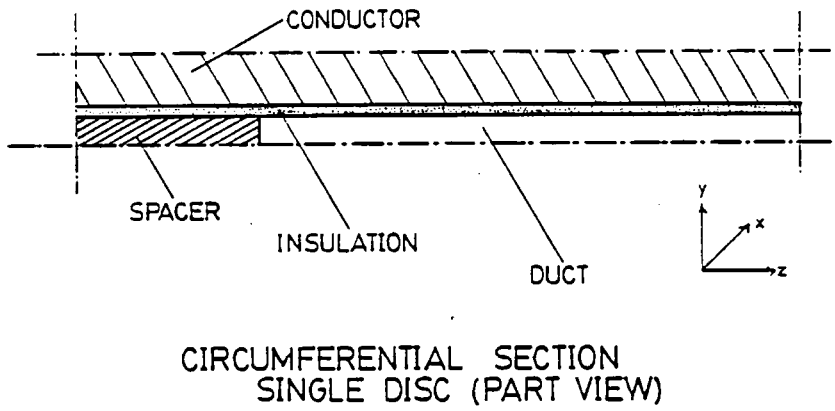


Fig. 14.1 System for Analysis of Circumferential Heat Flow

The only satisfactory solution would appear to be to analyse the full 3-dimensional situation, a circumferential section of which is shown as Fig. 14.1. A quarter section of the duct, whose axis is normal to the page, is shown, surrounded by the paper-insulated conductor on top, and the pressboard spacer on the left. The thermal system is bounded on all sides by the respective centre-lines, presumed also to be lines of symmetry. As with the system shown in Fig. 7.1, Fig. 14.1 presents a conjugated problem because of circumferential heat conduction in the solid areas.

A first step in the analysis might be to assume fully-developed velocity and temperature profiles. Although the latter is unlikely to occur in a relatively short duct with high Prandtl number fluids, such a preliminary analysis would indicate roughly how much heat flows through the spacers in the positive z-direction (most heat flow would be expected to flow through the conductor insulation in the negative y-direction, see Fig. 14.1). A similar analysis was applied to layer

windings by Allen and Allan (1963).

Relaxing the assumption of fully-developed thermal profiles would represent a substantial escalation of computing costs if a fully elliptical formulation such as DUCT were used. Adequate information could probably be obtained from a solution procedure which 'marched' in the x-direction. One such, especially developed for high Prandtl number fluids is the 'truncation' method, due to Allen and Finn (1969).

Irrespective of the method used, the solution would yield 1.) the percent heat flow through the spacers: the 'masking factor', as a function of duct, conductor and spacer dimensions and 2.) the temperature difference in the conductor between the spacer and duct centre-lines (extreme left and right, respectively, of Fig. 14.1) as a function of the 'masking factor' and the dissipation rate. A more accurate prediction of the hot-spot temperature could then be made.

14.3 Radial Flow between Parallel Discs As seen in the plan view of a typical disc winding, Fig. 2.1, the horizontal ducts are not of uniform circumferential width, and consequently some deceleration/acceleration in outward/inward flowing oil will occur. The pressure drop will not be as in the parallel plane geometry; in particular, pressure regain will compensate friction losses in decelerating outward flows, while additional pressure drops due to acceleration will add to friction losses in inward flows. As L/R increases, the effect may be expected to be more pronounced. This might occur in practice in windings with relatively small mean radii.

The problem can still be simplified to 2 dimensions, as shown in

Fig. 14.2, the coordinates being r and y rather than x and y. Assuming laminar, incompressible, purely radial, constant property flow, the continuity and momentum equations become

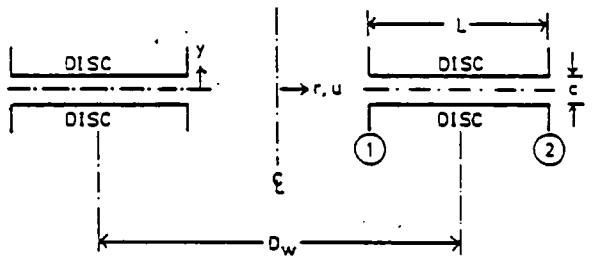


Fig. 14.2 Radial Flow between Parallel Discs

$$\frac{\partial u}{\partial r} + \frac{u}{r} = 0, \tag{14.1}$$

and

$$\rho u \frac{\partial u}{\partial r} = - \frac{\partial p}{\partial r} + \mu\left(\frac{\partial^2 u}{\partial r^2} + \frac{1}{r}\frac{\partial u}{\partial r} - \frac{u}{r^2} + \frac{\partial^2 u}{\partial y^2}\right). \tag{14.2}$$

Kreith (1966) presented a series solution of these equations, also solving the energy equation with constant disc wall temperatures, insulated (zero wall heat flux) discs, and combinations of these two. Jackson and Symmons (1965) presented experimental results, using air; Moller (1963) studied theoretically and experimentally air flow in both laminar and turbulent regimes. A preliminary grasp of the importance of the radial flow effect can be obtained from Livesey's (1960) simplified analysis. He pointed out that the inertia term $\rho u \frac{\partial u}{\partial r}$ in (14.2) may be neglected to first approximation in low Reynolds number flow. The resultant equation may then be easily solved for the radial velocity

profile:

$$u(r,y) = \frac{3Q}{\pi r c^3}\left[(c/2)^2 - y^2\right], \tag{14.3}$$

where Q is the flow rate, given by

$$Q = u_m 2\pi r c, \tag{14.4}$$

where u_m is the mean velocity and is of course a function of r. The pressure drop Δp from station 1 to 2 is then

$$\Delta p = \frac{6\mu Q}{\pi c^3} \ln\left[\frac{1 + L/D_w}{1 - L/D_w}\right], \tag{14.5}$$

where D_w is the mean winding diameter (see Fig. 14.2). Equation (14.3) is a parabolic velocity profile, similar to the parallel plane solution, but modified by a factor containing 1/r. The pressure drop given by (14.5) is thus logarithmic rather than linear. The degree of difference between the two may be seen by series expansion (Dwight (1961), p. 137) of (14.5):

$$\Delta p = \frac{12\mu Q}{\pi c^3}\frac{L}{D_w}\left[1 + \frac{(L/D_w)^2}{3} + \frac{(L/D_w)^4}{5} + \ldots\right]. \tag{14.6}$$

The first term is equivalent to the pressure drop for the parallel plane duct. The additional terms will be insignificant provided that $L/D_w \ll 1$.

An analytical solution in closed form to (14.2) has never been found, however an estimate of the importance of deceleration/acceleration to the pressure drop may be found by substituting (14.3) into (14.2) and integrating to obtain the pressure drop from station 1. to 2. The result is

$$\Delta p = \frac{12\mu Q}{\pi c^3}\frac{L}{D_w}\left\{\left[1 + \frac{(L/D_w)^2}{3} + \frac{(L/D_w)^4}{5} + \ldots\right]\right.$$

$$\left. - \frac{Re}{20}\frac{c}{R}\left[1 - 2(L/D_w)^3 + \ldots\right]\right\}, \qquad (14.7)$$

where the first series is the friction term (14.6) and the second series is the additional momentum term. Here,

$$Re = \frac{\rho Q}{\pi R \mu}. \qquad (14.8)$$

In both (14.6) and (14.7) Q is positive for outward flows, and negative for inward flows. Thus for $Q > 0$, the second term of (14.7) will decrease the pressure drop from station 1 to 2 (see Fig. 14.2). The importance of momentum will be slight provided that

$$\frac{Re}{20}\frac{c}{R} << 1. \qquad (14.9)$$

In most oil-immersed disc windings, (14.9) would probably hold along with $L/D_w << 1$; the effect was therefore not considered further here. It might however be usefully included in further research, especially if air-cooled windings were studied.

14.4 Conclusion The analytical tools developed in this thesis are really only the beginning of what could be accomplished in the computer-aided thermal design of large power transformers. Now that desk-top microcomputers are being made available which have a capacity comparable to medium-sized main frames, and at a low enough cost that every design engineer might have one for his personal use, the manufacturer should be able to specify the location and value of the hottest-spot temperature quite precisely. He should also be able to optimise the thermal design interactively with the electromagnetic and electrostatic design. The use of such methods will greatly increase the effectiveness, while lowering the cost, of the design process, and significantly reduce the cost per KVA of the final product.

CHAPTER 15

REFERENCES

Acrivos, A., B. D. Babcock and R. L. Pigford (1959): **Chem. Eng. Sci.**, Vol. 10, pp. 112-124

Akiyama, M., G. J. Hwang and K. C. Cheng (1971): "Experiments on the onset of longitudinal vortices in laminar forced convection between horizontal plates", ASME Paper 71-HT-1

Allen, P. H. G. (1957): "The thermal properties of high voltage insulants", IEE Monograph No. 250 M (105C, p.35)

Allen, P. H. G (1959): "Fluid thermal conductivity by a transient method", in "Thermodynamic and Transport Properties of Gases, Liquids and Solids", ASME, McGraw-Hill, New York, pp. 350-357

Allen, P. H. G. (1960): "Heat Transfer in Layer Type Windings in High Voltage Power Transformers", Ph.D. Thesis, University of London, 1960

Allen, P. H. G. and D. Allan (1963): **Proc. IEE**, Vol. 110, p.523

Allen, P. H. G. (1968): "Heat transfer in a simple vertical transformer oil duct", Proc. XIII International Colloquium, Technische Hochschule Ilmenau, Part 6, pp. 71-76

Allen, P. H. G. and A. H. Finn (1969): "Transformer winding thermal design by computer", IEE Conf. Pub. 51, pp. 589-599

Allen, P. H. G. and A. H. Finn (1970): **J. Heat Transfer**, May 1970, p. 299

Allen, P. H. G. and A. Tustin (1972): **IEEE Transactions on Electrical Insulation**, Vol. EI-7, No. 3, pp.153-157

Allen, P. H. G. (1972), discussion of Norris (1971): **Proc. IEE**, Vol. 119, No. 8, pp. 1183-1187

Allen, P. H. G. and K. Havlicek (1974): **Electrical Review**, 7/6/1974, pp. 647-650

Allen, P. H. G. (1975), discussion of Norris (1974): **Proc. IEE**, Vol. 122, p. 545

Allen, P. H. G. (1975), **Electrical Times**, 20/6/1975, pp. 10-11

Allen, P. H. G., O. Szpiro and E. Campero (1981): **Electric Machines and Electromechanics**, Vol. 6, pp. 1-11

Atkinson, B., M. P. Brocklebank, C. C. H. Card and J. M. Smith (1969): **AIChE Journal**, Vol. 15, pp. 548-553

Batchelor, G. K. (1967): "An Introduction to Fluid Dynamics", Cambridge University Press, Cambridge

Benedict, R. P. (1977): "Fundamentals of Temperature, Pressure and Flow Measurements", John Wiley and Sons, New York

Blest, D. C. (1972): **Proc. ASCE**, Vol. 98, HY1, pp. 171-179

Bertrand, J. and J. P. Couders (1978): **DISA Information**, No. 23, p. 28

Blowers, R. M. (1972): **Computer Physics Communications**, Vol. 4, pp. 64-72

Brechna, H. and M. Tschudi (1962): **Bull. Assoc. Suisse Elect.**, Vol. 53, No. 22, pp. 1069-1081

British Standard 148:1972

British Standard 171:Part 2:1978

CP 1010:1975 (Codes of Practice Committee for Electrical Engineering)

CRC Handbook of Chemistry and Physics, CRC, Cleveland, 1977

Carruthers, M. G. and E. T. Norris (1969): **Proc. IEE**, Vol. 116, No. 9, pp. 1564-1570

Cheng, K. C. and G. J. Hwang (1969): **J. Heat Transfer**, Feb. 1969, p. 59

Cheng, K. C., S. W. Hong and G. J. Hwang (1972): **Int. J. Heat and Mass Transfer**, Vol. 15, p. 1819

Collins, M. W., P. H. G. Allen and O. Szpiro (1977): **Proc. IME**, Vol. 191, pp. 19-29

DISA, Type 55M10 Instruction Manual, August 1977, Denmark

Dryden, H. L., F. D. Murnaghan and H. Bateman (1932): "Hydrodynamics" Bull. No. 84, pp. 197-201, Comm. Hydrodyn., Div. Phys. Sci., Natl. Res. Counc., Washington, D. C.; reprinted by Dover, New York, 1956

Dwight, H. B. (1961): "Tables of Integrals and Other Mathematical Data", 4th Ed., Macmillan, New York

EPRI Journal, September 1979

Eastgate, C. (1965): **Proc. IEE**, Vol. 112, pp. 1127-1134

Eckelmann, H. (1976): **DISA Information**, No. 13, p. 16

Favre, H. (1937): **Revue Universelle des Mines**, Vol. 13, No. 12, p. 502

Finn, A. H. (1971): "Futher Investigations into High Voltage Layer Type Winding Cooling", Ph.D. Thesis, University of London

Gibbs, J. B. (1950): "Transformer Principles and Practice", McGraw-Hill, New York

Gosman, A.D., B. E. Launder, F. C. Lockwood and G. J. Reece (1975): Imperial College of Science and Technology, Mechanical Engineering Dept., London SW7 2BX, series prepared under the auspices of the National Development Program in Computer Assisted Learning, 1975

Gourdon, C., J. Costes and S. Domenech (1981): **DISA Information**, No. 26, p. 19

Grubb, R. L., M. Hudis and A. R. Traut **IEEE PAS**, Vol. 100, No. 2, pp. 466-472

Haggblad, B. and M. Mattsson (1983): **ASEA Journal**, Vol. 56, No. 1, pp. 32-39

Hinze, J. O. (1959): "Turbulence", McGraw-Hill, New York

Hollasch, K. and B. Gebhart (1972): **J. Heat Transfer**, Vol. 94, pp. 17-22

Howe, A. F. (1978): **Proc. IEE**, Vol. 125, No. 10, p. 978

Imre, L. and G. Y. Dankó (1976): **Per. Pol. El. Eng.**, Vol. 20, p. 89

Imre, L. (1976): **Per. Pol. El. Eng.**, Vol. 20, p. 461

Imre, L., et al. (1978): Proc. Sixth Int'l Heat Transfer Conference, Toronto, Aug. 1978, Vol. II, Paper EC-20, pp. 123-128

Imre, L. and A. Bitai (1978): **Per. Pol. Mech. Eng.**, Vol. 23, p. 265

Imre, L. (1981): Chapter 3 of "Numerical Methods in Heat Transfer", ed. R. W. Lewis, K. Morgan and O. C. Zienkiewicz, John Wiley and Sons, New York

Jackson, J. D. and G. R. Symmons (1965): **Appl. Sci. Res.**, Vol. 15, pp. 59-75

Jamison, D. K. and J. R. Villemonte (1971): **Journal** ASCE, Vol. 97 (HY7) pp. 1045-1061

Kays, W. M. (1966): "Convective Heat and Mass Transfer", McGraw-Hill, New York

Keller, J. D. (1949): **J. Appl. Mech.**, Vol. 16, p. 77

King, L. V. (1914): **Phil. Trans. R. Soc. Lond.**, Vol. 214, Ser. A, pp. 373-432

Kramers, H. (1946): **Physica**, Vol. 12, pp. 61-80

Kreith, F. (1966): **Int. J. Heat and Mass Transfer**, Vol. 9, pp. 265-282

Lampe, W., B. G. Persson and T. Carlsson (1972): CIGRE Paper 12-02

Livesey, J. L. (1960): **Int. J. Mech. Sci.**, Vol. 1, pp.84-88

Lobenstein, G. (1967): **Elektrie**, Vol. 2, p. 53

McNown, J. S. and E.-Y. Hsu (1950): "Application of conformal mapping to

divided flow", Proc. of the First Midwestern Conference on Fluid Dynamics, pp. 143-155

McNutt, W. J., G. J. Kaufmann, A. P. Vitols and J. D. MacDonald (1979): "Short time failure mode considerations associated with power transformer overloading", IEEE PES Summer Meeting, Vancouver, Paper F 79 695-8

Marco, S. M. and L. S. Han (1955): **Trans.** ASME, Vol. 77, pp. 625-630

Moller, P. S. (1963): **Aero. Quart.**, Vol. 14, pp. 163-186

Muur, S. (1962): CIGRE Paper Vol. 2, p.

Natarajan, N. M. and S. M. Lakshmanan (1972): **Indian J. Technol.**, Vol. 10, pp. 435-438

Navier, C. L. M. H. **Memoires Acad. R. Sci.**, Paris, Vol. 6, pp. 389-416

Norris, E. T. (1971): **Proc. IEE**, Vol. 118, No. 11, pp. 1625-1629

Norris, E. T. (1974): **Proc. IEE**, Vol. 121, No. 8, pp. 840-844

Oliver, A. J. (1980): **Proc. IEE**, Vol. 127, Pt. c, No. 6, pp. 395-405

Patankar, S. V. and D. B. Spalding (1971): "A calculation prodedure for heat, mass and momentum transfer in three-dimensional parabolic flows", Imperial College of Science and Technology, Mechanical Engineering Department, Report BL/TN/A/45

Patankar, S. V. (1982): "Numerical methods in heat transfer", Proceedings 7th International Heat Transfer Conference, Munich, Sep. 6-10, 1982, Vol. 1, pp. 83-90

Perry, A. E. and G. L. Morrison (1971): **J. Fluid Mech.**, Vol. 47, Part 3, pp. 577-599

Pivrnec, M. and K. Havlicek (1972): **Electrotechn. Obz.**, Vol. 61, pp. 175-181

Pivrnec, M. (1973): **Electrotechn. Obz.**, Vol. 62, pp. 434-440

Pollard, A. and D. B. Spalding (1980): **Int. J. Heat and Mass Transfer**, Vol. 23, pp. 1605-1607

Pratt, F. C. (1972): contribution to Group 12 discussion, Proceedings CIGRE

Preiningerova, V. and P. H. G. Allen (1974): "Laminar flow entry length heat transfer with varying physical properties in simple and complex duct geometries", Proceedings 5th International Heat Transfer Conference, Tokyo, Paper NC5.4

Preiningerova, V. and M. Pivrnec (1977): **Proc. IEE**, Vol. 124, pp. 218-222

Preiningerova, V. (1983): **Electric Machines and Power Systems**, Vol. 8, No. 2, pp. 89-102

Schlichting, H. (1979): "Boundary-Layer Theory", 7th Ed., McGraw-Hill, New York

Shah, R. K. (1975): "Thermal entry length solutions for the circular tube and parallel plates", Proc. Natl. Heat Mass Transfer Conf., 3rd, Indian Inst. Technol., Bombay, Vol. I, Pap. No. HMT-11-75

Shah, R. K. and A. L. London (1978): "Laminar Flow Forced Convection in Ducts", Advances in Heat Transfer, Supplement 1, 1978

Simitovic, R. (1977): "Turbulent flow in a rectangular duct with an obliquely-introduced secondary jet", Ph.D. Thesis, University of London; also Imperial College of Science and Technology, Dept. of Mech. Engng., Heat Transfer Section, Report HTS/77/18

Spalding, D. B. (1972): **Int. J. Num. Meth. Engng.**, Vol. 4, pp. 551-559

Spalding, D. B. (1981): **Mathematics and Computers in Simulation**, North Holland Press, Vol. XXIII, pp. 267-276

Sparrow, E. M., J. L. Novotny and S. H. Lin (1963): **AIChE Journal**, Vol. 9, pp. 797-804

Strandring, W. G. and R. C. Hughes (1956): **Proc. IEE**, Vol. 103A, pp. 583-597

Steckler, Γ. (1928): **Elektrotechnik und Maschinenbau**, Vol. 46, pp. 285-287

Steckler, F. (1929): **Elektrotechnik und Maschinenbau**, Vol. 47, pp. 395-400

Stein, R. and W. T. Hunt, Jr. (1979): "Electric Power Systems and Components", Van Nostrand Reinhold Co., New York

Stokes, G. G. (1845): **Trans. Camb. Phil. Soc.**, Vol. 8, pp.287-308

Szpiro, O., "Research into Temperature and Oil Flow Distributions in Disc-Type Power Transformer Windings", Ph.D. Thesis, University of London

Szpiro, O., P. H. G. Allen and C. W. Richards (1982): "Coolant distributions in disc type transformer winding horizontal ducts and its influence on coil temperatures", Proceedings 7th International Heat Trnasfer Conference, Munich, Sep. 6-10, 1982, Vol. 6, pp. 251-256

Taylor, E. D., B. Berger and B. E. Western (1958): **Proc. IEE**, Vol. 105A, p. 141

Thiele, R. (1941): **Z. Tech. Phys.**, Vol. 22, pp. 287-300

Vlachos, N. S. (1978): "Laminar flow through a plane 90^{o} bifurcation, Imperial College of Science and Technology, Dept. of Mech. Engng. Report FS/78/30

Waters, M. (1966): "The Short-Circuit Strength of Power Transformers", MacDonald, London

White, C. M. (1929): **Proc. Roy. Soc. (London)**, Ser. A., Vol. 123, pp. 645-663

White, F. M. (1974): "Viscous Fluid Flow", McGraw-Hill, New York

Wills, J. A. B. (1962): **J. Fluid Mech.**, Vol. 12, pp. 388-396

Yamaguchi, M., T. Kumasaka, V. Inui and S. Ono (1981): **IEEE PAS**, Vol. 100, pp. 956-963

Yannucci, D. A. and J. M. Thompson (1979): "A passive hottest spot detector for transformers", Proc. 7th IEEE/PES Transmission and Distribution Conference and Exposition, April 1-6, 1979, pp. 192-199

APPENDIX A

THERMOPHYSICAL PROPERTIES

The thermophysical properties of transformer oil and oil-impregnated kraft paper insulation, needed for the computational work, are listed here. They were obtained by direct measurement in the Electrical Engineering Department at Imperial College, using identical or similar samples of the materials used in the experimental work. The difficulties associated with using published properties of transformer insulating materials has been described by Allen (1960), who pioneered, in particular, the measurement of thermal conductivity by a transient method (Allen (1957) and Allen (1959)).

The relevant thermophysical properties of the naphthenic transformer oil may be expressed by the following formulae:

$$\nu = \frac{\exp[\exp(A_1)(t + 273)^{A_2}] - 0.7}{10^6}, \tag{A1}$$

$$\varrho = A_3 + A_4 t, \tag{A2}$$

$$\mu = \nu\varrho, \tag{A3}$$

$$\varrho c_p = A_5 + A_6 t, \tag{A4}$$

$$k = A_7 + A_8 t, \tag{A5}$$

$$\alpha = \frac{k}{\varrho c} , \tag{A6}$$

$$Pr = \frac{\nu}{\alpha} , \tag{A7}$$

where t is the temperature in ^{o}C, exp stands for the exponential function, and A_1, A_2, ... A_8 are constants to be measured, and were, for the batch of reclaimed transformer oil (conforming to B.S. 148:1972) used in the experiments:

$$\begin{aligned} A_1 &= 24.656, \\ A_2 &= -4.1323, \\ A_3 &= 889.0 \text{ kg/m}^3, \\ A_4 &= -0.7 \text{ kg/m}^3\ ^{o}C, \\ A_5 &= 1.6 \times 10^6 \text{ J/m}^3\ ^{o}C, \\ A_6 &= 1.8 \times 10^3 \text{ J/m}^3\ ^{o}C^2, \\ A_7 &= 0.117 \text{ W/m}\ ^{o}C, \\ A_8 &= 0 \text{ W/m}\ ^{o}C^2. \end{aligned} \tag{A8}$$

Formula (A1) was obtained from Grubb, Hudis and Traut (1980), but similar formulae are in common use. By taking the natural logarithm of both sides of (A1) after some rearrangement, then doing so a second time, one obtains an equation of the form $y = mx + b$. Special graph paper is prepared on this basis so that ν vs. t plots as a straight line, and A_1 and A_2 may be read directly from the graph. In Figs. A1-A6, ν, ϱ, μ, c_p, α and Pr are plotted as a function of temperature.

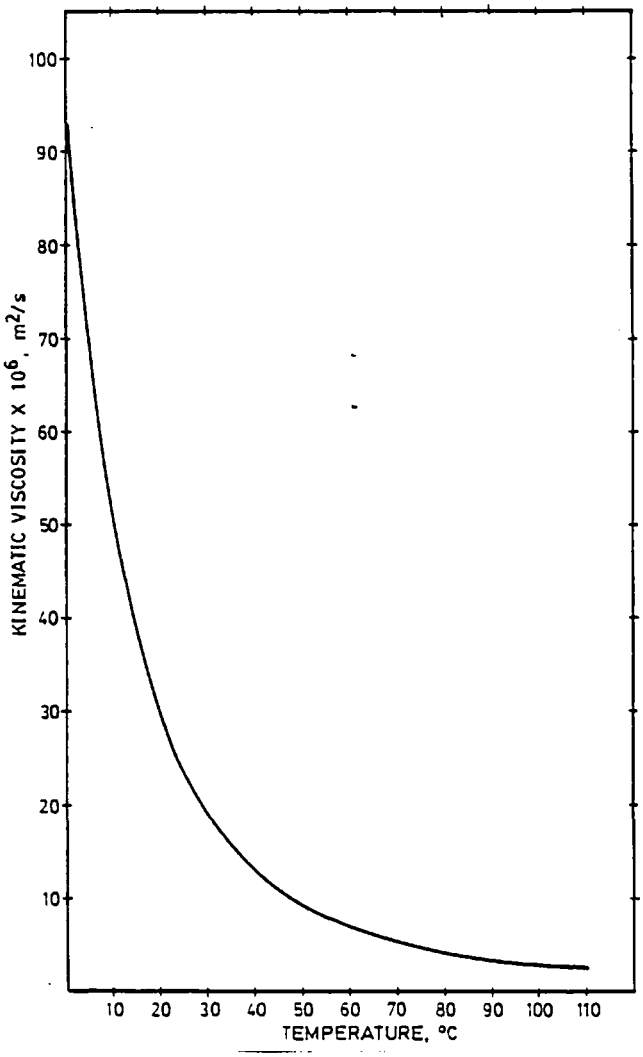


Fig. A1 Kinematic Viscosity vs. Temperature

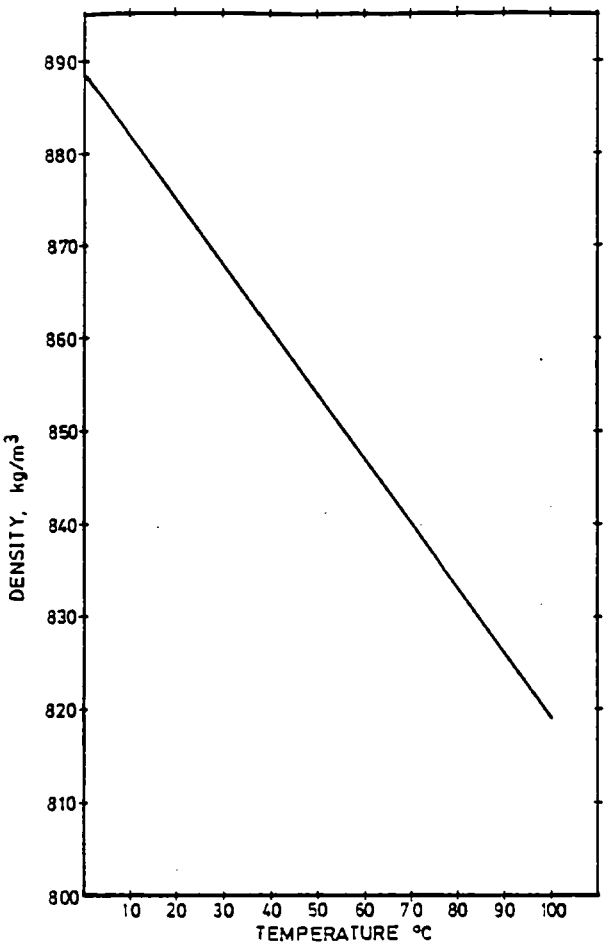


Fig. A2 Density vs. Temperature

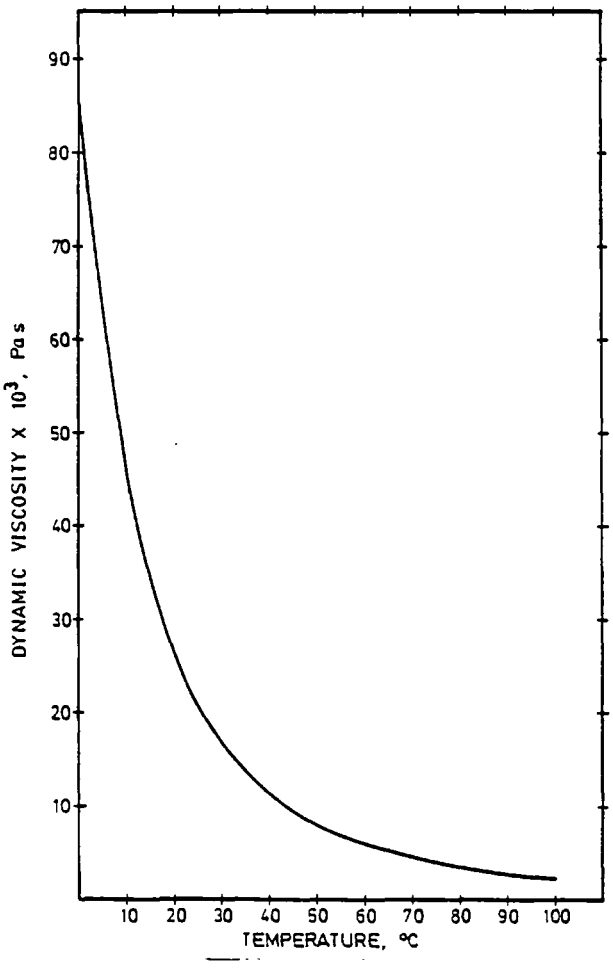


Fig. A3 Dynamic Viscosity vs. Temperature

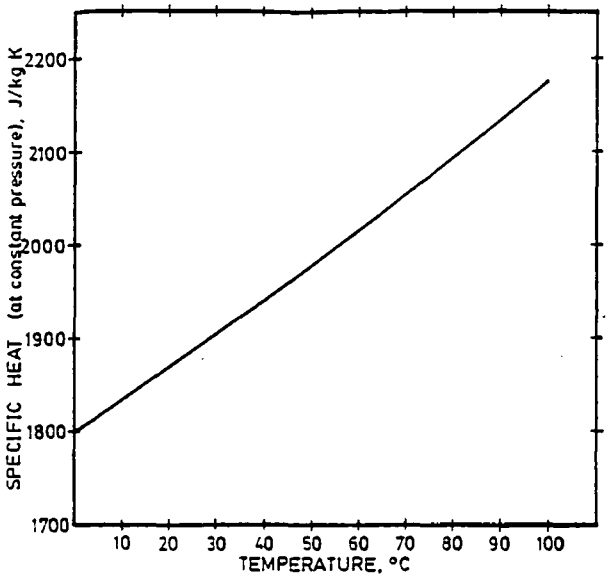


Fig. A4 Specific Heat vs. Temperature

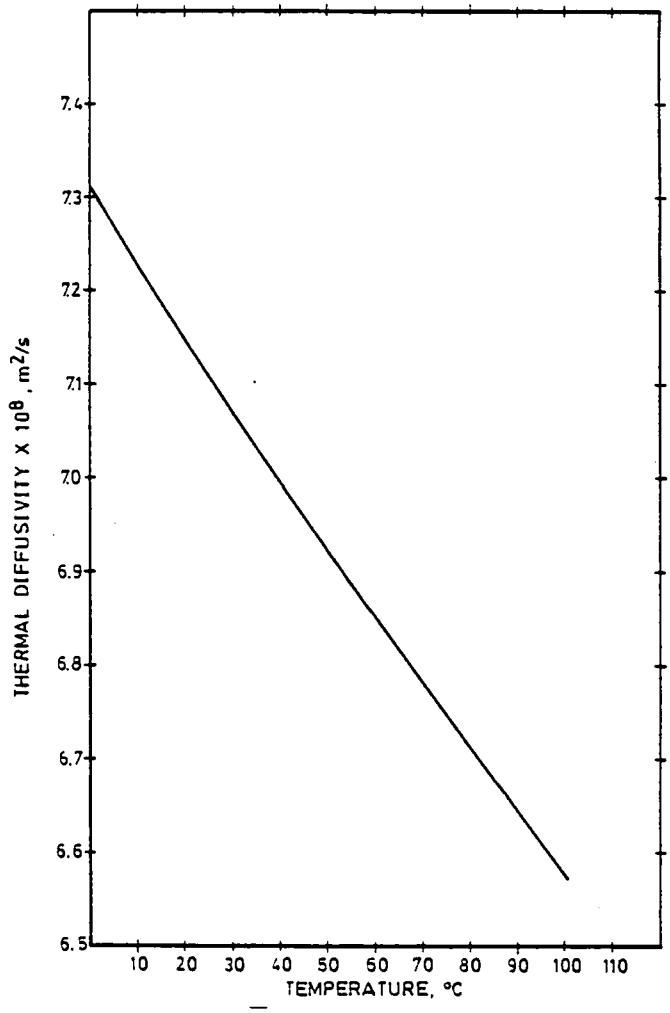


Fig. A5 Thermal Diffusivity vs. Temperature

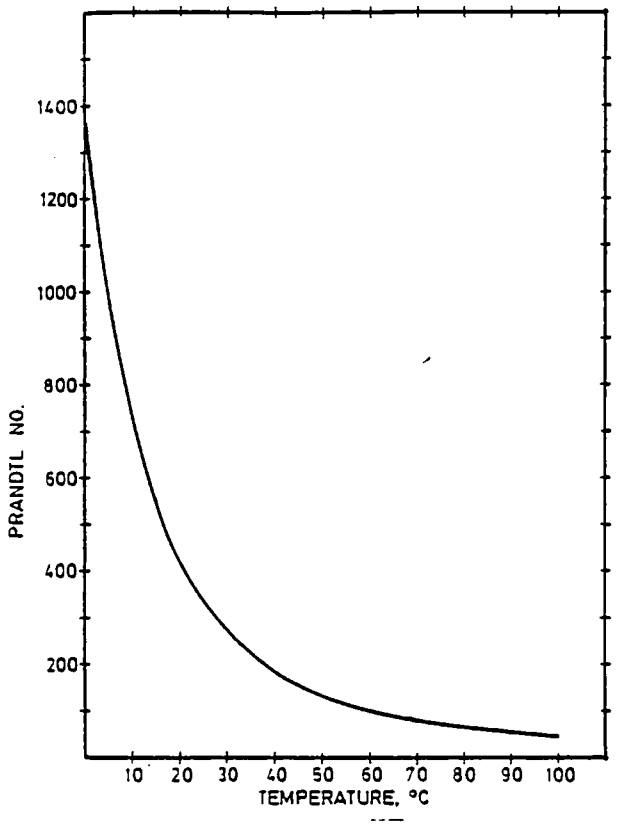


Fig. A6 Prandtl Number vs. Temperature

The value for the thermal conductivity k_p of the oil-impregnated kraft paper insulation was obtained from Finn (1971) who made measurements on material supplied by the same manufacturer who built the facsimile disc winding. The kraft paper has anisotropic thermal conductivity, however, in the calculations in DUCT, only k_p through the laminations was needed. The value used was

$$k_p = 0.172 \text{ W/m } ^{o}\text{C}. \qquad \text{(A9)}$$

Suitable values for the resistivity of copper and its temperature coefficient at 20 ^{o}C were obtained from the CRC Handbook (1977), p.

$$\varrho_{20} = 1.72 \times 10^{-8}\ \Omega\ m, \qquad (A10)$$

$$\alpha_{20} = 3.93 \times 10^{-3}\ {}^{o}C^{-1}. \qquad (A11)$$

APPENDIX B

MATHEMATICAL DETAILS OF EQUATION (4.18)

Equation (4.18) may be easily solved by introducing the following dimensionless variables:

$$\phi^* = \frac{\phi - \phi_W}{\phi_P - \phi_W}, \tag{B1}$$

and

$$x^* = \frac{x}{\delta x}. \tag{B2}$$

Substituting (B1) and (B2) into (4.18) yields

$$Pe \frac{d\phi^*}{dx^*} - \frac{d^2\phi^*}{dx^{*2}} = 0, \tag{B3}$$

$$\text{with b.c.'s } \phi^*(0) = 0, \ \phi^*(1) = 1,$$

the general solution of which is

$$\phi^* = Be^{Pex^*} + C. \tag{B4}$$

Application of the b.c.'s require

$$\begin{aligned} B &= -C \\ B &= \frac{1}{e^{Pe} - 1}, \end{aligned} \tag{B5}$$

hence

$$\phi^* = \frac{e^{Pex^*} - 1}{e^{Pe} - 1} . \qquad (B6)$$

Reverting to dimensional ϕ and x:

$$\phi = (\phi_P - \phi_W) \left[\frac{e^{Pex/\delta x} - 1}{e^{Pe} - 1} \right] + \phi_W , \qquad (B7)$$

and

$$\frac{d\phi}{dx} = \frac{(\phi_P - \phi_W)}{\delta x} Pe \left[\frac{e^{Pex/\delta x}}{e^{Pe} - 1} \right] . \qquad (B8)$$

If x is set to $\delta x/2$ in (B7) and (B8), (4.19) and (4.20) will result.

APPENDIX C

EQUIPMENT DETAILS

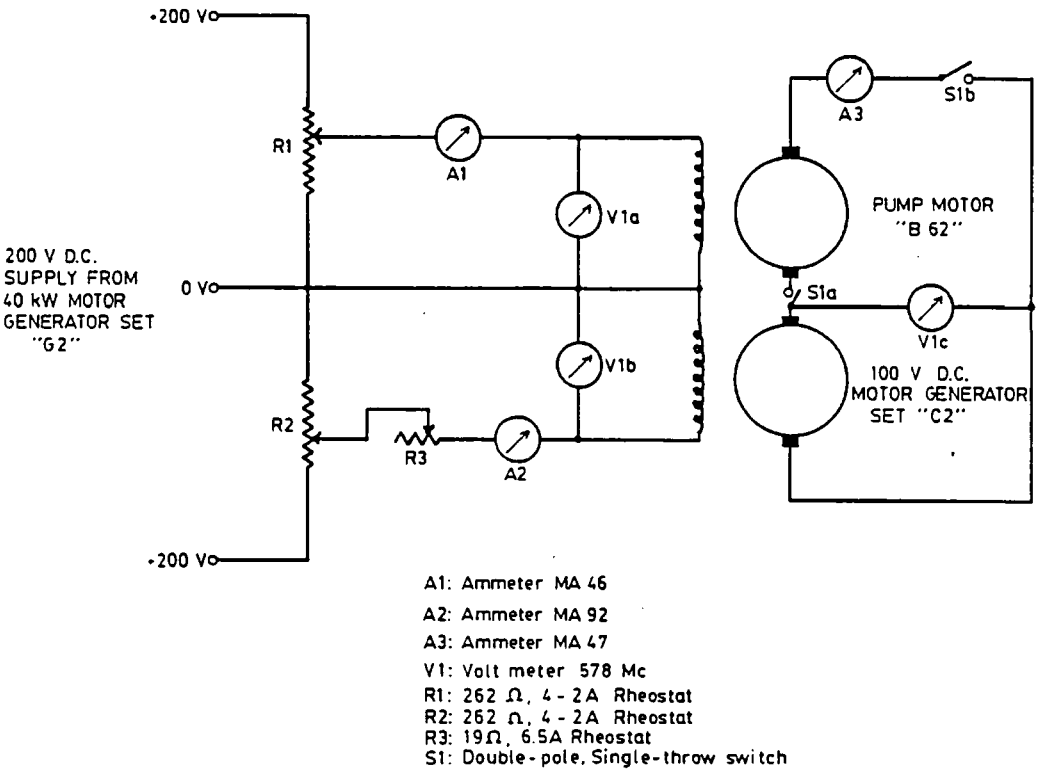
C1 Oil Cooling Circuit Further details of the equipment mentioned in Fig. 9.4 will be given in this section. The oil was pumped by an Autometric gear pump, rated by the manufacturer to deliver a maximum of 50 g.p.m. (3.79×10^{-3} m^3/s) at 800 R.P.M., against heads of up to 20 p.s.i.g. (144.8 kPa). It is designed to handle transformer oil at temperatures up to 90 ^{o}C. The pump shaft was fitted with a Fenner 72 L 100 pulley, the pump motor (B 62) shaft with a 18 L 050 pulley. The distance between the shaft centers was 240 mm. A 367 L 050 timing belt was used to couple the two, effecting a four-fold reduction in speed from motor to pump.

The pump motor B 62 was a Crompton-Parkinson D.C. compound wound motor, rated to run continuously at 1000 R.P.M., 200 V and 60 A. It was controlled using a Ward-Leonard system, as shown in Fig. C1.1. Typical operating conditions were:

```
Pump R.P.M.: 101.8,
B 62 R.P.M.: 407.2,
B 62 Armature Voltage: 62 V (V1c),                    (C1.1)
B 62 Armature Current: 2.8 A (A3),
B 62 Field Current: 0.7 A (A1),
C 2 Field Current: 0.5 A (A2).
```

The aluminium disc shown in Fig. 9.5 had 60 teeth which interrupted the infrared beam in the R.S. 304-560 Opto-Switch, the circuit diagram of which is shown as Fig. C1.2. The output at pin 5 was a square wave whose frequency, in Hz, was numerically equal to the pump

R.P.M. The frequency counter used (Venner Digital Counter Type TSA 6636/2M, Ser. AA002498) was set to count for 10 s, affording a read out to the nearest 0.1 R.P.M.



A1: Ammeter MA 46
A2: Ammeter MA 92
A3: Ammeter MA 47
V1: Volt meter 578 Mc
R1: 262 Ω, 4 - 2A Rheostat
R2: 262 Ω, 4 - 2A Rheostat
R3: 19Ω, 6.5A Rheostat
S1: Double - pole, Single - throw switch

Fig. C1.1 Control Circuit for Pump Motor

The R.P.M. vs. flow rate calibration was obtained using an Arkon Nutating Piston Positive Type flow meter (Fig. 9.4) and a digital stop watch. The calibration curve obtained is shown as Fig. C1.3. The characteristic is seen to be linear over the operating range of flow rates and oil temperatures.

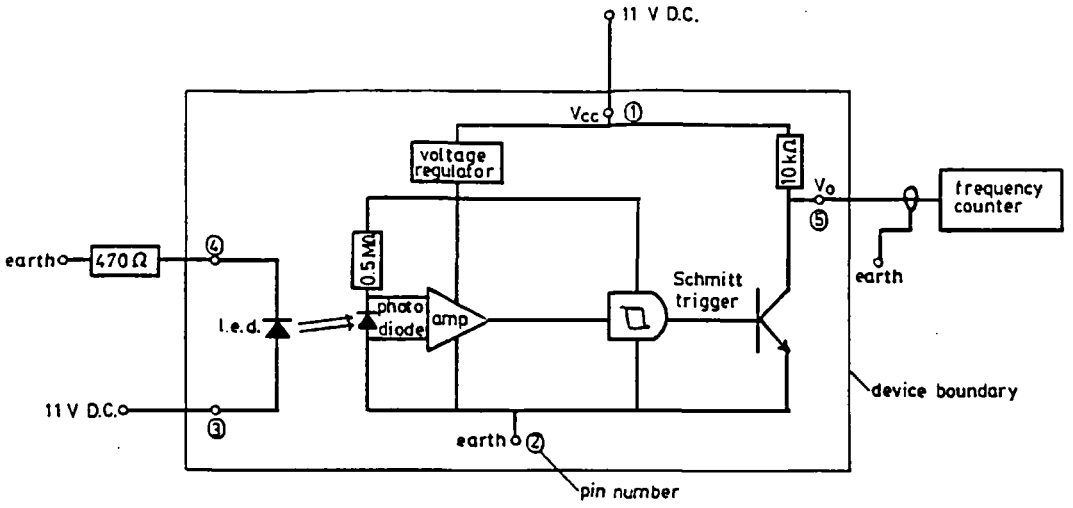


Fig. C1.2 Circuit Diagram of Opto-Switch

C2 Winding Heating and Temperature Measurement Equipment The D.C. supply to the winding was a Metropolitan Vickers motor-generator set. The induction motor had the following specifications:

$$\begin{array}{l} 440\ \text{V}, \\ 1475\ \text{R.P.M.}, \\ 50\ \text{Hz}, \\ 35\ \text{H.P. (26.1 kW)}, \\ 3\ \text{Phase}, \end{array} \qquad \text{(C2.1)}$$

and for the compound wound D.C. generator:

$$\begin{array}{l} 20\ \text{kW}, \\ 40\ \text{V}, \\ 500\ \text{A}, \\ 1475\ \text{R.P.M.} \end{array} \qquad \text{(C2.2)}$$

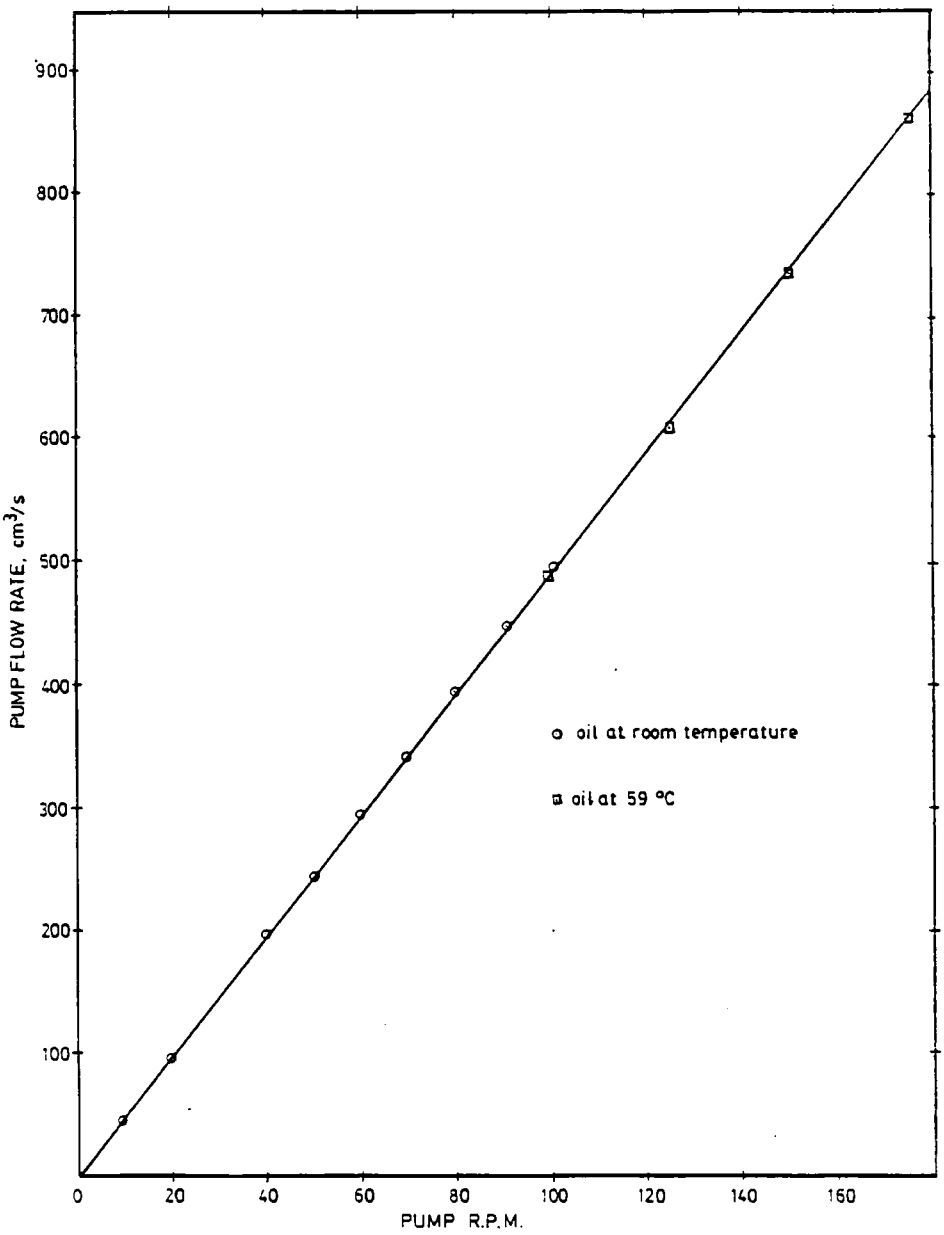


Fig. C1.3 Pump Flow Rate Calibration

A generator field current of 5A was typically required to supply 150 A to the winding.

The voltages from the winding taps, current shunt, and all t.c.'s were scanned by a Datron 1200 Signal Scanner (Ser. 02254). The voltages

were sent by the scanner to a Datron 1041 Multi-function DVM (Ser. 02357), which was calibrated by the manufacturer just before the experimental work was carried out. It provided resolution down to 1 μV. The accuracy of the DVM was checked with a standard cell. The only difficulty encountered was that the manufacturer had wired the 2-4 wire switch (intended for resistance measurements) incorrectly. To measure voltage, it was necessary to put the switch in the 4 wire position. There was a certain amount of A.C. noise on the embedded t.c. voltage readings (presumably caused by fluctuations in the winding current). This was adequately removed using the built in A.C. filter. Each channel voltage was then printed on the Datron 1230 Printer (Ser. 02358). The equipment is shown in the photograph, Fig. C2.1. In the background, on the panel rack, are the Datron units. To the right, on the bench, is the patch box (Fig. 11.4). In the foreground are the four rheostats for control of the pump motor and D.C. winding supply. Immediately to the right is the Δ-Y starter switch (Fig. 9.6).

The t.c. wires were each numbered as follows

winding t.c.'s: 1-99 (see Table C2.1),
bottom oil t.c.'s: 100, 101 (see Fig. 11.7), (C2.3)
top oil t.c.'s: 104-108 (see Fig. 11.8).

t.c.'s 102 and 103 were fitted to the tank outlet pipe but were not used. t.c.'s 109-124 were fitted to the three heat exchangers but were not used. The t.c. wire (iron-constantan, 33 SWG) was supplied in two batches by Saxonia Electrical Wire Co., Ltd.



Fig. C2.1 Data-Logging Equipment

	THERMOCOUPLE NUMBER					
Location: / Disc No.	After Turn No. From I.D.	Duct Centre Line	After Turn No. From I.D	Duct Spacer Corner	After Turn No. From I.D.	Spacer Centre Line
4	1	1	2	4	1	7
	10	2	9	5	10	8
	19	3	18	6	19	9
5	1	10	2	13	1	16
	10	11	9	14	10	17
	19	12	18	15	19	18
6	1	19	2	22	1	25
	10	20	9	23	10	26
	19	21	18	24	19	27
7	1	28	2	31	1	34
	10	29	9	32	10	35
	19	30	18	33	19	36
8	1	37	2	40	1	43
	10	38	9	41	10	44
	19	39	18	42	19	45
9	1	46	2	49	1	52
	10	47	9	50	10	53
	19	48	18	51	19	54
10	1	55	2	58	1	61
	10	56	9	59	10	62
	19	57	18	60	19	63
12	1	64	2	67	1	70
	10	65	9	68	10	71
	19	66	18	69	19	72
13	1	73	2	76	1	79
	10	74	9	77	10	80
	19	75	18	78	19	81
15	1	82	2	85	1	88
	10	83	9	86	10	89
	19	84	18	87	19	90
16	1	91	2	94	1	97
	10	92	9	95	10	98
	19	93	18	96	19	99

Table C2.1 Master List of Winding Thermocouples

C3 Hot Film Probe and Calibration Apparatus The DISA 55M system used comprised the following equipment:

55M05 Power Pack
55M01 Main Unit

55M10 CTA Standard Bridge (C3.1)
5 m Cable Compensation Unit
55R11 Quartz-Insulated Hot Film Probe

As the velocity and temperature fields were steady, the gain control was set to 1 (lowest setting) see DISA (1977).

The calibration system shown in Fig. 10.3 and 10.4 used an Opto-Switch circuit identical to that shown in Fig. C1.2. The aluminium wheel had 100 teeth, and for a readout numerically equal to R.P.M. x 10, a Racal 9521 Computing Counter (Ser. 1330) was set to count for 6 s. The Racal Counter did not cope well with square waves; it was necessary to add a simple RC low-pass filter to the output at pin 5 (Fig. C1.2). A 1kΩ resistor and a 0.47 μF capacitor worked adequately (they are not shown in Fig. C1.2).

The dimensioned drawings (reduced) for the calibration duct (Fig. 10.1) are shown as Figs. C3.1-C3.8.

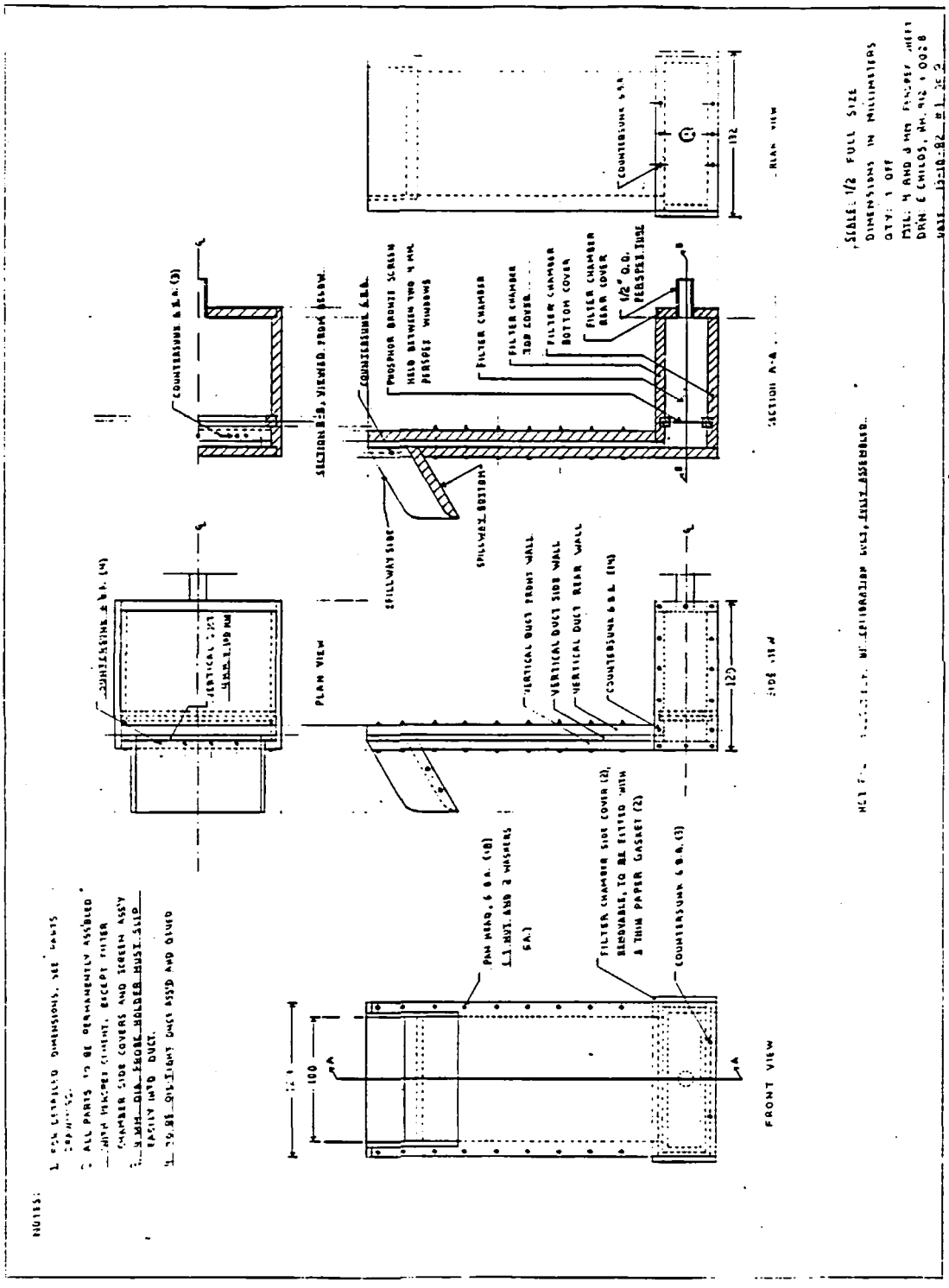


Fig. C3.1 Assembled Calibration Duct

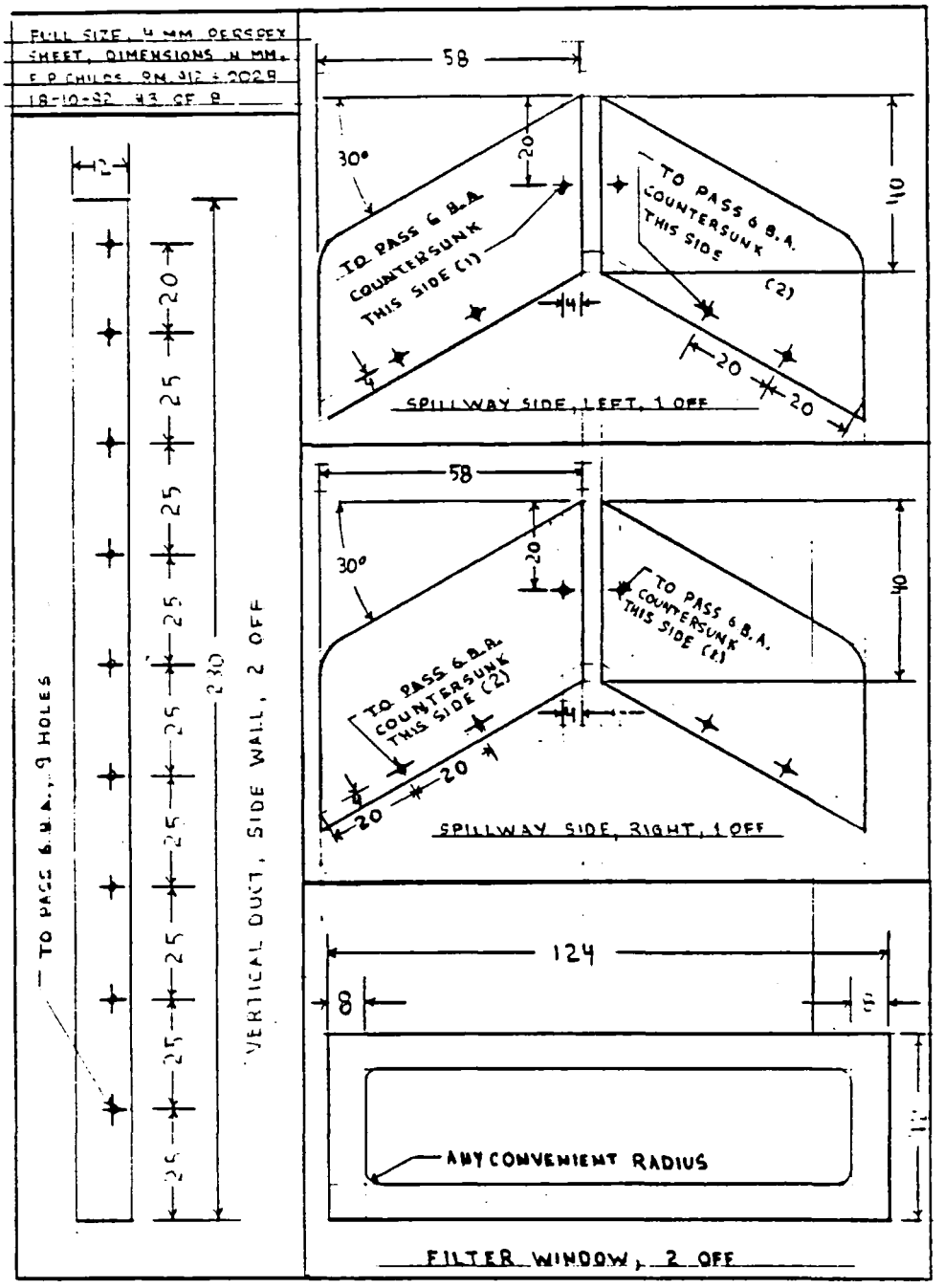


Fig. C3.2 Filter Window, Spillway Side and Vertical Duct Side Wall

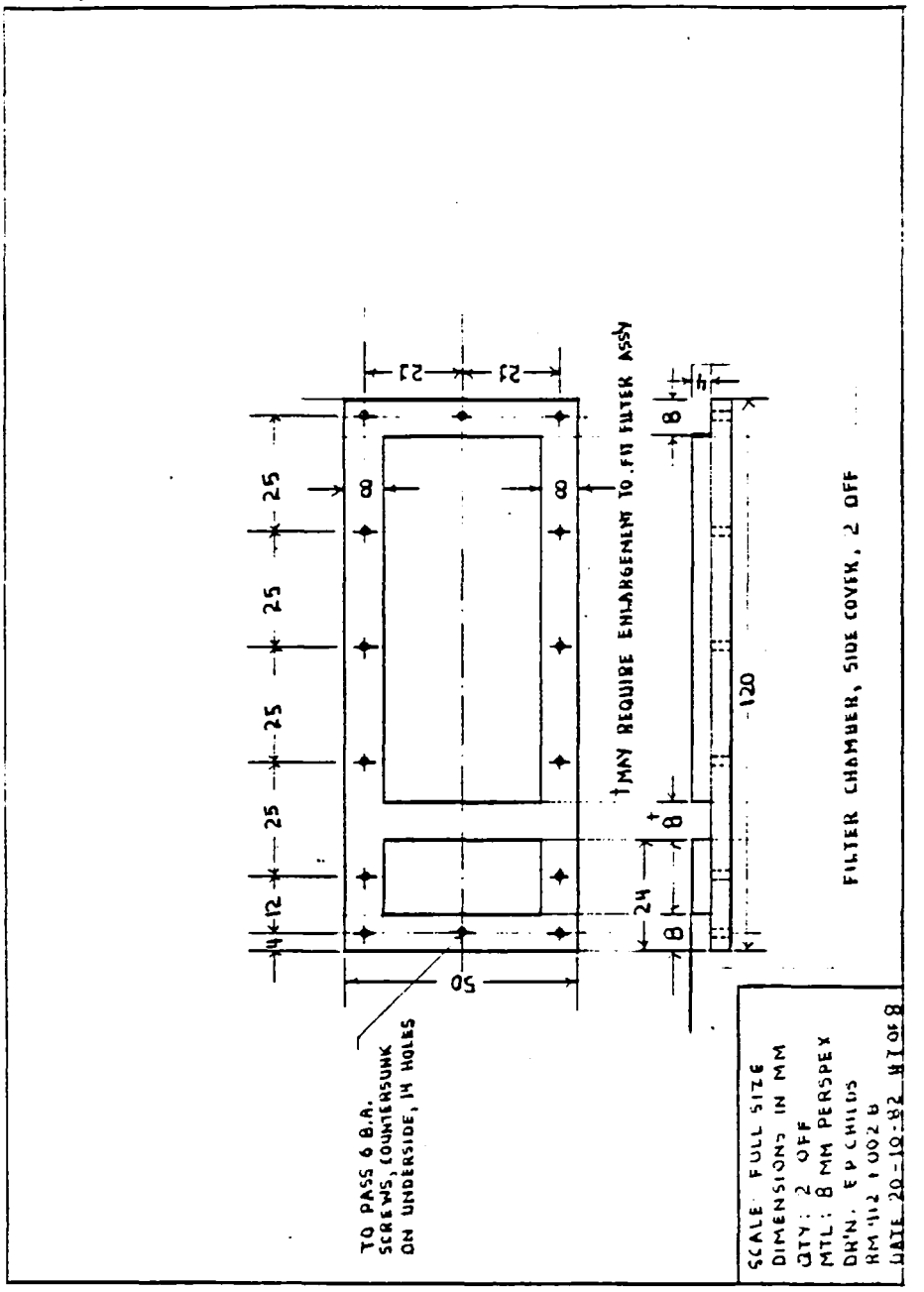


Fig. C3.3 Filter Chamber Side Cover

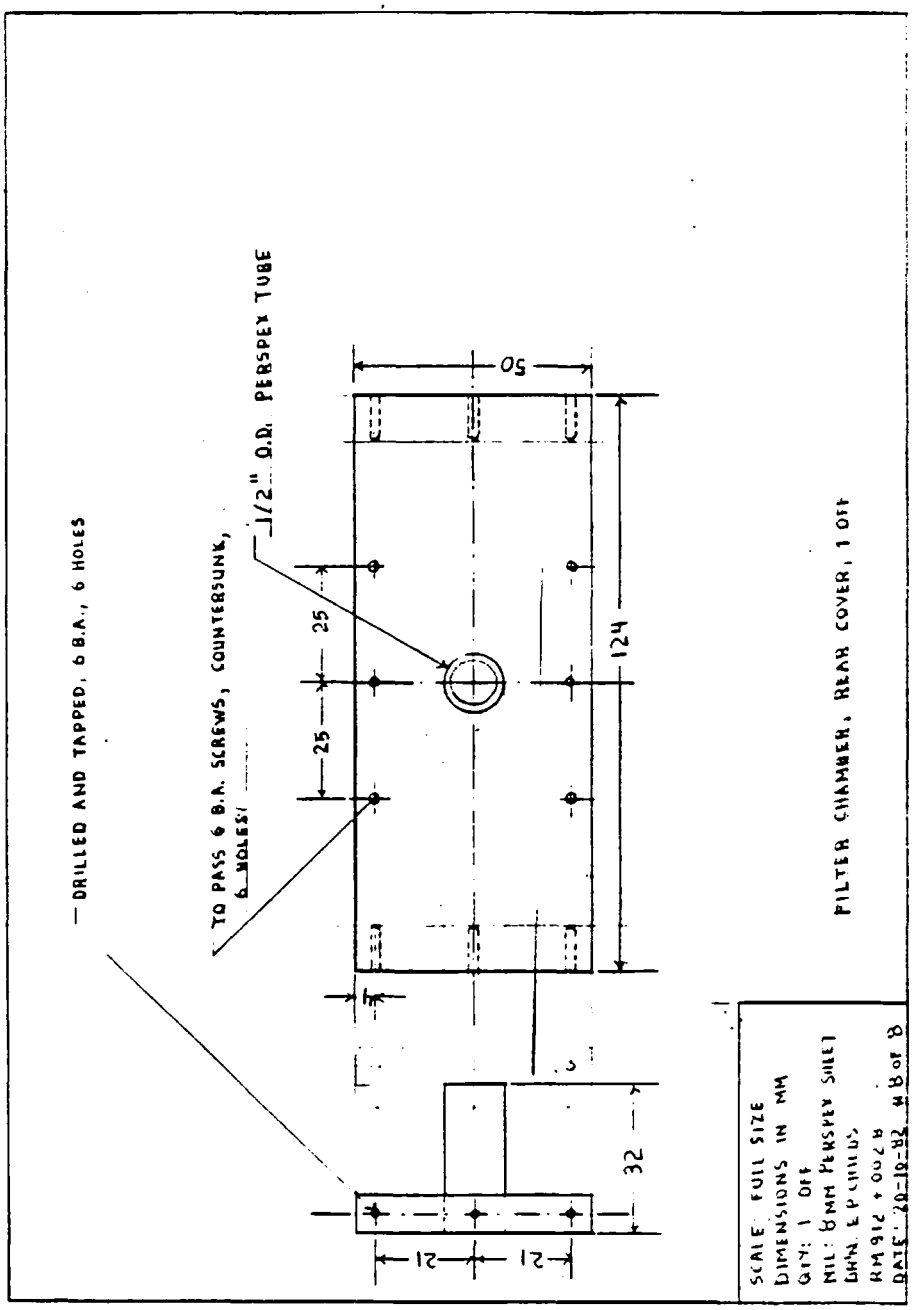


Fig. C3.4 Filter Chamber Rear Cover

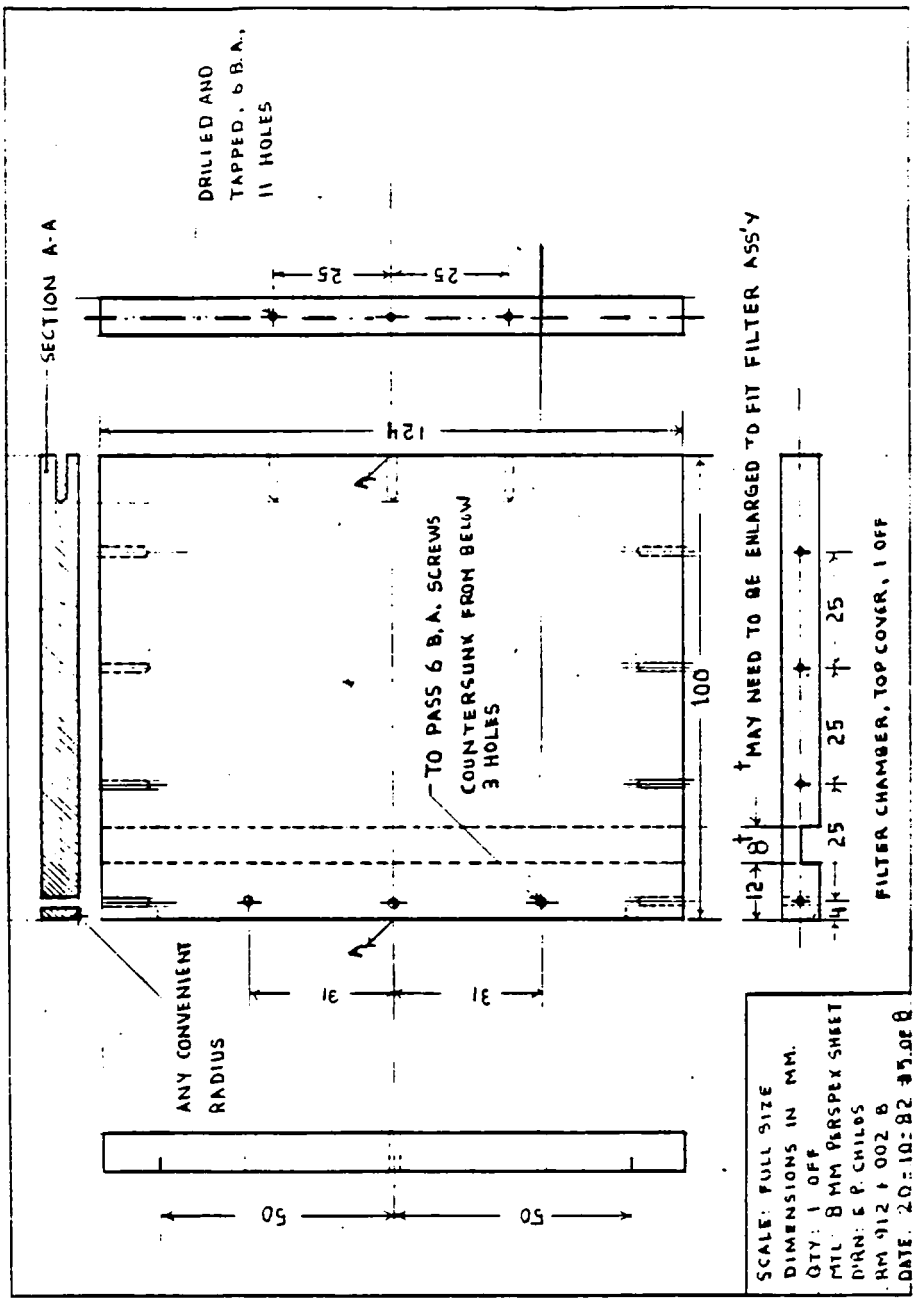


Fig. C3.5 Filter Chamber Top Cover

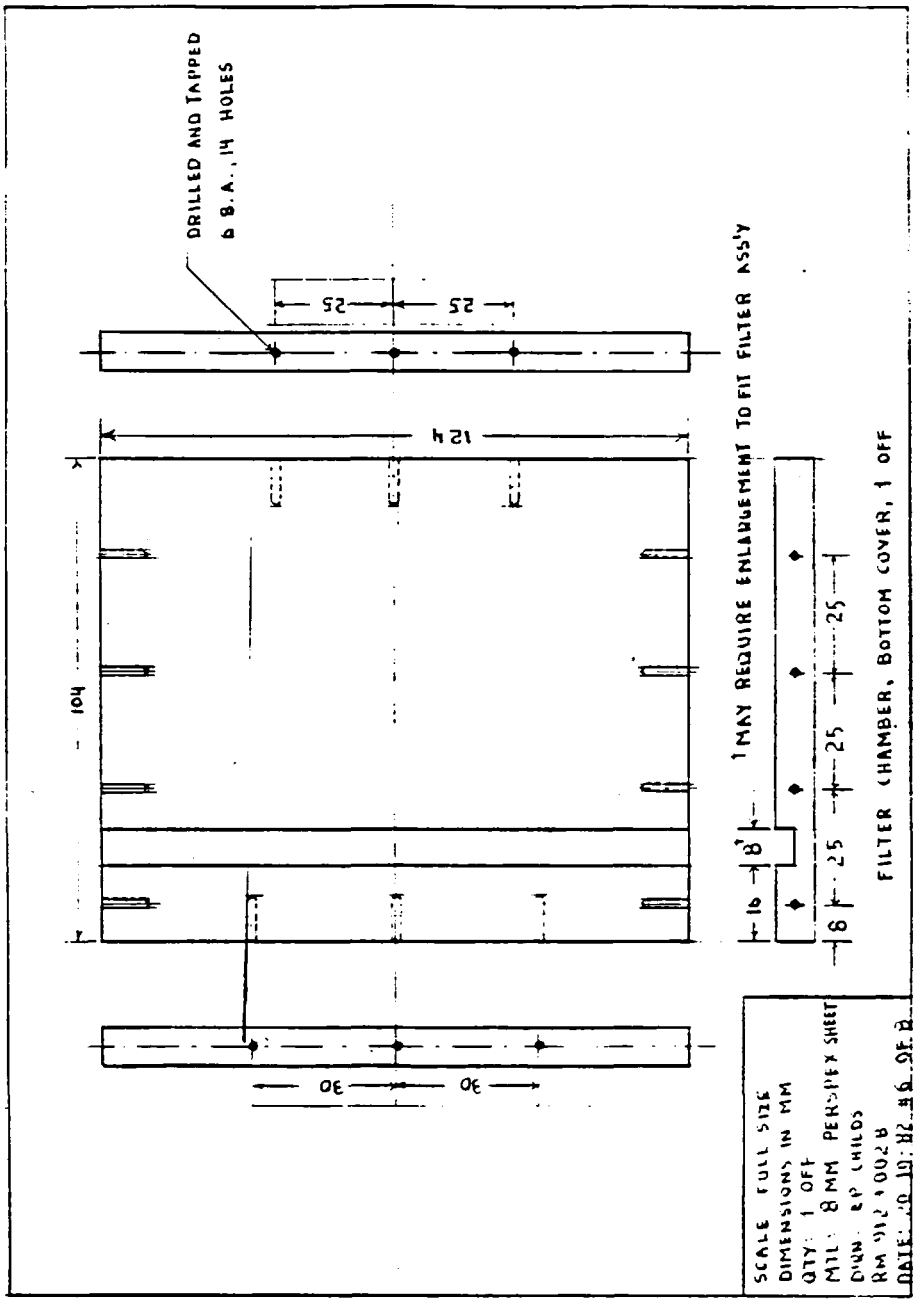


Fig. C3.6 Filter Chamber Bottom Cover

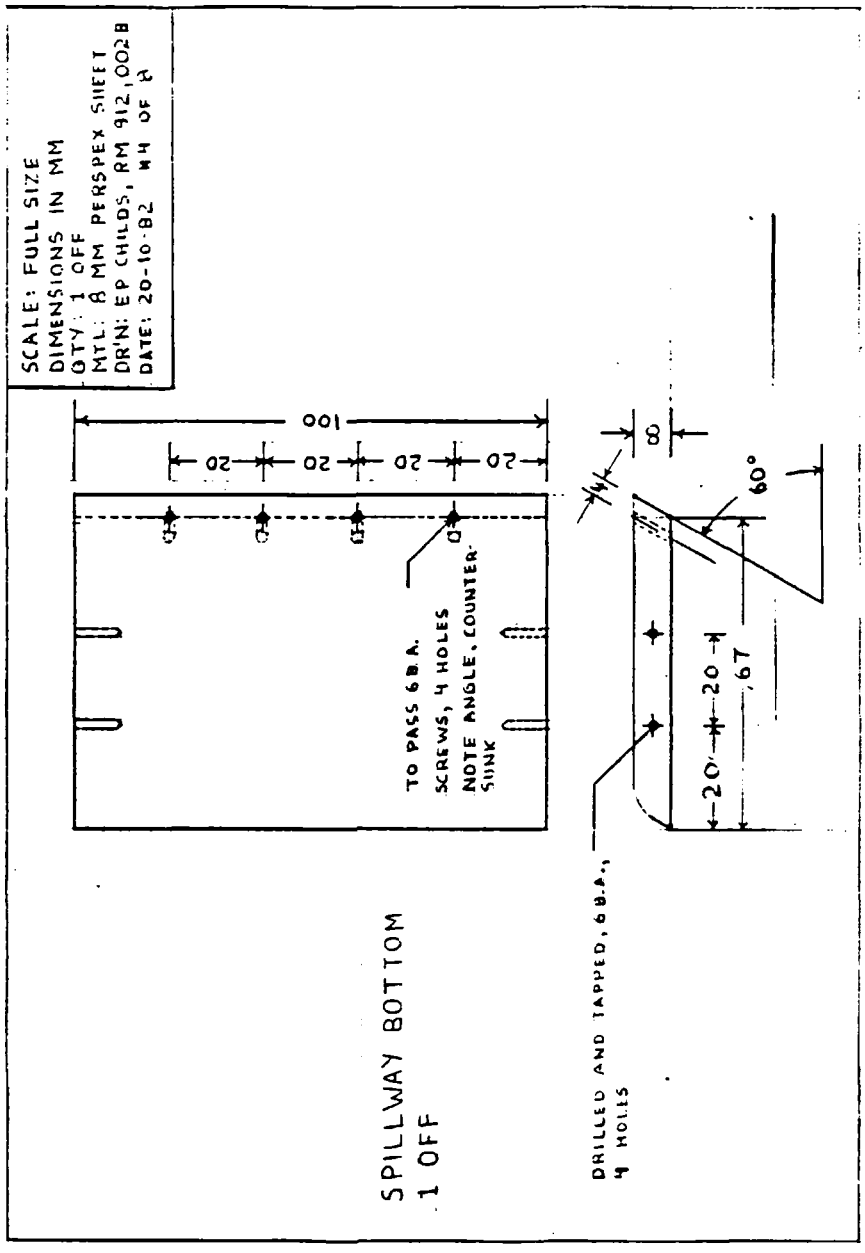


Fig. C3.7 Spillway Bottom

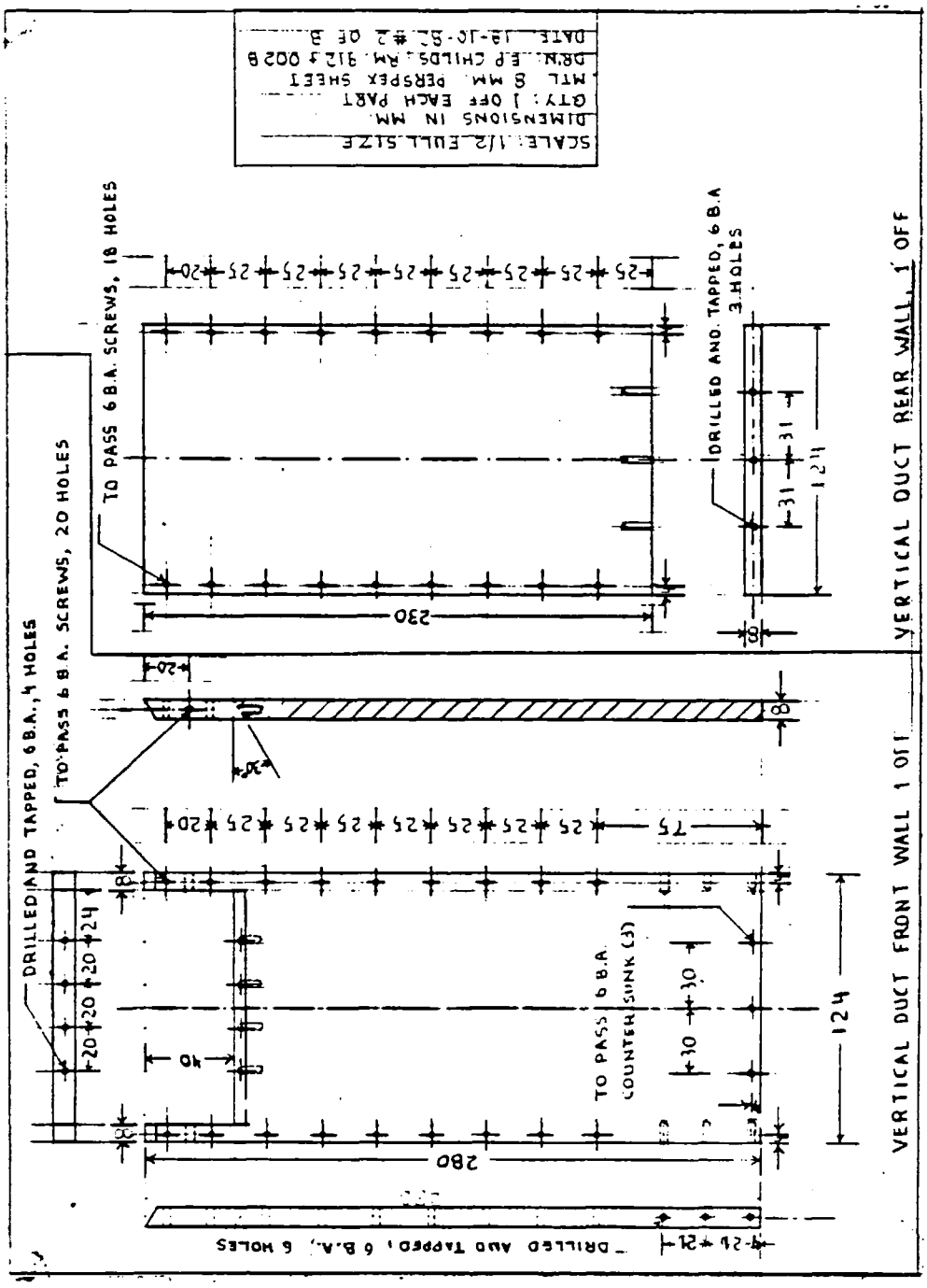


Fig. C3.8 Vertical Duct Front and Rear Walls

APPENDIX D

PROGRAM LISTINGS

D1 Simple Network The SN program, written in BASIC, was implemented on the Acorn 88C Model B Microcomputer. The program is a straightforward translation of the network equations in Chapter 3. A list of the BASIC variables, together with the program listing, follows. Interspersed comments (REM ...) outline the main points.

BASIC Variable	Definition
A(J)	t.d.m.a. coefficient
ALPHA	α
A1	A_1
A2	A_2
A3	A_3
A4	A_4
A5	A_5
A6	A_6
B(J)	t.d.m.a. coefficient
C(J)	t.d.m.a. coefficient
D(J)	t.d.m.a. coefficient
DH(J)	D_{hor} of duct J
DL	D_l
DR	D_r
I(J)	i_j (j = J)
K	k
N	number of ducts
NM1	N - 1

BASIC Variable	Definition
NU	ν
PR	Pr
Q	Q
Q2(J)	Q_2 in duct J
R(J)	R_j (j = J)
RHO	ϱ
RHOC	ϱc_p
TBULK(J)	$t_{mh,j}$ (j = J)
TBULKR(J)	$t_{m,j}$ (j = J)
THOT(J)	hottest surface temperature in duct J
TIN	$t_{m,in}$
VISCOS	μ
WHFLUX	$\dot{q}''_w$
X	L
Y	d

Basic Program

```
 10READ N:REM DISCNET PROGRAM FOR SIMPLE NETWORK MODEL
 20NM1=N-1:REM CONSTANT PROPERTIES, NEGLECTING JUNCTION AND CORNER LOSSES
 30DIM DH(N),I(NM1),R(N),Q2(N),THOT(N),TBULK(N),TBULKR(N),A(NM1),B(NM1),C(NM1),D(NM1)
 80FOR J=1 TO N
 90READ DH(J)
100NEXT J
110READ DL,DR,Y,X,Q,TIN,WHFLUX
120READ A1,A2,A3,A4,A5,A6,K
130RHO=A3+A4*TIN:REM CALCULATE FLUID PROPERTIES AT INLET TEMP.
140NU=(EXP(EXP(A1)*(TIN+273.)^A2)-.7)/1.E6
150VISCOS=NU*RHO
160RHOC=A5+A6*TIN
170ALPHA=K/RHOC
180PR=NU/ALPHA
190RL=96.*VISCOS*Y/DL^3:REM CALCULATE FLOW RESISTANCES
200RR=96.*VISCOS*Y/DR^3
220FOR J=1 TO N
230R(J)=96.*VISCOS*X/DH(J)^3
240NEXT J
250FOR J=1 TO NM1:REM SET UP TDMA COEFFICIENTS
260D(J)=R(J)+RR+R(J+1)+RL
270A(J)=R(J+1)
280NEXT J
290A(NM1)=0.
300B(1)=0.
310C(1)=-Q*(R(1)+RR)
320FOR J=2 TO NM1
330B(J)=A(J-1)
340C(J)=-Q*RR
350NEXT J
360A(1)=A(1)/D(1)
370C(1)=C(1)/D(1)
```

```
380FOR J=2 TO NM1
390TERM=1./(D(J)-B(J)*A(J-1))
400A(J)=A(J)*TERM
410C(J)=(C(J)+B(J)*C(J-1))*TERM
420NEXT J
430I(NM1)=C(NM1):REM CALCULATE LOOP CURRENTS BY BACK SUBSTITUTION
440FOR JJ=2 TO NM1
450J=N-JJ
460I(J)=A(J)*I(J+1)+C(J)
470NEXT JJ
480Q2(1)=Q+I(1)
490FOR J=2 TO NM1
500Q2(J)=I(J)-I(J-1)
510NEXT J
520Q2(N)=-I(NM1)
540FOR J=1 TO N:REM CALCULATE BULK FLUID AND HOT SPOT TEMPERATURES
550TBULK(J)=TIN+2.*WHFLUX*X/(RHOC*Q2(J))
560RE=2.*Q2(J)/NU
570PE=RE*PR
580XS=X/(DH(J)*PE)
590NUS=1.49*XS^(-1./3.):REM NUSSELT NUMBER EXPRESSIONS FROM SHAH AND LONDON
600IF XS>.0002 AND XS<=.001 THEN NUS=NUS+.4
610IF XS>.001 THEN NUS=8.233+8.68*(1000.*XS)^-.506*EXP(-164.*XS)
620H=K*NUS/DH(J)
630THOT(J)=TBULK(J)+WHFLUX/H
640NEXT J
650TBULKR(1)=TBULK(1):REM CALCULATE BULK TEMPERATURE IN RIGHT VERTICAL DUCTS
660QI=Q2(1)
670FOR J=2 TO N
680TBULKR(J)=(QI*TBULKR(J-1)+Q2(J)*TBULK(J))/(QI+Q2(J))
690QI=QI+Q2(J)
700NEXT J
710FLOSS=96.*Q2(1)*VISCOS*X/DH(1)^3+96.*Q*VISCOS*Y/DR^3
720QI=0.
730FOR J=1 TO N
740QI=QI+Q2(J)
750FLOSS=FLOSS+96.*QI*VISCOS*Y/DR^3
760NEXT J
770FBUOY=0.
780FOR J=1 TO N
790FBUOY=FBUOY-A4*9.80665*(.5*DH(J)+Y)*(TBULKR(J)-TIN)
800NEXT J
810@%=&20207
820PRINT "   DUCT  %FLOW    THOT TBULKR  TBULK"
830FOR J=N TO 1 STEP -1
840PRINT J,Q2(J)*100./Q,THOT(J),TBULKR(J),TBULK(J)
850NEXT J
860@%=10
870PRINT "FLOSS=",FLOSS," FBUOY=",FBUOY," DIFF=",FLOSS-FBUOY
980DATA 16
990DATA .00384,.00422,.00468,.0054,.00634,.00792,.01104,.02056,.02056,
        .01104,.00792,.00634,.0054,.00468,.00422,.00384
1000DATA .008,.008,.016,.1,1.2E-3,40.,3.E3
1010DATA 24.656,-4.1232,889.,-.7,1.6E6,1.8E3,.117
1020END
```

D2 FORTRAN Variable Definitions In this section, a list of the FORTRAN variables used in TEACH-L, JUNCTION, CORNER, DUCT, and DISCNET is presented. Each variable is defined with a short physical description, in terms of a symbol from the List of Symbols, or in terms of other FORTRAN variables. Scratch or dummy variables used only for programming convenience are not included. Occasionally a FORTRAN variable used in more than one program has several meanings and this is noted as necessary. For greater ease in understanding the variables related to geometry and grid-spacing, the reader is urged to consult Figs. 4.6, 5.2, 6.2 and 7.1.

FORTRAN Variable	Definition
A(J)	α_j
AE(I,J)	A_E (for U(I,J) in CALCU, etc.)
ALPHA	α_{20}
AN(I,J)	A_N (for U(I,J) in CALCU, etc.)
AP(I,J)	A_P (for U(I,J) in CALCU, etc.)
AS(I,J)	A_S (for U(I,J) in CALCU, etc.)
AW(I,J)	A_W (for U(I,J) in CALCU, etc.)
A1	A_1 in Appendix A
A2	A_2 in Appendix A
A3	A_3 in Appendix A
A4	A_4 in Appendix A
A5	A_5 in Appendix A
A6	A_6 in Appendix A
A7	A_7 in Appendix A
B(J)	β_j
C(J)	C_j

FORTRAN Variable	Definition
CURENT	I/2
D(J)	D_j
DELTAY	δ
DELTPS	Δp_s
DEN(I,J)	ϱ at X(I), Y(J)
DENSIT	ϱ at t_e in DUCT
	ϱ (constant) in JUNCTION and CORNER
DIVIDE	Logical variable: if .TRUE., JUNCTION assumes a dividing junction if .FALSE., JUNCTION assumes a combining junction
DL(I)	D_l of duct I
DLEN	L
DLTPCT	Δp_{ct}
DLTPDT	Δp_{dt}
DR(I)	D_r of vertical duct I
DU(I,J)	D_w for PP(I,J)
DV(I,J)	D_s for PP(I,J)
DXEPU(I)	XU(I+1) - XU(I)
DXPW(I)	X(I) - X(I-1)
DXPWU(I)	XU(I) - XU(I-1)
DYNP(J)	Y(J+1) - Y(J)
DYNPV(J)	YV(J+1) - YV(J)
DYPS(J)	Y(J) - Y(J-1)
DYPSV(J)	YV(J) - YV(J-1)
ENDROP	$(1.5\mu/r^3_{h,vert})Q_{in}\, L'_{entry}$
ENTFAC	dimensionless factor by which L_{entry} is modified for purposes of setting up the grid
ENTRLP	L'_{entry}
ENTRYL	L_{entry}

FORTRAN Variable	Definition
ENTRYP	L'_{entry}
EXITL	L_{exit}
EXTLP	L'_{exit}
FKC	K_c
FKCS	K_{cs}
FKCT	K_{ct}
FKDS	K_{ds}
FKDT	K_{dt}
FLOWIN	mass flow rate (per unit depth) at inlet
GAMH(I,J)	k/c_p at X(I), Y(J)
GC	G_c
GCF	$G_{c,f}$
GCP	$k_p z/\varepsilon$
GCPP	$k_p \sigma/\varepsilon$
GF	kz/δ
GL	G_l
GLP	$h_l \sigma$
GREAT	γ
GR	G_r
GRP	$h_r \sigma$
HEDDEN	as HEDU, for DEN(I,J)
HEDGAM	as HEDU, for GAMH(I,J)
HEDP	as HEDU, for P(I,J)
HEDT	as HEDU, for T(I,J)
HEDU	array containing character string used as heading for table of U(I,J)
HEDV	as HEDU, for V(I,J)
HEDVIS	as HEDU, for VIS(I,J)
HITCON	σ

FORTRAN Variable	Definition
HLEFT	h_l
HODROP	$(1.5\mu Q_2 L'_{horiz})/r^3_{h,horiz}$
HORIZL	L_{horiz}
HORZLP	L'_{horiz}
HORZP	L'_{horiz}
HRITE	h_r
IMON	I index of monitoring location
INCALP	as INCALU, for PP(I,J)
INCALT	as INCALU, for T(I,J)
INCALU	Logical variable, if .TRUE., solve for U(I,J) if .FALSE., don't
INCALV	as INCALU, for V(I,J)
INDPRI	number of iterations after which variable fields are printed out if other solution termination criteria have not been satisfied
INPRO	Logical variable, if .TRUE., variable properties if .FALSE., constant properties
IPREF	I index of reference pressure
ISTEP	I index of north-south grid line just east of corner nearest entrance. (ISTEP = 8, Fig. 6.2)
IST1	I index of north-south grid line just east of corner nearest entrance. (IST1 = 6, Fig. 5.2)
IST1M1	IST1 - 1
IST1M2	IST1 - 2
IST1P1	IST1 + 1
IST2	I index of north-south grid line just west of corner nearest exit. (IST2 = 12, Fig. 5.2)
IST2M1	IST2 - 1
IST2P1	IST2 + 1
IST2P2	IST2 + 2
IT	Dimension of I index in all arrays
JMON	J index of monitoring location

FORTRAN Variable	Definition
JPREF	J index of reference pressure
JSTEP (JUNCTION)	J index of east-west grid line just south of horizontal duct branch (JSTEP = 7, Fig. 5.2)
JSTEP (CORNER)	J index of east-west grid line just south of exit duct. (JSTEP = 8, Fig. 6.2)
JSTM1	JSTEP - 1
JSTP1	JSTEP + 1
JSTP2	JSTEP + 2
JT	Dimension of J index in all arrays
K(I)	K in horizontal duct I
KC(I,J)	K_c
KCS(I,J,K)	K_{cs}
KCT(I,J,K)	K_{ct}
KDS(I,J,K)	K_{ds}
KDT(I,J,K)	K_{dt}
KF(I)	K computed from X(2) to X(I)
KL(I)	K in left vertical duct I
KR(I)	K in right vertical duct I
MAXIT	maximum number of iterations in main loop
NDUCM1	NDUCT - 1
NDUCT	number of ducts in pass
NI	maximum value of I in solution domain
NIM1	NI - 1
NIM2	NI - 2
NITER	current iteration number
NJ	maximum value of J in solution domain
NJM1	NJ - 1
NJM2	NJ - 2
NSWPP	number of sweeps for pressure correction

FORTRAN Variable	Definition
NSWPT	Number of sweeps for temperature
NSWPU	Number of sweeps for U velocity
NSWPV	Number of sweeps for V velocity
NU(I)	Nu_x computed from X(2) to X(I)
NUMIT	Current iteration number
P(I,J))	pressure stored at X(I), Y(J)
PAVIN	p_{in}
PAV1	p_1
PAV2	p_2
PCTDFF	$\Delta\hat{p}_{ct}$
PDIFF	$\Delta\hat{p}_c$
PDTDFF	$\Delta\hat{p}_{dt}$
PEIN	Pe at t_e and u_m
PHI(I,J)	Dummy array used by LISOLV and PRINT to pass U(I,J), as a subroutine argument.
PP(I,J)	Pressure correction as X(I), Y(J)
PREF	Reference pressure
PRIN	Pr at t_e
PSDIFF	$\Delta\hat{p}_{ds}$ if DIVIDE = .TRUE. $\Delta\hat{p}_{cs}$ if DIVIDE = .FALSE.
QDOT	$\dot{Q}$
QDOTPP(I)	$\dot{Q}_i$ (i = I)
QIN	Q (in DISCNET)
QIN	Q_{in} (in JUNCTION and CORNER)
QIN	Q_2 (in DUCT)
QLOOP(I)	i_j (j = I)
QRATIO	Q_{in}/Q_2
Q2(I)	Q_2 in duct I
Q2OLD(I)	Q2(I) from previous iteration

FORTRAN Variable	Definition
R(I)	R_i (i = I)
RC	R_c
RCH	R_{ch}
RCL	R_{cl}
RCS(I)	R_{cs}
RCT(I)	R_{ct}
RDS(I)	R_{ds}
RDT(I)	R_{dt}
REIN	Re_{in} (in JUNCTION)
REIN	Re at t_e and u_m (in DUCT)
RESID	residual overall variation in flow distribution from one iteration to the next
RESMAX	Maximum fraction of Q permitted as sum of absolute values of variations in $Q_{2,i}$ from one iteration to the next in converged solution.
RESORU	R_u
RESORV	R_v
RESORM	S_{MP}
RESORT	R_t
RESTRT	Logical variable: if .TRUE., initial fields to be read from Unit 9 if .FALSE., initial fields to be set in program
RE1	Re_1
RE2	Re_2
RHORIZ	$r_{h,horiz}$
RHO20	ϱ_{20} (of copper)
RL(I)	$R_{l,i}$ (i = I)
RR(I)	$R_{r,i}$ (i = I)
RRATIO	$r_{h,vert}/r_{h,horiz}$
RVERT	$r_{h,vert}$

FORTRAN Variable	Definition
SEW(I)	east-west dimension of control volume for P(I,J) or T(I,J)
SEWU(I)	east-west dimension of control volume for U(I,J)
SMP	S_{MP}
SNORMM	Reference value for normalisation of RESORM
SNORMT	Reference value for normalisation of RESORT
SNORMU	Reference value for normalisation of RESORU
SNORMV	Reference value for normalisation of RESORV
SNS(J)	north-south dimension of control volume for P(I,J) or T(I,J)
SNSV(J)	north-south dimension of control volume for V(I,J)
SORCE	maximum of RESORU, etc.
SORMAX	maximum value of SORCE in converged solution
SP(I,J)	B for U(I,J), etc.
SPHEAT	c_p
SU(I,J)	C for U(I,J), etc.
TBULK(I)	t_m at X(I)
TC(I)	$t_{c,i}$ (i = I)
T(I,J)	temperature at X(I), Y(J)
THCOND	k
THCPAP	k_p
THKCON	η
TIN	$t_{m,in}$ (in DISCNET)
TIN	t_e (in DUCT)
TINSL	ε
TL(I)	t_m in left vertical duct
TLEFT	t_e
TOUT	$t_{m,r}$
TR(I)	$t_{m,i}$ (i = I)

FORTRAN Variable	Definition
TRITE	$t_{m,r}$
TWALL(J)	t_{wall} as X(I)
U(I,J)	u velocity at XU(I), Y()J)
URFP	f_p,
URFT	f_t
URFU	f_u
URFV	f_v
URFVIS	underrelaxation for viscosity (not used)
V(I,J)	v velocity at X(I), YV(J)
VIN	u_{in}
VIS(I,J)	μ at X(I), Y(J)
VISCOS	μ at t_e (in DUCT)
VISCOS	μ, constant (in JUNCTION and CORNER)
V1	u_1
WIDCON	z
WHFLUX	$\dot{q}''_w$
X(I)	x coordinate of north-south grid line I
XD(I)	L of duct I
XFRAC(I)	relative spacing between X(I) and X(I+1)
XSTAR	x^*
XU(I)	x coordinate of U(I,J)
Y(J)	y coordinate of east-west grid line J
YD(I)	d of vertical duct I
YFRAC(J)	relative spacing between Y(J) and Y(J+1)
YV(J)	y coordinate of V(I,J)

D3 TEACH-L The overall structure of TEACH-L is shown in Fig. D3.1. The main program (MAIN), in which the input data and initial ϕ fields are specified, and the subroutines MODU, MODV, MODP, MODT, in which the boundary conditions are set, are dependent for their content on the particular problem solved. Thus in the following sections, these 5 modules are listed for JUNCTION, CORNER and DUCT. The remaining 8 subroutines, which implement the basic solution procedure outlined in Chapter 4, are generally left unchanged by the user. A brief description of each is given, followed by listings.

In INIT, the x and y coordinates of the grid lines, which must be set by the user in MAIN, are used to compute all staggered variable locations (e.g. XU(I) and YV(J)) and all control volume dimensions (e.g. SEW(I), SNSV(J), see Fig. 4.6). All variable fields are set to zero and all fluid properties to a reference or initial value. INIT is only called once in the course of the calculation.

In CALCU and CALCV, the combined convection/diffusion coefficients AE(I,J), etc., sources SU(I,J) and SP(I,J) (including false sources), and DU(I,J) or DV(I,J) (for later use in CALCP) are computed using current variable fields. A call is made to MODU or MODV to alter the coefficients or sources at any point in the domain should boundary conditions so require. The sum of the absolute values of the residuals at each control volume is then computed (RESORU or RESORV) and finally, underrelaxation is implemented. LISOLV is then called to obtain the new U(I,J) or V(I,J) fields.

In CALCP, the SIMPLE algorithm is implemented (see Section 4.5).

AE(I,J), etc. are computed using DU(I,J) and DV(I,J) from CALCU and CALCV. SMP is determined at each control volume, the absolute sum of these over the whole domain yielding RESORM. MODP is called for user-imposed modifications to the pressure field, whereupon LISOLV is called to obtain the pressure correction field PP(I,J). The U(I,J), V(I,J) and P(I,J) fields are then corrected.

CALCT is very similar to CALCU and CALCV, only the source terms are not dependent on the pressure field P(I,J). The coefficients AE(I,J), etc. and sources SU(I,J) and SP(I,J) are assembled, modified if necessary by a call to MODT, used (together with prevailing T(I,J)) to determine RESORT, and finally input to LISOLV to obtain the new T(I,J) field.

If INPRO has been set to .TRUE., a call to PROPS will be made in which the fluid properties will be updated in accordance with formulae supplied by the user.

LISOLV is a straightforward implementation of the LBL (line-by-line) TDMA (tri-diagonal matrix algorithm) described in Section 4.4. PRINT is a clever subroutine which formats the tables of field variables in the sample output provided in Section D4, D5 and D6.

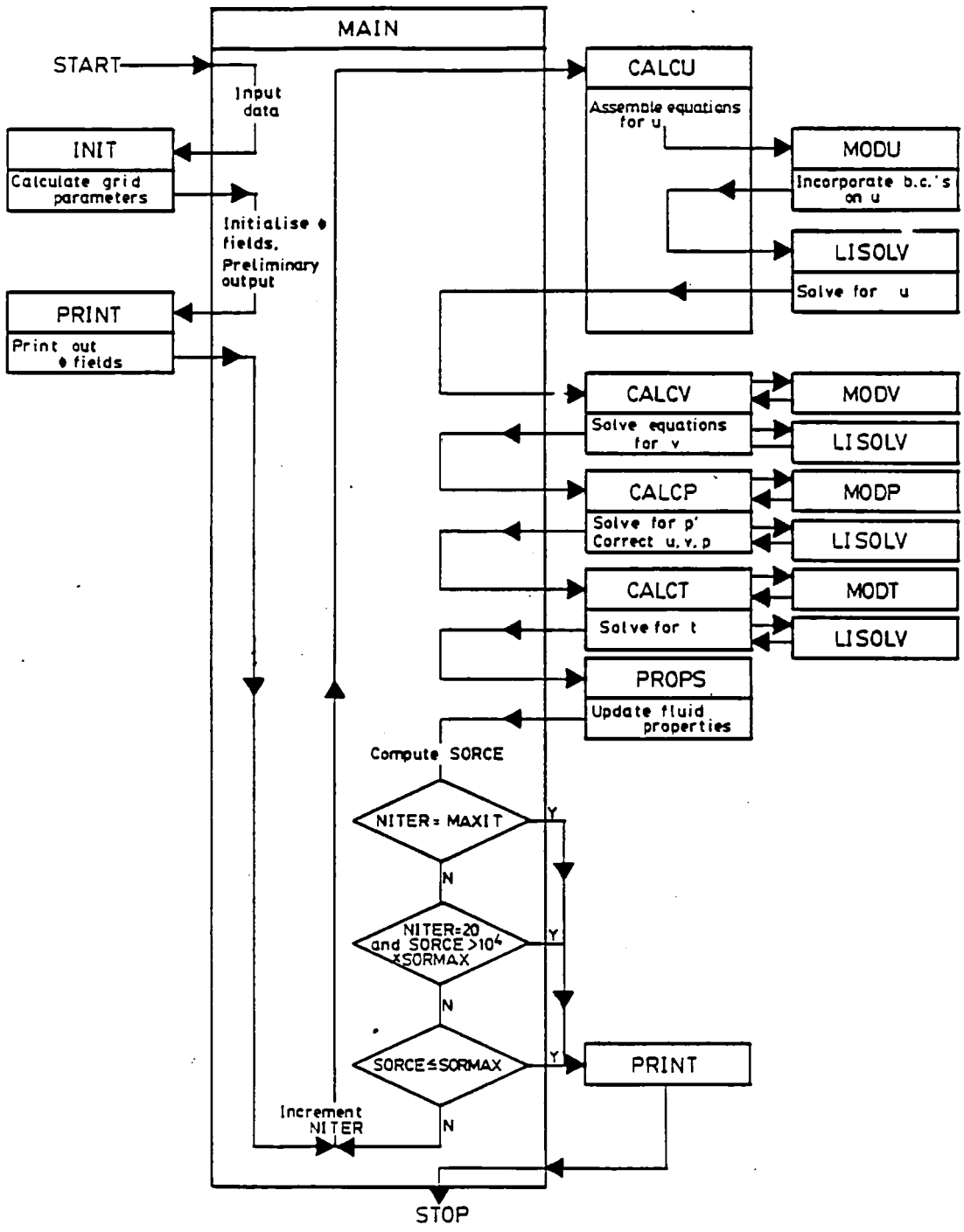


Fig. D3.1 Flow Chart of TEACH-L

SUBROUTINE INIT

```
      SUBROUTINE INIT
C
CHAPTER  0  0  0  0  0  0  0  0  PRELIMINARIES  0  0  0  0  0  0  0  0
C
      COMMON
     1/UVEL/RESORU,NSWPU,URFU,DXEPU(22),DXPWU(22),SEWU(22)
     1/VVEL/RESORV,NSWPV,URFV,DYNPV(9),DYPSV(9),SNSV(9)
     1/PCOR/RESORM,NSWPP,URFP,DU(22,9),DV(22,9),IPREF,JPREF
     1/TEMP/RESORT,NSWPT,URFT
     1/VAR/U(22,9),V(22,9),P(22,9),T(22,9),PP(22,9)
     1/ALL/IT,JT,NI,NJ,NIM1,NJM1,GREAT
     1/GEOM/X(22),Y(9),DXEP(22),DXPW(22),DYNP(9),DYPS(9),
     1       SNS(9),SEW(22),XU(22),YV(9)
     1/FLUPR/URFVIS,VISCOS,DENSIT,PRIN,DEN(22,9),VIS(22,9),
     1        CAMH(22,9),A1,A2,A3,A4,A5,A6,A7,SPHEAT,THCOND
     1/COEF/AP(22,9),AN(22,9),AS(22,9),AE(22,9),AW(22,9),SU(22,9),
     1       SP(22,9)
C
CHAPTER  1  1  1  1  1 CALCULATE GEOMETRICAL QUANTITIES  1  1  1  1  1
C
      DXPW(1)=0.0
      DXEP(NI)=0.0
      DO 101 I=1,NIM1
      DXEP(I)=X(I+1)-X(I)
  101 DXPW(I+1)=DXEP(I)
      DYPS(1)=0.0
      DYNP(NJ)=0.0
      DO 102 J=1,NJM1
      DYNP(J)=Y(J+1)-Y(J)
  102 DYPS(J+1)=DYNP(J)
      SEW(1)=0.0
      SEW(NI)=0.0
      DO 103 I=2,NIM1
  103 SEW(I)=0.5*(DXEP(I)+DXPW(I))
      SNS(1)=0.0
      SNS(NJ)=0.0
      DO 104 J=2,NJM1
  104 SNS(J)=0.5*(DYNP(J)+DYPS(J))
      XU(1)=0.0
      DO 105 I=2,NI
  105 XU(I)=0.5*(X(I)+X(I-1))
      DXPWU(1)=0.0
      DXPWU(2)=0.0
      DXEPU(1)=0.0
      DXEPU(NI)=0.0
      DO 106 I=2,NIM1
      DXEPU(I)=XU(I+1)-XU(I)
  106 DXPWU(I+1)=DXEPU(I)
      SEWU(1)=0.0
      SEWU(2)=0.0
      SEWU(NI)=0.0
      DO 107 I=3,NIM1
  107 SEWU(I)=0.5*(DXEPU(I)+DXPWU(I))
      YV(1)=0.0
      DO 108 J=2,NJ
  108 YV(J)=0.5*(Y(J)+Y(J-1))
      DYPSV(1)=0.0
      DYPSV(2)=0.0
      DYNPV(1)=0.0
      DYNPV(NJ)=0.0
      DO 109 J=2,NJM1
      DYNPV(J)=YV(J+1)-YV(J)
  109 DYPSV(J+1)=DYNPV(J)
      SNSV(1)=0.0
      SNSV(2)=0.0
      SNSV(NJ)=0.0
      DO 110 J=3,NJM1
  110 SNSV(J)=0.5*(DYNPV(J)+DYPSV(J))
C
CHAPTER  2  2  2  2  2  2 SET VARIABLES TO ZERO  2  2  2  2  2  2
C
      DO 200 I=1,NI
      DO 200 J=1,NJ
      U(I,J)=0.0
      V(I,J)=0.0
      P(I,J)=0.0
      PP(I,J)=0.0
```

```
      DEN(I,J)=DENSIT
      VIS(I,J)=VISCOS
      GAMH(I,J)=VISCOS/PRIN
      DU(I,J)=0.0
      DV(I,J)=0.0
      SU(I,J)=0.0
      SP(I,J)=0.0
  200 T(I,J)=0.0
      RETURN
      END
```

SUBROUTINE PROPS

```
      SUBROUTINE PROPS
C
CHAPTER  0  0  0  0  0  0  0  0  PRELIMINARIES  0  0  0  0  0  0  0  0
C
      COMMON
     1/VAR/U(22,9),V(22,9),P(22,9),T(22,9),PP(22,9)
     1/ALL/IT,JT,NI,NJ,NIM1,NJM1,GREAT
     1/FLUPR/URFVIS,VISCOS,DENSIT,PRIN,DEN(22,9),VIS(22,9),
     1       GAMH(22,9),A1,A2,A3,A4,A5,A6,A7,SPHEAT,THCOND
C
CHAPTER  1  1  DENSITY,VISCOSITY AND THERMAL EXCHANGE COEFFICIENT  1  1
C
C-----CALCULATE FLUID PROPERTIES FROM FORMULAE USING COEFFICIENTS
C-----A1,A2,...A7, READ IN FROM FILE DATIN.DAT (UNIT 8)
      EXPA1=EXP(A1)
      DO 100 I=2,NIM1
      DO 100 J=2,NJM1
      ENU=(EXP(EXPA1*(T(I,J)+273.)**A2)-.7)/1.E6
      DEN(I,J)=A3+A4*T(I,J)
      VIS(I,J)=ENU*DEN(I,J)
      RHOC=A5+A6*T(I,J)
      SPHEAT=RHOC/DEN(I,J)
  100 GAMH(I,J)=THCOND/SPHEAT
      RETURN
      END
```

SUBROUTINE CALCU

```
      SUBROUTINE CALCU
      COMMON
     1/UVEL/RESORU,NSWPU,URFU,DXEPU(22),DXPWU(22),SEWU(22)
     1/PCOR/RESORM,NSWPP,URFP,DU(22,9),DV(22,9),IPREF,JPREF
     1/TEMP/RESORT,NSWPT,URFT
     1/VAR/U(22,9),V(22,9),P(22,9),T(22,9),PP(22,9)
     1/ALL/IT,JT,NI,NJ,NIM1,NJM1,GREAT
     1/GEOM/X(22),Y(9),DXEP(22),DXPW(22),DYNP(9),DYPS(9),
     1       SNS(9),SEW(22),XU(22),YV(9)
     1/FLUPR/URFVIS,VISCOS,DENSIT,PRIN,DEN(22,9),VIS(22,9),
     1       GAMH(22,9),A1,A2,A3,A4,A5,A6,A7,SPHEAT,THCOND
     1/COEF/AP(22,9),AN(22,9),AS(22,9),AE(22,9),AW(22,9),SU(22,9),
     1       SP(22,9)
C
CHAPTER  0  0  0  0  0  0  0  0  PRELIMINARIES  0  0  0  0  0  0  0  0
C
C
CHAPTER  1  1  1  1  1  1  ASSEMBLY OF COEFFICIENTS  1  1  1  1  1  1  1
C
      DO 100 I=3,NIM1
      DO 101 J=2,NJM1
C-----COMPUTE AREAS AND VOLUME
      AREAN=SEWU(I)
      AREAS=SEWU(I)
      AREAEW=SNS(J)
      VOL=SEWU(I)*SNS(J)
C-----CALCULATE CONVECTION COEFFICIENTS
      GN=0.5*(DEN(I,J+1)+DEN(I,J))*V(I,J+1)
      GNW=0.5*(DEN(I-1,J)+DEN(I-1,J+1))*V(I-1,J+1)
      GS=0.5*(DEN(I,J-1)+DEN(I,J))*V(I,J)
      GSW=0.5*(DEN(I-1,J)+DEN(I-1,J-1))*V(I-1,J)
      GE=0.5*(DEN(I+1,J)+DEN(I,J))*U(I+1,J)
      GP=0.5*(DEN(I,J)+DEN(I-1,J))*U(I,J)
      GW=0.5*(DEN(I-1,J)+DEN(I-2,J))*U(I-1,J)
      CN=0.5*(GN+GNW)*AREAN
```

```
      CS=0.5*(CS+CSW)*AREAS
      CE=0.5*(CE+CP)*AREAEW
      CW=0.5*(CP+CW)*AREAEW
C-----CALCULATE DIFFUSION COEFFICIENTS
      VISN=0.25*(VIS(I,J)+VIS(I,J+1)+VIS(I-1,J)+VIS(I-1,J+1))
      VISS=0.25*(VIS(I,J)+VIS(I,J-1)+VIS(I-1,J)+VIS(I-1,J-1))
      DN=VISN*AREAN/DYNP(J)
      DS=VISS*AREAS/DYPS(J)
      DE=VIS(I,J)*AREAEW/DXEPU(I)
      DW=VIS(I-1,J)*AREAEW/DXEPU(I)
C-----CALCULATE COEFFICIENTS OF SOURCE TERMS
      SMP=CN-CS+CE-CW
      CP=AMAX1(0.0,SMP)
      CPO=CP
C-----ASSEMBLE MAIN COEFFICIENTS
      AN(I,J)=AMAX1(ABS(0.5*CN),DN)-0.5*CN
      AS(I,J)=AMAX1(ABS(0.5*CS),DS)+0.5*CS
      AE(I,J)=AMAX1(ABS(0.5*CE),DE)-0.5*CE
      AW(I,J)=AMAX1(ABS(0.5*CW),DW)-0.5*CW
      DU(I,J)=AREAEW
      SU(I,J)=CPO*U(I,J)+DU(I,J)*(P(I-1,J)-P(I,J))
      SP(I,J)=-CP
  101 CONTINUE
  100 CONTINUE
C
C  CHAPTER  2  2  2  2  2  2  2  PROBLEM MODIFICATIONS  2  2  2  2  2  2  2
C
      CALL MODU
C
C  CHAPTER  3  FINAL COEFF. ASSEMBLY AND RESIDUAL SOURCE CALCULATION  3  3
C
      RESORU=0.0
      DO 300 I=3,NIM1
      DO 301 J=2,NJM1
      AP(I,J)=AN(I,J)+AS(I,J)+AE(I,J)+AW(I,J)-SP(I,J)
      DU(I,J)=DU(I,J)/AP(I,J)
      RESOR=AN(I,J)*U(I,J+1)+AS(I,J)*U(I,J-1)+AE(I,J)*U(I+1,J)
     1      +AW(I,J)*U(I-1,J)-AP(I,J)*U(I,J)+SU(I,J)
      VOL=SEW(I)*SNS(J)
      SORVOL=GREAT*VOL
      IF(-SP(I,J).GT.0.5*SORVOL) RESOR=RESOR/SORVOL
      RESORU=RESORU+ABS(RESOR)
C-----UNDER-RELAXATION
      AP(I,J)=AP(I,J)/URFU
      SU(I,J)=SU(I,J)+(1.-URFU)*AP(I,J)*U(I,J)
      DU(I,J)=DU(I,J)*URFU
  301 CONTINUE
  300 CONTINUE
C
C  CHAPTER  4  4  4  SOLUTION OF DIFFERENCE EQUATION  4  4  4  4  4  4  4
C
      DO 400 N=1,NSWPU
  400 CALL LISOLV(3,2,NI,NJ,IT,JT,U)
      RETURN
      END
```

SUBROUTINE CALCV

```
      SUBROUTINE CALCV
      COMMON
     1/VVEL/RESORV,NSWPV,URFV,DYNPV(9),DYPSV(9),SNSV(9)
     1/PCOR/RESORM,NSWPP,URFP,DU(22,9),DV(22,9),IPREF,JPREF
     1/VAR/U(22,9),V(22,9),P(22,9),T(22,9),PP(22,9)
     1/ALL/IT,JT,NI,NJ,NIM1,NJM1,GREAT
     1/GEOM/X(22),Y(9),DXEP(22),DXPW(22),DYNP(9),DYPS(9),
     1       SNS(9),SEW(22),XU(22),YV(9)
     1/FLUPR/URFVIS,VISCOS,DENSIT,PRIN,DEN(22,9),VIS(22,9),
     1       GAMH(22,9),A1,A2,A3,A4,A5,A6,A7,SPHEAT,THCOND
     1/COEF/AP(22,9),AN(22,9),AS(22,9),AE(22,9),AW(22,9),SU(22,9),
     1       SP(22,9)
C
C  CHAPTER  0  0  0  0  0  0  0  0  PRELIMINARIES  0  0  0  0  0  0  0  0
C
C
C  CHAPTER  1  1  1  1  1  1  ASSEMBLY OF COEFFICIENTS  1  1  1  1  1  1  1
C
```

```
      DO 100 I=2,NIM1
      DO 101 J=2,NJM1
C-----COMPUTE AREAS AND VOLUME
      AREAN=SEW(I)
      AREAS=SEW(I)
      AREAEW=SNSV(J)
      VOL=SEW(I)*SNSV(J)
C-----CALCULATE CONVECTION COEFFICIENTS
      CN=0.5*(DEN(I,J+1)+DEN(I,J))*V(I,J+1)
      CP=0.5*(DEN(I,J)+DEN(I,J-1))*V(I,J)
      CS=0.5*(DEN(I,J-1)+DEN(I,J-2))*V(I,J-1)
      CE=0.5*(DEN(I+1,J)+DEN(I,J))*U(I+1,J)
      CSE=0.5*(DEN(I,J-1)+DEN(I+1,J-1))*U(I+1,J-1)
      CW=0.5*(DEN(I,J)+DEN(I-1,J))*U(I,J)
      CSW=0.5*(DEN(I,J-1)+DEN(I-1,J-1))*U(I,J-1)
      CN=0.5*(CN+CP)*AREAN
      CS=0.5*(CP+CS)*AREAS
      CE=0.5*(CE+CSE)*AREAEW
      CW=0.5*(CW+CSW)*AREAEW
C-----CALCULATE DIFFUSION COEFFICIENTS
      VISE=0.25*(VIS(I,J)+VIS(I+1,J)+VIS(I,J-1)+VIS(I+1,J-1))
      VISW=0.25*(VIS(I,J)+VIS(I-1,J)+VIS(I,J-1)+VIS(I-1,J-1))
      DN=VIS(I,J)*AREAN/DYNPV(J)
      DS=VIS(I,J-1)*AREAS/DYPSV(J)
      DE=VISE*AREAEW/DXEP(I)
      DW=VISW*AREAEW/DXPW(I)
C-----CALCULATE COEFFICIENTS OF SOURCE TERMS
      SMP=CN-CS+CE-CW
      CP=AMAX1(0.0,SMP)
      CPO=CP
C-----ASSEMBLE MAIN COEFFICIENTS
      AN(I,J)=AMAX1(ABS(0.5*CN),DN)-0.5*CN
      AS(I,J)=AMAX1(ABS(0.5*CS),DS)+0.5*CS
      AE(I,J)=AMAX1(ABS(0.5*CE),DE)-0.5*CE
      AW(I,J)=AMAX1(ABS(0.5*CW),DW)+0.5*CW
      DV(I,J)=0.5*(AREAN+AREAS)
      SU(I,J)=CPO*V(I,J)+DV(I,J)*(P(I,J-1)-P(I,J))
      SP(I,J)=-CP
  101 CONTINUE
  100 CONTINUE
C
C CHAPTER  2  2  2  2  2  2  2  PROBLEM MODIFICATIONS  2  2  2  2  2  2  2
C
      CALL MODV
C
C CHAPTER  3  FINAL COEFF. ASSEMBLY AND RESIDUAL SOURCE CALCULATION  3  3
C
      RESORV=0.0
      DO 300 I=2,NIM1
      DO 301 J=2,NJM1
      AP(I,J)=AN(I,J)+AS(I,J)+AE(I,J)+AW(I,J)-SP(I,J)
      DV(I,J)=DV(I,J)/AP(I,J)
      RESOR=AN(I,J)*V(I,J+1)+AS(I,J)*V(I,J-1)+AE(I,J)*V(I+1,J)
     1      +AW(I,J)*V(I-1,J)-AP(I,J)*V(I,J)+SU(I,J)
      VOL=SEW(I)*SNS(J)
      SORVOL=GREAT*VOL
      IF(-SP(I,J).GT.0.5*SORVOL) RESOR=RESOR/SORVOL
      RESORV=RESORV+ABS(RESOR)
C-----UNDER-RELAXATION
      AP(I,J)=AP(I,J)/URFV
      SU(I,J)=SU(I,J)+(1.-URFV)*AP(I,J)*V(I,J)
      DV(I,J)=DV(I,J)*URFV
  301 CONTINUE
  300 CONTINUE
C
C CHAPTER  4  4  4  SOLUTION OF DIFFERENCE EQUATION  4  4  4  4  4  4  4
C
      DO 400 N=1,NSWPV
  400 CALL LISOLV(2,3,NI,NJ,IT,JT,V)
      RETURN
      END
```

SUBROUTINE CALCP

```
      SUBROUTINE CALCP
      COMMON
     1/PCOR/RESORM,NEWPP,URFP,DU(22,9),DV(22,9),IPREF,JPREF
     1/VAR/U(22,9),V(22,9),P(22,9),T(22,9),PP(22,9)
     1/ALL/IT,JT,NI,NJ,NIM1,NJM1,GREAT
     1/GEOM/X(22),Y(9),DXEP(22),DXPW(22),DYNP(9),DYPS(9),
     1       SNS(9),SEW(22),XU(22),YV(9)
     1/FLUPR/URFVIS,VISCOS,DENSIT,PRIN,DEN(22,9),VIS(22,9),
     1       GAMH(22,9),A1,A2,A3,A4,A5,A6,A7,SPHEAT,THCOND
     1/COEF/AP(22,9),AN(22,9),AS(22,9),AE(22,9),AW(22,9),SU(22,9),
     1       SP(22,9)
C
CHAPTER  0  0  0  0  0  0  0  0  PRELIMINARIES  0  0  0  0  0  0  0  0
C
      RESORM=0.0
C
CHAPTER  1  1  1  1  1  1  ASSEMBLY OF COEFFICIENTS  1  1  1  1  1  1  1
C
      DO 100 I=2,NIM1
      DO 101 J=2,NJM1
C-----COMPUTE AREAS AND VOLUME
      AREAN=SEW(I)
      AREAS=SEW(I)
      AREAEW=SNS(J)
      VOL=SNS(J)*SEW(I)
C-----CALCULATE COEFFICIENTS
      DENN=0.5*(DEN(I,J)+DEN(I,J+1))
      DENS=0.5*(DEN(I,J)+DEN(I,J-1))
      DENE=0.5*(DEN(I,J)+DEN(I+1,J))
      DENW=0.5*(DEN(I,J)+DEN(I-1,J))
      AN(I,J)=DENN*AREAN*DV(I,J+1)
      AS(I,J)=DENS*AREAS*DV(I,J)
      AE(I,J)=DENE*AREAEW*DU(I+1,J)
      AW(I,J)=DENW*AREAEW*DU(I,J)
C-----CALCULATE SOURCE TERMS
      CN=DENN*V(I,J+1)*AREAN
      CS=DENS*V(I,J)*AREAS
      CE=DENE*U(I+1,J)*AREAEW
      CW=DENW*U(I,J)*AREAEW
      SMP=CN-CS+CE-CW
      SP(I,J)=0.0
      SU(I,J)=-SMP
C-----COMPUTE SUM OF ABSOLUTE MASS SOURCES
      RESORM=RESORM+ABS(SMP)
  101 CONTINUE
  100 CONTINUE
C
CHAPTER  2  2  2  2  2  2  2  PROBLEM MODIFICATIONS  2  2  2  2  2  2  2
C
      CALL MODP
C
CHAPTER  3  3  3  3  3  FINAL COEFFICIENT ASSEMBLY  3  3  3  3  3  3  3
C
      DO 300 I=2,NIM1
      DO 301 J=2,NJM1
  301 AP(I,J)=AN(I,J)+AS(I,J)+AE(I,J)+AW(I,J)-SP(I,J)
  300 CONTINUE
C
CHAPTER  4  4  4  4  4  SOLUTION OF DIFFERENCE EQUATIONS  4  4  4  4  4
C
      DO 400 N=1,NEWPP
  400 CALL LISOLV(2,2,NI,NJ,IT,JT,PP)
C
CHAPTER  5  5  5  5  CORRECT VELOCITIES AND PRESSURE  5  5  5  5  5  5
C
C-----VELOCITIES
      DO 500 I=2,NIM1
      DO 501 J=2,NJM1
      IF(I.NE.2) U(I,J)=U(I,J)+DU(I,J)*(PP(I-1,J)-PP(I,J))
      IF(J.NE.2) V(I,J)=V(I,J)+DV(I,J)*(PP(I,J-1)-PP(I,J))
  501 CONTINUE
  500 CONTINUE
C-----PRESSURES (WITH PROVISION FOR UNDER-RELAXATION)
      PPREF=PP(IPREF,JPREF)
      DO 502 I=2,NIM1
      DO 502 J=2,NJM1
      P(I,J)=P(I,J)+URFP*(PP(I,J)-PPREF)
```

```
      PP(I,J)=0.0
  503 CONTINUE
  502 CONTINUE
      RETURN
      END
```

SUBROUTINE CALCT

```
      SUBROUTINE CALCT
C
CHAPTER  0  0  0  0  0  0  0  PRELIMINARIES  0  0  0  0  0  0  0
C
      COMMON
     1/TEMP/RESORT,NSWPT,URFT
     1/VAR/U(22,9),V(22,9),P(22,9),T(22,9),PP(22,9)
     1/ALL/IT,JT,N1,NJ,NIM1,NJM1,GREAT
     1/GEOM/X(22),Y(9),DXEP(22),DXPW(22),DYNP(9),DYPS(9),
     1       SNS(9),SEW(22),XU(22),YV(9)
     1/FLUPR/UPPVIS,VISCOS,DENSIT,PRIN,DEN(22,9),VIS(22,9),
     1       GAMH(22,9),A1,A2,A3,A4,A5,A6,A7,SPHEAT,THCOND
     1/COEF/AP(22,9),AN(22,9),AS(22,9),AE(22,9),AW(22,9),SU(22,9),
     1       SP(22,9)
C
CHAPTER  1  1  1  1  1  1  ASSEMBLY OF COEFFICIENTS  1  1  1  1  1  1
C
      DO 100 I=2,NIM1
      DO 101 J=2,NJM1
C-----COMPUTE AREAS AND VOLUME
      AREAN=SEW(I)
      AREAS=SEW(I)
      AREAEW=SNS(J)
      VOL=SNS(J)*SEW(I)
C-----CALCULATE CONVECTION COEFFICIENTS
      GN=0.5*(DEN(I,J)+DEN(I,J+1))*V(I,J+1)
      GS=0.5*(DEN(I,J)+DEN(I,J-1))*V(I,J)
      GE=0.5*(DEN(I,J)+DEN(I+1,J))*U(I+1,J)
      GW=0.5*(DEN(I,J)+DEN(I-1,J))*U(I,J)
      CN=GN*AREAN
      CS=GS*AREAS
      CE=GE*AREAEW
      CW=GW*AREAEW
C-----CALCULATE DIFFUSION COEFFICIENTS
      GAMN=0.5*(GAMH(I,J)+GAMH(I,J+1))
      GAMS=0.5*(GAMH(I,J)+GAMH(I,J-1))
      GAME=0.5*(GAMH(I,J)+GAMH(I+1,J))
      GAMW=0.5*(GAMH(I,J)+GAMH(I-1,J))
      DN=GAMN*AREAN/DYNP(J)
      DS=GAMS*AREAS/DYPS(J)
      DE=GAME*AREAEW/DXEP(I)
       DW=GAMW*AREAEW/DXPW(I)
C-----SOURCE TERMS
      SMP=CN-CS+CE-CW
      CP=AMAX1(0.0,SMP)
      CPO=CP
C-----ASSEMBLE MAIN COEFFICIENTS
      AN(I,J)=AMAX1(ABS(0.5*CN),DN)-0.5*CN
      AS(I,J)=AMAX1(ABS(0.5*CS),DS)+0.5*CS
      AE(I,J)=AMAX1(ABS(0.5*CE),DE)-0.5*CE
      AW(I,J)=AMAX1(ABS(0.5*CW),DW)+0.5*CW
      SU(I,J)=CPO*T(I,J)
      SP(I,J)=-CP
  101 CONTINUE
  100 CONTINUE
C
CHAPTER  2  2  2  2  2  2  PROBLEM MODIFICATIONS  2  2  2  2  2  2
C
      CALL MODT
C
CHAPTER 3 FINAL COEFFICIENT ASSEMBLY AND RESIDUAL SOURCE CALCULATION 3
C
      RESORT=0.0
      DO 300 I=2,NIM1
      DO 301 J=2,NJM1
      AP(I,J)=AN(I,J)+AS(I,J)+AE(I,J)+AW(I,J)-SP(I,J)
      RESOR=AN(I,J)*T(I,J+1)+AS(I,J)*T(I,J-1)+AE(I,J)*T(I+1,J)
```

```
68:      1      +AW(I,J)*T(I-1,J)-AP(I,J)*T(I,J)+SU(I,J)
69:       VOL=SEW(I)*SNS(J)
70:       SORVOL=GREAT*VOL
71:       IF(-SP(I,J).GT.0.5*SORVOL) RESOR=RESOR/SORVOL
72:       RESORT=RESORT+ABS(RESOR)
73: C-----UNDER-RELAXATION
74:       AP(I,J)=AP(I,J)/URFT
75:       SU(I,J)=SU(I,J)+(1.-URFT)*AP(I,J)*T(I,J)
76:   301 CONTINUE
77:   300 CONTINUE
78: C
79: CHAPTER  4  4  4  4  4  SOLUTION OF DIFFERENCE EQUATIONS  4  4  4  4  4
80: C
81:       DO 400 N=1,NSWPT
82:   400 CALL LISOLV(2,2,NI,NJ,IT,JT,T)
83:       RETURN
84:       END
```

SUBROUTINE LISOLV

```
 1:       SUBROUTINE LISOLV(ISTART,JSTART,NI,NJ,IT,JT,PHI)
 2: C
 3: CHAPTER  0  0  0  0  0  0  0  0  PRELIMINARIES  0  0  0  0  0  0  0  0
 4: C
 5:       DIMENSION PHI(IT,JT),A(9),B(9),C(9),D(9)
 6:       COMMON
 7:      1/COEF/AP(22,9),AN(22,9),AS(22,9),AE(22,9),AW(22,9),SU(22,9),
 8:      1      SP(22,9)
 9:       NIM1=NI-1
10:       NJM1=NJ-1
11:       JSTM1=JSTART-1
12:       A(JSTM1)=0.0
13: C-----COMMENCE W-E SWEEP
14:       DO 100 I=ISTART,NIM1
15:       C(JSTM1)=PHI(I,JSTM1)
16: C-----COMMENCE S-N TRAVERSE
17:       DO 101 J=JSTART,NJM1
18: C-----ASSEMBLE TDMA COEFFICIENTS
19:       A(J)=AN(I,J)
20:       B(J)=AS(I,J)
21:       C(J)=AE(I,J)*PHI(I+1,J)+AW(I,J)*PHI(I-1,J)+SU(I,J)
22:       D(J)=AP(I,J)
23: C-----CALCULATE COEFFICIENTS OF RECURRENCE FORMULA
24:       TERM=1./(D(J)-B(J)*A(J-1))
25:       A(J)=A(J)*TERM
26:   101 C(J)=(C(J)+B(J)*C(J-1))*TERM
27: C-----OBTAIN NEW PHI'S
28:       DO 102 JJ=JSTART,NJM1
29:       J=NJ+JSTM1-JJ
30:   102 PHI(I,J)=A(J)*PHI(I,J+1)+C(J)
31:   100 CONTINUE
32:       RETURN
33:       END
```

SUBROUTINE PRINT

```
      SUBROUTINE PRINT(ISTART,JSTART,NI,NJ,IT,JT,X,Y,PHI,HEAD)
      DIMENSION PHI(IT,JT),X(IT),Y(JT),HEAD(6),STORE(50)
      DIMENSION F(7),F4(11)
      DATA F/4H(1H ,4H,A6,,4HI3, ,4H11I ,4H10, ,4H7X, ,
     14HA6) /
      DATA F4/4H 1I ,4H 2I ,4H 3I ,4H 4I ,4H 5I ,4H 6I ,
     1        4H 7I ,4H 8I ,4H 9I ,4H10I ,4H11I /
      DATA HI,HY/6H  I = , 6H Y =  /
      ISKIP=1
      JSKIP=1
      WRITE(6,110)HEAD
      ISTA=ISTART-12
  100 CONTINUE
      ISTA=ISTA+12
      IEND=ISTA+11
      IEND=MIN0(NI,IEND)
      IDIF=IEND-ISTA
      F(4)=F4(IDIF)
      WRITE(6,F) HI, (I,I=ISTA,IEND,ISKIP), HY
      WRITE(6,112)
      DO 101 JJ=JSTART,NJ,JSKIP
      J=JSTART+NJ-JJ
      DO 120 I=ISTA,IEND
      A=PHI(I,J)
      IF(ABS(A).LT.1.E-20) A=0.0
  120 STORE(I)=A
  101 WRITE(6,113)  J,(STORE(I),I=ISTA,IEND,ISKIP),Y(J)
      WRITE(6,114) (X(I),I=ISTA,IEND,ISKIP)
C-----------------------------------------------
      IF(IEND.LT.NI)GO TO 100
      RETURN
  110 FORMAT(1H0,20(2H*-),7X,6A4,7X,20(2H-*))
  111 FORMAT(1H0,5H  I = ,I3,11I10,7X,' Y = ')
  112 FORMAT(3H  J)
  113 FORMAT(1H ,I3,1P12E10.2,0PF7.5)
  114 FORMAT(6H0X=   ,F7.5,11F10.5)
      END
```

D4 JUNCTION In lines 1-90 of MAIN (see listings which follow), the necessary data is read in from unit 8 and written to the VDU and the output file (unit 6) for verification. In lines 93-158, the X(I) and Y(J) arrays are set, using the input values of XFRAC(I) and YFRAC(J). The process is involved; ENTRYL, EXITL and HORIZL must be adjusted according to REIN, RE1 and RE2, and the grid refined near corners and solid boundaries (see Fig. 5.2). In lines 184-218, the initial fields U(I,J), V(I,J) and P(I,J) are set (if not available as the output of a prior calculation). Lines 258-284 comprise the main iteration loop. The friction constants KDS, KDT, KCS and KCT are computed in lines 292-328, in accordance with Sec. 5.5.

In MODU, the boundary conditions on U are set. Within all solid areas, U(I,J) is forced to zero using the device desceribed in equations (5.1) and (5.2) (lines 16-23). When this is done, care must be taken to avoid generating large values of RESORU. This is avoided, in CALCU (see Sec. D3), in lines 75-76. The 'no-slip' wall boundary condition on U (Fig. 5.3), and the special corner condition (Fig. 5.4) are set in lines 24-39. In MODV, similar comments apply, and in MODP, only the PP(I,J) field within the solid areas has been forced to zero. Following the listings, sample output is provided.

PROGRAM MAIN

```
      PROGRAM MAIN
      SUBROUTINE CONTRO
C
CHAPTER  0  0  0  0  0  0  0  0  PRELIMINARIES  0  0  0  0  0  0  0  0
C
      DIMENSION HEDU(6),HEDV(6),HEDP(6),HEDT(6)
      DIMENSION XFRAC(17),YFRAC(13)
      LOGICAL INCALU,INCALV
      LOGICAL RESTRT,DIVIDE
       COMMON
     1/UVEL/RESORU,NSWPU,URFU,DXEPU(17),DXPWU(17),SEWU(17)
     1/VVEL/RESORV,NSWPV,URFV,DYNPV(13),DYPSV(13),SNSV(13)
     1/PCOR/RESORM,NSWPP,URFP,DU(17,13),DV(17,13),IPREF,JPREF
     1/VAR/U(17,13),V(17,13),P(17,13),PP(17,13)
     1/ALL/NI,NJ,NIM1,NJM1,GREAT
     1/GEOM/X(17),Y(13),DXEP(17),DXPW(17),DYNP(13),DYPS(13),
     1       SNS(13),SEW(17),XU(17),YV(13)
     1/FLUPR/VISCOS,DENSIT
     1/JUN/IST1,IST2,JSTEP,IST1M1,IST2M1,IST1M2,IST2P1,NIM2,
     1      JSTP1,NJM2,IST2P2,JSTP2,JSTM1,IST1P1
       CALL OPEN(6,'RESULT  DAT',2)
       CALL OPEN(8,'DATIN   DAT',2)
       CALL OPEN(9,'INTERMEDDAT',2)
       GREAT=1.0E30
       PI=4.*ATAN(1.)
       NITER=0
       READ(8,011) VISCOS,DENSIT,QIN,QRATIO,ENTFAC
       WRITE(4,025) VISCOS,DENSIT,QIN,QRATIO,ENTFAC
       READ(8,012) RVERT,RRATIO,IST1,IST2,NI,NJ,JSTEP
       WRITE(4,026) RVERT,RRATIO,IST1,IST2,NI,NJ,JSTEP
       NIM1=NI-1
       NJM1=NJ-1
       READ(8,024) (XFRAC(I),I=1,NIM1)
       WRITE(4,027) (XFRAC(I),I=1,NIM1)
       READ(8,024) (YFRAC(J),J=1,NJM1)
       WRITE(4,027) (YFRAC(J),J=1,NJM1)
       READ(8,013) NSWPU,NSWPV,NSWPP,MAXIT,INDPRI
       WRITE(4,028) NSWPU,NSWPV,NSWPP,MAXIT,INDPRI
       READ(8,014) URFU,URFV,URFP,SORMAX
       WRITE(4,029) URFU,URFV,URFP,SORMAX
       READ(8,015) RESTRT,DIVIDE
       WRITE(4,030) RESTRT,DIVIDE
       READ(8,010) HEDU,HEDV,HEDP
       WRITE(4,031) HEDU,HEDV,HEDP
C-----WRITE OUT SOLUTION CONTROL PARAMETERS
       WRITE(6,2000)
       WRITE(6,017) NSWPU,NSWPV,NSWPP,MAXIT,
      1URFU,URFV,URFP,SORMAX
       IF(RESTRT) WRITE(6,018)
       IF(.NOT.RESTRT) WRITE(6,019)
       WRITE(6,2000)
       WRITE(6,020) ENTFAC,IST1,IST2,JSTEP
       WRITE(6,021)
       WRITE(6,022) (XFRAC(I),I=1,NIM1)
       WRITE(6,023)
       WRITE(6,022) (YFRAC(J),J=1,NJM1)
  010 FORMAT(6A4)
  031 FORMAT(1X,6A4)
  011 FORMAT(5E12.3)
  025 FORMAT(1X,5E12.3)
  012 FORMAT(2F5.4,5I3)
  026 FORMAT(1X,2F6.4,5I3)
  013 FORMAT(5I2)
  028 FORMAT(1X,5I3)
  014 FORMAT(4F6.4)
  029 FORMAT(1X,4F6.4)
  015 FORMAT(2L5)
  030 FORMAT(1X,2L5)
  017 FORMAT('0',5X,'SOLUTION CONTROL PARAMETERS'/
     1/5X,'NSWPU----------=',I3
     1/5X,'NSWPV----------=',I3
     1/5X,'NSWPP----------=',I3
     1/5X,'MAXIT----------=',I4
     1/5X,'URFU-----------=',F5.2
     1/5X,'URFV-----------=',F5.2
     1/5X,'URFP-----------=',F5.2
     1/5X,'SORMAX---------=',F6.3)
```

```
  018 FORMAT('0','INITIAL FIELDS HAVE BEEN READ IN FROM UNIT 9')
  019 FORMAT('0','INITIAL FIELDS HAVE BEEN SET IN MAIN PROGRAM')
  020 FORMAT('0',5X,'GEOMETRICAL PARAMETERS'//
     1/5X,'ENTFAC----------=',F5.2
     1/5X,'IST1------------=',I3
     1/5X,'IST2------------=',I3
     1/5X,'JSTEP-----------=',I3)
  021 FORMAT('0','XFRAC(I)=')
  022 FORMAT(10X,5F7.3)
  023 FORMAT('0','YFRAC(J)=')
  024 FORMAT(17F7.3)
  027 FORMAT(1X,10F7.3)
C
CHAPTER  1  1  1  1  1  PARAMETERS AND CONTROL INDICES  1  1  1  1  1  1
C
      Q2=QIN/QRATIO
      IF(DIVIDE)Q1=QIN-Q2
      IF(.NOT.DIVIDE)Q1=QIN+Q2
      REIN=QIN*2.*DENSIT/VISCOS
      RE1=Q1*2.*DENSIT/VISCOS
      RE2=Q2*2.*DENSIT/VISCOS
C-----COMPUTE DUCT LENGTHS BASED ON HYDRODYNAMIC ENTRY LENGTH
      RHORIZ=RVERT/RRATIO
      ENTRYL=4.*RVERT*ENTFAC*(.3125+.011*REIN)
      EXITL=4.*RVERT*ENTFAC*(.3125+.011*RE1)
      HORIZL=4.*RHORIZ*ENTFAC*(.3125+.011*RE2)
C-----COMPUTE ALL INDICES
      NIM2=NI-2
      NJM2=NJ-2
      IST1M1=IST1-1
      IST1M2=IST1-2
      IST2M1=IST2-1
      IST1P1=IST1+1
      IST2P1=IST2+1
      IST2P2=IST2+2
      JSTP1=JSTEP+1
      JSTP2=JSTEP+2
      JSTM1=JSTEP-1
C-----COMPUTE SMALLEST DX IN HORIZONTAL BRANCH REGION
      XSUM=XFRAC(IST1M1)/2.
      DO 100 I=IST1,IST2M1
  100 XSUM=XSUM+XFRAC(I)
      XSUM=XSUM+XFRAC(IST2)/2.
      DXSM2=2.*RHORIZ/XSUM
C-----COMPUTE SMALLEST DX IN VERTICAL DUCT ENTRANCE REGION
      XSUM=XFRAC(1)/2.
      DO 105 I=2,IST1M2
  105 XSUM=XSUM+XFRAC(I)
      DXSM1=(ENTRYL-.5*XFRAC(IST1M1)*DXSM2)/XSUM
C-----COMPUTE SMALLEST DX IN VERTICAL DUCT EXIT REGION
      XSUM=0.
      DO 110 I=IST2P1,NIM2
  110 XSUM=XSUM+XFRAC(I)
      XSUM=XSUM+XFRAC(NIM1)/2.
      DXSM3=(EXITL-.5*XFRAC(IST2)*DXSM2)/XSUM
C-----COMPUTE SMALLEST DY IN VERTICAL DUCT REGION
      YSUM=YFRAC(1)/2.
      DO 115 J=2,JSTM1
  115 YSUM=YSUM+YFRAC(J)
      YSUM=YSUM+YFRAC(JSTEP)/2.
      DYSM1=2.*RVERT/YSUM
C-----COMPUTE SMALLEST DY IN HORIZONTAL BRANCH REGION
      YSUM=0.
      DO 120 J=JSTP1,NJM2
  120 YSUM=YSUM+YFRAC(J)
      YSUM=YSUM+YFRAC(NJM1)/2.
      DYSM2=(HORIZL-.5*YFRAC(JSTEP)*DYSM1)/YSUM
C-----SET UP X-ARRAY
      X(1)=-XFRAC(1)*DXSM1/2.
      DO 125 I=2,IST1M1
  125 X(I)=X(I-1)+XFRAC(I-1)*DXSM1
      DO 130 I=IST1,IST2P1
  130 X(I)=X(I-1)+XFRAC(I-1)*DXSM2
      DO 135 I=IST2P2,NI
  135 X(I)=X(I-1)+XFRAC(I-1)*DXSM3
C-----SET UP Y-ARRAY
      Y(1)=-YFRAC(1)*DYSM1/2.
      DO 140 J=2,JSTP1
  140 Y(J)=Y(J-1)+YFRAC(J-1)*DYSM1
      DO 145 J=JSTP2,NJ
  145 Y(J)=Y(J-1)+YFRAC(J-1)*DYSM2
C-----DEPENDENT VARIABLE SELECTION
```

```
      INCALU=.TRUE.
      INCALV=.TRUE.
      INCALP=.TRUE.
C-----BOUNDARY VALUES
C-----PRESSURE CALCULATION
      PREF=1.0
      IPREF=2
      JPREF=2
C-----PROGRAM CONTROL AND MONITOR
      IMON=IST1
      JMON=JSTEP
      NUMPRI=1
C
CHAPTER  2  2  2  2  2  2  INITIAL OPERATIONS  2  2  2  2  2  2  2  2  2
C
C-----CALCULATE GEOMETRICAL QUANTITIES AND SET VARIABLES TO ZERO
      CALL INIT
C-----INITIALISE VARIABLE FIELDS
C-----READ IN INITIAL FIELDS IF AVAILABLE FROM PREVIOUS RUN
      VIN=QIN/(RVERT*2.)
      V1=Q1/(RVERT*2.)
      IF(.NOT.RESTRT) GO TO 199
      CALL REST
      GO TO 235
C-----ASSUME PARABOLIC INLET AND OUTLET PROFILES
C-----ASSUME PARABOLIC INITIAL DISTRIBUTIONS
  199 DO 200 I=2,IST1
      DO 200 J=2,JSTEP
  200 U(I,J)=3.*VIN*(Y(J)/RVERT-.5*(Y(J)/RVERT)**2)
      DO 205 I=IST1P1,NI
      DO 205 J=2,JSTEP
  205 U(I,J)=3.*V1*(Y(J)/RVERT-.5*(Y(J)/RVERT)**2)
      IF(DIVIDE)V2=Q2/(RHORIZ*2.)
      IF(.NOT.DIVIDE)V2=-Q2/(RHORIZ*2.)
      DO 210 I=IST1,IST2
      XP=X(I)-XU(IST1)
      DO 210 J=JSTP1,NJ
  210 V(I,J)=3.*V2*(XP/RHORIZ-.5*(XP/RHORIZ)**2)
C-----ASSUME PRESSURE DISTRIBUTIONS FOR FULLY DEVELOPED FLOW
      DO 215 J=2,JSTEP
  215 P(2,J)=PREF
      FACTOR=1.5*VISCOS*QIN/RVERT**3
      DO 220 I=3,IST1
      XDIST=X(I)-X(2)
      DO 220 J=2,JSTEP
  220 P(I,J)=PREF-XDIST*FACTOR
      FACTOR=1.5*VISCOS*Q1/RVERT**3
      DO 225 I=IST1P1,NIM1
      XDIST=X(I)-X(IST1)
      DO 225 J=2,JSTEP
  225 P(I,J)=P(IST1,J)-XDIST*FACTOR
      DO 230 I=IST1P1,IST2
  230 P(I,JSTEP)=P(IST1,JSTEP)
      FACTOR=1.5*VISCOS*Q2/RHORIZ**3
      DO 235 J=JSTP1,NJM1
      YDIST=Y(J)-Y(JSTEP)
      DO 235 I=IST1,IST2
      IF(DIVIDE)P(I,J)=P(IST1,JSTEP)-FACTOR*YDIST
      IF(.NOT.DIVIDE) P(I,J)=P(IST1,JSTEP)+FACTOR*YDIST
  235 CONTINUE
C-----CALCULATE SOURCE-NORMALISATION FACTORS
      IF(DIVIDE)SNORMM=DENSIT*QIN
      IF(.NOT.DIVIDE)SNORMM=DENSIT*Q1
      IF(DIVIDE)SNORMU=SNORMM*VIN
      IF(.NOT.DIVIDE)SNORMU=SNORMM*V1
      SNORMV=SNORMU
C-----INITIAL OUTPUT
      WRITE(6,2000)
      IF(DIVIDE)WRITE(6,2010)
      IF(.NOT.DIVIDE)WRITE(6,2020)
      WRITE(6,2030)QIN,Q1,Q2,QRATIO,VISCOS,DENSIT,REIN,RE1,RE2,
     1RVERT,RHORIZ,PRATIO,ENTRYL,EXITL,HORIZL
      WRITE(6,2000)
      IF(INCALU) CALL PRINT(2,2,NI,NJ,17,18,XU,Y,U,HEDU)
      IF(INCALV) CALL PRINT(2,2,NI,NJ,17,18,X,YV,V,HEDV)
      IF(INCALP) CALL PRINT(2,2,NI,NJ,17,18,X,Y,P,HEDP)
 2000 FORMAT('///'0',120('*')///)
 2010 FORMAT('0',5X,'JUNCTION PRESSURE DROP, DIVIDING FLOW'//)
 2020 FORMAT('0',5X,'JUNCTION PRESSURE DROP, COMBINING FLOW'//)
```

```
239 2030 FORMAT('0',5X,'FLOW PARAMETERS'//
240     1/5X,'VERTICAL DUCT INLET FLOW RATE---------=',1PE12.3,' M**3/S'
241     1/5X,'VERTICAL DUCT EXIT FLOW RATE----------=',1PE12.3,' M**3/S'
242     1/5X,'HORIZONTAL DUCT FLOW RATE-------------=',1PE12.3,' M**3/S'
243     1/5X,'RATIO Q1N/Q2--------------------------=',1PE12.3
244     1/5X,'VISCOSITY-----------------------------=',1PE12.3,' KG/M*S'
245     1/5X,'DENSITY-------------------------------=',1PE12.3,' KG/M**3'
246     1/5X,'INLET REYNOLDS NO.--------------------=',1PE12.3
247     1/5X,'EXIT REYNOLDS NO.---------------------=',1PE12.3
248     1/5X,'HORIZONTAL DUCT REYNOLDS NO.----------=',1PE12.3
249     1/5X,'VERTICAL DUCT HYDRAULIC RADIUS--------=',1PE12.3,' M'
250     1/5X,'HORIZONTAL DUCT HYDRAULIC RADIUS------=',1PE12.3,' M'
251     1/5X,'RATIO, VERT. TO HOR. DUCT RADII-------=',1PE12.3
252     1/5X,'VERTICAL DUCT INLET LENGTH------------=',1PE12.3,' M'
253     1/5X,'VERTICAL DUCT EXIT LENGTH-------------=',1PE12.3,' M'
254     1/5X,'HORIZONTAL DUCT LENGTH----------------=',1PE12.3,' M')
255C
256CHAPTER  3  3  3  3  3  3  3  ITERATION LOOP  3  3  3  3  3  3  3  3  3
257C
258       WRITE(6,310) IMON,JMON
259   300 NITER=NITER+1
260C-----UPDATE MAIN DEPENDENT VARIABLES
261       IF(INCALU) CALL CALCU
262       IF(INCALV) CALL CALCV
263       IF(INCALP) CALL CALCP
264C-----INTERMEDIATE OUTPUT
265       RESORU=RESORU/SNORMU
266       RESORV=RESORV/SNORMV
267       RESORM=RESORM/SNORMM
268       WRITE(4,310) IMON,JMON
269       WRITE(6,311) NITER,RESORU,RESORV,RESORM,U(IMON,JMON),
270      1             V(IMON,JMON),P(IMON,JMON)
271       WRITE(4,311) NITER,RESORU,RESORV,RESORM,U(IMON,JMON),
272      1             V(IMON,JMON),P(IMON,JMON)
273       IF(MOD(NITER,INDPRI).NE.0) GO TO 301
274       IF(INCALU) CALL PRINT(2,2,NI,NJ,17,18,XU,Y,U,HEDU)
275       IF(INCALV) CALL PRINT(2,2,NI,NJ,17,18,X,YV,V,HEDV)
276       IF(INCALP) CALL PRINT(2,2,NI,NJ,17,18,X,Y,P,HEDP)
277       WRITE(6,310) IMON,JMON
278   301 CONTINUE
279C-----TERMINATION TESTS
280       SORCE=AMAX1(RESORU,RESORV,RESORM)
281       IF(NITER.EQ.MAXIT) GO TO 302
282       IF(NITER.EQ.20.AND.SORCE.GT.1.0E4*SORMAX) GO TO 302
283       IF(SORCE.GT.SORMAX) GO TO 300
284   302 CONTINUE
285C
286CHAPTER  4  4  4  4  4  4  FINAL OPERATIONS AND OUTPUT  4  4  4  4  4  4
287C
288       IF(INCALU) CALL PRINT(2,2,NI,NJ,17,18,XU,Y,U,HEDU)
289       IF(INCALV) CALL PRINT(2,2,NI,NJ,17,18,X,YV,V,HEDV)
290       IF(INCALP) CALL PRINT(2,2,NI,NJ,17,18,X,Y,P,HEDP)
291C-----DUMP ALL VARIABLE ARRAYS TO TAPE30 FOR LATER USE
292C-----COMPUTE AVERAGE JUNCTION INLET PRESSURE
293       PAVIN=PREF
294       I=NIM1
295       PAV1=0.
296C-----COMPUTE AVERAGE JUNCTION EXIT PRESSURE
297       DO 405 J=2,JSTEP
298   405 PAV1=PAV1+P(I,J)
```

```
      PAV1=PAV1/FLOAT(JSTM1)
C-----COMPUTE AVERAGE JUNCTION BRANCH PRESSURE
      J=NJM1
      PAV2=0.
      DO 410 I=IST1,IST2
  410 PAV2=PAV2+P(I,J)
      ITEMP=IST2-IST1+1
      PAV2=PAV2/FLOAT(ITEMP)
C-----COMPUTE TURNING AND STRAIGHT PRESSURE DROPS DUE TO FRICTION ALONE
      ENTRLP=ENTRYL-X(2)
      EXTLP=EXITL-(XU(NI)-X(NIM1))
      HORZLP=HORIZL-(YV(NJ)-Y(NJM1))
      DELTPS=(1.5*VISCOS/RVERT**3)*(QIN*ENTRLP+Q1*EXTLP)
      PSDIFF=(PAVIN-PAV1)-DELTPS
C-----COMPUTE TURNING AND STRAIGHT PRESSURE DROPS
      IF(.NOT.DIVIDE) GO TO 415
      DLTPDT=1.5*VISCOS*(QIN*ENTRLP/RVERT**3+Q2*HORZLP/RHORIZ**3)
      PDTDFF=(PAVIN-PAV2)-DLTPDT
      FACTOR=8.*RVERT**2/(VISCOS*QIN)
      FKDT=PDTDFF*FACTOR
      FKDS=PSDIFF*FACTOR
      GO TO 420
  415 DLTPCT=1.5*VISCOS*(Q2*HORZLP/RHORIZ**3+Q1*EXTLP/RVERT**3)
      PCTDFF=(PAV2-PAV1)-DLTPCT
      FACTOR=8.*RVERT**2/(VISCOS*Q1)
      FKCT=PCTDFF*FACTOR
      FKCS=PSDIFF*FACTOR
C-----WRITE OUT THE APPARENT FRICTION CONSTANTS
  420 IF(DIVIDE)WRITE(6,4000)FKDT,FKDS
      IF(.NOT.DIVIDE)WRITE(6,4005)FKCT,FKCS
      CALL DUMP
      STOP
C-----FORMAT STATEMENTS
 4000 FORMAT('0',5X,'FRICTION CONSTANTS FOR DIVIDING FLOW:'/
     1/5X,'KDT=',1PE12.3
     1/5X,'KDS=',1PE12.3)
 4005 FORMAT('0',5X,'FRICTION CONSTANTS FOR COMBINING FLOW:'/
     1/5X,'KCT=',1PE12.3
     1/5X,'KCS=',1PE12.3)
  310 FORMAT('0','ITER    ','I-----ABSOLUTE RESIDUAL SOURCE SUM',
     1'S-----I     I-FIELD VALUES AT MONITORING LOCATION',1X,
     1'(',I2,',',I2,')',' I'/2X,'NO.',6X,'UMOM',6X,'VMOM',6X,
     1'MASS',,12X,'U',9X,'V',9X,'P',9X/)
  311 FORMAT(1H ,I3,3X,1P3E10.3,5X,1P3E10.3)
      END
```

SUBROUTINE MODU

```
      SUBROUTINE MODU
      COMMON
     1/UVEL/RESORU,NSWPU,URFU,DXEPU(17),DXPWU(17),SEWU(17)
     1/VVEL/RESORV,NSWPV,URFV,DYNPV(13),DYPSV(13),SNSV(13)
     1/PCOR/RESORM,NSWPP,URFP,DU(17,13),DV(17,13),IPREF,JPREF
     1/VAR/U(17,13),V(17,13),P(17,13),PP(17,13)
     1/ALL/NI,NJ,NIM1,NJM1,GREAT
     1/GEOM/X(17),Y(13),DXEP(17),DXPW(17),DYNP(13),DYPS(13),
     1      SNS(13),SEW(17),XU(17),YV(13)
      1/FLUPR/VISCOS,DENSIT
      1/COEF/AP(17,13),AN(17,13),AS(17,13),AE(17,13),AW(17,13),SU(17,13),
      1      SP(17,13)
      1/JUN/IST1,IST2,JSTEP,IST1M1,IST2M1,IST1M2,IST2P1,NIM2,
      1JSTP1,NJM2,IST2P2,JSTP2,JSTM1,IST1P1
C-----SET U-VELOCITIES IN SOLID AREAS TO ZERO
      DO 200 I=3,IST1
      DO 200 J=JSTP1,NJM1
      SU(I,J)=0.
  200 SP(I,J)=-GREAT
      DO 205 I=IST2P1,NIM1
      DO 205 J=JSTP1,NJM1
      SU(I,J)=0.
  205 SP(I,J)=-GREAT
C-----NO SLIP WALL BOUNDARY CONDITIONS ON U
      J=JSTEP
      YDELT=YV(JSTP1)-Y(J)
      DO 210 I=3,IST1M1
      AN(I,J)=0.
  210 SP(I,J)=SP(I,J)-VISCOS*SEWU(I)/YDELT
C-----ALLOW FOR CORNERS
      I=IST1
      AN(I,J)=.5*AN(I,J)
      SP(I,J)=SP(I,J)-VISCOS*.5*SEWU(I)/YDELT
      I=IST2P1
      AN(I,J)=.5*AN(I,J)
      SP(I,J)=SP(I,J)-VISCOS*.5*SEWU(I)/YDELT
      DO 215 I=IST2P2,NIM1
      AN(I,J)=0.
  215 SP(I,J)=SP(I,J)-VISCOS*SEWU(I)/YDELT
C-----BOTTOM WALL
      J=2
      YDELT=Y(J)-YV(J)
      DO 220 I=3,NIM1
      AS(I,J)=0.
  220 SP(I,J)=SP(I,J)-VISCOS*SEWU(I)/YDELT
      RETURN
      END
```

SUBROUTINE MODV

```
      SUBROUTINE MODV
      COMMON
     1/UVEL/RESORU,NSWPU,URFU,DXEPU(17),DXPWU(17),SEWU(17)
     1/VVEL/RESORV,NSWPV,URFV,DYNPV(13),DYPSV(13),SNSV(13)
     1/PCOR/RESORM,NSWPP,URFP,DU(17,13),DV(17,13),IPREF,JPREF
     1/VAR/U(17,13),V(17,13),P(17,13),PP(17,13)
     1/ALL/NI,NJ,NIM1,NJM1,GREAT
     1/GEOM/X(17),Y(13),DXEP(17),DXPW(17),DYNP(13),DYPS(13),
     1       SNS(13),SEW(17),XU(17),YV(13)
      1/FLUPR/VISCOS,DENSIT
      1/COEF/AP(17,13),AN(17,13),AS(17,13),AE(17,13),AW(17,13),SU(17,13),
     1       SP(17,13)
      1/JUN/IST1,IST2,JSTEP,IST1M1,IST2M1,IST1M2,IST2P1,NIM2,
     1JSTP1,NJM2,IST2P2,JSTP2,JSTM1,IST1P1
C-----SET V-VELOCITIES IN SOLID AREAS TO ZERO
      DO 300 I=2,IST1M1
      DO 300 J=JSTP1,NJM1
      SU(I,J)=0.
  300 SP(I,J)=-GREAT
      DO 305 I=IST2P1,NIM1
      DO 305 J=JSTP1,NJM1
      SU(I,J)=0.
  305 SP(I,J)=-GREAT
C-----NO SLIP BOUNDARY CONDITIONS ON V
      I=IST1
C-----ALLOW FOR CORNERS
      XDELT=X(I)-XU(I)
      J=JSTP1
      AW(I,J)=.5*AW(I,J)
      SP(I,J)=SP(I,J)-VISCOS*.5*SNSV(J)/XDELT
      DO 310 J=JSTP2,NJM1
      AW(I,J)=0.
  310 SP(I,J)=SP(I,J)-VISCOS*SNSV(J)/XDELT
      I=IST2
      XDELT=XU(IST2P1)-X(I)
      J=JSTP1
      AE(I,J)=.5*AE(I,J)
      SP(I,J)=SP(I,J)-VISCOS*.5*SNSV(J)/XDELT
      DO 315 J=JSTP2,NJM1
      AE(I,J)=0.
  315 SP(I,J)=SP(I,J)-VISCOS*SNSV(J)/XDELT
      RETURN
      END
```

SUBROUTINE MODP

```
C
CHAPTER  4  4  4  4  4  4  PRESSURE CORRECTION  4  4  4  4  4  4  4  4
C
      SUBROUTINE MODP
      COMMON
     1/UVEL/RESORU,NSWPU,URFU,DXEPU(17),DXPWU(17),SEWU(17)
     1/VVEL/RESORV,NSWPV,URFV,DYNPV(13),DYPSV(13),SNSV(13)
     1/PCOR/RESORM,NSWPP,URFP,DU(17,13),DV(17,13),IPREF,JPREF
     1/VAR/U(17,13),V(17,13),P(17,13),PP(17,13)
      1/ALL/NI,NJ,NIM1,NJM1,GREAT
      1/GEOM/X(17),Y(13),DXEP(17),DXPW(17),DYNP(13),DYPS(13),
      1       SNS(13),SEW(17),XU(17),YV(13)
      1/FLUPR/VISCOS,DENSIT
      1/COEF/AP(17,13),AN(17,13),AS(17,13),AE(17,13),AW(17,13),SU(17,13),
      1       SP(17,13)
      1/JUN/IST1,IST2,JSTEP,IST1M1,IST2M1,IST1M2,IST2P1,NIM2,
      1JSTP1,NJM2,IST2P2,JSTP2,JSTM1,IST1P1
C-----SET PRESSURE CORRECTIONS IN SOLID AREAS TO 0
      DO 400 I=2,IST1M1
      DO 400 J=JSTP1,NJM1
      SU(I,J)=0.
  400 SP(I,J)=-GREAT
      DO 405 I=IST2P1,NIM1
      DO 405 J=JSTP1,NJM1
      SU(I,J)=0.
  405 SP(I,J)=-GREAT
      RETURN
      END
```

Input File DATIN.DAT

```
8.78E-3,8.51E+2,3.73E-5,4.00E+0,1.50E+0
0.006,3.000,6,12,17,13,7
5.0,2.5,1.25,1.0,1.0,2.0,2.5,5.0,5.0,2.5,2.0,1.0,1.0,1.25,2.5,5.0
1.25,1.25,2.5,2.5,1.25,1.0,1.0,2.0,2.5,2.5,5.0,10.0
2,2,10,99,50
0.5,0.5,1.000,0.010
FAL  FAL
      U VELOCITY
      V VELOCITY
      PRESSURE
```

Output File RESULT.DAT follows on next pages.

SOLUTION CONTROL PARAMETERS

NSURFU----------= 2
NSURFV----------= 2
NSURFP----------= 10
MAXIT-----------= 99
URFU------------= .50
URFV------------= .50
URFP------------= 1.00
SORMAX----------= .010

INITIAL FIELDS HAVE BEEN SET IN MAIN PROGRAM

GEOMETRICAL PARAMETERS

EXPFAC----------= 1.50
IST1------------= 6
IST2------------= 12
JSTEP-----------= 7

XFRAC(I)=

5.000 2.500 1.250 1.000 1.000
2.000 2.500 5.000 5.000 2.500
2.000 1.000 1.000 1.250 2.500
5.000

YFRAC(J)=

1.250 1.250 2.500 2.500 1.250
1.000 1.000 2.000 2.500 2.500
5.000 10.000

JUNCTION PRESSURE DROP, COMBINING FLOW

FLOW PARAMETERS

VERTICAL DUCT INLET FLOW RATE	=	3.730E-05 M**2/S
VERTICAL DUCT EXIT FLOW RATE	=	4.662E-05 M**2/S
HORIZONTAL DUCT FLOW RATE	=	9.325E-06 M**2/S
RATIO QIN/Q2	=	4.000E+00
VISCOSITY	=	6.780E-03 KG/M*S
DENSITY	=	8.510E+02 KG/M**3
INLET REYNOLDS NO.	=	9.364E+00
EXIT REYNOLDS NO.	=	1.170E+01
HORIZONTAL DUCT REYNOLDS NO.	=	2.341E+00
VERTICAL DUCT HYDRAULIC RADIUS	=	6.000E-03 M
HORIZONTAL DUCT HYDRAULIC RADIUS	=	2.000E-03 M
RATIO, VERT. TO HOR. DUCT RADII	=	3.000E+00
VERTICAL DUCT INLET LENGTH	=	1.496E-02 M
VERTICAL DUCT EXIT LENGTH	=	1.588E-02 M
HORIZONTAL DUCT LENGTH	=	4.059E-03 M

U VELOCITY

J	1	2	3	4	5	6	7	8	9	10	11	12	13	Y =
13	0.00E+00	0.00E+00	0.00E+00	0.00E+00	0.00E+00	0.00E+00	0.00E+00	0.00E+00	0.00E+00	0.00E+00	0.00E+00	0.00E+00	0.00E+00	.01707
12	0.00E+00	0.00E+00	0.00E+00	0.00E+00	0.00E+00	0.00E+00	0.00E+00	0.00E+00	0.00E+00	0.00E+00	0.00E+00	0.00E+00	0.00E+00	.01505
11	0.00E+00	0.00E+00	0.00E+00	0.00E+00	0.00E+00	0.00E+00	0.00E+00	0.00E+00	0.00E+00	0.00E+00	0.00E+00	0.00E+00	0.00E+00	.01404
10	0.00E+00	0.00E+00	0.00E+00	0.00E+00	0.00E+00	0.00E+00	0.00E+00	0.00E+00	0.00E+00	0.00E+00	0.00E+00	0.00E+00	0.00E+00	.01353
9	0.00E+00	0.00E+00	0.00E+00	0.00E+00	0.00E+00	0.00E+00	0.00E+00	0.00E+00	0.00E+00	0.00E+00	0.00E+00	0.00E+00	0.00E+00	.01707
8	0.00E+00	0.00E+00	0.00E+00	0.00E+00	0.00E+00	0.00E+00	0.00E+00	0.00E+00	0.00E+00	0.00E+00	0.00E+00	0.00E+00	0.00E+00	.01505
7	9.19E-04	9.19E-04	9.19E-04	9.19E-04	9.19E-04	1.15E-03	1.15E-03	1.15E-03	1.15E-03	1.15E-03	1.15E-03	1.15E-03	1.15E-03	.01404
6	2.45E-03	2.45E-03	2.45E-03	2.45E-03	2.45E-03	3.07E-03	3.07E-03	3.07E-03	3.07E-03	3.07E-03	3.07E-03	3.07E-03	3.07E-03	.01353
5	3.81E-03	3.81E-03	3.81E-03	3.81E-03	3.81E-03	4.76E-03	4.76E-03	4.76E-03	4.76E-03	4.76E-03	4.76E-03	4.76E-03	4.76E-03	.00827
4	4.62E-03	4.62E-03	4.62E-03	4.62E-03	4.62E-03	5.78E-03	5.78E-03	5.78E-03	5.78E-03	5.78E-03	5.78E-03	5.78E-03	5.78E-03	.00419

3	2.93E-03	2.93E-03	2.93E-03	2.93E-03	2.93E-03	3.66E-03	3.66E-03	3.66E-03	3.66E-03	3.66E-03	3.66E-03	3.66E-03	.00274
2	1.13E-03	1.13E-03	1.13E-03	1.13E-03	1.13E-03	1.42E-03	1.42E-03	1.42E-03	1.42E-03	1.42E-03	1.42E-03	1.42E-03	.00079

X=	0.00600	.0 769	.01153	.01383	.01496	.01526	.01571	.01646	.01746	.01821	.01866	.01896
	I 14	15	16	17	Y =							
J												
13	0.00E+00	0.00E+00	0.00E+00	0.00E+00	1.71E-02							
12	0.00E+00	0.00E+00	0.00E+00	0.00E+00	1.50E-02							
11	0.00E+00	0.00E+00	0.00E+00	0.00E+00	1.40E-02							
10	0.00E+00	0.00E+00	0.00E+00	0.00E+00	1.35E-02							
9	0.00E+00	0.00E+00	0.00E+00	0.00E+00	1.30E-02							
8	0.00E+00	0.00E+00	0.00E+00	0.00E+00	1.26E-02							
7	1.13E-03	1.15E-03	1.15E-03	1.15E-03	1.14E-02							
6	3.07E-03	3.07E-03	3.07E-03	3.07E-03	1.01E-02							
5	4.76E-03	4.76E-03	4.76E-03	4.76E-03	8.57E-03							
4	5.78E-03	5.78E-03	5.78E-03	5.78E-03	5.45E-03							
3	3.66E-03	3.66E-03	3.66E-03	3.66E-03	2.34E-03							
2	1.42E-03	1.42E-03	1.42E-03	1.42E-03	7.79E-04							

X=	.02015	.02260	.02668	.03484

V VELOCITY

	I 2	3	4	5	6	7	8	9	10	11	12	13	Y =
J													
13	0.00E+00	0.00E+00	0.00E+00	0.00E+00	-3.41E-04	-1.53E-03	-2.62E-03	-3.50E-03	-2.62E-03	-1.53E-03	-3.41E-04	0.00E+00	.01664
12	0.00E+00	0.00E+00	0.00E+00	0.00E+00	-3.41E-04	-1.53E-03	-2.62E-03	-3.50E-03	-2.62E-03	-1.53E-03	-3.41E-04	0.00E+00	.01454
11	0.00E+00	0.00E+00	0.00E+00	0.00E+00	-3.41E-04	-1.53E-03	-2.62E-03	-3.50E-03	-2.62E-03	-1.53E-03	-3.41E-04	0.00E+00	.01357
10	0.00E+00	0.00E+00	0.00E+00	0.00E+00	-3.41E-04	-1.53E-03	-2.62E-03	-3.50E-03	-2.62E-03	-1.53E-03	-3.41E-04	0.00E+00	.01308
9	0.00E+00	0.00E+00	0.00E+00	0.00E+00	-3.41E-04	-1.53E-03	-2.62E-03	-3.50E-03	-2.62E-03	-1.53E-03	-3.41E-04	0.00E+00	.01263
8	0.00E+00	0.00E+00	0.00E+00	0.00E+00	-3.41E-04	-1.53E-03	-2.62E-03	-3.50E-03	-2.62E-03	-1.53E-03	-3.41E-04	0.00E+00	.01220
7	0.00E+00	0.00E+00	0.00E+00	0.00E+00	0.00E+00	0.00E+00	0.00E+00	0.00E+00	0.00E+00	0.00E+00	0.00E+00	0.00E+00	.01075
6	0.00E+00	0.00E+00	0.00E+00	0.00E+00	0.00E+00	0.00E+00	0.00E+00	0.00E+00	0.00E+00	0.00E+00	0.00E+00	0.00E+00	.00875
5	0.00E+00	0.00E+00	0.00E+00	0.00E+00	0.00E+00	0.00E+00	0.00E+00	0.00E+00	0.00E+00	0.00E+00	0.00E+00	0.00E+00	.00701
4	0.00E+00	0.00E+00	0.00E+00	0.00E+00	0.00E+00	0.00E+00	0.00E+00	0.00E+00	0.00E+00	0.00E+00	0.00E+00	0.00E+00	.00550
3	0.00E+00	0.00E+00	0.00E+00	0.00E+00	0.00E+00	0.00E+00	0.00E+00	0.00E+00	0.00E+00	0.00E+00	0.00E+00	0.00E+00	.00415
2	0.00E+00	0.00E+00	0.00E+00	0.00E+00	0.00E+00	0.00E+00	0.00E+00	0.00E+00	0.00E+00	0.00E+00	0.00E+00	0.00E+00	.00303

X=	.00912	.01025	.01281	.01486	.01506	.01546	.01596	.01696	.01796	.01846	.01886	.01906
	I 14	15	16	17	Y =							
J												
13	0.00E+00	0.00E+00	0.00E+00	0.00E+00	1.61E-02							
12	0.00E+00	0.00E+00	0.00E+00	0.00E+00	1.45E-02							
11	0.00E+00	0.00E+00	0.00E+00	0.00E+00	1.38E-02							
10	0.00E+00	0.00E+00	0.00E+00	0.00E+00	1.37E-02							
9	0.00E+00	0.00E+00	0.00E+00	0.00E+00	1.28E-02							
8	0.00E+00	0.00E+00	0.00E+00	0.00E+00	1.20E-02							
7	0.00E+00	0.00E+00	0.00E+00	0.00E+00	1.08E-02							
6	0.00E+00	0.00E+00	0.00E+00	0.00E+00	9.35E-03							
5	0.00E+00	0.00E+00	0.00E+00	0.00E+00	7.01E-03							

4	0.00E+00	0.00E+00	0.00E+00	0.00E+00	3.90E-03
3	0.00E+00	0.00E+00	0.00E+00	0.00E+00	1.56E-02
2	0.00E+00	0.00E+00	0.00E+00	0.00E+00	0.00E+00

X= .02124 .02396 .02940 .04029

PRESSURE

J \ I	1	2	3	4	5	6	7	8	9	10	11	12	13	Y =
13	0.00E+00	0.00E+00	0.00E+00	0.00E+00	0.00E+00	0.00E+00	0.00E+00	0.00E+00	0.00E+00	0.00E+00	0.00E+00	0.00E+00	0.00E+00	.01707
12	0.00E+00	0.00E+00	0.00E+00	0.00E+00	1.03E+00	1.03E+00	1.03E+00	1.03E+00	1.03E+00	1.03E+00	1.03E+00	1.03E+00	0.00E+00	.01505
11	0.00E+00	0.00E+00	0.00E+00	0.00E+00	1.01E+00	1.01E+00	1.01E+00	1.01E+00	1.01E+00	1.01E+00	1.01E+00	1.01E+00	0.00E+00	.01404
10	0.00E+00	0.00E+00	0.00E+00	0.00E+00	1.01E+00	1.01E+00	1.01E+00	1.01E+00	1.01E+00	1.01E+00	1.01E+00	1.01E+00	0.00E+00	.01353
9	0.00E+00	0.00E+00	0.00E+00	0.00E+00	1.00E+00	1.00E+00	1.00E+00	1.00E+00	1.00E+00	1.00E+00	1.00E+00	1.00E+00	0.00E+00	.01303
8	0.00E+00	0.00E+00	0.00E+00	0.00E+00	9.97E-01	9.97E-01	9.97E-01	9.97E-01	9.97E-01	9.97E-01	9.97E-01	9.97E-01	0.00E+00	.01262
7	1.00E+00	9.91E-01	9.87E-01	9.83E-01	9.83E-01	9.83E-01	9.83E-01	9.83E-01	9.83E-01	9.83E-01	9.83E-01	9.83E-01	9.74E-01	.01138
6	1.00E+00	9.91E-01	9.87E-01	9.83E-01	9.83E-01	9.83E-01	9.82E-01	9.81E-01	9.78E-01	9.76E-01	9.75E-01	9.74E-01	9.74E-01	.01013
5	1.00E+00	9.91E-01	9.87E-01	9.83E-01	9.83E-01	9.82E-01	9.82E-01	9.81E-01	9.78E-01	9.76E-01	9.75E-01	9.74E-01	9.74E-01	.00857
4	1.00E+00	9.91E-01	9.87E-01	9.83E-01	9.83E-01	9.82E-01	9.82E-01	9.81E-01	9.78E-01	9.76E-01	9.75E-01	9.74E-01	9.74E-01	.00645
3	1.00E+00	9.91E-01	9.87E-01	9.83E-01	9.83E-01	9.82E-01	9.82E-01	9.81E-01	9.78E-01	9.76E-01	9.75E-01	9.74E-01	9.74E-01	.00374
2	1.00E+00	9.91E-01	9.87E-01	9.83E-01	9.83E-01	9.82E-01	9.82E-01	9.81E-01	9.78E-01	9.76E-01	9.75E-01	9.74E-01	9.74E-01	.00078

X= .00512 .01025 .01281 .01486 .01506 .01546 .01596 .01696 .01796 .01846 .01886 .01906

J \ I	14	15	16	17	Y =
13	0.00E+00	0.00E+00	0.00E+00	0.00E+00	1.71E-02
12	0.00E+00	0.00E+00	0.00E+00	0.00E+00	1.50E-02
11	0.00E+00	0.00E+00	0.00E+00	0.00E+00	1.40E-02
10	0.00E+00	0.00E+00	0.00E+00	0.00E+00	1.35E-02
9	0.00E+00	0.00E+00	0.00E+00	0.00E+00	1.30E-02
8	0.00E+00	0.00E+00	0.00E+00	0.00E+00	1.26E-02
7	9.69E-01	9.63E-01	9.51E-01	0.00E+00	1.14E-02
6	9.69E-01	9.63E-01	9.51E-01	0.00E+00	1.01E-02
5	9.69E-01	9.63E-01	9.51E-01	0.00E+00	8.57E-03
4	9.69E-01	9.63E-01	9.51E-01	0.00E+00	5.45E-03
3	9.69E-01	9.63E-01	9.51E-01	0.00E+00	2.34E-03
2	9.69E-01	9.63E-01	9.51E-01	0.00E+00	7.79E-04

X= .02124 .02396 .02940 .04029

ITER NO.	I-----ABSOLUTE RESIDUAL SOURCE SUMS-----I UNORM	VNORM	MASS	I-FIELD VALUES AT MONITORING LOCATION (6, 7)-I U	V	P
1	3.531E+00	9.191E-01	4.504E-01	3.137E-04	-1.422E-04	1.056E+00
2	1.090E+01	9.667E+00	7.855E-01	-1.601E-04	-4.298E-04	1.059E+00
3	6.784E+00	5.805E+00	5.036E-01	-1.702E-04	-5.592E-04	9.824E-01
4	3.247E+00	3.957E+00	2.682E-01	-1.735E-04	-6.335E-04	1.007E+00
5	1.698E+00	1.683E+00	1.572E-01	-3.477E-05	-6.945E-04	9.770E-01
6	1.996E+00	1.335E+00	6.722E-02	1.710E-04	-6.949E-04	9.708E-01

7	2.196E+00	1.605E+00	6.023E-02	3.569E-04	-6.714E-04	9.692E-01
8	1.330E+00	1.392E+00	6.242E-02	4.529E-04	-6.394E-04	9.774E-01
9	6.853E-01	8.148E-01	4.723E-02	4.667E-04	-6.202E-04	9.840E-01
10	9.020E-01	3.054E-01	2.812E-02	4.370E-04	-6.169E-04	9.877E-01
11	8.541E-01	7.234E-01	2.687E-02	4.053E-04	-6.254E-04	9.874E-01
12	4.648E-01	8.456E-01	2.549E-02	3.974E-04	-6.372E-04	9.847E-01
13	2.951E-01	6.819E-01	1.866E-02	4.170E-04	-6.454E-04	9.817E-01
14	4.668E-01	3.950E-01	1.353E-02	4.527E-04	-6.468E-04	9.797E-01
15	3.934E-01	3.254E-01	1.531E-02	4.889E-04	-6.423E-04	9.792E-01
16	2.631E-01	3.685E-01	1.054E-02	5.154E-04	-6.349E-04	9.797E-01
17	2.786E-01	3.270E-01	7.821E-03	5.295E-04	-6.277E-04	9.806E-01
18	2.680E-01	2.296E-01	7.759E-03	5.348E-04	-6.227E-04	9.812E-01
19	1.840E-01	1.624E-01	7.840E-03	5.366E-04	-6.203E-04	9.814E-01
20	1.264E-01	2.190E-01	5.361E-03	5.392E-04	-6.196E-04	9.812E-01
21	1.205E-01	2.282E-01	3.103E-03	5.443E-04	-6.194E-04	9.809E-01
22	1.231E-01	1.922E-01	3.635E-03	5.515E-04	-6.189E-04	9.806E-01
23	1.048E-01	1.397E-01	4.177E-03	5.594E-04	-6.176E-04	9.804E-01
24	9.972E-02	1.290E-01	3.332E-03	5.668E-04	-6.156E-04	9.803E-01
25	1.066E-01	1.301E-01	2.649E-03	5.731E-04	-6.132E-04	9.803E-01
26	1.005E-01	1.170E-01	2.900E-03	5.782E-04	-6.110E-04	9.803E-01
27	8.486E-02	9.738E-02	2.946E-03	5.824E-04	-6.090E-04	9.803E-01
28	7.264E-02	8.696E-02	2.646E-03	5.858E-04	-6.075E-04	9.804E-01
29	6.618E-02	8.976E-02	2.453E-03	5.887E-04	-6.064E-04	9.804E-01
30	6.118E-02	8.555E-02	2.468E-03	5.915E-04	-6.054E-04	9.804E-01
31	5.678E-02	7.534E-02	2.462E-03	5.942E-04	-6.045E-04	9.803E-01
32	5.451E-02	6.443E-02	2.441E-03	5.969E-04	-6.035E-04	9.803E-01
33	5.303E-02	6.043E-02	2.439E-03	5.997E-04	-6.025E-04	9.802E-01
34	5.040E-02	5.741E-02	2.434E-03	6.024E-04	-6.014E-04	9.802E-01
35	4.868E-02	5.317E-02	2.432E-03	6.049E-04	-6.003E-04	9.802E-01
36	4.300E-02	4.852E-02	2.432E-03	6.071E-04	-5.994E-04	9.802E-01
37	4.007E-02	4.499E-02	2.430E-03	6.089E-04	-5.985E-04	9.802E-01
38	3.754E-02	4.297E-02	2.426E-03	6.105E-04	-5.977E-04	9.802E-01
39	3.528E-02	4.022E-02	2.425E-03	6.119E-04	-5.971E-04	9.802E-01
40	3.340E-02	3.698E-02	2.425E-03	6.134E-04	-5.964E-04	9.802E-01
41	3.175E-02	3.396E-02	2.423E-03	6.148E-04	-5.958E-04	9.802E-01
42	3.021E-02	3.208E-02	2.423E-03	6.162E-04	-5.952E-04	9.802E-01
43	2.867E-02	3.027E-02	2.422E-03	6.175E-04	-5.945E-04	9.801E-01
44	2.707E-02	2.830E-02	2.422E-03	6.187E-04	-5.939E-04	9.801E-01
45	2.561E-02	2.628E-02	2.422E-03	6.198E-04	-5.934E-04	9.801E-01
46	2.434E-02	2.449E-02	2.420E-03	6.207E-04	-5.929E-04	9.801E-01
47	2.321E-02	2.297E-02	2.420E-03	6.216E-04	-5.924E-04	9.801E-01
48	2.213E-02	2.148E-02	2.421E-03	6.224E-04	-5.920E-04	9.801E-01
49	2.106E-02	2.002E-02	2.422E-03	6.232E-04	-5.915E-04	9.801E-01
50	2.001E-02	1.872E-02	2.419E-03	6.240E-04	-5.911E-04	9.801E-01

U VELOCITY

J	I 2	3	4	5	6	7	8	9	10	11	12	13	Y =
13	0.00E+00	0.00E+00	0.00E+00	0.00E+00	0.00E+00	0.00E+00	0.00E+00	0.00E+00	0.00E+00	0.00E+00	0.00E+00	0.00E+00	.01707

12	0.00E+00	0.00E+00	0.00E+00	0.00E+00	0.00E+00	-2.06E-06	-7.48E-06	-1.60E-05	-1.38E-05	-4.65E-06	2.47E-07	0.00E+00	.01505
11	0.00E+00	0.00E+00	0.00E+00	0.00E+00	0.00E+00	-1.58E-06	-6.85E-06	-5.65E-06	4.96E-06	-3.92E-06	-2.04E-06	0.00E+00	.01404
10	0.00E+00	0.00E+00	0.00E+00	0.00E+00	0.00E+00	-2.51E-06	-1.82E-06	2.97E-05	6.55E-05	1.87E-05	-1.17E-06	0.00E+00	.01253
9	0.00E+00	0.00E+00	0.00E+00	0.00E+00	0.00E+00	-5.55E-06	1.46E-05	1.11E-04	2.05E-04	1.03E-04	1.84E-05	0.00E+00	.01303
8	0.00E+00	0.00E+00	0.00E+00	0.00E+00	0.00E+00	-1.45E-05	4.80E-05	2.31E-04	4.16E-04	2.88E-04	1.05E-04	0.00E+00	.01262
7	9.19E-04	9.47E-04	9.60E-04	9.65E-04	6.24E-04	5.81E-04	7.07E-04	1.13E-03	1.82E-03	2.23E-03	2.33E-03	2.21E-03	.01138
6	2.45E-03	2.45E-03	2.42E-03	2.29E-03	2.14E-03	2.13E-03	2.19E-03	2.47E-03	3.07E-03	3.42E-03	3.53E-03	3.53E-03	.01013
5	3.81E-03	3.78E-03	3.72E-03	3.64E-03	3.68E-03	3.70E-03	3.76E-03	3.92E-03	4.25E-03	4.47E-03	4.58E-03	4.57E-03	.00857
4	4.62E-03	4.60E-03	4.61E-03	4.65E-03	4.75E-03	4.77E-03	4.82E-03	4.92E-03	5.08E-03	5.21E-03	5.29E-03	5.33E-03	.00545
3	2.93E-03	2.94E-03	2.99E-03	3.07E-03	3.14E-03	3.17E-03	3.20E-03	3.26E-03	3.36E-03	3.43E-03	3.48E-03	3.50E-03	.00234
2	1.13E-03	1.18E-03	1.21E-03	1.25E-03	1.28E-03	1.29E-03	1.31E-03	1.34E-03	1.38E-03	1.41E-03	1.43E-03	1.44E-03	.00078

X=	0.00000	.00769	.01153	.01383	.01496	.01526	.01571	.01646	.01746	.01821	.01866	.01896
	I 14	15	16	17	Y =							
J												
13	0.00E+00	0.00E+00	0.00E+00	0.00E+00	1.71E-02							
12	0.00E+00	0.00E+00	0.00E+00	0.00E+00	1.50E-02							
11	0.00E+00	0.00E+00	0.00E+00	0.00E+00	1.40E-02							
10	0.00E+00	0.00E+00	0.00E+00	0.00E+00	1.35E-02							
9	0.00E+00	0.00E+00	0.00E+00	0.00E+00	1.30E-02							
8	0.00E+00	0.00E+00	0.00E+00	0.00E+00	1.26E-02							
7	1.38E-03	1.13E-03	1.15E-03	1.15E-03	1.14E-02							
6	3.35E-03	3.03E-03	3.00E-03	3.07E-03	1.01E-02							
5	4.80E-03	4.73E-03	4.68E-03	4.76E-03	8.57E-03							
4	5.52E-03	5.70E-03	5.75E-03	5.78E-03	5.45E-03							
3	3.61E-03	3.74E-03	3.74E-03	3.66E-03	2.34E-03							
2	1.49E-03	1.53E-03	1.52E-03	1.42E-03	7.79E-04							

X=	.02015	.02260	.02668	.03484

V VELOCITY

	I 2	3	4	5	6	7	8	9	10	11	12	13	Y =
J													
13	0.00E+00	0.00E+00	0.00E+00	0.00E+00	-3.41E-04	-1.53E-03	-2.62E-03	-3.50E-03	-2.62E-03	-1.53E-03	-3.41E-04	0.00E+00	.01606
12	0.00E+00	0.00E+00	0.00E+00	0.00E+00	-3.53E-04	-1.55E-03	-2.64E-03	-3.49E-03	-2.61E-03	-1.51E-03	-3.42E-04	0.00E+00	.01454
11	0.00E+00	0.00E+00	0.00E+00	0.00E+00	-3.58E-04	-1.56E-03	-2.64E-03	-3.49E-03	-2.61E-03	-1.51E-03	-3.37E-04	0.00E+00	.01379
10	0.00E+00	0.00E+00	0.00E+00	0.00E+00	-3.63E-04	-1.56E-03	-2.62E-03	-3.47E-03	-2.65E-03	-1.53E-03	-3.35E-04	0.00E+00	.01328
9	0.00E+00	0.00E+00	0.00E+00	0.00E+00	-3.71E-04	-1.54E-03	-2.56E-03	-3.43E-03	-2.71E-03	-1.62E-03	-3.63E-04	0.00E+00	.01283
8	0.00E+00	0.00E+00	0.00E+00	0.00E+00	-4.12E-04	-1.42E-03	-2.36E-03	-3.27E-03	-2.85E-03	-1.96E-03	-6.53E-04	0.00E+00	.01290
7	4.66E-06	4.15E-06	2.10E-06	-3.78E-04	-5.91E-04	-1.08E-03	-1.66E-03	-2.40E-03	-2.18E-03	-1.69E-03	-1.15E-03	-8.35E-04	.01075
6	3.89E-06	-5.95E-06	-7.94E-05	-5.64E-04	-6.60E-04	-8.73E-04	-1.15E-03	-1.56E-03	-1.52E-03	-1.35E-03	-1.17E-03	-1.06E-03	.00935
5	-4.97E-06	-4.04E-05	-1.68E-04	-4.67E-04	-5.01E-04	-5.69E-04	-6.53E-04	-7.92E-04	-8.19E-04	-7.95E-04	-7.63E-04	-7.47E-04	.00701
4	-1.48E-05	-3.77E-05	-1.05E-04	-2.08E-04	-2.17E-04	-2.25E-04	-2.55E-04	-2.86E-04	-2.90E-04	-2.82E-04	-2.73E-04	-2.69E-04	.00390
3	-1.03E-05	-9.90E-06	-2.52E-05	-4.92E-05	-5.10E-05	-5.48E-05	-5.90E-05	-6.49E-05	-6.45E-05	-6.22E-05	-5.98E-05	-5.84E-05	.00156
2	0.00E+00	0.00E+00	0.00E+00	0.00E+00	0.00E+00	0.00E+00	0.00E+00	0.00E+00	0.00E+00	0.00E+00	0.00E+00	0.00E+00	0.00000

X=	.00512	.01025	.01281	.01486	.01506	.01546	.01596	.01696	.01796	.01846	.01886	.01906
	I 14	15	16	17	Y =							
J												

13	0.00E+00	0.00E+00	0.00E+00	0.00E+00	1.61E-02
12	0.00E+00	0.00E+00	0.00E+00	0.00E+00	1.45E-02
11	0.00E+00	0.00E+00	0.00E+00	0.00E+00	1.38E-02
10	0.00E+00	0.00E+00	0.00E+00	0.00E+00	1.33E-02
9	0.00E+00	0.00E+00	0.00E+00	0.00E+00	1.28E-02
8	0.00E+00	0.00E+00	0.00E+00	0.00E+00	1.20E-02
7	-1.28E-04	4.87E-06	-8.47E-03	0.00E+00	1.08E-02
6	-3.11E-04	-5.17E-06	1.08E-05	0.00E+00	9.35E-03
5	-3.83E-04	-5.43E-05	3.37E-05	0.00E+00	7.01E-03
4	-1.50E-04	5.63E-06	4.34E-05	0.00E+00	3.90E-03
3	-3.02E-05	6.24E-06	1.97E-05	0.00E+00	1.56E-03
2	0.00E+00	0.00E+00	0.00E+00	0.00E+00	0.00E+00

X= .02124 .02396 .02940 .04029

PRESSURE

I / J	2	3	4	5	6	7	8	9	10	11	12	13	Y =
13	0.00E+00	0.00E+00	0.00E+00	0.00E+00	0.00E+00	0.00E+00	0.00E+00	0.00E+00	0.00E+00	0.00E+00	0.00E+00	0.00E+00	.01707
12	1.12E-02	1.12E-02	1.12E-02	1.12E-02	1.03E+00	1.03E+00	1.03E+00	1.03E+00	1.03E+00	1.03E+00	1.03E+00	1.12E-02	.01505
11	1.12E-02	1.12E-02	1.12E-02	1.12E-02	1.02E+00	1.03E+00	1.02E+00	1.02E+00	1.02E+00	1.02E+00	1.02E+00	1.12E-02	.01404
10	1.12E-02	1.12E-02	1.12E-02	1.12E-02	1.01E+00	1.01E+00	1.01E+00	1.01E+00	1.01E+00	1.01E+00	1.01E+00	1.12E-02	.01353
9	1.12E-02	1.12E-02	1.12E-02	1.12E-02	1.00E+00	1.00E+00	1.01E+00	1.01E+00	1.01E+00	1.01E+00	1.01E+00	1.12E-02	.01303
8	1.12E-02	1.12E-02	1.12E-02	1.12E-02	9.93E-01	9.96E-01	9.98E-01	1.00E+00	9.99E-01	1.00E+00	1.01E+00	1.12E-02	.01262
7	1.00E+00	9.90E-01	9.84E-01	9.77E-01	9.80E-01	9.84E-01	9.87E-01	9.83E-01	9.83E-01	9.77E-01	9.71E-01	9.63E-01	.01138
6	1.00E+00	9.90E-01	9.85E-01	9.83E-01	9.82E-01	9.83E-01	9.83E-01	9.81E-01	9.77E-01	9.73E-01	9.70E-01	9.68E-01	.01013
5	1.00E+00	9.90E-01	9.85E-01	9.83E-01	9.82E-01	9.81E-01	9.80E-01	9.78E-01	9.75E-01	9.73E-01	9.71E-01	9.69E-01	.00857
4	1.00E+00	9.90E-01	9.85E-01	9.83E-01	9.80E-01	9.80E-01	9.78E-01	9.76E-01	9.74E-01	9.73E-01	9.72E-01	9.70E-01	.00545
3	1.00E+00	9.90E-01	9.85E-01	9.82E-01	9.80E-01	9.79E-01	9.78E-01	9.76E-01	9.74E-01	9.73E-01	9.72E-01	9.70E-01	.00234
2	1.00E+00	9.90E-01	9.85E-01	9.82E-01	9.80E-01	9.80E-01	9.78E-01	9.77E-01	9.75E-01	9.73E-01	9.72E-01	9.71E-01	.00073

X= .00512 .01025 .01281 .01486 .01506 .01546 .01596 .01696 .01796 .01846 .01886 .01906

I / J	14	15	16	17	Y =
13	0.00E+00	0.00E+00	0.00E+00	0.00E+00	1.71E-02
12	1.12E-02	1.12E-02	1.12E-02	0.00E+00	1.50E-02
11	1.12E-02	1.12E-02	1.12E-02	0.00E+00	1.40E-02
10	1.12E-02	1.12E-02	1.12E-02	0.00E+00	1.35E-02
9	1.12E-02	1.12E-02	1.12E-02	0.00E+00	1.30E-02
8	1.12E-02	1.12E-02	1.12E-02	0.00E+00	1.26E-02
7	9.60E-01	9.54E-01	9.44E-01	0.00E+00	1.14E-02
6	9.62E-01	9.56E-01	9.44E-01	0.00E+00	1.01E-02
5	9.64E-01	9.57E-01	9.44E-01	0.00E+00	8.57E-03
4	9.65E-01	9.58E-01	9.44E-01	0.00E+00	5.45E-03
3	9.66E-01	9.58E-01	9.44E-01	0.00E+00	2.34E-03
2	9.66E-01	9.58E-01	9.44E-01	0.00E+00	7.79E-04

X= .02124 .02396 .02940 .04029

ITER	I-----ABSOLUTE RESIDUAL SOURCE SUMS-----I			I-FIELD VALUES AT MONITORING LOCATION (6, 7)-I		
NO.	UMOM	VMOM	MASS	U	V	P
51	1.900E-02	1.757E-02	2.421E-03	6.247E-04	-5.908E-04	9.801E-01
52	1.805E-02	1.651E-02	2.420E-03	6.254E-04	-5.904E-04	9.801E-01
53	1.715E-02	1.552E-02	2.421E-03	6.260E-04	-5.900E-04	9.801E-01
54	1.631E-02	1.461E-02	2.421E-03	6.266E-04	-5.897E-04	9.801E-01
55	1.551E-02	1.380E-02	2.419E-03	6.271E-04	-5.894E-04	9.801E-01
56	1.474E-02	1.305E-02	2.419E-03	6.276E-04	-5.891E-04	9.801E-01
57	1.401E-02	1.239E-02	2.419E-03	6.281E-04	-5.888E-04	9.801E-01
58	1.329E-02	1.176E-02	2.420E-03	6.285E-04	-5.885E-04	9.801E-01
59	1.262E-02	1.120E-02	2.421E-03	6.289E-04	-5.883E-04	9.801E-01
60	1.199E-02	1.064E-02	2.420E-03	6.293E-04	-5.880E-04	9.801E-01
61	1.139E-02	1.011E-02	2.420E-03	6.297E-04	-5.878E-04	9.801E-01
62	1.082E-02	9.592E-03	2.419E-03	6.300E-04	-5.876E-04	9.801E-01
63	1.029E-02	9.101E-03	2.419E-03	6.303E-04	-5.874E-04	9.801E-01
64	9.767E-03	8.636E-03	2.419E-03	6.306E-04	-5.872E-04	9.801E-01

U VELOCITY

J	I 2	3	4	5	6	7	8	9	10	11	12	13	Y =
13	0.00E+00	0.00E+00	0.00E+00	0.00E+00	0.00E+00	0.00E+00	0.00E+00	0.00E+00	0.00E+00	0.00E+00	0.00E+00	0.00E+00	.01767
12	0.00E+00	0.00E+00	0.00E+00	0.00E+00	0.00E+00	-2.08E-06	-7.54E-06	-1.61E-05	-1.39E-05	-4.70E-06	2.37E-07	0.00E+00	.01505
11	0.00E+00	0.00E+00	0.00E+00	0.00E+00	0.00E+00	-1.59E-06	-6.65E-06	-5.51E-06	5.14E-06	-3.89E-06	-2.04E-06	0.00E+00	.01404
10	0.00E+00	0.00E+00	0.00E+00	0.00E+00	0.00E+00	-2.62E-06	-1.67E-06	3.03E-05	8.62E-05	1.39E-05	-1.18E-06	0.00E+00	.01353
9	0.00E+00	0.00E+00	0.00E+00	0.00E+00	0.00E+00	-5.48E-06	1.52E-05	1.12E-04	2.06E-04	1.07E-04	1.85E-05	0.00E+00	.01302
8	0.00E+00	0.00E+00	0.00E+00	0.00E+00	0.00E+00	-1.42E-05	4.92E-05	2.34E-04	4.19E-04	2.89E-04	1.06E-04	0.00E+00	.01252
7	9.19E-04	9.48E-04	9.62E-04	9.63E-04	6.31E-04	5.89E-04	7.15E-04	1.14E-03	1.84E-03	2.24E-03	2.34E-03	2.22E-03	.01178
6	2.43E-03	2.45E-03	2.43E-03	2.30E-03	2.15E-03	2.14E-03	2.20E-03	2.48E-03	3.08E-03	3.44E-03	3.55E-03	3.54E-03	.01013
5	3.81E-03	3.78E-03	3.73E-03	3.64E-03	3.69E-03	3.71E-03	3.77E-03	3.93E-03	4.26E-03	4.48E-03	4.59E-03	4.54E-03	.00857
4	4.62E-03	4.60E-03	4.60E-03	4.65E-03	4.74E-03	4.77E-03	4.82E-03	4.91E-03	5.07E-03	5.20E-03	5.28E-03	5.31E-03	.00545
3	2.92E-03	2.94E-03	2.98E-03	3.06E-03	3.14E-03	3.16E-03	3.19E-03	3.26E-03	3.35E-03	3.43E-03	3.47E-03	3.50E-03	.00224
2	1.13E-03	1.18E-03	1.21E-03	1.24E-03	1.28E-03	1.29E-03	1.30E-03	1.33E-03	1.38E-03	1.41E-03	1.43E-03	1.44E-03	.00078

X= 0.00000 .00769 .01153 .01383 .01496 .01526 .01571 .01646 .01746 .01821 .01866 .01893

J	I 14	15	16	17	Y =
13	0.00E+00	0.00E+00	0.00E+00	0.00E+00	1.71E-02
12	0.00E+00	0.00E+00	0.00E+00	0.00E+00	1.50E-02
11	0.00E+00	0.00E+00	0.00E+00	0.00E+00	1.40E-02
10	0.00E+00	0.00E+00	0.00E+00	0.00E+00	1.35E-02
9	0.00E+00	0.00E+00	0.00E+00	0.00E+00	1.30E-02
8	0.00E+00	0.00E+00	0.00E+00	0.00E+00	1.25E-02
7	1.39E-03	1.12E-03	1.15E-03	1.15E-03	1.14E-02
6	3.36E-03	3.03E-03	3.00E-03	3.07E-03	1.01E-02
5	4.81E-03	4.73E-03	4.68E-03	4.76E-03	8.57E-03
4	5.51E-03	5.70E-03	5.75E-03	5.78E-03	5.45E-03
3	3.61E-03	3.74E-03	3.74E-03	3.66E-03	2.34E-03
2	1.49E-03	1.54E-03	1.52E-03	1.42E-03	7.79E-04

X= .02015 .02260 .02668 .03484

V VELOCITY

J	I 2	3	4	5	6	7	8	9	10	11	12	13	Y =
13	0.00E+00	0.00E+00	0.00E+00	0.00E+00	-3.41E-04	-1.53E-03	-2.62E-03	-3.50E-03	-2.62E-03	-1.53E-03	-3.41E-04	0.00E+00	.01606
12	0.00E+00	0.00E+00	0.00E+00	0.00E+00	-3.53E-04	-1.55E-03	-2.64E-03	-3.49E-03	-2.61E-03	-1.51E-03	-3.42E-04	0.00E+00	.01454
11	0.00E+00	0.00E+00	0.00E+00	0.00E+00	-3.58E-04	-1.56E-03	-2.64E-03	-3.49E-03	-2.61E-03	-1.51E-03	-3.37E-04	0.00E+00	.01379
10	0.00E+00	0.00E+00	0.00E+00	0.00E+00	-3.63E-04	-1.56E-03	-2.62E-03	-3.47E-03	-2.65E-03	-1.53E-03	-3.35E-04	0.00E+00	.01328
9	0.00E+00	0.00E+00	0.00E+00	0.00E+00	-3.71E-04	-1.54E-03	-2.56E-03	-3.43E-03	-2.71E-03	-1.62E-03	-3.63E-04	0.00E+00	.01283
8	0.00E+00	0.00E+00	0.00E+00	0.00E+00	-4.11E-04	-1.43E-03	-2.36E-03	-3.27E-03	-2.85E-03	-1.96E-03	-6.54E-04	0.00E+00	.01230
7	4.72E-06	4.54E-06	3.14E-06	-3.75E-04	-5.87E-04	-1.07E-03	-1.66E-03	-2.40E-03	-2.19E-03	-1.70E-03	-1.15E-03	-8.70E-04	.01075
6	4.13E-06	-4.54E-06	-7.60E-05	-5.57E-04	-6.53E-04	-8.66E-04	-1.14E-03	-1.56E-03	-1.52E-03	-1.36E-03	-1.18E-03	-1.09E-03	.00979
5	-4.42E-06	-3.72E-05	-1.61E-04	-4.57E-04	-4.91E-04	-5.60E-04	-6.46E-04	-7.90E-04	-8.25E-04	-8.07E-04	-7.79E-04	-7.64E-04	.00701
4	-1.44E-05	-3.51E-05	-1.00E-04	-2.05E-04	-2.15E-04	-2.33E-04	-2.55E-04	-2.88E-04	-2.96E-04	-2.91E-04	-2.83E-04	-2.79E-04	.00390
3	-1.02E-05	-9.17E-06	-2.39E-05	-4.91E-05	-5.11E-05	-5.48E-05	-5.90E-05	-6.53E-05	-6.64E-05	-6.49E-05	-6.30E-05	-6.19E-05	.00156
2	0.00E+00	0.00E+00	0.00E+00	0.00E+00	0.00E+00	0.00E+00	0.00E+00	0.00E+00	0.00E+00	0.00E+00	0.00E+00	0.00E+00	.00000

X= .00512 .01025 .01281 .01486 .01506 .01546 .01596 .01696 .01796 .01846 .01886 .01906

J	I 14	15	16	17	Y =
13	0.00E+00	0.00E+00	0.00E+00	0.00E+00	1.61E-02
12	0.00E+00	0.00E+00	0.00E+00	0.00E+00	1.45E-02
11	0.00E+00	0.00E+00	0.00E+00	0.00E+00	1.38E-02
10	0.00E+00	0.00E+00	0.00E+00	0.00E+00	1.33E-02
9	0.00E+00	0.00E+00	0.00E+00	0.00E+00	1.28E-02
8	0.00E+00	0.00E+00	0.00E+00	0.00E+00	1.20E-02
7	1.30E-04	4.80E-06	4.42E-03	0.00E+00	1.08E-02
6	-3.16E-04	-5.68E-06	1.12E-05	0.00E+00	9.39E-03
5	-3.07E-04	-2.53E-05	3.45E-05	0.00E+00	7.01E-03
4	-1.55E-04	5.35E-06	4.43E-05	0.00E+00	3.90E-03
3	-3.12E-05	6.50E-06	1.99E-05	0.00E+00	1.56E-03
2	0.00E+00	0.00E+00	0.00E+00	0.00E+00	0.00E+00

X= .02124 .02396 .02940 .04029

PRESSURE

J	I 2	3	4	5	6	7	8	9	10	11	12	13	Y =
13	0.00E+00	0.00E+00	0.00E+00	0.00E+00	0.00E+00	0.00E+00	0.00E+00	0.00E+00	0.00E+00	0.00E+00	0.00E+00	0.00E+00	.01707
12	1.50E-02	1.50E-02	1.50E-02	1.50E-02	1.03E+00	1.03E+00	1.03E+00	1.03E+00	1.03E+00	1.03E+00	1.03E+00	1.50E-02	.01505
11	1.50E-02	1.50E-02	1.50E-02	1.50E-02	1.02E+00	1.02E+00	1.02E+00	1.02E+00	1.02E+00	1.02E+00	1.02E+00	1.50E-02	.01404
10	1.50E-02	1.50E-02	1.50E-02	1.50E-02	1.01E+00	1.01E+00	1.01E+00	1.01E+00	1.01E+00	1.01E+00	1.01E+00	1.50E-02	.01353
9	1.50E-02	1.50E-02	1.50E-02	1.50E-02	1.00E+00	1.00E+00	1.01E+00	1.01E+00	1.01E+00	1.01E+00	1.01E+00	1.50E-02	.01303
8	1.50E-02	1.50E-02	1.50E-02	1.50E-02	9.93E-01	9.96E-01	9.98E-01	1.00E+00	9.99E-01	1.00E+00	1.01E+00	1.50E-02	.01252
7	1.00E+00	9.90E-01	9.84E-01	9.77E-01	9.80E-01	9.84E-01	9.87E-01	9.88E-01	9.83E-01	9.77E-01	9.71E-01	9.62E-01	.01138
6	1.00E+00	9.90E-01	9.85E-01	9.83E-01	9.82E-01	9.83E-01	9.83E-01	9.81E-01	9.77E-01	9.73E-01	9.70E-01	9.38E-01	.01013

5	1.00E+00	9.90E-01	9.85E-01	9.83E-01	9.82E-01	9.81E-01	9.80E-01	9.78E-01	9.75E-01	9.73E-01	9.71E-01	9.69E-01	.00657
4	1.00E+00	9.90E-01	9.85E-01	9.82E-01	9.80E-01	9.80E-01	9.78E-01	9.76E-01	9.74E-01	9.73E-01	9.72E-01	9.70E-01	.00545
3	1.00E+00	9.90E-01	9.85E-01	9.82E-01	9.80E-01	9.79E-01	9.78E-01	9.76E-01	9.74E-01	9.73E-01	9.72E-01	9.71E-01	.00234
2	1.00E+00	9.90E-01	9.85E-01	9.82E-01	9.80E-01	9.80E-01	9.78E-01	9.77E-01	9.75E-01	9.73E-01	9.73E-01	9.71E-01	.00078

X=	.00512	.01025	.01281	.01486	.01506	.01546	.01596	.01696	.01796	.01846	.01886	.01904
	I 14	15	16	17	Y =							
J												
13	0.00E+00	0.00E+00	0.00E+00	0.00E+00	1.71E-02							
12	1.50E-02	1.50E-02	1.50E-02	0.00E+00	1.50E-02							
11	1.50E-02	1.50E-02	1.50E-02	0.00E+00	1.40E-02							
10	1.50E-02	1.50E-02	1.50E-02	0.00E+00	1.35E-02							
9	1.50E-02	1.50E-02	1.50E-02	0.00E+00	1.30E-02							
8	1.50E-02	1.50E-02	1.50E-02	0.00E+00	1.26E-02							
7	9.60E-01	9.56E-01	9.44E-01	0.00E+00	1.14E-02							
6	9.62E-01	9.58E-01	9.44E-01	0.00E+00	1.01E-02							
5	9.64E-01	9.57E-01	9.44E-01	0.00E+00	8.57E-03							
4	9.65E-01	9.58E-01	9.44E-01	0.00E+00	5.45E-03							
3	9.66E-01	9.58E-01	9.44E-01	0.00E+00	2.34E-03							
2	9.66E-01	9.58E-01	9.44E-01	0.00E+00	7.79E-04							

X=	.02124	.02396	.02940	.04029

FRICTION CONSTANTS FOR COMBINING FLOW:

KCT= 2.761E+01
KCB= 1.434E+01

D5 CORNER The procedure in CORNER is analogous to that in JUNCTION in every way, only, of course, it is simpler. Listings and sample output follow.

PROGRAM MAIN

```
      PROGRAM MAIN
      SUBROUTINE CONTRO
C
CHAPTER  0  0  0  0  0  0  0  0  PRELIMINARIES  0  0  0  0  0  0  0  0
C
      DIMENSION HEDU(6),HEDV(6),HEDP(6),HEDT(6)
      DIMENSION XFRAC(15),YFRAC(15)
      REAL HODROP
      LOGICAL INCALU,INCALV
       LOGICAL RESTRT
       COMMON
     1/UVEL/RESORU,NSWPU,URFU,DXEPU(15),DXPWU(15),SEWU(15)
     1/VVEL/RESORV,NSWPV,URFV,DYNPV(15),DYPSV(15),SNSV(15)
     1/PCOR/RESORM,NSWPP,URFP,DU(15,15),DV(15,15),IPREF,JPREF
     1/VAR/U(15,15),V(15,15),P(15,15),PP(15,15)
     1/ALL/NI,NJ,NIM1,NJM1,GREAT
     1/GEOM/X(15),Y(15),DXEP(15),DXPW(15),DYNP(15),DYPS(15),
     1       SNS(15),SEW(15),XU(15),YV(15)
     1/FLUPR/VISCOS,DENSIT
     1/JUN/ISTEP,JSTEP,ISTPM1,ISTPM2,NIM2,
     1      JSTP1,NJM2,JSTP2,JSTM1,ISTPP1
      CALL OPEN(6,'RESULT  DAT',2)
      CALL OPEN(8,'CORNDAT DAT',2)
      CALL OPEN(9,'INTERMEDDAT',2)
      GREAT=1.0E30
      PI=4.*ATAN(1.)
      NITER=0
      READ(8,011) VISCOS,DENSIT,QIN,ENTFAC
      WRITE(4,025) VISCOS,DENSIT,QIN,ENTFAC
      READ(8,012) RVERT,RRATIO,ISTEP,NI,NJ,JSTEP
      WRITE(4,026) RVERT,RRATIO,ISTEP,NI,NJ,JSTEP
      NIM1=NI-1
      NJM1=NJ-1
      READ(8,024) (XFRAC(I),I=1,NIM1)
      WRITE(4,027) (XFRAC(I),I=1,NIM1)
      READ(8,024) (YFRAC(J),J=1,NJM1)
      WRITE(4,027) (YFRAC(J),J=1,NJM1)
      READ(8,013) NSWPU,NSWPV,NSWPP,MAXIT,INDPRI
      WRITE(4,028) NSWPU,NSWPV,NSWPP,MAXIT,INDPRI
      READ(8,014) URFU,URFV,URFP,SORMAX
      WRITE(4,029) URFU,URFV,URFP,SORMAX
      READ(8,015) RESTRT
      WRITE(4,030) RESTRT
      READ(8,010) HEDU,HEDV,HEDP
      WRITE(4,031) HEDU,HEDV,HEDP
C-----WRITE OUT SOLUTION CONTROL PARAMETERS
      WRITE(6,2000)
      WRITE(6,017) NSWPU,NSWPV,NSWPP,MAXIT,
     1URFU,URFV,URFP,SORMAX
      IF(RESTRT) WRITE(6,018)
      IF(.NOT.RESTRT) WRITE(6,019)
      WRITE(6,2000)
      WRITE(6,020) ENTFAC,ISTEP,JSTEP
      WRITE(6,021)
      WRITE(6,022) (XFRAC(I),I=1,NIM1)
      WRITE(6,023)
      WRITE(6,022) (YFRAC(J),J=1,NJM1)
  010 FORMAT(6A4)
```

```
  021 FORMAT(1X,9A4)
  011 FORMAT(4E12.3)
  025 FORMAT(1X,4E12.3)
  012 FORMAT(2F6.4,4I3)
  026 FORMAT(1X,2F6.4,4I3)
  013 FORMAT(5I3)
  022 FORMAT(1X,5I3)
  014 FORMAT(4F5.4)
  029 FORMAT(1X,4F6.4)
  015 FORMAT(L5)
  030 FORMAT(1X,L5)
  017 FORMAT('0',5X,'SOLUTION CONTROL PARAMETERS'/
     1/5X,'NSWPU----------=',I3
     1/5X,'NSWPV----------=',I3
     1/5X,'NSWPP----------=',I3
     1/5X,'MAXIT----------=',I4
     1/5X,'URFU----------=',F5.2
     1/5X,'URFV----------=',F5.2
     1/5X,'URFP----------=',F5.2
     1/5X,'SORMAX---------=',F6.3)
  018 FORMAT('0','INITIAL FIELDS HAVE BEEN READ IN FROM UNIT 9')
  019 FORMAT('0','INITIAL FIELDS HAVE BEEN SET IN MAIN PROGRAM')
  020 FORMAT('0',5X,'GEOMETRICAL PARAMETERS'/
     1/5X,'ENTFAC----------=',F5.2
     1/5X,'ISTEP----------= ',I3
     1/5X,'JSTEP----------=',I3)
  021 FORMAT('0','XFRAC(I)=')
  022 FORMAT(10X,5F7.3)
  023 FORMAT('0','YFRAC(J)=')
  024 FORMAT(17F7.3)
  027 FORMAT(1X,10F7.3)
C
CHAPTER  1  1  1  1  1  PARAMETERS AND CONTROL INDICES  1  1  1  1  1  1
C
      Q2=QIN
      REIN=QIN*2.*DENSIT/VISCOS
      RE2=Q2*2.*DENSIT/VISCOS
C-----COMPUTE DUCT LENGTHS BASED ON HYDRODYNAMIC ENTRY LENGTH
      RHORIZ=RVERT/RRATIO
      ENTRYL=4.*RVERT*ENTFAC*(.3125+.011*REIN)
      HORIZL=4.*RHORIZ*ENTFAC*(.3125+.011*RE2)
C-----COMPUTE ALL INDICES
       NIM2=NI-2
       NJM2=NJ-2
       ISTPM1=ISTEP-1
       ISTPM2=ISTEP-2
       ISTPP1=ISTEP+1
       JSTP1=JSTEP+1
       JSTP2=JSTEP+2
       JSTM1=JSTEP-1
C-----COMPUTE SMALLEST DX IN HORIZONTAL BRANCH REGION
       XSUM=XFRAC(ISTPM1)/2.
       DO 100 I=ISTEP,NIM2
  100  XSUM=XSUM+XFRAC(I)
       XSUM=XSUM+XFRAC(NIM1)/2.
       DXSM2=2.*RHORIZ/XSUM
C-----COMPUTE SMALLEST DX IN VERTICAL DUCT ENTRANCE REGION
       XSUM=XFRAC(1)/2.
       DO 105 I=2,ISTPM2
  105  XSUM=XSUM+XFRAC(I)
```

```
      DXSM1=(ENTRYL-.5*XFRAC(ISTPM1)*DXSM2)/XSUM
C-----COMPUTE SMALLEST DY IN VERTICAL DUCT REGION
      YSUM=YFRAC(1)/2.
      DO 115 J=2,JSTM1
  115 YSUM=YSUM+YFRAC(J)
      YSUM=YSUM+YFRAC(JSTEP)/2.
      DYSM1=2.*RVERT/YSUM
C-----COMPUTE SMALLEST DY IN HORIZONTAL BRANCH REGION
      YSUM=0.
      DO 120 J=JSTP1,NJM2
  120 YSUM=YSUM+YFRAC(J)
      YSUM=YSUM+YFRAC(NJM1)/2.
      DYSM2=(HORIZL-.5*YFRAC(JSTEP)*DYSM1)/YSUM
C-----SET UP X-ARRAY
      X(1)=-XFRAC(1)*DXSM1/2.
      DO 125 I=2,ISTPM1
  125 X(I)=X(I-1)+XFRAC(I-1)*DXSM1
      DO 130 I=ISTEP,NI
  130 X(I)=X(I-1)+XFRAC(I-1)*DXSM2
C-----SET UP Y-ARRAY
      Y(1)=-YFRAC(1)*DYSM1/2.
      DO 140 J=2,JSTP1
  140 Y(J)=Y(J-1)+YFRAC(J-1)*DYSM1
      DO 145 J=JSTP2,NJ
  145 Y(J)=Y(J-1)+YFRAC(J-1)*DYSM2
C-----DEPENDENT VARIABLE SELECTION
      INCALU=.TRUE.
      INCALV=.TRUE.
      INCALP=.TRUE.
C-----BOUNDARY VALUES
C-----PRESSURE CALCULATION
      PREF=1.0
      IPREF=2
      JPREF=2
C-----PROGRAM CONTROL AND MONITOR
      IMON=ISTEP
      JMON=JSTEP
      NUMPRI=1
C
CHAPTER  2  2  2  2  2  2  INITIAL OPERATIONS  2  2  2  2  2  2  2  2  2
C
C-----CALCULATE GEOMETRICAL QUANTITIES AND SET VARIABLES TO ZERO
      CALL INIT
C-----INITIALISE VARIABLE FIELDS
C-----READ IN INITIAL FIELDS IF AVAILABLE FROM PREVIOUS RUN
      VIN=Q1N/(RVERT*2.)
      IF(.NOT.RESTRT) GO TO 199
      CALL REST
      GO TO 235
C-----ASSUME PARABOLIC INLET AND OUTLET PROFILES
C-----ASSUME PARABOLIC INITIAL DISTRIBUTIONS
  199 DO 200 I=2,ISTEP
      DO 200 J=2,JSTEP
  200 U(I,J)=3.*VIN*(Y(J)/RVERT-.5*(Y(J)/RVERT)**2)
      V2=Q2/(RHORIZ*2.)
      DO 210 I=ISTEP,NIM1
      XP=X(I)-XU(ISTEP)
      DO 210 J=JSTP1,NJ
  210 V(I,J)=3.*V2*(XP/RHORIZ-.5*(XP/RHORIZ)**2)
C-----ASSUME PRESSURE DISTRIBUTIONS FOR FULLY DEVELOPED FLOW
```

```
      DO 215 J=2,JSTEP
  215 P(2,J)=PREF
      FACTOR=1.5*VISCOS*QIN/RVERT**3
      DO 220 I=3,ISTEP
      XDIST=X(I)-X(2)
      DO 220 J=2,JSTEP
  220 P(I,J)=PREF-XDIST*FACTOR
      DO 230 I=ISTPP1,NIM1
      DO 230 J=2,JSTEP
  230 P(I,J)=P(ISTEP,JSTEP)
      FACTOR=1.5*VISCOS*Q2/RHORIZ**3
      DO 235 J=JSTP1,NJM1
      YDIST=Y(J)-Y(JSTEP)
      DO 235 I=ISTEP,NIM1
      P(I,J)=P(ISTEP,JSTEP)-FACTOR*YDIST
  235 CONTINUE
C-----CALCULATE SOURCE-NORMALISATION FACTORS
      SNORMM=DENSIT*QIN
      SNORMU=SNORMM*VIN
      SNORMV=SNORMU
C-----INITIAL OUTPUT
      WRITE(6,2000)
      WRITE(6,2010)
      WRITE(6,2030)QIN,Q2,VISCOS,DENSIT,REIN,RE2,
     1RVERT,RHORIZ,RRATIO,ENTRYL,HORIZL
      WRITE(6,2000)
      IF(INCALU) CALL PRINT(2,2,NI,NJ,15,15,XU,Y,U,HEDU)
      IF(INCALV) CALL PRINT(2,2,NI,NJ,15,15,X,YV,V,HEDV)
      IF(INCALP) CALL PRINT(2,2,NI,NJ,15,15,X,Y,P,HEDP)
 2000 FORMAT(///'0',120('*')///)
 2010 FORMAT('0',5X,'JUNCTION PRESSURE DROP, CORNER FLOW'/)
 2030 FORMAT('0',5X,'FLOW PARAMETERS'//
     1/5X,'VERTICAL DUCT INLET FLOW RATE---------=',1PE12.3,' M**3/S'
     1/5X,'HORIZONTAL DUCT FLOW RATE-------------=',1PE12.3,' M**2/S'
     1/5X,'VISCOSITY-----------------------------=',1PE12.3,' KG/M*S'
     1/5X,'DENSITY-------------------------------=',1PE12.3,' KG/M**3'
     1/5X,'INLET REYNOLDS NO.--------------------=',1PE12.3
     1/5X,'HORIZONTAL DUCT REYNOLDS NO.----------=',1PE12.3
     1/5X,'VERTICAL DUCT HYDRAULIC RADIUS--------=',1PE12.3,' M'
     1/5X,'HORIZONTAL DUCT HYDRAULIC RADIUS------=',1PE12.3,' M'
     1/5X,'RATIO, VERT. TO HOR. DUCT RADII-------=',1PE12.3
     1/5X,'VERTICAL DUCT INLET LENGTH------------=',1PE12.3,' M'
     1/5X,'HORIZONTAL DUCT LENGTH----------------=',1PE12.3,' M')

C-----CHAPTER 3 3 3 3 3 3 3 ITERATION LOOP 3 3 3 3 3 3 3 3 3
C
      WRITE(6,310) IMON,JMON
  300 NITER=NITER+1
C-----UPDATE MAIN DEPENDENT VARIABLES
      IF(INCALU) CALL CALCU
      IF(INCALV) CALL CALCV
      IF(INCALP) CALL CALCP
C-----INTERMEDIATE OUTPUT
      RESORU=RESORU/SNORMU
      RESORV=RESORV/SNORMV
      RESORM=RESORM/SNORMM
      WRITE(4,310) IMON,JMON
      WRITE(6,311) NITER,RESORU,RESORV,RESORM,U(IMON,JMON),
     1             V(IMON,JMON),P(IMON,JMON)
      WRITE(4,311) NITER,RESORU,RESORV,RESORM,U(IMON,JMON),
```

```
     1              V(IMON,JMON),P(IMON,JMON)
      IF(MOD(NITER,INDPRI).NE.0) GO TO 301
      IF(INCALU) CALL PRINT(2,2,NI,NJ,15,15,XU,Y,U,HEDU)
      IF(INCALV) CALL PRINT(2,2,NI,NJ,15,15,X,YV,V,HEDV)
      IF(INCALP) CALL PRINT(2,2,NI,NJ,15,15,X,Y,P,HEDP)
      WRITE(6,310) IMON,JMON
  301 CONTINUE
C-----TERMINATION TESTS
      SORCE=AMAX1(RESORU,RESORV,RESORM)
      IF(NITER.EQ.MAXIT) GO TO 302
      IF(NITER.EQ.20.AND.SORCE.GT.1.0E4*SORMAX) GO TO 302
      IF(SORCE.GT.SORMAX) GO TO 300
  302 CONTINUE
C
CHAPTER  4  4  4  4  4  4  FINAL OPERATIONS AND OUTPUT  4  4  4  4  4  4
C
      IF(INCALU) CALL PRINT(2,2,NI,NJ,15,15,XU,Y,U,HEDU)
      IF(INCALV) CALL PRINT(2,2,NI,NJ,15,15,X,YV,V,HEDV)
      IF(INCALP) CALL PRINT(2,2,NI,NJ,15,15,X,Y,P,HEDP)
C-----COMPUTE AVERAGE CORNER INLET PRESSURE
      ENTRYP=ENTRYL-X(2)
      HORIZP=HORIZL-(YV(NI)-Y(NIM1))
      ENDROP=(1.5*VISCOS/RVERT**3)*Q1N*ENTRYP
      HODROP=(1.5*VISCOS/RHORIZ**3)*Q2*HORIZP
      PAVIN=0.
      I=2
      DO 400 J=2,JSTEP
  400 PAVIN=PAVIN+P(I,J)
      PAVIN=PAVIN/FLOAT(JSTM1)
C-----COMPUTE AVERAGE CORNER BRANCH PRESSURE
      J=NJM1
      PAV2=0.
      DO 410 I=ISTEP,NIM1
  410 PAV2=PAV2+P(I,J)
      ITEMP=NIM1-ISTEP+1
      PAV2=PAV2/FLOAT(ITEMP)
      PDIFF=PAVIN-PAV2-(ENDROP+HODROP)
      FKC=8.*PDIFF*RVERT**2/(VISCOS*Q1N)
C-----WRITE OUT THE APPARENT FRICTION CONSTANT
      WRITE(6,4000)FKC
C-----DUMP ALL VARIABLE ARRAYS TO TAPE20 FOR LATER USE
      CALL DUMP
      STOP
C-----FORMAT STATEMENTS
 4000 FORMAT('0',5X,'FRICTION CONSTANT FOR CORNER FLOW:'/
     . 1/5X,'KC=',1PE12.3)
  310 FORMAT('0','ITER    ','I-----ABSOLUTE RESIDUAL SOURCE SUM',
     1'S-----I      I-FIELD VALUES AT MONITORING LOCATION',1X,
     1'(',I2,',',I2,')','-I'/2X,'NO.',6X,'UMOM',8X,'VMOM',6X,
     1'MASS',,12X,'U',9X,'V',9X,'P',9X/)
  311 FORMAT(1H ,I3,5X,1P3E10.3,5X,1P3E10.3)
      END
```

SUBROUTINE MODU

```
      SUBROUTINE MODU
      COMMON
     1/UVEL/RESORU,NSWPU,URFU,DXEPU(15),DXPWU(15),SEWU(15)
     1/VVEL/RESORV,NSWPV,URFV,DYNPV(15),DYPSV(15),SNSV(15)
     1/PCOR/RESORM,NSWPP,URFP,DU(15,15),DV(15,15),IPREF,JPREF
     1/VAR/U(15,15),V(15,15),P(15,15),PP(15,15)
     1/ALL/NI,NJ,NIM1,NJM1,GREAT
     1/GEOM/X(15),Y(15),DXEP(15),DXPW(15),DYNP(15),DYPS(15),
     1       SNS(15),SEW(15),XU(15),YV(15)
      1/FLUPR/VISCOS,DENSIT
      1/COEF/AP(15,15),AN(15,15),AS(15,15),AE(15,15),AW(15,15),SU(15,15),
      1       SP(15,15)
      1/JUN/ISTEP,JSTEP,ISTPM1,ISTPM2,NIM2,
      1JSTP1,NJM2,JSTP2,JSTM1,ISTPP1
C-----SET U-VELOCITIES IN SOLID AREAS TO ZERO
       DO 200 I=3,ISTEP
       DO 200 J=JSTP1,NJM1
       SU(I,J)=0.
  200  SP(I,J)=-GREAT
C-----NO SLIP WALL BOUNDARY CONDITIONS ON U
       J=JSTEP
       YDELT=YV(JSTP1)-Y(J)
       DO 210 I=3,ISTPM1
       AN(I,J)=0.
  210  SP(I,J)=SP(I,J)-VISCOS*SEWU(I)/YDELT
C-----ALLOW FOR CORNERS
       I=ISTEP
       AN(I,J)=.5*AN(I,J)
       SP(I,J)=SP(I,J)-VISCOS*.5*SEWU(I)/YDELT
C-----BOTTOM WALL
       J=2
       YDELT=Y(J)-YV(J)
       DO 220 I=3,NIM1
       AS(I,J)=0.
  220  SP(I,J)=SP(I.J)-VISCOS*SEWU(I)/YDELT
       RETURN
       END
```

SUBROUTINE MODV

```
      SUBROUTINE MODV
      COMMON
     1/UVEL/RESORU,NSWPU,URFU,DXEPU(15),DXPWU(15),SEWU(15)
     1/VVEL/RESORV,NSWPV,URFV,DYNPV(15),DYPSV(15),SNSV(15)
     1/PCOR/RESORM,NSWPP,URFP,DU(15,15),DV(15,15),IPREF,JPREF
     1/VAR/U(15,15),V(15,15),P(15,15),PP(15,15)
     1/ALL/NI,NJ,NIM1,NJM1,GREAT
     1/GEOM/X(15),Y(15),DXEP(15),DXPW(15),DYNP(15),DYPS(15),
     1       SNS(15),SEW(15),XU(15),YV(15)
      1/FLUPR/VISCOS,DENSIT
      1/COEF/AP(15,15),AN(15,15),AS(15,15),AE(15,15),AW(15,15),SU(15,15),
      1       SP(15,15)
      1/JUN/ISTEP,JSTEP,ISTPM1,ISTPM2,NIM2,
     1JSTP1,NJM2,JSTP2,JSTM1,ISTPP1
C-----SET V-VELOCITIES IN SOLID AREAS TO ZERO
       DO 300 I=2,ISTPM1
       DO 300 J=JSTP1,NJM1
       SU(I,J)=0.
  300 SP(I,J)=-GREAT
C-----NO SLIP BOUNDARY CONDITIONS ON V
       I=ISTEP
C-----ALLOW FOR CORNERS
       XDELT=X(I)-XU(I)
       J=JSTP1
       AW(I,J)=.5*AW(I,J)
       SP(I,J)=SP(I,J)-VISCOS*.5*SNSV(J)/XDELT
       DO 310 J=JSTP2,NJM1
       AW(I,J)=0.
  310 SP(I,J)=SP(I,J)-VISCOS*SNSV(J)/XDELT
       I=NIM1
       XDELT=XU(NI)-X(I)
       DO 315 J=3,NJM1
       AE(I,J)=0.
  315 SP(I,J)=SP(I,J)-VISCOS*SNSV(J)/XDELT
       RETURN
       END
```

SUBROUTINE MODP

```
1C
2CHAPTER  4  4  4  4  4  4  PRESSURE CORRECTION  4  4  4  4  4  4  4  4
3C
4       SUBROUTINE MODP
5       COMMON
6      1/UVEL/RESORU,NSWPU,URFU,DXEPU(15),DXPWU(15),SEWU(15)
7      1/VVEL/RESORV,NSWPV,URFV,DYNPV(15),DYPSV(15),SNSV(15)
8      1/PCOR/RESORM,NSWPP,URFP,DU(15,15),DV(15,15),IPREF,JPREF
9      1/VAR/U(15,15),V(15,15),P(15,15),PP(15,15)
10      1/ALL/NI,NJ,NIM1,NJM1,GREAT
11      1/GEOM/X(15),Y(15),DXEP(15),DXPW(15),DYNP(15),DYPS(15),
12      1       SNS(15),SEW(15),XU(15),YV(15)
13      1/FLUPR/VISCOS,DENSIT
14      1/COEF/AP(15,15),AN(15,15),AS(15,15),AE(15,15),AW(15,15),SU(15,15),
15      1       SP(15,15)
16      1/JUN/ISTEP,JSTEP,ISTPM1,ISTPM2,NIM2,
17      1JSTP1,NJM2,JSTP2,JSTM1,ISTPP1
18C-----SET PRESSURE CORRECTIONS IN SOLID AREAS TO 0
19       DO 400 I=2,ISTPM1
20       DO 400 J=JSTP1,NJM1
21       SU(I,J)=0.
22  400 SP(I,J)=-GREAT
23       RETURN
24       END
```

SUBROUTINE DUMP

```
1       SUBROUTINE DUMP
2       COMMON
3      1/ALL/NI,NJ,NIM1,NJM1,GREAT
4      1/VAR/U(15,15),V(15,15),P(15,15),PP(15,15)
5       IT=15
6       JT=15
7       REWIND 9
8       WRITE(9,100) IT,JT,NI,NJ
9       WRITE(9,200) ((U(I,J),I=1,NI),J=1,NJ)
10       WRITE(9,200) ((V(I,J),I=1,NI),J=1,NJ)
11       WRITE(9,200) ((P(I,J),I=1,NI),J=1,NJ)
12  100 FORMAT(1X,4I3)
13  200 FORMAT(1X,5E16.8)
14       RETURN
15       END
```

SUBROUTINE REST

```
1       SUBROUTINE REST
2       COMMON
3      1/ALL/NI,NJ,NIM1,NJM1,GREAT
4      1/VAR/U(15,15),V(15,15),P(15,15),PP(15,15)
5       READ(9,100)IMAX,JMAX,ILAST,JLAST
6       READ(9,200) ((U(I,J),I=1,NI),J=1,NJ)
7       READ(9,200) ((V(I,J),I=1,NI),J=1,NJ)
8       READ(9,200) ((P(I,J),I=1,NI),J=1,NJ)
9   100 FORMAT(4I3)
10   200 FORMAT(5E16.8)
11       RETURN
12       END
```

Input File CORNDAT.DAT

```
8.73E-3,8.51E+2,3.73E-5,1.50E+0
0.006,3.000,8,15,15,8
5.,2.5,2.0,1.5,1.25,1.,1.,2.0,2.5,5..5.,2.5,2.,1.
1.,2.,2.5,5.,5.,5.,2.5,2.,1.,1.,1.25,1.5,2.,2.5,5.
2,2,10.99,50
0.3,0.5,1.0,0.01
FAL
     U VELOCITY
     V VELOCITY
     PRESSURE
```

Output file RESULT.DAT follows on next pages.

```
**********************************************************************************************************************************

      SOLUTION CONTROL PARAMETERS

     NSWPU-----------=  2
     NSWPV-----------=  2
     NSWPP-----------= 10
     MAXIT-----------=  99
     URFU------------=  .50
     URFV------------=  .50
     URFP------------= 1.00
     SORMAX----------=  .010

INITIAL FIELDS HAVE BEEN SET IN MAIN PROGRAM

**********************************************************************************************************************************

      GEOMETRICAL PARAMETERS

     ENTFAC----------= 1.50
     ISTEP-----------=  8
     JSTEP-----------=  8

XFRAC(I)=
            5.000   2.500   2.000   1.500   1.250
            1.000   1.000   2.000   2.500   5.000
            5.000   2.500   2.000   1.000

YFRAC(J)=
            1.000   2.000   2.500   5.000   5.000
            2.500   2.000   1.000   1.000   1.250
            1.500   2.000   2.500   5.000

**********************************************************************************************************************************
```

JUNCTION PRESSURE DROP, CORNER FLOW

FLOW PARAMETERS

VERTICAL DUCT INLET FLOW RATE---------=	3.730E-05	M**2/S
HORIZONTAL DUCT FLOW RATE-------------=	3.730E-05	M**2/S
VISCOSITY-----------------------------=	6.780E-03	KG/M*S
DENSITY-------------------------------=	8.510E+02	KG/M**3
INLET REYNOLDS NO.--------------------=	9.364E+00	
HORIZONTAL DUCT REYNOLDS NO.----------=	9.364E+00	
VERTICAL DUCT HYDRAULIC RADIUS--------=	6.000E-03	M
HORIZONTAL DUCT HYDRAULIC RADIUS------=	2.000E-03	M
RATIO, VERT. TO HOR. DUCT RADII-------=	3.000E+00	
VERTICAL DUCT INLET LENGTH------------=	1.496E-02	M
HORIZONTAL DUCT LENGTH----------------=	4.986E-03	M

U VELOCITY

J	I 1	2	3	4	5	6	7	8	9	10	11	12	13	Y =
15	0.00E+00	0.00E+00	0.00E+00	0.00E+00	0.00E+00	0.00E+00	0.00E+00	0.00E+00	0.00E+00	0.00E+00	0.00E+00	0.00E+00	0.00E+00	.01808
14	0.00E+00	0.00E+00	0.00E+00	0.00E+00	0.00E+00	0.00E+00	0.00E+00	0.00E+00	0.00E+00	0.00E+00	0.00E+00	0.00E+00	0.00E+00	.01570
13	0.00E+00	0.00E+00	0.00E+00	0.00E+00	0.00E+00	0.00E+00	0.00E+00	0.00E+00	0.00E+00	0.00E+00	0.00E+00	0.00E+00	0.00E+00	.01481
12	0.00E+00	0.00E+00	0.00E+00	0.00E+00	0.00E+00	0.00E+00	0.00E+00	0.00E+00	0.00E+00	0.00E+00	0.00E+00	0.00E+00	0.00E+00	.01393
11	0.00E+00	0.00E+00	0.00E+00	0.00E+00	0.00E+00	0.00E+00	0.00E+00	0.00E+00	0.00E+00	0.00E+00	0.00E+00	0.00E+00	0.00E+00	.01328
10	0.00E+00	0.00E+00	0.00E+00	0.00E+00	0.00E+00	0.00E+00	0.00E+00	0.00E+00	0.00E+00	0.00E+00	0.00E+00	0.00E+00	0.00E+00	.01274
9	0.00E+00	0.00E+00	0.00E+00	0.00E+00	0.00E+00	0.00E+00	0.00E+00	0.00E+00	0.00E+00	0.00E+00	0.00E+00	0.00E+00	0.00E+00	.01230
8	4.55E-04	4.55E-04	4.55E-04	4.55E-04	4.55E-04	4.55E-04	4.55E-04	4.55E-04	0.00E+00	0.00E+00	0.00E+00	0.00E+00	0.00E+00	.01170
7	2.04E-03	2.04E-03	2.04E-03	2.04E-03	2.04E-03	2.04E-03	2.04E-03	2.04E-03	0.00E+00	0.00E+00	0.00E+00	0.00E+00	0.00E+00	.01050
6	3.50E-03	3.50E-03	3.50E-03	3.50E-03	3.50E-03	3.50E-03	3.50E-03	3.50E-03	0.00E+00	0.00E+00	0.00E+00	0.00E+00	0.00E+00	.00900
5	4.66E-03	4.66E-03	4.66E-03	4.66E-03	4.66E-03	4.66E-03	4.66E-03	4.66E-03	0.00E+00	0.00E+00	0.00E+00	0.00E+00	0.00E+00	.00600
4	3.50E-03	3.50E-03	3.50E-03	3.50E-03	3.50E-03	3.50E-03	3.50E-03	3.50E-03	0.00E+00	0.00E+00	0.00E+00	0.00E+00	0.00E+00	.00300
3	2.04E-03	2.04E-03	2.04E-03	2.04E-03	2.04E-03	2.04E-03	2.04E-03	2.04E-03	0.00E+00	0.00E+00	0.00E+00	0.00E+00	0.00E+00	.00150
2	4.55E-04	4.55E-04	4.55E-04	4.55E-04	4.55E-04	4.55E-04	4.55E-04	4.55E-04	0.00E+00	0.00E+00	0.00E+00	0.00E+00	0.00E+00	.00030
X=	0.00000	.00518	.00829	.01071	.01261	.01417	.01496	.01526	.01571	.01646	.01746	.01821		

I	14	15	Y =
J			
15	0.00E+00	0.00E+00	1.81E-02
14	0.00E+00	0.00E+00	1.59E-02
13	0.00E+00	0.00E+00	1.48E-02
12	0.00E+00	0.00E+00	1.39E-02
11	0.00E+00	0.00E+00	1.33E-02
10	0.00E+00	0.00E+00	1.27E-02
9	0.00E+00	0.00E+00	1.23E-02
8	0.00E+00	0.00E+00	1.17E-02
7	0.00E+00	0.00E+00	1.05E-02
6	0.00E+00	0.00E+00	9.00E-03
5	0.00E+00	0.00E+00	6.00E-03
4	0.00E+00	0.00E+00	3.00E-03
3	0.00E+00	0.00E+00	1.50E-03
2	0.00E+00	0.00E+00	3.00E-04

X= .01366 .01896

V VELOCITY

I	2	3	4	5	6	7	8	9	10	11	12	13	Y =
J													
15	0.00E+00	0.00E+00	0.00E+00	0.00E+00	0.00E+00	0.00E+00	1.36E-03	6.12E-03	1.05E-02	1.40E-02	1.05E-02	6.12E-03	.01699
14	0.00E+00	0.00E+00	0.00E+00	0.00E+00	0.00E+00	0.00E+00	1.36E-03	6.12E-03	1.05E-02	1.40E-02	1.05E-02	6.12E-03	.01535
13	0.00E+00	0.00E+00	0.00E+00	0.00E+00	0.00E+00	0.00E+00	1.36E-03	6.12E-03	1.05E-02	1.40E-02	1.05E-02	6.12E-03	.01437
12	0.00E+00	0.00E+00	0.00E+00	0.00E+00	0.00E+00	0.00E+00	1.36E-03	6.12E-03	1.05E-02	1.40E-02	1.05E-02	6.12E-03	.01361
11	0.00E+00	0.00E+00	0.00E+00	0.00E+00	0.00E+00	0.00E+00	1.36E-03	6.12E-03	1.05E-02	1.40E-02	1.05E-02	6.12E-03	.01301
10	0.00E+00	0.00E+00	0.00E+00	0.00E+00	0.00E+00	0.00E+00	1.36E-03	6.12E-03	1.05E-02	1.40E-02	1.05E-02	6.12E-03	.01251
9	0.00E+00	0.00E+00	0.00E+00	0.00E+00	0.00E+00	0.00E+00	1.36E-03	6.12E-03	1.05E-02	1.40E-02	1.05E-02	6.12E-03	.01200
8	0.00E+00	0.00E+00	0.00E+00	0.00E+00	0.00E+00	0.00E+00	0.00E+00	0.00E+00	0.00E+00	0.00E+00	0.00E+00	0.00E+00	.01110
7	0.00E+00	0.00E+00	0.00E+00	0.00E+00	0.00E+00	0.00E+00	0.00E+00	0.00E+00	0.00E+00	0.00E+00	0.00E+00	0.00E+00	.00975
6	0.00E+00	0.00E+00	0.00E+00	0.00E+00	0.00E+00	0.00E+00	0.00E+00	0.00E+00	0.00E+00	0.00E+00	0.00E+00	0.00E+00	.00750
5	0.00E+00	0.00E+00	0.00E+00	0.00E+00	0.00E+00	0.00E+00	0.00E+00	0.00E+00	0.00E+00	0.00E+00	0.00E+00	0.00E+00	.00450
4	0.00E+00	0.00E+00	0.00E+00	0.00E+00	0.00E+00	0.00E+00	0.00E+00	0.00E+00	0.00E+00	0.00E+00	0.00E+00	0.00E+00	.00225
3	0.00E+00	0.00E+00	0.00E+00	0.00E+00	0.00E+00	0.00E+00	0.00E+00	0.00E+00	0.00E+00	0.00E+00	0.00E+00	0.00E+00	.00090
2	0.00E+00	0.00E+00	0.00E+00	0.00E+00	0.00E+00	0.00E+00	0.00E+00	0.00E+00	0.00E+00	0.00E+00	0.00E+00	0.00E+000	.00060

X= .00346 .00691 .00967 .01175 .01348 .01486 .01506 .01546 .01596 .01696 .01796 .01846

I	14	15	Y =
J			
15	1.36E-03	0.00E+00	1.70E-02
14	1.36E-03	0.00E+00	1.54E-02
13	1.36E-03	0.00E+00	1.44E-02
12	1.36E-03	0.00E+00	1.36E-02
11	1.36E-03	0.00E+00	1.30E-02
10	1.36E-03	0.00E+00	1.25E-02
9	1.36E-03	0.00E+00	1.20E-02
8	0.00E+00	0.00E+00	1.11E-02
7	0.00E+00	0.00E+00	9.75E-03

6	0.00E+00	0.00E+00	7.50E-03
5	0.00E+00	0.00E+00	4.50E-03
4	0.00E+00	0.00E+00	2.25E-03
3	0.00E+00	0.00E+00	9.00E-04
2	0.00E+00	0.00E+00	0.00E+00

X= .01836 .01906

PRESSURE

J \ I	2	3	4	5	6	7	8	9	10	11	12	13	Y =
15	0.00E+00	0.00E+00	0.00E+00	0.00E+00	0.00E+00	0.00E+00	0.00E+00	0.00E+00	0.00E+00	0.00E+00	0.00E+00	0.00E+00	.01808
14	0.00E+00	0.00E+00	0.00E+00	0.00E+00	0.00E+00	0.00E+00	7.81E-01	7.81E-01	7.81E-01	7.81E-01	7.81E-01	7.81E-01	.01590
13	0.00E+00	0.00E+00	0.00E+00	0.00E+00	0.00E+00	0.00E+00	8.32E-01	8.32E-01	8.32E-01	8.32E-01	8.32E-01	8.32E-01	.01481
12	0.00E+00	0.00E+00	0.00E+00	0.00E+00	0.00E+00	0.00E+00	8.74E-01	8.74E-01	8.74E-01	8.74E-01	8.74E-01	8.74E-01	.01393
11	0.00E+00	0.00E+00	0.00E+00	0.00E+00	0.00E+00	0.00E+00	9.05E-01	9.05E-01	9.05E-01	9.05E-01	9.05E-01	9.05E-01	.01328
10	0.00E+00	0.00E+00	0.00E+00	0.00E+00	0.00E+00	0.00E+00	9.31E-01	9.31E-01	9.31E-01	9.31E-01	9.31E-01	9.31E-01	.01274
9	0.00E+00	0.00E+00	0.00E+00	0.00E+00	0.00E+00	0.00E+00	9.51E-01	9.51E-01	9.51E-01	9.51E-01	9.51E-01	9.51E-01	.01230
8	1.00E+00	9.94E-01	9.89E-01	9.85E-01	9.82E-01	9.80E-01	9.80E-01	9.80E-01	9.80E-01	9.80E-01	9.80E-01	9.80E-01	.01170
7	1.00E+00	9.94E-01	9.89E-01	9.85E-01	9.82E-01	9.80E-01	9.80E-01	9.80E-01	9.80E-01	9.80E-01	9.80E-01	9.80E-01	.01050
6	1.00E+00	9.94E-01	9.89E-01	9.85E-01	9.82E-01	9.80E-01	9.80E-01	9.80E-01	9.80E-01	9.80E-01	9.80E-01	9.80E-01	.00900
5	1.00E+00	9.94E-01	9.89E-01	9.85E-01	9.82E-01	9.80E-01	9.80E-01	9.80E-01	9.80E-01	9.80E-01	9.80E-01	9.80E-01	.00600
4	1.00E+00	9.94E-01	9.89E-01	9.85E-01	9.82E-01	9.80E-01	9.80E-01	9.80E-01	9.80E-01	9.80E-01	9.80E-01	9.80E-01	.00300
3	1.00E+00	9.94E-01	9.89E-01	9.85E-01	9.82E-01	9.80E-01	9.80E-01	9.80E-01	9.80E-01	9.80E-01	9.80E-01	9.80E-01	.00150
2	1.00E+00	9.94E-01	9.89E-01	9.85E-01	9.82E-01	9.80E-01	9.80E-01	9.80E-01	9.80E-	9.80E-01	9.80E-01	9.80E-01	.00030

X= .00346 .00691 .00967 .01175 .01348 .01486 .01506 .01546 .01596 .01696 .01796 .01846

J \ I	14	15	Y =
15	0.00E+00	0.00E+00	1.81E-02
14	7.81E-01	0.00E+00	1.59E-02
13	8.32E-01	0.00E+00	1.48E-02
12	8.74E-01	0.00E+00	1.39E-02
11	9.05E-01	0.00E+00	1.33E-02
10	9.31E-01	0.00E+00	1.27E-02
9	9.51E-01	0.00E+00	1.23E-02
8	9.80E-01	0.00E+00	1.17E-02
7	9.80E-01	0.00E+00	1.05E-02
6	9.80E-01	0.00E+00	9.00E-03
5	9.80E-01	0.00E+00	6.00E-03
4	9.80E-01	0.00E+00	3.00E-03
3	9.80E-01	0.00E+00	1.50E-03
2	9.80E-01	0.00E+00	3.00E-04

X= .01836 .01906

ITER NO.	I-----ABSOLUTE RESIDUAL SOURCE SUMS-----I UMOM	VMOM	MASS	I-FIELD VALUES AT MONITORING LOCATION (8, 8)-I U	V	P

1	1.680E+01	6.39?E+00	1.94?E+00	3.217E-03	8.570E-04	5.663E-01
2	5.?6?E+01	7.745E+01	4.429E+00	4.885E-03	2.139E-03	5.192E-01
3	3.85?E+01	4.374E+01	2.588E+00	5.294E-03	2.732E-03	8.322E-01
4	1.8?0E+01	3.059E+01	1.176E+00	5.903E-03	3.280E-03	7.376E-01
5	1.184E+01	2.462E+01	7.919E-01	6.139E-03	3.848E-03	7.824E-01
6	8.104E+00	1.256E+01	5.749E-01	6.216E-03	4.192E-03	8.154E-01
7	5.251E+00	6.827E+00	4.658E-01	5.960E-03	4.374E-03	8.678E-01
8	3.928E+00	1.007E+01	3.396E-01	5.493E-03	4.386E-03	9.322E-01
9	5.056E+00	1.224E+01	1.225E-01	4.996E-03	4.299E-03	9.525E-01
10	5.515E+00	1.133E+01	1.215E-01	4.611E-03	4.178E-03	9.531E-01
11	4.123E+00	7.745E+00	1.998E-01	4.431E-03	4.083E-03	9.286E-01
12	1.843E+00	3.445E+00	2.030E-01	4.442E-03	4.048E-03	9.025E-01
13	6.072E-01	1.632E+00	1.568E-01	4.590E-03	4.070E-03	8.794E-01
14	1.983E+00	4.120E+00	8.505E-02	4.795E-03	4.159E-03	8.656E-01
15	2.652E+00	5.401E+00	2.275E-02	4.989E-03	4.267E-03	8.620E-01
16	1.9?2E+00	5.03?E+00	5.990E-02	5.122E-03	4.373E-03	8.671E-01
17	1.255E+00	3.53?E+00	8.933E-02	5.174E-03	4.455E-03	8.790E-01
18	4.432E-01	1.544E+00	8.935E-02	5.150E-03	4.505E-03	8.907E-01
19	4.?28E-01	1.417E+00	6.732E-02	5.075E-03	4.521E-03	9.010E-01
20	9.034E-01	2.176E+00	3.374E-02	4.981E-03	4.513E-03	9.074E-01
21	1.051E+00	2.338E+00	1.086E-02	4.897E-03	4.493E-03	9.092E-01
22	9.178E-01	1.921E+00	2.894E-02	4.842E-03	4.472E-03	9.071E-01
23	6.?05E-01	1.1?2E+00	3.873E-02	4.824E-03	4.4?0E-03	9.027E-01
24	3.?0?E-01	4.128E-01	3.?01E-02	4.838E-03	4.460E-03	8.979E-01
25	2.394E-01	?.5?7E-01	2.449E-02	4.872E-03	4.472E-03	8.942E-01
26	3.978E-01	1.054E+00	9.524E-03	4.910E-03	4.491E-03	8.924E-01
27	4.187E-01	1.134E+00	?.?13E-03	4.943E-03	4.513E-03	8.926E-01
28	3.20?E-01	9.367E-01	1.484E-02	4.959E-03	4.533E-03	8.943E-01
29	1.?08E-01	5.?08E-01	1.789E-02	4.961E-03	4.547E-03	8.967E-01
30	9.?9?E-02	2.429E-01	1.574E-02	4.950E-03	4.555E-03	8.991E-01
31	1.?61E-01	3.?70E-01	1.022E-02	4.931E-03	4.55?E-03	9.009E-01
32	2.338E-01	4.701E-01	3.?6?E-03	4.912E-03	4.554E-03	9.017E-01
33	2.34?E-01	4.435E-01	3.?67E-03	4.897E-03	1.550E-03	9.018E-01
34	1.913E-01	3.?89E-01	?.?53E-03	4.889E-03	4.546E-03	9.012E-01
35	1.?69E-01	1.819E-01	7.492E-03	4.887E-03	4.547E-03	9.003E-01
36	9.107E-02	1.195E-01	?.?65E-03	4.891E-03	4.549E-03	8.995E-01
37	7.?91E-02	2.11?E-01	3.378E-03	4.898E-03	4.552E-03	8.990E-01
38	7.91?E-02	2.?54E-01	7.389E-04	4.904E-03	4.557E-03	8.988E-01
39	7.193E-02	2.404E-01	2.098E-03	4.908E-03	4.561E-03	8.990E-01
40	4.997E-02	1.?25E-01	3.299E-03	4.909E-03	4.565E-03	8.995E-01
41	4.?50E-02	1.09?E-01	3.413E-03	4.908E-03	4.568E-03	9.000E-01
42	5.074E-02	8.?0?E-02	2.668E-03	4.904E-03	4.569E-03	9.004E-01
43	?.110E-02	?.957E-02	1.504E-03	4.900E-03	4.569E-03	9.007E-01
44	6.43?E-02	1.035E-01	5.390E-04	4.896E-03	4.569E-03	9.008E-01
45	5.?8?E-02	8.855E-02	1.069E-03	4.893E-03	4.568E-03	9.008E-01
46	5.045E-02	?.301E-02	1.438E-03	4.892E-03	4.568E-03	9.007E-01
47	3.?3?E-02	4.237E-02	1.365E-03	4.892E-03	4.568E-03	9.005E-01
48	3.088E-02	4.857E-02	9.557E-04	4.893E-03	4.569E-03	9.004E-01
49	2.60?E-02	?.139E-02	4.?40E-04	4.894E-03	4.570E-03	9.004E-01
50	2.?0?E-02	6.299E-02	2.?70E-04	4.894E-03	4.571E-03	9.004E-01

U VELOCITY

J \ I	2	3	4	5	6	7	8	9	10	11	12	13	Y =
15	0.00E+00	0.00E+00	0.00E+00	0.00E+00	0.00E+00	0.00E+00	0.00E+00	0.00E+00	0.00E+00	0.00E+00	0.00E+00	0.00E+00	.01808
14	0.00E+00	0.00E+00	0.00E+00	0.00E+00	0.00E+00	0.00E+00	0.00E+00	-1.29E-06	-3.66E-05	-1.19E-04	-1.27E-04	-4.96E-05	.01590
13	0.00E+00	0.00E+00	0.00E+00	0.00E+00	0.00E+00	0.00E+00	0.00E+00	-1.48E-05	-7.96E-05	-1.72E-04	-1.76E-04	-7.06E-05	.01481
12	0.00E+00	0.00E+00	0.00E+00	0.00E+00	0.00E+00	0.00E+00	0.00E+00	-2.04E-05	-5.77E-05	-1.29E-05	-6.38E-05	-4.32E-05	.01373
11	0.00E+00	0.00E+00	0.00E+00	0.00E+00	0.00E+00	0.00E+00	0.00E+00	-1.06E-05	1.16E-04	4.52E-04	2.30E-04	4.61E-05	.01328
10	0.00E+00	0.00E+00	0.00E+00	0.00E+00	0.00E+00	0.00E+00	0.00E+00	1.20E-04	6.78E-04	1.25E-03	6.56E-04	1.81E-04	.01274
9	0.00E+00	0.00E+00	0.00E+00	0.00E+00	0.00E+00	0.00E+00	0.00E+00	8.29E-04	1.90E-03	2.23E-03	1.09E-03	3.15E-04	.01230
8	4.55E-04	4.81E-04	5.22E-04	6.23E-04	9.03E-04	1.95E-03	4.89E-03	5.46E-03	5.11E-03	3.80E-03	1.69E-03	4.98E-04	.01170
7	2.04E-03	2.11E-03	2.29E-03	2.72E-03	3.62E-03	5.29E-03	6.06E-03	6.19E-03	5.87E-03	4.55E-03	2.14E-03	6.51E-04	.01050
6	3.50E-03	3.59E-03	3.80E-03	4.22E-03	4.78E-03	5.15E-03	4.80E-03	4.62E-03	4.20E-03	3.20E-03	1.49E-03	4.43E-04	.00900
5	4.66E-03	4.65E-03	4.61E-03	4.47E-03	4.11E-03	3.42E-03	2.84E-03	2.61E-03	2.22E-03	1.54E-03	6.48E-04	1.83E-04	.00600
4	3.50E-03	3.41E-03	3.22E-03	2.86E-03	2.35E-03	1.74E-03	1.38E-03	1.23E-03	1.02E-03	6.70E-04	2.63E-04	7.19E-05	.00300
3	2.04E-03	1.98E-03	1.85E-03	1.60E-03	1.27E-03	8.98E-04	6.89E-04	6.10E-04	4.92E-04	3.05E-04	1.08E-04	2.77E-05	.00150
2	4.55E-04	4.49E-04	4.18E-04	3.59E-04	2.79E-04	1.88E-04	1.36E-04	1.17E-04	8.79E-05	4.20E-05	9.88E-08	-4.47E-06	.00030

X= 0.00000 .00518 .00829 .01071 .01261 .01417 .01496 .01526 .01571 .01646 .01746 .01821

J \ I	14	15	Y =
15	0.00E+00	0.00E+00	1.81E-02
14	-1.12E-05	0.00E+00	1.59E-02
13	-1.22E-05	0.00E+00	1.48E-02
12	-1.05E-05	0.00E+00	1.39E-02
11	8.57E-07	0.00E+00	1.33E-02
10	2.11E-05	0.00E+00	1.27E-02
9	4.07E-05	0.00E+00	1.23E-02
8	6.08E-05	0.00E+00	1.17E-02
7	9.26E-05	0.00E+00	1.05E-02
6	6.00E-05	0.00E+00	9.00E-03
5	2.35E-05	0.00E+00	6.00E-03
4	8.98E-06	0.00E+00	3.00E-03
3	3.31E-06	0.00E+00	1.50E-03
2	-1.48E-06	0.00E+00	3.00E-04

X= .01866 .01896

V VELOCITY

J \ I	2	3	4	5	6	7	8	9	10	11	12	13	Y =
15	0.00E+00	0.00E+00	0.00E+00	0.00E+00	0.00E+00	0.00E+00	1.36E-03	6.12E-03	1.05E-02	1.40E-02	1.05E-02	6.12E-03	.01699
14	0.00E+00	0.00E+00	0.00E+00	0.00E+00	0.00E+00	0.00E+00	1.36E-03	5.99E-03	1.03E-02	1.40E-02	1.07E-02	6.26E-03	.01535
13	0.00E+00	0.00E+00	0.00E+00	0.00E+00	0.00E+00	0.00E+00	1.31E-03	5.85E-03	1.02E-02	1.40E-02	1.08E-02	6.39E-03	.01437
12	0.00E+00	0.00E+00	0.00E+00	0.00E+00	0.00E+00	0.00E+00	1.26E-03	5.79E-03	1.02E-02	1.39E-02	1.08E-02	6.44E-03	.01361
11	0.00E+00	0.00E+00	0.00E+00	0.00E+00	0.00E+00	0.00E+00	1.24E-03	5.96E-03	1.05E-02	1.38E-02	1.07E-02	6.38E-03	.01301
10	0.00E+00	0.00E+00	0.00E+00	0.00E+00	0.00E+00	0.00E+00	1.43E-03	6.53E-03	1.09E-02	1.35E-02	1.04E-02	6.21E-03	.01252

7	0.00E+00	0.00E+00	0.00E+00	0.00E+00	0.00E+00	0.00E+00	2.86E-03	7.80E-03	1.11E-02	1.29E-02	9.83E-03	5.89E-03	.01200
8	4.55E-06	1.18E-05	3.97E-05	1.30E-04	6.05E-04	3.35E-03	4.57E-03	7.09E-03	9.54E-03	1.10E-02	8.40E-03	5.03E-03	.01110
7	2.39E-05	8.75E-05	2.78E-04	7.70E-04	2.06E-03	4.68E-03	5.16E-03	6.13E-03	7.16E-03	7.75E-03	5.72E-03	3.36E-03	.00975
6	6.32E-05	2.39E-04	6.68E-04	1.44E-03	2.59E-03	3.68E-03	3.80E-03	4.02E-03	4.13E-03	3.90E-03	2.56E-03	1.44E-03	.00750
5	5.68E-05	2.02E-04	4.91E-04	8.75E-04	1.26E-03	1.46E-03	1.47E-03	1.48E-03	1.45E-03	1.22E-03	7.23E-04	3.83E-04	.00450
4	1.74E-05	6.63E-05	1.59E-04	2.73E-04	3.75E-04	4.16E-04	4.15E-04	4.10E-04	3.92E-04	3.04E-04	1.50E-04	6.73E-05	.00225
3	1.05E-06	8.84E-06	2.19E-05	3.80E-05	5.23E-05	5.84E-05	5.84E-05	5.79E-05	5.51E-05	3.77E-05	5.49E-06	-5.96E-06	.00090
2	0.00E+00	0.00E+00	0.00E+00	0.00E+00	0.00E+00	0.00E+00	0.00E+00	0.00E+00	0.00E+00	0.00E+00	0.00E+00	0.00E+000	.00000

X= .00346 .00691 .00967 .01175 .01348 .01486 .01506 .01546 .01596 .01696 .01796 .01843

I 14 15 Y =

J			
15	1.36E-03	0.00E+00	1.70E-02
14	1.42E-03	0.00E+00	1.54E-02
13	1.47E-03	0.00E+00	1.44E-02
12	1.49E-03	0.00E+00	1.36E-02
11	1.49E-03	0.00E+00	1.30E-02
10	1.46E-03	0.00E+00	1.25E-02
9	1.39E-03	0.00E+00	1.20E-02
8	1.18E-03	0.00E+00	1.11E-02
7	7.63E-04	0.00E+00	9.75E-03
6	3.13E-04	0.00E+00	7.50E-03
5	7.78E-05	0.00E+00	4.50E-03
4	1.05E-05	0.00E+00	2.25E-03
3	-4.44E-06	0.00E+00	9.00E-04
2	0.00E+00	0.00E+00	0.00E+00

X= .01836 .01906

PRESSURE

J	1	2	3	4	5	6	7	8	9	10	11	12	13	Y =
15	0.00E+00	0.00E+00	0.00E+00	0.00E+00	0.00E+00	0.00E+00	0.00E+00	0.00E+00	0.00E+00	0.00E+00	0.00E+00	0.00E+00	0.00E+00	.01808
14	-2.26E-02	-2.26E-02	-2.26E-02	-2.26E-02	-2.26E-02	-2.26E-02	6.14E-01	6.14E-01	6.14E-01	6.14E-01	6.14E-01	6.14E-01	6.14E-01	.01590
13	-2.26E-02	-2.26E-02	-2.26E-02	-2.26E-02	-2.26E-02	-2.26E-02	6.73E-01	6.73E-01	6.73E-01	6.76E-01	6.78E-01	6.78E-01	6.78E-01	.01481
12	-2.26E-02	-2.26E-02	-2.26E-02	-2.26E-02	-2.26E-02	-2.26E-02	7.08E-01	7.08E-01	7.11E-01	7.18E-01	7.23E-01	7.24E-01	7.24E-01	.01393
11	-2.26E-02	-2.26E-02	-2.26E-02	-2.26E-02	-2.26E-02	-2.26E-02	7.27E-01	7.30E-01	7.39E-01	7.52E-01	7.60E-01	7.63E-01	7.63E-01	.01328
10	-2.26E-02	-2.26E-02	-2.26E-02	-2.26E-02	-2.26E-02	-2.26E-02	7.31E-01	7.45E-01	7.64E-01	7.81E-01	7.91E-01	7.95E-01	7.95E-01	.01274
9	-2.26E-02	-2.26E-02	-2.26E-02	-2.26E-02	-2.26E-02	-2.26E-02	7.33E-01	7.68E-01	7.94E-01	8.10E-01	8.20E-01	8.25E-01	8.25E-01	.01230
8	1.00E+00	9.93E-01	9.87E-01	9.82E-01	9.76E-01	9.63E-01	9.00E-01	8.67E-01	8.53E-01	8.53E-01	8.60E-01	8.63E-01	8.63E-01	.01170
7	1.00E+00	9.93E-01	9.86E-01	9.79E-01	9.67E-01	9.47E-01	9.36E-01	9.25E-01	9.15E-01	9.10E-01	9.14E-01	9.19E-01	9.19E-01	.01050
6	1.00E+00	9.93E-01	9.86E-01	9.79E-01	9.72E-01	9.64E-01	9.63E-01	9.61E-01	9.60E-01	9.59E-01	9.62E-01	9.66E-01	9.66E-01	.00900
5	1.00E+00	9.93E-01	9.88E-01	9.85E-01	9.83E-01	9.81E-01	9.82E-01	9.81E-01	9.81E-01	9.82E-01	9.84E-01	9.86E-01	9.86E-01	.00660
4	1.00E+00	9.93E-01	9.87E-01	9.87E-01	9.86E-01	9.86E-01	9.86E-01	9.86E-01	9.86E-01	9.86E-01	9.87E-01	9.88E-01	9.88E-01	.00360
3	1.00E+00	9.93E-01	9.89E-01	9.87E-01	9.86E-01	9.85E-01	9.85E-01	9.85E-01	9.85E-01	9.86E-01	9.87E-01	9.87E-01	9.87E-01	.00150
2	1.00E+00	9.93E-01	9.89E-01	9.88E-01	9.84E-01	9.84E-01	9.84E-01	9.84E-01	9.84E-01	9.85E-01	9.86E-01	9.86E-01	9.86E-01	.00070

X= .00346 .00691 .00967 .01175 .01348 .01486 .01506 .01546 .01596 .01696 .01796 .01846

I 14 15 Y =

J			
15	0.00E+00	0.00E+00	1.81E-02
14	6.14E-01	0.00E+00	1.59E-02
13	6.73E-01	0.00E+00	1.48E-02
12	7.24E-01	0.00E+00	1.39E-02
11	7.64E-01	0.00E+00	1.33E-02
10	7.97E-01	0.00E+00	1.27E-02
9	8.23E-01	0.00E+00	1.23E-02
8	8.70E-01	0.00E+00	1.17E-02
7	9.25E-01	0.00E+00	1.05E-02
6	9.71E-01	0.00E+00	9.00E-03
5	9.88E-01	0.00E+00	6.00E-03
4	9.94E-01	0.00E+00	3.00E-03
3	9.97E-01	0.00E+00	1.50E-03
2	9.98E-01	0.00E+00	3.00E-04

Y= .01886 .01906

ITER NO.	I-----ABSOLUTE RESIDUAL SOURCE SUMS-----I UMOM	VMOM	MASS	I-FIELD VALUES AT MONITORING LOCATION (8, 8)-I U	V	P
51	2.009E-02	5.482E-02	5.608E-04	4.895E-03	4.572E-03	9.004E-01
52	1.861E-02	4.084E-02	6.982E-04	4.895E-03	4.573E-03	9.006E-01
53	1.854E-02	2.780E-02	6.409E-04	4.894E-03	4.573E-03	9.007E-01
54	2.012E-02	2.725E-02	4.540E-04	4.893E-03	4.574E-03	9.007E-01
55	2.069E-02	2.772E-02	2.295E-04	4.892E-03	4.574E-03	9.008E-01
56	1.989E-02	2.561E-02	1.663E-04	4.891E-03	4.574E-03	9.008E-01
57	1.789E-02	2.153E-02	2.618E-04	4.890E-03	4.574E-03	9.008E-01
58	1.526E-02	1.692E-02	2.898E-04	4.890E-03	4.574E-03	9.008E-01
59	1.262E-02	1.492E-02	2.419E-04	4.890E-03	4.574E-03	9.008E-01
60	1.060E-02	1.663E-02	1.465E-04	4.890E-03	4.574E-03	9.007E-01
61	9.306E-03	1.758E-02	6.660E-05	4.890E-03	4.575E-03	9.007E-01
62	8.337E-03	1.651E-02	9.981E-05	4.890E-03	4.575E-03	9.008E-01
63	7.609E-03	1.392E-02	1.420E-04	4.890E-03	4.575E-03	9.008E-01
64	7.291E-03	1.089E-02	1.490E-04	4.890E-03	4.575E-03	9.008E-01
65	7.222E-03	9.229E-03	1.250E-04	4.890E-03	4.575E-03	9.008E-01

U VELOCITY

I	2	3	4	5	6	7	8	9	10	11	12	13	Y =
J													
15	0.00E+00	0.00E+00	0.00E+00	0.00E+00	0.00E+00	0.00E+00	0.00E+00	0.00E+00	0.00E+00	0.00E+00	0.00E+00	0.00E+00	.01808
14	0.00E+00	0.00E+00	0.00E+00	0.00E+00	0.00E+00	0.00E+00	0.00E+00	-1.23E-06	-3.64E-05	-1.19E-04	-1.26E-04	-4.95E-05	.01590
13	0.00E+00	0.00E+00	0.00E+00	0.00E+00	0.00E+00	0.00E+00	0.00E+00	-1.47E-05	-7.92E-05	-1.71E-04	-1.75E-04	-7.03E-05	.01481
12	0.00E+00	0.00E+00	0.00E+00	0.00E+00	0.00E+00	0.00E+00	0.00E+00	-2.03E-05	-5.72E-05	-1.16E-05	-6.25E-05	-4.27E-05	.01393
11	0.00E+00	0.00E+00	0.00E+00	0.00E+00	0.00E+00	0.00E+00	0.00E+00	-1.05E-05	1.16E-04	4.54E-04	2.31E-04	4.66E-05	.01328
10	0.00E+00	0.00E+00	0.00E+00	0.00E+00	0.00E+00	0.00E+00	0.00E+00	1.20E-04	6.79E-04	1.25E-03	6.57E-04	1.81E-04	.01274
9	0.00E+00	0.00E+00	0.00E+00	0.00E+00	0.00E+00	0.00E+00	0.00E+00	8.29E-04	1.90E-03	2.23E-03	1.09E-03	3.15E-04	.01230
8	4.55E-04	4.81E-04	5.21E-04	6.26E-04	8.[illegible]E-04	1.94E-03	4.89E-03	5.46E-03	5.11E-03	3.79E-03	1.69E-03	4.[illegible]E-04	.01170
7	2.04E-03	2.11E-03	2.29E-03	2.71E-03	3.[illegible]E-03	5.27E-03	6.05E-03	6.18E-03	5.06E-03	4.55E-03	2.13E-03	5.50E-04	.01050

6	3.50E-03	3.59E-03	3.79E-03	4.21E-03	4.77E-03	5.14E-03	4.78E-03	4.61E-03	4.19E-03	3.19E-03	1.49E-03	4.42E-04	.00900
5	4.66E-03	4.65E-03	4.61E-03	4.47E-03	4.12E-03	3.43E-03	2.85E-03	2.61E-03	2.23E-03	1.55E-03	6.50E-04	1.84E-04	.00600
4	3.50E-03	3.41E-03	3.22E-03	2.87E-03	2.36E-03	1.76E-03	1.39E-03	1.24E-03	1.03E-03	6.74E-04	2.65E-04	7.24E-05	.00300
3	2.04E-03	1.98E-03	1.85E-03	1.61E-03	1.28E-03	9.07E-04	6.95E-04	6.15E-04	4.96E-04	3.07E-04	1.08E-04	2.77E-05	.00150
2	4.55E-04	4.49E-04	4.19E-04	3.61E-04	2.81E-04	1.90E-04	1.37E-04	1.17E-04	8.79E-05	4.15E-05	-3.03E-07	-4.63E-06	.00030

X=	0.00000	.00518	.00829	.01071	.01261	.01417	.01496	.01526	.01571	.01646	.01746	.01821

I	14	15	Y =
J			
15	0.00E+00	0.00E+00	1.81E-02
14	-1.12E-05	0.00E+00	1.59E-02
13	-1.23E-05	0.00E+00	1.48E-02
12	-1.04E-05	0.00E+00	1.39E-02
11	9.60E-07	0.00E+00	1.33E-02
10	2.12E-05	0.00E+00	1.27E-02
9	4.07E-05	0.00E+00	1.23E-02
8	6.85E-05	0.00E+00	1.17E-02
7	9.24E-05	0.00E+00	1.05E-02
6	5.98E-05	0.00E+00	9.00E-03
5	2.36E-05	0.00E+00	6.00E-03
4	9.05E-06	0.00E+00	3.00E-03
3	3.21E-06	0.00E+00	1.50E-03
2	-1.51E-06	0.00E+00	3.00E-04

X=	.01866	.01896

V VELOCITY

I	2	3	4	5	6	7	8	9	10	11	12	13	Y =
J													
15	0.00E+00	0.00E+00	0.00E+00	0.00E+00	0.00E+00	0.00E+00	1.36E-03	6.12E-03	1.05E-02	1.40E-02	1.05E-02	6.12E-03	.01699
14	0.00E+00	0.00E+00	0.00E+00	0.00E+00	0.00E+00	0.00E+00	1.36E-03	5.99E-03	1.03E-02	1.40E-02	1.07E-02	6.26E-03	.01535
13	0.00E+00	0.00E+00	0.00E+00	0.00E+00	0.00E+00	0.00E+00	1.31E-03	5.85E-03	1.02E-02	1.40E-02	1.08E-02	6.39E-03	.01437
12	0.00E+00	0.00E+00	0.00E+00	0.00E+00	0.00E+00	0.00E+00	1.26E-03	5.79E-03	1.02E-02	1.39E-02	1.08E-02	6.44E-03	.01361
11	0.00E+00	0.00E+00	0.00E+00	0.00E+00	0.00E+00	0.00E+00	1.24E-03	5.96E-03	1.05E-02	1.38E-02	1.07E-02	6.38E-03	.01301
10	0.00E+00	0.00E+00	0.00E+00	0.00E+00	0.00E+00	0.00E+00	1.43E-03	6.57E-03	1.09E-02	1.35E-02	1.04E-02	6.21E-03	.01252
9	0.00E+00	0.00E+00	0.00E+00	0.00E+00	0.00E+00	0.00E+00	2.86E-03	7.80E-03	1.11E-02	1.29E-02	9.82E-03	5.89E-03	.01200
8	4.50E-06	1.17E-05	3.91E-05	1.29E-04	6.04E-04	3.35E-03	4.58E-03	7.09E-03	9.54E-03	1.10E-02	8.39E-03	5.03E-03	.01110
7	6.36E-05	8.62E-05	2.75E-04	7.65E-04	2.05E-03	4.68E-03	5.16E-03	6.14E-03	7.17E-03	7.76E-03	5.73E-03	3.36E-03	.00975
6	4.23E-05	2.36E-04	6.61E-04	1.43E-03	2.58E-03	3.69E-03	3.82E-03	4.04E-03	4.19E-03	3.92E-03	2.59E-03	1.45E-03	.00750
5	5.59E-05	2.00E-04	4.85E-04	8.68E-04	1.26E-03	1.47E-03	1.49E-03	1.49E-03	1.46E-03	1.23E-03	7.28E-04	3.84E-04	.00450
4	1.71E-05	6.53E-05	1.57E-04	2.70E-04	3.75E-04	4.21E-04	4.21E-04	4.15E-04	3.96E-04	3.06E-04	1.50E-04	6.71E-05	.00225
3	1.01E-06	8.70E-06	2.16E-05	3.76E-05	5.29E-05	5.99E-05	5.99E-05	5.89E-05	5.56E-05	3.77E-05	5.20E-06	-6.22E-06	.00090
2	0.00E+00	0.00E+00	0.00E+00	0.00E+00	0.00E+00	0.00E+00	0.00E+00	0.00E+00	0.00E+00	0.00E+00	0.00E+00	0.00E+000	.00000

X=	.00346	.00691	.00967	.01175	.01348	.01486	.01506	.01546	.01596	.01696	.01796	.01846

I	14	15	Y =
J			
15	1.36E-03	0.00E+00	1.70E-02
14	1.42E-03	0.00E+00	1.54E-02

13	1.46E-03	0.00E+00	1.44E-02
12	1.49E-03	0.00E+00	1.36E-02
11	1.49E-03	0.00E+00	1.30E-02
10	1.45E-03	0.00E+00	1.25E-02
9	1.38E-03	0.00E+00	1.20E-02
8	1.18E-03	0.00E+00	1.11E-02
7	7.63E-04	0.00E+00	9.75E-03
6	3.14E-04	0.00E+00	7.50E-03
5	7.83E-05	0.00E+00	4.50E-03
4	1.04E-05	0.00E+00	2.25E-03
3	-4.53E-06	0.00E+00	9.00E-04
2	0.00E+00	0.00E+00	0.00E+00

X= .01886 .01906

PRESSURE

J	1	2	3	4	5	6	7	8	9	10	11	12	13	Y =
15	0.00E+00	0.00E+00	0.00E+00	0.00E+00	0.00E+00	0.00E+00	0.00E+00	0.00E+00	0.00E+00	0.00E+00	0.00E+00	0.00E+00	0.00E+00	.01808
14	-2.24E-02	-2.24E-02	-2.24E-02	-2.24E-02	-2.24E-02	-2.24E-02	6.15E-01	6.15E-01	6.14E-01	6.15E-01	6.15E-01	6.15E-01	6.15E-01	.01590
13	-2.24E-02	-2.24E-02	-2.24E-02	-2.24E-02	-2.24E-02	-2.24E-02	6.74E-01	6.74E-01	6.74E-01	6.77E-01	6.79E-01	6.79E-01	6.79E-01	.01481
12	-2.24E-02	-2.24E-02	-2.24E-02	-2.24E-02	-2.24E-02	-2.24E-02	7.09E-01	7.09E-01	7.11E-01	7.18E-01	7.24E-01	7.25E-01	7.25E-01	.01393
11	-2.24E-02	-2.24E-02	-2.24E-02	-2.24E-02	-2.24E-02	-2.24E-02	7.28E-01	7.31E-01	7.40E-01	7.52E-01	7.61E-01	7.63E-01	7.63E-01	.01328
10	-2.24E-02	-2.24E-02	-2.24E-02	-2.24E-02	-2.24E-02	-2.24E-02	7.32E-01	7.46E-01	7.65E-01	7.81E-01	7.92E-01	7.95E-01	7.95E-01	.01274
9	-2.24E-02	-2.24E-02	-2.24E-02	-2.24E-02	-2.24E-02	-2.24E-02	7.33E-01	7.68E-01	7.94E-01	8.10E-01	8.21E-01	8.25E-01	8.25E-01	.01230
8	1.00E+00	9.92E-01	9.87E-01	9.82E-01	9.76E-01	9.63E-01	9.01E-01	8.67E-01	8.53E-01	8.53E-01	8.60E-01	8.65E-01	8.65E-01	.01170
7	1.00E+00	9.92E-01	9.86E-01	9.79E-01	9.67E-01	9.47E-01	9.36E-01	9.25E-01	9.16E-01	9.10E-01	9.14E-01	9.19E-01	9.19E-01	.01050
6	1.00E+00	9.92E-01	9.86E-01	9.79E-01	9.72E-01	9.64E-01	9.63E-01	9.62E-01	9.60E-01	9.59E-01	9.62E-01	9.64E-01	9.64E-01	.00900
5	1.00E+00	9.93E-01	9.88E-01	9.85E-01	9.82E-01	9.81E-01	9.82E-01	9.81E-01	9.81E-01	9.82E-01	9.84E-01	9.84E-01	9.84E-01	.00600
4	1.00E+00	9.93E-01	9.89E-01	9.87E-01	9.86E-01	9.85E-01	9.86E-01	9.86E-01	9.86E-01	9.86E-01	9.87E-01	9.88E-01	9.88E-01	.00300
3	1.00E+00	9.93E-01	9.89E-01	9.87E-01	9.85E-01	9.85E-01	9.85E-01	9.85E-01	9.85E-01	9.86E-01	9.87E-01	9.87E-01	9.87E-01	.00150
2	1.00E+00	9.93E-01	9.89E-01	9.86E-01	9.84E-01	9.84E-01	9.84E-01	9.84E-01	9.84E-01	9.85E-01	9.86E-01	9.86E-01	9.86E-01	.00030

X= .00346 .00691 .00967 .01175 .01343 .01486 .01506 .01546 .01596 .01696 .01796 .01846

J	1	14	15	Y =
15	0.00E+00	0.00E+00	1.81E-02	
14	6.15E-01	0.00E+00	1.59E-02	
13	6.79E-01	0.00E+00	1.48E-02	
12	7.25E-01	0.00E+00	1.39E-02	
11	7.64E-01	0.00E+00	1.33E-02	
10	7.98E-01	0.00E+00	1.27E-02	
9	8.28E-01	0.00E+00	1.23E-02	
8	8.70E-01	0.00E+00	1.17E-02	
7	9.25E-01	0.00E+00	1.05E-02	
6	9.71E-01	0.00E+00	9.00E-03	
5	9.88E-01	0.00E+00	6.00E-03	
4	9.89E-01	0.00E+00	3.00E-03	
3	9.87E-01	0.00E+00	1.50E-03	

```
  2  9.86E-01  0.00E+00  3.00E-04
X=     .01886     .01906
      FRICTION CONSTANT FOR CORNER FLOW:
     KC=    2.050E+02
```

D6 DUCT In DUCT, variable fluid properties are allowed for in PROPS, which is called after the temperature field T(I,J) has been updated. The input, grid specification and field initialisation routines are similar to JUNCTION and CORNER. In lines 170-200, the various conductances between the disc conductors and surrounding ducts are computed in accordance with Sec. 7.3 (see Fig. 7.1). After all of the initial output and the main iteration loop, the friction factor KF(I), and local Nusselt number NU(I) are computed in lines 387-415.

In subroutine MODU, the no-slip conditions are specified (lines 21-28). In lines 29-38, the velocity profile at the exit is adjusted from an overall continuity condition. The procedure appears to cause some minor convergence problems at the lowest flow rates. MODV and MODP introduce no additional boundary contitions and merely act as dummy subroutines. In MODT, the heat fluxes for each conductor QDOTPP(I) are determined in accordance with equations (7.14). These become the thermal boundary conditions as explained by equation (7.15) and (7.16). Listings and sample output follow.

PROGRAM MAIN

```
      PROGRAM MAIN
C     SUBROUTINE CONTRO
C
CHAPTER  0  0  0  0  0  0  0  0  PRELIMINARIES  0  0  0  0  0  0  0  0
C
      DIMENSION HEDU(6),HEDV(6),HEDP(6),HEDT(6),HEDVIS(6),HEDGAM(6)
      DIMENSION HEDDEN(6)
      DIMENSION XFRAC(22),YFRAC(9)
      REAL KF(22),NU(22),TBULK(22),TWALL(22)
      LOGICAL INCALU,INCALV,INCALP,INCALT,INPRO
      COMMON
     1/UVEL/RESORU,NSWPU,URFU,DXEPU(22),DXPWU(22),SEWU(22)
     1/VVEL/RESORV,NSWPV,URFV,DYNPV(9),DYPSV(9),SNSV(9)
     1/PCOR/RESORM,NSWPP,URFP,DU(22,9),DV(22,9),IPREF,JPREF
     1/TEMP/RESORT,NSWPT,URFT
     1/VAR/U(22,9),V(22,9),P(22,9),T(22,9),PP(22,9)
     1/ALL/IT,JT,NI,NJ,NIM1,NJM1,GREAT
     1/GEOM/X(22),Y(9),DXEP(22),DXPW(22),DYNP(9),DYPS(9),
     1       SNS(9),SEW(22),XU(22),YV(9)
     1/FLUPR/URFVIS,VISCOS,DENSIT,PRIN,DEN(22,9),VIS(22,9),
     1       GAMH(22,9),A1,A2,A3,A4,A5,A6,A7,SPHEAT,THCOND
     1/DUCT/DLEN,RHORIZ,TIN,QIN,TOUT,WHFLUX,NIM2,NJM2,FLOWIN
     1/DISC/THCPAP,WIDCON,TINSL,HITCON,HLEFT,HRITE,TLEFT,
     1       TRITE,RHO20,ALPHA,CURENT,THKCON,GC,GCP,GF,GCF,
     1       GLP,GCPP,GL,GRP,GR,RC,QDOT,TC(22),QDOTPP(22),
     1       DELTAY
      DATA HEDU /'     ','   U','  VEL','OCIT','Y   ','     '/
      DATA HEDV /'     ','   V','  VEL','OCIT','Y   ','     '/
      DATA HEDP /'     ','    ','PRES','SURE','    ','     '/
      DATA HEDT /'     ','  TE','MPER','ATUR','E   ','     '/
      DATA HEDVIS /'    ','DYNA','MIC ','VISC','OSIT','Y   '/
      DATA HEDGAM /'   T','HERM','AL E','XCH.',' COE','F.  '/
      DATA HEDDEN/'     ','    ','DENS','ITY ','    ','     '/
C-----RML 380Z FILE HANDLING STATEMENTS
      CALL OPEN(6,'RESULT  DAT',0)
      CALL OPEN(8,'DATIN   DAT',0)
      GREAT=1.0E30
C-----INITIALIZE ITERATION COUNTER
      NITER=0
C-----READ IN GRID INFORMATION DATA
      READ(8,010)IT,JT,NI,NJ
      WRITE(4,011)IT,JT,NI,NJ
      NIM1=NI-1
      NJM1=NJ-1
      READ(8,020) (XFRAC(I),I=1,NIM1)
      WRITE(4,021) (XFRAC(I),I=1,NIM1)
      READ(8,020) (YFRAC(J),J=1,NJM1)
      WRITE(4,021) (YFRAC(J),J=1,NJM1)
      READ(8,030) DLEN,RHORIZ
      WRITE(4,031) DLEN,RHORIZ
C-----READ IN SOLUTION CONTROL PARAMETERS
      READ(8,040) NSWPU,NSWPV,NSWPP,NSWPT,MAXIT,IPREF,JPREF
      WRITE(4,041) NSWPU,NSWPV,NSWPP,NSWPT,MAXIT,IPREF,JPREF
      READ(8,050) URFU,URFV,URFP,URFT,PREF,SORMAX
      WRITE(4,051) URFU,URFV,URFP,URFT,PREF,SORMAX
      READ(8,060) INCALU,INCALV,INCALP
      WRITE(4,061) INCALU,INCALV,INCALP
      READ(8,060) INCALT,INPRO
      WRITE(4,061) INCALT,INPRO
C-----READ IN FLUID PROPERTY DATA
```

```
      READ(8,070) A1,A2,A3,A4,A5,A6,A7
      WRITE(4,071) A1,A2,A3,A4,A5,A6,A7
C-----READ IN OPERATING CONDITIONS
      READ(8,080) TIN,TOUT,QIN
      WRITE(4,081) TIN,TOUT,QIN
C-----READ IN OUTPUT CONTROL PARAMETERS
      READ(8,090) IMON,JMON,INDPRI
      WRITE(4,091) IMON,JMON,INDPRI
C-----READ IN DISC PARAMETERS
      READ(8,095)THCPAP,WIDCON,TINSL,HITCON,QLEFT,QRITE,TLEFT,TRITE,
     1           RHO20,ALPHA,CURENT,THKCON,DLEFT,DRITE
      WRITE(4,096)THCPAP,WIDCON,TINSL,HITCON,QLEFT,QRITE,TLEFT,TRITE,
     1           RHO20,ALPHA,CURENT,THKCON,DLEFT,DRITE
C-----FORMAT STATEMENTS FOR CHAPTER ZERO
  010 FORMAT(4I6)
  020 FORMAT(10F8.5)
  030 FORMAT(2F8.6)
  040 FORMAT(7I6)
  050 FORMAT(6F8.6)
  060 FORMAT(3L5)
  070 FORMAT(7E13.4)
  080 FORMAT(4E13.4)
  090 FORMAT(3I6)
  095 FORMAT(7E13.4)
  011 FORMAT(1X,4I6)
  021 FORMAT(1X,10F8.5)
  031 FORMAT(1X,2F8.6)
  041 FORMAT(1X,7I6)
  051 FORMAT(1X,6F8.6)
  061 FORMAT(1X,3L5)
  071 FORMAT(1X,7E13.4)
  081 FORMAT(1X,4E13.4)
  091 FORMAT(1X,3I6)
  096 FORMAT(1X,7E13.4)
C
CHAPTER  1  1  1  1  1  SET UP GRID   1  1  1  1  1  1
C
      NIM2=NIM1-1
      NJM2=NJM1-1
C-----COMPUTE SMALLEST DX
      XSUM=XFRAC(1)/2.
      DO 100 I=2,NIM2
  100 XSUM=XSUM+XFRAC(I)
      XSUM=XSUM+XFRAC(NIM1)/2.
      DXSM=DLEN/XSUM
C-----COMPUTE SMALLEST DY
      YSUM=YFRAC(1)/2.
      DO 105 J=2,NJM2
  105 YSUM=YSUM+YFRAC(J)
      YSUM=YSUM+YFRAC(NJM1)/2.
      DYSM=RHORIZ/YSUM
C-----SET UP X-ARRAY
      X(1)=-XFRAC(1)*DXSM/2.
      DO 110 I=2,NI
  110 X(I)=X(I-1)+XFRAC(I-1)*DXSM
C-----SET UP Y-ARRAY
      Y(1)=-YFRAC(1)*DYSM/2.
      DO 115 J=2,NJ
  115 Y(J)=Y(J-1)+YFRAC(J-1)*DYSM
C
```

```
121: CHAPTER  2  2  2  2  2  2  INITIAL OPERATIONS  2  2  2  2  2  2  2  2  2
122: C
123: C-----CALCULATE INLET PROPERTY VALUES
124:       ENUIN=(EXP(EXP(A1)*(TIN+273.)**A2)-.7)/1.E8
125:       DENSIT=A3+A4*TIN
126:       VISCOS=DENSIT*ENUIN
127:       RHOCIN=A5+A6*TIN
128:       THCOND=A7
129:       SPHEAT=RHOCIN/DENSIT
130:       PRIN=VISCOS*SPHEAT/THCOND
131: C-----CALCULATE GEOMETRICAL QUANTITIES AND SET VARIABLES TO ZERO
132:       CALL INIT
133: C-----INITIALISE VARIABLE FIELDS
134: C-----ASSUME PARABOLIC VELOCITY PROFILE
135:       VIN=QIN/(RHORIZ*2.)
136:       DO 200 I=2,NI
137:       DO 200 J=2,NJM1
138:   200 U(I,J)=1.5*VIN*(1-(Y(J)/RHORIZ)**2)
139: C-----DETERMINE MASS FLOW RATE FROM ASSUMED INLET VELOCITY
140: C-----PROFILE -- THIS WILL BE USED FOR ESTABLISHING
141: C-----AN OVERALL CONTINUITY CONDITION AT THE EXIT
142:       FLOWIN=0.
143:       DO 201 J=2,NJM1
144:   201 FLOWIN=FLOWIN+SNS(J)*DENSIT*U(2,J)
145: C-----ASSUME PRESSURE FIELD IN ACCORDANCE WITH PARABOLIC
146: C-----U-VELOCITY PROFILE
147: C-----SET INLET PRESSURE UNIFORM AND EQUAL TO PREF
148:       I=2
149:       DO 202 J=2,NJM1
150:   202 P(I,J)=PREF
151: C-----CALCULATE PRESSURE DROP FROM THE STANDARD FRICTION
152: C-----FACTOR FORMULA (F=24/RE)
153:       FACTOR=1.5*VISCOS*QIN/RHORIZ**3
154:       DO 204 I=3,NIM1
155:       XDIST=X(I)-X(2)
156:       DO 204 J=2,NJM1
157:   204 P(I,J)=PREF-XDIST*FACTOR
158: C-----ASSUME UNIFORM TEMPERATURES
159:       DO 210 I=1,NIM1
160:       DO 210 J=2,NJM1
161:   210 T(I,J)=TIN
162: C-----EXIT TEMPERATURE
163:       I=NI
164:       DO 220 J=2,NJM1
165:   220 T(I,J)=TOUT
166: C-----INITIALIZE CONDUCTOR TEMPERATURES AND HEAT FLUXES TO ZERO
167:       DO 230 I=1,NI
168:       TC(I)=0.
169:   230 QDOTPP(I)=0.
170: C-----SET UP LEFT AND RIGHT EDGE CONVECTION CONDUCTANCES
171:       YD=2*(THKCON+HTCON)
172: C-----QLEFT OR QRITE EQUAL TO ZERO TO BE TAKEN AS
173: C-----AN INDICATION THAT HLEFT OR HRITE ARE TO BE SET TO
174: C-----ZERO.(FOR CONSTANT WALL HEAT FLUX RUNS)
175:      * HLEFT=0.
176:       HRITE=0.
177:       IF(QLEFT .GT. 0.)XLEFT=YD/(DLEFT*PE(QLEFT,TLEFT))
178:       IF(QRITE .GT. 0.)XRITE=YD/(DRITE*PE(QRITE,TRITE))
179:       IF(QLEFT .GT. 0.)HLEFT=HCOEF(DLEFT,XLEFT)
180:       IF(QRITE .GT. 0.)HRITE=HCOEF(DRITE,XRITE)
```

```
C-----CALCULATE CONDUCTANCES BETWEEN NODES WITHIN THE DISC
C-----FROM GEOMETRICAL AND THERMAL DATA
      DELTAY=Y(NJ)-Y(NJM1)
      GC=THCPAP*HITCON/(2.*TINSL)
      WRITE(6,2090)GC
      GCP=THCPAP*WIDCON/TINSL
      GF=THCOND*WIDCON/DELTAY
      GCF=GCP*GF/(GCP+GF)
      WRITE(6,2100)GCF
      GLP=HLEFT*HITCON
      GCPP=THCPAP*HITCON/TINSL
      GL=GLP*GCPP/(GLP+GCPP)
      WRITE(6,2110)GL
      GRP=HRITE*HITCON
      GR=GRP*GCPP/(GRP+GCPP)
      WRITE(6,2120)GR
      RC=RHO20*ALPHA*CURENT**2/(THKCON*HITCON)
      WRITE(6,2130)RC
      QDOT=RHO20*(1.-20.*ALPHA)*CURENT**2/(THKCON*HITCON)
      WRITE(6,2140)QDOT
C-----CALCULATE REYNOLDS,PRANDTL AND PECLET NUMBERS
      REIN=QIN*2.*DENSIT/VISCOS
      PRIN=VISCOS*SPHEAT/THCOND
      PEIN=REIN*PRIN
C-----INITIAL OUTPUT
      WRITE(6,2000)
      WRITE(6,2001)
C-----GRID INFORMATION DATA
      WRITE(6,2005) IT,JT,NI,NJ,DLEN,RHORIZ
      WRITE(6,2010)
      WRITE(6,2020) (XFRAC(I),I=1,NIM1)
      WRITE(6,2030)
      WRITE(6,2020) (YFRAC(J),J=1,NJM1)
C-----SOLUTION CONTROL PARAMETERS
      WRITE(6,2000)
      WRITE(6,2040) NSWPU,NSWPV,NSWPP,NSWPT,MAXIT,IPREF,JPREF,
     1URFU,URFV,URFP,URFT,PREF,SORMAX,INCALU,INCALV,INCALP,
     1INCALT,INPRO
C-----FLUID PROPERTY DATA
      WRITE(6,2000)
      WRITE(6,2050) A1,A2,A3,A4,A5,A6,A7,VISCOS,DENSIT,SPHEAT,THCOND
C-----OPERATING CONDITIONS
      WRITE(6,2060) TIN,TOUT,QIN,REIN,PRIN,PEIN
C-----OUTPUT CONTROL PARAMETERS
      WRITE(6,2000)
      WRITE(6,2070) IMON,JMON,INDPRI
      WRITE(6,2000)
      WRITE(6,2080)THCPAP,WIDCON,TINSL,HITCON,THKCON,RHO20,ALPHA,
     1              CURENT,HLEFT,HRITE,TLEFT,TRITE,
     1              QLEFT,QRITE,DLEFT,DRITE
      WRITE(6,2000)
      IF(INCALU) CALL PRINT(2,2,NI,NJ,IT,JT,XU,Y,U,HEDU)
      IF(INCALV) CALL PRINT(2,2,NI,NJ,IT,JT,X,YV,V,HEDV)
      IF(INCALP) CALL PRINT(2,2,NI,NJ,IT,JT,X,Y,P,HEDP)
      IF(INCALT) CALL PRINT(2,2,NI,NJ,IT,JT,X,Y,T,HEDT)
      IF(INPRO) CALL PRINT(2,2,NI,NJ,IT,JT,X,Y,VIS,HEDVIS)
      IF(INPRO) CALL PRINT(2,2,NI,NJ,IT,JT,X,Y,GAMH,HEDGAM)
      IF(INPRO) CALL PRINT(2,2,NI,NJ,IT,JT,X,Y,DEN,HEDDEN)
C-----FORMAT STATEMENTS FOR CHAPTER 2
 2000 FORMAT('1',120('*')/)
```

```
 2001 FORMAT('0',5X,'PARALLEL PLANE DUCT HEAT TRANSFER
     1 AND PRESSURE DROP')
 2005 FORMAT('0',5X,'GRID INFORMATION DATA'//
     1/5X,'IT-----------------------------------=',I5
     1/5X,'JT-----------------------------------=',I6
     1/5X,'NI-----------------------------------=',I5
     1/5X,'NJ-----------------------------------=',I6
     1/5X,'DUCT LENGTH--------------------------=',1PE12.3,' M'
     1/5X,'DUCT HYDRAULIC RADIUS----------------=',1PE12.3,' M')
 2010 FORMAT('0','XFRAC(I)=')
 2020 FORMAT(10X,5F7.3)
 2030 FORMAT('0','YFRAC(J)=')
 2040 FORMAT('0',5X,'SOLUTION CONTROL PARAMETERS'//
     1/5X,'NSWPU--------------------------------=',I6
     1/5X,'NSWPV--------------------------------=',I6
     1/5X,'NSWPP--------------------------------=',I6
     1/5X,'NSWPT--------------------------------=',I6
     1/5X,'MAXIT--------------------------------=',I5
     1/5X,'IPREF-------------------------- -------=',I6
     1/5X,'JPREF--------------------------------=',I6
     1/5X,'URFU---------------------------------=',1PE12.3
     1/5X,'URFV---------------------------------=',1PE12.3
     1/5X,'URFP---------------------------------=',1PE12.3
     1/5X,'URFT---------------------------------=',1PE12.3
     1/5X,'PREF---------------------------------=',1PE12.3,' PA'
     1/5X,'SORMAX-------------------------------=',1PE12.3
     1/5X,'INCALU-------------------------------=',L1
     1/5X,'INCALV-------------------------------=',L1
     1/5X,'INCALP-------------------------------=',L1
     1/5X,'INCALT-------------------------------=',L1
     1/5X,'INPRO--------------------------------=',L1)
 2050 FORMAT('0',5X,'FLUID PROPERTY DATA'//
     1/5X,'A1, VISCOSITY COEFFICIENT------------=',1PE12.3
     1/5X,'A2, VISCOSITY COEFFICIENT------------=',1PE12.3
     1/5X,'A3, DENSITY COEFFICIENT--------------=',1PE12.3,' KG/M**3'
     1/5X,'A4, DENSITY COEFFICIENT--------------=',1PE12.3,' KG/K-M**3'
     1/5X,'A5, RHO*CP COEFFICIENT---------------= ,1PE12.3,' J/K-M**3'
     1/5X,'A6, RHO*CP COEFFICIENT---------------=',1PE12.3,' J/K**2
     1-M**3'
     1/5X,'A7, THERMAL CONDUCTIVITY COEFFICIENT--=',1PE12.3,' W/M-K'
     1/5X,'INLET DYNAMIC VISCOSITY--------------=',1PE12.3,' PA-S'
     1/5X,'INLET DENSITY------------------------=',1PE12.3,' KG/M**3'
     1/5X,'INLET SPECIFIC HEAT------------------=',1PE12.3,' J/KG-K'
     1/5X,'INLET THERMAL CONDUCTIVITY-----------=',1PE12.3,' W/M-K')
 2060 FORMAT('0',5X,'OPERATING CONDITIONS'//
     1/5X,'INLET TEMPERATURE--------------------=',1PE12.3,' DEG. C'
     1/5X,'OUTLET TEMPERATURE-------------------=',1PE12.3,' DEG. C'
     1/5X,'INLET FLOW RATE----------------------=',1PE12.3,' M**2/SEC'
     1/5X,'INLET REYNOLDS NUMBER----------------=',1PE12.3
     1/5X,'INLET PRANDTL NUMBER-----------------=',1PE12.3
     1/5X,'INLET PECLET NUMBER------------------=',1PE12.3)
 2070 FORMAT('0',5X,'OUTPUT CONTROL PARAMETERS'//
     1/5X,'IMON---------------------------------=',I6
     1/5X,'JMON---------------------------------=',I5
     1/5X,'INDPPI-------------------------------=',I6)
 2080 FORMAT('0',5X,'DISC PARAMETERS'//
     1/5X,'THERMAL CONDUCTIVITY, INSULATION-----=',1PE12.3,' W/M-K'
     1/5X,'WIDTH OF INSULATED CONDUCTOR---------=',1PE12.3,' M'
     1/5X,'INSULATION THICKNESS-----------------=',1PE12.3,' M'
     1/5X,'HALF-HEIGHT OF COPPER CONDUCTOR------=',1PE12.3,' M'
```

```
      1/5X,'WIDTH OF COPPER CONDUCTOR-------------=',1PE12.3,' M'
      1/5X,'RESISTIVITY OF COPPER AT 20 DEG. C----=',1PE12.3,' OHM-M'
      1/5X,'TEMPERATURE RESISTIVITY COEFFICIENT---=',1PE12.3,' K**-1'
      1/5X,'WINDING CURRENT-----------------------=',1PE12.3,' AMPS'
      1/5X,'LEFT DISC EDGE CONVECTION CONDUCTANCE-=',1PE12.3,' W/M**2
     1-K'
      1/5X,'RIGHT DISC EDGE CONVECTION CONDUCTANCE=',1PE12.3,' W/M**2
     1-K'
      1/5X,'LEFT VERTICAL DUCT BULK FLUID TEMP.---=',1PE12.3,' DEG. C'
      1/5X,'RIGHT VERTICAL DUCT BULK FLUID TEMP---=',1PE12.3,' DEG. C'
      1/5X,'LEFT VERTICAL DUCT FLOW RATE----------=',1PE12.3,' M**2/SEC'
      1/5X,'RIGHT VERTICAL DUCT FLOW RATE---------=',1PE12.3,' M**2/SEC'
      1/5X,'LEFT VERTICAL DUCT HYDRAULIC DIA.-----=',1PE12.3,' M'
      1/5X,'RIGHT VERTICAL DUCT HYDRAULIC DIA.----=',1PE12.3,' M')
 2090 FORMAT(1X,'GC=',1PE12.3)
 2100 FORMAT(1X,'GCF=',1PE12.3)
 2110 FORMAT(1X,'GL=',1PE12.3)
 2120 FORMAT(1X,'GR=',1PE12.3)
 2130 FORMAT(1X,'RC=',1PE12.3)
 2140 FORMAT(1X,'QDOT=',1PE12.3)
C
CHAPTER  3  3  3  3  3  3  3  ITERATION LOOP  3  3  3  3  3  3  3  3  3
C
      WRITE(6,310) IMON,JMON
      WRITE(4,310) IMON,JMON
C-----INCREMENT ITERATION COUNTER
  300 NITER=NITER+1
C-----UPDATE MAIN DEPENDENT VARIABLES
      IF(INCALU) CALL CALCU
      IF(INCALV) CALL CALCV
      IF(INCALP) CALL CALCP
      IF(INCALT) CALL CALCT
C-----UPDATE FLUID PROPERITIES
      IF(INPRO) CALL PROPS
C-----CALCULATE SOURCE-NORMALIZATION FACTORS
      SNORMM=DENSIT*QIN/2.
      SNORMU=SNORMM*VIN
      SNORMV=SNORMU
C-----CALCULATE NORMALIZED SOURCES
      IF(INCALU) RESORU=RESORU/SNORMU
      IF(.NOT.INCALU) RESORU=0.
      IF(INCALV) RESORV=RESORV/SNORMV
      IF(.NOT.INCALV) RESORV=0.
      IF(INCALP) RESORM=RESORM/SNORMM
      IF(.NOT.INCALP) RESORM=0.
C-----ADJUST SNORMT FOR CHANGES IN TOTAL WALL HEAT FLUX
      WHFLUX=0.
      DO 315 I=2,NIM1
  315 WHFLUX=WHFLUX+QDOTPP(I)
      WHFLUX=WHFLUX/FLOAT(NIM2)
      SNORMT=WHFLUX*DLEN/SPHEAT
      IF(INCALT) RESORT=RESORT/SNORMT
      IF(.NOT.INCALT) RESORT=0.
C-----INTERMEDIATE OUTPUT
      WRITE(6,311) NITER,RESORU,RESORV,RESORM,RESORT,SNORMT,
     1         U(IMON,JMON),V(IMON,JMON),P(IMON,JMON),T(IMON,JMON),
     2         TC(IMON)
      WRITE(4,311) NITER,RESORU,RESORV,RESORM,RESORT,SNORMT,
     1         U(IMON,JMON),V(IMON,JMON),P(IMON,JMON),T(IMON,JMON),
     2         TC(IMON)
```

```
      IF(MOD(NITER,INDPRI).NE.0) GO TO 301
      IF(INCALU) CALL PRINT(2,2,NI,NJ,IT,JT,XU,Y,U,HEDU)
      IF(INCALV) CALL PRINT(2,2,NI,NJ,IT,JT,X,YV,V,HEDV)
      IF(INCALP) CALL PRINT(2,2,NI,NJ,IT,JT,X,Y,P,HEDP)
      IF(INCALT) CALL PRINT(2,2,NI,NJ,IT,JT,X,Y,T,HEDT)
      IF(INPRO) CALL PRINT(2,2,NI,NJ,IT,JT,X,Y,VIS,HEDVIS)
      IF(INPRO) CALL PRINT(2,2,NI,NJ,IT,JT,X,Y,GAMH,HEDGAM)
      IF(INPRO) CALL PRINT(2,2,NI,NJ,IT,JT,X,Y,DEN,HEDDEN)
      WRITE(6,310) IMON,JMON
  301 CONTINUE
C-----TERMINATION TESTS
      SORCE=AMAX1(RESORU,RESORV,RESORM,RESORT)
      IF(NITER.EQ.MAXIT) GO TO 302
      IF(NITER.EQ.20.AND.SORCE.GT.1.0E4*SORMAX) GO TO 302
      IF(SORCE.GT.SORMAX) GO TO 300
  302 CONTINUE
C
C  CHAPTER  4  4  4  4  4  4  FINAL OPERATIONS AND OUTPUT  4  4  4  4  4  4
C
      IF(INCALU) CALL PRINT(2,2,NI,NJ,IT,JT,XU,Y,U,HEDU)
      IF(INCALV) CALL PRINT(2,2,NI,NJ,IT,JT,X,YV,V,HEDV)
      IF(INCALP) CALL PRINT(2,2,NI,NJ,IT,JT,X,Y,P,HEDP)
      IF(INCALT) CALL PRINT(2,2,NI,NJ,IT,JT,X,Y,T,HEDT)
      IF(INPRO) CALL PRINT(2,2,NI,NJ,IT,JT,X,Y,VIS,HEDVIS)
      IF(INPRO) CALL PRINT(2,2,NI,NJ,IT,JT,X,Y,GAMH,HEDGAM)
      IF(INPRO) CALL PRINT(2,2,NI,NJ,IT,JT,X,Y,DEN,HEDDEN)
C-----CALCULATE PRESSURE DROP NORMALIZATION FACTOR
      PFAC=(4.*RHORIZ)**2/(2.*VIN*VISCOS)
C     CALCULATE AVERAGE PRESSURE DROP AND FRICTION CONSTANT
      DO 400 I=3,NIM1
      XDIST=X(I)-X(2)
      PAVI=0.
      DO 405 J=2,NJM1
  405 PAVI=PAVI+P(I,J)
      PAVI=PAVI/FLOAT(NJM2)
  400 KF(I)=(PREF-PAVI)*PFAC/XDIST
C-----CALCULATE WALL TEMPERATURE ASSUMING A LINEAR TEMPERATURE
C-----PROFILE NEAR THE WALL
      DO 410 I=2,NIM1
      DELTAT=QDOTPP(I)*DELTAY/THCOND
  410 TWALL(I)=T(I,NJM1)+DELTAT
C-----CALCULATE BULK FLUID TEMPERATURE BY NUMERICAL INTEGRATION
C-----OF THE VELOCITY TEMPERATURE PRODUCT
      DO 420 I=2,NIM1
      TSUM=0.
      VMEAN=0.
      DO 425 J=2,NJM1
      UAV=0.5*(U(I,J)+U(I+1,J))
      TSUM=TSUM+SNS(J)*UAV*T(I,J)
  425 VMEAN=VMEAN+SNS(J)*UAV/RHORIZ
  420 TBULK(I)=TSUM/(VMEAN*RHORIZ)
C-----CALCULATE NUSSELT NUMBER
      DO 430 I=2,NIM1
      H=QDOTPP(I)/(TWALL(I)-TBULK(I))
  430 NU(I)=H*4.*RHORIZ/THCOND
C-----FINAL OUTPUT
      WRITE(6,2000)
      WRITE(6,4000)
      KF(2)=0.
      DO 440 I=2,NIM1
```

```
C-----CALCULATE THERMAL ENTRY LENGTH DIMENSIONLESS DISTANCE
      XSTAR=X(I)/(4.*RHORIZ*PEIN)
  440 WRITE(6,4010) X(I),XSTAR,TWALL(I),TBULK(I),NU(I),RF(I)
C-----WRITE OUT CONDUCTOR TEMPERATURES
      WRITE(6,4015)
      DO 450 I=2,NIM1
  450 WRITE(6,4020)X(I),TC(I),QDOTPP(I)
      STOP
C-----FORMAT STATEMENTS
310   FORMAT(1H0,'ITER   ','I--------------ABSOLUTE RESIDUAL SOURCE SUM
     1S--------------I   I-------FIELD VALUES AT MONITORING LOCATION' '
     2(',I2,',',I2,')','--------I' / 2X,'NO.',5X,'UMOM',6X,'VMOM',6X,'MA
     3SS',6X,'ENER',6X,'SNORMT',4X,'     ',10X,'U',9X,'V',9X,'P',9X,
     4'T',9X,'TC',8X,' ')
311   FORMAT(1H ,I3,3X,1P5E10.3,15X,1P5E10.3)
4000  FORMAT(23X,'HEAT TRANSFER AND PRESSURE DROP SUMMARY'
     1//'0',5X,'X',8X,'X*',7X,'WALL TEMPERATURE',4X,'BULK FLUID
     1 TEMPERATURE',4X,'NUSSELT NUMBER',4X,'FRICTION CONSTANT'//)
4010  FORMAT(1X,F7.5,' M',3X,F9.1,4X,F7.2,' DEG C',10X,F7.2,' DEG C',
     110X,F8.3,11X,F8.3)
4015  FORMAT(23X,'WINDING TEMPERATURES AND HEAT FLUXES'
     1//'0',5X,'X',8X,'CONDUCTOR TEMPERATURE',4X,'CONDUCTOR
     1 HEAT FLUX'//)
4020  FORMAT(1X,F7.5,' M',11X,F7.2,' DEG. C',4X,1PE12.3,' W/M**2')
      END
```

SUBROUTINE MODU

```
      SUBROUTINE MODU
      COMMON
     1/UVEL/RESORU,NSWPU,URFU,DXEPU(22),DXPWU(22),SEWU(22)
     1/PCOR/RESORM,NSWPP,URFP,DU(22,9),DV(22,9),IPREF,JPREF
     1/TEMP/RESORT,NSWPT,URFT
     1/VAR/U(22,9),V(22,9),P(22,9),T(22,9),PP(22,9)
     1/ALL/IT,JT,NI,NJ,NIM1,NJM1,GREAT
     1/GEOM/X(22),Y(9),DXEP(22),DXPW(22),DYNP(9),DYPS(9),
     1       SNS(9),SEW(22),XU(22),YV(9)
      1/FLUPR/URFVIS,VISCOS,DENSIT,PRIN,DEN(22,9),VIS(22,9),
      1        GAMH(22,9),A1,A2,A3,A4,A5,A6,A7,SPHEAT,THCOND
      1/DUCT/DLEN,RHORIZ,TIN,QIN,TOUT,WHFLUX,NIM2,NJM2,FLOWIN
      1/COEF/AP(22,9),AN(22,9),AS(22,9),AE(22,9),AW(22,9),SU(22,9),
      1       SP(22,9)
C-----SYMMETRY CONDITION AT DUCT CENTRE-LINE
C-----SET SOUTH COMBINED CONVECTION/DIFFUSION COEFFICIENT
C-----TO ZERO
       J=2
       DO 100 I=3,NIM1
  100 AS(I,J)=0.
C-----NO SLIP CONDITION ON U-VELOCITIES AT DUCT WALL
C-----CALCULATE DISTANCE FROM U(I,NJM1) TO WALL
       J=NJM1
       YDELT=YV(NJ)-Y(NJM1)
C-----INSERT WALL INFLUENCE AS A MOMENTUM SINK
       DO 110 I=3,NIM1
       AN(I,J)=0.
  110 SP(I,J)=SP(I,J)-VIS(I,J)*SEWU(I)/YDELT
C-----DETERMINE OUTLET VELOCITIES FROM OVER ALL CONTINUITY CONDITION
       ARDEN=0.
       FLOW=0.
       DO 120 J=2,NJM1
       DENAR=0.5*(DEN(NIM1,J)+DEN(NIM2,J))*SNS(J)
       ARDEN=ARDEN+DENAR
  120 FLOW=FLOW+DENAR*U(NIM1,J)
       UINC=(FLOWIN-FLOW)/ARDEN
       DO 130 J=2,NJM1
  130 U(NI,J)=U(NIM1,J)+UINC
       RETURN
       END
```

SUBROUTINE MODV

```
      SUBROUTINE MODV
      COMMON
     1/VVEL/RESORV,NSWPV,URFV,DYNPV(9),DYPSV(9),SNSV(9)
     1/TEMP/RESORT,NSWPT,URFT
     1/VAR/U(22,9),V(22,9),P(22,9),T(22,9),PP(22,9)
     1/ALL/IT,JT,NI,NJ,NIM1,NJM1,GREAT
     1/GEOM/X(22),Y(9),DXEP(22),DXPW(22),DYNP(9),DYPS(9),
     1       SNS(9),SEW(22),XU(22),YV(9)
     1/FLUPR/URFVIS,VISCOS,DENSIT,PRIN,DEN(22,9),VIS(22,9),
      1        GAMH(22,9),A1,A2,A3,A4,A5,A6,A7,SPHEAT,THCOND
      1/DUCT/DLEN,RHORIZ,TIN,QIN,TOUT,WHFLUX,NIM2,NJM2,FLOWIN
      1/COEF/AP(22,9),AN(22,9),AS(22,9),AE(22,9),AW(22,9),SU(22,9),
      1       SP(22,9)
C-----NO MODIFICATIONS FOR THIS PROBLEM
       RETURN
       END
```

SUBROUTINE MODP

```
      SUBROUTINE MODP
      COMMON
     1/FCOR/RESORM,NEWPP,URFP,DU(22,9),DV(22,9),IPREF,JPREF
     1/VAR/U(22,9),V(22,9),P(22,9),T(22,9),PP(22,9)
     1/ALL/IT,JT,NI,NJ,NIM1,NJM1,GREAT
     1/GEOM/X(22),Y(9),DXEP(22),DXPW(22),DYNP(9),DYPS(9),
     1       SNS(9),SEW(22),XU(22),YV(9)
     1/FLUPR/URFVIS,VISCOS,DENSIT,PRIN,DEN(22,9),VIS(22,9),
     1        GAMH(22,9),A1,A2,A3,A4,A5,A6,A7,SPHEAT,THCOND
      1/DUCT/DLEN,RHORIC,TIN,QIN,TOUT,WHFLUX,NIM2,NJM2,FLOWIN
      1/COEF/AP(22,9),AN(22,9),AS(22,9),AE(22,9),AW(22,9),SU(22,9),
     1       SP(22,9)
C-----NO MODIFICATIONS FOR THIS PROBLEM
      RETURN
      END
```

SUBROUTINE MODT

```
      SUBROUTINE MODT
      DIMENSION A(22),B(22),C(22),D(22)
      COMMON
     1/UVEL/RESORU,NSWPU,URFU,DXEPU(22),DXPWU(22),SEWU(22)
     1/VVEL/RESORV,NSWPV,URFV,DYNPV(9),DYPSV(9),SNSV(9)
     1/PCOR/RESORM,NSWPP,URFP,DU(22,9),DV(22,9),IPREF,JPREF
     1/TEMP/RESORT,NSWPT,URFT
     1/VAR/U(22,9),V(22,9),P(22,9),T(22,9),PP(22,9)
     1/ALL/IT,JT,NI,NJ,NIM1,NJM1,GREAT
      1/GEOM/X(22),Y(9),DXEP(22),DXPW(22),DYNP(9),DYPS(9),
     1       SNS(9),SEW(22),XU(22),YV(9)
      1/FLUPR/URFVIS,VISCOS,DENSIT,PRIN,DEN(22,9),VIS(22,9),
     1        GAMH(22,9),A1,A2,A3,A4,A5,A6,A7,SPHEAT,THCOND
      1/DUCT/DLEN,RHORIZ,TIN,QIN,TOUT,WHFLUX,NIM2,NJM2,FLOWIN
      1/COEF/AP(22,9),AN(22,9),AS(22,9),AE(22,9),AW(22,9),SU(22,9),
     1       SP(22,9)
      1/DISC/THCPAP,WIDCON,TINSL,HITCON,HLEFT,HRITE,TLEFT,
     1       TRITE,RHO20,ALPHA,CURENT,THKCON,GC,GCP,GF,GCF,
     1       GLP,GCPP,GL,GRP,GR,RC,QDOT,TC(22),QDOTPP(22),
     1       DELTAY
C-----SET NORTH COMBINED CONVECTION/DIFFUSION
C-----COEFFICIENT TO ZERO
      J=NJM1
      DO 100 I=2,NIM1
  100 AN(I,J)=0.
C-----SYMMETRY CONDITION AT DUCT CENTRE-LINE
      J=2
      DO 105 I=2,NIM1
  105 AS(I,J)=0.
C-----DETERMINE WALL HEAT FLUXES FROM
C-----SOLVING THE CONDUCTION IN THE
C-----DISC, USING EACH CONDUCTOR AS
C-----NODE. THE TDMA WILL BE USED TO
C-----SOLVE FOR THE CONDUCTOR TEMPERATURES.
      A(1)=0.
      A(2)=GC
      B(1)=0.
      B(2)=0.
      C(1)=0.
      C(2)=QDOT+GL*TLEFT+GCF*T(2,NJM1)
      D(1)=0.
      D(2)=GC+GCF+GL-RC
      DO 110 I=3,NIM2
      D(I)=2*GC+GCF-RC
      A(I)=GC
      B(I)=GC
  110 C(I)=QDOT+GCF*T(I,NJM1)
      A(NIM1)=0.
      A(NI)=0.
      B(NIM1)=GC
      B(NI)=0.
      C(NIM1)=QDOT+GR*TRITE+GCF*T(NIM1,NJM1)
      C(NI)=0.
      D(NIM1)=GC+GCF+GR-RC
      D(NI)=0.
      DO 120 I=2,NIM1
      TERM=1./(D(I)-B(I)*A(I-1))
      A(I)=A(I)*TERM
  120 C(I)=(C(I)+B(I)*C(I-1))*TERM
      DO 130 II=2,NIM1
      I=NI+1-II
  130 TC(I)=A(I)*TC(I+1)+C(I)
      DO 140 I=2,NIM1
  140 QDOTPP(I)=GCF*(TC(I)-T(I,NJM1))/WIDCON
      J=NJM1
      DO 150 I=2,NIM1
      TERM=GAMH(I,J)*SEW(I)/THCOND
  150 SU(I,J)=SU(I,J)+TERM*QDOTPP(I)
      RETURN
      END
```

Output file RESULT.DAT follows. Since, in DUCT, all input data is printed in RESULT.DAT, DATIN.DAT has not been included here.

```
GC=    5.160E-01
GCF=    8.282E-01
GL=    7.905E-01
GR=    6.181E-01
RC=    3.570E-02
QDOT=     8.370E+00
```

****

PARALLEL PLANE DUCT HEAT TRANSFER AND PRESSURE DROP

GRID INFORMATION DATA

```
    IT-----------------------------------=     22
    JT-----------------------------------=      9
    NI-----------------------------------=     22
    NJ-----------------------------------=      9
    DUCT LENGTH--------------------------=   1.000E-01 M
    DUCT HYDRAULIC RADIUS----------------=   2.270E-03 M

XFRAC(I)=
           1.000  1.000  1.000  1.000  1.000
           1.000  1.000  1.000  1.000  1.000
           1.000  1.000  1.000  1.000  1.000
           1.000  1.000  1.000  1.000  1.000
           1.000

YFRAC(J)=
          16.000 12.000  8.000  6.000  4.000
           3.000  2.000  1.000
```

****

SOLUTION CONTROL PARAMETERS

```
    NSWPU--------------------------------=      5
```

```
NSWPV-------------------------------=     2
NSWPP-------------------------------=    20
NSWPT-------------------------------=     2
MAXIT-------------------------------=   200
IPREF-------------------------------=     2
JPREF-------------------------------=     2
URFU--------------------------------=   5.000E-01
URFV--------------------------------=   5.000E-01
URFP--------------------------------=   1.000E+00
URFT--------------------------------=   1.000E+00
PREF--------------------------------=   1.000E+00 PA
SORMAX------------------------------=   1.000E-02
INCALU-----------------------------=T
INCALV-----------------------------=T
INCALP-----------------------------=T
INCALT-----------------------------=T
INPRO------------------------------=T
```

****

FLUID PROPERTY DATA

```
A1, VISCOSITY COEFFICIENT-----------=   2.466E+01
A2, VISCOSITY COEFFICIENT-----------=  -4.123E+00
A3, DENSITY COEFFICIENT-------------=   8.890E+02 KG/M**3
A4, DENSITY COEFFICIENT-------------=  -7.000E-01 KG/K-M**3
A5, RHO*CP COEFFICIENT--------------=   1.600E+06 J/K-M**3
A6, RHO*CP COEFFICIENT--------------=   1.800E+03 J/K**2-M**3
A7, THERMAL CONDUCTIVITY COEFFICIENT--=   1.170E-01 W/M-K
INLET DYNAMIC VISCOSITY-------------=   6.042E-03 PA-S
INLET DENSITY-----------------------=   8.478E+02 KG/M**3
INLET SPECIFIC HEAT-----------------=   2.012E+03 J/KG-K
INLET THERMAL CONDUCTIVITY----------=   1.170E-01 W/M-K
```

OPERATING CONDITIONS

```
INLET TEMPERATURE-------------------=   5.890E+01 DEG. C
OUTLET TEMPERATURE------------------=   6.050E+01 DEG. C
INLET FLOW RATE---------------------=   1.524E-04 M**2/SEC
INLET REYNOLDS NUMBER---------------=   4.277E+01
INLET PRANDTL NUMBER----------------=   1.039E+02
INLET PECLET NUMBER-----------------=   4.444E+03
```

****

OUTPUT CONTROL PARAMETERS

INON	21
JMON	8
INDPRI	100

****

DISC PARAMETERS

THERMAL CONDUCTIVITY, INSULATION	1.720E-01	W/M-K
WIDTH OF INSULATED CONDUCTOR	5.000E-03	M
INSULATION THICKNESS	1.000E-03	M
HALF-HEIGHT OF COPPER CONDUCTOR	6.000E-03	M
WIDTH OF COPPER CONDUCTOR	3.000E-03	M
RESISTIVITY OF COPPER AT 20 DEG. C	1.720E-08	OHM-M
TEMPERATURE RESISTIVITY COEFFICIENT	3.930E-03	K**-1
WINDING CURRENT	9.750E+01	AMPS
LEFT DISC EDGE CONVECTION CONDUCTANCE	5.631E+02	W/M**2-K
RIGHT DISC EDGE CONVECTION CONDUCTANCE	2.569E+02	W/M**2-K
LEFT VERTICAL DUCT BULK FLUID TEMP.	5.890E+01	DEG. C
RIGHT VERTICAL DUCT BULK FLUID TEMP	6.050E+01	DEG. C
LEFT VERTICAL DUCT FLOW RATE	3.940E-04	M**2/SEC
RIGHT VERTICAL DUCT FLOW RATE	1.520E-04	M**2/SEC
LEFT VERTICAL DUCT HYDRAULIC DIA.	8.000E-03	M
RIGHT VERTICAL DUCT HYDRAULIC DIA.	1.614E-02	M

****

U VELOCITY

J \ I	2	3	4	5	6	7	8	9	10	11	12	13	Y =
9	0.00E+00	0.00E+00	0.00E+00	0.00E+00	0.00E+00	0.00E+00	0.00E+00	0.00E+00	0.00E+00	0.00E+00	0.00E+00	0.00E+00	.00230
8	1.15E-03	1.15E-03	1.15E-03	1.15E-03	1.15E-03	1.15E-03	1.15E-03	1.15E-03	1.15E-03	1.15E-03	1.15E-03	1.15E-03	.00224
7	5.62E-03	5.62E-03	5.62E-03	5.62E-03	5.62E-03	5.62E-03	5.62E-03	5.62E-03	5.62E-03	5.62E-03	5.62E-03	5.62E-03	.00211
6	1.19E-02	1.19E-02	1.19E-02	1.19E-02	1.19E-02	1.19E-02	1.19E-02	1.19E-02	1.19E-02	1.19E-02	1.19E-02	1.19E-02	.00198
5	1.96E-02	1.96E-02	1.96E-02	1.96E-02	1.96E-02	1.96E-02	1.96E-02	1.96E-02	1.96E-02	1.96E-02	1.96E-02	1.96E-02	.00177
4	2.95E-02	2.95E-02	2.95E-02	2.95E-02	2.95E-02	2.95E-02	2.95E-02	2.95E-02	2.95E-02	2.95E-02	2.95E-02	2.95E-02	.00146
3	3.97E-02	3.97E-02	3.97E-02	3.97E-02	3.97E-02	3.97E-02	3.97E-02	3.97E-02	3.97E-02	3.97E-02	3.97E-02	3.97E-02	.00104
2	4.86E-02	4.86E-02	4.86E-02	4.86E-02	4.86E-02	4.86E-02	4.86E-02	4.86E-02	4.86E-02	4.86E-02	4.86E-02	4.86E-02	.00042

X=	0.00000	.00500	.01000	.01500	.02000	.02500	.03000	.03500	.04000	.04500	.05000	.05500

J \ I	14	15	16	17	18	19	20	21	22	Y =
9	0.00E+00	0.00E+00	0.00E+00	0.00E+00	0.00E+00	0.00E+00	0.00E+00	0.00E+00	0.00E+00	2.30E-03
8	1.15E-03	1.15E-03	1.15E-03	1.15E-03	1.15E-03	1.15E-03	1.15E-03	1.15E-03	1.15E-03	2.24E-03
7	5.62E-03	5.62E-03	5.62E-03	5.62E-03	5.62E-03	5.62E-03	5.62E-03	5.62E-03	5.62E-03	2.14E-03
6	1.19E-02	1.19E-02	1.19E-02	1.19E-02	1.19E-02	1.19E-02	1.19E-02	1.19E-02	1.19E-02	1.98E-03
5	1.96E-02	1.96E-02	1.96E-02	1.96E-02	1.96E-02	1.96E-02	1.96E-02	1.96E-02	1.96E-02	1.77E-03
4	2.95E-02	2.95E-02	2.95E-02	2.95E-02	2.95E-02	2.95E-02	2.95E-02	2.95E-02	2.95E-02	1.46E-03
3	3.97E-02	3.97E-02	3.97E-02	3.97E-02	3.97E-02	3.97E-02	3.97E-02	3.97E-02	3.97E-02	1.04E-03
2	4.86E-02	4.86E-02	4.86E-02	4.86E-02	4.86E-02	4.86E-02	4.86E-02	4.86E-02	4.86E-02	4.17E-04

X=	.06000	.06500	.07000	.07500	.08000	.08500	.09000	.09500	.10000

V VELOCITY

J \ I	2	3	4	5	6	7	8	9	10	11	12	13	Y =
9	0.00E+00	0.00E+00	0.00E+00	0.00E+00	0.00E+00	0.00E+00	0.00E+00	0.00E+00	0.00E+00	0.00E+00	0.00E+00	0.00E+00	.00227
8	0.00E+00	0.00E+00	0.00E+00	0.00E+00	0.00E+00	0.00E+00	0.00E+00	0.00E+00	0.00E+00	0.00E+00	0.00E+00	0.00E+00	.00219
7	0.00E+00	0.00E+00	0.00E+00	0.00E+00	0.00E+00	0.00E+00	0.00E+00	0.00E+00	0.00E+00	0.00E+00	0.00E+00	0.00E+00	.00206
6	0.00E+00	0.00E+00	0.00E+00	0.00E+00	0.00E+00	0.00E+00	0.00E+00	0.00E+00	0.00E+00	0.00E+00	0.00E+00	0.00E+00	.00188
5	0.00E+00	0.00E+00	0.00E+00	0.00E+00	0.00E+00	0.00E+00	0.00E+00	0.00E+00	0.00E+00	0.00E+00	0.00E+00	0.00E+00	.00162
4	0.00E+00	0.00E+00	0.00E+00	0.00E+00	0.00E+00	0.00E+00	0.00E+00	0.00E+00	0.00E+00	0.00E+00	0.00E+00	0.00E+00	.00125
3	0.00E+00	0.00E+00	0.00E+00	0.00E+00	0.00E+00	0.00E+00	0.00E+00	0.00E+00	0.00E+00	0.00E+00	0.00E+00	0.00E+00	.00073
2	0.00E+00	0.00E+00	0.00E+00	0.00E+00	0.00E+00	0.00E+00	0.00E+00	0.00E+00	0.00E+00	0.00E+00	0.00E+00	0.00E+000	.00000

X=	.00250	.00750	.01250	.01750	.02250	.02750	.03250	.03750	.04250	.04750	.05250	.05750

J \ I	14	15	16	17	18	19	20	21	22	Y =
9	0.00E+00	0.00E+00	0.00E+00	0.00E+00	0.00E+00	0.00E+00	0.00E+00	0.00E+00	0.00E+00	2.27E-03
8	0.00E+00	0.00E+00	0.00E+00	0.00E+00	0.00E+00	0.00E+00	0.00E+00	0.00E+00	0.00E+00	2.19E-03
7	0.00E+00	0.00E+00	0.00E+00	0.00E+00	0.00E+00	0.00E+00	0.00E+00	0.00E+00	0.00E+00	2.06E-03
6	0.00E+00	0.00E+00	0.00E+00	0.00E+00	0.00E+00	0.00E+00	0.00E+00	0.00E+00	0.00E+00	1.88E-03
5	0.00E+00	0.00E+00	0.00E+00	0.00E+00	0.00E+00	0.00E+00	0.00E+00	0.00E+00	0.00E+00	1.62E-03
4	0.00E+00	0.00E+00	0.00E+00	0.00E+00	0.00E+00	0.00E+00	0.00E+00	0.00E+00	0.00E+00	1.25E-03
3	0.00E+00	0.00E+00	0.00E+00	0.00E+00	0.00E+00	0.00E+00	0.00E+00	0.00E+00	0.00E+00	7.31E-04

2	0.00E+00	0.00E+00	0.00E+00	0.00E+00	0.00E+00	0.00E+00	0.00E+00	0.00E+00	0.00E+00	0.00E+00

X=	.06250	.06750	.07250	.07750	.08250	.08750	.09250	.09750	.10250

PRESSURE

I	2	3	4	5	6	7	8	9	10	11	12	13	Y =
J													
9	0.00E+00	0.00E+00	0.00E+00	0.00E+00	0.00E+00	0.00E+00	0.00E+00	0.00E+00	0.00E+00	0.00E+00	0.00E+00	0.00E+00	.00230
8	1.00E+00	4.10E-01	-1.81E-01	-7.71E-01	-1.36E+00	-1.95E+00	-2.54E+00	-3.13E+00	-3.72E+00	-4.31E+00	-4.90E+00	-5.49E+00	.00224
7	1.00E+00	4.10E-01	-1.81E-01	-7.71E-01	-1.36E+00	-1.95E+00	-2.54E+00	-3.13E+00	-3.72E+00	-4.31E+00	-4.90E+00	-5.49E+00	.00214
6	1.00E+00	4.10E-01	-1.81E-01	-7.71E-01	-1.36E+00	-1.95E+00	-2.54E+00	-3.13E+00	-3.72E+00	-4.31E+00	-4.90E+00	-5.49E+00	.00198
5	1.00E+00	4.10E-01	-1.81E-01	-7.71E-01	-1.36E+00	-1.95E+00	-2.54E+00	-3.13E+00	-3.72E+00	-4.31E+00	-4.90E+00	-5.49E+00	.00177
4	1.00E+00	4.10E-01	-1.81E-01	-7.71E-01	-1.36E+00	-1.95E+00	-2.54E+00	-3.13E+00	-3.72E+00	-4.31E+00	-4.90E+00	-5.49E+00	.00146
3	1.00E+00	4.10E-01	-1.81E-01	-7.71E-01	-1.36E+00	-1.95E+00	-2.54E+00	-3.13E+00	-3.72E+00	-4.31E+00	-4.90E+00	-5.49E+00	.00104
2	1.00E+00	4.10E-01	-1.81E-01	-7.71E-01	-1.36E+00	-1.95E+00	-2.54E+00	-3.13E+00	-3.72E+00	-4.31E+00	-4.90E+00	-5.49E+00	.00012

X=	.00250	.00750	.01250	.01750	.02250	.02750	.03250	.03750	.04250	.04750	.05250	.05750

I	14	15	16	17	18	19	20	21	22	Y =
J										
9	0.00E+00	0.00E+00	0.00E+00	0.00E+00	0.00E+00	0.00E+00	0.00E+00	0.00E+00	0.00E+00	2.30E-03
8	-6.08E+00	-6.67E+00	-7.27E+00	-7.86E+00	-8.45E+00	-9.04E+00	-9.63E+00	-1.02E+01	0.00E+00	2.24E-03
7	-6.08E+00	-6.67E+00	-7.27E+00	-7.86E+00	-8.45E+00	-9.04E+00	-9.63E+00	-1.02E+01	0.00E+00	2.14E-03
6	-6.08E+00	-6.67E+00	-7.27E+00	-7.86E+00	-8.45E+00	-9.04E+00	-9.63E+00	-1.02E+01	0.00E+00	1.98E-03
5	-6.08E+00	-6.67E+00	-7.27E+00	-7.86E+00	-8.45E+00	-9.04E+00	-9.63E+00	-1.02E+01	0.00E+00	1.77E-03
4	-6.08E+00	-6.67E+00	-7.27E+00	-7.86E+00	-8.45E+00	-9.04E+00	-9.63E+00	-1.02E+01	0.00E+00	1.46E-03
3	-6.08E+00	-6.67E+00	-7.27E+00	-7.86E+00	-8.45E+00	-9.04E+00	-9.63E+00	-1.02E+01	0.00E+00	1.04E-03
2	-6.08E+00	-6.67E+00	-7.27E+00	-7.86E+00	-8.45E+00	-9.04E+00	-9.63E+00	-1.02E+01	0.00E+00	4.17E-04

X=	.06250	.06750	.07250	.07750	.08250	.08750	.09250	.09750	.10250

TEMPERATURE

I	2	3	4	5	6	7	8	9	10	11	12	13	Y =
J													
9	0.00E+00	0.00E+00	0.00E+00	0.00E+00	0.00E+00	0.00E+00	0.00E+00	0.00E+00	0.00E+00	0.00E+00	0.00E+00	0.00E+00	.00230
8	5.89E+01	5.89E+01	5.89E+01	5.89E+01	5.89E+01	5.89E+01	5.89E+01	5.89E+01	5.89E+01	5.89E+01	5.89E+01	5.89E+01	.00224
7	5.89E+01	5.89E+01	5.89E+01	5.89E+01	5.89E+01	5.89E+01	5.89E+01	5.89E+01	5.89E+01	5.89E+01	5.89E+01	5.89E+01	.00214
6	5.89E+01	5.89E+01	5.89E+01	5.89E+01	5.89E+01	5.89E+01	5.89E+01	5.89E+01	5.89E+01	5.89E+01	5.89E+01	5.89E+01	.00198
5	5.89E+01	5.89E+01	5.89E+01	5.89E+01	5.89E+01	5.89E+01	5.89E+01	5.89E+01	5.89E+01	5.89E+01	5.89E+01	5.89E+01	.00177
4	5.89E+01	5.89E+01	5.89E+01	5.89E+01	5.89E+01	5.89E+01	5.89E+01	5.89E+01	5.89E+01	5.89E+01	5.89E+01	5.89E+01	.00146
3	5.89E+01	5.89E+01	5.89E+01	5.89E+01	5.89E+01	5.89E+01	5.89E+01	5.89E+01	5.89E+01	5.89E+01	5.89E+01	5.89E+01	.00104
2	5.89E+01	5.89E+01	5.89E+01	5.89E+01	5.89E+01	5.89E+01	5.89E+01	5.89E+01	5.89E+01	5.89E+01	5.89E+01	5.89E+01	.00012

X=	.00250	.00750	.01250	.01750	.02250	.02750	.03250	.03750	.04250	.04750	.05250	.05750

I	14	15	16	17	18	19	20	21	22	Y =
J										
9	0.00E+00	0.00E+00	0.00E+00	0.00E+00	0.00E+00	0.00E+00	0.00E+00	0.00E+00	0.00E+00	2.30E-03
8	5.89E+01	5.89E+01	5.89E+01	5.89E+01	5.89E+01	5.89E+01	5.89E+01	5.89E+01	6.05E+01	2.24E-03
7	5.89E+01	5.89E+01	5.89E+01	5.89E+01	5.89E+01	5.89E+01	5.89E+01	5.89E+01	6.05E+01	2.14E-03
6	5.89E+01	5.89E+01	5.89E+01	5.89E+01	5.89E+01	5.89E+01	5.89E+01	5.89E+01	6.05E+01	1.98E-03
5	5.89E+01	5.89E+01	5.89E+01	5.89E+01	5.89E+01	5.89E+01	5.89E+01	5.89E+01	6.05E+01	1.77E-03

4	5.89E+01	5.89E+01	5.89E+01	5.89E+01	5.89E+01	5.89E+01	5.89E+01	5.89E+01	6.05E+01	1.46E-03
3	5.89E+01	5.89E+01	5.89E+01	5.89E+01	5.89E+01	5.89E+01	5.89E+01	5.89E+01	6.05E+01	1.04E-03
2	5.89E+01	5.89E+01	5.89E+01	5.89E+01	5.89E+01	5.89E+01	5.89E+01	5.89E+01	6.05E+01	4.17E-04

X= .06250 .06750 .07250 .07750 .08250 .08750 .09250 .09750 .10250

DYNAMIC VISCOSITY

J \ I	2	3	4	5	6	7	8	9	10	11	12	13	Y =
9	6.04E-03	6.04E-03	6.04E-03	6.04E-03	6.04E-03	6.04E-03	6.04E-03	6.04E-03	6.04E-03	6.04E-03	6.04E-03	6.04E-03	.00230
8	6.04E-03	6.04E-03	6.04E-03	6.04E-03	6.04E-03	6.04E-03	6.04E-03	6.04E-03	6.04E-03	6.04E-03	6.04E-03	6.04E-03	.00224
7	6.04E-03	6.04E-03	6.04E-03	6.04E-03	6.04E-03	6.04E-03	6.04E-03	6.04E-03	6.04E-03	6.04E-03	6.04E-03	6.04E-03	.00214
6	6.04E-03	6.04E-03	6.04E-03	6.04E-03	6.04E-03	6.04E-03	6.04E-03	6.04E-03	6.04E-03	6.04E-03	6.04E-03	6.04E-03	.00198
5	6.04E-03	6.04E-03	6.04E-03	6.04E-03	6.04E-03	6.04E-03	6.04E-03	6.04E-03	6.04E-03	6.04E-03	6.04E-03	6.04E-03	.00177
4	6.04E-03	6.04E-03	6.04E-03	6.04E-03	6.04E-03	6.04E-03	6.04E-03	6.04E-03	6.04E-03	6.04E-03	6.04E-03	6.04E-03	.00146
3	6.04E-03	6.04E-03	6.04E-03	6.04E-03	6.04E-03	6.04E-03	6.04E-03	6.04E-03	6.04E-03	6.04E-03	6.04E-03	6.04E-03	.00104
2	6.04E-03	6.04E-03	6.04E-03	6.04E-03	6.04E-03	6.04E-03	6.04E-03	6.04E-03	6.04E-03	6.04E-03	6.04E-03	6.04E-03	.00042

X= .00250 .00750 .01250 .01750 .02250 .02750 .03250 .03750 .04250 .04750 .05250 .05750

J \ I	14	15	16	17	18	19	20	21	22	Y =
9	6.04E-03	6.04E-03	6.04E-03	6.04E-03	6.04E-03	6.04E-03	6.04E-03	6.04E-03	6.04E-03	2.30E-03
8	6.04E-03	6.04E-03	6.04E-03	6.04E-03	6.04E-03	6.04E-03	6.04E-03	6.04E-03	6.04E-03	2.24E-03
7	6.04E-03	6.04E-03	6.04E-03	6.04E-03	6.04E-03	6.04E-03	6.04E-03	6.04E-03	6.04E-03	2.14E-03
6	6.04E-03	6.04E-03	6.04E-03	6.04E-03	6.04E-03	6.04E-03	6.04E-03	6.04E-03	6.04E-03	1.98E-03
5	6.04E-03	6.04E-03	6.04E-03	6.04E-03	6.04E-03	6.04E-03	6.04E-03	6.04E-03	6.04E-03	1.77E-03
4	6.04E-03	6.04E-03	6.04E-03	6.04E-03	6.04E-03	6.04E-03	6.04E-03	6.04E-03	6.04E-03	1.46E-03
3	6.04E-03	6.04E-03	6.04E-03	6.04E-03	6.04E-03	6.04E-03	6.04E-03	6.04E-03	6.04E-03	1.04E-03
2	6.04E-03	6.04E-03	6.04E-03	6.04E-03	6.04E-03	6.04E-03	6.04E-03	6.04E-03	6.04E-03	4.17E-04

X= .06250 .06750 .07250 .07750 .08250 .08750 .09250 .09750 .10250

THERMAL EXCH. COEF.

J \ I	2	3	4	5	6	7	8	9	10	11	12	13	Y =
9	5.81E-05	5.81E-05	5.81E-05	5.81E-05	5.81E-05	5.81E-05	5.81E-05	5.81E-05	5.81E-05	5.81E-05	5.81E-05	5.81E-05	.00230
8	5.81E-05	5.81E-05	5.81E-05	5.81E-05	5.81E-05	5.81E-05	5.81E-05	5.81E-05	5.81E-05	5.81E-05	5.81E-05	5.81E-05	.00224
7	5.81E-05	5.81E-05	5.81E-05	5.81E-05	5.81E-05	5.81E-05	5.81E-05	5.81E-05	5.81E-05	5.81E-05	5.81E-05	5.81E-05	.00214
6	5.81E-05	5.81E-05	5.81E-05	5.81E-05	5.81E-05	5.81E-05	5.81E-05	5.81E-05	5.81E-05	5.81E-05	5.81E-05	5.81E-05	.00198
5	5.81E-05	5.81E-05	5.81E-05	5.81E-05	5.81E-05	5.81E-05	5.81E-05	5.81E-05	5.81E-05	5.81E-05	5.81E-05	5.81E-05	.00177
4	5.81E-05	5.81E-05	5.81E-05	5.81E-05	5.81E-05	5.81E-05	5.81E-05	5.81E-05	5.81E-05	5.81E-05	5.81E-05	5.81E-05	.00146
3	5.81E-05	5.81E-05	5.81E-05	5.81E-05	5.81E-05	5.81E-05	5.81E-05	5.81E-05	5.81E-05	5.81E-05	5.81E-05	5.81E-05	.00104
2	5.81E-05	5.81E-05	5.81E-05	5.81E-05	5.81E-05	5.81E-05	5.81E-05	5.81E-05	5.81E-05	5.81E-05	5.81E-05	5.81E-05	.00042

X= .00250 .00750 .01250 .01750 .02250 .02750 .03250 .03750 .04250 .04750 .05250 .05750

J \ I	14	15	16	17	18	19	20	21	22	Y =
9	5.81E-05	5.81E-05	5.81E-05	5.81E-05	5.81E-05	5.81E-05	5.81E-05	5.81E-05	5.81E-05	2.30E-03
8	5.81E-05	5.81E-05	5.81E-05	5.81E-05	5.81E-05	5.81E-05	5.81E-05	5.81E-05	5.81E-05	2.24E-03
7	5.81E-05	5.81E-05	5.81E-05	5.81E-05	5.81E-05	5.81E-05	5.81E-05	5.81E-05	5.81E-05	2.14E-03

6	5.81E-05	5.81E-05	5.81E-05	5.81E-05	5.81E-05	5.81E-05	5.81E-05	5.81E-05	5.81E-05	1.98E-03
5	5.81E-05	5.81E-05	5.81E-05	5.81E-05	5.81E-05	5.81E-05	5.81E-05	5.81E-05	5.81E-05	1.77E-03
4	5.81E-05	5.81E-05	5.81E-05	5.81E-05	5.81E-05	5.81E-05	5.81E-05	5.81E-05	5.81E-05	1.46E-03
3	5.81E-05	5.81E-05	5.81E-05	5.81E-05	5.81E-05	5.81E-05	5.81E-05	5.81E-05	5.81E-05	1.04E-03
2	5.81E-05	5.81E-05	5.81E-05	5.81E-05	5.81E-05	5.81E-05	5.81E-05	5.81E-05	5.81E-05	4.17E-04

X= .06250 .06750 .07250 .07750 .08250 .08750 .09250 .09750 .10250

DENSITY

I / J	1	2	3	4	5	6	7	8	9	10	11	12	13	Y =
9	8.48E+02	8.48E+02	8.48E+02	8.48E+02	8.48E+02	8.48E+02	8.48E+02	8.48E+02	8.48E+02	8.48E+02	8.48E+02	8.48E+02	8.48E+02	.00230
8	8.48E+02	8.48E+02	8.48E+02	8.48E+02	8.48E+02	8.48E+02	8.48E+02	8.48E+02	8.48E+02	8.48E+02	8.48E+02	8.48E+02	8.48E+02	.00224
7	8.48E+02	8.48E+02	8.48E+02	8.48E+02	8.48E+02	8.48E+02	8.48E+02	8.48E+02	8.48E+02	8.48E+02	8.48E+02	8.48E+02	8.48E+02	.00214
6	8.48E+02	8.48E+02	8.48E+02	8.48E+02	8.48E+02	8.48E+02	8.48E+02	8.48E+02	8.48E+02	8.48E+02	8.48E+02	8.48E+02	8.48E+02	.00198
5	8.48E+02	8.48E+02	8.48E+02	8.48E+02	8.48E+02	8.48E+02	8.48E+02	8.48E+02	8.48E+02	8.48E+02	8.48E+02	8.48E+02	8.48E+02	.00177
4	8.48E+02	8.48E+02	8.48E+02	8.48E+02	8.48E+02	8.48E+02	8.48E+02	8.48E+02	8.48E+02	8.48E+02	8.48E+02	8.48E+02	8.48E+02	.00146
3	8.48E+02	8.48E+02	8.48E+02	8.48E+02	8.48E+02	8.48E+02	8.48E+02	8.48E+02	8.48E+02	8.48E+02	8.48E+02	8.48E+02	8.48E+02	.00104
2	8.48E+02	8.48E+02	8.48E+02	8.48E+02	8.48E+02	8.48E+02	8.48E+02	8.48E+02	8.48E+02	8.48E+02	8.48E+02	8.48E+02	8.48E+02	.00042

X= .00250 .00750 .01250 .01750 .02250 .02750 .03250 .03750 .04250 .04750 .05250 .05750

I / J	14	15	16	17	18	19	20	21	22	Y =
9	8.48E+02	8.48E+02	8.48E+02	8.48E+02	8.48E+02	8.48E+02	8.48E+02	8.48E+02	8.48E+02	2.30E-03
8	8.48E+02	8.48E+02	8.48E+02	8.48E+02	8.48E+02	8.48E+02	8.48E+02	8.48E+02	8.48E+02	2.24E-03
7	8.48E+02	8.48E+02	8.48E+02	8.48E+02	8.48E+02	8.48E+02	8.48E+02	8.48E+02	8.48E+02	2.14E-03
6	8.48E+02	8.48E+02	8.48E+02	8.48E+02	8.48E+02	8.48E+02	8.48E+02	8.48E+02	8.48E+02	1.98E-03
5	8.48E+02	8.48E+02	8.48E+02	8.48E+02	8.48E+02	8.48E+02	8.48E+02	8.48E+02	8.48E+02	1.77E-03
4	8.48E+02	8.48E+02	8.48E+02	8.48E+02	8.48E+02	8.48E+02	8.48E+02	8.48E+02	8.48E+02	1.46E-03
3	8.48E+02	8.48E+02	8.48E+02	8.48E+02	8.48E+02	8.48E+02	8.48E+02	8.48E+02	8.48E+02	1.04E-03
2	8.48E+02	8.48E+02	8.48E+02	8.48E+02	8.48E+02	8.48E+02	8.48E+02	8.48E+02	8.48E+02	4.17E-04

X= .06250 .06750 .07250 .07750 .08250 .08750 .09250 .09750 .10250

ITER NO.	ABSOLUTE RESIDUAL SOURCE SUMS: UMOM	VMOM	MASS	ENER	SNORMT	FIELD VALUES AT MONITORING LOCATION (21, 8): U	V	P	T	TC
1	6.756E-02	0.000E+00	1.159E-05	1.026E+00	1.005E-01	1.154E-03	-4.295E-08	-1.022E+01	7.249E+01	6.805E+01
2	3.112E+00	1.826E-04	1.335E-02	8.809E-02	1.009E-01	1.180E-03	3.895E-07	-9.637E+00	7.088E+01	7.746E+01
3	2.475E+00	3.612E-02	2.577E-02	1.966E-02	1.012E-01	1.192E-03	-4.374E-07	-9.193E+00	7.110E+01	7.665E+01
4	2.024E+00	2.101E-02	1.106E-02	1.156E-02	1.012E-01	1.210E-03	-5.177E-07	-8.866E+00	7.101E+01	7.673E+01
5	1.662E+00	2.119E-02	6.676E-03	9.432E-03	1.012E-01	1.227E-03	-4.912E-07	-8.924E+00	7.099E+01	7.668E+01
6	1.331E+00	1.455E-02	6.687E-03	7.319E-03	1.012E-01	1.242E-03	-4.716E-07	-9.032E+00	7.096E+01	7.666E+01
7	1.061E+00	1.390E-02	4.416E-03	6.671E-03	1.012E-01	1.256E-03	-4.401E-07	-9.082E+00	7.093E+01	7.664E+01
8	8.674E-01	1.004E-02	2.792E-03	5.337E-03	1.012E-01	1.267E-03	-4.108E-07	-9.032E+00	7.091E+01	7.663E+01
9	7.142E-01	8.793E-03	3.459E-03	4.352E-03	1.012E-01	1.277E-03	-3.819E-07	-8.949E+00	7.089E+01	7.661E+01
10	5.900E-01	6.390E-03	2.382E-03	3.331E-03	1.012E-01	1.286E-03	-3.565E-07	-8.890E+00	7.088E+01	7.659E+01
11	4.837E-01	5.459E-03	1.815E-03	2.671E-03	1.012E-01	1.293E-03	-3.341E-07	-8.875E+00	7.087E+01	7.658E+01
12	3.924E-01	3.779E-03	1.202E-03	2.163E-03	1.012E-01	1.299E-03	-3.148E-07	-8.881E+00	7.086E+01	7.658E+01
13	3.160E-01	3.366E-03	1.356E-03	1.830E-03	1.012E-01	1.304E-03	-2.984E-07	-8.886E+00	7.086E+01	7.657E+01

14	2.561E-01	2.321E-03	8.928E-04	1.526E-03	1.012E-01	1.308E-03	-2.844E-07	-8.878E+00	7.085E+01	7.657E+01
15	2.092E-01	2.088E-03	1.055E-03	1.239E-03	1.012E-01	1.311E-03	-2.731E-07	-8.865E+00	7.084E+01	7.656E+01
16	1.718E-01	1.427E-03	7.793E-04	1.000E-03	1.012E-01	1.314E-03	-2.632E-07	-8.853E+00	7.084E+01	7.656E+01
17	1.406E-01	1.301E-03	8.794E-04	7.959E-04	1.012E-01	1.316E-03	-2.552E-07	-8.846E+00	7.084E+01	7.655E+01
18	1.145E-01	8.550E-04	7.214E-04	6.556E-04	1.012E-01	1.318E-03	-2.485E-07	-8.844E+00	7.084E+01	7.655E+01
19	9.274E-02	8.241E-04	7.837E-04	5.528E-04	1.012E-01	1.320E-03	-2.432E-07	-8.844E+00	7.083E+01	7.655E+01
20	7.527E-02	5.246E-04	6.907E-04	4.584E-04	1.012E-01	1.321E-03	-2.387E-07	-8.842E+00	7.083E+01	7.655E+01
21	6.127E-02	5.335E-04	7.292E-04	3.748E-04	1.012E-01	1.322E-03	-2.350E-07	-8.839E+00	7.083E+01	7.655E+01
22	5.009E-02	3.362E-04	6.748E-04	3.149E-04	1.012E-01	1.323E-03	-2.319E-07	-8.837E+00	7.083E+01	7.655E+01
23	4.092E-02	3.456E-04	6.948E-04	2.463E-04	1.012E-01	1.324E-03	-2.294E-07	-8.835E+00	7.083E+01	7.655E+01
24	3.334E-02	2.135E-04	6.706E-04	2.244E-04	1.012E-01	1.324E-03	-2.274E-07	-8.834E+00	7.083E+01	7.654E+01
25	2.709E-02	2.322E-04	6.780E-04	1.819E-04	1.012E-01	1.325E-03	-2.256E-07	-8.833E+00	7.083E+01	7.654E+01
26	2.203E-02	1.430E-04	6.648E-04	1.529E-04	1.012E-01	1.325E-03	-2.242E-07	-8.833E+00	7.083E+01	7.654E+01
27	1.791E-02	1.516E-04	6.672E-04	1.356E-04	1.012E-01	1.325E-03	-2.231E-07	-8.832E+00	7.083E+01	7.654E+01
28	1.459E-02	9.632E-05	6.622E-04	1.216E-04	1.012E-01	1.326E-03	-2.222E-07	-8.831E+00	7.082E+01	7.654E+01
29	1.192E-02	1.070E-04	6.629E-04	9.878E-05	1.012E-01	1.326E-03	-2.215E-07	-8.831E+00	7.082E+01	7.654E+01
30	9.699E-03	6.673E-05	6.585E-04	8.994E-05	1.012E-01	1.326E-03	-2.208E-07	-8.831E+00	7.082E+01	7.654E+01

U VELOCITY

I	2	3	4	5	6	7	8	9	10	11	12	13	Y =
J													
9	0.00E+00	0.00E+00	0.00E+00	0.00E+00	0.00E+00	0.00E+00	0.00E+00	0.00E+00	0.00E+00	0.00E+00	0.00E+00	0.00E+00	.00230
8	1.15E-03	1.28E-03	1.31E-03	1.33E-03	1.35E-03	1.36E-03	1.37E-03	1.37E-03	1.38E-03	1.38E-03	1.39E-03	1.39E-03	.00224
7	5.62E-03	5.99E-03	6.17E-03	6.28E-03	6.36E-03	6.42E-03	6.46E-03	6.50E-03	6.53E-03	6.55E-03	6.57E-03	6.59E-03	.00214
6	1.19E-02	1.24E-02	1.27E-02	1.29E-02	1.30E-02	1.31E-02	1.32E-02	1.33E-02	1.34E-02	1.34E-02	1.34E-02	1.35E-02	.00190
5	1.96E-02	2.00E-02	2.02E-02	2.04E-02	2.06E-02	2.07E-02	2.09E-02	2.10E-02	2.10E-02	2.11E-02	2.12E-02	2.12E-02	.00177
4	2.95E-02	2.96E-02	2.98E-02	2.99E-02	3.00E-02	3.01E-02	3.02E-02	3.02E-02	3.03E-02	3.04E-02	3.04E-02	3.05E-02	.00146
3	3.97E-02	3.96E-02	3.95E-02	3.95E-02	3.95E-02	3.95E-02	3.95E-02	3.95E-02	3.95E-02	3.95E-02	3.95E-02	3.95E-02	.00104
2	4.86E-02	4.83E-02	4.81E-02	4.80E-02	4.78E-02	4.77E-02	4.76E-02	4.75E-02	4.74E-02	4.74E-02	4.73E-02	4.73E-02	.00042
X=	0.00000	.00500	.01000	.01500	.02000	.02500	.03000	.03500	.04000	.04500	.05000	.05500	

I	14	15	16	17	18	19	20	21	22	Y =
J										
9	0.00E+00	0.00E+00	0.00E+00	0.00E+00	0.00E+00	0.00E+00	0.00E+00	0.00E+00	0.00E+00	2.30E-03
8	1.39E-03	1.40E-03	1.40E-03	1.40E-03	1.40E-03	1.39E-03	1.38E-03	1.33E-03	1.30E-03	2.24E-03
7	6.61E-03	6.62E-03	6.64E-03	6.65E-03	6.65E-03	6.64E-03	6.60E-03	6.48E-03	6.45E-03	2.14E-03
6	1.35E-02	1.36E-02	1.36E-02	1.36E-02	1.36E-02	1.36E-02	1.36E-02	1.34E-02	1.34E-02	1.98E-03
5	2.13E-02	2.13E-02	2.14E-02	2.14E-02	2.14E-02	2.15E-02	2.14E-02	2.14E-02	2.13E-02	1.77E-03
4	3.05E-02	3.06E-02	3.06E-02	3.06E-02	3.07E-02	3.07E-02	3.07E-02	3.07E-02	3.07E-02	1.46E-03
3	3.95E-02	3.95E-02	3.95E-02	3.95E-02	3.95E-02	3.96E-02	3.96E-02	3.96E-02	3.96E-02	1.04E-03
2	4.72E-02	4.72E-02	4.71E-02	4.71E-02	4.71E-02	4.70E-02	4.70E-02	4.71E-02	4.71E-02	4.17E-04
X=	.06000	.06500	.07000	.07500	.08000	.08500	.09000	.09500	.10000	

V VELOCITY

I	2	3	4	5	6	7	8	9	10	11	12	13	Y =
J													
9	0.00E+00	0.00E+00	0.00E+00	0.00E+00	0.00E+00	0.00E+00	0.00E+00	0.00E+00	0.00E+00	0.00E+00	0.00E+00	0.00E+00	.00227
8	2.01E-06	4.74E-07	2.86E-07	1.95E-07	1.43E-07	1.10E-07	8.91E-08	7.40E-08	6.28E-08	5.41E-08	4.72E-08	4.07E-08	.00219
7	1.15E-05	4.85E-06	3.08E-06	2.10E-06	1.52E-06	1.16E-06	9.27E-07	7.64E-07	6.45E-07	5.54E-07	4.82E-07	4.21E-07	.00206

6	2.84E-05	1.47E-05	9.96E-06	7.08E-06	5.27E-06	4.10E-06	3.31E-06	2.75E-06	2.34E-06	2.02E-06	1.76E-06	1.55E-06	.00188
5	4.76E-05	2.85E-05	2.06E-05	1.54E-05	1.20E-05	9.59E-06	7.92E-06	6.69E-06	5.76E-06	5.02E-06	4.43E-06	3.93E-06	.00162
4	5.69E-05	3.83E-05	2.92E-05	2.29E-05	1.85E-05	1.53E-05	1.30E-05	1.12E-05	9.84E-06	8.72E-06	7.80E-06	7.01E-06	.00125
3	4.43E-05	3.29E-05	2.60E-05	2.09E-05	1.73E-05	1.47E-05	1.28E-05	1.12E-05	1.00E-05	9.05E-06	8.21E-06	7.50E-06	.00073
2	0.00E+00	0.00E+00	0.00E+00	0.00E+00	0.00E+00	0.00E+00	0.00E+00	0.00E+00	0.00E+00	0.00E+00	0.00E+00	0.00E+00	.00000

X=	.00250	.00750	.01250	.01750	.02250	.02750	.03250	.03750	.04250	.04750	.05250	.05750
I	14	15	16	17	18	19	20	21	22	Y =		
J												
9	0.00E+00	0.00E+00	0.00E+00	0.00E+00	0.00E+00	0.00E+00	0.00E+00	0.00E+00	0.00E+00	2.27E-03		
8	3.52E-08	2.78E-08	1.57E-08	-1.16E-08	-8.04E-08	-2.65E-07	-7.69E-07	-2.21E-07	0.00E+00	2.19E-03		
7	3.67E-07	3.10E-07	2.28E-07	6.76E-08	-3.15E-07	-1.32E-06	-4.00E-06	4.96E-08	0.00E+00	2.06E-03		
6	1.37E-06	1.18E-06	9.44E-07	5.25E-07	-4.26E-07	-2.87E-06	-9.25E-06	1.18E-06	0.00E+00	1.88E-03		
5	3.49E-06	3.08E-06	2.60E-06	1.83E-06	1.95E-07	-3.88E-06	-1.42E-05	2.97E-06	0.00E+00	1.62E-03		
4	6.33E-06	5.68E-06	4.97E-06	3.94E-06	1.90E-06	-2.99E-06	-1.50E-05	3.97E-06	0.00E+00	1.25E-03		
3	6.87E-06	6.27E-06	5.63E-06	4.75E-06	3.09E-06	-7.81E-07	-9.86E-06	2.84E-06	0.00E+00	7.31E-04		
2	0.00E+00	0.00E+00	0.00E+00	0.00E+00	0.00E+00	0.00E+00	0.00E+00	0.00E+00	0.00E+00	0.00E+00		

X=	.06250	.06750	.07250	.07750	.08250	.08750	.09250	.09750	.10250

PRESSURE

I	2	3	4	5	6	7	8	9	10	11	12	13	Y =
J													
9	0.00E+00	0.00E+00	0.00E+00	0.00E+00	0.00E+00	0.00E+00	0.00E+00	0.00E+00	0.00E+00	0.00E+00	0.00E+00	0.00E+00	.00230
8	9.99E-01	4.35E-01	-1.22E-01	-6.72E-01	-1.21E+00	-1.75E+00	-2.28E+00	-2.81E+00	-3.33E+00	-3.85E+00	-4.36E+00	-4.87E+00	.00224
7	9.99E-01	4.35E-01	-1.22E-01	-6.72E-01	-1.21E+00	-1.75E+00	-2.28E+00	-2.81E+00	-3.33E+00	-3.85E+00	-4.36E+00	-4.87E+00	.00214
6	9.99E-01	4.34E-01	-1.23E-01	-6.72E-01	-1.22E+00	-1.75E+00	-2.28E+00	-2.81E+00	-3.33E+00	-3.85E+00	-4.36E+00	-4.87E+00	.00198
5	9.99E-01	4.34E-01	-1.23E-01	-6.72E-01	-1.22E+00	-1.75E+00	-2.28E+00	-2.81E+00	-3.33E+00	-3.85E+00	-4.36E+00	-4.87E+00	.00177
4	9.99E-01	4.35E-01	-1.23E-01	-6.72E-01	-1.22E+00	-1.75E+00	-2.28E+00	-2.81E+00	-3.33E+00	-3.85E+00	-4.36E+00	-4.87E+00	.00146
3	1.00E+00	4.35E-01	-1.22E-01	-6.72E-01	-1.21E+00	-1.75E+00	-2.28E+00	-2.81E+00	-3.33E+00	-3.85E+00	-4.36E+00	-4.87E+00	.00104
2	1.00E+00	4.35E-01	-1.22E-01	-6.72E-01	-1.21E+00	-1.75E+00	-2.28E+00	-2.81E+00	-3.33E+00	-3.85E+00	-4.36E+00	-4.87E+00	.00042

X=	.00250	.00750	.01250	.01750	.02250	.02750	.03250	.03750	.04250	.04750	.05250	.05750
I	14	15	16	17	18	19	20	21	22	Y =		
J												
9	0.00E+00	0.00E+00	0.00E+00	0.00E+00	0.00E+00	0.00E+00	0.00E+00	0.00E+00	0.00E+00	2.30E-03		
8	-5.37E+00	-5.88E+00	-6.37E+00	-6.87E+00	-7.36E+00	-7.85E+00	-8.34E+00	-8.83E+00	0.00E+00	2.24E-03		
7	-5.37E+00	-5.88E+00	-6.37E+00	-6.87E+00	-7.36E+00	-7.85E+00	-8.34E+00	-8.83E+00	0.00E+00	2.14E-03		
6	-5.37E+00	-5.88E+00	-6.37E+00	-6.87E+00	-7.36E+00	-7.85E+00	-8.34E+00	-8.83E+00	0.00E+00	1.98E-03		
5	-5.37E+00	-5.88E+00	-6.37E+00	-6.87E+00	-7.36E+00	-7.85E+00	-8.34E+00	-8.83E+00	0.00E+00	1.77E-03		
4	-5.37E+00	-5.88E+00	-6.37E+00	-6.87E+00	-7.36E+00	-7.85E+00	-8.34E+00	-8.83E+00	0.00E+00	1.46E-03		
3	-5.37E+00	-5.88E+00	-6.37E+00	-6.87E+00	-7.36E+00	-7.85E+00	-8.34E+00	-8.83E+00	0.00E+00	1.04E-03		
2	-5.37E+00	-5.88E+00	-6.37E+00	-6.87E+00	-7.36E+00	-7.85E+00	-8.34E+00	-8.83E+00	0.00E+00	4.17E-04		

X=	.06250	.06750	.07250	.07750	.08250	.08750	.09250	.09750	.10250

TEMPERATURE

I	2	3	4	5	6	7	8	9	10	11	12	13	Y =
J													
9	0.00E+00	0.00E+00	0.00E+00	0.00E+00	0.00E+00	0.00E+00	0.00E+00	0.00E+00	0.00E+00	0.00E+00	0.00E+00	0.00E+00	.00230

8	6.15E+01	6.38E+01	6.53E+01	6.65E+01	6.74E+01	6.81E+01	6.88E+01	6.93E+01	6.99E+01	7.04E+01	7.08E+01	7.12E+01	.00221
7	6.05E+01	6.22E+01	6.35E+01	6.46E+01	6.54E+01	6.61E+01	6.68E+01	6.74E+01	6.79E+01	6.84E+01	6.88E+01	6.92E+01	.00211
6	5.95E+01	6.04E+01	6.13E+01	6.21E+01	6.28E+01	6.35E+01	6.41E+01	6.46E+01	6.51E+01	6.56E+01	6.60E+01	6.64E+01	.00198
5	5.90E+01	5.93E+01	5.96E+01	6.01E+01	6.05E+01	6.09E+01	6.13E+01	6.18E+01	6.22E+01	6.25E+01	6.29E+01	6.32E+01	.00177
4	5.89E+01	5.89E+01	5.90E+01	5.91E+01	5.92E+01	5.93E+01	5.95E+01	5.96E+01	5.98E+01	6.00E+01	6.01E+01	6.03E+01	.00146
3	5.89E+01	5.89E+01	5.89E+01	5.89E+01	5.89E+01	5.89E+01	5.90E+01	5.90E+01	5.90E+01	5.90E+01	5.91E+01	5.91E+01	.00104
2	5.89E+01	5.89E+01	5.89E+01	5.89E+01	5.89E+01	5.89E+01	5.89E+01	5.89E+01	5.89E+01	5.89E+01	5.89E+01	5.89E+01	.00042

X=	.00250	.00750	.01250	.01750	.02250	.02750	.03250	.03750	.04250	.04750	.05250	.05750	
I	14	15	16	17	18	19	20	21	22	Y =			
J													
9	0.00E+00	0.00E+00	0.00E+00	0.00E+00	0.00E+00	0.00E+00	0.00E+00	0.00E+00	0.00E+00	2.30E-03			
8	7.16E+01	7.20E+01	7.24E+01	7.27E+01	7.29E+01	7.30E+01	7.26E+01	7.08E+01	6.05E+01	2.24E-03			
7	6.96E+01	7.00E+01	7.03E+01	7.07E+01	7.09E+01	7.11E+01	7.10E+01	6.99E+01	6.05E+01	2.14E-03			
6	6.68E+01	6.71E+01	6.75E+01	6.78E+01	6.81E+01	6.83E+01	6.85E+01	6.82E+01	6.05E+01	1.98E-03			
5	6.36E+01	6.39E+01	6.42E+01	6.45E+01	6.48E+01	6.51E+01	6.53E+01	6.54E+01	6.05E+01	1.77E-03			
4	6.05E+01	6.07E+01	6.09E+01	6.11E+01	6.13E+01	6.15E+01	6.17E+01	6.19E+01	6.05E+01	1.46E-03			
3	5.92E+01	5.92E+01	5.93E+01	5.93E+01	5.94E+01	5.95E+01	5.95E+01	5.96E+01	6.05E+01	1.04E-03			
2	5.89E+01	5.89E+01	5.89E+01	5.89E+01	5.89E+01	5.89E+01	5.90E+01	5.90E+01	6.05E+01	4.17E-04			

X=	.06250	.06750	.07250	.07750	.08250	.08750	.09250	.09750	.10250

DYNAMIC VISCOSITY

I	2	3	4	5	6	7	8	9	10	11	12	13	Y =
J													
9	6.04E-03	6.04E-03	6.04E-03	6.04E-03	6.04E-03	6.04E-03	6.04E-03	6.04E-03	6.04E-03	6.04E-03	6.04E-03	6.04E-03	.00230
8	5.61E-03	5.27E-03	5.05E-03	4.90E-03	4.79E-03	4.70E-03	4.62E-03	4.55E-03	4.49E-03	4.44E-03	4.39E-03	4.34E-03	.00224
7	5.78E-03	5.51E-03	5.31E-03	5.16E-03	5.04E-03	4.95E-03	4.86E-03	4.79E-03	4.73E-03	4.67E-03	4.61E-03	4.57E-03	.00214
6	5.94E-03	5.79E-03	5.65E-03	5.52E-03	5.41E-03	5.31E-03	5.23E-03	5.15E-03	5.09E-03	5.02E-03	4.97E-03	4.91E-03	.00198
5	6.02E-03	5.98E-03	5.91E-03	5.84E-03	5.77E-03	5.70E-03	5.63E-03	5.57E-03	5.51E-03	5.45E-03	5.40E-03	5.35E-03	.00177
4	6.04E-03	6.04E-03	6.03E-03	6.01E-03	5.99E-03	5.97E-03	5.95E-03	5.92E-03	5.89E-03	5.86E-03	5.83E-03	5.80E-03	.00146
3	6.04E-03	6.04E-03	6.04E-03	6.04E-03	6.04E-03	6.04E-03	6.03E-03	6.03E-03	6.02E-03	6.02E-03	6.01E-03	6.00E-03	.00101
2	6.04E-03	6.04E-03	6.04E-03	6.04E-03	6.04E-03	6.04E-03	6.04E-03	6.04E-03	6.04E-03	6.04E-03	6.04E-03	6.04E-03	.00042

X=	.00250	.00750	.01250	.01750	.02250	.02750	.03250	.03750	.04250	.04750	.05250	.05750	
I	14	15	16	17	18	19	20	21	22	Y =			
J													
9	6.04E-03	6.04E-03	6.04E-03	6.04E-03	6.04E-03	6.04E-03	6.04E-03	6.04E-03	6.04E-03	2.30E-03			
8	4.30E-03	4.26E-03	4.22E-03	4.19E-03	4.16E-03	4.16E-03	4.20E-03	4.38E-03	6.04E-03	2.24E-03			
7	4.52E-03	4.48E-03	4.44E-03	4.40E-03	4.37E-03	4.35E-03	4.37E-03	4.48E-03	6.04E-03	2.14E-03			
6	4.86E-03	4.82E-03	4.78E-03	4.74E-03	4.70E-03	4.67E-03	4.65E-03	4.69E-03	6.04E-03	1.98E-03			
5	5.30E-03	5.25E-03	5.21E-03	5.17E-03	5.13E-03	5.09E-03	5.06E-03	5.04E-03	6.04E-03	1.77E-03			
4	5.77E-03	5.73E-03	5.70E-03	5.67E-03	5.64E-03	5.61E-03	5.58E-03	5.55E-03	6.04E-03	1.46E-03			
3	6.00E-03	5.99E-03	5.98E-03	5.97E-03	5.96E-03	5.95E-03	5.93E-03	5.92E-03	6.04E-03	1.04E-03			
2	6.04E-03	6.04E-03	6.04E-03	6.04E-03	6.04E-03	6.03E-03	6.03E-03	6.03E-03	6.04E-03	4.17E-04			

X=	.06250	.06750	.07250	.07750	.08250	.08750	.09250	.09750	.10250

THERMAL EXCH. COEF.

I	2	3	4	5	6	7	8	9	10	11	12	13	Y =

J													
9	5.81E-05	5.81E-05	5.81E-05	5.81E-05	5.81E-05	5.81E-05	5.81E-05	5.81E-05	5.81E-05	5.81E-05	5.81E-05	5.81E-05	.00230
8	5.79E-05	5.76E-05	5.74E-05	5.73E-05	5.72E-05	5.71E-05	5.71E-05	5.70E-05	5.70E-05	5.69E-05	5.69E-05	5.68E-05	.00224
7	5.80E-05	5.78E-05	5.76E-05	5.75E-05	5.74E-05	5.74E-05	5.73E-05	5.72E-05	5.72E-05	5.71E-05	5.71E-05	5.70E-05	.00211
6	5.81E-05	5.80E-05	5.79E-05	5.78E-05	5.77E-05	5.76E-05	5.76E-05	5.75E-05	5.75E-05	5.74E-05	5.74E-05	5.73E-05	.00198
5	5.81E-05	5.81E-05	5.81E-05	5.80E-05	5.80E-05	5.80E-05	5.79E-05	5.79E-05	5.78E-05	5.78E-05	5.77E-05	5.77E-05	.00177
4	5.81E-05	5.81E-05	5.81E-05	5.81E-05	5.81E-05	5.81E-05	5.81E-05	5.81E-05	5.80E-05	5.80E-05	5.80E-05	5.80E-05	.00146
3	5.81E-05	5.81E-05	5.81E-05	5.81E-05	5.81E-05	5.81E-05	5.81E-05	5.81E-05	5.81E-05	5.81E-05	5.81E-05	5.81E-05	.00104
2	5.81E-05	5.81E-05	5.81E-05	5.81E-05	5.81E-05	5.81E-05	5.81E-05	5.81E-05	5.81E-05	5.81E-05	5.81E-05	5.81E-05	.00043

X=	.00250	.00750	.01250	.01750	.02250	.02750	.03250	.03750	.04250	.04750	.05250	.05750	
I	14	15	16	17	18	19	20	21	22	Y =			
J													
9	5.81E-05	5.81E-05	5.81E-05	5.81E-05	5.81E-05	5.81E-05	5.81E-05	5.81E-05	5.81E-05	2.30E-03			
8	5.68E-05	5.67E-05	5.67E-05	5.67E-05	5.66E-05	5.66E-05	5.67E-05	5.69E-05	5.81E-05	2.24E-03			
7	5.70E-05	5.69E-05	5.69E-05	5.69E-05	5.68E-05	5.68E-05	5.68E-05	5.69E-05	5.81E-05	2.14E-03			
6	5.73E-05	5.72E-05	5.72E-05	5.72E-05	5.71E-05	5.71E-05	5.71E-05	5.71E-05	5.81E-05	1.98E-03			
5	5.76E-05	5.76E-05	5.76E-05	5.75E-05	5.75E-05	5.75E-05	5.74E-05	5.74E-05	5.81E-05	1.77E-03			
4	5.80E-05	5.79E-05	5.79E-05	5.79E-05	5.79E-05	5.79E-05	5.78E-05	5.78E-05	5.81E-05	1.46E-03			
3	5.81E-05	5.81E-05	5.81E-05	5.81E-05	5.81E-05	5.81E-05	5.81E-05	5.81E-05	5.81E-05	1.04E-03			
2	5.81E-05	5.81E-05	5.81E-05	5.81E-05	5.81E-05	5.81E-05	5.81E-05	5.81E-05	5.81E-05	4.17E-04			

X=	.06250	.06750	.07250	.07750	.08250	.08750	.09250	.09750	.10250

DENSITY

I	2	3	4	5	6	7	8	9	10	11	12	13	Y =
J													
9	8.48E+02	8.48E+02	8.48E+02	8.48E+02	8.48E+02	8.48E+02	8.48E+02	8.48E+02	8.48E+02	8.48E+02	8.48E+02	8.48E+02	.00230
8	8.46E+02	8.44E+02	8.43E+02	8.42E+02	8.42E+02	8.41E+02	8.41E+02	8.40E+02	8.40E+02	8.40E+02	8.39E+02	8.39E+02	.00224
7	8.47E+02	8.45E+02	8.45E+02	8.44E+02	8.43E+02	8.43E+02	8.42E+02	8.42E+02	8.41E+02	8.41E+02	8.41E+02	8.41E+02	.00211
6	8.47E+02	8.47E+02	8.46E+02	8.46E+02	8.45E+02	8.45E+02	8.44E+02	8.44E+02	8.43E+02	8.43E+02	8.43E+02	8.43E+02	.00198
5	8.48E+02	8.48E+02	8.47E+02	8.47E+02	8.47E+02	8.46E+02	8.46E+02	8.46E+02	8.45E+02	8.45E+02	8.45E+02	8.45E+02	.00177
4	8.48E+02	8.48E+02	8.48E+02	8.48E+02	8.48E+02	8.47E+02	8.47E+02	8.47E+02	8.47E+02	8.47E+02	8.47E+02	8.47E+02	.00146
3	8.48E+02	8.48E+02	8.48E+02	8.48E+02	8.48E+02	8.48E+02	8.48E+02	8.48E+02	8.48E+02	8.48E+02	8.48E+02	8.48E+02	.00101
2	8.48E+02	8.48E+02	8.48E+02	8.48E+02	8.48E+02	8.48E+02	8.48E+02	8.48E+02	8.48E+02	8.48E+02	8.48E+02	8.48E+02	.00043

X=	.00250	.00750	.01250	.01750	.02250	.02750	.03250	.03750	.04250	.04750	.05250	.05750	
I	14	15	16	17	18	19	20	21	22	Y =			
J													
9	8.48E+02	8.48E+02	8.48E+02	8.48E+02	8.48E+02	8.48E+02	8.48E+02	8.48E+02	8.48E+02	2.30E-03			
8	8.39E+02	8.39E+02	8.38E+02	8.38E+02	8.38E+02	8.38E+02	8.38E+02	8.39E+02	8.48E+02	2.24E-03			
7	8.40E+02	8.40E+02	8.40E+02	8.40E+02	8.39E+02	8.39E+02	8.39E+02	8.40E+02	8.48E+02	2.14E-03			
6	8.42E+02	8.42E+02	8.42E+02	8.42E+02	8.41E+02	8.41E+02	8.41E+02	8.41E+02	8.48E+02	1.98E-03			
5	8.45E+02	8.44E+02	8.44E+02	8.44E+02	8.44E+02	8.43E+02	8.43E+02	8.43E+02	8.48E+02	1.77E-03			
4	8.47E+02	8.46E+02	8.46E+02	8.46E+02	8.46E+02	8.46E+02	8.46E+02	8.46E+02	8.48E+02	1.46E-03			
3	8.48E+02	8.48E+02	8.48E+02	8.47E+02	8.47E+02	8.47E+02	8.47E+02	8.47E+02	8.48E+02	1.04E-03			
2	8.48E+02	8.48E+02	8.48E+02	8.48E+02	8.48E+02	8.48E+02	8.48E+02	8.48E+02	8.48E+02	4.17E-04			

X=	.06250	.06750	.07250	.07750	.08250	.08750	.09250	.09750	.10250

****

HEAT TRANSFER AND PRESSURE DROP SUMMARY

X	X*	WALL TEMPERATURE	BULK FLUID TEMPERATURE	NUSSELT NUMBER	FRICTION CONSTANT
.00250 M	.0000619	61.77 DEG C	58.95 DEG C	33.673	0.000
.00750 M	.0001858	64.18 DEG C	59.02 DEG C	28.186	22.982
.01250 M	.0003097	65.79 DEG C	59.10 DEG C	24.359	22.815
.01750 M	.0004336	66.95 DEG C	59.18 DEG C	21.841	22.657
.02250 M	.0005575	67.86 DEG C	59.27 DEG C	20.085	22.511
.02750 M	.0006814	68.62 DEG C	59.36 DEG C	18.791	22.374
.03250 M	.0008053	69.27 DEG C	59.44 DEG C	17.793	22.245
.03750 M	.0009292	69.85 DEG C	59.53 DEG C	16.995	22.123
.04250 M	.0010531	70.38 DEG C	59.62 DEG C	16.338	22.007
.04750 M	.0011770	70.87 DEG C	59.70 DEG C	15.785	21.897
.05250 M	.0013009	71.32 DEG C	59.79 DEG C	15.310	21.792
.05750 M	.0014248	71.74 DEG C	59.88 DEG C	14.897	21.691
.06250 M	.0015487	72.14 DEG C	59.96 DEG C	14.531	21.594
.06750 M	.0016726	72.52 DEG C	60.05 DEG C	14.201	21.500
.07250 M	.0017965	72.87 DEG C	60.14 DEG C	13.891	21.410
.07750 M	.0019204	73.18 DEG C	60.23 DEG C	13.576	21.323
.08250 M	.0020443	73.41 DEG C	60.31 DEG C	13.191	21.239
.08750 M	.0021682	73.44 DEG C	60.39 DEG C	12.561	21.161
.09250 M	.0022921	72.97 DEG C	60.46 DEG C	11.155	21.089
.09750 M	.0024160	71.04 DEG C	60.49 DEG C	6.972	21.033

WINDING TEMPERATURES AND HEAT FLUXES

X	CONDUCTOR TEMPERATURE	CONDUCTOR HEAT FLUX
.00250 M	68.89 DEG. C	1.225E+03 W/M**2
.00750 M	75.07 DEG. C	1.874E+03 W/M**2
.01250 M	78.00 DEG. C	2.100E+03 W/M**2
.01750 M	79.67 DEG. C	2.187E+03 W/M**2
.02250 M	80.79 DEG. C	2.224E+03 W/M**2
.02750 M	81.65 DEG. C	2.242E+03 W/M**2
.03250 M	82.37 DEG. C	2.253E+03 W/M**2
.03750 M	82.99 DEG. C	2.260E+03 W/M**2
.04250 M	83.55 DEG. C	2.266E+03 W/M**2
.04750 M	84.07 DEG. C	2.270E+03 W/M**2
.05250 M	84.54 DEG. C	2.274E+03 W/M**2
.05750 M	84.99 DEG. C	2.278E+03 W/M**2
.06250 M	85.40 DEG. C	2.280E+03 W/M**2

.06750 M	85.78 DEG. C	2.281E+03 W/M**2
.07250 M	86.12 DEG. C	2.279E+03 W/M**2
.07750 M	86.35 DEG. C	2.266E+03 W/M**2
.08250 M	86.35 DEG. C	2.226E+03 W/M**2
.08750 M	85.73 DEG. C	2.113E+03 W/M**2
.09250 M	83.42 DEG. C	1.798E+03 W/M**2
.09750 M	76.54 DEG. C	9.471E+02 W/M**2

D7 DISCNET The structure of DISCNET is highly modular, consisting of 10 subroutines and 4 functions, each of which are relatively short. An overall flow chart for DISCNET is shown as Fig. D7.1. The brief descriptions of the subroutines in each box require little elaboration. Subroutine HDUCT is just a 6x6 grid version of DUCT, configured so as to be called as a subroutine. The listings for HDUCT and the TEACH-L subroutines are not duplicated here.

Four functions are provided to perform frequently needed tasks. FUNCTION H(DHOR, XSTAR) computes a duct-averaged convective heat transfer coefficient using equations (7.7). FUNCTIONs PE (FLORAT,TEMP), and RE(FLORAT,TEMP) compute local Peclet and Reynolds numbers. FUNCTION VISC(TEMP) computes the local fluid viscosity. Listings and sample output follow.

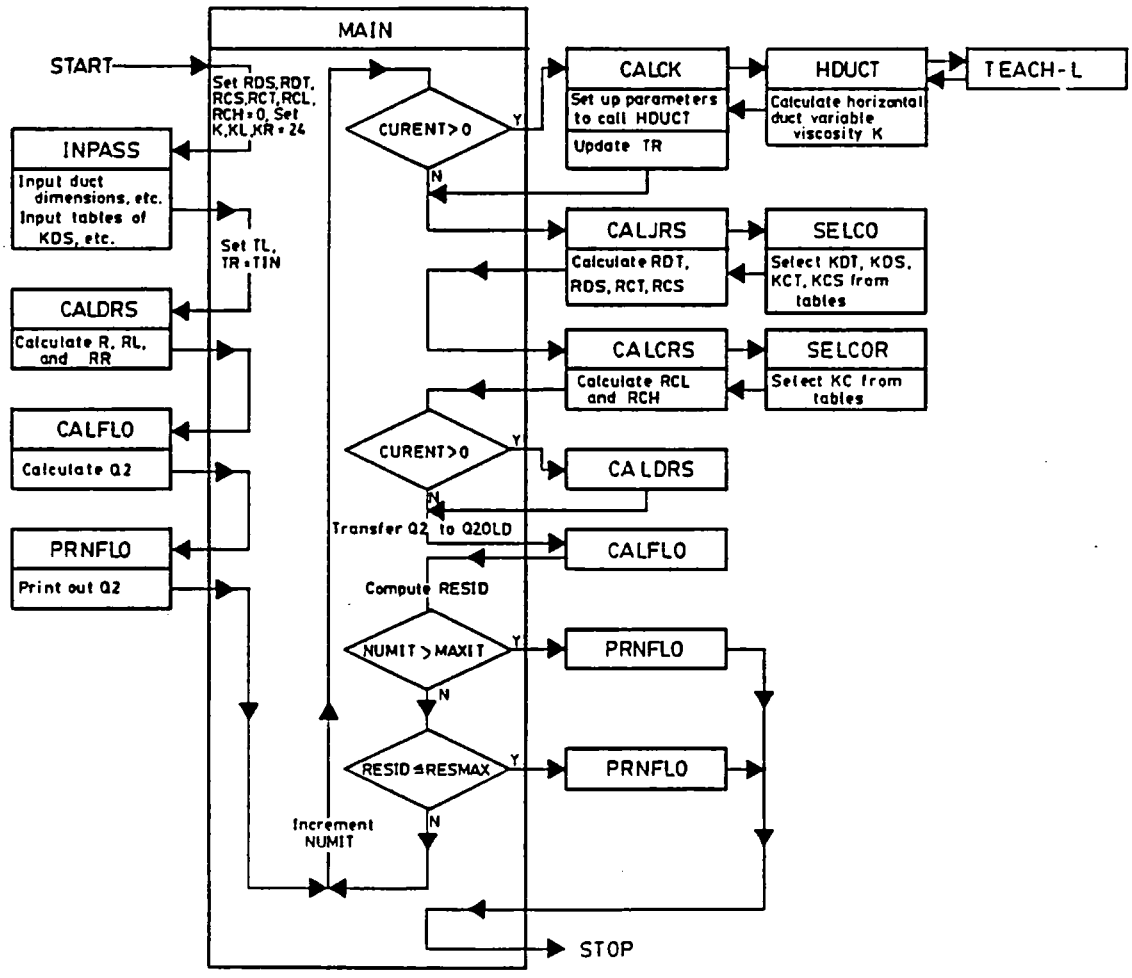


Fig. D7.1 Flow Chart of DISCNET

PROGRAM MAIN

```
      PROGRAM MAIN
      DIMENSION Q2OLD(15)
      REAL KDT(6,5,4),KDS(5,5,4),KCT(6,5,4),KCS(6,5,4),
     1KC(5,4),K(16),KL(15),KR(15)
      COMMON
     1/FCON/KDT,KDS,KCT,KCS,KC,K,KL,KR
     1/PASDAT/XD(15),YD(15),DL(15),DR(15),DH(16),QIN,TIN,NDUCT,NDUCM1

     1/FLOW/Q2(16),RDT(16),RDS(15),RCT(16),RCS(16),RCL,RCH,
     1R(16),RL(15),RR(15),TL(16),TR(16)
     1/FLUPR/URFVIS,VISCOS,DENSIT,PRIN,DEN(6,6),VIS(6,6),
     1GAMH(6,6),A1,A2,A3,A4,A5,A6,A7,SPHEAT,THCOND
     1/DISC/THCPAP,WIDCON,TINSL,HITCON,HLEFT,HRITE,TLEFT,
     1       TRITE,RHO20,ALPHA,CURENT,THKCON,GC,GCP,GF,GCF,
     1       GLP,GCPP,GL,GRP,GR,RC,QDOT,TC(6),QDOTPP(6),
     1       DELTAY
      DATA K,KL,KR /46*24./
      DATA RDT,RDS,RCT,RCS,RCL,RCH /65*0.0/
      CALL OPEN(6,'RESULT  DAT',0)
      CALL OPEN(5,'DATIN   DAT',0)
      CALL INPASS
C-----INITIALIZE TEMPERATURES
      DO 10 I=1,NDUCT
      TL(I)=TIN
   10 TR(I)=TIN
      MAXIT=10
      NUMIT=0
      RESMAX=.01
      CALL CALDRS
      CALL CALFLO
      WRITE(4,1000)
      WRITE(6,1000)
      CALL PRNFLO
  100 NUMIT=NUMIT+1
      IF(CURENT .NE. 0.) CALL CALCK
      CALL CALJRS
      CALL CALCRS
      IF(CURENT .NE. 0.) CALL CALDRS
      DO 200 I=1,NDUCT
  200 Q2OLD(I)=Q2(I)
      CALL CALFLO
      RESID=0.
      DO 210 I=1,NDUCT
      TEMP=ABS(Q2OLD(I)-Q2(I))
  210 RESID=RESID+TEMP
      RESID=RESID/QIN
      WRITE(6,1010) NUMIT,RESID
      WRITE(4,1010) NUMIT,RESID
      IF(NUMIT.GT.MAXIT) GO TO 300
      IF(RESID.GT.RESMAX) GO TO 100
  300 CONTINUE
      WRITE(4,1020) NUMIT
      WRITE(6,1020) NUMIT
      CALL PRNFLO
      STOP
 1000 FORMAT(1X,'INITIAL DISTRIBUTION')
 1010 FORMAT(1X,'RESIDUAL AFTER',I4,' ITERATIONS IS ',1PE12.3)
 1020 FORMAT(1X,'FINAL DISTRIBUTION AFTER',I4,' ITERATIONS:'//)
      END
```

SUBROUTINE INPASS

```
      SUBROUTINE INPASS
      REAL KDT(6,5,4),KDS(6,5,4),KCT(6,5,4),KCS(6,5,4),
     1KC(5,4),K(15),KL(15),KR(15)
      COMMON
     1/FCON/KDT,KDS,KCT,KCS,KC,K,KL,KR
     1/PASDAT/XD(15),YD(15),DL(15),DR(15),DH(15),QIN,TIN,NDUCT,NDUCM1
     1/FLUPR/URFVIS,VISCOS,DENSIT,PRIN,DEN(6,6),VIS(6,6),
     1GAMH(6,6),A1,A2,A3,A4,A5,A6,A7,SPHEAT,THCOND
     1/DISC/THCPAP,WIDCON,TINSL,HITCON,HLEFT,HRITE,TLEFT,
     1       TRITE,RHO20,ALPHA,CURENT,THKCON,GC,GCP,GF,GCF,
     1       GLP,GCPP,GL,GRP,GR,RC,QDOT,TC(5),QDOTPP(5),
     1       DELTAY
      READ(8,900) NDUCT
      NDUCM1=NDUCT-1
      READ(8,1000) (XD(I),I=1,NDUCM1)
      READ(8,1000) (YD(I),I=1,NDUCM1)
      READ(8,1000) (DL(I),I=1,NDUCM1)
      READ(8,1000) (DR(I),I=1,NDUCM1)
      READ(8,1000) (DH(I),I=1,NDUCT)
      READ(8,1005) QIN,TIN,A1,A2,A3,A4,A5,A6,A7
      READ(8,1005) THCPAP,WIDCON,TINSL,HITCON,RHO20,
     1             ALPHA,CURENT,THKCON
      READ(8,1002) KCS
      READ(8,1002) KCT
      READ(8,1002) KDS
      READ(8,1002) KDT
      DO 200 I=1,5
  200 READ(8,1007) (KC(I,J),J=1,4)
      WRITE(6,1010) QIN,TIN,CURENT,NDUCT
C-----FORMAT STATEMENTS
  900 FORMAT(I3)
 1000 FORMAT(6F8.5)
 1002 FORMAT(6F8.3)
 1005 FORMAT(9E13.4)
 1007 FORMAT(4F8.3)
 1010 FORMAT(' QIN    = ',1PE12.3,' M**2/SEC'/
     1       ' TIN    = ',1PE12.3,' DEG. C'/
     1       ' CURRENT= ',1PE12.3,' AMPS'/
     1       ' NDUCT  =',I3)
      RETURN
      END
```

SUBROUTINE CALDRS

```
 1:       SUBROUTINE CALDRS
 2:       REAL KDT(6,5,4),KDS(6,5,4),KCT(6,5,4),KCS(6,5,4),
 3:      1KC(5,4),K(15),KL(15),KR(15)
 4:       COMMON
 5:      1/FCON/KDT,KDS,KCT,KCS,KC,K,KL,KR
 6:      1/PASDAT/XD(15),YD(15),DL(15),DR(15),DH(16),QIN,TIN,NDUCT,NDUCM1
 7:
 8:      1/FLOW/Q2(15),RDT(16),RDS(15),RCT(16),RCS(15),RCL,RCH,
 9:      1R(16),RL(15),RR(15),TL(16),TR(16)
10: C-----CALCULATE RESISTANCES IN HORIZONTAL DUCTS
11:       R(1)=4.*K(1)*VISC(TL(1))*XD(1)/DH(1)**3
12:       DO 10 I=2,NDUCM1
13:    10 R(I)=4.*K(I)*VISC(TL(I))*.5*(XD(I-1)+XD(I))/DH(I)**3
14:       R(NDUCT)=4.*K(NDUCT)*VISC(TL(NDUCT))*XD(NDUCM1)/DH(NDUCT)**3
15: C-----CALCULATE RESISTANCES IN LEFT AND RIGHT DUCTS
16:       DO 20 I=1,NDUCM1
17:       RL(I)=4.*KL(I)*VISC(TL(I))*YD(I)/DL(I)**3
18:    20 RR(I)=4.*KR(I)*VISC(TR(I))*YD(I)/DR(I)**3
19:       WRITE(6,1000) R
20:       WRITE(6,1010) RL
21:       WRITE(6,1020) RR
22:       RETURN
23:  1000 FORMAT(/1X,'R= '/4E13.4/4E13.4/)
24:  1010 FORMAT(/1X,'RL= '/4E13.4/4E13.4/)
25:  1020 FORMAT(/1X,'RR= '/4E13.4/4E13.4/)
26:       END
```

SUBROUTINE CALFLO

```
      SUBROUTINE CALFLO
      DIMENSION QLOOP(15),A(15),B(15),C(15),D(15)
      COMMON
     1/FLOW/Q2(16),RDT(16),RDS(15),RCT(15),RCS(15),RCL,RCH,
     1R(16),RL(15),RR(15),TL(16),TR(16)
     1/PASDAT/XD(15),YD(15),DL(15),DR(15),DH(15),QIN,TIN,NDUCT,NDUCM1
C-----SET UP COEFFICIENTS
      RCT(1)=RCL
      RDT(NDUCT)=RCH
      DO 10 I=1,NDUCM1
      RPL=RDT(I)+R(I)+RCT(I)
      RRP=RR(I)+RCS(I+1)
      RPH=RCT(I+1)+R(I+1)+RDT(I+1)
      RLP=RL(I)+RDS(I)
      D(I)=RPL+RRP+RPH+RLP
   10 A(I)=RPH
      A(NDUCM1)=0.
      B(1)=0.
      C(1)=-QIN*(RDT(1)+R(1)+RCL+RR(1)+RCS(2))
      DO 20 I=2,NDUCM1
      B(I)=A(I-1)
   20 C(I)=-QIN*(RR(I)+RCS(I+1))
C-----BEGIN RECURRENCE PROCEDURE
      A(1)=A(1)/D(1)
      C(1)=C(1)/D(1)
      DO 30 I=2,NDUCM1
      TERM=1./(D(I)-B(I)*A(I-1))
      A(I)=A(I)*TERM
   30 C(I)=(C(I)+B(I)*C(I-1))*TERM
C-----OBTAIN LOOP FLOW RATES BY BACK SUBSTITUTION
      QLOOP(NDUCM1)=C(NDUCM1)
      DO 40 II=2,NDUCM1
      I=NDUCT-II
   40 QLOOP(I)=A(I)*QLOOP(I+1)+C(I)
C-----NOW CALCULATE FLOW RATE IN EACH DUCT
      Q2(1)=QIN+QLOOP(1)
      DO 50 I=2,NDUCM1
   50 Q2(I)=QLOOP(I)-QLOOP(I-1)
      Q2(NDUCT)=-QLOOP(NDUCM1)
      RETURN
      END
```

SUBROUTINE PRNFLO

```
      SUBROUTINE PRNFLO
      COMMON
     1/PASDAT/XD(15),YD(15),DL(15),DR(15),DH(15),QIN,TIN,NDUCT,NDUCM1
     1/FLOW/Q2(15),RDT(15),RDS(15),RCT(15),RCS(15),RCL,RCH,
     1R(16),RL(15),PR(15),TL(16),TR(16)
      DO 10 I=1,NDUCT
      PFLOW=Q2(I)*100./QIN
      WRITE(4,1000) I,PFLOW
   10 WRITE(6,1000) I,PFLOW
      DO 20 I=1,NDUCT
   20 WRITE(6,1010) I,Q2(I)
      RETURN
 1000 FORMAT(1X,'PERCENT FLOW IN DUCT NO. ',I2,' IS ',F5.2)
 1010 FORMAT(1X,'FLOW RATE IN DUCT NO. ',I2,' IS ',1PE12.3,' M**3/SEC')
      END
```

SUBROUTINE CALCK

```
      SUBROUTINE CALCK
      REAL KDT(6,5,4),KDS(6,5,4),KCT(6,5,4),KCS(6,5,4),
     1KC(5,4),K(15),KL(15),KR(15)
      COMMON
     1/FICN/KDT,KDS,KCT,KCS,KC,K,KL,KR
     1/PASDAT/XD(15),YD(15),DL(15),DR(15),DH(16),QIN,TIN,NDUCT,NDUCM1
     1/FLOW/Q2(16),RDT(16),RDS(15),RCT(16),RCS(16),RCL,RCH,
     1R(16),RL(15),RR(15),TL(16),TR(16)
     1/DISC/THCPAP,WIDCON,TINSL,HITCON,HLEFT,HRITE,TLEFT,
     1       TRITE,RHO20,ALPHA,CURENT,THKCON,GC,GCP,GF,GCF,
     1       GLP,GCPP,GL,GRP,GR,RC,QDOT,TC(6),QDOTPP(6),
     1       DELTAY
C-----START AT BOTTOM OF PASS
      DLEN=XD(1)
      RHORIZ=DH(1)/4.
      WRITE(6,1005)
C-----CALCULATE CONVECTION COEFFICIENTS HLEFT AND HRITE USING
C-----MEAN NUSSELT NUMBER FROM SHAH
C-----CALCULATE FLOW RATE ON LEFT AND RIGHT EDGES
      QL=QIN-Q2(1)
      QR=Q2(1)
      XLEFT=.5*YD(1)/(DL(1)*PE(QL,TL(1)))
      XRITE=.5*YD(1)/(DR(1)*PE(QR,TR(1)))
      HLEFT=H(DL(1),XLEFT)
      HRITE=H(DR(1),XRITE)
C-----USE EXISTING TL'S AND TR'S BUT UPDATE THEM AFTER
C-----CALLING HDUCT
      NDUC=1
      WRITE(4,1000) NDUC
      WRITE(6,1030) NDUC,XLEFT,HLEFT,XRITE,HRITE,QL,QR
      CALL HDUCT(DLEN,RHORIZ,TL(1),TR(1),Q2(1),K(1),TBOUT)
      TR(1)=TBOUT
      QI=Q2(1)
      DO 10 I=2,NDUCM1
      DLEN=0.5*(XD(I)+XD(I-1))
      RHORIZ=DH(I)/4.
      QL=QL-Q2(I)
      QR=QR+Q2(I)
      XLEFT=.5*YD(I)/(DL(I)*PE(QL,TL(I)))
      XRITE=.5*YD(I)/(DR(I)*PE(QR,TR(I)))
      HLEFT=H(DL(I),XLEFT)
      HRITE=H(DR(I),XRITE)
      NDUC=I
      WRITE(4,1000) NDUC
      WRITE(6,1030) NDUC,XLEFT,HLEFT,XRITE,HRITE,QL,QR
      CALL HDUCT(DLEN,RHORIZ,TL(I),TR(I),Q2(I),K(I),TBOUT)
      QI=Q2(I)+QI
      TR(I)=(TBOUT*Q2(I)+TR(I-1)*QI)/QI
   10 QI=QI
      DLEN=XD(NDUCM1)
      RHORIZ=DH(NDUCT)/4.
      QR=QIN
      XLEFT=0.
      HLEFT=0.
      XRITE=.5*YD(NDUCM1)/(DR(NDUCM1)*PE(QR,TR(8)))
      HRITE=H(DR(7),XRITE)
      NDUC=NDUCT
      WRITE(4,1000) NDUC
      WRITE(6,1030) NDUC,XLEFT,HLEFT,XRITE,HRITE,QL,QR
      CALL HDUCT(DLEN,RHORIZ,TL(NDUCT),TR(NDUCT),
     1Q2(NDUCT),K(NDUCT),TBOUT)
      QI=Q2(NDUCT)+QI
      TR(NDUCT)=(TBOUT*Q2(NDUCT)+TR(NDUCM1)*QI)/QI
      WRITE(6,1010) TR
      WRITE(6,1020) K
      RETURN
 1000 FORMAT(1X,'CALCULATION PROCEEDING IN DUCT NO. ',I4)
 1005 FORMAT('0',1X,'DUCT NO.',5X,'XLEFT',7X,'HLEFT',7X,'XRITE',
     1 7X,'HRITE',7X,'QLEFT',7X,'QRITE')
 1010 FORMAT(1X,'TR='/4E18.4/4E18.4)
 1020 FORMAT(1X,'K='/4E18.4/4E18.4)
 1030 FORMAT(7X,I2,2X,1P6E12.3)
      END
```

SUBROUTINE CALJRS

```
      SUBROUTINE CALJRS
      REAL KDT(6,5,4),KDS(6,5,4),KCT(6,5,4),KCS(6,5,4),
     1KC(5,4),K(16),KL(15),KR(15)
      COMMON
     1/FCON/KDT,KDS,KCT,KCS,KC,K,KL,KR
     1/PASDAT/XD(15),YD(15),DL(15),DR(15),DH(16),QIN,TIN,NDUCT,NDUCM1

     1/FLOW/Q2(16),RDT(16),RDS(15),RCT(16),RCS(16),RCL,RCH,
     1R(16),RL(15),RR(15),TL(16),TR(16)
     1/FLUPR/URFVIS,VISCOS,DENSIT,PRIN,DEN(6,5),VIS(6,6),
     1GAMH(6,6),A1,A2,A3,A4,A5,A6,A7,SPHEAT,THCOND
C-----CALCULATE DIVIDING JUNCTION RESISTANCES
      QI=QIN
      WRITE(6,1040)
      DO 10 I=1,NDUCM1
      QRATIO=QI/Q2(I)
      RRATIO=DL(I)/DH(I)
      CALL SELCO(KDT,QRATIO,RRATIO,RE(QI,TL(I)),FKDT)
      CALL SELCO(KDS,QRATIO,RRATIO,RE(QI,TL(I)),FKDS)
      REYN=RE(QI,TL(I))
      WRITE(6,1050) I,QRATIO,RRATIO,REYN,FKDT,FKDS
      RDT(I)=2.*FKDT*QRATIO*VISC(TL(I))/DL(I)**2
      RDS(I)=2.*FKDS*(1./(1.-1./QRATIO))*VISC(TL(I))/DL(I)**2
   10 QI=QI-Q2(I)
C-----CALCULATE COMBINING JUNCTION RESISTANCES
      QI=Q2(1)
      WRITE(6,1060)
      DO 20 I=2,NDUCT
      QRATIO=QI/Q2(I)
      RRATIO=DR(I-1)/DH(I)
      CALL SELCO(KCT,QRATIO,RRATIO,RE(QI,TR(I)),FKCT)
      CALL SELCO(KCS,QRATIO,RRATIO,RE(QI,TR(I)),FKCS)
      REYN=RE(QI,TR(I))
      WRITE(6,1050) I,QRATIO,RRATIO,REYN,FKCT,FKCS
      RCT(I)=2.*FKCT*(QRATIO+1.)*VISC(TR(I))/DR(I-1)**2
      RCS(I)=2.*FKCS*(1.+1./QRATIO)*VISC(TR(I))/DR(I-1)**2
   20 QI=QI+Q2(I)
      WRITE(6,1000) RDT
      WRITE(6,1010) RDS
      WRITE(6,1020) RCT
      WRITE(6,1030) RCS
      RETURN
 1000 FORMAT(1X,'RDT= '/4E13.4/4E13.4/)
 1010 FORMAT(1X,'RDS= '/4E13.4/4E13.4/)
 1020 FORMAT(1X,'RCT= '/4E13.4/4E13.4/)
 1030 FORMAT(1X,'RCS= '/4E13.4/4E13.4/)
 1040 FORMAT(1X,'DIVIDING JUNCTIONS'/
     1' DUCT NO.',2X,'QRATIO',3X,'RRATIO',2X,'RE',
     1 5X,'KDT',5X,'KDS')
 1050 FORMAT(3X,I2,4X,5F8.2)
 1060 FORMAT(1X,'COMBINING JUNCTIONS'/
     1' DUCT NO.',2X,'QRATIO',3X,'RRATIO',2X,'RE',
     1 5X,'KCT',5X,'KCS')
      END
```

SUBROUTINE CALCRS

```
      SUBROUTINE CALCRS
      REAL KDT(6,5,4),KDS(6,5,4),KCT(6,5,4),KCS(6,5,4),
     1KC(5,4),K(15),KL(15),KR(15)
      COMMON
     1/FCON/KDT,KDS,KCT,KCS,KC,K,KL,KR
     1/PASDAT/XD(15),YD(15),DL(15),DR(15),DH(16),QIN,TIN,NDUCT,NDUCM1

     1/FLOW/Q2(16),RDT(16),RDS(15),RCT(16),RCS(16),RCL,RCH,
     1R(15),RL(15),RR(15),TL(16),TR(16)
C-----CALCULATE BOTTOM CORNER RESISTANCE
      RRATIO=DH(1)/DR(1)
      CALL SELCOR(KC,RRATIO,RE(Q2(1),TR(1)),FKCL)
      RCL=2.*FKCL*VISC(TR(1))/DH(1)**2
      REYN=RE(Q2(1),TR(1))
      WRITE(6,1010) RRATIO,REYN,FKCL
C-----CALCULATE TOP CORNER RESISTANCE
      RRATIO=DL(NDUCM1)/DH(NDUCT)
      CALL SELCOR(KC,RRATIO,RE(Q2(NDUCT),TL(NDUCT)),FKCH)
      RCH=2.*FKCH*VISC(TL(NDUCT))/DL(NDUCM1)**2
      REYN=RE(Q2(NDUCT),TL(NDUCT))
      WRITE(6,1020) RRATIO,REYN,FKCH
      WRITE(6,1000) RCL,RCH
      RETURN
 1000 FORMAT(1X,'RCL= ',E13.4,' RCH= ',E13.4/)
 1010 FORMAT(1X,'BOTTOM CORNER'/
     1' RRATIO',5X,'RE',6X,'KCL'/1X,3F8.2)
 1020 FORMAT(1X,'TOP CORNER'/
     1' RRATIO',5X,'RE',6X,'KCH'/1X,3F8.2)
      END
```

SUBROUTINE SELCOR

```
      SUBROUTINE SELCOR(KFAC,RRATIO,RE,F)
      DIMENSION REYN(5),RRAT(4),F2(2)
      REAL KFAC(5,4)
      DATA REYN/9.384,17.57,51.96,93.64,175.7/
      DATA RRAT/.5,1.,2.,3./
      JL=1
      DO 20 J=1,5
   20 IF(RE.GE.REYN(J)) JL=J
      IF(JL.EQ.5) JL=4
      JH=JL+1
      KL=1
      DO 30 K=1,4
   30 IF(RRATIO.GE.RRAT(K)) KL=K
      IF(KL.EQ.4) KL=3
      KH=KL+1
      DO 40 K=1,2
      KK=KL+K-1
   40 F2(K)=KFAC(JL,KK)+((RE-REYN(JL))/(REYN(JH)-REYN(JL)))
     1*(KFAC(JH,KK)-KFAC(JL,KK))
      F=F2(1)+((RRATIO-RRAT(KL))/(RRAT(KH)-RRAT(KL)))
     1*(F2(2)-F2(1))
      RETURN
      END
```

SUBROUTINE SELCO

```
      SUBROUTINE SELCO(KFAC,QRATIO,FRATIO,RE,F)
      DIMENSION QRAT(6),REYN(5),RRAT(4),F1(2,2),F2(2)
      REAL KFAC(6,5,4)
      DATA QRAT/1.5,2.14,4.,6.,8.,10./
      DATA REYN/9.864,17.57,31.96,93.64,175.7/
      DATA RRAT/.5,1.,2.,3./
C-----DETERMINE INDICES OF ADJACENT TABLE VALUES FOR
C-----INTERPOLATION ROUTINE
C-----INITIALLY ASSUME THAT VALUE IS IN LOWER EXTRAPOLATION
C-----RANGE
      IL=1
      DO 10 I=1,6
   10 IF(QRATIO .GE. QRAT(I))IL=I
C-----CHECK FOR UPPER EXTRAPOLATION RANGE
      IF(IL .EQ. 6)IL=5
      IH=IL+1
      JL=1
      DO 20 J=1,5
   20 IF(RE .GE. REYN(J))JL=J
      IF(JL .EQ. 5)JL=4
      JH=JL+1
      KL=1
      DO 30 K=1,4
   30 IF(RRATIO .GE. RRAT(K)) KL=K
      IF(KL .EQ. 4) KL=3
      KH=KL+1
C-----COMMENCE FIRST INTERPOLATION
      DO 40 K=1,2
      KK=KL+K-1
      DO 45 J=1,2
      JJ=JL+J-1
      F1(J,K)=KFAC(IL,JJ,KK)+((QRATIO-QRAT(IL))/(QRAT(IH)-QRAT(IL)))
     1*(KFAC(IH,JJ,KK)-KFAC(IL,JJ,KK))
   45 CONTINUE
   40 CONTINUE
C-----COMMENCE SECOND INTERPOLATION
      DO 50 K=1,2
   50 F2(K)=F1(1,K)+((RE-REYN(JL))/(REYN(JH)-REYN(JL)))
     1*(F1(2,K)-F1(1,K))
C-----DO FINAL INTERPOLATION FOR DESIRED FRICTION CONSTANT
      F=F2(1)+((RRATIO-RRAT(KL))/(RRAT(KH)-RRAT(KL)))*
     1(F2(2)-F2(1))
      RETURN
```

FUNCTION H

```
      FUNCTION H(DHOR,XSTAR)
      REAL NU
      COMMON
     1/FLUPR/URFVIS,VISCOS,DENSIT,PRIN,DEN(6,6),VIS(6,6),
     1       GAMH(6,6),A1,A2,A3,A4,A5,A6,A7,SPHEAT,THCOND
      NU=2.235*XSTAR**(-1./3.)
      IF(XSTAR.GT.0.001.AND.XSTAR.LT.0.01)NU=NU+.3
      IF(XSTAR.GE.0.01)NU=0.235+.0364/XSTAR
      H=(A7/DHOR)*NU
      RETURN
      END
```

FUNCTION PE

```
      FUNCTION PE(FLORAT,TEMP)
      COMMON
     1/FLUPR/URFVIS,VISCOS,DENSIT,PRIN,DEN(6,6),VIS(6,6),
     1       GAMH(6,6),A1,A2,A3,A4,A5,A6,A7,SPHEAT,THCOND
      DENS=A3+A4*TEMP
      RHOCP=A5+A6*TEMP
      CP=RHOCP/DENS
      PR=VISC(TEMP)*CP/A7
      PE=RE(FLORAT,TEMP)*PR
      RETURN
      END
```

FUNCTION RE

```
      FUNCTION RE(FLORAT,TEMP)
      COMMON
     1/FLUPR/URFVIS,VISCOS,DENSIT,PRIN,DEN(6,6),VIS(6,6),
     1GAMH(6,6),A1,A2,A3,A4,A5,A6,A7,SPHEAT,THCOND
      DENS=A3+A4*TEMP
      RE=FLORAT*2.*DENS/VISC(TEMP)
      RETURN
      END
```

FUNCTION VISC

```
      FUNCTION VISC(TEMP)
      COMMON
     1/FLUPR/URFVIS,VISCOS,DENSIT,PRIN,DEN(6,6),VIS(6,6),
     1GAMH(6,6),A1,A2,A3,A4,A5,A6,A7,SPHEAT,THCOND
      DENS=A3+A4*TEMP
      ENUIN=(EXP(EXP(A1)*(TEMP+273.)**A2)-.7)/1.E6
      VISC=DENS*ENUIN
      RETURN
      END
```

Input File DATIN.DAT

```
8
.1024,.1024,.1024,.1024,.1024,.1024,.1024,
.01374,.01374,.01374,.01374,.01374,.01374,.01374
.008,.008,.008,.008,.008,.008,.008
.01614,.01614,.01614,.01614,.01614,.01614,.01614
.00908,.00788,.00804,.00764,.00864,.0082,.00936,.00716
5.46E-4,58.9,24.656,-4.1232,889.,-.7,1.6E6,1.8E3,.117
.172,.025,.001,.006,1.72E-8,3.93E-3,603.5,.023
32.56,31.34,30.29,30.01,29.9,29.89
42.85,39.28,35.81,34.36,33.64,33.24
89.72,75.24,58.99,52.71,49.78,47.42
151.86,121.92,87.74,74.2,66.99,63.3
286.7,223.4,148.2,117.9,102.37,93.7
26.7,25.,23.33,22.7,22.37,22.19
36.32,32.47,28.05,26.25,25.34,24.75
81.17,66.49,48.74,41.77,38.26,36.
142.88,111.08,75.98,61.5,53.89,49.84
278.9,212.75,135.2,104.4,88.44,78.85
21.4,19.34,16.76,15.97,15.26,15.25
32.29,26.94,21.68,19.40,18.3,17.58
76.,60.7,42.02,34.5,30.47,28.26
137.91,105.9,69.28,54.2,46.44,41.55
282.4,211.1,129.4,97.66,80.8,70.44
19.27,17.42,14.39,13.39,12.84,12.68
29.53,24.39,19.41,16.97,15.69,14.63
74.74,59.15,40.01,32.15,28.67,25.57
137.43,105.1,67.81,51.8,43.85,39.02
290.2,213.8,129.2,95.07,78.6,68.2
26.37,24.54,22.56,21.73,21.4,21.15
37.37,33.52,29.52,27.8,26.89,26.45
84.51,70.21,53.76,47.62,44.51,42.16
146.5,116.33,81.99,68.28,61.02,57.24
280.1,217.,141.2,110.2,94.26,85.6
22.88,20.79,18.07,16.88,16.19,15.81
32.34,28.26,23.43,21.4,20.21,19.5
75.45,62.09,44.84,38.04,34.43,32.14
138.08,108.13,73.26,58.4,50.36,46.41
274.8,208.77,133.7,101.7,84.92,74.90
28.36,23.93,18.19,16.4,14.29,13.59
33.93,29.13,22.57,19.36,18.3,16.05
68.91,57.01,41.39,34.84,30.53,27.61
128.1,102.,51.13,53.54,46.34,40.68
266.3,202.8,127.6,98.02,81.6,70.65
39.32,37.24,27.61,22.09,18.83,16.21
43.04,37.23,27.85,24.,18.73,18.4
68.15,58.92,44.52,36.43,32.23,28.67
121.17,98.6,70.8,55.6,47.4,41.56
263.2,198.,125.6,95.25,81.7,71.5
12.86,17.09,22.42,24.72,25.91,26.58
8.08,13.55,21.02,24.34,25.06,27.18
-10.62,-1.54,13.84,21.63,25.65,28.13
-31.,-20.04,3.356,15.71,22.61,27.56
-64.02,-52.03,-19.38,1.695,13.46,21.85
6.53,10.09,14.81,16.88,17.96,18.69
.688,5.39,12.33,15.38,17.1,18.14
-20.18,-13.07,1.2,8.73,12.82,15.52
-39.14,-31.67,-11.47,.477,7.38,11.82
-70.11,-61.78,-33.12,-15.4,-3.62,4.098
1.12,3.9,7.94,9.58,10.62,11.58
-5.38,-1.3,5.07,8.01,9.45,10.56
-25.94,-20.34,-7.02,.23,4.361,6.99
-43.7,-38.08,-20.08,-8.64,-1.76,2.82
-73.68,-66.9,-41.4,-24.67,-13.51,-6.06
1.033,1.22,5.28,6.74,8.05,8.61
-7.43,-4.07,2.308,4.73,6.49,7.53
-28.17,-23.05,-10.26,-2.75,1.15,3.69
-45.72,-40.78,-23.11,-12.,-5.23,-.8
-75.23,-69.7,-45.2,-27.53,-17.04,-9.93
10.26,9.96,9.65,9.52,9.58,9.56
7.6,7.2,7.11,7.12,7.19,7.16
3.961,3.44,4.07,4.43,4.69,4.83
6.24,3.32,4.3,5.1,5.42,5.59
```

```
16.22,19.09,7.73,7.56,8.03,8.27
14.94,11.91,9.43,8.7,8.29,8.22
14.29,10.3,7.53,6.81,6.53,6.38
20.25,10.49,5.53,4.47,4.14,4.03
37.87,19.02,7.32,5.56,4.97,4.79
86.15,42.14,16.47,11.8,9.64,9.24
45.05,20.18,17.01,12.69,10.6,9.35
54.57,33.76,16.82,12.15,10.,8.64
106.6,55.41,21.03,12.8,9.82,8.30
189.3,94.65,32.91,18.4,13.56,11.52
384.4,197.7,62.92,35.1,24.62,19.59
100.5,64.88,33.68,23.06,17.39,14.64
126.35,76.27,35.48,23.42,18.04,14.52
259.13,138.54,51.09,29.47,20.53,16.5
446.24,229.2,76.8,40.77,27.65,21.59
861.42,448.8,141.6,74.58,48.58,36.74
11.28,22.32,86.1,205.0
8.58,23.94,109.3,266.5
5.612,44.46,235.6,578.5
9.23,78.25,408.3,990.6
23.42,167.6,805.6,1902.
```

Output file RESULT.DAT follows on next pages.

```
QIN     =     5.460E-04 M**2/SEC
TIN     =     5.890E+01 DEG. C
CURRENT=     6.035E+02 AMPS
NDUCT   =  8

R=
    .7934E+05     .1214E+06     .1143E+06     .1332E+06
    .9209E+05     .1077E+06     .7243E+05     .1618E+06


P=
    .0000E+01     .0000E+01     .0000E+01     .0000E+01
    .0000E+01     .0000E+01     .0000E+01     .0000E+01


RL=
    .1556E+05     .1556E+05     .1556E+05     .1556E+05
    .1556E+05     .1556E+05     .1556E+05     .0000E+01


PL=
    .0000E+01     .0000E+01     .0000E+01     .0000E+01
    .0000E+01     .0000E+01     .0000E+01

RR=
    .1895E+04     .1895E+04     .1895E+04     .1895E+04
    .1895E+04     .1895E+04     .1895E+04     .0000E+01


RR=
    .0000E+01     .0000E+01     .0000E+01     .0000E+01
    .0000E+01     .0000E+01     .0000E+01
INITIAL DISTRIBUTION
PERCENT FLOW IN DUCT NO.   1 IS 37.06
PERCENT FLOW IN DUCT NO.   2 IS 16.73
PERCENT FLOW IN DUCT NO.   3 IS 12.37
PERCENT FLOW IN DUCT NO.   4 IS  7.60
PERCENT FLOW IN DUCT NO.   5 IS  8.07
PERCENT FLOW IN DUCT NO.   6 IS  5.72
PERCENT FLOW IN DUCT NO.   7 IS  8.12
PERCENT FLOW IN DUCT NO.   8 IS  4.34
FLOW RATE IN DUCT NO.   1 IS    2.023E-04 M**2/SEC
FLOW RATE IN DUCT NO.   2 IS    9.135E-05 M**2/SEC
FLOW RATE IN DUCT NO.   3 IS    6.753E-05 M**2/SEC
FLOW RATE IN DUCT NO.   4 IS    4.149E-05 M**2/SEC
FLOW RATE IN DUCT NO.   5 IS    4.408E-05 M**2/SEC
FLOW RATE IN DUCT NO.   6 IS    3.121E-05 M**2/SEC
FLOW RATE IN DUCT NO.   7 IS    4.432E-05 M**2/SEC
FLOW RATE IN DUCT NO.   8 IS    2.368E-05 M**2/SEC
```

DUCT NO.	XLEFT	HLEFT	XRITE	HRITE	QLEFT	QRITE
1	8.569E-05	7.418E+02	7.213E-05	8.894E+02	8.437E-04	2.023E-04
2	1.167E-04	6.692E+02	4.970E-05	4.409E+02	2.523E-04	2.937E-04
3	1.594E-04	6.032E+02	4.041E-05	4.724E+02	1.848E-04	3.612E-04
4	2.055E-04	5.541E+02	3.624E-05	4.898E+02	1.483E-04	4.027E-04
5	2.968E-04	4.902E+02	3.267E-05	5.070E+02	9.320E-05	4.468E-04
6	4.391E-04	4.322E+02	3.053E-05	5.186E+02	6.799E-05	4.780E-04
7	1.244E-03	3.173E+02	2.794E-05	5.341E+02	2.368E-05	5.223E-04
8	0.000E+00	0.000E+00	2.673E-05	5.421E+02	2.368E-05	5.460E-04

TR=

.6011E+02	.6056E+02	.6091E+02	.6130E+02
.6159E+02	.6191E+02	.6211E+02	.6244E+02

TR=

.0000E+01	.0000E+01	.0000E+01	.0000E+01
.0000E+01	.0000E+01	.0000E+01	.0000E+01

K=

.2122E+02	.2018E+02	.1958E+02	.1862E+02
.1852E+02	.1775E+02	.1834E+02	.1668E+02

K=

.2400E+02	.2400E+02	.2400E+02	.2400E+02
.2400E+02	.2400E+02	.2400E+02	.2400E+02

DIVIDING JUNCTIONS

DUCT NO.	QRATIO	RRATIO	RE	KDT	KDS
1	2.70	.88	158.23	25.26	-42.92
2	3.76	1.02	96.44	9.69	-14.96
3	3.74	1.00	70.81	7.44	-6.80
4	4.45	1.05	51.86	5.95	2.55
5	3.25	.93	40.21	7.47	1.88
6	3.18	.98	27.84	8.33	5.44
7	1.53	.85	19.08	12.32	2.22

COMBINING JUNCTIONS

DUCT NO.	QRATIO	RRATIO	RE	KCT	KCS
2	2.22	2.05	59.46	64.27	67.88
3	4.35	2.01	87.15	49.93	62.60
4	8.71	2.11	108.81	50.41	50.23
5	9.14	1.87	121.73	54.77	55.41
6	14.32	1.97	136.22	38.34	40.18
7	10.79	1.72	146.53	57.88	59.25
8	22.06	2.25	161.54	6.08	8.06

RDT=

.1287E+05	.8884E+04	.5249E+04	.5002E+04
.4586E+04	.5001E+04	.3568E+04	.0000E+01

RDT=

.0000E+01	.0000E+01	.0000E+01	.0000E+01
.0000E+01	.0000E+01	.0000E+01	.0000E-01

RDS=

-.1287E+05	-.8846E+04	-.1753E+04	.6302E+03
.5126E+03	.1499E+04	.1202E+04	.0000E+01

```
RDS=
   .0000E+01     .0000E+01     .0000E+01     .0000E+01
   .0000E+01     .0000E+01     .0000E+01
RCT=
   .0000E+01     .9142E+04     .1170E+05     .2120E+05
   .2386E+05     .2501E+05     .2889E+05     .5880E+04

RCT=
   .0000E+01     .0000E+01     .0000E+01     .0000E+01
   .0000E+01     .0000E+01     .0000E+01     .0000E+01

RCS=
   .0000E+01     .4359E+04     .3372E+04     .2426E+04
   .2642E+04     .1831E+04     .2742E+04     .3536E+03

RCS=
   .0000E+01     .0000E+01     .0000E+01     .0000E+01
   .0000E+01     .0000E+01     .0000E+01     .0000E+01

BOTTOM CORNER
RRATIO      RE        KCL
     .56    58.73     11.68
TOP CORNER
RRATIO      RE        KCH
    1.12     6.64     28.41
RCL=      .1653E+04 RCH=      .5363E+04


R=
   .7014E+05     .1020E+06     .9323E 05     .1033E+06
   .7107E+05     .7968E+05     .5536E+05     .1124E+06


R=
   .0000E+01     .0000E+01     .0000E+01     .0000E+01
   .0000E+01     .0000E+01     .0000E+01     .0000E+01


RL=
   .1556E+05     .1556E+05     .1556E+05     .1556E+05
   .1556E+05     .1556E+05     .1556E+05     .0000E+01


RL=
   .0000E+01     .0000E+01     .0000E+01     .0000E+01
   .0000E+01     .0000E+01     .0000E+01

RR=
   .1831E+04     .1808E+04     .1790E+04     .1770E+04
```

```
   .1756E+04     .1740E+04     .1731E+04     .0000E+01

RR=
   .0000E+01     .0000E+01     .0000E+01     .0000E+01
   .0000E+01     .0000E+01     .0000E+01
RESIDUAL AFTER   1 ITERATIONS IS    2.477E-01

 DUCT NO.       XLEFT         HLEFT         XRITE         HRITE         QLEFT         QRITE
        1     7.160E-05     7.375E+02     1.082E-04     3.401E+02     4.113E-04     1.347E-04
        2     9.289E-05     7.221E+02     6.362E-05     4.060E+02     3.170E-04     2.290E-04
        3     1.233E-04     6.571E+02     4.743E-05     4.478E+02     2.389E-04     3.071E-04
        4     1.567E-04     6.066E+02     4.066E-05     4.714E+02     1.880E-04     3.580E-04
        5     2.160E-04     5.451E+02     3.553E-05     4.931E+02     1.364E-04     4.096E-04
        6     3.063E-04     4.851E+02     3.234E-05     5.087E+02     9.613E-05     4.499E-04
        7     7.081E-04     3.669E+02     2.884E-05     5.286E+02     4.159E-05     5.044E-04
        8     0.000E+00     0.000E+00     2.663E-05     5.428E+02     4.159E-05     5.460E-04
TR=
   .6071E+02     .6103E+02     .6128E+02     .6161E+02
   .6186E+02     .6213E+02     .6226E+02     .6248E+02
TR=
   .0000E+01     .0000E+01     .0000E+01     .0000E+01
   .0000E+01     .0000E+01     .0000E+01     .0000E+01
K=
   .2063E+02     .2022E+02     .1985E+02     .1907E+02
   .1887E+02     .1838E+02     .1882E+02     .1826E+02
K=
   .2400E+02     .2400E+02     .2400E+02     .2400E+02
   .2400E+02     .2400E+02     .2400E+02     .2400E+02
DIVIDING JUNCTIONS
DUCT NO.   QRATIO    RRATIO   RE       KDT      KDS
   1         4.05       .88   153.29    12.18   -23.41
   2         4.36      1.02   115.42     9.72   -14.91
   3         4.06      1.00    88.96     7.04    -9.56
   4         4.69      1.05    67.05     6.48     -.64
   5         3.64       .93    52.75     6.16      .04
   6         3.39       .98    38.27     7.55     2.43
   7         1.78       .85    26.98    11.54     -.37
COMBINING JUNCTIONS
DUCT NO.   QRATIO    RRATIO   RE       KCT      KCS
   2         1.43      2.05    40.10    58.02    62.17
   3         2.93      2.01    68.64    62.38    57.75
   4         6.03      2.11    92.88    58.33    53.46
   5         6.94      1.87   109.01    58.25    58.87
   6        10.18      1.97   125.63    51.82    52.44
   7         8.25      1.72   138.45    65.58    66.33
   8        12.19      2.25   156.16    53.56    53.33
PDT=
   .9321E+04     .8006E+04     .5997E+04     .5736E+04
   .4235E+04     .4829E+04     .3841E+04     .5363E+04
```

```
FDT=
   .0000E+01     .0000E+01     .0000E+01     .0000E+01
   .0000E+01     .0000E+01     .0000E+01     .0000E+01

RDS=
  -.5867E+04    -.3652E+04    -.2395E+04    -.1537E+03
   .1006E+02     .6512E+03    -.1613E+03     .0000E+01

RDS=
   .0000E+01     .0000E+01     .0000E+01     .0000E+01
   .0000E+01     .0000E+01     .0000E+01
RCT=
   .1653E+04     .6152E+04     .1063E+05     .1609E+05
   .1972E+05     .2453E+05     .2558E+05     .2948E+05

RCT=
   .0000E+01     .0000E+01     .0000E+01     .0000E+01
   .0000E+01     .0000E+01     .0000E+01     .0000E+01

RCS=
   .0000E+01     .4613E+04     .3938E+04     .2677E+04
   .2873E+04     .2438E+04     .3137E+04     .2420E+04

RCS=
   .0000E+01     .0000E+01     .0000E+01     .0000E+01
   .0000E+01     .0000E+01     .0000E+01     .0000E+01

BOTTOM CORNER
RRATIO      RE        KCL
    .56    39.76     10.48
TOP CORNER
PRATIO      RE        KCH
   1.12    11.67     30.99
RCL=      .1459E+04 RCH=      .5850E+04


R=
   .6821E+05     .1023E+06     .9453E+05     .1058E+06
   .7241E+05     .8250E+05     .5679E+05     .1231E+06


R=
   .0000E+01     .0000E+01     .0000E+01     .0000E+01
   .0000E+01     .0000E+01     .0000E+01     .0000E+01


RL=
   .1556E+05     .1556E+05     .1556E+05     .1556E+05
   .1556E+05     .1556E+05     .1556E+05     .0000E+01
```

```
RL=
   .0000E+01     .0000E+01     .0000E+01     .0000E+01
   .0000E+01     .0000E+01     .0000E+01

RR=
   .1800E+04     .1784E+04     .1771E+04     .1755E+04
   .1748E+04     .1730E+04     .1724E+04     .0000E+01


RR=
   .0000E+01     .0000E+01     .0000E+01     .0000E+01
   .0000E+01     .0000E+01     .0000E+01
RESIDUAL AFTER   2 ITERATIONS IS     1.002E-01

 DUCT NO.       XLEFT         HLEFT         XRITE         HRITE         QLEFT         QRITE
       1     7.614E-05    7.715E+02.    9.147E-05    3.597E+02    3.867E-04    1.593E-04
       2     9.746E-05    7.106E+02     5.972E-05    4.147E+02    3.021E-04    2.439E-04
       3     1.254E-04    6.516E+02     4.651E-05    4.507E+02    2.330E-04    3.130E-04
       4     1.582E-04    6.047E+02     4.045E-05    4.722E+02    1.862E-04    3.598E-04
       5     2.154E-04    5.455E+02     3.555E-05    4.930E+02    1.367E-04    4.093E-04
       6     3.010E-04    4.880E+02     3.246E-05    5.081E+02    9.783E-05    4.482E-04
       7     7.274E-04    3.636E+02     2.877E-05    5.290E+02    4.048E-05    5.055E-04
       8     0.000E+00    0.000E+00     2.663E-05    5.428E+02    4.048E-05    5.460E-04
TR=
   .6044E+02     .6090E+02     .6123E+02     .6160E+02
   .6186E+02     .6214E+02     .6225E+02     .6248E+02
TR=
   .0000E+01     .0000E+01     .0000E+01     .0000E+01
   .0000E+01     .0000E+01     .0000E+01     .0000E+01
K=
   .2088E+02     .2003E+02     .1962E+02     .1888E+02
   .1878E+02     .1830E+02     .1893E+02     .1820E+02
K=
   .2400E+02     .2400E+02     .2400E+02     .2400E+02
   .2400E+02     .2400E+02     .2400E+02     .2400E+02
DIVIDING JUNCTIONS
DUCT NO.   QRATIO    RRATIO   RE       KDT      KDS
   1         3.43       .88   153.23   17.97   -32.23
   2         4.57      1.02   108.53    8.71   -11.82
   3         4.37      1.00    84.79    6.62    -6.61
   4         4.88      1.05    65.38    6.15     1.10
   5         3.76       .93    52.25    5.85     1.15
   6         3.52       .98    38.37    7.28     3.17
   7         1.71       .85    27.45   11.93    -1.14
COMBINING JUNCTIONS
DUCT NO.   QRATIO    RRATIO   RE       KCT      KCS
   2         1.88      2.05    47.35   57.69    61.61
   3         3.53      2.01    78.00   54.91    62.84
```

```
   4         6.69     2.11    94.64    51.75    51.74
   5         7.27     1.87   109.56    56.99    57.54
   6        10.53     1.97   125.56    50.48    51.21
   7         7.82     1.72   137.30    67.50    68.21
   8        12.49     2.25   156.51    51.95    51.80
RDT=
   .1163E+05     .7518E+04     .5460E+04     .5785E+04
   .4160E+04     .4832E+04     .3842E+04     .5850E+04

RDT=
   .0000E+01     .0000E+01     .0000E+01     .0000E+01
   .0000E+01     .0000E+01     .0000E+01     .0000E+01

RDS=
  -.8590E+04    -.2857E+04    -.1619E+04     .2605E+03
   .2948E+03     .8367E+03    -.5205E+03     .0000E+01

RDS=
   .0000E+01     .0000E+01     .0000E+01     .0000E+01
   .0000E+01     .0000E+01     .0000E+01
RCT=
   .1459E+04     .7283E+04     .1079E+05     .1710E+05
   .2011E+05     .2463E+05     .2510E+05     .2937E+05

RCT=
   .0000E+01     .0000E+01     .0000E+01     .0000E+01
   .0000E+01     .0000E+01     .0000E+01     .0000E+01

RCS=
   .0000E+01     .4132E+04     .3501E+04     .2555E+04
   .2791E+04     .2373E+04     .3246E+04     .2345E+04

RCS=
   .0000E+01     .0000E+01     .0000E+01     .0000E+01
   .0000E+01     .0000E+01     .0000E+01     .0000E+01

BOTTOM CORNER
RRATIO      RE       KCL
     .56   45.65    10.48
TOP CORNER
RRATIO      RE       KCH
    1.12   11.36    30.83
RCL=      .1463E+04 RCH=      .5820E+04


R=
   .6904E+05     .1013E+06     .3941E+05     .1048E+06
   .7205E+05     .8213E+05     .5713E+05     .1227E+06
```

```
R=
    .0000E+01     .0000E+01     .0000E+01     .0000E+01
    .0000E+01     .0000E+01     .0000E+01     .0000E+01

RL=
    .1556E+05     .1556E+05     .1556E+05     .1556E+05
    .1556E+05     .1556E+05     .1556E+05     .0000E+01

RL=
    .0000E+01     .0000E+01     .0000E+01     .0000E+01
    .0000E+01     .0000E+01     .0000E+01

RR=
    .1814E+04     .1790E+04     .1774E+04     .1755E+04
    .1743E+04     .1729E+04     .1724E+04     .0000E+01

RR=
    .0000E+01     .0000E+01     .0000E+01     .0000E+01
    .0000E+01     .0000E+01     .0000E+01
RESIDUAL AFTER   3 ITERATIONS IS    3.516E-02

 DUCT NO.       XLEFT         HLEFT         XRITE         HRITE         QLEFT         QRITE
        1    7.449E-05    7.772E+02    9.669E-05    3.532E+02    3.953E-04    1.507E-04
        2    9.664E-05    7.126E+02    6.036E-05    4.132E+02    3.047E-04    2.413E-04
        3    1.267E-04    6.511E+02    4.643E-05    4.510E+02    2.824E-04    3.136E-04
        4    1.591E-04    6.036E+02    4.033E-05    4.726E+02    1.851E-04    3.609E-04
        5    2.168E-04    5.444E+02    3.547E-05    4.933E+02    1.358E-04    4.102E-04
        6    3.022E-04    4.873E+02    3.243E-05    5.083E+02    9.745E-05    4.486E-04
        7    7.301E-04    3.632E+02    2.876E-05    5.290E+02    4.033E-05    5.057E-04
        8    0.000E+00    0.000E+00    2.663E-05    5.428E+02    4.033E-05    5.460E-04
TR=
    .6053E+02     .6092E+02     .6123E+02     .6159E+02
    .6185E+02     .6214E+02     .6225E+02     .6248E+02
TR=
    .0000E+01     .0000E+01     .0000E+01     .0000E+01
    .0000E+01     .0000E+01     .0000E+01     .0000E+01
K=
    .2080E+02     .2015E+02     .1970E+02     .1890E+02
    .1877E+02     .1827E+02     .1892E+02     .1919E+02
K=
    .2400E+02     .2400E+02     .2400E+02     .2400E+02
    .2400E+02     .2400E+02     .2400E+02     .2400E+02
DIVIDING JUNCTIONS
DUCT NO.   QRATIO    RRATIO   RE        KDT      KDS
    1         3.52       .88   158.23    16.09   -29.38
    2         4.36      1.02   110.99     9.23   -18.77
    3         4.22      1.00    85.51     6.77    -7.65
```

```
   4         4.91     1.05    65.23     6.20      .85
   5         3.75      .93    51.96     5.86     1.17
   6         3.54      .98    38.12     7.24     3.40
   7         1.71      .85    27.85    11.92    -1.08
COMBINING JUNCTIONS
DUCT NO.   QRATIO    RRATIO   RE       KCT      KCS
   2         1.66     2.05    44.74    58.99    63.37
   3         3.34     2.01    72.23    57.82    64.99
   4         6.69     2.11    94.78    52.05    52.05
   5         7.32     1.87   109.86    56.93    57.46
   6        10.69     1.97   125.82    49.96    50.74
   7         7.85     1.72   138.01    67.31    68.02
   8        12.54     2.25   156.55    51.72    51.58
RDT=
   .1096E+05     .7606E+04     .5390E+04     .5755E+04
   .4153E+04     .4839E+04     .3840E^4      .5820E+04

RDT=
   .0000E+01     .0000E+01     .0000E+01     .0000E+01
   .0000E+01     .0000E+01     .0000E+01     .0000E+01

RDS=
  -.7561E+04    -.3374E+04    -.1894E+04     .2005E+03
   .3014E+03     .8952E+03    -.4920E+03     .0000E+01

RDS=
   .0000E+01     .0000E+01     .0000E+01     .0000E+01
   .0000E+01     .0000E+01     .0000E+01
RCT=
   .1469E+04     .5879E+04     .1089E+05     .1706E+05
   .2020E+05     .2471E+05     .2514E+05     .2935E+05

RCT=
   .0000E+01     .0000E+01     .0000E+01     .0000E+01
   .0000E+01     .0000E+01     .0000E+01     .0000E+01

RCS=
   .0000E+01     .4442E+04     .3666E+04     .2574E+04
   .2786E+04     .2948E+04     .3235E+04     .2935E+04

RCS=
   .0000E+01     .0000E+01     .0000E+01     .0000E+01
   .0000E+01     .0000E+01     .0000E+01     .0000E+01

BOTTOM CORNER
RRATIO     RE       KCL
    .55    44.25    10.48
TOP CORNER
RRATIO     RE       KCH
   1.12    11.92    30.81
```

```
RCL=      .1466E+04 RCH=      .5816E+04

R=
    .6877E+05     .1019E+06     .9381E+05     .1049E+06
    .7202E+05     .8199E+05     .5711E+05     .1226E+06

R=
    .0000E+01     .0000E+01     .0000E+01     .0000E+01
    .0000E+01     .0000E+01     .0000E+01     .0000E+01

RL=
    .1556E+05     .1556E+05     .1556E+05     .1556E+05
    .1556E+05     .1556E+05     .1556E+05     .0000E+01

RL=
    .0000E+01     .0000E+01     .0000E+01     .0000E+01
    .0000E+01     .0000E+01     .0000E+01

RR=
    .1809E+04     .1789E+04     .1774E+04     .1756E+04
    .1743E+04     .1729E+04     .1724E+04     .0000E+01

RR=
    .0000E+01     .0000E+01     .0000E+01     .0000E+01
    .0000E+01     .0000E+01     .0000E+01
RESIDUAL AFTER    4 ITERATIONS IS     1.063E-02
```

DUCT NO.	XLEFT	HLEFT	XRITE	HRITE	QLEFT	QRITE
1	7.494E-05	7.756E+02	9.518E-05	3.550E+02	3.929E-04	1.531E-04
2	9.668E-05	7.125E+02	6.033E-05	4.133E+02	3.046E-04	2.414E-04
3	1.264E-04	6.516E+02	4.651E-05	4.507E+02	2.330E-04	3.130E-04
4	1.587E-04	6.040E+02	4.037E-05	4.725E+02	1.855E-04	3.605E-04
5	2.166E-04	5.445E+02	3.548E-05	4.933E+02	1.360E-04	4.100E-04
6	3.022E-04	4.873E+02	3.243E-05	5.083E+02	9.745E-05	4.486E-04
7	7.302E-04	3.631E+02	2.876E-05	5.290E+02	4.033E-05	5.057E-04
8	0.000E+00	0.000E+00	2.663E-05	5.428E+02	4.033E-05	5.460E-04

```
TR=
    .6050E+02     .6092E+02     .6133E+02     .6160E+02
    .6186E+02     .6214E+02     .6225E+02     .6248E+02
TR=
    .0000E+01     .0000E+01     .0000E+01     .0000E+01
    .0000E+01     .0000E+01     .0000E+01     .0000E+01
K=
    .2083E-02     .2011E+02     .1969E+02     .1891E+02
    .1878E+02     .1828E+02     .1893E+02     .1819E+02
```

```
K=
   .2400E+02     .2400E+02     .2400E+02     .2400E+02
   .2400E+02     .2400E+02     .2400E+02     .2400E+02
DIVIDING JUNCTIONS
DUCT NO.   QRATIO    RRATIO   RE        KDT      KDS
   1         3.57       .88   153.23    16.59   -30.20
   2         4.45      1.02   110.27     9.05   -13.05
   3         4.25      1.00    85.48     6.74    -7.45
   4         4.91      1.05    65.38     6.21      .78
   5         3.74       .93    52.06     5.89     1.06
   6         3.53       .98    38.15     7.26     3.34
   7         1.71       .85    27.35    11.92    -1.08
COMBINING JUNCTIONS
DUCT NO.   QRATIO    RRATIO   PE        KCT      KCS
   2         1.73      2.05    45.44    58.52    62.75
   3         3.37      2.01    72.27    57.30    64.57
   4         6.59      2.11    94.63    52.10    52.11
   5         7.28      1.87   109.75    57.07    57.61
   6        10.65      1.97   125.78    50.09    50.86
   7         7.85      1.72   138.01    67.32    68.09
   8        12.54      2.25   156.56    51.71    51.57
PDT=
   .1117E+05     .7601E+04     .5412E+04     .5759E+04
   .4162E+04     .4838E+04     .3840E+04     .5816E+04

RDT=
   .0000E+01     .0000E+01     .0000E+01     .0000E+01
   .0000E+01     .0000E+01     .0000E+01     .0000E+01

PDS=
  -.7923E+04    -.3178E+04    -.1838E+04     .1860E+03
   .2722E+03     .8794E+03    -.4932E+03     .0000E+01

RDS=
   .0000E+01     .0000E+01     .0000E+01     .0000E+01
   .0000E+01     .0000E+01     .0000E+01
PCT=
   .1466E+04     .7002E+04     .1087E+05     .1700E+05
   .2015E+05     .2469E+05     .2514E+05     .2935E+05

RCT=
   .0000E+01     .0000E+01     .0000E+01     .0000E+01
   .0000E+01     .0000E+01     .0000E+01     .0000E+01

PCS=
   .0000E+01     .4333E+04     .3634E+04     .2573E+04
   .2795E+04     .2355E+04     .3236E+04     .2334E+04

RCS=
   .0000E+01     .0000E+01     .0000E+01     .0000E+01
```

```
   .0000E+01     .0000E+01     .0000E+01     .0000E+01

BOTTOM CORNER
RRATIO      RE       KCL
    .56    44.92    10.48
TOP CORNER
RRATIO      RE       KCH
   1.12    11.32    30.80
RCL=      .1467E+04 RCH=      .5816E+04


R=
   .6885E+05     .1017E+06     .9373E+05     .1049E+06
   .7206E+05     .8202E+05     .5711E+05     .1226E+06


R=
   .0000E+01     .0000E+01     .0000E+01     .0000E+01
   .0000E+01     .0000E+01     .0000E+01     .0000E+01


RL=
   .1556E+05     .1555E+05     .1556E+05     .1556E+05
   .1556E+05     .1556E+05     .1556E+05     .0000E+01


RL=
   .0000E+01     .0000E+01     .0000E+01     .0000E+01
   .0000E+01     .0000E+01     .0000E+01

RR=
   .1811E+04     .1789E+04     .1773E+04     .1756E+04
   .1743E+04     .1729E+04     .1724E+04     .0000E+01


RR=
   .0000E+01     .0000E+01     .0000E+01     .0000E+01
   .0000E+01     .0000E+01     .0000E+01
RESIDUAL AFTER   5 ITERATIONS IS    2.812E-03
FINAL DISTRIBUTION AFTER   5 ITERATIONS:


PERCENT FLOW IN DUCT NO.  1 IS 27.92
PERCENT FLOW IN DUCT NO.  2 IS 16.30
PERCENT FLOW IN DUCT NO.  3 IS 13.13
PERCENT FLOW IN DUCT NO.  4 IS  8.68
PERCENT FLOW IN DUCT NO.  5 IS  9.07
PERCENT FLOW IN DUCT NO.  6 IS  7.05
PERCENT FLOW IN DUCT NO.  7 IS 10.47
PERCENT FLOW IN DUCT NO.  8 IS  7.39
```

```
FLOW RATE IN DUCT NO.   1 IS     1.524E-04 M**2/SEC
FLOW RATE IN DUCT NO.   2 IS     8.899E-05 M**2/SEC
FLOW RATE IN DUCT NO.   3 IS     7.168E-05 M**2/SEC
FLOW RATE IN DUCT NO.   4 IS     4.739E-05 M**2/SEC
FLOW RATE IN DUCT NO.   5 IS     4.950E-05 M**2/SEC
FLOW RATE IN DUCT NO.   6 IS     3.851E-05 M**2/SEC
FLOW RATE IN DUCT NO.   7 IS     5.715E-05 M**2/SEC
FLOW RATE IN DUCT NO.   8 IS     4.034E-05 M**2/SEC
```